Advances in Neurobiology 33

Zhao-Wen Wang *Editor*

Molecular Mechanisms of Neurotransmitter Release

Second Edition

Springer

Advances in Neurobiology

Volume 33

Series Editor

Arne Schousboe
Department of Drug Design & Pharmacology
University of Copenhagen
Copenhagen, Denmark

Advances in Neurobiology covers basic research in neurobiology and neurochemistry. It provides in-depth, book-length treatment of some of the most important topics in neuroscience including molecular and pharmacological aspects. The main audiences of the series are basic science researchers and graduate students as well as clinicians including neuroscientists (neurobiologists and neurochemists) and neurologists. *Advances in Neurobiology* is indexed in PubMed, Google Scholar, and the Thompson Reuters Book Citation Index.

Zhao-Wen Wang
Editor

Molecular Mechanisms of Neurotransmitter Release

Second Edition

Springer

Editor
Zhao-Wen Wang
Department of Neuroscience
University of Connecticut School of Medicine
Farmington, CT, USA

ISSN 2190-5215 ISSN 2190-5223 (electronic)
Advances in Neurobiology
ISBN 978-3-031-34228-8 ISBN 978-3-031-34229-5 (eBook)
https://doi.org/10.1007/978-3-031-34229-5

This Springer imprint is published by the registered company Springer Nature Switzerland AG
The registered company address is: Gewerbestrasse 11, 6330 Cham, Switzerland

Paper in this product is recylable.

Preface

Neurotransmitter release is a fundamental process that underpins the physiological functions of the nervous system. This book is intended for graduate students and neuroscientists who are interested in understanding the molecular mechanisms that govern this critical process. Recent breakthroughs and discoveries have shed new light on the diverse roles played by different proteins in regulating neurotransmitter release. The second edition of this book builds upon the success of the first edition, with important chapters substantially updated and new chapters added to reflect the latest advances in the field.

The updated chapters cover a wide range of topics, including the architecture of presynaptic release sites, modes of synaptic vesicle fusion and retrieval, the role of SNARE proteins in synaptic vesicle fusion, the sources and roles of calcium in synaptic exocytosis, the regulation of presynaptic calcium channels, the roles of UNC-13/Munc13 and UNC-18/Munc18 in synaptic exocytosis, and the regulation of neurotransmitter release by potassium channels, cell adhesion molecules, and lipids. The book also includes several new chapters that describe the roles of calcium sensors, tomosyn, complexins, and regulators of presynaptic ryanodine receptors (aryl hydrocarbon receptor-interacting protein, presenilins, and calstabins) in synaptic exocytosis, as well as a chapter on the components and functions of presynaptic cytomatrix proteins.

I would like to express my gratitude to the contributors of the book chapters, who are leading experts on the topics related to their chapters. It is an honor and a privilege to have such an outstanding group of scientists as contributors. I also thank Springer Nature for their support and for providing me with the opportunity to publish this new edition. I want to extend special thanks to William Lamsback, Senior Editor of Neuroscience at Springer Nature, for his encouragement and for inviting me to publish this second edition. I am also grateful to Vyshnavi Kalanath and Kate Lazaro, Project Coordinators at Springer Nature, for their assistance and support throughout the publication process.

Lastly, I want to acknowledge the readers of the previous edition for their feedback, which has helped to make this second edition possible. I hope that this new edition will continue to serve as a valuable resource for those interested in understanding the molecular mechanisms of neurotransmitter release.

I am forever grateful to my wife, Mingfu Yu, whose love and support have been a constant source of inspiration throughout my career.

Farmington, CT, USA Zhao-Wen Wang

Contents

Contributors

Isaac O. Akefe Clem Jones Centre for Ageing Dementia Research, Queensland Brain Institute, The University of Queensland, St Lucia, QLD, Australia

Chun Hin Chow Division of Experimental & Translational Neuroscience, Krembil Brain Institute, University Health Network, Toronto, ON, Canada

Faculty of Medicine, Department of Physiology, University of Toronto, Toronto, ON, Canada

Kensuke Futai Brudnick Neuropsychiatric Research Institute, Department of Neurobiology, University of Massachusetts Medical School, Worcester, MA, USA

Yasunori Hayashi Department of Pharmacology, Kyoto University Graduate School of Medicine, Kyoto, Japan

Zhitao Hu Clem Jones Centre for Ageing Dementia Research (CJCADR), Queensland Brain Institute, The University of Queensland, Brisbane, QLD, Australia

Mengjia Huang Division of Experimental & Translational Neuroscience, Krembil Brain Institute, University Health Network, Toronto, ON, Canada

Faculty of Medicine, Department of Physiology, University of Toronto, Toronto, ON, Canada

Yishi Jin Department of Neurobiology, School of Biological Sciences, University of California San Diego, La Jolla, CA, USA

Erik M. Jorgensen School of Biological Sciences, and Howard Hughes Medical Institute, University of Utah, Salt Lake City, UT, USA

Francisco José López-Murcia Department of Pathology and Experimental Therapy, Institute of Neurosciences, University of Barcelona, Barcelona, Spain

Bellvitge Biomedical Research Institute (IDIBELL), Barcelona, Spain

Benjamin Matthews Clem Jones Centre for Ageing Dementia Research, Queensland Brain Institute, The University of Queensland, St Lucia, QLD, Australia

Frédéric A. Meunier Clem Jones Centre for Ageing Dementia Research (CJCADR), Queensland Brain Institute, The University of Queensland, St Lucia, QLD, Australia

Longgang Niu Department of Neuroscience, University of Connecticut School of Medicine, Farmington, CT, USA

Shona L. Osborne ARC Training Centre for Innovation in Biomedical Imaging Technology (CIBIT), The University of Queensland, St Lucia, QLD, Australia

Mark T. Palfreyman School of Biological Sciences, and Howard Hughes Medical Institute, University of Utah, Salt Lake City, UT, USA

Kerstin Reim Department of Molecular Neurobiology, Max Planck Institute for Multidisciplinary Sciences, Göttingen, Germany

Sadaf Riaz Department of Neuroscience, University of Connecticut School of Medicine, Farmington, CT, USA

Shuzo Sugita Division of Experimental & Translational Neuroscience, Krembil Brain Institute, University Health Network, Toronto, ON, Canada

Faculty of Medicine, Department of Physiology, University of Toronto, Toronto, ON, Canada

Holger Taschenberger Department of Molecular Neurobiology, Max Planck Institute for Multidisciplinary Sciences, Göttingen, Germany

Laurence O. Trussell Oregon Hearing Research Center & Vollum Institute, Oregon Health and Science University, Portland, OR, USA

Motokazu Uchigashima Department of Cellular Neuropathology, Brain Research Institute, Niigata University, Niigata, Japan

Kiranmayi Vedantham Department of Neuroscience, University of Connecticut School of Medicine, Farmington, CT, USA

Tristan P. Wallis Clem Jones Centre for Ageing Dementia Research, Queensland Brain Institute, The University of Queensland, St Lucia, QLD, Australia

Zhao-Wen Wang Department of Neuroscience, University of Connecticut School of Medicine, Farmington, CT, USA

Sam E. West School of Biological Sciences, and Howard Hughes Medical Institute, University of Utah, Salt Lake City, UT, USA

Ling-Gang Wu National Institute of Neurological Disorders and Stroke, Bethesda, MD, USA

Xin-Sheng Wu National Institute of Neurological Disorders and Stroke, Bethesda, MD, USA

Lixia Yue Department of Cell Biology, Calhoun Cardiology Center, University of Connecticut School of Medicine, Farmington, CT, USA

R. Grace Zhai Department of Molecular and Cellular Pharmacology, Leonard M. Miller School of Medicine, University of Miami, Miami, FL, USA

Qiangjun Zhou Department of Cell and Developmental Biology, Vanderbilt Brain Institute, Vanderbilt University, Nashville, TN, USA

Pengyu Zong Department of Cell Biology, Calhoun Cardiology Center, University of Connecticut School of Medicine, Farmington, CT, USA

The Architecture of the Presynaptic Release Site

R. Grace Zhai

Abstract The architecture of the presynaptic release site is exquisitely designed to facilitate and regulate synaptic vesicle exocytosis. With the identification of some of the building blocks of the active zone and the advent of super resolution imaging techniques, we are beginning to understand the morphological and functional properties of synapses in great detail. Presynaptic release sites consist of the plasma membrane, the cytomatrix, and dense projections. These three components are morphologically distinct but intimately connected with each other and with postsynaptic specializations, ensuring the fidelity of synaptic vesicle tethering, docking, and fusion, as well as signal detection. Although the morphology and molecular compositions of active zones may vary among species, tissues, and cells, global architectural design of the release sites is highly conserved.

Keywords Ribbon synapse · T-bar · Dense projection · Cytomatrix · Neuromuscular junction

1 Introduction

In 1897, Sir Charles Sherrington introduced the term "synapse" to explain a delay of the spinal reflex at the junction between neurons [1], as he "felt the need of some name to call the junction between nerve-cell and nerve-cell, because the place of junction now entered physiology as carrying functional importance" [2]. The notion of synapse contributed to the birth of the concept of chemical transmission, firstly with adrenalin [3] and secondly with acetylcholine (ACh) [4, 5].

R. G. Zhai (✉)
Department of Molecular and Cellular Pharmacology, Leonard M. Miller School of Medicine, University of Miami, Miami, FL, USA
e-mail: gzhai@med.miami.edu

Z.-W. Wang (ed.), *Molecular Mechanisms of Neurotransmitter Release*, Advances in Neurobiology 33, https://doi.org/10.1007/978-3-031-34229-5_1

In the early 1900s, Ramón y Cajal proposed his neuron doctrine, which predicted that pre- and postsynaptic structures are constructed from distinct cells that do not have cytoplasmic continuity with each other. It was not until the mid-1940s that René Couteaux, a great French histologist, first morphologically identified synapses [6]. By staining with a special dye, Janus Green B, Couteaux revealed a membranous "subneural apparatus" related to the "synaptic gutter" [7, 8]. This discovery gave a morphological basis to the physiological term and defined synapses as specialized cell–cell contacts where signals are transduced from a neuron to its target cell. Soon after, in the 1950s, seminal work using electron microscopy (EM) from two teams, De Robertis and Bennett [9], and Palade and Palay [10], provided ultrastructural evidence for synapses.

At chemical synapses, signal transduction is achieved by converting an electrical signal into a chemical signal that diffuses between cells. This signal conversion occurs primarily at active zones, which are highly specialized sites at the presynaptic nerve terminal. The term "active zone" was coined by Couteaux and Pecot-Dechavassine in 1970 [11] during their ultrastructural studies of partially contracted frog muscles, where they observed profiles of open synaptic vesicles immediately adjacent to presynaptic dense bands, which they designated "les zones actives." Subsequently, similar structures were observed in other types of synapses. Ultrastructural studies of synapses in different organisms have revealed the following conserved morphological features among active zones, regardless of their size, location, neuron type, and postsynaptic partner. First, the plasma membrane of the active zone appears to be electron-dense, suggesting a proteinaceous nature. Second, synaptic vesicles cluster, tether, and fuse at the active zone [11, 12]. Third, the active zone is closely and precisely aligned with a postsynaptic density (PSD) area of another neuron in such a way that the active zone spans the same width as the PSD, and the extracellular space between the two membranes (synaptic cleft) is as narrow as 20–30 nm [13]. The latter two morphological characteristics led to the suggestion that active zones function as sites of synaptic vesicle exocytosis and neurotransmitter release. This hypothesis has gained strong support from many studies of synaptic vesicle exocytosis and postsynaptic neurotransmitter receptor function since it was proposed about three decades ago. It is important to note that more recent studies have suggested that neuronal exocytosis can also occur at sites that are distant from active zones, the so-called "ectopic release" sites [14], indicating that cellular communication in the nervous system may be more versatile and dynamic than we have already known.

Here, I discuss the structural organization of active zones in different types of synapses found in a variety of organisms, summarize recent advances in the molecular characterization of the active zone assembly, and propose that all active zones are organized following similar principles. At the end, I also discuss the possible structural bases of ectopic release.

2 The Structure of Active Zones

Active zones are defined morphologically as sites of synaptic vesicle docking and fusion, and physiologically as sites of neurotransmitter release. The active zone can be divided into three morphologically distinct components: (1) the plasma membrane juxtaposed to the PSD where synaptic vesicle fusion occurs, (2) the cytomatrix immediately internal to the plasma membrane where synaptic vesicles dock, and (3) electron-dense projections extending from the cytomatrix into the cytoplasm with tethered synaptic vesicles. All active zones have these three components although they may vary in appearance, especially in the size and shape of dense projections. Figure 1 illustrates the ultrastructure of active zones found in nine different types of synapses, as well as the schematic representation of the three components in each type of active zone. Figure 2 provides three-dimensional (3-D) reconstruction models of frog neuromuscular junction (NMJ) and mammalian central nervous system (CNS) synapses as examples of active zone architecture. In the following, I discuss the molecular and functional properties of each component of the active zone.

2.1 The Plasma Membrane of the Active Zone

Besides separating the cytosol from the extracellular environment, the plasma membrane of the active zone has two "gates" essential for neurotransmission, one for Ca^{2+} "entry," which is the voltage-gated Ca^{2+} channel, and the other for neurotransmitter "exit," which is the synaptic vesicle fusion site. These two gates are thought to be in close proximity with each other based on several observations. First, the time delay between Ca^{2+} entry and synaptic vesicle fusion is only 0.2 ms [15, 16]. Second, theoretical analyses of calcium diffusion dynamics and quantal secretion have shown that the probability of secretion of a synaptic vesicle decreases threefold with doubling of the distance between the calcium channel and the synaptic vesicle from 25 to 50 nm [17]. It is thus likely that in most synapses the space between calcium channels and docked synaptic vesicles at the active zone is less than 50 nm [16, 18]. Numerous immunohistochemical studies have demonstrated the localization of calcium channels near the active zone [19–21]; however, the organization and arrangement of calcium channels at active zones are best suggested by freeze-fracture studies on frog, lizard, and mammalian neuromuscular junctions (NMJs) [22–24]. On freeze-fracture replicas of NMJ boutons, double rows of prominent intramembranous particles of 10–12 nm in diameter can be seen with occasional synaptic vesicles clustered closely beside them (Figs. 1m and 2c). These rows of particles are in exact register with postsynaptic folds in the underlying muscle [23] and are postulated to be voltage-gated calcium channels [20, 25, 26]. The most direct evidence supporting this view comes from atomic force microscopy on the large calyciform synapse of the chick ciliary ganglion, showing a row-like arrangement of the immunolabeled calcium channels [27].

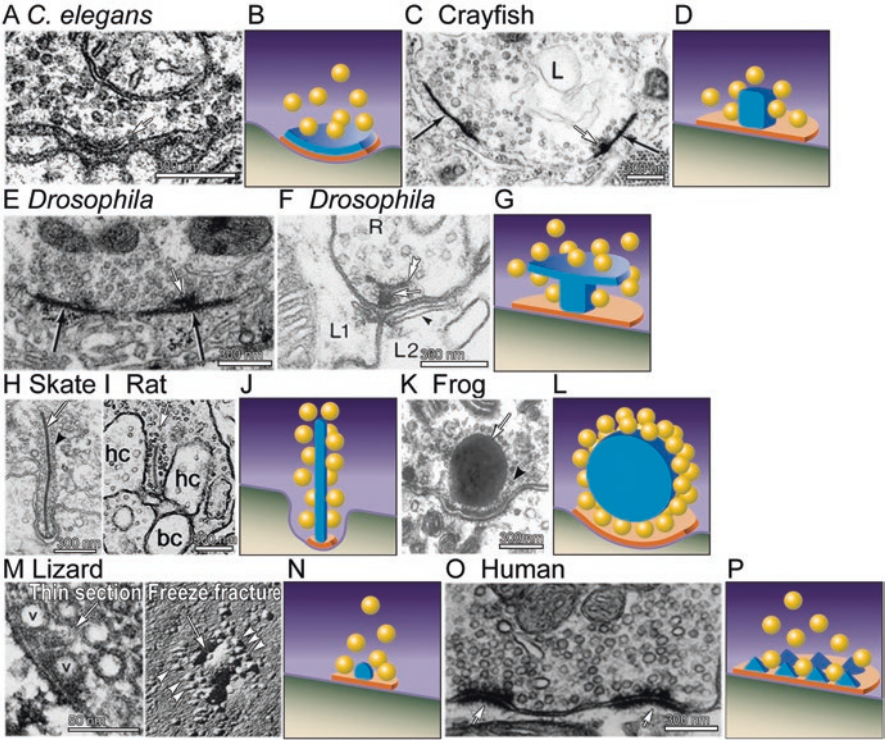

Fig. 1 Electron micrographs and schematic representations of the active zone structures found in different synapses of various organisms. (**a**, **c**, **e**, **f**, **h**, **i**, **k**, **m**, **o**) Electron micrographs of synapses in various species. (**b**, **d**, **g**, **j**, **l**, **n**, **p**) Schematic diagrams of the active zone structure in the corresponding synaptic terminals. (**a**) A neuromuscular junction (NMJ) terminal in *Caenorhabditis elegans* [93] with a plaque-like active zone projection (arrow). (**c**) An NMJ terminal in crayfish [108] with a dense projection (white arrow). (**e**) An NMJ terminal in *Drosophila* [131] with a dense projection called "T-bar"(white arrow). (**f**) A tetrad synapse between photoreceptor (R) and lamina monopolar cells (L1 and L2) in *Drosophila* [94]. The T-bar consists of a platform (double arrowhead) and a pedestal (white arrow). (**h**) An electroreceptor in skate [91] with a long ribbon-like dense projection (arrow) and a halo of synaptic vesicles (arrowhead). (**i**) A triadic photoreceptor ribbon synapse between rod photoreceptor and horizontal cell (hc) and a rod bipolar cell (bc) in rat [101]. (**k**) A saccular hair cell in frog [91] with a spherical dense projection (arrow) and attached vesicles (arrowhead). (**m**) A thin section and a freeze-fracture image of an NMJ terminal in lizard [24]. The dense projection is marked by arrows in both images, and the intramembranous particles are marked by arrowheads. (**p**) An excitatory synaptic terminal in human hippocampus [87] with two active zones (arrows)

Great advances have been made in the recent years in super-resolution imaging techniques, including structured illumination microscopy (SIM), stimulated emission depletion (STED), photo-activated localization microscopy (PALM), and stochastic optical reconstruction microscopy (STORM). These techniques overcome the diffraction limit imposed by Abbe's principle and have revealed the synaptic structure at unprecedented resolution [28, 29]. Studies using these techniques have

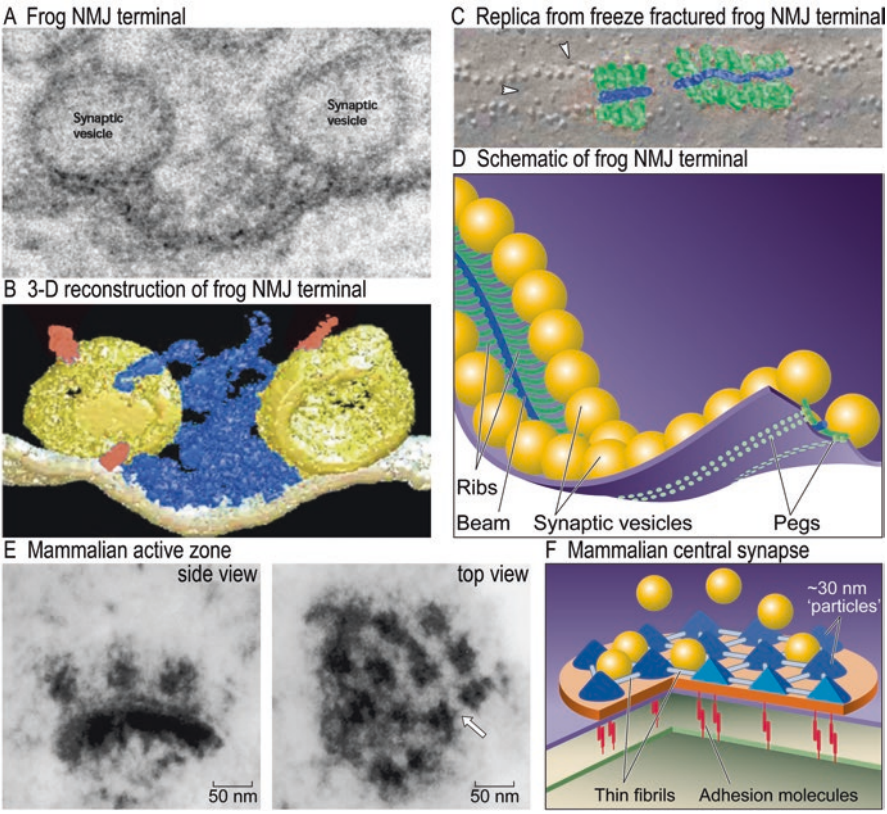

Fig. 2 Models of the active zone structure in frog neuromuscular junction (NMJ) and mammalian central nervous system (CNS) synapses. (**a**–**d**) Models of the active zone structure in frog NMJs [67]. (**e**–**f**) Models of the active zone structure in mammalian CNS synapses [68]. (**a**) TEM micrograph of frog NMJ, where synaptic vesicles are docked to the plasma membrane through dense projections. (**b**) 3-D reconstructed and surface-rendered view of the active zone material and docked vesicles. (**c**) A replica from a freeze-fractured frog's NMJ showing a series of particles/macromolecules on each slope of a ridge with surface-rendered rib and beam assemblies. (**d**) Schematic diagram of the arrangement of ribs, beams, and synaptic vesicles at frog NMJs. (**e**) TEM micrographs of purified active zones from mammalian CNS in side-view and top-view. Thin fibrils can be seen (arrow in top-view). (**f**) Schematic diagram of the active zone structure of mammalian central synapses

found that calcium channel distribution can be variable at mammalian synapses. For example, at cerebellar parallel fiber synapses, the calcium channel $Ca_V2.1$ is enriched at the active zones, close to Bassoon and metabotropic glutamate 4 receptors, but can also be detected outside the active zone [28], while at the excitatory hippocampal synapses, $Ca_V2.1$ clusters were found to be segregated from Bassoon clusters [30]. In addition to the variable localization patterns, calcium channels have also been found to be dynamic and mobile. In cultured hippocampal neurons, significant proportion of exogenously expressed Cav2.1 channels are mobile in the

presynaptic membrane with confined movement and the movement can be reduced by buffering basal calcium [31]. The dynamic localization of calcium channels with regulated motility therefore allows rapid equalization of calcium density among release sites with docked vesicles.

If the calcium channels are organized in orderly arrays at active zones, one would expect the other gates—the synaptic vesicle fusion sites—to be organized in a corresponding manner. The vesicle fusion sites are specialized to allow the lipid bilayers of synaptic vesicles and active zone plasma membrane to come together and form a hydrophilic fusion pore. The SNARE (soluble NSF attachment receptor) complex has been thought to be the driving force for bringing the membranes together, facilitating lipid bilayer mixing and subsequent membrane fusion [32, 33]. The t-SNAREs syntaxin and SNAP-25 are localized to the presynaptic plasma membrane, although their distribution is not restricted to the active zone [34–36]. Biochemical analyses have demonstrated direct interactions among syntaxin, SNAP-25, and calcium channels [37–40]. This might be a mechanism for the physical closeness between the fusion machinery and the calcium channels required for Ca^{2+}-dependent exocytosis. Recent studies using super resolution microscopy approaches have confirmed the biochemical findings of enrichment of SNARE proteins at the synapse [41]. Specifically, these studies show that SNAP-25, syntaxin-1, and Munc18 colocalize in clusters of 100 nm or less along the axonal membrane in cultured neurons, [42], and that the distance between the v-SNARE protein synaptobrevin 2 and the active zone scaffold protein intersect 1 is reduced during synaptic activity, indicating the SNARE complex association with active zone during exocytosis [43].

Interestingly, a study with PC12 cells, a neurosecretory cell line, has shown that syntaxin and SNAP-25 form cholesterol-dependent clusters in the plasma membrane, and these clusters seem to define sites where secretory vesicles dock and fuse with high preference. Cholesterol depletion causes dispersion of the clusters and inhibition of exocytosis [44]. These results suggest that lipids might play a role in active zone plasma membrane specification.

Other important components of the plasma membrane are adhesion molecules, which most likely mediate the precise alignment of the active zone with the PSD. Several classes of adhesion molecules exist at the active zone: cadherins [45, 46], protocadherins [47], nectins [48, 49], neural cell adhesion molecule (NCAM) [50], fasciclin II [51], apCAM [52], DsCAM [53], syndecans [54], L1-CAM/neuroglian [55], integrins [56], neurexins [57], neuroligin [58], and sidekicks [58, 59]. All adhesion molecules share common protein motifs: an extracellular domain that mediates binding with the postsynaptic counterparts or extracellular matrix, a single-pass transmembrane domain or membrane anchor, and often an intracellular domain that binds to the cytoskeleton or the intracellular scaffolding proteins [60, 61]. All of these adhesion molecules except neurexin, which is expressed presynaptically and binds its postsynaptic receptor neuroligin [58], are expressed both pre- and postsynaptically, and bridge the gap between the pre- and postsynaptic membranes through homophilic interactions. Adhesion molecules at the active zone are more than just a “glue.” They also mediate signaling within and between nerve

terminals, and modulate neurotransmission. Numerous reviews have commented on the detailed mechanisms of these molecules in synapse adhesion and regulation [49, 62–64].

In summary, the primary function of the plasma membrane at the active zone during neurotransmitter release is to mediate fusion of synaptic vesicles upon calcium entry. This is achieved by an array-like organization of calcium channels and the localization of the fusion machinery at the membrane.

2.2 The Cytomatrix Underlying the Plasma Membrane of the Active Zone

When viewed by electron microscopy, the cytomatrix of the active zone is electron-dense and displays a "web"-like pattern, which was first noticed by Bloom and Aghajanian [65] and subsequently by Pfenninger and colleagues [66]. Elegant ultrastructural studies have provided the first three-dimensional views of the cytomatrix at the active zone of frog NMJs and mammalian central nervous system (CNS) synapses. By means of electron microscope tomography, Harlow and colleagues [67] revealed a striking array-like structure at the frog NMJ consisting of "beams" and "ribs" that connect docked synaptic vesicles to putative calcium channels (Fig. 2a–d). A beam runs in the midline of the presynaptic ridge along the ridge's long axis, and ribs extend laterally from the beam and connect to synaptic vesicles located at the vesicle–plasma membrane interface. In addition, the ribs are connected to pegs (Fig. 2d), which resemble the putative calcium channels seen in freeze-fracture studies, and form arrays lateral to but in parallel with the beam (Figs. 1m and 2c). With this organization, each docked vesicle is perfectly aligned with at least one calcium channel, which would allow high-fidelity coupling between them. A picture of the mammalian CNS synapse was revealed by Phillips and colleagues [68]. In this study, they purified a presynaptic "particle web" consisting of pyramidally shaped particles (~30 nm in dimension) interconnected by fibrils (Fig. 2e). The "particles" are evenly spaced by the fibrils at ~50–100 nm intervals, forming a web of 50–100 nm slots for synaptic vesicles to dock and fuse (Fig. 2f).

The electron-dense nature of the cytomatrix underlying the plasma membrane suggests that many proteins are localized there and that the cytomatrix at the active zone is important in regulating vesicle docking and fusion. In searching for the building blocks of this specialized cytomatrix, a number of protein components have been identified. Based on their established or putative functions, the proteins identified in the active zone cytomatrix can be classified into three categories: (1) Classical cytoskeletal proteins, such as actin, tubulin, myosin, spectrin α chain and β chain, and β-catenin [68–70]: These proteins are the fundamental elements of the framework of active zone cytomatrix. (2) Scaffold proteins, including SAP90/PSD95/Dlg, SAP97, and CASK/LIN-2 [71–74]: These proteins probably link ion channels and the fusion machinery onto grids formed by the cytoskeletal proteins to

ensure proper active zone function [75–77]. For example, CASK interacts with β-neurexin, syndecan 2, calcium channels, the cytosolic protein Veli/LIN-7, and the Munc18/n-Sec1-interacting protein Mint1 [71, 78–80]. However, functions of scaffold proteins are not restricted to active zones because they also participate in clustering postsynaptic receptors and organizing cellular junctions. (3) Active-zone-specific proteins, including RIM1, RIM-BP, Munc13/unc13, Bassoon, Piccolo/Aczonin, Liprin, and ELKS/CAST/ERCs [81–86]: As described in detail in Chapter "Presynaptic Cytomatrix Proteins", the active-zone-specific localization and their multidomain structure allow them to form large protein complexes and participate in modulating synaptic vesicle docking, priming, and fusion, as well as initiation of the assembly of the active zone structure. Physiological studies indicate that some of these proteins are involved in vesicle priming as well as synaptic transmission regulation [87–89].

In summary, the primary function of the cytomatrix at the active zone is to mediate docking of synaptic vesicles. The cytoskeletal and scaffolding proteins form a "web"-like structure consisting of "slots" for synaptic vesicle docking, and components of the cytomatrix regulate vesicle priming and fusion.

2.3 Synaptic Ribbons: The Electron-Dense Projections Extending from the Cytomatrix of the Active Zone

Some active zones have very prominent electron-dense projections extending from the cytomatrix into the cytoplasm. They were first described and characterized in vertebrate sensory synapses involved in vision, hearing, and balance [90–92]. These dense projections, or synaptic ribbons, are ribbon-like or spherical, extend 0.5–1 μm into the cytoplasm, and always have a "halo" of synaptic vesicles tethered to their surface (Fig. 1h–l, [91]). Due to their remarkable appearance, it has been thought that ribbon synapses are different from all other synapses, and the "synaptic ribbons" are exclusive to ribbon synapses in order to mediate the graded and sustained neurotransmitter release of these synapses [91, 92]. However, through careful examination and comparison of different types of synapses, a hypothesis has emerged that electron-dense projections are not unique to ribbon synapses but rather an integral part of the active zone with evolutionarily conserved structures to perform the conserved function of tethering synaptic vesicles at active zones.

Morphologically, dense projections have been observed in different types of synapses in a variety of species. At *Caenorhabditis elegans* NMJs, dense projections in the shape of a plaque have been described (Fig. 1a, [93]). In *Drosophila*, T-shaped dense projections can be seen in NMJs, tetrad synapses of the visual system (Fig. 1e–g), and CNS synapses [94, 95]. In crustacean NMJs, dense projections appear cylindrical (Fig. 1c, [96]). In vertebrate NMJs, dense projections have been described in frog, lizard, and mammals (Fig. 1m–n [12, 22, 24]). In mammalian CNS synapses, dense projections were noted in EM studies as early as the 1960s,

and were recently purified and visualized in great detail (Fig. 2e [65, 68]). Based on the size of dense projections, we can divide different types of active zones into two groups: those with prominent dense projections, including invertebrate synapses with T-bars and vertebrate ribbon synapses, and those with less prominent dense projections, including vertebrate NMJs and CNS synapses. Because dense projections in these latter active zones are not very prominent and project less than 100 nm into the cytoplasm, they have generally been considered being a part of the cytomatrix at the active zone [13, 87, 97].

Physiologically, numerous studies have demonstrated the tethering function of dense projections. In vertebrate sensory synapses, the motor protein KIF3A, which is a component of ribbons, likely mediates the tethering of synaptic vesicles [98]. In tomographic images, synaptic vesicles in frog NMJs are clearly tethered through "ribs" to the "beams" corresponding to the dense projections [67]. In *Drosophila* and crayfish, synaptic vesicles cluster around T-bars (Fig. 1a–g). However, the mechanism of tethering is essentially unknown. Recently, dense projections of mammalian CNS active zones were biochemically purified and molecularly characterized [68]. They are ~50 nm in size and pyramid-like in appearance (Figs. 1p and 2e), and contain synaptic vesicle binding proteins such as synapsin and RIM [68, 85, 99]. Therefore, the pyramid-like dense projections of mammalian CNS synapses are thought to tether and cluster synaptic vesicles to the active zone. Despite their proposed function of tethering synaptic vesicles, dense projections do not appear to be essential to neurotransmitter release, as suggested by several knockout studies that disrupted dense projections. For example, in the mammalian retina, Bassoon is a component of photoreceptor ribbon synapse [100]. In the retina of homozygous *bassoon* mutant mice, photoreceptors have a greatly reduced number of ribbons, and the remaining ribbons float freely in the cytoplasm with synaptic vesicles attached to them. Electroretinogram recordings from these photoreceptors showed that neurotransmission is maintained at low-intensity light stimulation but dramatically reduced at high-intensity light stimulation [101], suggesting that ribbon anchorage to the plasma membrane is not essential to synaptic vesicle exocytosis but is required for strong and continuous exocytosis. In *Drosophila*, a coiled-coil domain protein Bruchpilot (BRP) is required for dense projection (T-bar) assembly. At brp mutant active zones, T-bars are entirely lost, and individual receptor fields for glutamate on the postsynaptic membrane are enlarged. Consistent with the morphological change, amplitudes of evoked excitatory junctional currents are drastically decreased whereas the mean amplitude of miniature excitatory junctional currents resulting from spontaneous single vesicle fusion events is increased [102]. This study suggests that dense projections facilitate efficient and localized transmitter release. In mice, knockout studies of synapsin suggest that it may not be required for the vesicle fusion step, but rather for the synapsin-dependent cluster of vesicles. This clustering is apparently required for sustained release of neurotransmitter in response to high levels of neuronal activity [99].

If the function of dense projections was to tether synaptic vesicles, what would be the physiological advantage of varying their size and shape? One possibility is that larger dense projections may increase the number of synaptic vesicles tethered

at the active zone and therefore enlarge the size of the readily releasable pool. This possibility is favored by observations at ribbon synapses. For example, the number of synaptic vesicles attached to a ribbon (~400) is much more than that contacting the active zone (~100) at a ribbon synapse of frog saccular hair cells (Fig. 1k), and all the vesicles attached to ribbons in saccular hair cells may be released upon strong stimulation [103–105]. Therefore, these large dense projections allow an increase in the size of the readily releasable pool without necessitating an enlargement of the active zone.

The close connection between the shape of dense projections and the function of synapses is further demonstrated in studies characterizing mutant phenotypes of a short isoform of Piccolo, Piccolino. Piccolino was found to be a critical component of the sensory ribbon synapses of the eye and ear [106]. In Piccolino loss-of-function synapses, the ribbons adopt a small and spherical shape instead of the normal large plate shape, indicating a defect in the maturation of synaptic ribbons [107].

Larger dense projections or synaptic ribbons are often observed in sensory synapses, where sustained release upon continuous stimulation requires a huge readily releasable pool and a highly efficient synaptic vesicle replenishment capability but the confined space representation of individual sensory neurons in the visual or auditory field restricts the size of each terminal. In contrast, smaller dense projections are often associated with NMJs, where stimulation is noncontinuous and nerve terminal size is not spatially restricted during development. Interestingly, at *Drosophila* and crustacean NMJs, active zones with prominent T-bars are often adjacent to those without T-bars within the same presynaptic nerve terminal (Fig. 1c, e). It has been proposed that active zones with prominent T-bars have a stronger output because more synaptic vesicles may be released upon stimulation. In support of this notion, crustacean NMJ terminals of high output have a threefold higher density of dense projections than those of low output in the same excitatory motor axon despite that they have similar total synaptic surface areas [96, 108].

Thus, although dense projections vary greatly in morphology in different types of synapses, they may serve the same primary function of tethering synaptic vesicles to the active zone. Larger dense projections tether more synaptic vesicles and therefore increase the size of the readily releasable pool.

3 Active Zone Assembly and the Regulation of Active Zone Density and Spacing

Active zone assembly begins upon axon-target recognition and contact, and ends with the establishment of functional neurotransmitter release sites. In cultured hippocampal neurons, active zone assembly takes about 30 minutes [109, 110]. According to a recently proposed unitary assembly model, active-zone-specific proteins are packaged into transport vesicles for delivery to the nascent synaptic contact site. Upon fusion of such vesicles with the plasma membrane, the active zone

proteins are deposited and localized [111, 112]. In cultured hippocampal synapses, one active zone forms from two to three transport vesicles [112, 113]. Considering that on average each active zone has 10–15 synaptic vesicle release sites or "grid units," each transport vesicle should carry the building material for 4–5 synaptic vesicle release sites. This model suggests that active zone assembly occurs within an hour, which allows rapid synaptogenesis during development and synapse expansion during activity-dependent long-term potentiation.

Genetic analyses in *C. elegans* and *Drosophila* have identified mutations of several genes that affect active zone assembly. In *C. elegans*, the *syd-2* gene and its positive regulator *syd-1* are required for the assembly of numerous presynaptic components [114]. In *syd-2* loss-of-function mutants, active zones of NMJ terminals are lengthened and less electron-dense [115]. The SYD-2 protein is localized to active zones and is a member of the Liprin-α protein family, which contains coiled-coil and sterile alpha motif domains [116]. Liprins interact with the Lar family of receptor protein tyrosine phosphatases (RPTPs) and cluster RPTPs to focal adhesions [116]. *Drosophila* Liprin-α (DLiprin) is also localized to active zones at NMJs. In mutants of either DLiprin or its associated protein DLar (a receptor protein tyrosine phosphatase), the size of active zones in motor neurons is ~2.5-fold larger than normal and the morphology is less compact [117]. In *Drosophila*, loss of *wishful thinking* (*wit*) causes a reduced number of boutons, an increased number of active zones per bouton, and freely floating T-bar structures in the cytoplasm [118]. Wit is a BMP type II receptor that is expressed in a subset of neurons, including motor neurons. However, its molecular mechanism of regulating active zone assembly is not understood [118, 119].

Recent advances in the characterization of dynamic protein–protein interactions and biomolecular condensates (BMCs) have highlighted an emerging role of liquid–liquid phase separation (LLPS) in driving the assembly of transmitter release machineries at the active zone [120]. Purified RIM, RIM-BP, and ELKS proteins can assemble into liquid-like protein condensates and undergo LLPS in vitro [121, 122]. These RIM-containing BMCs are dynamic liquid droplets that allow fast material exchange with the surrounding solution and rapid fusion with each other upon contact, a process that would facilitate the clustering of active zone materials on the plasma membrane [123]. A study with *C. elegans* showed that phase separation of Liprin-α and ELKS is required for the recruitment and assembly of other active zone components such as UNC-10/RIM and UNC-13/Munc-13 in vivo [124]. A detailed discussion of the function and protein structures of many of these cytomatrix proteins is included in Chapter "Presynaptic Cytomatrix Proteins".

Active zones are not static but rather plastic structures. In tetrad synapses of the *Drosophila* visual system, the number of presynaptic ribbons/T-bars changes with alterations in light stimulation [125, 126]. In crustacean NMJs, high-frequency stimulation-induced long-term facilitation is accompanied by increased numbers of active zones and dense projections [127]. In mammalian hippocampal neurons, long-term potentiation is associated with an expansion or "division" of active zones [128, 129]. At *Drosophila* larval NMJs, persistent augmentation of synaptic vesicle release relies on an increased number of presynaptic boutons with the density of

active zones similar to that in wild type [130]. The same study also showed that an increase in active zone density without an expansion of the bouton size may lead to only a transient increase in evoked vesicle release in response to single action potentials but not the release evoked by high-frequency stimulation. Therefore, long-term potentiation requires both the assembly of new active zones and the expansion of bouton size to keep the density of active zones constant.

Ultrastructural observations from *Drosophila* and *Sarcophaga* have also suggested that the density of active zones is tightly regulated and that there is a minimum spacing required between neighboring active zones [131], presumably allowing each active zone to have sufficient and equal access to synaptic vesicle pools and/or recycling machinery. Nevertheless, the density of active zones may also change under certain conditions. For example, in *Drosophila* mutants of *synaptojanin*, an inositol phosphatase that promotes synaptic vesicle uncoating during endocytosis, there are more active zones per unit area of synaptic boutons and more T-bars within these active zones [132]. Thus, activity-dependent active zone plasticity may be associated with changes in either active zone density or synaptic bouton size depending on synapses or experimental/physiological conditions.

In addition to neuronal activity, active zone stability is also regulated by protein turnover and autophagy. The most important players identified so far in active zone turnover are the large scaffolding proteins Bassoon and Piccolo. In addition to their well-characterized roles in the formation and function of the presynaptic active zone [133], Bassoon and Piccolo are also critical regulators of protein and structural homeostasis of the active zone. Loss of Bassoon and Piccolo leads to aberrant degradation of several active zone proteins including SNAP-25 and Munc-13, which are mediated in part by the E3 ubiquitin ligase Siah1 [134]. Besides the ubiquitin-mediated protein degradation, Piccolo and Bassoon also regulate presynaptic autophagy [135]. Depletion of Bassoon and Piccolo in primary neuron culture results in the formation of presynaptic autophagosomes and the degradation of synaptic vesicles [135, 136]. Specifically, the CC2 domain of Bassoon selectively binds to ATG5, an E3-like ligase essential for autophagy, to inhibit the induction of autophagy [136]. Therefore, Bassoon and Piccolo are important for stabilizing the active zone by inhibiting synaptic autophagy and degradation.

4 Ectopic Release Sites

Vesicular release from neuronal membranes that lack morphological specialization has long been recognized but thought to be restricted to large dense-core vesicles. This view is changing as accumulating evidence supports “ectopic release” of small synaptic vesicles at sites distant from morphologically defined synapses [14]. Evidence for the ectopic release of small synaptic vesicles first came from freeze-fracture studies of the frog NMJ, where exocytosis evoked by an elevated extracellular potassium concentration resulted in almost uniformly distributed fusion sites along the presynaptic membrane independent of the position of active zones [137].

Direct visual observation of ectopic release of small synaptic vesicles comes from evanescent-wave microscopy of isolated retinal bipolar cell terminals, where stimulated exocytosis of vesicles loaded with the fluorescent dye FM1-43 could be observed in the presynaptic plasma membrane [138, 139]. Although most of these fusion events (64%) clustered at sites corresponding to active zones, the remaining fusion events were randomly distributed along the presynaptic membrane, indicating the presence of ectopic exocytosis.

The three SNARE proteins, including the t-SNAREs syntaxin 1 and SNAP-25 (synaptosome-associated protein 25 kDa), and the v-SNARE synaptobrevin, are the minimum proteins required for the fusion of synaptic vesicles [140]. Both SNAP-25 and syntaxin 1 are expressed throughout the plasma membrane [34]; therefore, the fusion event can occur wherever the SNARE complex is formed. It remains to be determined how the ectopic sites are organized, which proteins that participate in the synaptic vesicle cycling are present at the ectopic sites, and how ectopic release is regulated. Physiological significance of ectopic release also awaits elucidation.

5 Summary

The active zone in the presynaptic nerve terminal is a complex and highly organized structure. Its morphology dynamically adapts to the rate of neurotransmitter release. Nature has presented elaborate variations of active zones, from the ~30 nm pyramid in vertebrate central neurons to the ~400 nm sphere in vertebrate hair cells. Nevertheless, all active zones share key structural features that facilitate the efficient and regulated synaptic vesicle release cycle. Their differences in size and shape appear to have evolved to suit synapse-specific kinetic needs of transmitter release.

References

1. Sherrington CS. The central nervous system. In: Foster M, editor. A text book of physiology, vol. 3. London: Macmillan and Co.; 1897. p. 929.
2. Fulton JF. Physiology of the nervous system. London: Oxford University Press; 1938.
3. Elliott TR. On the action of adrenalin. J Physiol (London). 1904;31:20P.
4. Loewi O. Ueber humorale uebertragbarkeit der Herznervenwirkung (II. Miteilung). Pflugers Arch Gesamte Physio Menschen Tirer. 1921;193:201–13.
5. Dale HH. The action of certain esters and ethers of choline, and their relation to muscarine. J Pharmacol. 1914;6:147–90.
6. Tsuji S. Rene Couteaux (1909-1999) and the morphological identification of synapses. Biol Cell. 2006;98:503–9. https://doi.org/10.1042/BC20050036.
7. Couteaux R. Nouvelles observations sur la structure de la plaque motrice et interprétation des rapports myo-neuraux. C R Soc Biol. 1944;138:976–9.
8. Couteaux R. *Sur Les Gouttieres Synaptiques Du Muscle Strie. Comptes Rendus Des Seances De La Societe De Biologie Et De Ses Filiales. 1946;140:270–1.

9. De Robertis ED, Bennett HS. Some features of the submicroscopic morphology of synapses in frog and earthworm. J Biophys Biochem Cytol. 1955;1:47–58. https://doi.org/10.1083/jcb.1.1.47.
10. Palay SL, Palade GE. The fine structure of neurons. J Biophys Biochem Cytol. 1955;1:69–88. https://doi.org/10.1083/jcb.1.1.69.
11. Couteaux R, Pecot-Dechavassine M. Synaptic vesicles and pouches at the level of "active zones" of the neuromuscular junction. C R Acad Sci Hebd Seances Acad Sci D. 1970;271:2346–9.
12. Heuser JE, Reese TS. Evidence for recycling of synaptic vesicle membrane during transmitter release at the frog neuromuscular junction. J Cell Biol. 1973;57:315–44. https://doi.org/10.1083/jcb.57.2.315.
13. Landis DM, Hall AK, Weinstein LA, Reese TS. The organization of cytoplasm at the presynaptic active zone of a central nervous system synapse. Neuron. 1988;1:201–9. https://doi.org/10.1016/0896-6273(88)90140-7.
14. Matsui K, Jahr CE. Exocytosis unbound. Curr Opin Neurobiol. 2006;16:305–11. https://doi.org/10.1016/j.conb.2006.04.001.
15. Parsegian VA. Approaches to the cell biology of neurons. In: Cowan WW, Ferrendelli JA, editors. . Bethesda: Society for Neuroscience; 1977. p. 161–71.
16. Stanley EF. The calcium channel and the organization of the presynaptic transmitter release face. Trends Neurosci. 1997;20:404–9. https://doi.org/10.1016/s0166-2236(97)01091-6.
17. Bennett MR, Farnell L, Gibson WG. The probability of quantal secretion near a single calcium channel of an active zone. Biophys J. 2000;78:2201–21. https://doi.org/10.1016/S0006-3495(00)76769-5.
18. Atwood HL, Karunanithi S. Diversification of synaptic strength: presynaptic elements. Nat Rev Neurosci. 2002;3:497–516. https://doi.org/10.1038/nrn876.
19. Kawasaki F, Zou B, Xu X, Ordway RW. Active zone localization of presynaptic calcium channels encoded by the cacophony locus of Drosophila. J Neurosci. 2004;24:282–5. https://doi.org/10.1523/JNEUROSCI.3553-03.2004.
20. Robitaille R, Adler EM, Charlton MP. Strategic location of calcium channels at transmitter release sites of frog neuromuscular synapses. Neuron. 1990;5:773–9. https://doi.org/10.1016/0896-6273(90)90336-e.
21. Zhang L, Volknandt W, Gundelfinger ED, Zimmermann H. A comparison of synaptic protein localization in hippocampal mossy fiber terminals and neurosecretory endings of the neurohypophysis using the cryo-immunogold technique. J Neurocytol. 2000;29:19–30. https://doi.org/10.1023/a:1007108012667.
22. Ellisman MH, Rash JE, Staehelin LA, Porter KR. Studies of excitable membranes. II. A comparison of specializations at neuromuscular junctions and nonjunctional sarcolemmas of mammalian fast and slow twitch muscle fibers. J Cell Biol. 1976;68:752–74. https://doi.org/10.1083/jcb.68.3.752.
23. Heuser JE, Reese TS, Landis DM. Functional changes in frog neuromuscular junctions studied with freeze-fracture. J Neurocytol. 1974;3:109–31. https://doi.org/10.1007/BF01111936.
24. Walrond JP, Reese TS. Structure of axon terminals and active zones at synapses on lizard twitch and tonic muscle fibers. J Neurosci. 1985;5:1118–31. https://doi.org/10.1523/JNEUROSCI.05-05-01118.1985.
25. Cohen MW, Jones OT, Angelides KJ. Distribution of Ca2+ channels on frog motor nerve terminals revealed by fluorescent omega-conotoxin. J Neurosci. 1991;11:1032–9. https://doi.org/10.1523/JNEUROSCI.11-04-01032.1991.
26. Pumplin DW, Reese TS, Llinas R. Are the presynaptic membrane particles the calcium channels? Proc Natl Acad Sci U S A. 1981;78:7210–3. https://doi.org/10.1073/pnas.78.11.7210.
27. Haydon PG, Henderson E, Stanley EF. Localization of individual calcium channels at the release face of a presynaptic nerve terminal. Neuron. 1994;13:1275–80. https://doi.org/10.1016/0896-6273(94)90414-6.

28. Siddig S, Aufmkolk S, Doose S, Jobin ML, Werner C, Sauer M, et al. Super-resolution imaging reveals the nanoscale organization of metabotropic glutamate receptors at presynaptic active zones. Sci Adv. 2020;6:eaay7193. https://doi.org/10.1126/sciadv.aay7193.
29. Carvalhais LG, Martinho VC, Ferreiro E, Pinheiro PS. Unraveling the nanoscopic organization and function of central mammalian Presynapses with super-resolution microscopy. Front Neurosci. 2020;14:578409. https://doi.org/10.3389/fnins.2020.578409.
30. Grauel MK, Maglione M, Reddy-Alla S, Willmes CG, Brockmann MM, Trimbuch T, et al. RIM-binding protein 2 regulates release probability by fine-tuning calcium channel localization at murine hippocampal synapses. Proc Natl Acad Sci U S A. 2016;113:11615–20. https://doi.org/10.1073/pnas.1605256113.
31. Schneider R, Hosy E, Kohl J, Klueva J, Choquet D, Thomas U, et al. Mobility of calcium channels in the presynaptic membrane. Neuron. 2015;86:672–9. https://doi.org/10.1016/j.neuron.2015.03.050.
32. Jahn R, Lang T, Sudhof TC. Membrane fusion. Cell. 2003;112:519–33. https://doi.org/10.1016/s0092-8674(03)00112-0.
33. Rizo J. SNARE function revisited. Nat Struct Biol. 2003;10:417–9. https://doi.org/10.1038/nsb0603-417.
34. Garcia EP, McPherson PS, Chilcote TJ, Takei K, De Camilli P. rbSec1A and B colocalize with syntaxin 1 and SNAP-25 throughout the axon, but are not in a stable complex with syntaxin. J Cell Biol. 1995;129:105–20. https://doi.org/10.1083/jcb.129.1.105.
35. Hiesinger PR, Scholz M, Meinertzhagen IA, Fischbach KF, Obermayer K. Visualization of synaptic markers in the optic neuropils of Drosophila using a new constrained deconvolution method. J Comp Neurol. 2001;429:277–88. https://doi.org/10.1002/1096-9861(20000108)429:2<277::aid-cne8>3.0.co;2-8.
36. Schulze KL, Broadie K, Perin MS, Bellen HJ. Genetic and electrophysiological studies of Drosophila syntaxin-1A demonstrate its role in nonneuronal secretion and neurotransmission. Cell. 1995;80:311–20. https://doi.org/10.1016/0092-8674(95)90414-x.
37. Jarvis SE, Barr W, Feng ZP, Hamid J, Zamponi GW. Molecular determinants of syntaxin 1 modulation of N-type calcium channels. J Biol Chem. 2002;277:44399–407. https://doi.org/10.1074/jbc.M206902200.
38. Taverna E, Saba E, Rowe J, Francolini M, Clementi F, Rosa P. Role of lipid microdomains in P/Q-type calcium channel (Cav2.1) clustering and function in presynaptic membranes. J Biol Chem. 2004;279:5127–34. https://doi.org/10.1074/jbc.M308798200.
39. Catterall WA. Interactions of presynaptic Ca2+ channels and snare proteins in neurotransmitter release. Ann N Y Acad Sci. 1999;868:144–59. https://doi.org/10.1111/j.1749-6632.1999.tb11284.x.
40. Martin-Moutot N, Charvin N, Leveque C, Sato K, Nishiki T, Kozaki S, et al. Interaction of SNARE complexes with P/Q-type calcium channels in rat cerebellar synaptosomes. J Biol Chem. 1996;271:6567–70. https://doi.org/10.1074/jbc.271.12.6567.
41. Wilhelm BG, Mandad S, Truckenbrodt S, Krohnert K, Schafer C, Rammner B, et al. Composition of isolated synaptic boutons reveals the amounts of vesicle trafficking proteins. Science. 2014;344:1023–8. https://doi.org/10.1126/science.1252884.
42. Pertsinidis A, Mukherjee K, Sharma M, Pang ZP, Park SR, Zhang Y, et al. Ultrahigh-resolution imaging reveals formation of neuronal SNARE/Munc18 complexes in situ. Proc Natl Acad Sci U S A. 2013;110:E2812–20. https://doi.org/10.1073/pnas.1310654110.
43. Japel M, Gerth F, Sakaba T, Bacetic J, Yao L, Koo SJ, et al. Intersectin-mediated clearance of SNARE complexes is required for fast neurotransmission. Cell Rep. 2020;30:409–420 e406. https://doi.org/10.1016/j.celrep.2019.12.035.
44. Lang T, Bruns D, Wenzel D, Riedel D, Holroyd P, Thiele C, et al. SNAREs are concentrated in cholesterol-dependent clusters that define docking and fusion sites for exocytosis. EMBO J. 2001;20:2202–13. https://doi.org/10.1093/emboj/20.9.2202.
45. Shapiro L, Colman DR. The diversity of cadherins and implications for a synaptic adhesive code in the CNS. Neuron. 1999;23:427–30. https://doi.org/10.1016/s0896-6273(00)80796-5.

46. Yagi T, Takeichi M. Cadherin superfamily genes: functions, genomic organization, and neurologic diversity. Genes Dev. 2000;14:1169–80. https://doi.org/10.1101/gad.14.10.1169.
47. Frank M, Kemler R. Protocadherins. Curr Opin Cell Biol. 2002;14:557–62. https://doi.org/10.1016/s0955-0674(02)00365-4.
48. Mizoguchi A, Nakanishi H, Kimura K, Matsubara K, Ozaki-Kuroda K, Katata T, et al. Nectin: an adhesion molecule involved in formation of synapses. J Cell Biol. 2002;156:555–65. https://doi.org/10.1083/jcb.200103113.
49. Takai Y, Shimizu K, Ohtsuka T. The roles of cadherins and nectins in interneuronal synapse formation. Curr Opin Neurobiol. 2003;13:520–6. https://doi.org/10.1016/j.conb.2003.09.003.
50. Rougon G, Hobert O. New insights into the diversity and function of neuronal immunoglobulin superfamily molecules. Annu Rev Neurosci. 2003;26:207–38. https://doi.org/10.1146/annurev.neuro.26.041002.131014.
51. Davis GW, Schuster CM, Goodman CS. Genetic analysis of the mechanisms controlling target selection: target-derived Fasciclin II regulates the pattern of synapse formation. Neuron. 1997;19:561–73. https://doi.org/10.1016/s0896-6273(00)80372-4.
52. Mayford M, Barzilai A, Keller F, Schacher S, Kandel ER. Modulation of an NCAM-related adhesion molecule with long-term synaptic plasticity in Aplysia. Science. 1992;256:638–44. https://doi.org/10.1126/science.1585176.
53. Schmucker D, Clemens JC, Shu H, Worby CA, Xiao J, Muda M, et al. Drosophila Dscam is an axon guidance receptor exhibiting extraordinary molecular diversity. Cell. 2000;101:671–84. https://doi.org/10.1016/s0092-8674(00)80878-8.
54. Hsueh YP, Sheng M. Regulated expression and subcellular localization of syndecan heparan sulfate proteoglycans and the syndecan-binding protein CASK/LIN-2 during rat brain development. J Neurosci. 1999;19:7415–25. https://doi.org/10.1523/JNEUROSCI.19-17-07415.1999.
55. Walsh FS, Doherty P. Neural cell adhesion molecules of the immunoglobulin superfamily: role in axon growth and guidance. Annu Rev Cell Dev Biol. 1997;13:425–56. https://doi.org/10.1146/annurev.cellbio.13.1.425.
56. Chavis P, Westbrook G. Integrins mediate functional pre- and postsynaptic maturation at a hippocampal synapse. Nature. 2001;411:317–21. https://doi.org/10.1038/35077101.
57. Missler M, Sudhof TC. Neurexins: three genes and 1001 products. Trends Genet. 1998;14:20–6. https://doi.org/10.1016/S0168-9525(97)01324-3.
58. Yamagata M, Sanes JR, Weiner JA. Synaptic adhesion molecules. Curr Opin Cell Biol. 2003;15:621–32. https://doi.org/10.1016/s0955-0674(03)00107-8.
59. Yamagata M, Weiner JA, Sanes JR. Sidekicks: synaptic adhesion molecules that promote lamina-specific connectivity in the retina. Cell. 2002;110:649–60. https://doi.org/10.1016/s0092-8674(02)00910-8.
60. Gottardi CJ, Gumbiner BM. Adhesion signaling: how beta-catenin interacts with its partners. Curr Biol. 2001;11:R792–4. https://doi.org/10.1016/s0960-9822(01)00473-0.
61. Sheng M, Sala C. PDZ domains and the organization of supramolecular complexes. Annu Rev Neurosci. 2001;24:1–29. https://doi.org/10.1146/annurev.neuro.24.1.1.
62. Packard M, Mathew D, Budnik V. FASt remodeling of synapses in Drosophila. Curr Opin Neurobiol. 2003;13:527–34. https://doi.org/10.1016/j.conb.2003.09.008.
63. Scheiffele P. Cell-cell signaling during synapse formation in the CNS. Annu Rev Neurosci. 2003;26:485–508. https://doi.org/10.1146/annurev.neuro.26.043002.094940.
64. Ferreira A, Paganoni S. The formation of synapses in the central nervous system. Mol Neurobiol. 2002;26:69–79. https://doi.org/10.1385/MN:26:1:069.
65. Bloom FE, Aghajanian GK. Fine structural and cytochemical analysis of the staining of synaptic junctions with phosphotungstic acid. J Ultrastruct Res. 1968;22:361–75. https://doi.org/10.1016/s0022-5320(68)90027-0.
66. Pfenninger K, Akert K, Moor H, Sandri C. The fine structure of freeze-fractured presynaptic membranes. J Neurocytol. 1972;1:129–49. https://doi.org/10.1007/BF01099180.

67. Harlow ML, Ress D, Stoschek A, Marshall RM, McMahan UJ. The architecture of active zone material at the frog's neuromuscular junction. Nature. 2001;409:479–84. https://doi.org/10.1038/35054000.
68. Phillips GR, Huang JK, Wang Y, Tanaka H, Shapiro L, Zhang W, et al. The presynaptic particle web: ultrastructure, composition, dissolution, and reconstitution. Neuron. 2001;32:63–77. https://doi.org/10.1016/s0896-6273(01)00450-0.
69. Burns ME, Augustine GJ. Synaptic structure and function: dynamic organization yields architectural precision. Cell. 1995;83:187–94. https://doi.org/10.1016/0092-8674(95)90160-4.
70. Hirokawa N, Sobue K, Kanda K, Harada A, Yorifuji H. The cytoskeletal architecture of the presynaptic terminal and molecular structure of synapsin 1. J Cell Biol. 1989;108:111–26. https://doi.org/10.1083/jcb.108.1.111.
71. Hata Y, Butz S, Sudhof TC. CASK: a novel dlg/PSD95 homolog with an N-terminal calmodulin-dependent protein kinase domain identified by interaction with neurexins. J Neurosci. 1996;16:2488–94. https://doi.org/10.1523/JNEUROSCI.16-08-02488.1996.
72. Kistner U, Wenzel BM, Veh RW, Cases-Langhoff C, Garner AM, Appeltauer U, et al. SAP90, a rat presynaptic protein related to the product of the Drosophila tumor suppressor gene dlg-A. J Biol Chem. 1993;268:4580–3. https://doi.org/10.1016/S0021-9258(18)53433-5.
73. Koulen P, Fletcher EL, Craven SE, Bredt DS, Wassle H. Immunocytochemical localization of the postsynaptic density protein PSD-95 in the mammalian retina. J Neurosci. 1998;18:10136–49. https://doi.org/10.1523/JNEUROSCI.18-23-10136.1998.
74. Muller BM, Kistner U, Veh RW, Cases-Langhoff C, Becker B, Gundelfinger ED, et al. Molecular characterization and spatial distribution of SAP97, a novel presynaptic protein homologous to SAP90 and the Drosophila discs-large tumor suppressor protein. J Neurosci. 1995;15:2354–66. https://doi.org/10.1523/JNEUROSCI.15-03-02354.1995.
75. Fanning AS, Anderson JM. PDZ domains: fundamental building blocks in the organization of protein complexes at the plasma membrane. J Clin Invest. 1999;103:767–72. https://doi.org/10.1172/JCI6509.
76. Garner CC, Nash J, Huganir RL. PDZ domains in synapse assembly and signalling. Trends Cell Biol. 2000;10:274–80. https://doi.org/10.1016/s0962-8924(00)01783-9.
77. O'Brien RJ, Lau LF, Huganir RL. Molecular mechanisms of glutamate receptor clustering at excitatory synapses. Curr Opin Neurobiol. 1998;8:364–9. https://doi.org/10.1016/s0959-4388(98)80062-7.
78. Butz S, Okamoto M, Sudhof TC. A tripartite protein complex with the potential to couple synaptic vesicle exocytosis to cell adhesion in brain. Cell. 1998;94:773–82. https://doi.org/10.1016/s0092-8674(00)81736-5.
79. Hsueh YP, Yang FC, Kharazia V, Naisbitt S, Cohen AR, Weinberg RJ, et al. Direct interaction of CASK/LIN-2 and syndecan heparan sulfate proteoglycan and their overlapping distribution in neuronal synapses. J Cell Biol. 1998;142:139–51. https://doi.org/10.1083/jcb.142.1.139.
80. Maximov A, Sudhof TC, Bezprozvanny I. Association of neuronal calcium channels with modular adaptor proteins. J Biol Chem. 1999;274:24453–6. https://doi.org/10.1074/jbc.274.35.24453.
81. tom Dieck S, Sanmarti-Vila L, Langnaese K, Richter K, Kindler S, Soyke A, et al. Bassoon, a novel zinc-finger CAG/glutamine-repeat protein selectively localized at the active zone of presynaptic nerve terminals. J Cell Biol. 1998;142:499–509. https://doi.org/10.1083/jcb.142.2.499.
82. Fenster SD, Chung WJ, Zhai R, Cases-Langhoff C, Voss B, Garner AM, et al. Piccolo, a presynaptic zinc finger protein structurally related to bassoon. Neuron. 2000;25:203–14. https://doi.org/10.1016/s0896-6273(00)80883-1.
83. Wang X, Kibschull M, Laue MM, Lichte B, Petrasch-Parwez E, Kilimann MW. Aczonin, a 550-kD putative scaffolding protein of presynaptic active zones, shares homology regions with Rim and Bassoon and binds profilin. J Cell Biol. 1999;147:151–62. https://doi.org/10.1083/jcb.147.1.151.

84. Wang Y, Liu X, Biederer T, Sudhof TC. A family of RIM-binding proteins regulated by alternative splicing: implications for the genesis of synaptic active zones. Proc Natl Acad Sci U S A. 2002;99:14464–9. https://doi.org/10.1073/pnas.182532999.
85. Wang Y, Okamoto M, Schmitz F, Hofmann K, Sudhof TC. Rim is a putative Rab3 effector in regulating synaptic-vesicle fusion. Nature. 1997;388:593–8. https://doi.org/10.1038/41580.
86. Brose N, Hofmann K, Hata Y, Sudhof TC. Mammalian homologues of Caenorhabditis elegans unc-13 gene define novel family of C2-domain proteins. J Biol Chem. 1995;270:25273–80. https://doi.org/10.1074/jbc.270.42.25273.
87. Dresbach T, Qualmann B, Kessels MM, Garner CC, Gundelfinger ED. The presynaptic cytomatrix of brain synapses. Cell Mol Life Sci. 2001;58:94–116. https://doi.org/10.1007/PL00000781.
88. Rosenmund C, Rettig J, Brose N. Molecular mechanisms of active zone function. Curr Opin Neurobiol. 2003;13:509–19. https://doi.org/10.1016/j.conb.2003.09.011.
89. Takao-Rikitsu E, Mochida S, Inoue E, Deguchi-Tawarada M, Inoue M, Ohtsuka T, et al. Physical and functional interaction of the active zone proteins, CAST, RIM1, and Bassoon, in neurotransmitter release. J Cell Biol. 2004;164:301–11. https://doi.org/10.1083/jcb.200307101.
90. Lagnado L. Ribbon synapses. Curr Biol. 2003;13:R631. https://doi.org/10.1016/s0960-9822(03)00566-9.
91. Lenzi D, von Gersdorff H. Structure suggests function: the case for synaptic ribbons as exocytotic nanomachines. BioEssays. 2001;23:831–40. https://doi.org/10.1002/bies.1118.
92. von Gersdorff H. Synaptic ribbons: versatile signal transducers. Neuron. 2001;29:7–10. https://doi.org/10.1016/s0896-6273(01)00175-1.
93. Hallam SJ, Goncharov A, McEwen J, Baran R, Jin Y. SYD-1, a presynaptic protein with PDZ, C2 and rhoGAP-like domains, specifies axon identity in C. elegans. Nat Neurosci. 2002;5:1137–46. https://doi.org/10.1038/nn959.
94. Meinertzhagen IA. Ultrastructure and quantification of synapses in the insect nervous system. J Neurosci Methods. 1996;69:59–73. https://doi.org/10.1016/S0165-0270(96)00021-0.
95. Yasuyama K, Meinertzhagen IA, Schurmann FW. Synaptic organization of the mushroom body calyx in Drosophila melanogaster. J Comp Neurol. 2002;445:211–26. https://doi.org/10.1002/cne.10155.
96. Govind CK, Meiss DE. Quantitative comparison of low- and high-output neuromuscular synapses from a motoneuron of the lobster (Homarus americanus). Cell Tissue Res. 1979;198:455–63. https://doi.org/10.1007/BF00234190.
97. Garner CC, Kindler S, Gundelfinger ED. Molecular determinants of presynaptic active zones. Curr Opin Neurobiol. 2000;10:321–7. https://doi.org/10.1016/s0959-4388(00)00093-3.
98. Muresan V, Lyass A, Schnapp BJ. The kinesin motor KIF3A is a component of the presynaptic ribbon in vertebrate photoreceptors. J Neurosci. 1999;19:1027–37. https://doi.org/10.1523/JNEUROSCI.19-03-01027.1999.
99. Hilfiker S, Pieribone VA, Czernik AJ, Kao HT, Augustine GJ, Greengard P. Synapsins as regulators of neurotransmitter release. Philos Trans R Soc Lond Ser B Biol Sci. 1999;354:269–79. https://doi.org/10.1098/rstb.1999.0378.
100. Brandstatter JH, Fletcher EL, Garner CC, Gundelfinger ED, Wassle H. Differential expression of the presynaptic cytomatrix protein bassoon among ribbon synapses in the mammalian retina. Eur J Neurosci. 1999;11:3683–93. https://doi.org/10.1046/j.1460-9568.1999.00793.x.
101. Dick O, tom Dieck S, Altrock WD, Ammermuller J, Weiler R, Garner CC, et al. The presynaptic active zone protein bassoon is essential for photoreceptor ribbon synapse formation in the retina. Neuron. 2003;37:775–86. https://doi.org/10.1016/s0896-6273(03)00086-2.
102. Kittel RJ, Wichmann C, Rasse TM, Fouquet W, Schmidt M, Schmid A, et al. Bruchpilot promotes active zone assembly, Ca2+ channel clustering, and vesicle release. Science. 2006;312:1051–4. https://doi.org/10.1126/science.1126308.

103. Lenzi D, Crum J, Ellisman MH, Roberts WM. Depolarization redistributes synaptic membrane and creates a gradient of vesicles on the synaptic body at a ribbon synapse. Neuron. 2002;36:649–59. https://doi.org/10.1016/s0896-6273(02)01025-5.
104. Lenzi D, Runyeon JW, Crum J, Ellisman MH, Roberts WM. Synaptic vesicle populations in saccular hair cells reconstructed by electron tomography. J Neurosci. 1999;19:119–32. https://doi.org/10.1523/JNEUROSCI.19-01-00119.1999.
105. Matthews G. Synaptic mechanisms of bipolar cell terminals. Vis Res. 1999;39:2469–76. https://doi.org/10.1016/s0042-6989(98)00249-1.
106. Regus-Leidig H, Ott C, Lohner M, Atorf J, Fuchs M, Sedmak T, et al. Identification and immunocytochemical characterization of Piccolino, a novel Piccolo splice variant selectively expressed at sensory ribbon synapses of the eye and ear. PLoS One. 2013;8:e70373. https://doi.org/10.1371/journal.pone.0070373.
107. Regus-Leidig H, Fuchs M, Lohner M, Leist SR, Leal-Ortiz S, Chiodo VA, et al. In vivo knockdown of Piccolino disrupts presynaptic ribbon morphology in mouse photoreceptor synapses. Front Cell Neurosci. 2014;8:259. https://doi.org/10.3389/fncel.2014.00259.
108. Govind CK, Quigley PA, Pearce J. Synaptic differentiation between two phasic motoneurons to a crayfish fast muscle. Invertebr Neurosci. 2001;4:77–84. https://doi.org/10.1007/s101580100009.
109. Ahmari SE, Buchanan J, Smith SJ. Assembly of presynaptic active zones from cytoplasmic transport packets. Nat Neurosci. 2000;3:445–51. https://doi.org/10.1038/74814.
110. Friedman HV, Bresler T, Garner CC, Ziv NE. Assembly of new individual excitatory synapses: time course and temporal order of synaptic molecule recruitment. Neuron. 2000;27:57–69. https://doi.org/10.1016/s0896-6273(00)00009-x.
111. Dresbach T, Torres V, Wittenmayer N, Altrock WD, Zamorano P, Zuschratter W, et al. Assembly of active zone precursor vesicles: obligatory trafficking of presynaptic cytomatrix proteins Bassoon and Piccolo via a trans-Golgi compartment. J Biol Chem. 2006;281:6038–47. https://doi.org/10.1074/jbc.M508784200.
112. Zhai RG, Vardinon-Friedman H, Cases-Langhoff C, Becker B, Gundelfinger ED, Ziv NE, et al. Assembling the presynaptic active zone: a characterization of an active one precursor vesicle. Neuron. 2001;29:131–43. https://doi.org/10.1016/s0896-6273(01)00185-4.
113. Shapira M, Zhai RG, Dresbach T, Bresler T, Torres VI, Gundelfinger ED, et al. Unitary assembly of presynaptic active zones from Piccolo-Bassoon transport vesicles. Neuron. 2003;38:237–52. https://doi.org/10.1016/s0896-6273(03)00207-1.
114. Patel MR, Lehrman EK, Poon VY, Crump JG, Zhen M, Bargmann CI, et al. Hierarchical assembly of presynaptic components in defined C. elegans synapses. Nat Neurosci. 2006;9:1488–98. https://doi.org/10.1038/nn1806.
115. Zhen M, Jin Y. The liprin protein SYD-2 regulates the differentiation of presynaptic termini in C. elegans. Nature. 1999;401:371–5. https://doi.org/10.1038/43886.
116. Serra-Pages C, Medley QG, Tang M, Hart A, Streuli M. Liprins, a family of LAR transmembrane protein-tyrosine phosphatase-interacting proteins. J Biol Chem. 1998;273:15611–20. https://doi.org/10.1074/jbc.273.25.15611.
117. Kaufmann N, DeProto J, Ranjan R, Wan H, Van Vactor D. Drosophila liprin-alpha and the receptor phosphatase Dlar control synapse morphogenesis. Neuron. 2002;34:27–38. https://doi.org/10.1016/s0896-6273(02)00643-8.
118. Aberle H, Haghighi AP, Fetter RD, McCabe BD, Magalhaes TR, Goodman CS. Wishful thinking encodes a BMP type II receptor that regulates synaptic growth in Drosophila. Neuron. 2002;33:545–58. https://doi.org/10.1016/s0896-6273(02)00589-5.
119. Marques G, Bao H, Haerry TE, Shimell MJ, Duchek P, Zhang B, et al. The Drosophila BMP type II receptor Wishful Thinking regulates neuromuscular synapse morphology and function. Neuron. 2002;33:529–43. https://doi.org/10.1016/s0896-6273(02)00595-0.
120. Chen X, Wu X, Wu H, Zhang M. Phase separation at the synapse. Nat Neurosci. 2020;23:301–10. https://doi.org/10.1038/s41593-019-0579-9.

121. Wu X, Cai Q, Feng Z, Zhang M. Liquid-liquid phase separation in neuronal development and synaptic signaling. Dev Cell. 2020;55:18–29. https://doi.org/10.1016/j.devcel.2020.06.012.
122. Wu X, Cai Q, Shen Z, Chen X, Zeng M, Du S, et al. RIM and RIM-BP form presynaptic active-zone-like condensates via phase separation. Mol Cell. 2019;73:971–984 e975. https://doi.org/10.1016/j.molcel.2018.12.007.
123. Wu X, Ganzella M, Zhou J, Zhu S, Jahn R, Zhang M. Vesicle tethering on the surface of phase-separated active zone condensates. Mol Cell. 2021;81:13–24 e17. https://doi.org/10.1016/j.molcel.2020.10.029.
124. McDonald NA, Fetter RD, Shen K. Assembly of synaptic active zones requires phase separation of scaffold molecules. Nature. 2020;588:454–8. https://doi.org/10.1038/s41586-020-2942-0.
125. Brandstatter JH, Meinertzhagen IA. The rapid assembly of synaptic sites in photoreceptor terminals of the fly's optic lobe recovering from cold shock. Proc Natl Acad Sci U S A. 1995;92:2677–81. https://doi.org/10.1073/pnas.92.7.2677.
126. Rybak J, Meinertzhagen IA. The effects of light reversals on photoreceptor synaptogenesis in the fly Musca domestica. Eur J Neurosci. 1997;9:319–33. https://doi.org/10.1111/j.1460-9568.1997.tb01402.x.
127. Wojtowicz JM, Marin L, Atwood HL. Activity-induced changes in synaptic release sites at the crayfish neuromuscular junction. J Neurosci. 1994;14:3688–703.
128. Harris KM, Fiala JC, Ostroff L. Structural changes at dendritic spine synapses during long-term potentiation. Philos Trans R Soc Lond Ser B Biol Sci. 2003;358:745–8. https://doi.org/10.1098/rstb.2002.1254.
129. Weeks AC, Ivanco TL, Leboutillier JC, Racine RJ, Petit TL. Sequential changes in the synaptic structural profile following long-term potentiation in the rat dentate gyrus. II. Induction/early maintenance phase. Synapse. 2000;36:286–96. https://doi.org/10.1002/(SICI)1098-2396(20000615)36:4<286::AID-SYN5>3.0.CO;2-T.
130. Reiff DF, Thiel PR, Schuster CM. Differential regulation of active zone density during long-term strengthening of Drosophila neuromuscular junctions. J Neurosci. 2002;22:9399–409. https://doi.org/10.1523/JNEUROSCI.22-21-09399.2002.
131. Meinertzhagen IA, Govind CK, Stewart BA, Carter JM, Atwood HL. Regulated spacing of synapses and presynaptic active zones at larval neuromuscular junctions in different genotypes of the flies Drosophila and Sarcophaga. J Comp Neurol. 1998;393:482–92. https://doi.org/10.1002/(sici)1096-9861(19980420)393:4<482::aid-cne7>3.0.co;2-x.
132. Dickman DK, Lu Z, Meinertzhagen IA, Schwarz TL. Altered synaptic development and active zone spacing in endocytosis mutants. Curr Biol. 2006;16:591–8. https://doi.org/10.1016/j.cub.2006.02.058.
133. Gundelfinger ED, Reissner C, Garner CC. Role of Bassoon and Piccolo in assembly and molecular organization of the active zone. Front Synap Neurosci. 2015;7:19. https://doi.org/10.3389/fnsyn.2015.00019.
134. Waites CL, Leal-Ortiz SA, Okerlund N, Dalke H, Fejtova A, Altrock WD, et al. Bassoon and Piccolo maintain synapse integrity by regulating protein ubiquitination and degradation. EMBO J. 2013;32:954–69. https://doi.org/10.1038/emboj.2013.27.
135. Montenegro-Venegas C, Annamneedi A, Hoffmann-Conaway S, Gundelfinger ED, Garner CC. BSN (bassoon) and PRKN/parkin in concert control presynaptic vesicle autophagy. Autophagy. 2020;16:1732–3. https://doi.org/10.1080/15548627.2020.1801259.
136. Okerlund ND, Schneider K, Leal-Ortiz S, Montenegro-Venegas C, Kim SA, Garner LC, et al. Bassoon controls presynaptic autophagy through Atg5. Neuron. 2017;93:897–913 e897. https://doi.org/10.1016/j.neuron.2017.01.026.
137. Ceccarelli B, Fesce R, Grohovaz F, Haimann C. The effect of potassium on exocytosis of transmitter at the frog neuromuscular junction. J Physiol. 1988;401:163–83. https://doi.org/10.1113/jphysiol.1988.sp017156.

138. Zenisek D, Davila V, Wan L, Almers W. Imaging calcium entry sites and ribbon structures in two presynaptic cells. J Neurosci. 2003;23:2538–48. https://doi.org/10.1523/JNEUROSCI.23-07-02538.2003.
139. Zenisek D, Steyer JA, Almers W. Transport, capture and exocytosis of single synaptic vesicles at active zones. Nature. 2000;406:849–54. https://doi.org/10.1038/35022500.
140. Sudhof TC. The synaptic vesicle cycle. Annu Rev Neurosci. 2004;27:509–47. https://doi.org/10.1146/annurev.neuro.26.041002.131412.

Presynaptic Cytomatrix Proteins

Yishi Jin and R. Grace Zhai

Abstract The Cytomatrix Assembled at the active Zone (CAZ) of a presynaptic terminal displays electron-dense appearance and defines the center of the synaptic vesicle release. The protein constituents of CAZ are multiple-domain scaffolds that interact extensively with each other and also with an ensemble of synaptic vesicle proteins to ensure docking, fusion, and recycling. Reflecting the central roles of the active zone in synaptic transmission, CAZ proteins are highly conserved throughout evolution. As the nervous system increases complexity and diversity in types of neurons and synapses, CAZ proteins expand in the number of gene and protein isoforms and interacting partners. This chapter summarizes the discovery of the core CAZ proteins and current knowledge of their functions.

Keywords Presynaptic active zone · Munc13 · UNC-13 · Rim · UNC-10 · RIM-BP · ELKS · Bruchpilot · Fife · CLA-1 · Bassoon · Piccolo · Liprin-α · SYD-2 · SYD-1 · CASK

1 Introduction

The appearance of an electron-dense matrix associated with patches of the axonal plasma membrane and surrounded by small clusters of vesicles under electron microscopy has been taken as the morphological landmark of a presynaptic terminal, often named active zone (Chapter "The Architecture of the Presynaptic Release

Y. Jin (✉)
Department of Neurobiology, School of Biological Sciences, University of California San Diego, La Jolla, CA, USA
e-mail: yijin@ucsd.edu

R. G. Zhai (✉)
Department of Molecular and Cellular Pharmacology, Leonard M. Miller School of Medicine, University of Miami, Miami, FL, USA
e-mail: gzhai@med.miami.edu

Z.-W. Wang (ed.), *Molecular Mechanisms of Neurotransmitter Release*, Advances in Neurobiology 33, https://doi.org/10.1007/978-3-031-34229-5_2

Site"). Molecular identification of presynaptic components began with the ingenious invention of biochemical preparation of synaptosomes, developed by Victor Whittaker and coworkers [1]. Combined with technology advances in mass spectrometry proteomics, thousands of distinct presynaptic proteins have been identified, culminating to a landmark study by Reinhart Jahn and coworkers, which reports 410 proteins associated with a single synaptic vesicle [2]. However, the constituents of the Cytomatrix Assembled at the active Zone (CAZ) tend to be insoluble in biochemical purifications, and some proteins may be present in selective types of synapses or transiently associate with synapses. It took additional approaches, such as antibody-based protein expression screening, protein-interaction screening, and molecular genetics in model organisms, to unveil the identities of CAZ proteins.

It is generally agreed that CAZ proteins fall into three main functional categories. First are the classical cytoskeletal proteins corresponding to actin, tubulin, myosin, spectrin α chain and β chain, and β-catenin. They are the fundamental elements of the cytoskeletal framework of active zone cytomatrix. Second are the adaptor and scaffold proteins, such as SAP90/PSD95/DLG4, SAP97/DLG1, and CASK/LIN-2. These proteins are not restricted to presynaptic active zones, also participate in clustering postsynaptic receptors, and are involved in the organization of a variety of cell junctions. If the cytoskeleton proteins form a grid-like structure at the active zone, these proteins probably link the ion channels and the synaptic vesicle fusion machinery onto the grid to ensure proper active zone function. Third are the active-zone-specific CAZ proteins, represented by six evolutionarily conserved families known as Munc13/UNC-13, RIM, RIM-BP (RIM-binding protein), ELKS, Bassoon and Piccolo, and Liprin-α [3]. This chapter will focus on the discovery and function of these active-zone-specific CAZ components.

2 Experimental Approaches Used in the Identification of CAZ Proteins

We begin by offering a brief overview of the key approaches used to identify CAZ proteins.

2.1 Antibody-Based Protein Expression Screen

When researchers realized that the protein constituents of the electron-dense matrix in presynaptic terminals were low in abundance and problematic with solubility in biochemical purification, they sought to obtain antibodies against brain synaptic junctional proteins. The antibodies were used in immunocytochemistry on either brain tissues or cells to determine if the corresponding antigens were localized to presynaptic terminals [4, 5]. To search for the molecules that encode the antigens,

researchers relied on a powerful technique, developed in the late 1980s, that enabled the production of any proteins in bacteriophage lambda [6]. In essence, mRNAs isolated from brain tissues were made into cDNAs, which were cloned into special expression vectors for protein production in bacteriophage lambda. The synapse-specific antibodies were used to recognize proteins produced from lambda. The amino acid sequences for candidate proteins were then deduced from the DNA sequences of the corresponding cDNA. This approach led to the identification of the CAZ proteins Bassoon and Piccolo in mammals [7, 8], and Bruchpilot in *Drosophila* [9].

2.2 Protein-Interaction-Based Screen

Around late 1980s, another powerful technique was developed to detect protein–protein interactions in yeast, named yeast-two-hybrid (Y2H) interaction assay [10]. The Y2H design was based on the finding that the transcriptional activity of the yeast protein Gal4 requires two modular protein domains, a DNA-binding (DB) domain and a transcription-activation domain (AD). When the DB and AD domains are in close proximity, transcription of genes encoding enzymes of galactose utilization can be activated, thereby allowing yeast to grow in galactose selection media. In a Y2H assay, a bait protein X, which can be either the full length or a fragment of the protein of interest, is fused to the Gal4(DB) domain, and potential prey proteins (Y) are fused to the Gal4(AD) domain. Upon co-expression in yeast, if protein X binds to protein Y, it will lead to reconstitution of Gal4 transcriptional activity. Thus, the Y2H assay does not rely on either solubility or abundance of target proteins and can be carried out on a large scale when a library of prey is used. However, the resulting candidate binding partners need to be verified using other biochemical assays and validated for expression in brain tissues. This approach led to the identification of the CAZ proteins RIM [11], RIM-Binding Protein [12], and ELKS [13].

2.3 Forward Genetic Screen for Mutants Affecting Synaptic Transmission

Around 1960s, the nematode *Caenorhabditis elegans* was chosen by the Nobel Laureate Sydney Brenner to study the development and function of the nervous system. He carried out the first forward genetic screen and isolated a large number of mutants that displayed a variety of abnormal patterns of movement, categorized as *unc*oordinated [14]. Subsequent molecular cloning of the genes related to the *unc* phenotypes and physiological studies began to uncover the synaptic basis of the uncoordinated movement [15]. By early 1990s, it became clear that genes acting in synaptic transmission are evolutionarily conserved. This notion fueled the

efforts to search for homologs of *C. elegans unc* genes in mammals and other species based on DNA sequence similarity. For example, *C. elegans unc-13* (*uncoordinated-13*) mutants are paralyzed and resistant to drugs that perturb synaptic transmission. Molecular cloning of *unc-13* revealed that the predicted UNC-13 protein contains domains, known as C1 and C2, that can bind to Ca^{2+}, phospholipids, and diacylglycerol [16]. Using *unc-13* cDNA to screen a rat brain cDNA library then led to the discovery of its mammalian member named as Munc13 [17]. Protein expression studies further showed that Munc13 and UNC-13 localize to presynaptic active zone.

The nervous system of *C. elegans* is fully reconstructed at the ultrastructural level, providing the precise knowledge on the synapse number, position, and pattern for each neuron [18]. *C. elegans* is also optically transparent. With the advent of using GFP and other fluorescent proteins as non-invasive reporters in living *C. elegans* [19], researchers can observe any cellular morphology and compartment. In particular, transgenic reporters expressing chimeric proteins, in which GFP is fused in-frame to synaptic vesicle proteins, such as Synaptobrevin-1 (SNB-1::GFP), enabled the visualization of synapses [20, 21]. Combined with genome-wide chemical mutagenesis, mutants that displayed abnormal synapse morphology, position, and number were subsequently isolated [22]. Molecular cloning and expression studies of the corresponding genes showed that many proteins are localized to sub-compartments of presynaptic terminals. This approach led to the identification of the CAZ protein SYD-2/Liprin-α [23].

3 Summary of CAZ Proteins and Function

The active-zone-specific CAZ proteins are composed of multiple domains known for protein–protein, protein–lipid, and protein–ion bindings (Fig. 1a). They exhibit homomeric interactions and also bind extensively with other CAZ proteins, the synaptic plasma membrane, components of the synaptic cytoskeleton, and the synaptic vesicle recycling machinery (Fig. 1b). Like the conserved nature of synapse ultrastructure (Chapter "The Architecture of the Presynaptic Release Site"), CAZ proteins are highly conserved from invertebrates to human. Each family of CAZ proteins is typically encoded by a single gene in invertebrates, but multiple genes in vertebrates, reflecting the expansion of genomes in gene number and regulatory capacity. Regardless of species, each CAZ gene can produce several protein isoforms through the use of alternative promoters and alternative splicing, and these protein isoforms often show distinct dynamics and binding interactions depending on synapse type and neuronal activity state. Functional investigation of CAZ proteins using genetic malleable invertebrates has offered key insights into evolutionarily conserved mechanisms, while studies of CAZ proteins in mammalian nervous systems have both validated the commonality and also uncovered additional divergent themes. Here, we summarize general knowledge of each CAZ protein family (Fig. 1).

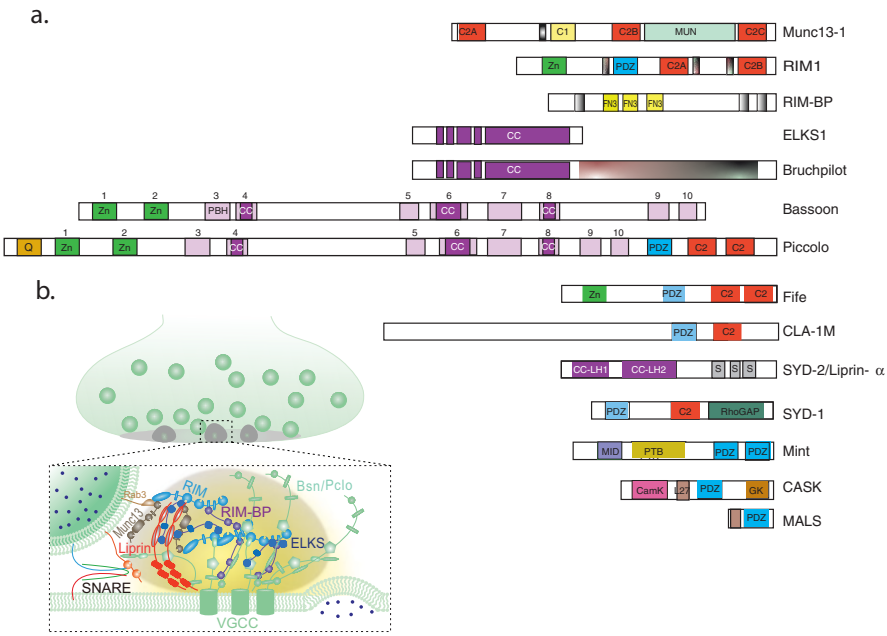

Fig. 1 (**a**) Schematics of presynaptic CAZ proteins, using a representative full-length protein isoform for each family. Functional domains are marked following conventional designation (see main text and Ref. [3]). (**b**) Graphic illustration of CAZ protein-interacting network at the presynaptic active zone. (Modified from the graphic abstract in Ref. [47], provided by Mingjie Zhang)

3.1 Munc13/UNC-13

The Munc13/UNC-13 proteins are characterized by an ordered arrangement of three C2 domains (designated as C2A, C2B, C2C), a calmodulin-binding domain, a C1 domain that binds lipid, and an MUN domain that binds to the SNARE protein syntaxin and the SM protein Munc18/UNC-18 [24, 25] (Fig. 1a). Mammals have five *Munc13* genes, with *Munc13-1, -2*, and *-3* being abundantly expressed in CNS synapses. Alternative protein isoforms produced from each gene can vary in the amino acid linker sequences between the identified domains and in the number of C2 domains. *C. elegans* and *Drosophila* each has only one such gene, which also produces several protein isoforms. Munc13/UNC-13 proteins decorate the center of the presynaptic active zone.

The key function of this protein family is to prime synaptic vesicles for fast exocytosis. The first evidence came from electrophysiological studies of the *unc-13* mutants, which revealed a complete abolishment of neurotransmitter release [26]. Subsequent studies of *Drosophila unc-13* mutants and mouse *Munc13-1* knockout supported their essential role in synaptic vesicle exocytosis [27, 28]. Knockout of other *Munc13* genes also resulted in similar effects in a variety of synapses [3]. However, in the absence of any Munc13/UNC-13 member, the morphological

organization of synapses and the assembly of dense projection are grossly normal, except that the precise docking pattern of synaptic vesicles is altered in a way that is consistent with changes in exocytosis dynamics [29].

Biochemical studies of Munc13/UNC-13 proteins have uncovered a complex protein-interaction network involving each domain of Munc13/UNC-13 [3]. For example, the most N-terminal C2A domain binds the Zinc Finger of RIM [30]. In different synapses and organisms, C2A domain is shown to be important for synapse vesicle docking and priming [31, 32], release probability [33], and kinetics [34], partly through regulating the spatial proximity of Munc13/UNC-13 to the calcium channels [35]. The C2B domain binds Ca^{2+} and anionic phospholipid, and works together with the C1 domain, which binds diacylglycerol and phorbol esters, to inhibit Ca^{2+}-dependent neurotransmitter release [36]. The C2C domain at the C-terminus is shown to function as a vesicle or endosome adaptor [37]. With the many protein isoforms that often display subtle differences in their binding affinities and binding partners, a major remaining puzzle is how Munc13/UNC-13 protein diversity endorses the physiological specificity of the synaptic vesicle release.

3.2 RIM

The first member of RIM (for Rab3-interacting molecule) proteins, RIM1, was identified in a yeast-two-hybrid protein-interaction screen using an activated form of the small GTPase RAB3 [11]. Vertebrates have four *Rim* genes, with *Rim1* and *Rim2* broadly expressed in synapses, and *C. elegans* and *Drosophila* has one gene each, known as *unc-10* and *Rim*, respectively. RIM proteins contain a Zinc Finger at N-terminus, a PDZ domain in the middle, two C2 domains at the C-terminus, and a proline-rich region in between the C2 domains (Fig. 1a). Each domain binds to specific proteins. The N-terminus of RIM binds to GTP-bound RAB3 associated with the synaptic vesicles, the Zinc Finger binds to the C2A domain of Munc13 [30], the PDZ domain binds to the CAZ protein ELKS [13], the proline-rich region binds to the CAZ protein RIM-BP [12], and the C2 domains mediate interactions with SNAREs, calcium channels [38], and the CAZ protein Liprin-α [39]. Thus, Rim acts as scaffolds at the presynaptic cytomatrix to organize synaptic vesicles and other proteins in the presynaptic release machinery (Fig. 1b).

Studies of *C. elegans unc-10* mutants provided first functional evidence for a role of RIM in synaptic vesicle release. In *unc-10* mutants the morphology of the presynaptic density and the docking pattern of synaptic vesicles are grossly normal, but there is greatly diminished neurotransmitter release [40]. Analyses of *Drosophila Rim* mutants revealed similar synaptic transmission deficits, and further showed reduced readily release pool of synaptic vesicles and reduced clustering of calcium channels at the active zone [41, 42]. In mice *Rim 1* and *Rim 2* each produces at least two protein isoforms through alternative splicing, with RIM1a being more abundant than RIM1b at presynaptic sites. Knockout of *Rim1a* caused a selective reduction in Munc13-1 expression at synapses, altered release probability, and short-term

synaptic plasticity, but normal synaptic morphology [39]. Conditional knockout of both *Rim 1* and *Rim 2* led to further reduced readily releasable pool of vesicles and calcium channels at the Calyx of Held synapse [43]. These functional effects of RIM are consistent with the extensive molecular interactions between RIM and other CAZ proteins (Fig. 1b).

3.3 RIM-BP

As implied by its name, RIM-BP (RIM-binding protein) binds to RIM, originally isolated by yeast-two-hybrid screening [12]. RIM-BP proteins contain three SRC homology 3 (SH3) domains and three fibronectin III domains (Fig. 1a). The two C-terminal SH3 domains bind the proline-rich motifs of RIM and a number of voltage-gated calcium channels [44, 45], and the N-terminal SH3 domain binds the proline-rich motif of the CAZ protein Bassoon [46]. Mammals express three *Rim-BP* genes, while *C. elegans* and *Drosophila* each has one gene known as *rimb-1* and *Rim-BP*. In vitro biochemical studies show that the binding between RIM and RIM-BP displays liquid–liquid phase separation, forming dynamic and condensed assemblies. In the presence of voltage-gated calcium channels, the RIM and RIM-BP condensates can enrich the channels [47]. Such mode of protein interactions may underlie the appearance of small clusters of vesicle release sites observed in neuronal synapses [48]. Genetic knockout studies with mice, *Drosophila*, and *C. elegans* have supported the functional significance of protein binding between Rim-BP and calcium channels, such that the mutant synapses have reduced number of calcium channels. Double mutants of *Rim-BP* and *Rim* show more severe synaptic deficits, revealing some overlapping roles of Rim and Rim-BP in synaptic vesicle docking, the morphology of presynaptic dense projections, and the number of calcium channels at the active zone [49–51]. In mice, a complete loss of *Rim-BP1* leads to motor abnormalities reminiscent of dystonia, decreased Purkinje cell dendritic arborization, and a reduced number of cerebellar synapses. Interestingly, several loss-of-function mutations in human TSPOAP1/Rim-BP are recently reported to cause autosomal recessive dystonia [52]. These findings form the basis for further broadening our understanding of RIM-BPs.

3.4 ELKS

The name of ELKS proteins reflects the fact that these proteins are rich in E (Glutamate), L (Leucine), K (Lysine), and S (Serine) amino acid residues. ELKS1 was initially identified as a fusion protein with the receptor tyrosine kinase RET in thyroid carcinomas [53]. Mammals have two *Elks* genes that produce several isoforms; and *C. elegans* expresses a single ortholog ELKS-1, whereas *Drosophila* expresses an ELKS-like molecule called Bruchpilot (Fig. 1a). ELKS proteins

contain mostly coiled-coil domains, and interact with a multitude of proteins, hence given different names in the literatures, including Rab6IP2 (Rab6-interacting protein 2) [54], CAST (CAZ-associated structural protein) [55], and ERC (ELKS/Rab6IP2/CAST) [13]. At synapses, ELKS/ELKS-1/Bruchpilot can bind to multiple CAZ proteins, including Rim via the coiled-coil region in C-termini [13], Bassoon and Piccolo via the central coiled-coil region [55], and Liprin-α via the N-terminal coiled-coil region [56].

Functional studies of individual ELKS genes using genetic knockout animals in different species show no major synapse defects. *C. elegans elks-1* null animals have normal synapse architecture and CAZ protein expression [57]. However, as described below, in a gain-of-function SYD-2/Liprin-α mutant, ELKS-1 is required for the function and morphological integrity of certain synapses [58]. *Elks* single knockout mice also show no major synapse defects [59]. However, when both *Rim1* and *Rim2* and both *Elks1* and *Elks2* were deleted, neurons showed overall normal synaptic organization, but an absence of docked synaptic vesicles and a strong reduction in Munc13, Bassoon, Piccolo, and RIM-BP at the active zone, indicating disassembly of the presynaptic active zone [60]. These data show that ELKS proteins alone are not essential for formation of presynaptic terminals, but can modulate presynaptic active zone under specific conditions.

Drosophila Bruchpilot is a large protein that contains an ELKS homology region at the N-terminus and lacks the RIM-interacting domain, instead acquires a unique large C-terminal extension that bears features of cytoskeletal proteins such as plectin and myosin (Fig. 1a) [9]. Bruchpilot has received extensive attention as it was the first CAZ protein with its precise localization revealed by the STimulated Emission Depletion (STED) super-resolution microscopy. At the neuromuscular junction (NMJ), the N-terminus of Bruchpilot is close to the presynaptic plasma membrane, and its C-terminus extends into synaptic vesicle clusters. The ring-like T-bar structure is formed by two protein isoforms of Bruchpilot arranged in an alternating pattern in a circular array. Such an array creates "slots" for calcium channels and synaptic vesicle docking sites allowing efficient neurotransmission [61]. Loss of Bruchpilot alone causes dramatic effects on the formation of the platform of the T-bar structure at the presynaptic active zone (see diagram in Chapter "The Architecture of the Presynaptic Release Site", Fig. 1), and is required for the clustering of calcium channels at the "pedestal" of T-bar at the center of active zone, ensuring the close proximity of calcium influx to the synaptic vesicle fusion machinery [62, 63]. It is possible that the different effects of eliminating Bruchpilot and ELKS on synaptic morphology are due to their differences in molecular structures.

3.5 Bassoon and Piccolo

These two very large proteins of greater than 450 kDa were identified using an antibody-based expression cloning method, and were among the first group of proteins to define the CAZ of presynaptic terminals in the vertebrate nervous system [7,

8, 64]. Bassoon and Piccolo share related protein structures, namely, repeated homologous regions called Piccolo Bassoon homology domain (PBH domains), of unknown function, coiled-coil regions, and two Zinc Finger domains (Fig. 1a). Additionally, Piccolo has a single PDZ domain and two C2 domains at its C-terminal (Fig. 1a). Given their large sizes, it is not surprising that they have many binding partners, ranging from components of the synaptic actin cytoskeleton to synaptic vesicle-associated proteins, such as the prenylated Rab acceptor PRA1 [64], other CAZ proteins (e.g., Rim, Rim-BP, ELKS, and Munc13) [65], and voltage-gated calcium channels [46]. The CC2 domain Bassoon also directly binds to an ubiquitin E3 ligase molecule Atg5 [66].

Although Bassoon and Piccolo were initially thought to be unique to CNS synapses, subsequent analyses show that they are also present at neuromuscular junctions, ribbon synapses, and other peripheral synapses [67, 68]. Bassoon and Piccolo show differential distributions within presynaptic terminals and play distinct roles in different types of synapses. In glutamatergic synapses of mammalian CNS, Bassoon clusters detected by immune-EM are often present above the filaments emanating from the plasma membrane at the active zone [69]. Super-resolution imaging using STED microscopy reveals that the C-terminus of Bassoon is close to the presynaptic plasma membrane and N-terminus extended into the presynaptic cytoplasm [70] (Fig. 1b). The mammalian photoreceptor ribbon synapse has two sub-compartments: a dense projection from the plasma membrane, and an electron-dense ribbon extending from the SV release site into the presynaptic cytoplasm [71]. Bassoon localizes at the junction between these two sub-compartments, while Piccolo associates with the ribbon, and Rim, Munc13, and ELKS exist at the presynaptic density [72].

At least two mutant mouse strains of Bassoon (*Bsn*) have been reported. A *Bsn* in-frame deletion mutant, which expresses a protein of 180 kd that includes the N-terminal and C-terminal regions but lacks the central part of Bassoon, shows unanchored ribbons in the presynaptic terminal of retina photoreceptors [73]. In these *Bsn* mutant mice, the inner hair cell ribbon synapses in the cochlea also exhibit loss of fast neurotransmitter release [74], while CNS excitatory synapses exhibit impaired synaptic transmission but apparently normal synaptic morphology [75]. These data establish the importance of Bassoon in ribbon synaptic architecture and suggest Bassoon's role may vary depending on synapse type. In a *Bsn* null mutant, cerebellar mossy fiber synapses show enhanced short-term synaptic depression but largely normal basal synaptic transmission and the number of synaptic vesicles [76]. In the endbulb synapses of auditory nerve fibers, the replenishment of synaptic vesicles at the release sites is significantly reduced [77]. Bassoon promotes vesicle replenishment in part through inhibiting presynaptic autophagy [66].

Piccolo also exhibits synapse-type specific effects. For example, a short isoform of Piccolo, Piccolino, is found to be predominantly expressed at sensory ribbon synapses in the eye and ear [78]. Piccolino is required for the formation of the plate-shaped ribbons, as loss of Piccolino in rodents results in spherical ribbons and a disruption of the maturation of ribbons [79, 80]. At the rat calyx of the Held synapse, Piccolo deficiency results in a defect in replenishment of readily releasable

synaptic vesicles during prolonged and intense firing activities, and smaller synapses [81]. The Piccolo knockout rats (Pclotgt/gt) also exhibit abnormal brain morphology and altered cerebellar neural circuitry [82]. Interestingly, loss-of-function mutations of human Piccolo (PCLO) have been associated with type 3 pontocerebellar hypoplasia (PCH3), also known as cerebellar atrophy with progressive microcephaly [83]. Knockdown of both Bassoon and Piccolo in hippocampal and cortical neurons led to a reduction in synaptic vesicles, but did not alter synapse physiology, supporting their partially overlapping functions [84].

For a period of time, it was thought that proteins similar to Bassoon and Piccolo were not present in synapses of invertebrates. Through careful molecular phylogeny analysis, in combination with expression and genetic studies, the *Drosophila* Fife and *C. elegans* CLA-1/Clarinet are reported to share features similar to Piccolo and Rim [85]. Both Fife and CLA-1 are large proteins that contain Zinc Finger, C2, and PDZ domains, along with numerous unique repeats. Both genes produce multiple protein isoforms, which exhibit distinctive localization in the presynaptic cytomatrix, forming nanodomains and interacting with other CAZ proteins [86, 87]. Genetic studies of *fife* and *cla-1* mutants show that different isoforms display synapse-type specificity to regulate presynaptic terminal structural and functional integrity [85–87]. CLA-1 has recently been linked to autophagy (bioRxiv 2021.08.19.457026), supporting mechanistic conservation with Bassoon.

3.6 Liprin-Alpha

Liprin (for Lar-interacting-protein-related protein) proteins were named because of their initial identification by Y2H assay as proteins interacting with the intracellular phosphatase domain of LAR and closely related receptor tyrosine phosphatases [88]. Liprin proteins include three subfamilies: alpha, beta, and gamma; however, only alpha proteins are extensively studied for their roles in synapses. The N-termini of Liprin-α proteins are characterized by multiple coiled-coil structures, with a stretch of ~100 amino acids, known as the LH1 (Liprin Homology) domain, which shares near 90% sequence identity from *C. elegans* to mammals; and the C-terminal half of Liprin-α contains three SAM domains (Fig. 1). The middle region of different isoforms of Liprin-α generally has low-complexity domains. *C. elegans* and *Drosophila* each expresses one Liprin-α gene, known as *syd-2* and DLiprin-α, respectively [23, 89]. Both are exclusively localized to presynaptic terminals. Vertebrates express four Liprin-α genes. Expression of Liprin-α1 and Liprin-α4 is seen in limited area in the brain and also outside of the nervous system. Liprin-α2 and Liprin-α3 are specifically and broadly expressed in the brain. Liprin-α3 shows strong localization to the presynaptic active zone [70], and Liprin-α2 is present at both pre- and postsynaptic sites [90].

Genetic studies of mutants in *C. elegans* and *Drosophila* provided the first evidence for roles of Liprin-α in structural integrity of the presynaptic active zone. *C. elegans syd-2* was identified from a forward genetic screen using an SNB-1::GFP

reporter, because loss of function in *syd-2* caused both reduced and diffused accumulation of SNB-1::GFP at neuromuscular synapses [23]. Subsequent findings from *Drosophila* showed that loss of *DLiprin-α* also altered morphology of neuromuscular synapses [89]. Ultrastructural analysis of both *syd-2* and *DLiprin-α* mutants revealed a primary effect on the length and shape of the presynaptic dense projection. Moreover, the CAZ proteins ELKS and RIM show diffuse and reduced accumulation at the presynaptic active zone [58, 91, 92]. In mouse hippocampal neuron synapses, knockout of Liprin-α3 alone causes subtle but significant alternation in presynaptic ultrastructure and CAZ protein compositions [70]. Knockout of both Liprin-α2 and α3 leads to stronger reductions in the protein machinery for docking and priming and in the pool of releasable vesicles at excitatory and inhibitory synapses, and increases in Ca^{2+} channels and release probability at excitatory but not inhibitory synapses [93].

Studies of a gain-of-function (gf) mutation in the *C. elegans* SYD-2 have provided an important clue to the understanding of how Liprin-α organizes presynaptic cytomatrix. The *syd-2(gf)* mutation changes Arg184 to Cys in the highly conserved LH1 domain and causes enlarged presynaptic dense projections [58, 94]. In biochemical studies, purified wild type LH1 domain forms dimers, whereas LH1 domain with the Arg184Cys mutation forms multimers [95]. The LH1 domain is predicted to form a coiled-coil structure. Crystal structure studies of the LH1 domain of the vertebrate Liprin-α2 reveals that the helix containing Arg194 (corresponding to Arg184 in SYD-2) forms a homo-tetramer [96]. Arg194 faces away from the tetramerization surface and stabilizes intramolecular interaction between orderly arranged helical dimers. The Arg194Cys mutation disrupts the interaction among positively charged amino acid residues and enhances the dimer to oligomer transition of the LH1 domain. Moreover, in both biochemical assays and living cells, oligomerized Liprin-α2 promotes formation of ELKS condensates via liquid–liquid phase separation, and such ELKS condensates recruit RIM1a, RIM-BP [58]. As described in Chapter "The Architecture of the Presynaptic Release Site", functional evidence from *C. elegans* and mice has supported the idea that the liquid–liquid phase separation property of CAZ proteins is important for presynaptic active zone assembly.

4 Intracellular Regulators of CAZ Proteins in Synapse Formation

The extensive interactive nature among CAZ proteins underlies the complex regulation of presynaptic assembly. Live imaging of CAZ proteins has probed into the dynamic processes of assembly of a presynaptic terminal. CAZ proteins translated in the soma must be sorted into the axon, and transported and delivered to the presynaptic terminal [97–99]. The transport and delivery of CAZ components involve diverse vesicular carriers that interact with Golgi apparatus, endosomes, and

lysosomal pathways [100, 101]. For example, ELKS can interact with Rab6 to mediate transport between endosome and Golgi [54]. Bassoon and Piccolo are transported in large dense core vesicles that contain other CAZ proteins and SNAREs [98]. Liprin-α interacts with the axonal motor proteins kinesin-1 and KIF1A/Unc104 [92, 102] as well as many intracellular and cell surface molecules to contribute to the delivery of other CAZ proteins and the nucleation of nascent active zone [62, 91, 103]. Here, we highlight two intracellular pathways that coordinate with CAZ proteins in synapse formation.

4.1 SYD-1/dSYD-1/SYDE

Molecular genetic studies from *C. elegans* and *Drosophila* have supported a functional hierarchy involving the conserved SYD-1/dSYD-1 proteins as an upstream regulator in the assembly of presynaptic active zone. *C. elegans syd-1* was identified from the forward genetic screen that yielded *syd-2*, based on similarly altered SNB-1::GFP patterns [104]. The invertebrate SYD-1 and dSYD-1 full-length proteins have an N-terminus PDZ domain, followed by a C2 domain and a Rho-GAP (GTPase Activating Protein) domain (Fig. 1a) [104, 105]. Mouse expresses two homologs, known as SYDE1 and SYDE2, containing only C2 and Rho-GAP domains [106], resembling a short isoform of *C. elegans* SYD-1. The C2 domain facilitates protein association with the membrane. However, the function of the GAP domain varies between species. *Drosophila* dSYD-1 has GAP activity on Rac1 [107] and mouse SYDE1/mSYD1A acts on CDC42 [106], whereas the GAP domain in *C. elegans* SYD-1 may not be active [104].

Evidence from both *C. elegans* and *Drosophila* supports a conclusion that *syd-1/dsyd-1* and *syd-2/Dliprin-α* act in a common molecular pathway to promote synapse formation [58, 105, 108, 109]. In *C. elegans*, double mutants of *syd-1* and *syd-2* resemble each single mutant. In the absence of *syd-1*, the *syd-2(gf)* mutation can induce synapse formation [58]. Synapse imaging studies in both *C. elegans* and *Drosophila* show that SYD-1/dSYD-1 arrives early at nascent sites of the presynaptic terminals and facilitates the accumulation of SYD-2/DLiprin-α and other CAZ proteins, such as ELKS-1/Bruchpilot [35, 110–112]. SYD-1/dSYD-1 can interact with neurexin via the PDZ domain [110], and also bind to other synaptic proteins such as spinophilin [113], neurabin [111], and RSY-1/PNISR [114]. Such complex interactions orchestrate early assembly processes at the *Drosophila* NMJs [110, 115]. Mice lacking *Syde1/mSYD1A* exhibit reduced docked vesicles and synaptic activities [106]. An intrinsically disordered region of SYDE1/mSYD1A interacts with multiple synapse proteins, including CAZ protein Liprin-α2, Munc18-1, and presynaptic receptor tyrosine phosphatases. Conceivably, such multi-protein interactions play a key role in tethering synaptic vesicles.

4.2 Tripartite Complex of CASK, Mint, and Veli

This tightly associated PDZ domain-containing protein complex has been studied in many cellular contexts and is present at both pre- and postsynaptic sites [116]. A presynaptic role for CASK/Mint/Veli was initially hinted at by the interactions with neurexins [117]. CASK/Mint/Veli also bind directly or indirectly to other synaptic proteins such as voltage-gated calcium channels, Liprin-α, and Cdk5 [118, 119], as well as several synaptic adhesion molecules [116]. A single member of each protein family is present in invertebrates; in mammals, Mint and Veli each is encoded by three genes. Knockout mice of either Mint or Veli die at an early stage, precluding a full examination of their roles in synapse formation [120, 121]. Nonetheless, it is generally agreed that these three proteins play regulatory roles in synaptic vesicle release, and may indirectly contribute to the transport of synaptic proteins and interaction with synaptic surface proteins to facilitate the development and maintenance of synaptic architecture.

5 Summary

Through consorted efforts using combinatorial approaches, research in the past two decades has revealed the shared core CAZ components. Despite their precise localization to the presynaptic active zone, functional studies have placed different families of CAZ proteins in a wide spectrum for their essentiality in synapse formation and function. Munc13/Unc-13 is essential for synaptic vesicle release, whereas ELKS has the least functional significance yet provides maladaptive regulation to many actions of presynaptic release. The interwoven protein-interaction network at CAZ remains a wonderland where conceptual creativity and technology innovation continue to push the boundary of our knowledge about the mystery of synapses.

Acknowledgments We thank many researchers for their beautiful work in the studies of CAZ proteins and apologize for selective citations due to space limit. We acknowledge funds from NIH that have supported the research in our laboratories.

References

1. Nagy A, Baker RR, Morris SJ, Whittaker VP. The preparation and characterization of synaptic vesicles of high purity. Brain Res. 1976;109:285–309. https://doi.org/10.1016/0006-8993(76)90531-x.
2. Takamori S, Holt M, Stenius K, Lemke EA, Gronborg M, Riedel D, et al. Molecular anatomy of a trafficking organelle. Cell. 2006;127:831–46. https://doi.org/10.1016/j.cell.2006.10.030.
3. Sudhof TC. The presynaptic active zone. Neuron. 2012;75:11–25. https://doi.org/10.1016/j.neuron.2012.06.012.

4. Kistner U, Wenzel BM, Veh RW, Cases-Langhoff C, Garner AM, Appeltauer U, et al. SAP90, a rat presynaptic protein related to the product of the Drosophila tumor suppressor gene dlg-A. J Biol Chem. 1993;268:4580–3.
5. Langnaese K, Seidenbecher C, Wex H, Seidel B, Hartung K, Appeltauer U, et al. Protein components of a rat brain synaptic junctional protein preparation. Brain Res Mol Brain Res. 1996;42:118–22. https://doi.org/10.1016/s0169-328x(96)00147-7.
6. Huse WD, Sastry L, Iverson SA, Kang AS, Alting-Mees M, Burton DR, et al. Generation of a large combinatorial library of the immunoglobulin repertoire in phage lambda. Science. 1989;246:1275–81. https://doi.org/10.1126/science.2531466.
7. tom Dieck S, Sanmarti-Vila L, Langnaese K, Richter K, Kindler S, Soyke A, et al. Bassoon, a novel zinc-finger CAG/glutamine-repeat protein selectively localized at the active zone of presynaptic nerve terminals. J Cell Biol. 1998;142:499–509. https://doi.org/10.1083/jcb.142.2.499.
8. Cases-Langhoff C, Voss B, Garner AM, Appeltauer U, Takei K, Kindler S, et al. Piccolo, a novel 420 kDa protein associated with the presynaptic cytomatrix. Eur J Cell Biol. 1996;69:214–23.
9. Wagh DA, Rasse TM, Asan E, Hofbauer A, Schwenkert I, Durrbeck H, et al. Bruchpilot, a protein with homology to ELKS/CAST, is required for structural integrity and function of synaptic active zones in Drosophila. Neuron. 2006;49:833–44. https://doi.org/10.1016/j.neuron.2006.02.008.
10. Fields S, Song O. A novel genetic system to detect protein-protein interactions. Nature. 1989;340:245–6. https://doi.org/10.1038/340245a0.
11. Wang Y, Okamoto M, Schmitz F, Hofmann K, Sudhof TC. Rim is a putative Rab3 effector in regulating synaptic-vesicle fusion. Nature. 1997;388:593–8. https://doi.org/10.1038/41580.
12. Wang Y, Sugita S, Sudhof TC. The RIM/NIM family of neuronal C2 domain proteins. Interactions with Rab3 and a new class of Src homology 3 domain proteins. J Biol Chem. 2000;275:20033–44. https://doi.org/10.1074/jbc.M909008199.
13. Wang Y, Liu X, Biederer T, Sudhof TC. A family of RIM-binding proteins regulated by alternative splicing: implications for the genesis of synaptic active zones. Proc Natl Acad Sci U S A. 2002;99:14464–9. https://doi.org/10.1073/pnas.182532999.
14. Brenner S. The genetics of *Caenorhabditis elegans*. Genetics. 1974;77:71–94. https://doi.org/10.1093/genetics/77.1.71.
15. Rand JB, Nonet ML. Synaptic transmission. In: Riddle DL, Blumenthal T, Meyer BJ, Priess JR, editors. C. elegans II. Cold Spring Harbor (NY); 1997.
16. Maruyama IN, Brenner S. A phorbol ester/diacylglycerol-binding protein encoded by the unc-13 gene of Caenorhabditis elegans. Proc Natl Acad Sci U S A. 1991;88:5729–33. https://doi.org/10.1073/pnas.88.13.5729.
17. Brose N, Hofmann K, Hata Y, Sudhof TC. Mammalian homologues of Caenorhabditis elegans unc-13 gene define novel family of C2-domain proteins. J Biol Chem. 1995;270:25273–80. https://doi.org/10.1074/jbc.270.42.25273.
18. White JG, Southgate E, Thomson JN, Brenner S. The structure of the nervous system of the nematode Caenorhabditis elegans. Philos Trans R Soc Lond Ser B Biol Sci. 1986;314:1–340. https://doi.org/10.1098/rstb.1986.0056.
19. Chalfie M, Tu Y, Euskirchen G, Ward WW, Prasher DC. Green fluorescent protein as a marker for gene expression. Science. 1994;263:802–5. https://doi.org/10.1126/science.8303295.
20. Nonet ML. Visualization of synaptic specializations in live C. elegans with synaptic vesicle protein-GFP fusions. J Neurosci Methods. 1999;89:33–40. https://doi.org/10.1016/s0165-0270(99)00031-x.
21. Jorgensen EM, Hartwieg E, Schuske K, Nonet ML, Jin Y, Horvitz HR. Defective recycling of synaptic vesicles in synaptotagmin mutants of Caenorhabditis elegans. Nature. 1995;378:196–9. https://doi.org/10.1038/378196a0.
22. Jin Y. Synaptogenesis. WormBook. 2005; https://doi.org/10.1895/wormbook.1.44.1.

23. Zhen M, Jin Y. The liprin protein SYD-2 regulates the differentiation of presynaptic termini in C. elegans. Nature. 1999;401:371–5. https://doi.org/10.1038/43886.
24. Betz A, Okamoto M, Benseler F, Brose N. Direct interaction of the rat unc-13 homologue Munc13-1 with the N terminus of syntaxin. J Biol Chem. 1997;272:2520–6. https://doi.org/10.1074/jbc.272.4.2520.
25. Lai Y, Choi UB, Leitz J, Rhee HJ, Lee C, Altas B, et al. Molecular mechanisms of synaptic vesicle priming by Munc13 and Munc18. Neuron. 2017;95:591–607 e510. https://doi.org/10.1016/j.neuron.2017.07.004.
26. Richmond JE, Davis WS, Jorgensen EM. UNC-13 is required for synaptic vesicle fusion in *C. elegans*. Nat Neurosci. 1999;2:959–64. https://doi.org/10.1038/14755.
27. Aravamudan B, Fergestad T, Davis WS, Rodesch CK, Broadie K. Drosophila UNC-13 is essential for synaptic transmission. Nat Neurosci. 1999;2:965–71. https://doi.org/10.1038/14764.
28. Augustin I, Rosenmund C, Sudhof TC, Brose N. Munc13-1 is essential for fusion competence of glutamatergic synaptic vesicles. Nature. 1999;400:457–61. https://doi.org/10.1038/22768.
29. Imig C, Min SW, Krinner S, Arancillo M, Rosenmund C, Sudhof TC, et al. The morphological and molecular nature of synaptic vesicle priming at presynaptic active zones. Neuron. 2014;84:416–31. https://doi.org/10.1016/j.neuron.2014.10.009.
30. Lu J, Machius M, Dulubova I, Dai H, Sudhof TC, Tomchick DR, et al. Structural basis for a Munc13-1 homodimer to Munc13-1/RIM heterodimer switch. PLoS Biol. 2006;4:e192. https://doi.org/10.1371/journal.pbio.0040192.
31. Deng L, Kaeser PS, Xu W, Sudhof TC. RIM proteins activate vesicle priming by reversing autoinhibitory homodimerization of Munc13. Neuron. 2011;69:317–31. https://doi.org/10.1016/j.neuron.2011.01.005.
32. Camacho M, Basu J, Trimbuch T, Chang S, Pulido-Lozano C, Chang SS, et al. Heterodimerization of Munc13 C2A domain with RIM regulates synaptic vesicle docking and priming. Nat Commun. 2017;8:15293. https://doi.org/10.1038/ncomms15293.
33. Zhou K, Stawicki TM, Goncharov A, Jin Y. Position of UNC-13 in the active zone regulates synaptic vesicle release probability and release kinetics. elife. 2013;2:e01180. https://doi.org/10.7554/eLife.01180.
34. Hu Z, Tong XJ, Kaplan JM. UNC-13L, UNC-13S, and Tomosyn form a protein code for fast and slow neurotransmitter release in Caenorhabditis elegans. elife. 2013;2:e00967. https://doi.org/10.7554/eLife.00967.
35. Bohme MA, Beis C, Reddy-Alla S, Reynolds E, Mampell MM, Grasskamp AT, et al. Active zone scaffolds differentially accumulate Unc13 isoforms to tune Ca(2+) channel-vesicle coupling. Nat Neurosci. 2016;19:1311–20. https://doi.org/10.1038/nn.4364.
36. Michelassi F, Liu H, Hu Z, Dittman JS. A C1-C2 module in Munc13 inhibits calcium-dependent neurotransmitter release. Neuron. 2017;95:577–590 e575. https://doi.org/10.1016/j.neuron.2017.07.015.
37. Padmanarayana M, Liu H, Michelassi F, Li L, Betensky D, Dominguez MJ, et al. A unique C2 domain at the C terminus of Munc13 promotes synaptic vesicle priming. Proc Natl Acad Sci U S A. 2021;118 https://doi.org/10.1073/pnas.2016276118.
38. Coppola T, Magnin-Luthi S, Perret-Menoud V, Gattesco S, Schiavo G, Regazzi R. Direct interaction of the Rab3 effector RIM with Ca2+ channels, SNAP-25, and synaptotagmin. J Biol Chem. 2001;276:32756–62. https://doi.org/10.1074/jbc.M100929200.
39. Schoch S, Castillo PE, Jo T, Mukherjee K, Geppert M, Wang Y, et al. RIM1alpha forms a protein scaffold for regulating neurotransmitter release at the active zone. Nature. 2002;415:321–6. https://doi.org/10.1038/415321a.
40. Koushika SP, Richmond JE, Hadwiger G, Weimer RM, Jorgensen EM, Nonet ML. A post-docking role for active zone protein Rim. Nat Neurosci. 2001;4:997–1005. https://doi.org/10.1038/nn732.
41. Graf ER, Valakh V, Wright CM, Wu C, Liu Z, Zhang YQ, et al. RIM promotes calcium channel accumulation at active zones of the Drosophila neuromuscular junction. J Neurosci. 2012;32:16586–96. https://doi.org/10.1523/JNEUROSCI.0965-12.2012.

42. Muller M, Liu KS, Sigrist SJ, Davis GW. RIM controls homeostatic plasticity through modulation of the readily-releasable vesicle pool. J Neurosci. 2012;32:16574–85. https://doi.org/10.1523/JNEUROSCI.0981-12.2012.
43. Han Y, Kaeser PS, Sudhof TC, Schneggenburger R. RIM determines Ca(2)+ channel density and vesicle docking at the presynaptic active zone. Neuron. 2011;69:304–16. https://doi.org/10.1016/j.neuron.2010.12.014.
44. Hibino H, Pironkova R, Onwumere O, Vologodskaia M, Hudspeth AJ, Lesage F. RIM binding proteins (RBPs) couple Rab3-interacting molecules (RIMs) to voltage-gated Ca(2+) channels. Neuron. 2002;34:411–23. https://doi.org/10.1016/s0896-6273(02)00667-0.
45. Kaeser PS, Deng L, Wang Y, Dulubova I, Liu X, Rizo J, et al. RIM proteins tether Ca2+ channels to presynaptic active zones via a direct PDZ-domain interaction. Cell. 2011;144:282–95. https://doi.org/10.1016/j.cell.2010.12.029.
46. Davydova D, Marini C, King C, Klueva J, Bischof F, Romorini S, et al. Bassoon specifically controls presynaptic P/Q-type Ca(2+) channels via RIM-binding protein. Neuron. 2014;82:181–94. https://doi.org/10.1016/j.neuron.2014.02.012.
47. Wu X, Cai Q, Shen Z, Chen X, Zeng M, Du S, et al. RIM and RIM-BP form presynaptic active-zone-like condensates via phase separation. Mol Cell. 2019;73:971–984 e975. https://doi.org/10.1016/j.molcel.2018.12.007.
48. Tang AH, Chen H, Li TP, Metzbower SR, MacGillavry HD, Blanpied TA. A trans-synaptic nanocolumn aligns neurotransmitter release to receptors. Nature. 2016;536:210–4. https://doi.org/10.1038/nature19058.
49. Petzoldt AG, Gotz TWB, Driller JH, Lutzkendorf J, Reddy-Alla S, Matkovic-Rachid T, et al. RIM-binding protein couples synaptic vesicle recruitment to release sites. J Cell Biol. 2020;219 https://doi.org/10.1083/jcb.201902059.
50. Acuna C, Liu X, Gonzalez A, Sudhof TC. RIM-BPs mediate tight coupling of action potentials to Ca(2+)-triggered neurotransmitter release. Neuron. 2015;87:1234–47. https://doi.org/10.1016/j.neuron.2015.08.027.
51. Kushibiki Y, Suzuki T, Jin Y, Taru H. RIMB-1/RIM-binding protein and UNC-10/RIM redundantly regulate presynaptic localization of the voltage-gated Calcium Channel in Caenorhabditis elegans. J Neurosci. 2019;39:8617–31. https://doi.org/10.1523/JNEUROSCI.0506-19.2019.
52. Mencacci NE, Brockmann MM, Dai J, Pajusalu S, Atasu B, Campos J, et al. Biallelic variants in TSPOAP1, encoding the active-zone protein RIMBP1, cause autosomal recessive dystonia. J Clin Invest. 2021;131 https://doi.org/10.1172/JCI140625.
53. Nakata T, Kitamura Y, Shimizu K, Tanaka S, Fujimori M, Yokoyama S, et al. Fusion of a novel gene, ELKS, to RET due to translocation t(10;12)(q11;p13) in a papillary thyroid carcinoma. Genes Chromosomes Cancer. 1999;25:97–103. https://doi.org/10.1002/(sici)1098-2264(199906)25:2<97::aid-gcc4>3.0.co;2-l.
54. Monier S, Jollivet F, Janoueix-Lerosey I, Johannes L, Goud B. Characterization of novel Rab6-interacting proteins involved in endosome-to-TGN transport. Traffic. 2002;3:289–97. https://doi.org/10.1034/j.1600-0854.2002.030406.x.
55. Ohtsuka T, Takao-Rikitsu E, Inoue E, Inoue M, Takeuchi M, Matsubara K, et al. Cast: a novel protein of the cytomatrix at the active zone of synapses that forms a ternary complex with RIM1 and munc13-1. J Cell Biol. 2002;158:577–90. https://doi.org/10.1083/jcb.200202083.
56. Ko J, Na M, Kim S, Lee JR, Kim E. Interaction of the ERC family of RIM-binding proteins with the liprin-alpha family of multidomain proteins. J Biol Chem. 2003;278:42377–85. https://doi.org/10.1074/jbc.M307561200.
57. Deken SL, Vincent R, Hadwiger G, Liu Q, Wang ZW, Nonet ML. Redundant localization mechanisms of RIM and ELKS in Caenorhabditis elegans. J Neurosci. 2005;25:5975–83. https://doi.org/10.1523/JNEUROSCI.0804-05.2005.
58. Dai Y, Taru H, Deken SL, Grill B, Ackley B, Nonet ML, et al. SYD-2 Liprin-alpha organizes presynaptic active zone formation through ELKS. Nat Neurosci. 2006;9:1479–87. https://doi.org/10.1038/nn1808.

59. Kaeser PS, Deng L, Chavez AE, Liu X, Castillo PE, Sudhof TC. ELKS2alpha/CAST deletion selectively increases neurotransmitter release at inhibitory synapses. Neuron. 2009;64:227–39. https://doi.org/10.1016/j.neuron.2009.09.019.
60. Wang SSH, Held RG, Wong MY, Liu C, Karakhanyan A, Kaeser PS. Fusion competent synaptic vesicles persist upon active zone disruption and loss of vesicle docking. Neuron. 2016;91:777–91. https://doi.org/10.1016/j.neuron.2016.07.005.
61. Matkovic T, Siebert M, Knoche E, Depner H, Mertel S, Owald D, et al. The Bruchpilot cytomatrix determines the size of the readily releasable pool of synaptic vesicles. J Cell Biol. 2013;202:667–83. https://doi.org/10.1083/jcb.201301072.
62. Fouquet W, Owald D, Wichmann C, Mertel S, Depner H, Dyba M, et al. Maturation of active zone assembly by Drosophila Bruchpilot. J Cell Biol. 2009;186:129–45. https://doi.org/10.1083/jcb.200812150.
63. Kittel RJ, Wichmann C, Rasse TM, Fouquet W, Schmidt M, Schmid A, et al. Bruchpilot promotes active zone assembly, Ca2+ channel clustering, and vesicle release. Science. 2006;312:1051–4. https://doi.org/10.1126/science.1126308.
64. Fenster SD, Chung WJ, Zhai R, Cases-Langhoff C, Voss B, Garner AM, et al. Piccolo, a presynaptic zinc finger protein structurally related to bassoon. Neuron. 2000;25:203–14. https://doi.org/10.1016/s0896-6273(00)80883-1.
65. Wang X, Hu B, Zieba A, Neumann NG, Kasper-Sonnenberg M, Honsbein A, et al. A protein interaction node at the neurotransmitter release site: domains of Aczonin/Piccolo, Bassoon, CAST, and rim converge on the N-terminal domain of Munc13-1. J Neurosci. 2009;29:12584–96. https://doi.org/10.1523/JNEUROSCI.1255-09.2009.
66. Okerlund ND, Schneider K, Leal-Ortiz S, Montenegro-Venegas C, Kim SA, Garner LC, et al. Bassoon controls presynaptic autophagy through Atg5. Neuron. 2018;97:727. https://doi.org/10.1016/j.neuron.2018.01.010.
67. Dick O, Hack I, Altrock WD, Garner CC, Gundelfinger ED, Brandstatter JH. Localization of the presynaptic cytomatrix protein Piccolo at ribbon and conventional synapses in the rat retina: comparison with Bassoon. J Comp Neurol. 2001;439:224–34. https://doi.org/10.1002/cne.1344.
68. Juranek J, Mukherjee K, Rickmann M, Martens H, Calka J, Sudhof TC, et al. Differential expression of active zone proteins in neuromuscular junctions suggests functional diversification. Eur J Neurosci. 2006;24:3043–52. https://doi.org/10.1111/j.1460-9568.2006.05183.x.
69. Siksou L, Rostaing P, Lechaire JP, Boudier T, Ohtsuka T, Fejtova A, et al. Three-dimensional architecture of presynaptic terminal cytomatrix. J Neurosci. 2007;27:6868–77. https://doi.org/10.1523/JNEUROSCI.1773-07.2007.
70. Wong MY, Liu C, Wang SSH, Roquas ACF, Fowler SC, Kaeser PS. Liprin-alpha3 controls vesicle docking and exocytosis at the active zone of hippocampal synapses. Proc Natl Acad Sci U S A. 2018;115:2234–9. https://doi.org/10.1073/pnas.1719012115.
71. Gray EG, Pease HL. On understanding the organisation of the retinal receptor synapses. Brain Res. 1971;35:1–15. https://doi.org/10.1016/0006-8993(71)90591-9.
72. tom Dieck S, Altrock WD, Kessels MM, Qualmann B, Regus H, Brauner D, et al. Molecular dissection of the photoreceptor ribbon synapse: physical interaction of Bassoon and RIBEYE is essential for the assembly of the ribbon complex. J Cell Biol. 2005;168:825–36. https://doi.org/10.1083/jcb.200408157.
73. Dick O, tom Dieck S, Altrock WD, Ammermuller J, Weiler R, Garner CC, et al. The presynaptic active zone protein bassoon is essential for photoreceptor ribbon synapse formation in the retina. Neuron. 2003;37:775–86. https://doi.org/10.1016/s0896-6273(03)00086-2.
74. Khimich D, Nouvian R, Pujol R, Tom Dieck S, Egner A, Gundelfinger ED, et al. Hair cell synaptic ribbons are essential for synchronous auditory signalling. Nature. 2005;434:889–94. https://doi.org/10.1038/nature03418.
75. Altrock WD, tom Dieck S, Sokolov M, Meyer AC, Sigler A, Brakebusch C, et al. Functional inactivation of a fraction of excitatory synapses in mice deficient for the active zone protein bassoon. Neuron. 2003;37:787–800. https://doi.org/10.1016/s0896-6273(03)00088-6.

76. Hallermann S, Fejtova A, Schmidt H, Weyhersmuller A, Silver RA, Gundelfinger ED, et al. Bassoon speeds vesicle reloading at a central excitatory synapse. Neuron. 2010;68:710–23. https://doi.org/10.1016/j.neuron.2010.10.026.
77. Mendoza Schulz A, Jing Z, Sanchez Caro JM, Wetzel F, Dresbach T, Strenzke N, et al. Bassoon-disruption slows vesicle replenishment and induces homeostatic plasticity at a CNS synapse. EMBO J. 2014;33:512–27. https://doi.org/10.1002/embj.201385887.
78. Regus-Leidig H, Ott C, Lohner M, Atorf J, Fuchs M, Sedmak T, et al. Identification and immunocytochemical characterization of Piccolino, a novel Piccolo splice variant selectively expressed at sensory ribbon synapses of the eye and ear. PLoS One. 2013;8:e70373. https://doi.org/10.1371/journal.pone.0070373.
79. Regus-Leidig H, Fuchs M, Lohner M, Leist SR, Leal-Ortiz S, Chiodo VA, et al. In vivo knockdown of Piccolino disrupts presynaptic ribbon morphology in mouse photoreceptor synapses. Front Cell Neurosci. 2014;8:259. https://doi.org/10.3389/fncel.2014.00259.
80. Muller TM, Gierke K, Joachimsthaler A, Sticht H, Izsvak Z, Hamra FK, et al. A multiple Piccolino-RIBEYE interaction supports plate-shaped synaptic ribbons in retinal neurons. J Neurosci. 2019;39:2606–19. https://doi.org/10.1523/JNEUROSCI.2038-18.2019.
81. Parthier D, Kuner T, Korber C. The presynaptic scaffolding protein Piccolo organizes the readily releasable pool at the calyx of Held. J Physiol. 2018;596:1485–99. https://doi.org/10.1113/JP274885.
82. Falck J, Bruns C, Hoffmann-Conaway S, Straub I, Plautz EJ, Orlando M, et al. Loss of Piccolo function in rats induces cerebellar network dysfunction and pontocerebellar hypoplasia type 3-like phenotypes. J Neurosci. 2020;40:2943–59. https://doi.org/10.1523/JNEUROSCI.2316-19.2020.
83. Ahmed MY, Chioza BA, Rajab A, Schmitz-Abe K, Al-Khayat A, Al-Turki S, et al. Loss of PCLO function underlies pontocerebellar hypoplasia type III. Neurology. 2015;84:1745–50. https://doi.org/10.1212/WNL.0000000000001523.
84. Mukherjee K, Yang X, Gerber SH, Kwon HB, Ho A, Castillo PE, et al. Piccolo and bassoon maintain synaptic vesicle clustering without directly participating in vesicle exocytosis. Proc Natl Acad Sci U S A. 2010;107:6504–9. https://doi.org/10.1073/pnas.1002307107.
85. Bruckner JJ, Gratz SJ, Slind JK, Geske RR, Cummings AM, Galindo SE, et al. Fife, a Drosophila Piccolo-RIM homolog, promotes active zone organization and neurotransmitter release. J Neurosci. 2012;32:17048–58. https://doi.org/10.1523/JNEUROSCI.3267-12.2012.
86. Bruckner JJ, Zhan H, Gratz SJ, Rao M, Ukken F, Zilberg G, et al. Fife organizes synaptic vesicles and calcium channels for high-probability neurotransmitter release. J Cell Biol. 2017;216:231–46. https://doi.org/10.1083/jcb.201601098.
87. Xuan Z, Manning L, Nelson J, Richmond JE, Colon-Ramos DA, Shen K, et al. Clarinet (CLA-1), a novel active zone protein required for synaptic vesicle clustering and release. elife. 2017;6 https://doi.org/10.7554/eLife.29276.
88. Serra-Pages C, Medley QG, Tang M, Hart A, Streuli M. Liprins, a family of LAR transmembrane protein-tyrosine phosphatase-interacting proteins. J Biol Chem. 1998;273:15611–20. https://doi.org/10.1074/jbc.273.25.15611.
89. Kaufmann N, DeProto J, Ranjan R, Wan H, Van Vactor D. Drosophila liprin-alpha and the receptor phosphatase Dlar control synapse morphogenesis. Neuron. 2002;34:27–38. https://doi.org/10.1016/s0896-6273(02)00643-8.
90. Wyszynski M, Kim E, Dunah AW, Passafaro M, Valtschanoff JG, Serra-Pages C, et al. Interaction between GRIP and liprin-alpha/SYD2 is required for AMPA receptor targeting. Neuron. 2002;34:39–52. https://doi.org/10.1016/s0896-6273(02)00640-2.
91. Ackley BD, Harrington RJ, Hudson ML, Williams L, Kenyon CJ, Chisholm AD, et al. The two isoforms of the Caenorhabditis elegans leukocyte-common antigen related receptor tyrosine phosphatase PTP-3 function independently in axon guidance and synapse formation. J Neurosci. 2005;25:7517–28. https://doi.org/10.1523/JNEUROSCI.2010-05.2005.

92. Miller KE, DeProto J, Kaufmann N, Patel BN, Duckworth A, Van Vactor D. Direct observation demonstrates that Liprin-alpha is required for trafficking of synaptic vesicles. Curr Biol. 2005;15:684–9. https://doi.org/10.1016/j.cub.2005.02.061.
93. Emperador-Melero J, Wong MY, Wang SSH, de Nola G, Nyitrai H, Kirchhausen T, et al. PKC-phosphorylation of Liprin-alpha3 triggers phase separation and controls presynaptic active zone structure. Nat Commun. 2021;12:3057. https://doi.org/10.1038/s41467-021-23116-w.
94. Kittelmann M, Hegermann J, Goncharov A, Taru H, Ellisman MH, Richmond JE, et al. Liprin-alpha/SYD-2 determines the size of dense projections in presynaptic active zones in C. elegans. J Cell Biol. 2013;203:849–63. https://doi.org/10.1083/jcb.201302022.
95. Taru H, Jin Y. The Liprin homology domain is essential for the homomeric interaction of SYD-2/Liprin-alpha protein in presynaptic assembly. J Neurosci. 2011;31:16261–8. https://doi.org/10.1523/JNEUROSCI.0002-11.2011.
96. Liang M, Jin G, Xie X, Zhang W, Li K, Niu F, et al. Oligomerized liprin-alpha promotes phase separation of ELKS for compartmentalization of presynaptic active zone proteins. Cell Rep. 2021;34:108901. https://doi.org/10.1016/j.celrep.2021.108901.
97. Ahmari SE, Buchanan J, Smith SJ. Assembly of presynaptic active zones from cytoplasmic transport packets. Nat Neurosci. 2000;3:445–51. https://doi.org/10.1038/74814.
98. Zhai RG, Vardinon-Friedman H, Cases-Langhoff C, Becker B, Gundelfinger ED, Ziv NE, et al. Assembling the presynaptic active zone: a characterization of an active one precursor vesicle. Neuron. 2001;29:131–43. https://doi.org/10.1016/s0896-6273(01)00185-4.
99. Garner CC, Zhai RG, Gundelfinger ED, Ziv NE. Molecular mechanisms of CNS synaptogenesis. Trends Neurosci. 2002;25:243–51. https://doi.org/10.1016/s0166-2236(02)02152-5.
100. Maas C, Torres VI, Altrock WD, Leal-Ortiz S, Wagh D, Terry-Lorenzo RT, et al. Formation of Golgi-derived active zone precursor vesicles. J Neurosci. 2012;32:11095–108. https://doi.org/10.1523/JNEUROSCI.0195-12.2012.
101. Vukoja A, Rey U, Petzoldt AG, Ott C, Vollweiter D, Quentin C, et al. Presynaptic biogenesis requires axonal transport of lysosome-related vesicles. Neuron. 2018;99:1216–1232 e1217. https://doi.org/10.1016/j.neuron.2018.08.004.
102. Wagner OI, Esposito A, Kohler B, Chen CW, Shen CP, Wu GH, et al. Synaptic scaffolding protein SYD-2 clusters and activates kinesin-3 UNC-104 in C. elegans. Proc Natl Acad Sci U S A. 2009;106:19605–10. https://doi.org/10.1073/pnas.0902949106.
103. Shin H, Wyszynski M, Huh KH, Valtschanoff JG, Lee JR, Ko J, et al. Association of the kinesin motor KIF1A with the multimodular protein liprin-alpha. J Biol Chem. 2003;278:11393–401. https://doi.org/10.1074/jbc.M211874200.
104. Hallam SJ, Goncharov A, McEwen J, Baran R, Jin Y. SYD-1, a presynaptic protein with PDZ, C2 and rhoGAP-like domains, specifies axon identity in C. elegans. Nat Neurosci. 2002;5:1137–46. https://doi.org/10.1038/nn959.
105. Owald D, Fouquet W, Schmidt M, Wichmann C, Mertel S, Depner H, et al. A Syd-1 homologue regulates pre- and postsynaptic maturation in Drosophila. J Cell Biol. 2010;188:565–79. https://doi.org/10.1083/jcb.200908055.
106. Wentzel C, Sommer JE, Nair R, Stiefvater A, Sibarita JB, Scheiffele P. mSYD1A, a mammalian synapse-defective-1 protein, regulates synaptogenic signaling and vesicle docking. Neuron. 2013;78:1012–23. https://doi.org/10.1016/j.neuron.2013.05.010.
107. Spinner MA, Walla DA, Herman TG. Drosophila Syd-1 Has RhoGAP activity that is required for presynaptic clustering of Bruchpilot/ELKS but not Neurexin-1. Genetics. 2018;208:705–16. https://doi.org/10.1534/genetics.117.300538.
108. Patel MR, Lehrman EK, Poon VY, Crump JG, Zhen M, Bargmann CI, et al. Hierarchical assembly of presynaptic components in defined C. elegans synapses. Nat Neurosci. 2006;9:1488–98. https://doi.org/10.1038/nn1806.
109. Li L, Tian X, Zhu M, Bulgari D, Bohme MA, Goettfert F, et al. Drosophila Syd-1, liprin-alpha, and protein phosphatase 2A B' subunit Wrd function in a linear pathway to prevent ectopic accumulation of synaptic materials in distal axons. J Neurosci. 2014;34:8474–87. https://doi.org/10.1523/JNEUROSCI.0409-14.2014.

110. Owald D, Khorramshahi O, Gupta VK, Banovic D, Depner H, Fouquet W, et al. Cooperation of Syd-1 with Neurexin synchronizes pre- with postsynaptic assembly. Nat Neurosci. 2012;15:1219–26. https://doi.org/10.1038/nn.3183.
111. Chia PH, Patel MR, Shen K. NAB-1 instructs synapse assembly by linking adhesion molecules and F-actin to active zone proteins. Nat Neurosci. 2012;15:234–42. https://doi.org/10.1038/nn.2991.
112. Fulterer A, Andlauer TFM, Ender A, Maglione M, Eyring K, Woitkuhn J, et al. Active Zone Scaffold protein ratios tune functional diversity across brain synapses. Cell Rep. 2018;23:1259–74. https://doi.org/10.1016/j.celrep.2018.03.126.
113. Muhammad K, Reddy-Alla S, Driller JH, Schreiner D, Rey U, Bohme MA, et al. Presynaptic spinophilin tunes neurexin signalling to control active zone architecture and function. Nat Commun. 2015;6:8362. https://doi.org/10.1038/ncomms9362.
114. Patel MR, Shen K. RSY-1 is a local inhibitor of presynaptic assembly in C. elegans. Science. 2009;323:1500–3. https://doi.org/10.1126/science.1169025.
115. Ramesh N, Escher MJF, Mampell MM, Bohme MA, Gotz TWB, Goel P, et al. Antagonistic interactions between two Neuroligins coordinate pre- and postsynaptic assembly. Curr Biol. 2021;31:1711–1725 e1715. https://doi.org/10.1016/j.cub.2021.01.093.
116. Hsueh YP. The role of the MAGUK protein CASK in neural development and synaptic function. Curr Med Chem. 2006;13:1915–27. https://doi.org/10.2174/092986706777585040.
117. Butz S, Okamoto M, Sudhof TC. A tripartite protein complex with the potential to couple synaptic vesicle exocytosis to cell adhesion in brain. Cell. 1998;94:773–82. https://doi.org/10.1016/s0092-8674(00)81736-5.
118. Olsen O, Moore KA, Fukata M, Kazuta T, Trinidad JC, Kauer FW, et al. Neurotransmitter release regulated by a MALS-liprin-alpha presynaptic complex. J Cell Biol. 2005;170:1127–34. https://doi.org/10.1083/jcb.200503011.
119. Samuels BA, Hsueh YP, Shu T, Liang H, Tseng HC, Hong CJ, et al. Cdk5 promotes synaptogenesis by regulating the subcellular distribution of the MAGUK family member CASK. Neuron. 2007;56:823–37. https://doi.org/10.1016/j.neuron.2007.09.035.
120. Atasoy D, Schoch S, Ho A, Nadasy KA, Liu X, Zhang W, et al. Deletion of CASK in mice is lethal and impairs synaptic function. Proc Natl Acad Sci U S A. 2007;104:2525–30. https://doi.org/10.1073/pnas.0611003104.
121. Ho A, Liu X, Sudhof TC. Deletion of Mint proteins decreases amyloid production in transgenic mouse models of Alzheimer's disease. J Neurosci. 2008;28:14392–400. https://doi.org/10.1523/JNEUROSCI.2481-08.2008.

Multiple Modes of Fusion and Retrieval at the Calyx of Held Synapse

Xin-Sheng Wu and Ling-Gang Wu

Abstract Neurotransmitter in vesicles is released through a fusion pore when vesicles fuse with the plasma membrane. Subsequent retrieval of the fused vesicle membrane is the key step in recycling exocytosed vesicles. Application of advanced electrophysiological techniques to a large nerve terminal, the calyx of Held, has led to recordings of endocytosis, individual vesicle fusion and retrieval, and the kinetics of the fusion pore opening process and the fission pore closure process. These studies have revealed three kinetically different forms of endocytosis—rapid, slow, and bulk—and two forms of fusion—full collapse and kiss-and-run. Calcium influx triggers all kinetically distinguishable forms of endocytosis at calyces by activation of calmodulin/calcineurin signaling pathway and protein kinase C, which may dephosphorylate and phosphorylate endocytic proteins. Polymerized actin may provide mechanical forces to bend the membrane, forming membrane pits, the precursor for generating vesicles. These research advancements are reviewed in this chapter.

Keywords Vesicle fusion · Vesicle endocytosis · Exocytosis · Full collapse fusion · Kiss-and-run · Cell-attached recording · Capacitance recording · Calyx of Held · Synaptic transmission · Quantal response

1 Introduction

Neurons release neurotransmitter through synaptic vesicle exocytosis, a specialized form of vesicle trafficking whereby synaptic vesicles fuse with the presynaptic plasma membrane at the active zone and release their contents into the synaptic cleft. Following exocytosis, vesicles are retrieved from the plasma membrane in a process called endocytosis and refilled with neurotransmitter, forming new vesicles

X.-S. Wu (✉) · L.-G. Wu (✉)
National Institute of Neurological Disorders and Stroke, Bethesda, MD, USA
e-mail: wux@ninds.nih.gov; wul@ninds.nih.gov

Z.-W. Wang (ed.), *Molecular Mechanisms of Neurotransmitter Release*,
Advances in Neurobiology 33, https://doi.org/10.1007/978-3-031-34229-5_3

that can be used for further release [1]. Thus, coordination of the exocytosis of neurotransmitter and the endocytosis of vesicular components sustains the membrane trafficking of synaptic vesicles.

The modes of exocytosis and endocytosis depend on the behavior of the fusion pore, a molecular structure that forms to connect vesicle membrane and presynaptic plasma membrane during synaptic vesicle fusion. The initial fusion pore may expand rapidly, allowing the vesicles to fully collapse into the plasma membrane [2]. This mode of exocytosis is called "full collapse" or "full fusion." Alternatively, the initial fusion pore opens for a short time without dilating and then closes again, allowing the vesicle to retain its integrity when it discharges its contents. This process is called "kiss-and-run" fusion [3, 4]. Full fusion leads to a rapid release of all neurotransmitter in a bolus, while kiss-and-run may regulate the rate of neurotransmitter discharge by opening the fusion pore to different degrees [5]. The rate of neurotransmitter release may affect the postsynaptic response, and possibly contribute to synaptic plasticity [6].

The modes of fusion may also determine a vesicle's fate after neurotransmitter release. It is thought that full collapse fusion is followed by compensatory endocytosis, a clathrin-mediated process in which vesicles are reformed from the plasma membrane and severed by the GTPase dynamin [1]. The endocytic rate is much slower than kiss-and-run endocytosis, which simply involves closing of the fusion pore. It is plausible that the differing rates of endocytosis may affect synaptic function, as endocytosis is critical for replenishment of various synaptic vesicle pools, which influences the ability of the nerve terminal to maintain transmitter release during repetitive firing [7]. Regulation of vesicle availability through the rate of endocytosis, and thus the rate of vesicle cycling, could contribute to the generation of some forms of synaptic plasticity [7]. Owing to these potential important roles, the kinetics of endocytosis and its regulation have been intensively studied in the past decade.

Both fusion and retrieval can be monitored in live synapses with imaging and electrophysiological techniques [8]. Compared to imaging techniques, electrophysiological techniques, including whole-cell and cell-attached capacitance recording techniques, provide faster time resolution and allow for the measurement of the fusion pore opening process and the fission pore closure kinetics. In the past two decades, these advanced electrophysiological techniques have been applied to a large nerve terminal, the calyx of Held, to study the rates and modes of endocytosis. These studies have provided recordings of fast endocytosis and individual vesicle fusion and retrieval at a central synapse. Further, the kinetics of the fusion pore opening process and the fission pore closure process has been measured. These results have not been reported at any other synapse, which is at least partly due to the small size of most other synapses that has precluded the application of the electrophysiological techniques. In this chapter, we will discuss what we have learned from electrophysiological studies of fusion and retrieval at the calyx of Held. We believe that the calyx of Held synapse is an excellent model for the study of vesicle fusion and retrieval, and hope that the results obtained at this large synapse can provide useful lessons for further studies of fusion and retrieval at most small conventional synapses.

2 The Calyx of Held Synapse and the Whole-Cell Capacitance Measurement

The calyx of Held is a glutamatergic nerve terminal that forms part of the relay pathway involved in sound localization in the auditory brainstem (Fig. 1a) [9]. The calyx of Held arises from globular bushy cells in the anterior ventral cochlear nucleus (aVCN), which project onto principal neurons of the contralateral medial nucleus of the trapezoid body (MNTB; Fig. 1b) [9]. EM reconstruction of the calyx of Held has shown the presence of ~300–700 individual active zones, each with about two morphologically docked vesicles [10, 11]. The large number of active zones helps ensure rapid signaling, as a presynaptic action potential (AP) releases hundreds of vesicles, generating a large excitatory postsynaptic current (EPSC) that rapidly depolarizes the postsynaptic neuron to the threshold for generating action potentials [9].

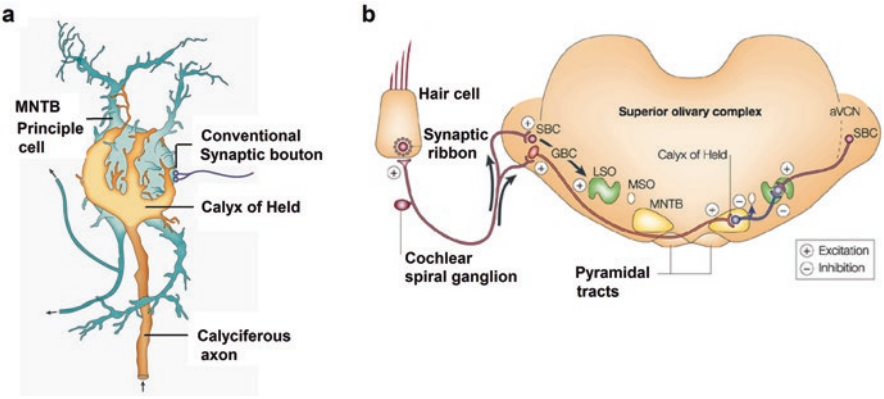

Fig. 1 Anatomy of the calyx of Held synapse. (**a**) A diagram of the adult calyx of Held, a glutamatergic synapse in the mammalian auditory brainstem. Notice the large-caliber axon (4–12 μm in diameter; brown) that gives rise to the calyx. The postsynaptic cell (blue) has relatively short dendrites and an axon with a collateral branch. MNTB, medial nucleus of the trapezoid body. (**b**) A diagram of the circuitry of the superior olivary complex (SOC), which is involved in computing sound localization from the auditory inputs from both ears. Auditory information from the cochlea is transmitted to the ipsilateral anterior ventral cochlear nucleus (aVCN) through excitatory synapses onto spherical bushy cells (SBCs) and globular bushy cells (GBCs). The GBCs synapse onto the contralateral medial nucleus of the trapezoid body (MNTB), which makes an inhibitory synapse onto the lateral superior olive (LSO). The LSO also receives excitatory input from the ipsilateral SBCs. It is at the level of the LSO that discharges evoked by interaural intensity differences are first represented as differences in the timing of excitatory and inhibitory inputs. So, the LSO is thought to function as a coincidence detector of binaural signals, whereas the main role of the MNTB is simply to act as a fast, sign-inverting relay station. The principal cells of the MNTB, however, also receive strong inhibitory input from unknown sources, and are organized in a tonotopic map of characteristic sound frequencies. The MNTB is therefore not a functionally homogeneous nucleus, and its output might be modulated by other brainstem nuclei. MSO, medial superior olive. (Figure adapted, with permission, from Ref. [9])

Except for the large size of the terminal and the large quantal synaptic output, the synapse acts in a similar way to a conventional fast synapse in the CNS. For example, the terminal releases glutamate in response to presynaptic action potential stimulation. The terminal contains many spherical, clear-core vesicles with a diameter of about 50 nm [10, 12]. The delay between the peak of a presynaptic action potential and the onset of the excitatory postsynaptic current (EPSC) is less than 1 ms [13]. Multiple types of voltage-dependent Ca^{2+} channels control transmitter release at single release sites in the MNTB synapse [14, 15], as in many other CNS synapses [16]. The synapse exhibits short-term synaptic depression and facilitation [9, 17]. Since the MNTB synapse functionally resembles other fast central synapses in many aspects, the experimental results obtained from this synapse may not only be applied to calyceal synapses, but also have a more general significance.

Presynaptic patch-clamp measurements of exocytosis and endocytosis rely on the increase in surface membrane area when vesicles fuse with the plasma membrane during exocytosis, and the decrease when membrane is retrieved by endocytosis. The changes in surface area can be monitored electrically as changes in membrane capacitance (Cm) [18]. Whole-cell capacitance measurement is best achieved in round cells that are electrically equivalent to a membrane capacitor in parallel with a membrane resistor (Fig. 2a) [18]. A series of studies demonstrated that this technique can also be applied to the calyx of Held [19–21]. Although the calyx is connected with an axon, simulation suggests that the axon does not significantly affect the measurement of the capacitance at the calyx when Lindau-Neher's technique, a test signal of a sinusoidal voltage used in estimating the membrane capacitance and membrane conductance by a two-phase lock-in amplifier, is used [20]; thus, changes in membrane size at the calyx can be accurately measured. Experimental results have confirmed this simulation result. First, when both the EPSC and the presynaptic capacitance were simultaneously recorded at the same synapse, the EPSC amplitude or the charge increased as the capacitance jump (ΔCm) increased (Fig. 2b). Their relationship could be fit by a linear regression line with a slope of about 148 pA/fF (Fig. 2b) [19]. Second, by averaging about 2.7 million spontaneous miniature EPSCs (mEPSCs) and the corresponding presynaptic capacitance traces from 459 individual synapses (Fig. 2c), we found that the presynaptic membrane capacitance jumped by about 65 aF within 1 ms before the onset of the mean mEPSC [22, 23]. As the specific membrane capacitance is 9 fF μm^{-2} [24], 65 aF corresponds to a vesicle with a diameter of 48 nm, which is similar to the estimate from electron microscopy [10]. We concluded that the capacitance jump accurately reflects vesicle fusion. Whole-cell recordings of fusion have advantages and drawbacks, compared to the more common measurement of postsynaptic currents induced by transmitter binding. The drawbacks are that the signal-to-noise ratio is not as good as postsynaptic current recordings, and recording release during a stimulus is not possible. However, one significant advantage is that capacitance measurements provide a better estimate of total release, since they are independent of the functional state of the postsynaptic receptors, while postsynaptic currents are complicated by the effects of receptor saturation, desensitization, and inactivation that skew the relationship between release and postsynaptic response. In addition to its utility in the study of vesicle fusion, time-resolved

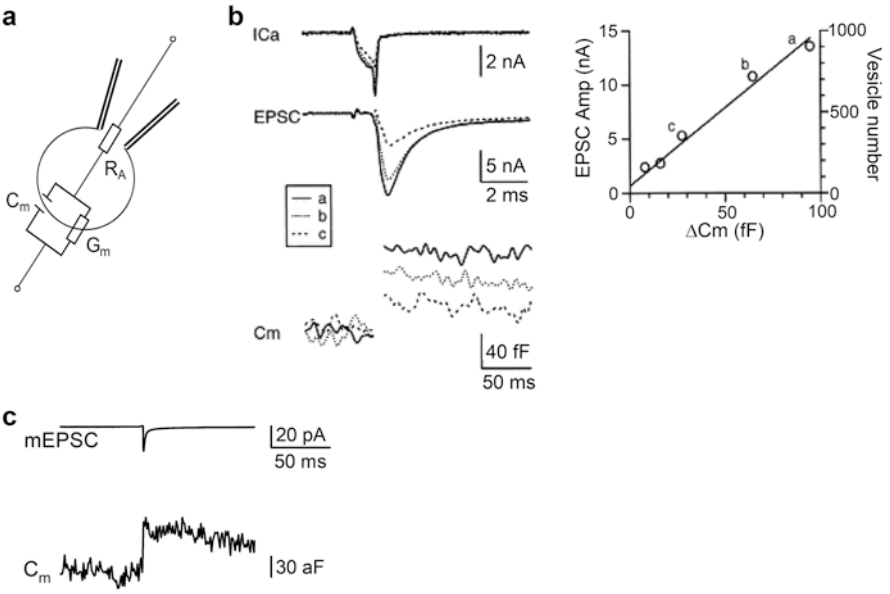

Fig. 2 Capacitance jumps reflect exocytosis at the calyx of Held. (**a**) An equivalent circuit of a cell in the whole-cell recording configuration. Cm is the membrane capacitance, R_a is the access resistance, and R_m is the membrane resistance. (**b**) The linear relation between the capacitance jump and the excitatory postsynaptic current (EPSC). Left: Sample recordings induced by 1 ms steps to +10 mV ((**a**), solid), 0 mV ((**b**), dotted), and −6 mV ((**c**), dashed), respectively. Presynaptic Ca^{2+} currents and EPSCs are plotted at the same time scale (applied to all other figures if not mentioned), whereas capacitance changes are plotted at a different time scale. Right: The relation between the EPSC amplitude (EPSC Amp, left *y* axis) and ΔCm evoked by a series of 1 ms step depolarizations from −80 mV to a voltage ranging from −10 to +20 mV at a synapse. (Panels (**a**) and (**b**) are adapted, with permission, from Ref. [19]). (**c**) The mean EPSC and Cm averaged from 2.66 million fusion events obtained from 459 paired recordings. Traces are shown without filtering. (Adapted from Ref. [23])

capacitance measurement at the calyx provides a powerful technique to study synaptic vesicle endocytosis at a central synapse.

3 A Linear Relation Between the Time Constant of Endocytosis and the Amount of Exocytosis

Synaptic vesicle endocytosis can be detected as the decay of the capacitance jump to baseline levels after a stimulus. At the calyx of Held this decay is exponential, and is described by the time constant (τ) in an exponential equation. The τ is the time at which ~63% of the jump has decayed. Studies at the calyx of Held showed that the time course of endocytosis, as measured by whole-cell capacitance recordings, depended on the stimulation intensity. After a single action potential-equivalent

(AP-e) stimulus, the capacitance change was measured by two labs, using slightly different stimuli. One lab used a 1-ms step depolarization from −80 to +7 mV (Fig. 3a), which induces the release of the same number of vesicles as an action potential [22]. After this stimulus, the capacitance jump was about 20 fF, and decayed with a τ of about 2.2 s [21]. Earlier measurements indicated that the decay was much faster (τ = ~115 ms [22]), but it was later shown that they were contaminated by the presence of an artifactual capacitance jump with a decay time in the hundreds of milliseconds, which persists after abolishing exocytosis with botulinum neurotoxin E [25] or C [21]. Another lab approximated an AP-e with a 4-ms step depolarization from −80 to +80 mV, followed by a 1-ms step to +40 mV [25]. This was found to evoke approximately three times the amount of release as an action potential [21], and induced a capacitance jump of about 60 fF. After this stimulus, the decay was fit with a τ of about 10.4 s when the first 500 ms after stimulation was ignored [25]. The difference in the τ reported by these two labs is at least partly due to the difference in the stimulation intensity and thus the capacitance jump, because when the first lab changed the stimulus protocol and increased the capacitance jump from about 20 fF to about 70 fF, the τ increased from about 2.2 to 4.2 s [21].

The τ after short AP-e trains increased in linear proportion to the net capacitance jump at the end of the stimulus (Fig. 3a–c) [21, 22]. This relationship cannot be attributed to an increase in stimulus frequency alone, as similar capacitance jumps elicited by AP-e trains at frequencies from 20 to 333 Hz had similar decay times [21, 22]. As further evidence, the trend was also seen when continuous step depolarizations from −80 to 0–10 mV with durations from 2 to 20 ms were used to evoke exocytosis [21, 22, 25]. The lengthening of the time constant also cannot be explained by the increase in global calcium influx due to increased stimulation, because EGTA, a slow-binding calcium chelator that eliminates the residual calcium transient, did not reduce the τ [22]. Moreover, clamping presynaptic calcium levels at ~1 μM, which exceeds the peak global calcium concentration after 10 AP-e at 333 Hz, did not lengthen the τ [22]. The duration of elevated local calcium domains can also be ruled out, as the τ was similar after 10-ms and 30-ms step depolarizations from −80 to +10 mV, which elicited similar capacitance jumps and similar time courses of endocytosis [22]. Thus, it appears that the net accumulation of fused vesicle membrane at the end of a stimulus is itself the cause of the increase in the τ.

This linear relationship is also seen at other synapses. FM dye studies at the frog neuromuscular junction show that the endocytic τ increases as the duration of a 30-Hz stimulus train of APs increases [26]. Similarly, at cultured hippocampal neuron boutons, studies using the genetically encoded exo-/endocytic marker synaptopHluorin demonstrated that the τ increased linearly with the number of APs in a 10-Hz train, from <10 s after 20 APs to ~90 s after 600 APs [27]. There is the question what happens at very mild stimulation, as another study with a similar marker, called sypHy, found that this linearity did not hold for trains of up to 40 APs at 20 Hz frequency [28]. However, the authors did see a lengthening of the τ with stronger stimulation.

A hypothesis to explain this correlation between τ and net exocytosis has been described [27]. In this model, the endocytic apparatus has a fixed rate and limited

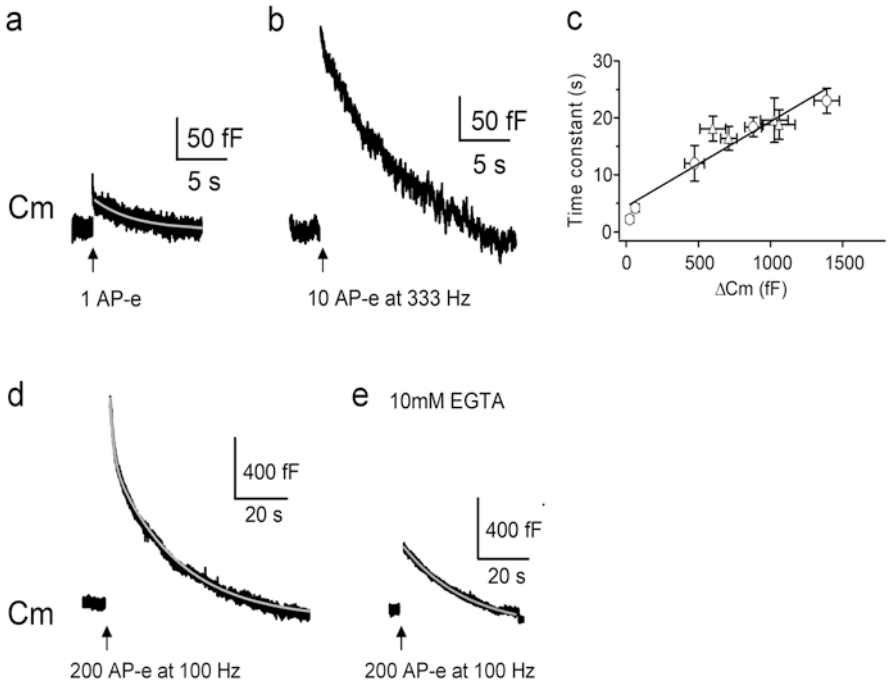

Fig. 3 Slow and rapid endocytoses at the calyx of Held. (**a**) Sampled whole-cell capacitance (Cm) response to an AP-e (1 ms step to +7 mV). The capacitance decay, starting from 200 ms after stimulation, was fit with an exponential function with a time constant of 2.9 s. (Adapted from Ref. [21]). (**b**) Sampled Cm response to 10 AP-e at 333 Hz. Note that the retrieval time is significantly longer than after 1 AP-e. (Adapted from Ref. [22]). (**c**) The relation between the time constant and the amplitude of endocytosis. A plot of endocytosis time constant versus its amplitude after various stimuli. The endocytosis component and stimuli included the slower component of endocytosis after 10 depolarizing pulses at 1 and 10 Hz (circles), endocytosis after a 20 ms depolarization (circle) and a 1 ms depolarization to +7 mV or 15–30 mV (circle), endocytosis after 50 AP-e at 100 Hz (triangle), and endocytosis after 200 AP-e at 100 Hz (triangle), 50 AP-e at 100 Hz repeated 5 times at 1 Hz (triangle), or 50 AP-e at 30 Hz repeated 5 times at 0.4 Hz (triangle). The data were fit with a linear regression line with a slope of 1.4 s/100 fF. (**d**) Sampled Cm response to 200 AP-e at 100 Hz (bars). The capacitance decay was fit with a bi-exponential function (gray, $\tau_1 = 1.8$ s [377 fF], $\tau_2 = 24.0$ s [1020 fF]). (**e**) Sampled Cm response to 200 AP-e at 100 Hz with 10 mM EGTA in the pipette. The capacitance decay was fit with a mono-exponential function (gray, $\tau = 24.7$ s). (Panels (**c**–**e**) are adapted from Ref. [21])

capacity; when the amount of fusion exceeds the capacity for retrieval, the plasma membrane is retrieved at a constant rate. Thus, addition of more fused vesicles will lengthen the τ in a linear fashion. This model predicts the observed linear relationship between the τ and the net exocytosis after mild-to-moderate stimulation at the calyx. However, it also predicts a linear decay, while at the calyx (and in cultured hippocampal neurons), membrane retrieval is best fit with an exponential function. Thus, this model may be similar, but not identical, to the physiological mechanism in the calyx of Held at mild-to-moderate stimulation.

4 Intense Stimulation Activates Rapid Endocytosis by Increasing the Calcium Influx

Under stronger stimulus conditions at the calyx, the linear relationship between the τ and net exocytosis no longer applies [21]. When a 20-ms pulse stimulus is repeated ten times at 10 Hz, a fast component with a τ of 1–2 s is evident immediately after the end of stimulation. After several seconds it gives way to slow endocytosis, and the total capacitance decline is well fit by a double exponential. The fast component can also be evoked by a train of 200 AP-e at 100 Hz (Fig. 3d), suggesting that it is physiologically important.

Slowing the frequency of the 20-ms pulses to 1 Hz allows capacitance measurements to be made between pulses, enabling an examination of how the fast component develops. Under this condition, the initial rate of endocytosis increased from about 28 fF/s after the first pulse to a plateau of about 208 fF/s after the sixth pulse, which corresponds to about six vesicles per second per active zone [21]. It is estimated that this high retrieval rate is mostly (two-thirds) due to rapid endocytosis, indicating that the fast component of endocytosis becomes dominant during stimulation.

The trigger for fast endocytosis is calcium. Moreover, 10 mM EGTA added to the presynaptic pipette blocked the fast component induction during a train of ten 20-ms pulses at 1 Hz (Fig. 3e). Likewise, lowering the range of depolarization voltage from 90 mV (−80 to +10 mV) to 75 mV (−80 to −5 mV) reduced the evoked calcium current and eliminated the fast component. Membrane accumulation is not the trigger for fast endocytosis, because 20 pulses at the reduced 75-mV jump at 1 Hz failed to elicit a fast component, though this stimulus caused a net accumulation (~1.5 pF) similar to the control condition (using the 90-mV pulse from −80 to +10 mV) in which fast endocytosis was observed [21].

The role of calcium in endocytosis has been investigated at several other synapses. At the frog neuromuscular junction, only a slow form of endocytosis is detected, and its rate is not sensitive to raised intracellular calcium levels [26]. In cultured hippocampal neurons, experiments using synaptopHluorin or sypHy showed that the rate of the single component is reduced when extracellular calcium is reduced, but raising the calcium level above physiological concentrations does not accelerate the endocytic process [29]. At goldfish bipolar cells, endocytosis is fast following a brief depolarization [30, 31], and can be slowed by adding EGTA or BAPTA, another calcium chelator, to the patch pipette. However, during intensive stimulation, fast endocytosis appears to be slowed down or even blocked [31, 32], which may be due to a buildup in intracellular calcium [31]. The reasons for this apparent discrepancy have not been discovered, but it has been proposed that intensive stimulation causes non-synchronous release to occur at sites far away from central active zones, and that these vesicles can only be retrieved through a slower pathway [32]. A flash photolysis study in mouse cochlear inner hair cells has shown that a fast form of endocytosis is activated at internal calcium concentrations above 15 μM, and that proportion of the fast component increases with increasing calcium

levels at calcium concentrations above this level, though the τ stays the same [33]. Thus, it appears that calcium regulation of endocytosis depends on the type of neurons.

5 Bulk Endocytosis and the Measurement of the Fission Pore Formation and Closure

An early pioneering study of endocytosis using electron microscopy noted the appearance of large endosome-like structures in the nerve terminal after strong stimulation, from which small vesicles bud off [2]. Further studies led to the widely held hypothesis that these endosome-like structures are generated slowly (~1 min) from the plasma membrane, a process called bulk endocytosis [34–39]. However, the kinetic evidence indicating the instant of bulk membrane fission is missing at synapses. In the following, we discuss a study at the calyx of Held that provides this missing piece of evidence [40].

Bulk membrane uptake could be detected after stimulation by step depolarizations and AP-e trains, and were characterized by downward capacitance shifts (DCSs) with a 10–90% decay time between 30 and 500 ms (Fig. 4a–c). The sizes of the DCSs ranged from the detection limit of ~20 fF up to 500 fF, with an average size of about 131 fF. These values were much larger than the membrane capacitance (~65 aF) of a single vesicle. Their size distribution was peaked at the detection limit of ~20 fF, suggesting that there were possibly many more events that were too small to be detected [40].

The occurrence of DCSs increased with stimulation. DCSs were detected at a frequency of ~0.003 Hz before stimulation, and the frequency increased to about 0.021 Hz in the first 10 s after ten pulses of 20-ms depolarization (from −80 to +10 mV) at 10 Hz (Fig. 4b). The frequency decayed to baseline levels within 80 s and had a half decay time of <20 s. Vesicle fusion was required for this increase, as the increase was not seen after stimulation when exocytosis was blocked by botulinum neurotoxin C. The proportion of retrieval conducted by bulk endocytosis was about 9% of the net exocytosis. This is likely an underestimate, since, as noted above, events below 20 fF in size could not be detected [40].

The diameter of the fission pore and the rate of closure were determined using the measured pore conductance, and with the assumption that the pore is cylindrical. The initial diameter ranged from 3 to 19 nm and decreased to undetectable levels within 500 ms (Fig. 4c). The slope of the 20–80% decrease in diameter was about 31 nm/s (Fig. 4c). This was not correlated with the DCS size, suggesting that the fission step is separate from the fission pore formation step. Consistent with this suggestion, bulk membrane fission can occur as early as a few seconds after stimulation, and the rate of fission pore closure is much smaller than the rate needed to form the fission pore in only a few seconds. Thus, bulk endocytosis is comprised of two kinetically different steps: a membrane invagination step that forms the fission pore, and the closure of the pore that completes the fission process [40].

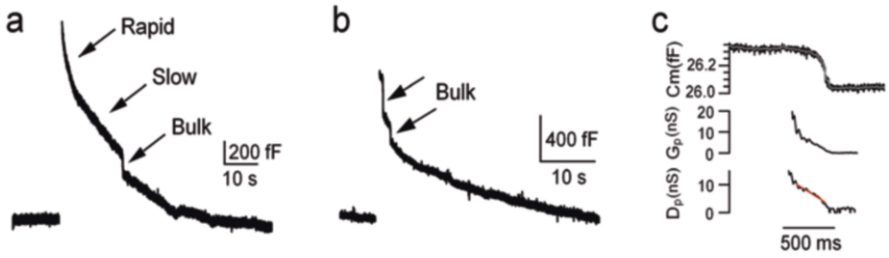

Fig. 4 Bulk endocytosis at the calyx of Held. (**a**) Three kinetic forms of endocytosis (arrows)—rapid, slow, and bulk—were observed by whole-cell capacitance (Cm) recordings at the calyx of Held. The stimulus was 10 depolarizing pulses of 20 ms from −80 to +10 mV at 10 Hz. (**b**) The whole-cell membrane capacitance (Cm) response to 10 depolarizing pulses at 10 Hz. The arrows indicate bulk endocytosis that occurred within a few seconds after the stimulus. (**c**) The whole-cell membrane capacitance (Cm), the fission pore conductance (G_p), and the fission pore diameter (D_p) during bulk endocytosis. The 20–80% decrease in D_p was fit with a linear regression line (red) with a slope (red) of −31 nm/s. Cm trace was low-pass filtered at 30 Hz (gray), from which G_p and D_p were calculated. (Panels (**a**–**c**) are adapted from Ref. [40])

It should be noted that the frequency of DCSs peaked in less than 10 s after stimulation. Some bulk endocytosis events occurred at only a few seconds after the stimulus (Fig. 4b). Such a rapid time course is in sharp contrast to the currently prevailing view that endosome-like structures are generated on a time scale of minutes [2, 37, 41, 42]. This discrepancy is likely due to methodological differences. The majority of previous studies have assessed the time course of bulk endocytosis by electron microscopy. Electron microscopy has a low time resolution, whereas the capacitance measurement technique used in the present work provides a time resolution of milliseconds. Electron microscopy measures the lifetime of endosome-like structures, whereas the capacitance measurement indicates the time course of generating endosome-like structures from the plasma membrane. We suggest modifying the current view to a rapid generation of endosome-like structures, followed by slow bud off of small vesicles from endosome-like structures.

6 Resolving Full Collapse Fusion and Kiss-and-Run with Cell-Attached Recordings

We have discovered at least three kinetic forms of endocytosis at the whole-cell configuration at the calyx of Held. These forms are rapid, slow, and bulk endocytoses (Fig. 4a). It has been suggested that rapid endocytosis represents a kiss-and-run form of fusion, whereas slow endocytosis is consistent with full collapse fusion [43]. However, other interpretations are possible. For example, imaging studies at goldfish retinal bipolar synapses raise the possibility that rapid endocytosis could be a result of full collapse fusion followed by rapid endocytosis [44]. The key difference between these two modes of fusion is that kiss-and-run opens a fusion pore and

closes the pore rapidly, whereas full collapse fusion fully expands the fusion pore. The only unambiguous way to distinguish these is to record fusion pore kinetics at synapses, which is technically challenging and rarely performed; correspondingly, whether kiss-and-run exists at synapses is currently under intense debate [17]. In the following, we describe a study that has resolved the fusion pore conductance at the calyx by using the cell-attached capacitance measurement technique [45].

The cell-attached capacitance measurement technique provides a high-enough resolution to detect single vesicle fusion events, which appear as unitary capacitance steps directly proportional to the vesicle size (Fig. 5a). Full vesicle incorporation into the plasma membrane produces an upward capacitance step, whereas kiss-and-run fusion produces an up-step followed within a few seconds by a down-step, called a capacitance flicker [5]. In some of these fusion events, fusion pore conductance can be measured, allowing for an estimate of the fusion pore size [5].

Measurements of capacitance steps during large dense core vesicle fusion in endocrine and immune cells have provided a detailed picture of exocytosis of this vesicle class in non-neuronal cells [5]. Extending this approach to synapses has been frustrated by two problems: First, the smaller size of vesicles makes resolving individual vesicle fusion more difficult. Second, the postsynaptic neuron apposing the presynaptic release site might make the release site inaccessible to the patch pipette. These two hurdles have been overcome in some studies. For example, in pituitary nerve terminals (which do not form synapses), fusion of individual micro-vesicles similar in size to synaptic vesicles was resolved, demonstrating that these small events can in fact be detected [46, 47]. About 5% of fusion events were capacitance flickers with a fusion pore conductance of ~19 pS, indicating the existence of kiss-and-run fusion [46]. Direct patch-clamp recordings of nerve terminals that are not associated with their postsynaptic counterpart have been made at a chick calyx-type synapse [48], synaptosomes [49], and the rat calyx of Held [45].

At the calyx of Held synapse, the release site can be exposed by pulling out the postsynaptic neuron using a large pipette (Fig. 5b). At the exposed release sites, cell-attached recordings reveal individual capacitance up-steps reflecting single vesicle fusion during high potassium application (Fig. 5c) [45]. About 20% of fusion events were capacitance flickers. The capacitance flicker duration ranged from 10 ms to 2 s with a mean of ~300 ms (Fig. 5d). For most capacitance flickers, the fusion pore conductance was larger than 288 pS. The exact size could not be detected owing to the resolution limit. In a small fraction of capacitance flickers, however, a fusion pore conductance ranging from 15 to 288 pS with a mean of ~66 pS was observed, which might correspond to a fusion pore with a mean diameter of ~1.1 nm (Fig. 5d). These results suggest that a minor fraction of fusion events is kiss-and-run during high potassium application [45].

Most capacitance up-steps are not followed in a brief time by an equal size down-step, and thus reflect full collapse fusion [45]. Their initial fusion pores were often too large to resolve (Fig. 5d). However, in a small fraction of up-steps, an initial fusion pore conductance of ~250 pS was resolved, which was followed in ~10–300 ms by a rapid pore expansion (Fig. 5e) [45]. These results provide the first kinetic evidence revealing the instant of full collapse fusion at synapses.

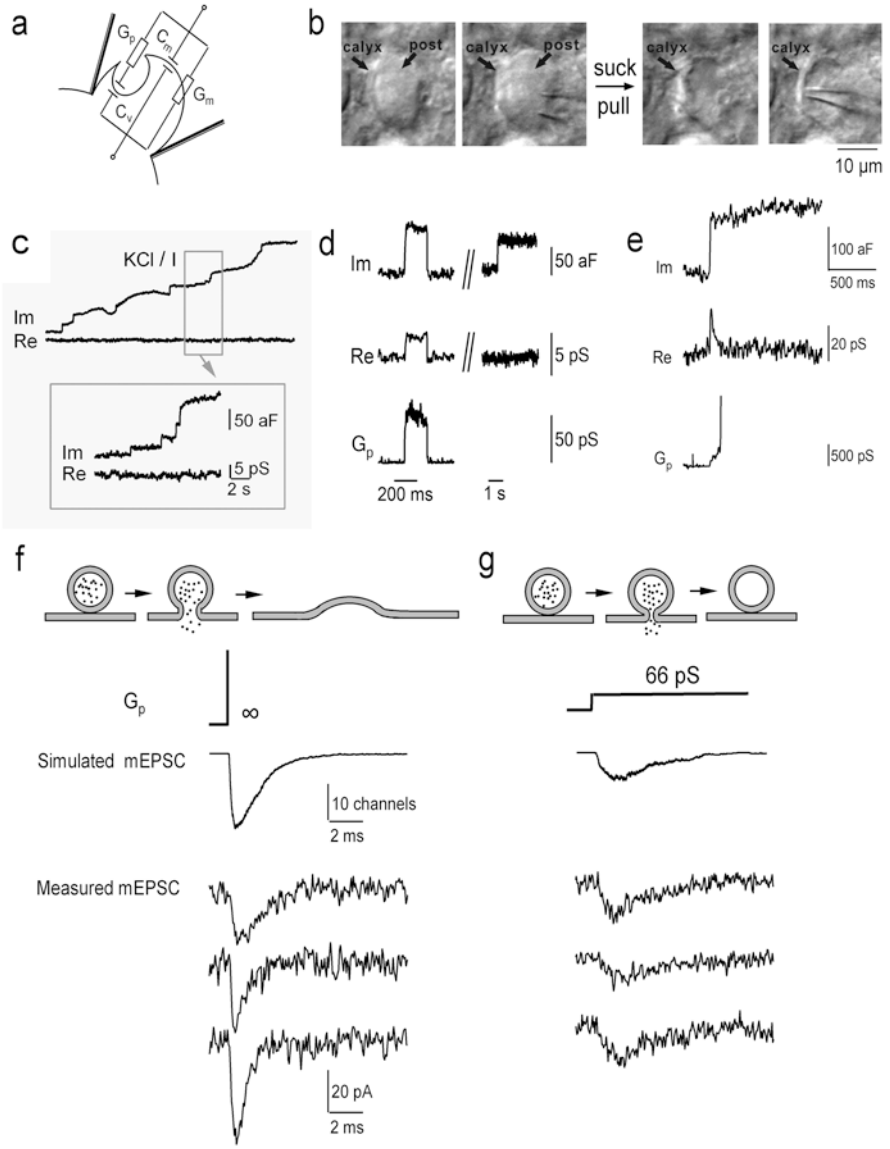

Fig. 5 Kiss-and-run and full collapse fusions recorded in the cell-attached mode at the calyx of Held. (**a**) Equivalent circuit of a patch in the cell-attached mode when a vesicle is fused with the plasma membrane and has opened a fusion pore. Double line indicates patch pipette. Cm *Gm*, *Cv*, and *Gp* are cell membrane capacitance, cell membrane conductance, vesicle capacitance, and fusion pore conductance, respectively. (**b**) The procedure to perform cell-attached recordings at the release face of a calyx. A calyx associated with a postsynaptic neuron was first identified (left). The postsynaptic neuron was sucked and pulled away by a pipette shown in the middle left (middle two panels). Another pipette was positioned at the release face of the calyx membrane (right) for cell-attached recordings, from which individual vesicle fusions such as those shown in (**c**) and (**d**) were

7 The Impact of Kiss-and-Run Fusion on the Quantal Response

Synapses that are able to use kiss-and-run fusion may have two advantages compared to those that use only full collapse. First, it allows rapid and economical vesicle recycling, perhaps preventing some of the rundown in release during strong stimulation. Second, its narrow fusion pore could limit the rate of transmitter discharge out of the vesicle, resulting in a slower and smaller quantal response (Fig. 5g) compared to full collapse fusion (Fig. 5f). Control over the amplitude and the kinetics of the quantal response by regulation of the two fusion modes may contribute to synaptic plasticity [6]. However, whether the fusion pore size is small enough to slow down transmitter diffusion was largely unclear. We have attempted to address this issue at the calyx-type synapse.

During capacitance flickers at the calyx-type synapse, the fusion pore conductance of most events was more than 288 pS, whereas the conductance in a minor fraction of events was on average ~66 pS. Knowing the fusion pore conductance (G_p), the fusion pore diameter (D_p) could be estimated by the equation [50, 51]: $D_p = [4G_p\rho\lambda/\pi]^{0.5}$, where ρ is the saline resistivity (100Vcm); λ, the pore length, is taken as the length of a gap junction channel (15 nm). According to this equation, kiss-and-run fusion with a G_p of 66 pS corresponds to a D_p of 1.1 nm, and kiss-and-run fusion with a G_p more than 288 pS corresponds to a D_p of more than 2.3 nm. The values of the fusion pore diameter can be used to estimate the time constant (τ_{glu_v}) of transmitter diffusion from the vesicle to the synaptic cleft by the equation $\tau_{glu\_v} = (\pi D_v^3/6)/(\rho K_d G_p)$, where D_v is the vesicle diameter and K_d, the diffusion constant, is 3.3×10^{-6} cm^2 s^{-1} for glutamate in the synaptic cleft. Based on this equation, τ_{glu_v} is 2.3 ms for a G_p of 66 pS, and 0.54 ms for a G_p of 288 pS. These calculations suggest that kiss-and-run with a small fusion pore can slow down the diffusion of transmitter out of the vesicle. This suggestion was further confirmed by Monte Carlo simulations of quantal events with MCell 2.50, a program that models the three-dimensional random walk diffusion and reaction kinetics in complex spatial environments reflecting realistic cellular ultrastructure [52]. The simulation

Fig. 5 (continued) obtained. (**c**) Im (imaginary component of the admittance, reflecting capacitance) and Re (real component of the admittance, reflecting conductance) traces from cell-attached recordings during application of 25 mM KCl. The inset shows discrete capacitance up-steps. (**d**) Im, Re, and G_p during a capacitance flicker. A non-flicker up-step (right) occurring 10 s later was not accompanied by detectable Re changes, indicating proper phase adjustment. (**e**) Im, Re, and G_p during a full collapse fusion. Note that G_p was detected in this fusion event. (**f**) Top: cartoon illustrating a full collapse event. Middle: the simulated mEPSC caused by a $G_p > 288$ pS, as observed in 97% of fusion events. This trace was the average of the simulated mEPSC resulting from initial G_p values of ∞ and 288 pS. The scale bars also apply to (**f**). Bottom: Three experimentally observed individual mEPSCs (thin) at the calyx of Held with a rapid rise time. The scale bars also apply to panel g. (**g**) Top: cartoon illustrating a kiss-and-run event. Middle: the simulated mEPSC caused by a G_p of 66 pS, as observed in 3% of fusion events. Bottom: three experimentally observed individual mEPSCs displaying a 10–90% rise time slower than 0.8 ms and an amplitude smaller than 25 pA. These represent about 1.1% of all observed events in Ref. [45], from which this figure is adapted

shows that kiss-and-run fusion with a D_p of 1.1 nm would cause an mEPSC with a much slower rise and decay, and a smaller amplitude as compared to full collapse fusion with a D_p that is too large and/or too fast to resolve (Fig. 5f, g). Since kiss-and-run with a D_p of about 1.1 nm was detected in only ~3% of the total fusion events, small mEPSCs with a slow rise and decay must represent a very minor fraction of mEPSCs. Consistent with this prediction, less than ~1% of the measured mEPSCs were small and slow in both rise and decay (Fig. 5f, g). These results suggest that kiss-and-run with a small fusion pore may induce small and slow mEPSCs.

It should be pointed out that a small and slow mEPSC is not necessarily the result of kiss-and-run fusion with a small fusion pore. Many other mechanisms may also determine the amplitudes and/or the kinetics of mEPSCs. These mechanisms include variation in the vesicle size [53–55], the vesicular transmitter content [56–59], the distance between release sites and glutamate receptor clusters [60], differences in receptor subunit compositions [61], and release from boutons other than the calyx that form synapses at the principal cell in the medial nucleus of the trapezoid body [62].

8 Regulation of Endocytosis

Endocytosis recycles vesicles and thus sustains synaptic transmission during repetitive activity [63]. Mechanisms that regulate endocytosis may thus regulate synaptic transmission. Here, we describe some mechanisms that may regulate endocytosis at calyces.

A study at calyces suggests that Ca^{2+} influx through voltage-dependent Ca^{2+} channels at the plasma membrane triggers slow endocytosis (>10 s), rapid endocytosis (1~2 s), bulk endocytosis (retrieving endosome-like structures larger than regular vesicles), and endocytosis overshoot (more endocytosis than exocytosis) [64]. For example, lowering extracellular Ca^{2+} or buffering Ca^{2+} with BAPTA reduces the rate of rapid and slow endocytoses by 50–1500 folds (Fig. 6a, b), whereas increasing calcium current charges increases the endocytosis rate by hundreds of folds. The comparable results are also confirmed by other labs [65, 66].

What is the Ca^{2+} sensor for the calcium-triggered endocytosis? Studies suggest that two calcium-binding proteins, namely, calmodulin (CaM) and protein kinase C are involved in mediating this process. Knockout of CaM 2 blocks slow and rapid endocytoses at calyces [67]. The inhibition induced by CaM 2 knockout can be rescued at hippocampal synapses by wild-type CaM 2, but not by a calcium-binding-deficient CaM 2. The results suggest that CaM 2 serves as a Ca^{2+} sensor for calcium-stimulated endocytosis at synapses (Fig. 6c). Supporting this suggestion, calcineurin (CaN), a phosphatase activated by Ca^{2+}/CaM, may dephosphorylate endocytic proteins and is involved in endocytosis. CaN catalytic subunits A_α and A_β are expressed in the brain. Knockout of CaN A_α inhibits rapid and slow endocytoses at calyces (Fig. 6d) [68]. Thus, calcium may activate CaM/CaN to dephosphorylate endocytic proteins, such as dynamin 1, to initiate and accelerate endocytosis.

Knockout of PKC α or β isoform (PKC_α, PKC_β) inhibited slow and rapid endocytoses after various stimulation protocols at calyceal nerve terminals (Fig. 6e) [67]. At hippocampal synapses, inhibition of endocytosis by PKC_α knockout can be rescued by the wild-type PKC_α, but not by a calcium-binding-deficient PKC_α. These results suggest that PKCs (PKC_α and PKC_β) serve as Ca^{2+} sensors for regulating Ca^{2+}-stimulated endocytosis at synapses. How PKC links to endocytosis remains unclear. Given that PKC mediates phosphorylation and CaM may activate CaN and MLCK to mediate dephosphorylation and phosphorylation, respectively, we suggest that calcium triggers and facilitates endocytosis by phosphorylating and dephosphorylating the endocytosis proteins. Since endocytosis may be composed of multiple steps, such as the formation of a membrane pit, the formation of a narrow pore, hemi-fission, and fission, it might be possible that PKC and CaM are involved in these different transitions.

Mechanical force provided by endocytic molecules mediates endocytosis, including membrane invagination, pit formation, and fission. A study found that knockout of either β-actin or γ-actin, two actin isoforms in the brain, inhibits slow, rapid, bulk, and overshoot endocytoses at the calyx of Held (Fig. 6f) [69]. The results suggest that polymerized actin may provide mechanical force essential for all kinetically distinguishable forms of endocytosis at calyx synapses. Measurements of fission pore conductance and electron microscopy suggest that polymerized actin may exert mechanical force to bend the membrane and thus generate membrane pits [69].

9 Conclusions

Both whole-cell and cell-attached capacitance measurements have been successfully applied to the calyx of Held synapse to investigate vesicle fusion and retrieval. Whole-cell recordings reveal three kinetically different forms of endocytosis: rapid, slow, and bulk endocytoses. Intense stimulation triggers rapid endocytosis by increasing the calcium influx, which may speed up vesicle recycling to catch up with the rapid rate of exocytosis. Bulk endocytosis was shown to occur faster than previously estimated, and to carry ~10% of the total endocytic load. Cell-attached recordings show two modes of fusion: kiss-and-run fusion and full collapse fusion. Kiss-and-run fusion is followed by rapid endocytosis, whereas full collapse fusion is not. Kiss-and-run with a small fusion pore is likely to produce a small and slow quantal response. Switch between kiss-and-run and full collapse may thus be a mechanism by which synaptic plasticity can be achieved. Calcium influx triggers endocytosis by activation of CaM/CaN and PKC that may dephosphorylate and phosphorylate endocytic proteins. Polymerized actin may provide mechanical forces to bend the membrane, forming membrane pits needed to form endocytic vesicles.

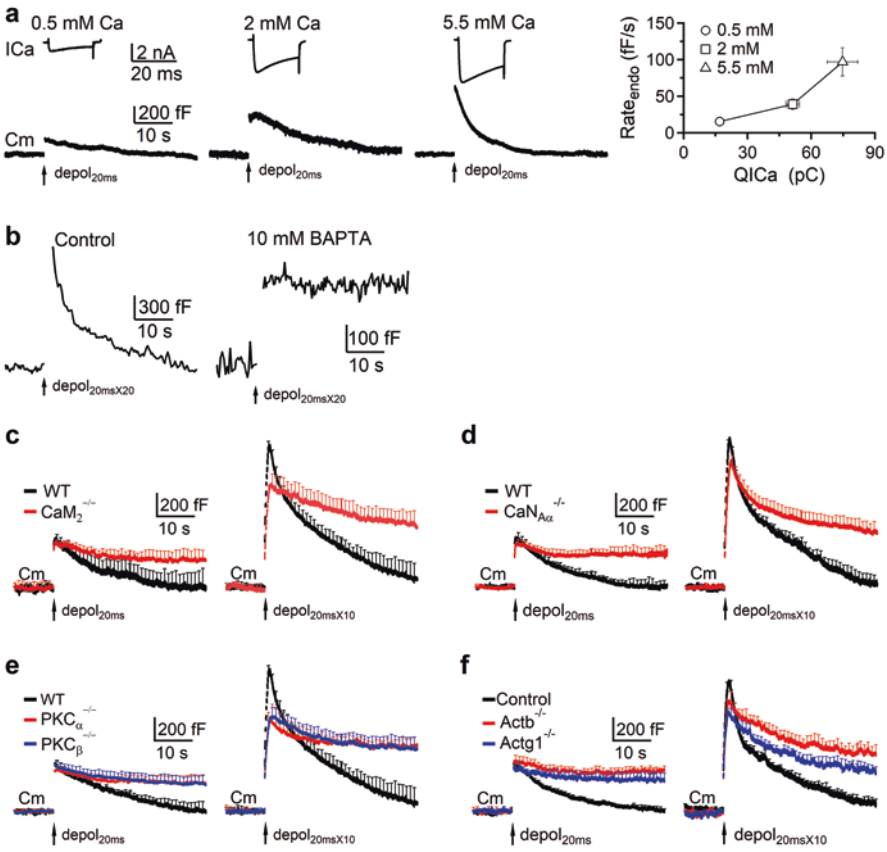

Fig. 6 Endocytosis triggered by Ca^{2+} influx and regulated by Ca^{2+}, calmodulin, calcineurin, PKC, and actin at calyces. (**a**) Sampled calcium channel current (ICa, upper) and capacitance change (Cm, lower) induced by a 20-ms depolarization from −80 to 10 mV ($depol_{20ms}$, arrow) at 0.5, 2, and 5.5 mM in bath solution. We use endocytosis decay rate ($Rate_{endo}$), Cm decay in the 1–5 s after stimulation, to estimate the endocytosis speed. A summary (in right) shows that $Rate_{endo}$ becomes fast as ICa charge (QICa) (and $[Ca^{2+}]_o$) increases. (This figure is adapted from Ref. [64]). (**b**) Sampled Cm induced by 20 20-ms depolarization at 10 Hz ($depol_{20msX20}$, arrow) in control or with 10 mM BAPTA in pipette solution. To reduce the noise, we used the software X-chart (HEKA) to monitor the change in Cm. Ca^{2+} in bath is 2 mM. (This figure is adapted from Ref. [64]). (**c**) Mean Cm trace (mean + s.e.m.) induced by $depol_{20ms}$ (arrow; left) or 10 $depol_{20ms}$ at 10 Hz ($depol_{20msX10}$, arrow; right) from WT (black) and calmodulin 2 KO ($CaM_2^{-/-}$) (red) calyces from P7–10 mice at 22–24 °C. The s.e.m. is plotted every 1 s. Ca^{2+} in bath is 2 mM. A $depol_{20ms}$ induces slow endocytosis with time constant (τ) of 15–25 s at WT calyces. A $depol_{20msX10}$ induces fast endocytosis with τ of 1–2 s at WT calyces. CaM_2 KO inhibits slow and fast endocytoses. Scale bar also applies for the right. (This figure is adapted from Ref. [67]). (**d**) Similar to (**c**), except from calcineurin A_α KO ($CaN_{A\alpha}^{-/-}$) (red). (This figure is adapted from Ref. [68]). (**e**) Similar to (**c**), except from PKC_α KO ($PKC_\alpha^{-/-}$) (red) or PKC_β KO ($PKC_\beta^{-/-}$) (blue). (This figure is adapted from Ref. [67]). (**f**) Similar to (**c**), except from β-actin KO ($Actb^{-/-}$) (red) or γ-actin KO ($Actg1^{-/-}$) (blue). (This figure is adapted from Ref. [69])

Acknowledgments This work was supported by the National Institute of Neurological Disorders and Stroke (NINDS) Intramural Research Program (ZIA NS003009-15 and ZIA NS003105-10, L.-G.W.).

References

1. De Camilli P, Slepnev VI, Shupliakov O, Brodin L. Synaptic vesicle endocytosis. In: Cowan WM, Sudhof TC, Stevens CF, editors. Synapses. Baltimore/London: The Johns Hopkins University Press; 2001. p. 217–74.
2. Heuser JE, Reese TS. Evidence for recycling of synaptic vesicle membrane during transmitter release at the frog neuromuscular junction. J Cell Biol. 1973;57:315–44. https://doi.org/10.1083/jcb.57.2.315.
3. Ceccarelli B, Hurlbut WP, Mauro A. Turnover of transmitter and synaptic vesicles at the frog neuromuscular junction. J Cell Biol. 1973;57:499–524. https://doi.org/10.1083/jcb.57.2.499.
4. Fesce R, Grohovaz F, Valtorta F, Meldolesi J. Neurotransmitter release: fusion or 'kiss-and-run'? Trends Cell Biol. 1994;4:1–4. https://doi.org/10.1016/0962-8924(94)90025-6.
5. Lindau M, Alvarez de Toledo G. The fusion pore. Biochim Biophys Acta. 2003;1641:167–73. https://doi.org/10.1016/s0167-4889(03)00085-5.
6. Choi S, Klingauf J, Tsien RW. Fusion pore modulation as a presynaptic mechanism contributing to expression of long-term potentiation. Philos Trans R Soc Lond Ser B Biol Sci. 2003;358:695–705. https://doi.org/10.1098/rstb.2002.1249.
7. Wu LG. Kinetic regulation of vesicle endocytosis at synapses. Trends Neurosci. 2004;27:548–54. https://doi.org/10.1016/j.tins.2004.07.001.
8. Betz WJ, Angleson JK. The synaptic vesicle cycle. Annu Rev Physiol. 1998;60:347–63. https://doi.org/10.1146/annurev.physiol.60.1.347.
9. von Gersdorff H, Borst JG. Short-term plasticity at the calyx of Held. Nat Rev Neurosci. 2002;3:53–64. https://doi.org/10.1038/nrn705.
10. Sätzler K, Söhl LF, Bollmann JH, Borst JG, Frotscher M, Sakmann B, et al. Three-dimensional reconstruction of a calyx of Held and its postsynaptic principal neuron in the medial nucleus of the trapezoid body. J Neurosci. 2002;22:10567–79. https://doi.org/10.1523/jneurosci.22-24-10567.2002.
11. Taschenberger H, Leão RM, Rowland KC, Spirou GA, von Gersdorff H. Optimizing synaptic architecture and efficiency for high-frequency transmission. Neuron. 2002;36:1127–43. https://doi.org/10.1016/s0896-6273(02)01137-6.
12. Lenn NJ, Reese TS. The fine structure of nerve endings in the nucleus of the trapezoid body and the ventral cochlear nucleus. Am J Anat. 1966;118:375–89. https://doi.org/10.1002/aja.1001180205.
13. Borst JG, Sakmann B. Calcium influx and transmitter release in a fast CNS synapse. Nature. 1996;383:431–4. https://doi.org/10.1038/383431a0.
14. Iwasaki S, Momiyama A, Uchitel OD, Takahashi T. Developmental changes in calcium channel types mediating central synaptic transmission. J Neurosci. 2000;20:59–65. https://doi.org/10.1523/jneurosci.20-01-00059.2000.
15. Wu LG, Westenbroek RE, Borst JG, Catterall WA, Sakmann B. Calcium channel types with distinct presynaptic localization couple differentially to transmitter release in single calyx-type synapses. J Neurosci. 1999;19:726–36. https://doi.org/10.1523/jneurosci.19-02-00726.1999.
16. Dunlap K, Luebke JI, Turner TJ. Exocytotic Ca2+ channels in mammalian central neurons. Trends Neurosci. 1995;18:89–98.
17. Xu J, He L, Wu LG. Role of Ca(2+) channels in short-term synaptic plasticity. Curr Opin Neurobiol. 2007;17:352–9. https://doi.org/10.1016/j.conb.2007.04.005.

18. Gillis KD. Techniques for membrane capacitance measurements. In: Sakmann B, Neher E, editors. Single-channel recording. New York: Plenum Press; 1995. p. 155–98.
19. Sun JY, Wu LG. Fast kinetics of exocytosis revealed by simultaneous measurements of presynaptic capacitance and postsynaptic currents at a central synapse. Neuron. 2001;30:171–82. https://doi.org/10.1016/s0896-6273(01)00271-9.
20. Sun JY, Wu XS, Wu W, Jin SX, Dondzillo A, Wu LG. Capacitance measurements at the calyx of Held in the medial nucleus of the trapezoid body. J Neurosci Methods. 2004;134:121–31. https://doi.org/10.1016/j.jneumeth.2003.11.018.
21. Wu W, Xu J, Wu XS, Wu LG. Activity-dependent acceleration of endocytosis at a central synapse. J Neurosci. 2005;25:11676–83. https://doi.org/10.1523/jneurosci.2972-05.2005.
22. Sun JY, Wu XS, Wu LG. Single and multiple vesicle fusion induce different rates of endocytosis at a central synapse. Nature. 2002;417:555–9. https://doi.org/10.1038/417555a.
23. Wu XS, Xue L, Mohan R, Paradiso K, Gillis KD, Wu LG. The origin of quantal size variation: vesicular glutamate concentration plays a significant role. J Neurosci. 2007;27:3046–56. https://doi.org/10.1523/jneurosci.4415-06.2007.
24. Gentet LJ, Stuart GJ, Clements JD. Direct measurement of specific membrane capacitance in neurons. Biophys J. 2000;79:314–20. https://doi.org/10.1016/s0006-3495(00)76293-x.
25. Yamashita T, Hige T, Takahashi T. Vesicle endocytosis requires dynamin-dependent GTP hydrolysis at a fast CNS synapse. Science. 2005;307:124–7. https://doi.org/10.1126/science.1103631.
26. Wu LG, Betz WJ. Nerve activity but not intracellular calcium determines the time course of endocytosis at the frog neuromuscular junction. Neuron. 1996;17:769–79. https://doi.org/10.1016/s0896-6273(00)80208-1.
27. Sankaranarayanan S, Ryan TA. Real-time measurements of vesicle-SNARE recycling in synapses of the central nervous system. Nat Cell Biol. 2000;2:197–204. https://doi.org/10.1038/35008615.
28. Granseth B, Odermatt B, Royle SJ, Lagnado L. Clathrin-mediated endocytosis is the dominant mechanism of vesicle retrieval at hippocampal synapses. Neuron. 2006;51:773–86. https://doi.org/10.1016/j.neuron.2006.08.029.
29. Sankaranarayanan S, Ryan TA. Calcium accelerates endocytosis of vSNAREs at hippocampal synapses. Nat Neurosci. 2001;4:129–36. https://doi.org/10.1038/83949.
30. Neves G, Lagnado L. The kinetics of exocytosis and endocytosis in the synaptic terminal of goldfish retinal bipolar cells. J Physiol. 1999;515(Pt 1):181–202. https://doi.org/10.1111/j.1469-7793.1999.181ad.x.
31. von Gersdorff H, Matthews G. Inhibition of endocytosis by elevated internal calcium in a synaptic terminal. Nature. 1994;370:652–5. https://doi.org/10.1038/370652a0.
32. Neves G, Gomis A, Lagnado L. Calcium influx selects the fast mode of endocytosis in the synaptic terminal of retinal bipolar cells. Proc Natl Acad Sci U S A. 2001;98:15282–7. https://doi.org/10.1073/pnas.261311698.
33. Beutner D, Voets T, Neher E, Moser T. Calcium dependence of exocytosis and endocytosis at the cochlear inner hair cell afferent synapse. Neuron. 2001;29:681–90. https://doi.org/10.1016/s0896-6273(01)00243-4.
34. Holt M, Cooke A, Wu MM, Lagnado L. Bulk membrane retrieval in the synaptic terminal of retinal bipolar cells. J Neurosci. 2003;23:1329–39. https://doi.org/10.1523/jneurosci.23-04-01329.2003.
35. Koenig JH, Ikeda K. Disappearance and reformation of synaptic vesicle membrane upon transmitter release observed under reversible blockage of membrane retrieval. J Neurosci. 1989;9:3844–60. https://doi.org/10.1523/jneurosci.09-11-03844.1989.
36. Koenig JH, Ikeda K. Synaptic vesicles have two distinct recycling pathways. J Cell Biol. 1996;135:797–808. https://doi.org/10.1083/jcb.135.3.797.
37. Richards DA, Guatimosim C, Betz WJ. Two endocytic recycling routes selectively fill two vesicle pools in frog motor nerve terminals. Neuron. 2000;27:551–9. https://doi.org/10.1016/s0896-6273(00)00065-9.

38. Takei K, Mundigl O, Daniell L, De Camilli P. The synaptic vesicle cycle: a single vesicle budding step involving clathrin and dynamin. J Cell Biol. 1996;133:1237–50. https://doi.org/10.1083/jcb.133.6.1237.
39. Teng H, Wilkinson RS. Clathrin-mediated endocytosis near active zones in snake motor boutons. J Neurosci. 2000;20:7986–93. https://doi.org/10.1523/jneurosci.20-21-07986.2000.
40. Wu W, Wu LG. Rapid bulk endocytosis and its kinetics of fission pore closure at a central synapse. Proc Natl Acad Sci U S A. 2007;104:10234–9. https://doi.org/10.1073/pnas.0611512104.
41. de Lange RP, de Roos AD, Borst JG. Two modes of vesicle recycling in the rat calyx of Held. J Neurosci. 2003;23:10164–73. https://doi.org/10.1523/jneurosci.23-31-10164.2003.
42. Richards DA, Guatimosim C, Rizzoli SO, Betz WJ. Synaptic vesicle pools at the frog neuromuscular junction. Neuron. 2003;39:529–41. https://doi.org/10.1016/s0896-6273(03)00405-7.
43. Elhamdani A, Azizi F, Artalejo CR. Double patch clamp reveals that transient fusion (kiss-and-run) is a major mechanism of secretion in calf adrenal chromaffin cells: high calcium shifts the mechanism from kiss-and-run to complete fusion. J Neurosci. 2006;26:3030–6. https://doi.org/10.1523/jneurosci.5275-05.2006.
44. Llobet A, Beaumont V, Lagnado L. Real-time measurement of exocytosis and endocytosis using interference of light. Neuron. 2003;40:1075–86. https://doi.org/10.1016/s0896-6273(03)00765-7.
45. He L, Wu XS, Mohan R, Wu LG. Two modes of fusion pore opening revealed by cell-attached recordings at a synapse. Nature. 2006;444:102–5. https://doi.org/10.1038/nature05250.
46. Debus K, Lindau M. Resolution of patch capacitance recordings and of fusion pore conductances in small vesicles. Biophys J. 2000;78:2983–97. https://doi.org/10.1016/s0006-3495(00)76837-8.
47. Klyachko VA, Jackson MB. Capacitance steps and fusion pores of small and large-dense-core vesicles in nerve terminals. Nature. 2002;418:89–92. https://doi.org/10.1038/nature00852.
48. Stanley EF. Single calcium channels and acetylcholine release at a presynaptic nerve terminal. Neuron. 1993;11:1007–11. https://doi.org/10.1016/0896-6273(93)90214-c.
49. Smith SM, Bergsman JB, Harata NC, Scheller RH, Tsien RW. Recordings from single neocortical nerve terminals reveal a nonselective cation channel activated by decreases in extracellular calcium. Neuron. 2004;41:243–56. https://doi.org/10.1016/s0896-6273(03)00837-7.
50. Almers W, Breckenridge LJ, Iwata A, Lee AK, Spruce AE, Tse FW. Millisecond studies of single membrane fusion events. Ann N Y Acad Sci. 1991;635:318–27. https://doi.org/10.1111/j.1749-6632.1991.tb36502.x.
51. Spruce AE, Breckenridge LJ, Lee AK, Almers W. Properties of the fusion pore that forms during exocytosis of a mast cell secretory vesicle. Neuron. 1990;4:643–54. https://doi.org/10.1016/0896-6273(90)90192-i.
52. Stiles JR, Bartol TB, Salpeter MM, Salpeter EE, Sejnowski TJ. Synaptic variability. In: Cowan WM, Sudhof TC, Stevens CF, editors. Synapses. Baltimore/London: The Johns Hopkins University Press; 2001. p. 681–732.
53. Bruns D, Riedel D, Klingauf J, Jahn R. Quantal release of serotonin. Neuron. 2000;28:205–20. https://doi.org/10.1016/s0896-6273(00)00097-0.
54. Karunanithi S, Marin L, Wong K, Atwood HL. Quantal size and variation determined by vesicle size in normal and mutant Drosophila glutamatergic synapses. J Neurosci. 2002;22:10267–76. https://doi.org/10.1523/jneurosci.22-23-10267.2002.
55. Zhang B, Koh YH, Beckstead RB, Budnik V, Ganetzky B, Bellen HJ. Synaptic vesicle size and number are regulated by a clathrin adaptor protein required for endocytosis. Neuron. 1998;21:1465–75. https://doi.org/10.1016/s0896-6273(00)80664-9.
56. Fremeau RT Jr, Kam K, Qureshi T, Johnson J, Copenhagen DR, Storm-Mathisen J, et al. Vesicular glutamate transporters 1 and 2 target to functionally distinct synaptic release sites. Science. 2004;304:1815–9. https://doi.org/10.1126/science.1097468.
57. Song H, Ming G, Fon E, Bellocchio E, Edwards RH, Poo M. Expression of a putative vesicular acetylcholine transporter facilitates quantal transmitter packaging. Neuron. 1997;18:815–26. https://doi.org/10.1016/s0896-6273(00)80320-7.

58. Wilson NR, Kang J, Hueske EV, Leung T, Varoqui H, Murnick JG, et al. Presynaptic regulation of quantal size by the vesicular glutamate transporter VGLUT1. J Neurosci. 2005;25:6221–34. https://doi.org/10.1523/jneurosci.3003-04.2005.
59. Wojcik SM, Rhee JS, Herzog E, Sigler A, Jahn R, Takamori S, et al. An essential role for vesicular glutamate transporter 1 (VGLUT1) in postnatal development and control of quantal size. Proc Natl Acad Sci U S A. 2004;101:7158–63. https://doi.org/10.1073/pnas.0401764101.
60. Nielsen TA, DiGregorio DA, Silver RA. Modulation of glutamate mobility reveals the mechanism underlying slow-rising AMPAR EPSCs and the diffusion coefficient in the synaptic cleft. Neuron. 2004;42:757–71. https://doi.org/10.1016/j.neuron.2004.04.003.
61. Jonas P. The time course of signaling at central glutamatergic synapses. News Physiol Sci. 2000;15:83–9. https://doi.org/10.1152/physiologyonline.2000.15.2.83.
62. Hamann M, Billups B, Forsythe ID. Non-calyceal excitatory inputs mediate low fidelity synaptic transmission in rat auditory brainstem slices. Eur J Neurosci. 2003;18:2899–902. https://doi.org/10.1111/j.1460-9568.2003.03017.x.
63. Wu LG, Hamid E, Shin W, Chiang HC. Exocytosis and endocytosis: modes, functions, and coupling mechanisms. Annu Rev Physiol. 2014;76:301–31. https://doi.org/10.1146/annurev-physiol-021113-170305.
64. Wu XS, McNeil BD, Xu J, Fan J, Xue L, Melicoff E, et al. Ca(2+) and calmodulin initiate all forms of endocytosis during depolarization at a nerve terminal. Nat Neurosci. 2009;12:1003–10. https://doi.org/10.1038/nn.2355.
65. Hosoi N, Holt M, Sakaba T. Calcium dependence of exo- and endocytotic coupling at a glutamatergic synapse. Neuron. 2009;63:216–29. https://doi.org/10.1016/j.neuron.2009.06.010.
66. Yamashita T, Eguchi K, Saitoh N, von Gersdorff H, Takahashi T. Developmental shift to a mechanism of synaptic vesicle endocytosis requiring nanodomain Ca2+. Nat Neurosci. 2010;13:838–44. https://doi.org/10.1038/nn.2576.
67. Jin YH, Wu XS, Shi B, Zhang Z, Guo X, Gan L, et al. Protein Kinase C and Calmodulin serve as calcium sensors for calcium-stimulated endocytosis at synapses. J Neurosci. 2019;39:9478–90. https://doi.org/10.1523/jneurosci.0182-19.2019.
68. Sun T, Wu XS, Xu J, McNeil BD, Pang ZP, Yang W, et al. The role of calcium/calmodulin-activated calcineurin in rapid and slow endocytosis at central synapses. J Neurosci. 2010;30:11838–47. https://doi.org/10.1523/jneurosci.1481-10.2010.
69. Wu XS, Lee SH, Sheng J, Zhang Z, Zhao WD, Wang D, et al. Actin is crucial for all kinetically distinguishable forms of endocytosis at synapses. Neuron. 2016;92:1020–35. https://doi.org/10.1016/j.neuron.2016.10.014.

SNARE Proteins in Synaptic Vesicle Fusion

Mark T. Palfreyman, Sam E. West, and Erik M. Jorgensen

Abstract Neurotransmitters are stored in small membrane-bound vesicles at synapses; a subset of synaptic vesicles is docked at release sites. Fusion of docked vesicles with the plasma membrane releases neurotransmitters. Membrane fusion at synapses, as well as all trafficking steps of the secretory pathway, is mediated by SNARE proteins. The SNAREs are the minimal fusion machinery. They zipper from N-termini to membrane-anchored C-termini to form a 4-helix bundle that forces the apposed membranes to fuse. At synapses, the SNAREs comprise a single helix from syntaxin and synaptobrevin; SNAP-25 contributes the other two helices to complete the bundle. Unc13 mediates synaptic vesicle docking and converts syntaxin into the permissive "open" configuration. The SM protein, Unc18, is required to initiate and proofread SNARE assembly. The SNAREs are then held in a half-zippered state by synaptotagmin and complexin. Calcium removes the synaptotagmin and complexin block, and the SNAREs drive vesicle fusion. After fusion, NSF and alpha-SNAP unwind the SNAREs and thereby recharge the system for further rounds of fusion. In this chapter, we will describe the discovery of the SNAREs, their relevant structural features, models for their function, and the central role of Unc18. In addition, we will touch upon the regulation of SNARE complex formation by Unc13, complexin, and synaptotagmin.

Keywords SNARE · Munc18 · Munc13 · Unc18 · Unc13 · Complexin · Synaptotagmin · SNAP-25 · Synaptobrevin · Syntaxin · NSF · Membrane fusion · Synaptic vesicle

M. T. Palfreyman · S. E. West · E. M. Jorgensen (✉)
School of Biological Sciences, and Howard Hughes Medical Institute, University of Utah, Salt Lake City, UT, USA
e-mail: jorgensen@biology.utah.edu

Z.-W. Wang (ed.), *Molecular Mechanisms of Neurotransmitter Release*,
Advances in Neurobiology 33, https://doi.org/10.1007/978-3-031-34229-5_4

Abbreviations

CATCHR	Complexes Associated with Tethering Containing Helical Rods
NSF	NEM-sensitive factor
RIM	Rab3-interacting molecule
SM proteins	Sec1/Munc18
SNARE	Soluble N-ethylmaleimide sensitive factor attachment protein receptor
Unc13	Uncoordinated-13
Unc18	Uncoordinated-18

1 SNARE DISCOVERY—A Convergence of Genetics and Biochemistry

To understand the mechanisms of synaptic vesicle fusion, it is useful to think about the evolution of neurotransmission. In prokaryotic cells, the cytoplasm comprises a single compartment, which limits the diversity of potential chemical reactions conducted in a cell. By contrast, eukaryotic cells segregate cellular functions into specialized membrane-bound compartments, or organelles. The contents of these organelles are moved between compartments by transport vesicles. To transfer cargo, the lipid bilayers of the vesicle and target organelle must fuse. Fusing negatively charged membranes is an energetically unfavorable process. SNARE proteins evolved to force membranes together and merge them, so that the cargo in the transport vesicle is transferred to the lumen of the target organelle. In some cases, cargo must be secreted into the extracellular space via exocytosis, in particular to signal to other cells in the environment. During evolution, it was perhaps a small step to couple SNARE-mediated fusion to membrane depolarization, but it was a giant leap for the diversity of life—the nervous system is arguably the universe's greatest invention.

The identification of SNAREs as the central players in membrane fusion arose from a convergence of independent scientific approaches: protein purification from brain, genetic studies in yeast, pharmacological approaches from toxicology, electrophysiological approaches in model organisms, and in vitro reconstitution assays for membrane fusion.

In the late 1980s, SNARE proteins were identified in the brain as components of the synapse. Specifically, synaptobrevin (also called VAMP—vesicle-associated membrane protein) was purified from synaptic vesicles from the electric ray *Torpedo* [1]. The other two SNARE proteins, syntaxin and SNAP25 (synaptosomal-associated protein of 25 kDa), were purified from rat brain [2–5]. The identification of homologs among the yeast *sec* genes (*sec*retion defective) linked the mechanisms of synaptic function to vesicular trafficking [6, 7] and hinted at the universality of membrane fusion in the trafficking pathways of all eukaryotic cells. However, at

this point there was no evidence that these proteins functioned in calcium-dependent exocytosis of synaptic vesicles. Evidence these proteins were required for neurotransmission came from the study of toxins found in bacteria.

Clostridia are anaerobic soil bacteria that can cause fatal infections in animals. A bizarre feature of such infections is that they produce toxins that can cause muscle paralysis lasting many days [8]. The groups of Heiner Niemann, Reinhard Jahn, and Cesare Montecucco identified the targets of the clostridial toxins at synapses. It was found that botulinum and tetanus toxins cleave synaptobrevin, syntaxin and SNAP25 demonstrating the central role of these proteins in synaptic vesicle release [9–12]. These were the first functional data that the SNAREs were involved in neurotransmission [13, 14]. The essential role of the SNAREs in neurotransmission would later be demonstrated from electrophysiological studies on null mutants in the SNARE proteins in *Drosophila*, mice, and *C. elegans* [15–20]. Thus, the functional data demonstrated that each of these SNARE proteins are required components of synaptic transmission, but their physical association as a complex was not yet known.

The discovery that these proteins formed a complex was demonstrated by experiments aiming to reconstitute membrane fusion. Jim Rothman's group was taking a biochemical approach to understand trafficking in the Golgi apparatus. The toxin N-ethylmaleimide (NEM) potently blocks Golgi trafficking [21, 22] by inhibiting NSF (NEM sensitive factor) [23], the mammalian homolog of the yeast gene *SEC18* [24–26]. NSF was found to bind, via the action of the soluble NSF adaptors (SNAPs) [27], to a set of proteins from brain detergent extracts called SNAREs (soluble N-ethylmaleimide sensitive factor attachment protein receptor) [28]. When these protein complexes were analyzed by mass spectroscopy, it was found that they comprised synaptobrevin, syntaxin, and SNAP25 (Fig. 1a). The perturbation experiments described above, combined with their physical association, convincingly linked these proteins to synaptic vesicle exocytosis, but a list of names in a complex did not constitute a model.

The first coherent model, called the "SNARE hypothesis," would arise from the melding of the genetic and biochemical observations described above. Although wrong in detail, it would catalyze a number of hypothesis-driven experiments that would lead to more accurate models. Based on the finding that a unique set of SNARE proteins were found at each of the trafficking steps [29, 30], Thomas Söllner and Jim Rothman proposed that SNARE interactions provided the specificity for vesicular trafficking by tethering the vesicle to its target membrane—essentially providing an addressing system within the cell [28, 31]. The SNAREs would then be acted on by the ATPase NSF which, by disassembling the SNAREs, would drive fusion [31, 32].

Experiments from Bill Wickner's lab, using a purified vacuole fusion assay, demonstrated that NSF acts not at the final step of fusion, but rather to recover monomeric SNAREs for use in further rounds of fusion [33–35]. Studies at synapses indicated that NSF acts after membrane fusion during the recovery of synaptic vesicles [36, 37]. These data indicated that SNARE assembly, not disassembly, catalyzes fusion.

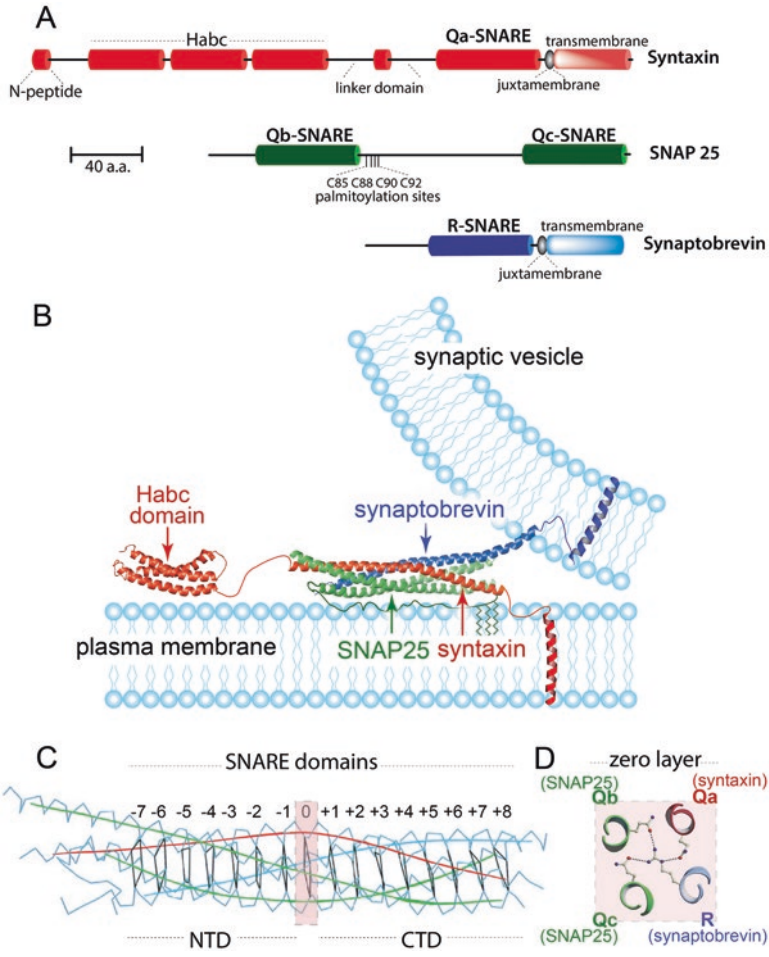

Fig. 1 Molecular description of the SNAREs. (**a**) *Synaptic SNARE proteins*. The SNARE motifs are 60–70 amino acid in length and form a four-helix bundle. Synaptobrevin (R-SNARE), and syntaxin (Qa) contribute one SNARE motif and SNAP25 contributes two SNARE motifs (Qb and Qc). Syntaxin contains an additional regulatory domain comprised of three alpha helices called the "Habc" domain. Syntaxin and synaptobrevin are tail-anchored transmembrane proteins while SNAP25 is attached to the membrane via palmitoylation of the linker region. (**b**) *Vesicle docking*. By assembling into a four-helix parallel bundle, the SNAREs bridge the gap between the two membranes destined to fuse. In the case of the neuronal SNAREs, syntaxin (red) and SNAP25 (green) are found on the plasma membrane and synaptobrevin (blue) is associated with the synaptic vesicle. The N-termini are at the left and the C-termini are at the right. (**c**) *SNARE complex*. The amino acids facing toward the center of this helix (denoted as layers −7 to +8) are largely hydrophobic in nature with the notable exception of the zero layer. (**d**) *Zero layer*. Charged residues are oriented toward the center of the helix: syntaxin contributes one glutamine (Qa), SNAP25 contributes two glutamines (Qb and Qc), and synaptobrevin contributes one arginine (R). (Illustration in (**b**) courtesy of Enfu Hui and Edwin R. Chapman. (**c**) is adapted from Ref. [40]. (**d**) is adapted from Ref. [456])

Proof that SNARE assembly could do active work on membranes came when Rothman's group demonstrated that the SNAREs alone could fuse membranes [38, 39]. Weber et al. incorporated SNAREs into vesicles composed of artificial lipid bilayers and demonstrated that donor vesicles containing synaptobrevin were capable of fusion with acceptor vesicles containing syntaxin and SNAP25 [38]. The SNAREs therefore function in the final steps of fusion and represent the minimal fusion machinery.

2 SNARE Structure

At each trafficking step in the secretory pathway, a unique SNARE complex is used [29]. The SNAREs can be classified functionally as vesicle SNAREs (v-SNAREs) or target SNAREs (t-SNAREs). The assembly of the SNARE complex bridges the vesicle and target membrane, forming what is known as a *trans* SNARE complex (Fig. 1b). The formation of the *trans* SNARE complex drives fusion.

Molecularly, the SNARE proteins are defined by the presence of a conserved 60–70 amino acid SNARE motif, and often also include an N-terminal regulatory domain and a C-terminal membrane anchor. The SNAREs comprise four different families that arose very early in eukaryotic evolution [29, 40–43]. They are defined at a molecular level as Qa-, Qb-, Qc-, and R-SNAREs based on the conserved residue at the center of the SNARE motif. The v-SNARE is usually an R-SNARE, and the t-SNAREs are usually the Qa-, Qb-, and Qc-SNAREs, although this arrangement is not universally true. Moreover, defining what is a "vesicle" and what is a "target" in fusion reactions is often meaningless; for example, transport vesicles fuse to generate a larger vesicle during homotypic fusion [44]. Therefore, we have adopted the Qabc and R nomenclature in this chapter.

The individual SNARE motifs are largely unstructured in solution [45–49], but when all four family members are mixed, the SNARE motifs come together to form a four-helix parallel bundle known as the core complex (Fig. 1b, c) [45, 50]. The SNARE complex is remarkably stable and can only be separated by boiling in the presence of sodium dodecyl sulfate (SDS) [51, 52]. The parallel orientation of the SNAREs [53], their assembly into a four-helix bundle [50], and the stability of the complex [52] led directly to the proposal that SNARE assembly might proceed by zippering from the N-termini to membrane-anchored C-termini.

Along the bore of the helix, the four alpha helical SNARE motifs are arranged in 16 layers of interacting residues (−7 to +8) (Fig. 1c). Fifteen of these layers (−7 to −1 and +1 to +8) consist of interacting hydrophobic residues; the "0" layer in the middle of the complex is formed by ionic interactions between an arginine (R) and three glutamines (Q) (Fig. 1c, d). The "0" layer residues are used to classify the four SNARE families as R- and Q- SNAREs, and can be further divided as Qa-, Qb-, and Qc-SNAREs based on their position in the four-helix core complex. In rare instances (Use1, Vti1, Sft1, and Bet1), an aspartate

(D) or a threonine (T) residue replaces one of the glutamines (Q) [29]. However, the presence of either aspartate or threonine is not conserved in all orthologs; for instance, Vti1 contains a D residue in yeast and mammals, but a Q residue in *Drosophila* and *C. elegans* [29]. The SNAREs used for synaptic vesicle exocytosis are synaptobrevin (R-SNARE, also called VAMP2), syntaxin 1a (Qa-SNARE, more generally known simply as syntaxin), and SNAP25 (which contains both the Qb- and Qc-SNARE motifs) (Fig. 1a) [1–4, 54].

In all SNARE-based fusion reactions, each of the two membranes destined to fuse must contain at least one SNARE with a transmembrane domain; otherwise, fusion will not occur [55]; membrane proximity alone is not sufficient to catalyze fusion [56]. When the transmembrane domain is truncated, mutated, or replaced with an artificial lipid anchor, fusion levels are reduced and, in most cases, no longer proceeds to complete membrane fusion [56–62]. Nevertheless, many of these perturbations still lead to a state in which lipids can exchange, suggesting hemifusion of the juxtaposed monolayers, or spontaneous flipping of individual lipids across the gap [58, 59, 61]. These findings are consistent with the energy requirements for fusion—the early steps of lipid exchange have been calculated to require less energy than the later stages of fusion pore formation and expansion [63].

In most fusion reactions, all four SNAREs possess a transmembrane domain and are encoded as individual proteins [29, 40, 43]. However, in the SNAREs used in post-Golgi trafficking, which include SNAP25, the Qb- and Qc-SNARE domains are coupled in a single protein lacking a transmembrane domain [64, 65]. SNAP25 is anchored via palmitoylation of cysteines in the linker connecting the two SNARE motifs (Fig. 1a). SNAP25 membrane association is not absolutely required for fusion, but mutation of the palmitoylated cysteines results in altered kinetics [66]. It is possible that fusing Qb- and Qc-SNAREs into a single polypeptide evolved to support the rapid calcium-triggered fusion of exocytic vesicles [66], although it is worth noting that several post-Golgi SNAREs including the yeast ortholog of SNAP25, Sec9p, also have coupled Qb- and Qc-SNAREs.

Many SNARE proteins have autonomously folding N-terminal regulatory domains [67]. All Qa-SNAREs, including the synaptic syntaxins, possess an Habc domain at the N-terminus [68]. Some R-SNAREs possess a Longin domain [69]. In rare instances, Qb- and Qc-SNAREs possess an Habc domain or other regulatory domains [70]. These exceptions have led to some confusion. Notoriously, “syntaxin 6” is not a Qa-SNARE; it is instead a Qc-SNARE by homology and behaves as a Qc-SNARE in complexes [71]. Syntaxin 6, despite its homology, was misnamed because it possesses an Habc domain like syntaxins/Qa-SNAREs [29, 70, 72]. Unfortunately, the name “syntaxin 6” stuck. At the synapse, syntaxin with its Habc domain is the only SNARE with an extended N-terminal domain (Fig. 1a, b). The R-SNARE homolog, synaptobrevin, does not have the evolutionarily more ancient Longin domain found in other R-SNAREs.

Both the Habc domain [73, 74] and the Longin domain [67, 75, 76] can fold over and occlude the SNARE motif of their respective proteins, although this mode of interaction is not conserved [67]. Adopting this occluded or "closed" state prevents the SNARE motif from prematurely interacting with other SNAREs [73, 76].

The simple model in which the main function of the Habc domain is to occlude SNARE interactions is not correct. First, in vivo, deletion of Habc dramatically decreases fusion rather than increasing fusion rates [77–80]. Second, Habc domains, as well as Longin domains, have been found on numerous non-SNARE proteins [75, 81, 82]. Third, the closed conformation is not generally conserved among syntaxin proteins [83]. Fourth, the Habc domain of syntaxin can function when SNARE motif and Habc domain are encoded as separate proteins (*in trans*) [80]. Fifth, the Habc is required to activate the SM protein Unc18 to initiate SNARE pairing, as described in detail below [84].

3 SNARE Genetic Redundancy

Perturbation of SNAREs in vivo usually fully eliminates a single trafficking step. However, in many cases the trafficking step was not completely eliminated. There are two possible explanations. First, it is possible that the SNAREs are not executing fusion—an unlikely interpretation given the wealth of data described above. Second, the SNAREs might be partially redundant. Evidence points to the latter interpretation. Knockout mice in synaptobrevin/VAMP2 were found to retain some synaptic activity in hippocampal neurons [17]. In chromaffin cells, this remnant activity could be attributed to the synaptobrevin paralog cellubrevin [85]. Redundancy can also explain the remaining fusion events in null mutants of n-Syb, the *Drosophila* equivalent of synaptobrevin. Syb, the *Drosophila* equivalent of cellubrevin, can functionally substitute for n-Syb when overexpressed in neurons [86]. Redundancy is also seen in the Q SNAREs. SNAP23, SNAP47, and SNAP24 can provide partial function when SNAP25 is absent [19, 87, 88]. Finally, redundancy might also explain the almost complete lack of phenotype in syntaxin 1a knockout mice [89], where it is likely that syntaxin 1b is sufficient to almost entirely replace syntaxin 1a [90]. These observations are supported by experiments in yeast where redundancy between SNAREs has also been conclusively demonstrated in numerous trafficking reactions [91–93]. By contrast, loss of syntaxin (*unc-64*) in *C. elegans* neurons results in a 500-fold reduction in neurotransmitter release with no apparent developmental defects [20]; UNC-64 is committed to synaptic vesicle fusion and is unlikely to have a redundant syntaxin, like in mice; nor is it involved in other cellular functions, like in flies [94]. In summary, the SNAREs largely function at single trafficking steps and are completely necessary for membrane fusion.

4 General Principles of SNARE-Based Trafficking

Before moving to synaptic vesicle fusion, we pause here to describe the four universally conserved steps in SNARE-based trafficking. Sequentially, they are as follows:

- Vesicles are tethered to target membrane
- SM proteins template SNARE assembly
- SNARE zippering drives fusion
- SNAREs are disassembled

4.1 Vesicle Tethering

Regulated trafficking requires a vesicle to first recognize and physically attach to its target—a step known as tethering (Box 1). Tethering is defined as a loose attachment to the membrane, and is visible by electron microscopy. Multisubunit

Box 1 Definitions: The World Turned Upside Down and Given a Good Shake

The nomenclature for steps in vesicle fusion relies on operational definitions. Unfortunately, the terms used by the synaptic community sometimes conflict with the nomenclature used by the yeast community, and have not always been used consistently by either the yeast or the synapse community.

Synaptic nomenclature:

- *Tethering*. Tethering is a morphological definition defined by electron microscopy. Often, physical tethers can be observed in electron micrographs as a darkly stained filament contacting the plasma and vesicle membranes [95]. More generally vesicles close to the plasma membrane, usually less than 20 nm, are considered tethered. Even vesicles that appear to touch the plasma membrane are considered tethered rather than docked, if they remain rounded and lack an electron dense contact site [95]. The precise molecular components of tethering are not yet known but are likely to include the active zone proteins: piccolo, bassoon, alpha-liprin, ELKS/CAST, RIM, RBP, Rab3/Rab27, and Unc13 [96]. Tethering is thought to be independent of SNAREs.
- *Docking*. Docked vesicles, also defined by ultrastructure, are vesicles in contact with the plasma membrane [95, 97–99]. In these fixed and stained samples, clearly distinguishable bilayers are not detected and the vesicle sometimes appears slightly flattened against the plasma membrane. This strict definition is backed up by genetic experiments indicating that docking requires SNAREs and Unc13.

- *Priming*. Priming is a molecular definition in which the SNARE proteins are engaged. SNARE engagement is required for morphologically defined docking, and for the electrophysiologically defined readily releasable vesicles. It is therefore likely that release-ready, docking, and priming define the same group of vesicles by different techniques [100]. What the precise molecular configuration is for primed vesicles is not yet known, although it must include SNAREs, synaptotagmin, complexin and probably includes Unc18 and Unc13. Moreover, priming is likely to include more than a single molecular state of SNARE assembly.
- *Readily releasable pool (RRP)*. The RRP is defined by electrophysiology. These are vesicles that can fuse, if they are exposed to calcium. A single action potential will not cause all release-ready vesicles to fuse due to the stochastic nature of calcium channel opening. However, the size of the pool can be determined by a succession of action potentials that exhaust the pool [101]. Vesicles in the readily releasable pool can also be driven to fuse in the absence of stimulation by applying hypertonic sucrose [102]. It is likely that hypertonic media dehydrates the cytoplasmic gap between the plasma and vesicle membranes of primed vesicles, stimulating SNARE-mediated fusion.

Yeast nomenclature:

- *Tethering*. In yeast, tethering is the first stage in membrane association. It is independent of SNARE proteins and dependent on small GTPases. Unlike the second stage—SNARE engagement—tethering is reversible. *Tethering* in yeast and synapses is roughly equivalent.
- *Docking*. Historically, docking in yeast refers to the entire process of membrane association of vesicles to their target membrane [103]. In the late 1990s, a reversible GTPase-dependent step that is independent of SNAREs was discovered and termed "*tethering*" [104]. Although docking is still sometimes used to refer to the entire process of membrane association, in recent years it has more often been applied to the *stable docking* step that follows tethering in which the SNAREs are engaged, thus falling in concert with the synaptic literature. A stable docked state, like that observed at synapses, is normally not observed in yeast, since SNARE engagement leads inexorably to fusion. However, stable docking can be observed in biochemical reconstitution experiments in which membrane fusion is prevented by reduced temperature.
- *Priming*. Priming in yeast nomenclature is defined as the separation of SNARE proteins by the ATPase NSF, so that the potential energy of unengaged SNAREs is now restored. This terminology is at odds with synaptic nomenclature and there is no equivalent terminology for SNARE separation in synapse nomenclature.

tethering complexes function at this step [105]. Loose membrane association proceeds to tight membrane association that is mediated by SNAREs. At synapses, this second stage is known as docking [20, 95]. Tethering factors and SNAREs serve overlapping roles in target recognition. Together their actions culminate in the initial N-terminal assembly of the SNAREs in diverse cellular trafficking events from yeast to vertebrates, from lysosomes to synaptic vesicles.

Multisubunit tethering complexes comprise a diverse collection of proteins. Broadly speaking, they can be divided into two general categories: CATCHR and non-CATCHR. CATCHR complexes (Complexes Associated with Tethering Containing Helical Rods) include Dsl1, COG, GARP, and exocyst. Non-CATCHR complexes include TRAPP I, II, III, HOPS, and CORVET. Despite the lack of sequence conservation, multisubunit tethering complexes share architectural features: they have common structural elements and subunit organization [106–108]. Some of these complexes have been verified to act as tethers, that is, they can physically link vesicle and target membranes; others may act indirectly in tethering by regulating SNARE assembly [109]. Most likely, multisubunit tethering complexes serve both functions: they physically link the vesicle to the target, and also regulate SNARE assembly.

Overlapping roles for factors mediating tethering and SNARE assembly have been observed in yeast [110–115]. For instance, *sec35,* a tethering protein for Golgi trafficking, can be partially bypassed by overexpression of the relevant SNARE proteins [113]. Similarly, mutations in the tethering complex for plasma membrane fusion can be bypassed by SNARE overexpression [111, 114]. Suppression is not bidirectional—SNARE overexpression can bypass tethering factors, but tethering factors cannot bypass SNAREs—demonstrating that SNAREs act downstream of tethering factors [115].

At synapses, the MUN domain proteins Unc13 and CAPS tether synaptic vesicles and dense core vesicles to fusion sites [5, 20, 100, 108, 116–120]. Structurally, the MUN domain resembles the CATCHR family used in trafficking to and from the Golgi [106, 117, 121, 122]. The C2 domains that flank the MUN domain bind to the synaptic vesicle and the plasma membrane, thereby bridging the two membranes destined to fuse [118]. Additionally, Unc13 plays an active role in SNARE assembly [20, 123–128]. Unc13 is thus a membrane tether and a regulator of SNARE-dependent docking.

At each trafficking step along the secretory pathway a unique SNARE complex is used, leading to the model that SNAREs *alone* could direct target specificity [28, 129–131]. This simple model is not correct. In vivo, tethering complexes bring vesicles to the correct fusion sites; in their absence, vesicles do not successfully reach their targets.

Nevertheless, SNARE compatibility is still an essential component for directing fusion to a specific target. When inserted in artificial membranes, SNAREs exhibit specificity in catalyzing fusion reactions [129, 130]. Specificity can also be seen in vivo; after cleavage of SNAP25 in PC12 cells, secretion could only be rescued by

SNAP25 itself and not by other SNAP25 homologs [131]. Finally, the removal of SNARE proteins results in defects in respective membrane attachment [20, 84, 95]. Despite early evidence to the contrary [13, 14, 16, 132], it is now clear that SNAREs can mediate the specificity and physical attachment of vesicles to their target membrane [20, 84, 95, 133–135]. In vivo, a combination of tethering factors and regulated SNAREs assembly is necessary to precisely dock synaptic vesicles at the active zone [44, 136–141]. The partially overlapping functions of tethering factors and SNAREs is needed to achieve the high level of spatial fidelity seen in vesicle fusion.

4.2 SM Proteins Template SNARE Assembly

SM proteins are conserved in all SNARE-based membrane fusion events [142]. They are the fifth Beatle to the four SNAREs—SNARE assembly cannot be considered without them. The importance of the SM proteins is underscored by their presence in every known SNARE-mediated membrane fusion reaction [143, 144], and the dramatic phenotypes that result from their absence [145–149]. In the case of synaptic vesicle fusion in mice, for instance, the removal of Munc18 results in a defect in synaptic vesicle fusion that is as profound as the removal of the SNAREs themselves [145].

SM proteins all have a common structure [74, 150–160]. Roughly speaking, they have a globular body with a protruding hairpin structure, domain 3a, that can be furled or unfurled [74, 154, 161–164] (see Fig. 4). Between the globular body and domain 3a lies a prominent groove. As such, the full structure looks like a mitten—the globular body representing the palm, and domain 3a the thumb. The first structure of an SM protein was of Unc18 gripping syntaxin in the closed state. Interestingly, this structure did not represent a conserved binding mode between SM proteins and syntaxin, but nevertheless, dominated thinking about the role of Unc18 in the years that followed.

The importance of SM proteins has been clear for many years, but understanding the role for SM proteins in SNARE assembly has been confounded by the numerous binding modes between SNAREs and SM proteins [165]. It is now clear that the different binding modes exist to allow SM proteins to regulate multiple steps during the trafficking and assembly of SNAREs. By binding SNAREs, SM proteins (1) block inappropriate SNARE interactions, (2) transport syntaxin, (3) template correct SNARE interactions, and (4) protect SNARE disassembly by NSF. Templating represents the universally conserved role of SM proteins. The relative importance of the other roles depends on the specific requirements of the membrane trafficking step. In the case of synaptic transmission, the SM protein Unc18 must get syntaxin to the synapse and prevent it from prematurely interacting with other SNAREs.

4.3 SNARE Zippering Drives Fusion

SNARE assembly proceeds via zippering from the N-termini to C-termini. The concept that SNARE zippering could drive membrane fusion came from three key observations: (1) the SNARE complex is remarkably stable [52], (2) the SNAREs assemble in a parallel orientation [53] and (3) assembled SNAREs form a coiled-coil structure [50]. The nucleation of the SNARE complex at the free N-termini followed by progressive assembly of the complex would pull the vesicle and the plasma membranes together to drive fusion (Fig. 1b) [53, 166–177].

The actual evidence for zippering came initially from two complementary experiments. First, biochemical and structural studies demonstrated that the membrane-proximal domain of syntaxin becomes sequentially more ordered upon binding synaptobrevin in a directed N- to C-terminal fashion [169, 178–180]. The temperatures for assembly and disassembly of SNARE complex differ by as much as 10 °C. Thus, assembly and dissociation follow different reaction pathways. Temperature hysteresis is evidence of a kinetic barrier between folded and unfolded states [51, 172, 173]. Mutations in the N-terminal hydrophobic core of the SNARE complex selectively slowed SNARE assembly while those in the C-termini did not [169, 181], suggesting that SNARE assembly is nucleated at the N-termini and that loose SNARE complexes might be a stable intermediate [182]. The second line of evidence for zippering came from in vivo disruption studies using clostridial toxins, antibodies directed toward the SNARE motifs, and mutations in the hydrophobic core of the SNARE complex [166, 168, 169, 183, 184]. These studies demonstrated that the N-termini of SNAREs become resistant to cleavage or antibody block at early stages of SNARE assembly, while C-termini are only resistant to disruptions at late stages.

Recent advances in technology, such as optical tweezers, have confirmed that SNARE assembly proceeds by zippering [171, 173–177]. Zippering proceeds in three distinct steps. Initial zippering takes place at the N-termini of the SNARE motif, this is followed by a pause at the half-zippered state, then zippering proceeds to the C-termini [173]. Zippering is an intrinsic property of SNARE proteins [171, 185] and does not require additional factors [172, 173].

4.4 SNARE Disassembly

After the two membranes have merged, the SNARE complex is located in a single membrane and is referred to as a *cis* SNARE complex. Repeated rounds of vesicle fusion require SNARE disassembly. NSF and SNAPs disassemble the *cis* SNARE complex, allowing the SNAREs to be repartitioned to their appropriate compartments. NSF uses ATP to disassemble the SNAREs, and much like a battery, the energy put into the system is stored in the monomeric SNARE proteins. This energy will be released during SNARE winding to fuse membranes. Together, NSF and the SNAPs are able to disassemble all SNARE complexes [186–189]. The ATPase NSF itself

does not directly bind SNAREs, instead it binds SNAREs through the action of the SNAPs [187, 190]. SNAP proteins (Soluble *N*-ethylmaleimide-Sensitive Factor Attachment Protein) are not related to the SNARE protein SNAP25. There are three SNAP proteins: αSNAP, βSNAP, and γSNAP [27]. αSNAP and βSNAP are closely related and became duplicated in the vertebrate lineage. αSNAP is ubiquitous, and βSNAP is brain specific [191]; they act together in regulated exocytosis in neuronal cells [192–194]. γSNAP is found in all phyla and is dedicated to SNAREs involved in endosome trafficking [195]. The SNAPs bind to the surface of the *cis* SNAREs around the central zero layer, which contains the conserved Q and R residues [190, 196]; although it is not clear whether these residues are important for disassembly [197, 198]. NSF does not disassemble SNAREs by pulling an unwound SNARE through the pore of the ATPase. Current models suggest that dislocation of the N-terminus of SNAP25 by the membrane-proximal ring of NSF, or reverse torque applied to the complex by the SNAP proteins, could cause the complex to disassemble [187, 188, 199].

NSF and αSNAP disassemble *cis* SNAREs and police the synapse for incorrectly assembled SNAREs that may have wandered astray during assembly. αSNAP and NSF can disassemble numerous off-pathway SNARE complexes, including non-cognate, antiparallel, and non-stoichiometric complexes [187]. Indeed, NSF can also disassemble productive *trans* SNARE complexes. In a physiological setting, the on-pathway SNAREs are protected from the action of NSF by Unc18, Unc13, complexin, and synatotagmin [200–202]. Disassembled syntaxin is also rapidly bound up by Unc18, the starting point for a new round of SNARE assembly and the release of another synaptic vesicle. Thus, NSF serves not only to recycle *cis* SNAREs but also as a quality control mechanism during SNARE assembly.

5 Assembling Snares at Synapses

Cycles of SNARE assembly and disassembly underlie rounds of vesicle fusion: assembly leads to vesicle fusion; disassembly prepares the SNAREs for another round (Fig. 2). At synapses, SNARE interactions must be tightly regulated to ensure the spatial and temporal fidelity of membrane fusion. The process of SNARE-mediated synaptic vesicle fusion can be divided into seven steps:

- *Transport: Unc18 chaperones syntaxin during trafficking*
- *Tethering: Unc13 tethers synaptic vesicles*
- *SNARE pairing: UNC-18 templates SNARE assembly*
- *Priming: synaptotagmin and complexin pause SNARE winding at the half-zippered state*
- *Disinhibition: calcium binds synaptotagmin and unleashes SNARE zippering*
- *Fusion: zippering of the SNARE C-termini transfers energy to the transmembrane domains and drives fusion*
- *Disassembly: NSF and αSNAP separate the SNARE complex*

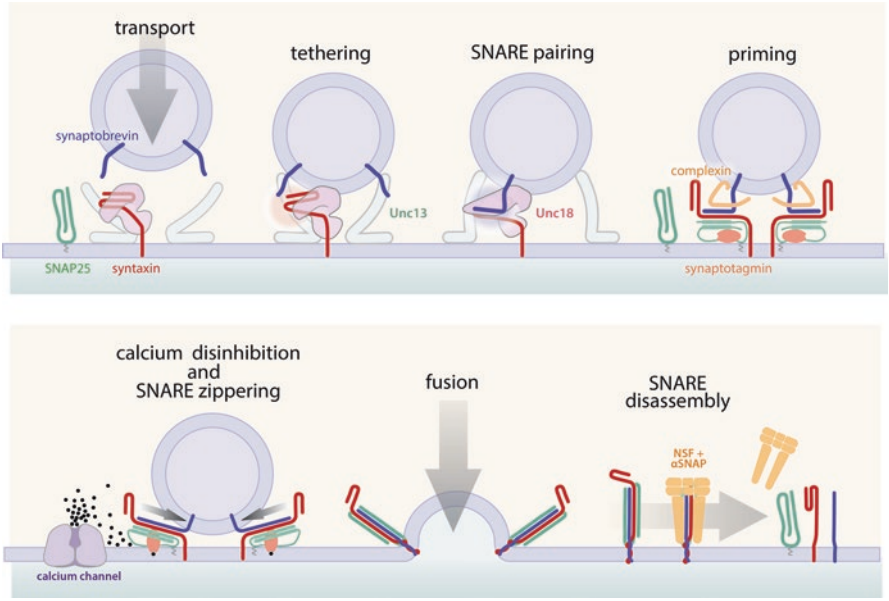

Fig. 2 Overview of SNARE assembly and membrane fusion at synapses. *Transport*, synaptobrevin is transported to the synapse by kinesin on synaptic vesicle precursors. Syntaxin and SNAP25 are broadly localized in axons. *Tethering*, the synaptic vesicle is recruited to a release site by Unc13 and syntaxin is converted to the open state. *SNARE pairing*, the open state of syntaxin stimulates Unc18 to template and proofread syntaxin and synaptobrevin pairing. *Priming*, Unc13 and Unc18 recruit SNAP25, and synaptotagmin and complexin hold the vesicle in the paused, half-zippered state. (Only the C2B domain of synaptotagmin is shown). *Calcium*, membrane depolarization opens calcium channels, calcium-binding releases the synaptotagmin block. *Fusion*, SNARE winding pulls the membranes together and creates a fusion pore. *SNARE diassembly*, alpha-SNAP binds the complex and the ATPase NSF separates the SNAREs

In the remainder of this chapter, we will go through each of these steps, detailing the proteins and membrane rearrangements that take place.

5.1 Transport and Trafficking SNAREs

Upon exit from the Golgi, synaptobrevin is sorted into synaptic vesicle precursors and transported by kinesin to the synapse within BLOC-One-Related Complexes (BORC) [203–213]. Syntaxin is transported on vesicles by the kinesin adaptor protein Fez1/UNC-76 [214]. The Qbc-SNARE SNAP25 lacks a transmembrane domain but is palmitoylated in the Golgi and is transported to the plasma membrane by the secretory pathway [215–217], perhaps in association with kinesin-1 [218]. The Qbc-SNARE SNAP25 is broadly localized to the plasma membrane of

the axon where it can be found in clusters [217, 219]. Syntaxin is also not specifically localized at synapses but rather decorates the axoplasm uniformly or in broad clusters [217, 219–222] and is transported there during growth cone extension [223, 224].

5.1.1 Unc18 Chaperones Syntaxin to the Axoplasm

Promiscuous assembly is an intrinsic property of SNARE proteins, and this presents a problem during transport. SNAREs can assemble with non-cognate SNAREs, they can assemble with the wrong stoichiometry, and they can assemble in antiparallel configurations [46, 201, 225–229]. SNAREs are sticky proteins and many identified binding partners are likely to be irrelevant or artifactual. On the other hand, legitimate binding targets include non-SNARE proteins that regulate trafficking or fusion [230]. It is clear these errant teenagers require a chaperone. At the cotillion of SNARE assembly, SM proteins ensure that only productive SNARE complexes are formed.

The first step is to simply exit the Golgi and to get to the plasma membrane of the axon without interacting with other SNARE proteins. In neurons, the SM protein Unc18 (UNC-18/ Munc18/nSec1) binds tightly to closed syntaxin [231] and transports syntaxin to the plasma membrane [232]. Unc18 binds syntaxin in the closed conformation with the Habc domain folded over the SNARE motif (see Fig. 4b) [74]. This conformation prevents premature interactions with other SNARE proteins [74, 231–236].

The mammalian homolog Munc18-1 binds syntaxin with a Kd of ~1–5 nM [74, 159, 235, 237–239]. This high-affinity binding led to the proposal that Unc18 inhibits vesicle fusion [240–242]. However, the genetic evidence is not consistent with this model. Moreover, this mode of binding is not universally conserved; the binding of Unc18 to closed syntaxin monomers appears to be a unique adaptation for synaptic vesicle release [83, 157, 243–245]. The strength of this interaction may reflect the importance of trafficking syntaxin and Unc18 in neurons. In the absence of Unc18, syntaxin accumulates in the soma and is unstable [78, 79, 84, 232–236, 246–248]. For a protein, the distance between cell body and synapse can be immense, and protecting syntaxin from inappropriate interactions during transport is likely to be particularly important.

By contrast, the distance that Qa-SNAREs must be transported in yeast is comparatively short. Perhaps as a consequence, the binding to closed syntaxin monomers may not be a priority. When SM proteins do interact with Qa monomers, it is often binding that promotes open syntaxin, rather than stabilizing the closed form [153, 249, 250]. For instance, Vps45, the SM protein used in yeast Golgi fusion binds to its syntaxin partner Tlg2 in an open conformation [153]. The contrasting priorities for transport are likely to explain the difficulties for the SNARE community in arriving at a consensus for SM protein function.

5.2 *Unc13 Tethers Synaptic Vesicles and Initiates SNARE Assembly*

Synaptic vesicles in the reserve pool feed vesicles to fusion sites in the active zone. These release sites are tightly coupled to calcium channels [251], and are organized by Unc13 [252, 253]. The C1-C2B-MUN-C2C fragment of Unc13 is conserved in all isoforms and is responsible for tethering vesicles and activating syntaxin [254] (Fig. 3a). The Unc13 C2C domain binds to lipids and to synaptobrevin on a synaptic vesicle [118, 255–257]; the C2B domain binds negatively charged lipids in the

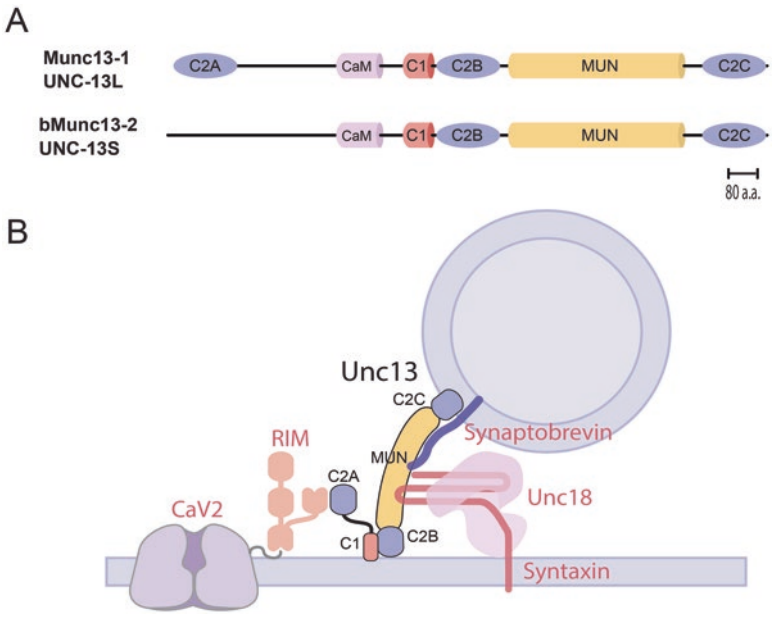

Fig. 3 Unc13 tethers synaptic vesicles and activates syntaxin. (**a**) *Domain architecture of Unc13*. All Unc13 isoforms contain a conserved C1-C2B-MUN-C2C fragment that is responsible for tethering vesicles and activating syntaxin. The C2C domain binds synaptic vesicles, the C2B domain binds the plasma membrane. C1 bind diacylglycerol (DAG) and modulates Unc13 activity. The MUN domain binds syntaxin. Along with this C-terminal fragment, Unc13 isoforms contain variable N-terminal extensions that are responsible for the organization of active zones, particularly the localization of calcium channels. The C2A domain of Unc13 binds Rab3-interacting molecule (RIM). Illustrated are the two predominant vertebrate Unc13 isoforms present in hippocampal neurons: Munc13-1 and bMunc13-2. *C. elegans* and *Drosophila* have two isoforms with similar architecture to Munc13-1 and bMunc13-2 [252, 253]. The N-termini are at the left and the C-termini are at the right. (**b**) *Unc13 organizes release sites*. Unc13 binds synaptic vesicle directly via C2C domains and indirectly by binding synaptobrevin. C2B domains bind the plasma membrane, tethering synaptic vesicles. Vesicle tethering is localized to calcium channels via the variable N-terminal of Unc13 that binds to RIM, which in turn binds the calcium channel CaV2. Interactions between the MUN domain and syntaxin activate syntaxin allowing it to form the 4-helix core SNARE complex

plasma membrane (Fig. 3b). Together, the C2C and C2B domains allow Unc13 to bridge vesicles and plasma membranes [118], likely keeping them ~20 nm apart [256]. In vivo, the absence of Unc13 eliminates tethering and docking [20, 95, 258]. Along with bridging synaptic vesicle and plasma membranes, Unc13 guides synaptic vesicles to calcium channels via variable N-terminal domains. Specifically, the C2A domain, present in some isoforms, is linked to a calcium channel via the active zone protein RIM [140, 259–262].

Unc13 also serves an active role in SNARE assembly: Unc13 converts syntaxin to an open state to promote formation of the SNARE complex [20, 123–127, 263]. The closed, inhibited, state of syntaxin is a specialized property of SNAREs used in exocytosis. Unc13 likely opens syntaxin by interacting with the linker domain separating the syntaxin SNARE motif from the regulatory Habc and N-peptide [264] (Fig. 1a). Mutations in the linker domain, the so called "LE" mutations, lead syntaxin to adopt an open conformation [73]. In the absence of Unc13, synaptic vesicle fusion is abolished [265–268]. However, the constitutively open form of syntaxin can partially restore fusion [20, 123, 269] and can fully rescue *unc-13* docking defects [20]. The discrepancy between full rescue of docked vesicles and partial rescue of fusion hints at potential roles for Unc13 downstream of docking. We will explore those in the coming sections.

Thus, Unc13 stands ready at release sites, cradling syntaxin bound tightly by Unc18. Recruitment of a synaptic vesicle from the reserve pool by the C2C domain signals to the MUN domain to convert syntaxin to the open state and offer it to synaptobrevin.

5.3 Unc18 Templates SNARE Assembly

In the closed state of syntaxin, Unc18 keeps the SNARE motif broken up into several smaller helices that are trapped in place by binding between the Habc domain and Unc18 [74] (Fig. 3a). This structure is incompatible with SNARE assembly and, it was theorized, would need to be dismantled for syntaxin to adopt the "open" form that would initiate SNARE assembly [73, 74].

Experimentally, however, Unc18 can bind both open and closed syntaxin [152, 236, 270]. Furthermore, the unfolding energies for Unc18 bound to closed syntaxin and bound to open syntaxin are 7.2 and 2.6 k_BT, respectively [271]. This implies that only 4.6 k_BT is required to open syntaxin, a figure far less than the ~22 k_BT that has been calculated to wrestle Unc18 free of syntaxin [159].

The opening of syntaxin does not involve the removal of Unc18, as was once envisioned; rather Unc18 remains associated with syntaxin. The structure of Unc18 bound to open syntaxin can be predicted from the structure of Vps45, the SM protein involved in vesicle fusion in the Golgi from yeast, bound to its syntaxin partner Tlg2 in an open conformation [153]. In the threaded structure, Unc18 remains attached to syntaxin via continued association with the Habc domain, the N-peptide of syntaxin bound to domain-1 of Unc18, and possibly via residues at the bottom of

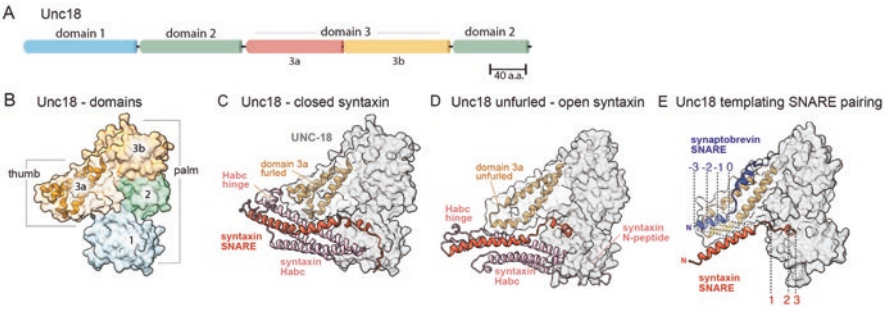

Fig. 4 SNARE templating by Unc18. (**a**) *Domain architecture of Unc18*. Unc18 can be divided into four domains; domain 3 is further divided into domain 3a and 3b. The N-termini are at the left and the C-termini are at the right. (**b**) *Unc18 structure*. Unc18 folds into a structure that roughly resembles a mitten. Domain 3a forms the thumb of the mitten; the other domains form the palm. (**c–e**) *Potential steps for nucleating pairing of syntaxin and synaptobrevin by Unc18, as predicted from molecular structures*. (**c**) *Syntaxin closed state*. Syntaxin resides on the plasma membrane and is bound by Unc18 in the closed state. The Habc domain occludes the N-terminal half of the SNARE motif. Unc18 domain 1 binds the C-terminal half of the SNARE motif. (**d**) *Open syntaxin unfurls Unc18*. Unc13 recruits a synaptic vesicle to a release site and acts on the hinge domain to open syntaxin. The Habc domain transduces this conformational change to Unc18, and a segment from domain 3a in Unc18 flips out to create the "unfurled" or "open" conformation. (**e**) *SNARE pairing*. The unfurled domain of Unc18 can recruit synaptobrevin and aligns the N-termini of the syntaxin and synaptobrevin SNARE motifs. For **a**, UNC-18 and syntaxin/UNC-64a sequences from *C. elegans* were threaded onto the crystal structure of Munc18-1 bound to closed syntaxin-1 (PDB ID: 3C98). For **b**, the sequence of UNC-18 was threaded onto Vps45p and UNC-64a was threaded onto Tlg2p from the yeast Vps45-Tlg2 complex (PDB ID: 6XM1). For **c**, the UNC-18 sequence was threaded onto Vps33p, UNC-64a was threaded onto Vam3p; SNB-1 was threaded onto Nyv1p from the yeast Vps33-Vam3-Nyv1 complex (PDB ID: 5BUZ, 5BV0). The unstructured and therefore missing sequences in Munc18, syntaxin and Nyv1 crystal structures were assigned unstructured regions by the threading program. Homology modeling was performed using SWISS-MODEL [457], and visualization was performed using ChimeraX [458]

domain 3a that interact with the SNARE motif of syntaxin [263] (Fig. 4b). The relative importance of these binding interfaces is still in dispute. Some studies indicate that removal of the N-peptide does not perturb SNARE assembly and fusion [78, 84, 272, 273], whereas others indicate the opposite [79, 274–276]. Much like the open form of syntaxin, the binding mode of SM proteins to the syntaxin N-terminal regulatory domain is not conserved: some SM proteins favor N-peptide association whereas others favor Habc interactions [277]. Irrespective of the exact mode of binding, it is clear that all SM proteins remain attached to SNAREs to template their assembly. In neurons, Unc13 catalyzes the transition between closed and open syntaxin.

In neurons, the tight binding between Unc18 and closed syntaxin monomers masked a weaker but far more central role for the SM proteins: templating SNARE assembly. Templating was discovered in yeast, where tight binding between SM proteins and syntaxin monomers is not seen. The transient templating interaction between SM proteins and SNAREs very likely represents the evolutionarily conserved central function of SM proteins [84, 278].

The first hints at a proofreading role for SM proteins came from studies of the SM protein, Sly1, and its cognate syntaxin partner, Sed5. In the absence of Sly1, Sed5 formed complexes with numerous non-cognate SNAREs [274, 279]. Peng and Gallwitz proposed that the SM protein, Sly1p, might be proofreading the assembly of the Qa-SNARE Sed5 and the R-SNARE Bet1 [279, 280]. They were remarkably prescient.

In 2007, the labs of Tom Melia and Jim Rothman showed that in a liposome fusion assay the SNAREs were activated by their cognate SM proteins [281]. The strong stimulation of fusion that they observed was dependent on direct contact between the SM proteins and the Qa- and R-SNAREs. They suggested that SM proteins proofread SNARE assembly.

In 2015, the lab of Fred Hughson provided the first visual evidence for the proofreading step when they crystalized two complexes: (1) the SM protein Vps33 with the Qa-SNARE Vam3, and (2) Vps33 with the R-SNARE Nyv1 [151]. A composite of the two structures—experimentally supported by the presence of the tripartite structure in size exclusion chromatography—showed that Vps33 provides a template for Qa- and R-SNARE assembly [151]. In this structure, the C-terminal halves of the Vam3 and Nyv1 SNARE motifs are splayed apart on the surface of the SM protein [151]. By contrast, the N-terminal half of the SNARE motifs are aligned along an extended 3a domain of Vps33. The structure looks like a half-zippered SNARE complex, with the N-terminal domains aligned [151].

The extension of domain 3a, seen in Baker et al., 2015, is a conserved feature of SM proteins and is now understood to initiate SNARE templating [84, 161–164]. Like Vps33, domain 3a of neuronal Munc18-1 transitions from a compact furled loop (closed state) to an extended helical structure (open state) [154]. The extended domain 3a of Unc18 opens the platform for the assembly of a half-zippered syntaxin-synaptobrevin SNARE complex—the C-terminal half of the SNARE motif lies in the palm, the N-terminal half along the extended thumb [151]. The tripartite templating complex, consisting of SM protein and Qa- and R-SNAREs, has been observed in vitro [151], and in vivo experiments support its functional importance [84, 282]. Optical trap experiments and site-directed mutagenesis indicate that neuronal Munc18-1 shares the same templating functions as Vps33 [271].

We can create a potential structural pathway for Unc18 function by threading the sequence of UNC-18 onto the structures of SM proteins in various binding modes (Fig. 4c–e). From transport through the initiation of SNARE assembly, Unc18 binds syntaxin in the closed state (Fig. 4c) [78, 79, 84, 232–236, 246–248, 283, 284]. At the active zone, vesicles are tethered and presented to the Unc18-syntaxin complex by Unc13. Unc13 converts syntaxin to the open state. Through an unknown mechanism, likely involving the Habc domain [84], the domain 3a of Unc18 becomes unfurled (Fig. 4d) exposing a platform for syntaxin and synaptobrevin SNARE motifs, templating their assembly (Fig. 4e).

It is important to note that VPS33 does not interact with the Qa-SNARE in a closed state. It is likely that the high-affinity binding of Unc18 to closed syntaxin blinded us to this essential function of Unc18. The templating complex has an unfolding free energy of 5.2 k_BT and a lifetime of 1.4 seconds. The transient nature

of the complex is consistent with its role in proofreading, and probably helps explain its elusiveness to experimentalists. SNARE assembly needs to only briefly pause on the way to fusion. A templating complex that is too stable will never transition to fusion and one that is not stable enough will not provide the time for proper proofreading. To stabilize the neuronal templating complex for structural studies, Jose Rizo's lab crosslinked an open form of Syntaxin 1A with synaptobrevin and crystalized it with the open form of Munc18-1 [285]. The structure they solved looks remarkably like the tripartite, templating, Vps33-Vam3-Nyv1 complex [151, 285]. A strong case for the universal templating function of SM proteins can be made from these in vitro data.

The physiological importance of templating in vivo has been tested by engineering directed mutants based on templating structures. Mutation of the residues in Munc-18-1, which interact with syntaxin and synaptobrevin, seriously impairs synaptic vesicle release [282]. More strikingly, the yeast SM protein, Sec1, which normally provides no rescue to worm synaptic vesicle release, can rescue synaptic transmission when it is engineered to template worm SNAREs, if it can also interact with the Habc domain of syntaxin [84]. The requirement for the Habc domain is consistent with the known in vitro stabilizing role for this domain in the templating complex [143, 271, 286]. After years of searching for the enigmatic, conserved, positive function of SM proteins, these in vitro and in vivo studies have finally provided the answer: SNARE templating.

5.3.1 Revisiting the t-SNARE Acceptor Complex

The templating complex—a 1:1:1 complex between an SM protein and the Qa- and R-SNARE—does not include the Qb- and Qc-SNARE motifs. This realization prompted a reassessment of the "acceptor t-SNARE complex" model in which a 1:1 complex between syntaxin and SNAP25 represents the first stage in SNARE assembly. The "acceptor complex" had become the default starting point for effectively all in vitro SNARE assembly reactions [178, 181, 228]. But is it the physiologically relevant starting point in vivo?

The dynamics of the acceptor complex are not optimal. In liposome fusion assays, the acceptor complex does speed up the assembly of the core complex [179]. The binding of the acceptor complex to synaptobrevin can be quite fast, ranging from rate constants of 6×10^3 to 5×10^5 M^{-1} s^{-1} [179, 287], compared to the minutes to hours that individually mixed SNAREs require to assemble [181]. However, even with the acceptor complex, fusion rates do not approach the rates seen in vivo. In assays where the rate of fusion is more closely mimicked, the acceptor complex did not speed fusion [288], and indeed in some cases could result in a docked state that would persist for as long as 30 minutes [289].

The acceptor complex also readily misfolds [290, 291]. It will rapidly incorporate another syntaxin molecule to form a dead-end Qaabc four-helix complex [179, 292, 293]. In addition, the acceptor complex will readily assemble with tomosyn [294–298], a negative regulator of fusion [299–302]. Thus, in vivo, the acceptor

complex represents, at best, a problematic on-pathway starting point for SNARE assembly. Instead, it is a highly reactive complex that can sometimes proceed to productive fusion, but more often gets shunted off to non-productive end points.

In vivo, Unc18 binding to syntaxin monomers shields syntaxin from incorporation into "acceptor" complexes. Complexes that escape the protection of Unc18 are likely to be quickly dealt with by αSNAP and NSF, that together can disassemble a wide range of SNARE complexes [200, 202, 303, 304]. There is still active debate about the assembly order of the SNAREs [305, 306]. But SNAP25 appears to have gone from the first SNARE to enter the complex to the last [255, 271, 307, 308]. Instead of the acceptor complex, it is probable the Unc18-syntaxin complex represents the true physiological starting point for SNARE assembly [283] (Fig. 2).

At synapses, it is possible that Unc18 templating is aided by Unc13 through a yet to be unraveled mechanism [309]. In an in vitro assay, absence of either Unc18 or Unc13 causes an increase in antiparallel SNARE complexes [143, 225]. When both proteins are lacking as many as 40% of the complexes are assembled in antiparallel orientation [225]. The central MUN domain of Unc13 is known to bind syntaxin, SNAP-25, and synaptobrevin [124, 128, 255, 264, 307] and may therefore help incorporate SNAP25 into SM templated syntaxin-synaptobrevin pairs. However, when and how SNAP25 is recruited to prime vesicles for fusion is not known.

5.4 Synaptotagmin and Complexin Hold the SNAREs in a Half-Zippered State

After the SNAREs have been aligned and the complex nucleated at their N-termini, SNARE assembly pauses at a half-zippered state [173, 182]. This pause is an intrinsic property of SNAREs [173, 182]—it occurs in the absence of other proteins—and is likely the result of two factors. First, the repulsive forces of closely apposed membranes maintain the half-zippered state [173]. Second, the conserved zero layer residues may disrupt zippering and leave the C-termini splayed open momentarily [166, 310].

Neurons have exploited this intrinsic pause in SNARE zippering to link calcium influx to rapid and synchronous membrane fusion. All membrane fusion events are facilitated by calcium. Facilitation can be indirect, for example by binding proteins such as calmodulin [311]. Alternatively, it can be direct: calcium is a divalent cation that can act directly on membranes, for example by neutralizing the negative charges of phosphatidylinositol 4,5-bisphosphate (PIP2) [312–317]. But only in neurons is calcium exquisitely tied to triggering SNARE-mediated fusion. Two changes make this possible: (1) synaptotagmin and complexin stabilize the half-zippered state and are disinhibited by calcium, and (2) voltage-gated calcium channels are tightly localized to synaptic vesicle fusion sites, minimizing calcium diffusion [251, 318]. Together these factors allow for the delay between the elevation of cytosolic calcium and the postsynaptic response to be as short as 60–200 μs [319].

Broadly speaking, complexin and synaptotagmin stabilize the half-zippered state; calcium relieves this inhibition (Fig. 5). Complexin and synaptotagmin are both brakes and facilitators of fusion, they resemble the anchor escape mechanism that synchronizes pendulum clocks. Calcium binding to synaptotagmin releases the catch and SNARE zippering rapidly propagates and pulls the membranes together [320–323]. We are only just beginning to understand the mechanism of stabilization. However, we do not understand the mechanism of disinhibition. The rapid structural changes that underlie calcium sensing represent one of the great remaining mysteries in synaptic transmission.

5.4.1 Synaptotagmin

Synaptotagmin is an integral membrane protein of the synaptic vesicle composed of tandem calcium-binding C2 domains: C2A and C2B [324–328] (Fig. 5a). Null mutants in synaptotagmin dramatically decrease calcium-triggered, evoked synaptic vesicle release with a concomitant increase in spontaneous fusion [327, 329]. Thus, synaptotagmin acts as a brake on spontaneous fusion, pushing the vesicle release machinery into a state that is preferentially geared to calcium triggering. Mutations that alter calcium-binding affinity of synaptotagmin-1 lead to parallel change in the calcium sensitivity of synaptic vesicle release [328, 330]. Calcium stimulated interactions between synaptotagmin and the phospholipid, PIP2, have a Kd of 10 μM calcium [326], which closely matches the EC50 measured for calcium to trigger vesicle fusion [331]. Synaptotagmin is therefore the major calcium sensor for vesicle fusion, and phospholipid binding is key to its function.

The C2 domains of synaptotagmin interact with SNAREs and membranes in both a calcium-dependent and a calcium-independent manner [332–336]. C2B mutations more severely impair evoked release than C2A mutations [337–339]; however, it is likely that both calcium-binding domains coordinate during vesicle fusion through as of yet unknown mechanisms [335, 340–342]. Calcium causes the C2B binding domain to toggle between two different membrane-binding conformations: In the absence of calcium, positively charged lysine residues on the "ventral" surface of the C2B domain bind acidic phospholipids and hold the C2B domain in a horizontal configuration [343–345] (Fig. 5b). In the presence of calcium, the hydrophobic lips that surround the calcium-binding pocket penetrate the phosphatidylinositol membrane and are likely to rotate the C2 domain into a vertical orientation [346, 347] (Fig. 5c).

Fig. 5 (continued) The accessory helix (AH) of complexin holds the C-termini of SNAP25 Qc (green) and synaptobrevin away from the other SNARE helices. The synaptotagmin C2B domain (gold) sits under the SNARE complex preventing zippering beyond the 0 layer, and interacts with the plasma membrane. (**c**) *Fusing vesicle*. Upon calcium binding (black dots), the calcium-binding loops of the synaptotagmin C2B domain rotate into the plasma membrane, driving synaptotagmin out from under the SNAREs. This removes the block to fusion, allowing the SNAREs to fully zipper leading to synaptic vesicle fusion

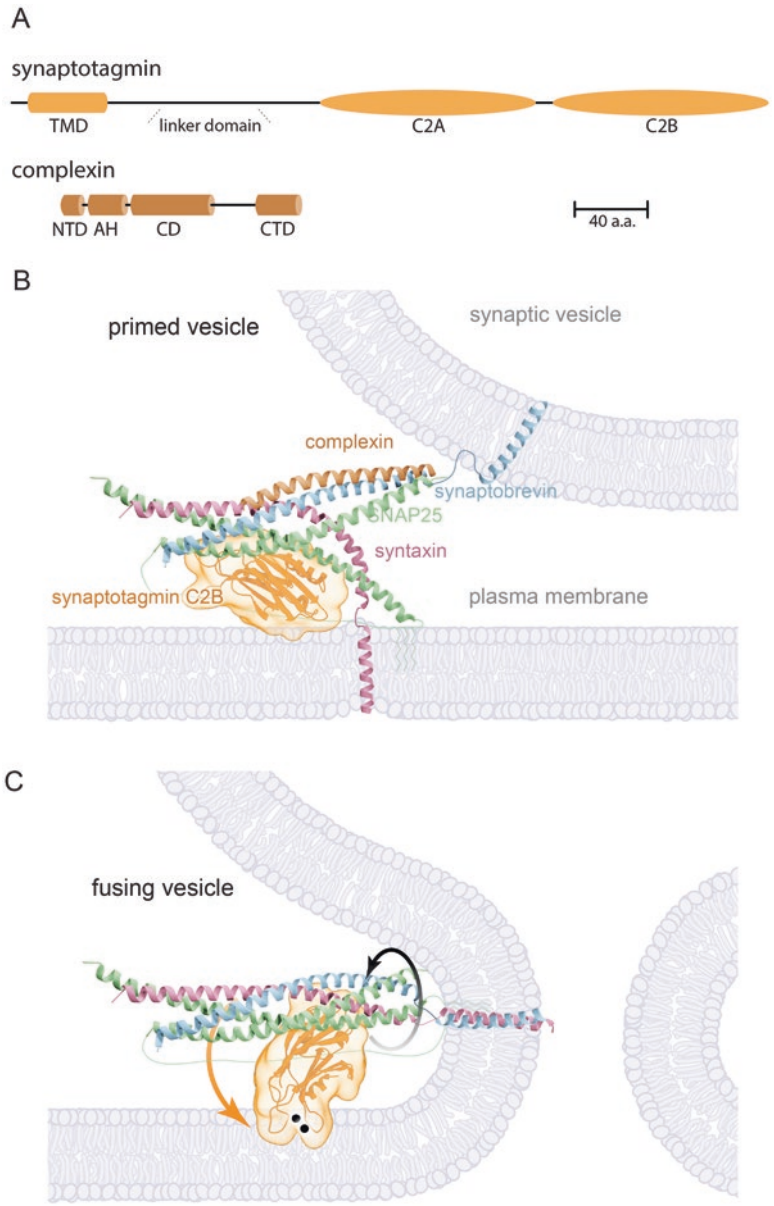

Fig. 5 Calcium disinhibits the paused state. (**a**) *Domain architecture of synaptotagmin and complexin*. Synaptotagmin is attached to synaptic vesicles via a transmembrane domain. A linker domain connects the transmembrane domain to two C2 domains. Complexin binds synaptic vesicles via its C-terminal domain (CTD). The central domain (CD) binds syntaxin and synaptobrevin across the zero layer, stabilizing the primed state. The accessory helix (AH) prevents SNARE zippering. (**b**) *Primed vesicle*. In the partially zippered SNARE complex, the central domain (CD) of complexin (brown) binds the groove between synaptobrevin (blue) and syntaxin (red).

In the horizontal configuration, the C2B domain binds the SNAP25 and syntaxin helices in the SNARE complex [348]. By binding membranes, through the polybasic ventral surface, and SNAREs via the dorsal surface, the horizontally configured C2B domain can serve as a bridge between the plasma membrane and the SNAREs [349]. Low-resolution Cryo-EM structures of C2AB fragments bound to SNARE complexes on lipid nanotubes further support the existence of this configuration [350].

The interaction between C2B and the SNARE complex is likely to mediate both positive and negative functions in membrane fusion. When reconstituted in an in vitro liposome fusion assay, synaptotagmin can act alone as both a fusion clamp in the absence of calcium, and an accelerator of fusion in the presence of calcium [351, 352].

Synaptotagmin likely promotes fusion by docking synaptic vesicles at release sites (Fig. 4a). By binding both the membrane and SNAP-25, synaptotagmin links synaptic vesicles to the plasma membrane [353]. Null mutants in synaptotagmin reduce vesicle docking by half ([354], but see also [95]), and mutations that disrupt either the membrane interface of the C2B domain or the dorsal SNAP25 interface dramatically reduce calcium-triggered evoked release [345, 348, 349, 354–356]. The calcium-independent binding of membranes and SNAREs by the C2B domain likely accounts for the positive role that synaptotagmin plays in fusion.

But this same horizontal configuration of the C2B domain might also inhibit SNARE-mediated fusion by preventing full zippering of the SNARE complex (Fig. 5b). Historically, it was believed that calcium facilitated fusion by triggering synaptotagmin to interact with SNAREs; however, it now appears that calcium instead dissociates synaptotagmin from the SNAREs to allow for rapid fusion [349]. Calcium acts as an electrostatic switch that tips the C2 domain into the membrane [346, 357]. This upright orientation would increase the tilt angle of the SNAREs [358], and might simultaneously break the contacts between the dorsal surface of C2B and SNAP-25 [349], and allow winding to proceed to the C-terminus and fusion of the membranes.

5.4.2 Complexin

Complexin is a small protein (130–150 residues). It consists of four domains: an N-terminal domain, an accessory helix, a central region, and a C-terminal domain that anchors complexin to the synaptic vesicle membrane [359, 360] (Fig. 5a). Complexin is largely unstructured in solution [361] but becomes partially helical upon interacting with membrane and the SNARE complex [362]. Except for a very weak interaction with syntaxin, complexin does not bind individual SNAREs [363]. Rather, the central region of complexin forms an α-helix that binds between syntaxin and synaptobrevin, across the zero layer. The accessory helix of complexin projects between the apposed vesicle and plasma membranes [363, 364]. Full zippering may be indirectly blocked by the steric hindrance between the accessory helix and vesicle membranes [365–367]. Alternatively, the accessory helix could interact with the membrane-proximal C-termini of synaptobrevin and the Qc-SNARE of SNAP25

[368] and stabilize a splayed configuration of SNARE C-termini (Fig. 5b). Irrespective of the precise mechanism, the key role of complexin is to stabilize the half-zippered state (Fig. 5b).

Genetic tests of complexin null mutants in both vertebrates and invertebrates indicate a positive role in vesicle priming. Together with synaptotagmin, complexin holds the vesicle in a primed but paused state. In the mouse complexin double knockout, evoked release is reduced to less than 50% [369–371]. In *Drosophila* knockouts, evoked responses are reduced to 40% [372]. In *C. elegans* knockouts, evoked responses are reduced to 10% [373, 374]. Mutations in the central helix eliminated activity of complexins from each species [374–376]. This positive role is evolutionarily ancient—complexin from sea anemone can rescue evoked responses in the mouse [377]. These data indicate that the positive role for complexin acts by binding the central helix, and stabilizing the SNARE complex.

Interestingly, complexin has a prominent role in stabilizing the docked state in worms and flies. In mammals, this role appears minimal. Complexin mutants in *C. elegans* exhibit a 73% reduction in docked vesicles as determined by electron microscopy [373]. Evoked release can be rescued by expression of constructs that contain the central helix, suggesting that complexin binding to syntaxin and synaptobrevin prevents the SNAREs from unwinding [373, 374]. Likewise, in *Drosophila,* the docked vesicles within the readily releasable pool are reduced by 50% in complexin mutants, and increased to 200% in animals overexpressing complexin [372] (see Box 1 for explanation of the readily releasable pool). In vitro studies show that vertebrate complexin can promote the docked state [378]. However, in mouse complexin mutants, vesicle docking in electron micrographs is not decreased [95, 369], and neither is the readily releasable pool as measured by hypertonic sucrose [369, 375]. In the mouse, stabilization of the docked state is less reliant on complexin, and instead may preferentially use another protein such as synaptotagmin [371, 379, 380]. In *Drosophila,* complexin and synaptotagmin mutants are additive [372]; in mouse, the double mutant resembles a synaptotagmin single mutant [371].

Along with a positive role in priming, complexin also plays a prominent role in inhibiting vesicle fusion in invertebrates. In *Drosophila* and *C. elegans*, knockouts of complexin exhibit *increased* rates of tonic miniature currents [372–374, 381]. Although tonic mini rates in the nematode are calcium-dependent, a fraction of fusions in the nematode complexin mutant are calcium-independent [373]. Inhibition of vesicle fusion is contributed by the N-terminal domain, accessory helix, amphipathic helix and C-terminal anchor [382, 383].

The inhibitory role appears to be minor in the vertebrate central nervous system. In most complexin knockout experiments, spontaneous fusion is unchanged or reduced [361, 362, 377]. However, in complexin knockdowns, an increase in spontaneous vesicle fusions has been observed in cultured neurons [384–387]. These contradictory results may arise due to differential levels of complexin, leading to different levels of vesicle priming. Alternatively, they may result from differences in the balance between the inhibitory and facilitatory functions of complexin in different organisms [362, 365–368].

What is the contribution of complexin to the primed state? When challenged with 500 mM sucrose the size of the readily releasable pool was unchanged in complexin mutants [369, 375]. By challenging with a reduced hyperosmotic challenge, 250 mM sucrose, the readily releasable pool was reduced to 50% in the complexin mutants [388]. Moreover, the profound loss of evoked release in complexin mutants could be restored by increasing calcium [375, 388]. Thus, the docked pool as measured by hypertonic sucrose is normal in total size, but the releasable pool is "reluctant" rather than "ready." These vesicles can only be recruited by either increasing calcium or by potentiating the synapse using multiple stimulations [388]. Similarly, in the calyx of Held, spontaneous release is decreased under resting conditions, but after a burst of action potentials asynchronous release is increased [389]. One possibility is that complexin plays a specific role in superpriming rather than more generally in all priming steps [390]. It is possible that high-frequency stimulation can bypass the requirement for complexin by acting on Unc13 proteins.

5.4.3 Unc13

In addition to its function in recruiting vesicles to fusion sites and opening syntaxin, Unc13 may also act again at the half-zippered stage. Unc13 is required for "superpriming" docked vesicles [391–393], in which the release machinery is poised for rapid fusion [394]. This transition is mediated by disinhibition of Unc13 by diacylglycercol (DAG) binding to the C1 domain or calcium binding to the C2 domain of Unc13 [395]. Superpriming decreases the latency between calcium influx and vesicle fusion and increases vesicle release probability [393, 396]. This transition appears to involve a large physical reorganization of Unc13 and the SNARE complex. Cryo-EM studies suggest that Unc13 can forms rings of six proteins between apposed membranes [256]. Within these rings, Unc13 can adopt two conformations: an upright orientation and a collapsed state. Because Unc13 is attached to both the synaptic vesicle and the plasma membrane, the switch in state should bring the membranes from ~21 nm apart to ~14 nm apart—a situation resembling the Rab GTPase-triggered collapse of the tethering factor EEA1 [397]. How this would alter the configuration of SNAREs and SNARE binding proteins is not known.

5.5 C-Terminal SNARE Zippering and Membrane Fusion

After the calcium-triggered release from the half-zippered state, the final steps are rapid and irreversible, involving only the SNARES and lipids themselves. C-terminal zippering releases the remaining energy stored in the SNARE proteins completing membrane fusion and delivering the membrane-bound cargo. In this section, we will briefly explain the forces preventing spontaneous membrane fusion and then describe how multimerized SNAREs might overcome these forces by guiding lipids

through a conserved set of rearrangements to merge membranes (Fig. 6). Importantly, membrane fusion must take place in an organized fashion so that lipid-bound cargo is not lost through burst membranes. Understanding the rapid interplay between SNAREs and lipids during fusion is experimentally challenging and remains one of the biggest mysteries in vesicle fusion.

Membranes do not spontaneously fuse. Membrane stabilizing forces include the hydrophobic core that minimizes solvent-exposed surfaces, elastic forces that resist

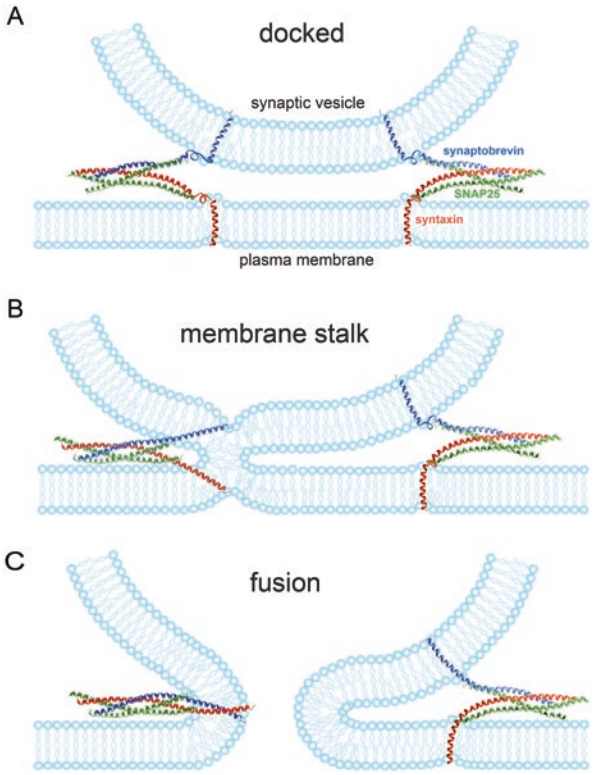

Fig. 6 Steps in membrane fusion. The high repulsive forces between lipid membranes prevent them from fusing. The SNAREs provide the energy that enables the lipid rearrangements required for fusion. This model assumes the SNAREs are not clustered in the center, but rather are in a ring at the edges of a contact zone. Such an arrangement might be required to accommodate large proteins, such as Unc13, associated with the primed state. (**a**) *Docking*. Pairing of the SNAREs brings the membranes into close proximity; winding of the SNAREs is paused at the half-zippered state. The juxtamembrane domains disrupt lipid packing locally but these unstructured regions cannot themselves drive fusion. (**b**) *Stalk formation*. Calcium binding to synaptotagmin (not shown) disinhibits SNARE winding, and propagates helix formation into the flexible juxtamembrane segments. Forcing the helices together brings the locally disrupted lipids to meet and causes the merger of the proximal leaflets into a lipid stalk. (**c**) *Fusion*. Full fusion of the two membranes requires the transfer of energy from the SNARE complex to the transmembrane domains. Coiling of the transmembrane domains of syntaxin and synaptobrevin drive charges at the C-termini into the membrane that cleaves the stalk. For simplicity the figure only shows a single SNARE winding and breaking the membrane. Vesicle fusion requires multiple, most likely flanking, SNAREs to fuse a synaptic vesicle

monolayer deformation, and repulsion generated by negatively charged phospholipid head groups [398, 399]. Charge repulsion, in particular, keeps membranes 1–2 nm apart, and this space must be dehydrated to bring the bilayers together [317]. The lipid rearrangements necessary for membrane fusion and the membrane stabilizing forces that must be overcome were initially predicted from mathematical modeling of pure lipids [400, 401]. Membrane fusion can be broken into three steps: (1) membranes are brought into proximity, (2) membrane deformation allows the merger of the proximal leaflets of the bilayer, and (3) the merger of the distal bilayers completes fusion.

To drive fusion, the stabilizing forces of lipid packing must be disrupted by deforming the membrane. Specifically, point-like protrusions lower the energy of hydration repulsion and enable the formation of a lipid stalk between the proximal leaves of the lipid bilayer [401–404]. Lipid stalks can proceed to full fusion or relax into an extended hemifused state. Intermediates in which the proximal membranes are fused can be observed by the exchange of lipids between membranes without lumenal content mixing [405–408]. In vitro, extended hemifusion intermediates can transition to full fusion [61, 409, 410]. However, in vivo, the lipid stalk likely transitions directly to full fusion [411–413]. These common lipid intermediates are present in all membrane fusion reactions [398, 414–416].

How might the SNAREs fuse membranes? The SNAREs are uniquely suited to overcome the stabilizing forces of membranes: they can force membranes together to dehydrate the intervening space, and they actively disrupt lipids by bending membranes (Fig. 6). Five characteristics of the SNAREs are central to the current models for their function in fusing membranes. First, productive SNAREs assemble in a parallel orientation [45, 50, 53, 167, 417]. Due to their parallel orientation, SNARE assembly leads to the close apposition of the transmembrane domains and hence the membranes themselves (Fig. 6a). Second, the SNARE complex must consist of at least two SNARE molecules with transmembrane domains [418]. The transmembrane domains must be inserted into both of the membranes destined to fuse [55, 56]. Third, SNAREs contain numerous basic residues in their juxtamembrane region that are likely to interact with the negatively charged head groups of lipids. Additionally, the synaptobrevin juxtamembrane region contains tandem tryptophan residues that are likely to insert into bilayers and disrupt their packing. Mutations or alterations in the positioning of these tryptophan residues disrupt fusion both in vitro [419] and in vivo [384, 420–424]. Fourth, the energy released by SNARE zippering is concentrated at the C-terminal end [171], where the transmembrane domains are located. Zippering of the SNARE proteins during core complex assembly transduces force to the transmembrane domains that can overcome barriers to fusion [56, 425]. As SNARE winding propagates to the C-termini, the transmembrane domains will be forced together and bring the lipids of vesicle and plasma membranes together and lead to the formation of a membrane stalk (Fig. 6b). Fifth, SNARE winding propagates into the helical transmembrane domains of synaptobrevin and syntaxin [171, 426–428], and thereby transfers energy generated from SNARE zippering into the vesicle and plasma membranes, and forces them together. Torque

on the transmembrane domains might force dimples in the lipid bilayer at regions of *trans* SNARE complex formation, perhaps corresponding to the point-like protrusions that are thought to be necessary to initiate the fusion of the proximal bilayers [399, 402, 418]. The transmembrane domains are therefore likely to directly disrupt lipids as SNARE assembly proceeds [56, 384, 425]. As the C-termini of the transmembrane domains of synaptobrevin and syntaxin wind around each other, they will merge the distal leaves of the bilayer, and break the barrier between vesicle lumen and extracellular space (Fig. 6c).

Together, these characteristics allow the SNAREs to dehydrate and disrupt lipid bilayers. In in vitro assays, a single SNARE complex is capable of catalyzing fusion [429, 430]. Nevertheless, this result has not been reproduced in vivo and the single SNARE complex is only sufficient to fuse highly fusogenic membranes and, even then, does so with very slow kinetics [429] and without the ability to maintain an open fusion pore [431]. This result is not surprising. Measurements of the energy released from zippering the entire SNARE motif range from 13 k_BT, for yeast exocytic SNAREs, to between 27 k_BT and 68 k_BT, for the neuronal SNAREs [171, 173, 175, 177, 432]. However, C-terminal zippering itself has only been measured to release a maximum of 27 k_BT of energy [173]. These figures are close to the theoretically calculated 40 k_BT to 100 k_BT that is needed for membrane fusion [63], but they are not quite enough. Physiologically, a single SNARE is not enough to fuse membranes. It must be getting help from some friends.

First among those friends are the SNAREs themselves, they form linked rings of complexes. Early electron microscopy studies demonstrated that SNAREs assembled into star-shaped structures with their transmembrane domains at the vertex [433]. Cryo-EM studies by Jim Rothman's group identified six SNAREs complexes sitting beneath a vesicle [434, 435]—a number that precisely matches the optimal number of SNAREs in modeling experiments [436]. Though the interactions are quite weak [437] it has been shown that both syntaxin and synaptobrevin form higher order multimers via conserved regions located in their transmembrane domains [438–440]. At the level of a fusion pore, membranes are largely rigid, thus SNAREs will be mechanically coupled, potentially allowing them to coordinate zippering [434, 436]. By aligning the transmembrane domains of the SNAREs at the vertex, the SNAREs are capable of delineating a patch of membrane where fusion can begin.

In vivo evidence for multimerization comes from a combination of the dose-dependent block provided by peptide blockers and botulinum neurotoxins as well as the cooperative action of the SNAREs themselves [441–447]. Together, these experiments have estimated between 2 and 15 SNARE complexes are needed for productive fusion [441, 444–447]. Titration of syntaxin in neurons indicated a Hill coefficient for cooperativity of 3 for the SNARE complex [90]. These data suggest that the Hill coefficient of 3–4 for calcium cooperativity [448] may not reflect calcium-binding cooperativity within synaptotagmin's C2 domains, but it rather reflects calcium-dependent conformational changes among the SNAREs [443].

5.6 Disassembly of SNARE Complexes

After vesicle fusion, the SNAREs are in the plasma membrane of the active zone in a *cis* SNARE complex. The SNAREs and other components of synaptic vesicles must be cleared from active zone to allow sustained vesicle fusion. The SNAREs must be separated from each other and sorted to their correct compartments. Studies of temperature-sensitive alleles at *Drosophila* synapses indicated that the ATPase NSF acts after membrane fusion during the recovery of synaptic vesicles [36, 449]. NSF does not directly bind the SNARE complex but binds via alpha-SNAP, which either acts as a stator to hold the complex as NSF unravels individual strands, or acts to apply reverse torque to open the complex like uncoiling a stranded rope [187, 199].

How is the *cis* SNARE complex prevented from instantly reforming? The chaperone Unc18 may remain attached to syntaxin during fusion by binding the N-terminal motif. Unc18 binding to syntaxin in the closed state would prevent it from rejoining the SNARE complex [283]. Synaptobrevin is sequestered by AP180 [450]. The EH domain protein intersectin binds synaptobrevin and SNAP-25 [451, 452]. It is not known where in the synapse the SNAREs are separated. NSF may act at the plasma membrane to unwind SNAREs; alternatively, disassembly may take places at synaptic endosomes [453].

6 Summary

Rounds of SNARE assembly and disassembly lie at the center of all vesicular trafficking [454]. Assembly of the SNAREs into a four-helix bundle drives fusion of synaptic vesicles with the plasma membrane and thereby mediates the release of neurotransmitter [455]. αSNAP and the ATPase NSF, meanwhile, survey the landscape for unproductive SNARE assembly—actively disassembling them. The assembly of SNAREs is carefully orchestrated by Unc18 and Unc13 [143]. Unc13 tethers vesicles and opens syntaxin, allowing SNARE assembly to begin. Unc18 provides a template on which syntaxin and synaptobrevin are proofread to ensure correct assembly. Together, Unc13 and Unc18 ensure that productive SNARE complexes are formed. The SNAREs are held in a half-zippered state by complexin and synaptotagmin until calcium triggers full SNARE zippering and membrane merger. After membrane fusion and release of neurotransmitter, the entwined *cis* SNAREs are pulled apart by NSF, which reenergizes the system for further rounds of fusion.

This model is generally accepted; nevertheless, controversies and mysteries still remain. An important lesson from the last few decades is that the strength of protein-protein interactions does not necessarily translate to conserved mechanistic features. For example, the templating role for SM proteins, despite its importance, was notoriously difficult to find due to its relatively transient nature. How complexin and synaptotagmin act on SNARE assembly also remains an enduring enigma, very

likely due to the rapid time scale between calcium entry and fusion. Perhaps the holy grail of mysteries remains how the assembly of SNAREs interacts with lipids to guide them through membrane fusion.

Acknowledgments We thank Enfu Hui and Edwin R. Chapman for providing versions of Figs. 1 and 3. Thanks also to Winfried Weissenhorn, Dirk Fasshauer, and Reinhard Jahn for allowing us to use and modify their images for Fig. 1. We thank M. Wayne Davis, Brian Mueller, and Britt Graham for reading the manuscript.

References

1. Trimble WS, Cowan DM, Scheller RH. VAMP-1: a synaptic vesicle-associated integral membrane protein. Proc Natl Acad Sci U S A. 1988;85:4538–42. https://doi.org/10.1073/pnas.85.12.4538.
2. Inoue A, Obata K, Akagawa K. Cloning and sequence analysis of cDNA for a neuronal cell membrane antigen, HPC-1. J Biol Chem. 1992;267:10613–9.
3. Bennett MK, Calakos N, Scheller RH. Syntaxin: a synaptic protein implicated in docking of synaptic vesicles at presynaptic active zones. Science. 1992;257:255–9. https://doi.org/10.1126/science.1321498.
4. Oyler GA, Higgins GA, Hart RA, Battenberg E, Billingsley M, Bloom FE, et al. The identification of a novel synaptosomal-associated protein, SNAP-25, differentially expressed by neuronal subpopulations. J Cell Biol. 1989;109:3039–52. https://doi.org/10.1083/jcb.109.6.3039.
5. Maus L, Lee C, Altas B, Sertel SM, Weyand K, Rizzoli SO, et al. Ultrastructural correlates of presynaptic functional heterogeneity in hippocampal synapses. Cell Rep. 2020;30:3632–43.e8. https://doi.org/10.1016/j.celrep.2020.02.083.
6. Brennwald P, Kearns B, Champion K, Keranen S, Bankaitis V, Novick P. Sec9 is a SNAP-25-like component of a yeast SNARE complex that may be the effector of Sec4 function in exocytosis. Cell. 1994;79:245–58. https://doi.org/10.1016/0092-8674(94)90194-5.
7. Novick P, Field C, Schekman R. Identification of 23 complementation groups required for post-translational events in the yeast secretory pathway. Cell. 1980;21:205–15. https://doi.org/10.1016/0092-8674(80)90128-2.
8. Burgen AS, Dickens F, Zatman LJ. The action of botulinum toxin on the neuro-muscular junction. J Physiol. 1949;109:10–24. https://doi.org/10.1113/jphysiol.1949.sp004364.
9. Blasi J, Chapman ER, Link E, Binz T, Yamasaki S, De Camilli P, et al. Botulinum neurotoxin A selectively cleaves the synaptic protein SNAP-25. Nature. 1993;365:160–3. https://doi.org/10.1038/365160a0.
10. Blasi J, Chapman ER, Yamasaki S, Binz T, Niemann H, Jahn R. Botulinum neurotoxin C1 blocks neurotransmitter release by means of cleaving HPC-1/syntaxin. EMBO J. 1993;12:4821–8. https://doi.org/10.1002/j.1460-2075.1993.tb06171.x.
11. Link E, Edelmann L, Chou JH, Binz T, Yamasaki S, Eisel U, et al. Tetanus toxin action: inhibition of neurotransmitter release linked to synaptobrevin proteolysis. Biochem Biophys Res Commun. 1992;189:1017–23. https://doi.org/10.1016/0006-291X(92)92305-H.
12. Schiavo G, Benfenati F, Poulain B, Rossetto O, Polverino de Laureto P, DasGupta BR, et al. Tetanus and botulinum-B neurotoxins block neurotransmitter release by proteolytic cleavage of synaptobrevin. Nature. 1992;359:832–5. https://doi.org/10.1038/359832a0.
13. Marsal J, Ruiz-Montasell B, Blasi J, Moreira JE, Contreras D, Sugimori M, et al. Block of transmitter release by botulinum C1 action on syntaxin at the squid giant synapse. Proc Natl Acad Sci U S A. 1997;94:14871–6. https://doi.org/10.1073/pnas.94.26.14871.

14. O'Connor V, Heuss C, De Bello WM, Dresbach T, Charlton MP, Hunt JH, et al. Disruption of syntaxin-mediated protein interactions blocks neurotransmitter secretion. Proc Natl Acad Sci U S A. 1997;94:12186–91. https://doi.org/10.1073/pnas.94.22.12186.
15. Deitcher DL, Ueda A, Stewart BA, Burgess RW, Kidokoro Y, Schwarz TL. Distinct requirements for evoked and spontaneous release of neurotransmitter are revealed by mutations in the Drosophila gene neuronal-synaptobrevin. J Neurosci. 1998;18:2028–39. https://doi.org/10.1523/JNEUROSCI.18-06-02028.1998.
16. Broadie K, Prokop A, Bellen HJ, O'Kane CJ, Schulze KL, Sweeney ST. Syntaxin and synaptobrevin function downstream of vesicle docking in *Drosophila*. Neuron. 1995;15:663–73. https://doi.org/10.1016/0896-6273(95)90154-X.
17. Schoch S, Deak F, Konigstorfer A, Mozhayeva M, Sara Y, Südhof TC, et al. SNARE function analyzed in synaptobrevin/VAMP knockout mice. Science. 2001;294:1117–22. https://doi.org/10.1126/science.1064335.
18. Washbourne P, Thompson PM, Carta M, Costa ET, Mathews JR, Lopez-Bendito G, et al. Genetic ablation of the t-SNARE SNAP-25 distinguishes mechanisms of neuroexocytosis. Nat Neurosci. 2002;5:19–26. https://doi.org/10.1038/nn783.
19. Vilinsky I, Stewart BA, Drummond JA, Robinson IM, Deitcher DL. A Drosophila SNAP-25 null mutant reveals context-dependent redundancy with SNAP-24 in neurotransmission. Genetics. 2002;162:259–71. https://doi.org/10.1093/genetics/162.1.259.
20. Hammarlund M, Palfreyman MT, Watanabe S, Olsen S, Jorgensen EM. Open syntaxin docks synaptic vesicles. PLoS Biol. 2007;5:e198. https://doi.org/10.1371/journal.pbio.0050198.
21. Balch WE, Dunphy WG, Braell WA, Rothman JE. Reconstitution of the transport of protein between successive compartments of the Golgi measured by the coupled incorporation of N-acetylglucosamine. Cell. 1984;39:405–16. https://doi.org/10.1016/0092-8674(84)90019-9.
22. Balch WE, Glick BS, Rothman JE. Sequential intermediates in the pathway of intercompartmental transport in a cell-free system. Cell. 1984;39:525–36. https://doi.org/10.1016/0092-8674(84)90459-8.
23. Block MR, Glick BS, Wilcox CA, Wieland FT, Rothman JE. Purification of an N-ethylmaleimide-sensitive protein catalyzing vesicular transport. Proc Natl Acad Sci U S A. 1988;85:7852–6. https://doi.org/10.1073/pnas.85.21.7852.
24. Wilson DW, Wilcox CA, Flynn GC, Chen E, Kuang WJ, Henzel WJ, et al. A fusion protein required for vesicle-mediated transport in both mammalian cells and yeast. Nature. 1989;339:355–9. https://doi.org/10.1038/339355a0.
25. Eakle KA, Bernstein M, Emr SD. Characterization of a component of the yeast secretion machinery: identification of the SEC18 gene product. Mol Cell Biol. 1988;8:4098–109. https://doi.org/10.1128/mcb.8.10.4098-4109.1988.
26. Ariel P, Ryan TA. New Insights Into Molecular Players Involved in Neurotransmitter Release. Physiology. 2012;27:15–24. https://doi.org/10.1152/physiol.00035.2011.
27. Clary DO, Griff IC, Rothman JE. SNAPs, a family of NSF attachment proteins involved in intracellular membrane fusion in animals and yeast. Cell. 1990;61:709–21. https://doi.org/10.1016/0092-8674(90)90482-T.
28. Söllner T, Whiteheart SW, Brunner M, Erdjument-Bromage H, Geromanos S, Tempst P, et al. SNAP receptors implicated in vesicle targeting and fusion. Nature. 1993;362:318–24. https://doi.org/10.1038/362318a0.
29. Bock JB, Matern HT, Peden AA, Scheller RH. A genomic perspective on membrane compartment organization. Nature. 2001;409:839–41. https://doi.org/10.1038/35057024.
30. Jahn R, Lang T, Südhof TC. Membrane fusion. Cell. 2003;112:519–33. https://doi.org/10.1016/S0092-8674(03)00112-0.
31. Rothman JE. Intracellular membrane fusion. Adv Second Messenger Phosphoprotein Res. 1994;29:81–96. https://doi.org/10.1016/s1040-7952(06)80008-x.
32. Söllner T, Bennett MK, Whiteheart SW, Scheller RH, Rothman JE. A protein assembly-disassembly pathway *in vitro* that may correspond to sequential steps of synaptic vesicle docking, activation, and fusion. Cell. 1993;75:409–18. https://doi.org/10.1016/0092-8674(93)90376-2.

33. Mayer A, Wickner W, Haas A. Sec18p (NSF)-driven release of Sec17p (alpha-SNAP) can precede docking and fusion of yeast vacuoles. Cell. 1996;85:83–94. https://doi.org/10.1016/S0092-8674(00)81084-3.
34. Nichols BJ, Ungermann C, Pelham HR, Wickner WT, Haas A. Homotypic vacuolar fusion mediated by t- and v-SNAREs. Nature. 1997;387:199–202. https://doi.org/10.1038/387199a0.
35. Grote E, Carr CM, Novick PJ. Ordering the final events in yeast exocytosis. J Cell Biol. 2000;151:439–52. https://doi.org/10.1083/jcb.151.2.439.
36. Littleton JT, Chapman ER, Kreber R, Garment MB, Carlson SD, Ganetzky B. Temperature-sensitive paralytic mutations demonstrate that synaptic exocytosis requires SNARE complex assembly and disassembly. Neuron. 1998;21:401–13. https://doi.org/10.1016/S0896-6273(00)80549-8.
37. Cao X, Ballew N, Barlowe C. Initial docking of ER-derived vesicles requires Uso1p and Ypt1p but is independent of SNARE proteins. EMBO J. 1998;17:2156–65. https://doi.org/10.1093/emboj/17.8.2156.
38. Weber T, Zemelman BV, McNew JA, Westermann B, Gmachl MJ, Parlati F, et al. SNAREpins: minimal machinery for membrane fusion. Cell. 1998;92:759–72. https://doi.org/10.1016/S0092-8674(00)81404-X.
39. Hu C, Ahmed M, Melia TJ, Söllner TH, Mayer T, Rothman JE. Fusion of cells by flipped SNAREs. Science. 2003;300:1745–9. https://doi.org/10.1126/science.1084909.
40. Fasshauer D, Sutton RB, Brunger AT, Jahn R. Conserved structural features of the synaptic fusion complex: SNARE proteins reclassified as Q-and R-SNAREs. Proc Natl Acad Sci U S A. 1998;95:15781–6. https://doi.org/10.1073/pnas.95.26.15781.
41. Kloepper TH, Kienle CN, Fasshauer D. SNAREing the basis of multicellularity: consequences of protein family expansion during evolution. Mol Biol Evol. 2008;25:2055. https://doi.org/10.1093/molbev/msn151.
42. Kloepper TH, Kienle CN, Fasshauer D. An elaborate classification of SNARE proteins sheds light on the conservation of the eukaryotic endomembrane system. Mol Biol Cell. 2007;18:3463–71. https://doi.org/10.1091/mbc.e07-03-0193.
43. Kienle N, Kloepper TH, Fasshauer D. Phylogeny of the SNARE vesicle fusion machinery yields insights into the conservation of the secretory pathway in fungi. BMC Evol Biol. 2009;9:19. https://doi.org/10.1186/1471-2148-9-19.
44. Hong W, Lev S. Tethering the assembly of SNARE complexes. Trends Cell Biol. 2014;24:35–43. https://doi.org/10.1016/j.tcb.2013.09.006.
45. Fasshauer D, Eliason WK, Brünger AT, Jahn R. Identification of a minimal core of the synaptic SNARE complex sufficient for reversible assembly and disassembly. Biochemistry. 1998;37:10354–62. https://doi.org/10.1021/bi980542h.
46. Fasshauer D, Antonin W, Margittai M, Pabst S, Jahn R. Mixed and non-cognate SNARE complexes. Characterization of assembly and biophysical properties. J Biol Chem. 1999;274:15440–6. https://doi.org/10.1074/jbc.274.22.15440.
47. Liang B, Kiessling V, Tamm LK. Prefusion structure of syntaxin-1A suggests pathway for folding into neuronal *trans*-SNARE complex fusion intermediate. Proc Natl Acad Sci U S A. 2013;110:19384–9. https://doi.org/10.1073/pnas.1314699110.
48. Lakomek N-A, Yavuz H, Jahn R, Pérez-Lara Á. Structural dynamics and transient lipid binding of synaptobrevin-2 tune SNARE assembly and membrane fusion. Proc Natl Acad Sci U S A. 2019;116:8699–708. https://doi.org/10.1073/pnas.1813194116.
49. Wang C, Tu J, Zhang S, Cai B, Liu Z, Hou S, et al. Different regions of synaptic vesicle membrane regulate VAMP2 conformation for the SNARE assembly. Nat Commun. 2020;11:1531. https://doi.org/10.1038/s41467-020-15270-4.
50. Sutton RB, Fasshauer D, Jahn R, Brunger AT. Crystal structure of a SNARE complex involved in synaptic exocytosis at 2.4 A resolution. Nature. 1998;395:347–53. https://doi.org/10.1038/26412.
51. Fasshauer D, Antonin W, Subramaniam V, Jahn R. SNARE assembly and disassembly exhibit a pronounced hysteresis. Nat Struct Biol. 2002;9:144–51. https://doi.org/10.1038/nsb750.

52. Hayashi T, McMahon H, Yamasaki S, Binz T, Hata Y, Südhof TC, et al. Synaptic vesicle membrane fusion complex: action of clostridial neurotoxins on assembly. EMBO J. 1994;13:5051–61. https://doi.org/10.1002/j.1460-2075.1994.tb06834.x.
53. Hanson PI, Roth R, Morisaki H, Jahn R, Heuser JE. Structure and conformational changes in NSF and its membrane receptor complexes visualized by quick-freeze/deep-etch electron microscopy. Cell. 1997;90:523–35. https://doi.org/10.1016/S0092-8674(00)80512-7.
54. Baumert M, Maycox PR, Navone F, De Camilli P, Jahn R. Synaptobrevin: an integral membrane protein of 18,000 daltons present in small synaptic vesicles of rat brain. EMBO J. 1989;8:379–84. https://doi.org/10.1002/j.1460-2075.1989.tb03388.x.
55. Parlati F, McNew JA, Fukuda R, Miller R, Söllner TH, Rothman JE. Topological restriction of SNARE-dependent membrane fusion. Nature. 2000;407:194–8. https://doi.org/10.1038/35025076.
56. McNew JA, Weber T, Parlati F, Johnston RJ, Melia TJ, Söllner TH, et al. Close is not enough: SNARE-dependent membrane fusion requires an active mechanism that transduces force to membrane anchors. J Cell Biol. 2000;150:105–17. https://doi.org/10.1083/jcb.150.1.105.
57. Fdez E, Martínez-Salvador M, Beard M, Woodman P, Hilfiker S. Transmembrane-domain determinants for SNARE-mediated membrane fusion. J Cell Sci. 2010;123:2473–80. https://doi.org/10.1242/jcs.061325.
58. Giraudo CG, Hu C, You D, Slovic AM, Mosharov EV, Sulzer D, et al. SNAREs can promote complete fusion and hemifusion as alternative outcomes. J Cell Biol. 2005;170:249–60. https://doi.org/10.1083/jcb.200501093.
59. Grote E, Baba M, Ohsumi Y, Novick PJ. Geranylgeranylated SNAREs are dominant inhibitors of membrane fusion. J Cell Biol. 2000;151:453–66. https://doi.org/10.1083/jcb.151.2.453.
60. Ngatchou AN, Kisler K, Fang Q, Walter AM, Zhao Y, Bruns D, et al. Role of the synaptobrevin C terminus in fusion pore formation. Proc Natl Acad Sci U S A. 2010;107:18463–8. https://doi.org/10.1073/pnas.100672710.
61. Xu Y, Zhang F, Su Z, McNew JA, Shin YK. Hemifusion in SNARE-mediated membrane fusion. Nat Struct Mol Biol. 2005;12:417–22. https://doi.org/10.1038/nsmb921.
62. Zhou P, Bacaj T, Yang X, Pang ZP, Südhof TC. Lipid-anchored SNAREs lacking transmembrane regions fully support membrane fusion during neurotransmitter release. Neuron. 2013;80:470–83. https://doi.org/10.1016/j.neuron.2013.09.010.
63. Cohen FS, Melikyan GB. The energetics of membrane fusion from binding, through hemifusion, pore formation, and pore enlargement. J Membr Biol. 2004;199:1–14. https://doi.org/10.1007/s00232-004-0669-8.
64. Kádková A, Radecke J, Sørensen JB. The SNAP-25 protein family. Neuroscience. 2019;420:50–71. https://doi.org/10.1016/j.neuroscience.2018.09.020.
65. Fukuda R, McNew JA, Weber T, Parlati F, Engel T, Nickel W, et al. Functional architecture of an intracellular membrane t-SNARE. Nature. 2000;407:198–202. https://doi.org/10.1038/35025084.
66. Nagy G, Milosevic I, Mohrmann R, Wiederhold K, Walter AM, Sørensen JB. The SNAP-25 linker as an adaptation toward fast exocytosis. Mol Biol Cell. 2008;19:3769–81. https://doi.org/10.1091/mbc.e07-12-1218.
67. Dietrich LE, Boeddinghaus C, LaGrassa TJ, Ungermann C. Control of eukaryotic membrane fusion by N-terminal domains of SNARE proteins. Biochim Biophys Acta. 1641;2003:111–9. https://doi.org/10.1016/S0167-4889(03)00094-6.
68. Fernandez I, Ubach J, Dulubova I, Zhang X, Südhof TC, Rizo J. Three-dimensional structure of an evolutionarily conserved N-terminal domain of syntaxin 1A. Cell. 1998;94:841–9. https://doi.org/10.1016/S0092-8674(00)81742-0.
69. Filippini F, Rossi V, Galli T, Budillon A, D'Urso M, D'Esposito M. Longins: a new evolutionary conserved VAMP family sharing a novel SNARE domain. Trends Biochem Sci. 2001;26:407–9. https://doi.org/10.1016/S0968-0004(01)01861-8.
70. Misura KM, Bock JB, Gonzalez LC Jr, Scheller RH, Weis WI. Three-dimensional structure of the amino-terminal domain of syntaxin 6, a SNAP-25 C homolog. Proc Natl Acad Sci U S A. 2002;99:9184–9. https://doi.org/10.1073/pnas.132274599.

71. Wade N, Bryant NJ, Connolly LM, Simpson RJ, Luzio JP, Piper RC, et al. Syntaxin 7 Complexes with Mouse Vps10p Tail Interactor 1b, Syntaxin 6, Vesicle-associated Membrane Protein (VAMP)8, and VAMP7 in B16 Melanoma Cells. J Biol Chem. 2001;276:19820–7. https://doi.org/10.1074/jbc.M010838200.
72. Bock JB, Lin RC, Scheller RH. A New Syntaxin Family Member Implicated in Targeting of Intracellular Transport Vesicles. J Biol Chem. 1996;271:17961–5. https://doi.org/10.1074/jbc.271.30.17961.
73. Dulubova I, Sugita S, Hill S, Hosaka M, Fernandez I, Südhof TC, et al. A conformational switch in syntaxin during exocytosis: role of munc18. EMBO J. 1999;18:4372–82. https://doi.org/10.1093/emboj/18.16.4372.
74. Misura KM, Scheller RH, Weis WI. Three-dimensional structure of the neuronal-Sec1-syntaxin 1a complex. Nature. 2000;404:355–62. https://doi.org/10.1038/35006120.
75. Daste F, Galli T, Tareste D. Structure and function of longin SNAREs. J Cell Sci. 2015;128:4263–72. https://doi.org/10.1242/jcs.178574.
76. Tochio H, Tsui MMK, Banfield DK, Zhang M. An Autoinhibitory mechanism for non-syntaxin SNARE proteins revealed by the structure of Ykt6p. Science. 2001;293:698–702. https://doi.org/10.1126/science.1062950.
77. Lürick A, Kuhlee A, Brocker C, Kummel D, Raunser S, Ungermann C. The Habc domain of the SNARE Vam3 interacts with the HOPS tethering complex to facilitate vacuole fusion. J Biol Chem. 2015;290:5405–13. https://doi.org/10.1074/jbc.M114.631465.
78. Vardar G, Salazar-Lázaro A, Brockmann M, Weber-Boyvat M, Zobel S, Kumbol VW-A, et al. Reexamination of N-terminal domains of syntaxin-1 in vesicle fusion from central murine synapses. elife. 2021;10:e69498. https://doi.org/10.7554/eLife.69498.
79. Zhou P, Pang ZP, Yang X, Zhang Y, Rosenmund C, Bacaj T, et al. Syntaxin-1 N-peptide and Habc-domain perform distinct essential functions in synaptic vesicle fusion. EMBO J. 2013;32:159–71. https://doi.org/10.1038/emboj.2012.307.
80. Rathore SS, Bend EG, Yu H, Hammarlund M, Jorgensen EM, Shen J. Syntaxin N-terminal peptide motif is an initiation factor for the assembly of the SNARE-Sec1/Munc18 membrane fusion complex. Proc Natl Acad Sci U S A. 2010;107:22399–406. https://doi.org/10.1073/pnas.1012997108.
81. De Franceschi N, Wild K, Schlacht A, Dacks JB, Sinning I, Filippini F. Longin and GAF domains: structural evolution and adaptation to the subcellular trafficking machinery: structure and evolution of longin domains. Traffic. 2014;15:104–21. https://doi.org/10.1111/tra.12124.
82. Suer S, Misra S, Saidi LF, Hurley JH. Structure of the GAT domain of human GGA1: a syntaxin amino-terminal domain fold in an endosomal trafficking adaptor. Proc Natl Acad Sci U S A. 2003;100:4451–6. https://doi.org/10.1073/pnas.0831133100.
83. Dulubova I, Yamaguchi T, Wang Y, Südhof TC, Rizo J. Vam3p structure reveals conserved and divergent properties of syntaxins. Nat Struct Biol. 2001;8:258–64. https://doi.org/10.1038/85012.
84. Parra-Rivas LA, Palfreyman MT, Vu TN, Jorgensen EM. Interspecies complementation identifies a pathway to assemble SNAREs. iScience. 2022;25:104506. https://doi.org/10.1016/j.isci.2022.104506.
85. Borisovska M, Zhao Y, Tsytsyura Y, Glyvuk N, Takamori S, Matti U, et al. v-SNAREs control exocytosis of vesicles from priming to fusion. EMBO J. 2005;24:2114–26. https://doi.org/10.1038/sj.emboj.7600696.
86. Bhattacharya S, Stewart BA, Niemeyer BA, Burgess RW, McCabe BD, Lin P, et al. Members of the synaptobrevin/vesicle-associated membrane protein (VAMP) family in *Drosophila* are functionally interchangeable *in vivo* for neurotransmitter release and cell viability. Proc Natl Acad Sci U S A. 2002;99:13867–72. https://doi.org/10.1073/pnas.202335999.
87. Holt M, Varoqueaux F, Wiederhold K, Takamori S, Urlaub H, Fasshauer D, et al. Identification of SNAP-47, a novel Qbc-SNARE with ubiquitous expression. J Biol Chem. 2006;281:17076–83. https://doi.org/10.1074/jbc.M513838200.

88. Sørensen JB, Nagy G, Varoqueaux F, Nehring RB, Brose N, Wilson MC, et al. Differential control of the releasable vesicle pools by SNAP-25 splice variants and SNAP-23. Cell. 2003;114:75–86. https://doi.org/10.1016/S0092-8674(03)00477-X.
89. Fujiwara T, Mishima T, Kofuji T, Chiba T, Tanaka K, Yamamoto A, et al. Analysis of knock-out mice to determine the role of HPC-1/syntaxin 1A in expressing synaptic plasticity. J Neurosci. 2006;26:5767–76. https://doi.org/10.1523/JNEUROSCI.0289-06.2006.
90. Arancillo M, Min SW, Gerber S, Munster-Wandowski A, Wu YJ, Herman M, et al. Titration of Syntaxin1 in mammalian synapses reveals multiple roles in vesicle docking, priming, and release probability. J Neurosci. 2013;33:16698–714. https://doi.org/10.1523/JNEUROSCI.0187-13.2013.
91. Liu Y, Barlowe C. Analysis of Sec22p in endoplasmic reticulum/Golgi transport reveals cellular redundancy in SNARE protein function. Mol Biol Cell. 2002;13:3314–24. https://doi.org/10.1091/mbc.e02-04-0204.
92. Fischer von Mollard G, Stevens TH. The *Saccharomyces cerevisiae* v-SNARE Vti1p is required for multiple membrane transport pathways to the vacuole. Mol Biol Cell. 1999;10:1719–32. https://doi.org/10.1091/mbc.10.6.1719.
93. Darsow T, Rieder SE, Emr SD. A multispecificity syntaxin homologue, Vam3p, essential for autophagic and biosynthetic protein transport to the vacuole. J Cell Biol. 1997;138:517–29. https://doi.org/10.1083/jcb.138.3.517.
94. Burgess RW, Deitcher DL, Schwarz TL. The synaptic protein syntaxin1 is required for cellularization of *Drosophila* embryos. J Cell Biol. 1997;138:861–75. https://doi.org/10.1083/jcb.138.4.861.
95. Imig C, Min S-W, Krinner S, Arancillo M, Rosenmund C, Südhof TC, et al. The morphological and molecular nature of synaptic vesicle priming at presynaptic active zones. Neuron. 2014;84:416–31. https://doi.org/10.1016/j.neuron.2014.10.009.
96. Emperador-Melero J, Kaeser PS. Assembly of the presynaptic active zone. Curr Opin Neurobiol. 2020;63:95–103. https://doi.org/10.1016/j.conb.2020.03.008.
97. Xu-Friedman MA, Harris KM, Regehr WG. Three-dimensional comparison of ultrastructural characteristics at depressing and facilitating synapses onto cerebellar Purkinje cells. J Neurosci. 2001;21:6666–72. https://doi.org/10.1523/JNEUROSCI.21-17-06666.2001.
98. Schikorski T, Stevens CF. Quantitative ultrastructural analysis of hippocampal excitatory synapses. J Neurosci. 1997;17:5858–67. https://doi.org/10.1523/JNEUROSCI.17-15-05858.1997.
99. Schikorski T, Stevens CF. Morphological correlates of functionally defined synaptic vesicle populations. Nat Neurosci. 2001;4:391–5. https://doi.org/10.1038/86042.
100. Siksou L, Varoqueaux F, Pascual O, Triller A, Brose N, Marty S. A common molecular basis for membrane docking and functional priming of synaptic vesicles. Eur J Neurosci. 2009;30:49–56. https://doi.org/10.1111/j.1460-9568.2009.06811.x.
101. Thanawala MS, Regehr WG. Determining synaptic parameters using high-frequency activation. J Neurosci Methods. 2016;264:136–52. https://doi.org/10.1016/j.jneumeth.2016.02.021.
102. Rosenmund C, Stevens CF. Definition of the readily releasable pool of vesicles at hippocampal synapses. Neuron. 1996;16:1197–207. https://doi.org/10.1016/S0896-6273(00)80146-4.
103. Price A, Wickner W, Ungermann C. Proteins needed for vesicle budding from the Golgi complex are also required for the docking step of homotypic vacuole fusion. J Cell Biol. 2000;148:1223–30. https://doi.org/10.1083/jcb.148.6.1223.
104. Ungermann C, Sato K, Wickner W. Defining the functions of *trans*-SNARE pairs. Nature. 1998;396:543–8. https://doi.org/10.1038/25069.
105. Yu IM, Hughson FM. Tethering factors as organizers of intracellular vesicular traffic. Annu Rev Cell Dev Biol. 2010;26:137–56. https://doi.org/10.1146/annurev.cellbio.042308.113327.
106. Santana-Molina C, Gutierrez F, Devos DP. Homology and modular evolution of CATCHR at the origin of the eukaryotic endomembrane system. Genome Biol Evol. 2021;13:evab125. https://doi.org/10.1093/gbe/evab125.

107. Chou H-T, Dukovski D, Chambers MG, Reinisch KM, Walz T. CATCHR, HOPS and CORVET tethering complexes share a similar architecture. Nat Struct Mol Biol. 2016;23:761–3. https://doi.org/10.1038/nsmb.3264.
108. James DJ, Martin TFJ. CAPS and Munc13: CATCHRs that SNARE vesicles. Front Endocrinol. 2013;4:187. https://doi.org/10.3389/fendo.2013.00187.
109. Brunet S, Sacher M. Are all multisubunit tethering complexes bona fide tethers? Traffic. 2014;15:1282–7. https://doi.org/10.1111/tra.12200.
110. Wiederkehr A, Du Y, Pypaert M, Ferro-Novick S, Novick P. Sec3p is needed for the spatial regulation of secretion and for the inheritance of the cortical endoplasmic reticulum. Mol Biol Cell. 2003;14:4770–82. https://doi.org/10.1091/mbc.e03-04-0229.
111. Wiederkehr A, De Craene JO, Ferro-Novick S, Novick P. Functional specialization within a vesicle tethering complex: bypass of a subset of exocyst deletion mutants by Sec1p or Sec4p. J Cell Biol. 2004;167:875–87. https://doi.org/10.1083/jcb.200408001.
112. Finger FP, Hughes TE, Novick P. Sec3p is a spatial landmark for polarized secretion in budding yeast. Cell. 1998;92:559–71. https://doi.org/10.1016/S0092-8674(00)80948-4.
113. VanRheenen SM, Cao X, Lupashin VV, Barlowe C, Waters MG. Sec35p, a novel peripheral membrane protein, is required for ER to Golgi vesicle docking. J Cell Biol. 1998;141:1107–19. https://doi.org/10.1083/jcb.141.5.1107.
114. Novick P, Medkova M, Dong G, Hutagalung A, Reinisch K, Grosshans B. Interactions between Rabs, tethers, SNAREs and their regulators in exocytosis. Biochem Soc Trans. 2006;34:683–6. https://doi.org/10.1042/BST0340683.
115. Sapperstein SK, Lupashin VV, Schmitt HD, Waters MG. Assembly of the ER to Golgi SNARE complex requires Uso1p. J Cell Biol. 1996;132:755–67. https://doi.org/10.1083/jcb.132.5.755.
116. Hammarlund M, Watanabe S, Schuske K, Jorgensen EM. CAPS and syntaxin dock dense core vesicles to the plasma membrane in neurons. J Cell Biol. 2008;180:483–91. https://doi.org/10.1083/jcb.200708018.
117. Li W, Ma C, Guan R, Xu Y, Tomchick Diana R, Rizo J. The crystal structure of a Munc13 C-terminal module exhibits a remarkable similarity to vesicle tethering factors. Structure. 2011;19:1443–55. https://doi.org/10.1016/j.str.2011.07.012.
118. Quade B, Camacho M, Zhao X, Orlando M, Trimbuch T, Xu J, et al. Membrane bridging by Munc13-1 is crucial for neurotransmitter release. elife. 2019;8:e42806. https://doi.org/10.7554/eLife.42806.
119. Liu X, Seven AB, Camacho M, Esser V, Xu J, Trimbuch T, et al. Functional synergy between the Munc13 C-terminal C1 and C2 domains. elife. 2016;5:e13696. https://doi.org/10.7554/eLife.13696.
120. Xu J, Camacho M, Xu Y, Esser V, Liu X, Trimbuch T, et al. Mechanistic insights into neurotransmitter release and presynaptic plasticity from the crystal structure of Munc13-1 C1C2BMUN. elife. 2017;6:e22567. https://doi.org/10.7554/eLife.22567.
121. Pei J, Ma C, Rizo J, Grishin NV. Remote homology between Munc13 MUN domain and vesicle tethering complexes. J Mol Biol. 2009;391:509–17. https://doi.org/10.1016/j.jmb.2009.06.054.
122. Ungermann C, Kümmel D. Structure of membrane tethers and their role in fusion. Traffic. 2019;20:479–90. https://doi.org/10.1111/tra.12655.
123. Richmond JE, Weimer RM, Jorgensen EM. An open form of syntaxin bypasses the requirement for UNC-13 in vesicle priming. Nature. 2001;412:338–41. https://doi.org/10.1038/35085583.
124. Ma C, Li W, Xu Y, Rizo J. Munc13 mediates the transition from the closed syntaxin-Munc18 complex to the SNARE complex. Nat Struct Mol Biol. 2011;18:542–9. https://doi.org/10.1038/nsmb.2047.
125. Gong J, Wang X, Cui C, Qin Y, Jin Z, Ma C, et al. Exploring the two coupled conformational changes that activate the Munc18-1/Syntaxin-1 complex. Front Mol Neurosci. 2021;14:785696. https://doi.org/10.3389/fnmol.2021.785696.

126. Magdziarek M, Bolembach AA, Stepien KP, Quade B, Liu X, Rizo J. Re-examining how Munc13-1 facilitates opening of syntaxin-1. Protein Sci. 2020;29:1440–58. https://doi.org/10.1002/pro.3844.
127. Yang X, Wang S, Sheng Y, Zhang M, Zou W, Wu L, et al. Syntaxin opening by the MUN domain underlies the function of Munc13 in synaptic-vesicle priming. Nat Struct Mol Biol. 2015;22:547–54. https://doi.org/10.1038/nsmb.3038.
128. Betz A, Okamoto M, Benseler F, Brose N. Direct interaction of the rat *unc-13* homologue Munc13-1 with the N terminus of syntaxin. J Biol Chem. 1997;272:2520–6. https://doi.org/10.1074/jbc.272.4.2520.
129. McNew JA, Parlati F, Fukuda R, Johnston RJ, Paz K, Paumet F, et al. Compartmental specificity of cellular membrane fusion encoded in SNARE proteins. Nature. 2000;407:153–9. https://doi.org/10.1038/35025000.
130. Parlati F, Varlamov O, Paz K, McNew JA, Hurtado D, Söllner TH, et al. Distinct SNARE complexes mediating membrane fusion in Golgi transport based on combinatorial specificity. Proc Natl Acad Sci U S A. 2002;99:5424–9. https://doi.org/10.1073/pnas.082100899.
131. Scales SJ, Chen YA, Yoo BY, Patel SM, Doung YC, Scheller RH. SNAREs contribute to the specificity of membrane fusion. Neuron. 2000;26:457–64. https://doi.org/10.1016/S0896-6273(00)81177-0.
132. Hunt JM, Bommert K, Charlton MP, Kistner A, Habermann E, Augustine GJ, et al. A post-docking role for synaptobrevin in synaptic vesicle fusion. Neuron. 1994;12:1269–79. https://doi.org/10.1016/0896-6273(94)90443-X.
133. Ohara-Imaizumi M, Fujiwara T, Nakamichi Y, Okamura T, Akimoto Y, Kawai J, et al. Imaging analysis reveals mechanistic differences between first- and second-phase insulin exocytosis. J Cell Biol. 2007;177:695–705. https://doi.org/10.1083/jcb.200608132.
134. de Wit H, Cornelisse LN, Toonen RF, Verhage M. Docking of secretory vesicles is syntaxin dependent. PLoS One. 2006;1:e126. https://doi.org/10.1371/journal.pone.0000126.
135. Toonen RF, Kochubey O, de Wit H, Gulyas-Kovacs A, Konijnenburg B, Sørensen JB, et al. Dissecting docking and tethering of secretory vesicles at the target membrane. EMBO J. 2006;25:3725–37. https://doi.org/10.1038/sj.emboj.7601256.
136. Sztul E, Lupashin V. Role of tethering factors in secretory membrane traffic. Am J Physiol Cell Physiol. 2006;290:C11–26. https://doi.org/10.1152/ajpcell.00293.2005.
137. Whyte JR, Munro S. Vesicle tethering complexes in membrane traffic. J Cell Sci. 2002;115:2627–37. https://doi.org/10.1242/jcs.115.13.2627.
138. Zerial M, McBride H. Rab proteins as membrane organizers. Nat Rev Mol Cell Biol. 2001;2:107–17. https://doi.org/10.1038/35052055.
139. Guo W, Sacher M, Barrowman J, Ferro-Novick S, Novick P. Protein complexes in transport vesicle targeting. Trends Cell Biol. 2000;10:251–5. https://doi.org/10.1016/S0962-8924(00)01754-2.
140. Tan C, Wang SSH, de Nola G, Kaeser PS. Rebuilding essential active zone functions within a synapse. Neuron. 2022;110:1498–515.e8. https://doi.org/10.1016/j.neuron.2022.01.026.
141. Xuan Z, Manning L, Nelson J, Richmond JE, Colón-Ramos DA, Shen K, et al. Clarinet (CLA-1), a novel active zone protein required for synaptic vesicle clustering and release. elife. 2017;6:e29276. https://doi.org/10.7554/eLife.29276.
142. Koumandou VL, Dacks JB, Coulson RM, Field MC. Control systems for membrane fusion in the ancestral eukaryote; evolution of tethering complexes and SM proteins. BMC Evol Biol. 2007;7:29. https://doi.org/10.1186/1471-2148-7-29.
143. Zhang Y, Hughson FM. Chaperoning SNARE folding and assembly. Annu Rev Biochem. 2021;90:581–603. https://doi.org/10.1146/annurev-biochem-081820-103615.
144. Hong W. SNAREs and traffic. Biochim Biophys Acta. 1744;2005:493–517. https://doi.org/10.1016/j.bbamcr.2005.03.014.
145. Verhage M, Maia AS, Plomp JJ, Brussaard AB, Heeroma JH, Vermeer H, et al. Synaptic assembly of the brain in the absence of neurotransmitter secretion. Science. 2000;287:864–9. https://doi.org/10.1126/science.287.5454.864.

146. Hosono R, Hekimi S, Kamiya Y, Sassa T, Murakami S, Nishiwaki K, et al. The *unc-18* gene encodes a novel protein affecting the kinetics of acetylcholine metabolism in the nematode *Caenorhabditis elegans*. J Neurochem. 1992;58:1517–25. https://doi.org/10.1111/j.1471-4159.1992.tb11373.x.
147. Weimer RM, Richmond JE, Davis WS, Hadwiger G, Nonet ML, Jorgensen EM. Defects in synaptic vesicle docking in *unc-18* mutants. Nat Neurosci. 2003;6:1023–30. https://doi.org/10.1038/nn1118.
148. Aalto MK, Ruohonen L, Hosono K, Keränen S. Cloning and sequencing of the yeast *Saccharomyces cerevisiae* SEC1 gene localized on chromosome IV. Yeast. 1991;7:643–50. https://doi.org/10.1002/yea.320070613.
149. Schulze KL, Littleton JT, Salzberg A, Halachmi N, Stern M, Lev Z, et al. Rop, a *Drosophila* homolog of yeast Sec1 and vertebrate n-Sect/Munc-18 proteins, is a negative regulator of neurotransmitter release *in vivo*. Neuron. 1994;13:1099–108. https://doi.org/10.1016/0896-6273(94)90048-5.
150. Baker RW, Jeffrey PD, Hughson FM. Crystal structures of the Sec1/Munc18 (SM) protein Vps33, alone and bound to the homotypic fusion and vacuolar protein sorting (HOPS) subunit Vps16. PLoS One. 2013;8:e67409. https://doi.org/10.1371/journal.pone.0067409.
151. Baker RW, Jeffrey PD, Zick M, Phillips BP, Wickner WT, Hughson FM. A direct role for the Sec1/Munc18-family protein Vps33 as a template for SNARE assembly. Science. 2015;349:1111–4. https://doi.org/10.1126/science.aac7906.
152. Colbert KN, Hattendorf DA, Weiss TM, Burkhardt P, Fasshauer D, Weis WI. Syntaxin1a variants lacking an N-peptide or bearing the LE mutation bind to Munc18a in a closed conformation. Proc Natl Acad Sci U S A. 2013;110:12637–42. https://doi.org/10.1073/pnas.1303753110.
153. Eisemann TJ, Allen F, Lau K, Shimamura GR, Jeffrey PD, Hughson FM. The Sec1/Munc18 protein Vps45 holds the Qa-SNARE Tlg2 in an open conformation. elife. 2020;9:e60724. https://doi.org/10.7554/eLife.60724.
154. Hu SH, Christie MP, Saez NJ, Latham CF, Jarrott R, Lua LH, et al. Possible roles for Munc18-1 domain 3a and Syntaxin1 N-peptide and C-terminal anchor in SNARE complex formation. Proc Natl Acad Sci U S A. 2011;108:1040–5. https://doi.org/10.1073/pnas.0914906108.
155. Graham SC, Wartosch L, Gray SR, Scourfield EJ, Deane JE, Luzio JP, et al. Structural basis of Vps33A recruitment to the human HOPS complex by Vps16. Proc Natl Acad Sci U S A. 2013;110:13345–50. https://doi.org/10.1073/pnas.1307074110.
156. Hackmann Y, Graham SC, Ehl S, Höning S, Lehmberg K, Aricò M, et al. Syntaxin binding mechanism and disease-causing mutations in Munc18-2. Proc Natl Acad Sci U S A. 2013;110:E4482–91. https://doi.org/10.1073/pnas.1313474110.
157. Bracher A, Weissenhorn W. Structural basis for the Golgi membrane recruitment of Sly1p by Sed5p. EMBO J. 2002;21:6114–24. https://doi.org/10.1093/emboj/cdf608.
158. Bracher A, Weissenhorn W. Crystal structures of neuronal squid Sec1 implicate inter-domain hinge movement in the release of t-SNAREs. J Mol Biol. 2001;306:7–13. https://doi.org/10.1006/jmbi.2000.4347.
159. Burkhardt P, Hattendorf DA, Weis WI, Fasshauer D. Munc18a controls SNARE assembly through its interaction with the syntaxin N-peptide. EMBO J. 2008;27:923–33. https://doi.org/10.1038/emboj.2008.37.
160. Burkhardt P, Stegmann CM, Cooper B, Kloepper TH, Imig C, Varoqueaux F, et al. Primordial neurosecretory apparatus identified in the choanoflagellate *Monosiga brevicollis*. Proc Natl Acad Sci U S A. 2011;108:15264–9. https://doi.org/10.1073/pnas.1106189108.
161. Han GA, Park S, Bin NR, Jung CH, Kim B, Chandrasegaram P, et al. A pivotal role for pro-335 in balancing the dual functions of Munc18-1 domain-3a in regulated exocytosis. J Biol Chem. 2014;289:33617–28. https://doi.org/10.1074/jbc.M114.584805.
162. Munch AS, Kedar GH, van Weering JR, Vazquez-Sanchez S, He E, Andre T, et al. Extension of helix 12 in Munc18-1 induces vesicle priming. J Neurosci. 2016;36:6881–91. https://doi.org/10.1523/JNEUROSCI.0007-16.2016.

163. Parisotto D, Pfau M, Scheutzow A, Wild K, Mayer MP, Malsam J, et al. An extended helical conformation in domain 3a of Munc18-1 provides a template for SNARE (soluble N-ethylmaleimide-sensitive factor attachment protein receptor) complex assembly. J Biol Chem. 2014;289:9639–50. https://doi.org/10.1074/jbc.M113.514273.
164. Park S, Bin NR, Yu B, Wong R, Sitarska E, Sugita K, et al. UNC-18 and tomosyn antagonistically control synaptic vesicle priming downstream of UNC-13 in *Caenorhabditis elegans*. J Neurosci. 2017;37:8797–815. https://doi.org/10.1523/JNEUROSCI.0338-17.2017.
165. Rizo J, David G, Fealey ME, Jaczynska K. On the difficulties of characterizing weak protein interactions that are critical for neurotransmitter release. FEBS Open Bio. 2022;12:1912. https://doi.org/10.1002/2211-5463.13473.
166. Chen YA, Scales SJ, Scheller RH. Sequential SNARE assembly underlies priming and triggering of exocytosis. Neuron. 2001;30:161–70. https://doi.org/10.1016/S0896-6273(01)00270-7.
167. Lin RC, Scheller RH. Structural organization of the synaptic exocytosis core complex. Neuron. 1997;19:1087–94. https://doi.org/10.1016/S0896-6273(00)80399-2.
168. Hua SY, Charlton MP. Activity-dependent changes in partial VAMP complexes during neurotransmitter release. Nat Neurosci. 1999;2:1078–83. https://doi.org/10.1038/16005.
169. Sørensen JB, Wiederhold K, Muller EM, Milosevic I, Nagy G, de Groot BL, et al. Sequential N- to C-terminal SNARE complex assembly drives priming and fusion of secretory vesicles. EMBO J. 2006;25:955–66. https://doi.org/10.1038/sj.emboj.7601003.
170. Xu T, Rammner B, Margittai M, Artalejo AR, Neher E, Jahn R. Inhibition of SNARE complex assembly differentially affects kinetic components of exocytosis. Cell. 1999;99:713–22. https://doi.org/10.1016/S0092-8674(00)81669-4.
171. Zorman S, Rebane AA, Ma L, Yang G, Molski MA, Coleman J, et al. Common intermediates and kinetics, but different energetics, in the assembly of SNARE proteins. elife. 2014;3:e03348. https://doi.org/10.7554/eLife.03348.
172. Min D, Kim K, Hyeon C, Cho YH, Shin YK, Yoon TY. Mechanical unzipping and rezipping of a single SNARE complex reveals hysteresis as a force-generating mechanism. Nat Commun. 2013;4:1705. https://doi.org/10.1038/ncomms2692.
173. Gao Y, Zorman S, Gundersen G, Xi Z, Ma L, Sirinakis G, et al. Single reconstituted neuronal SNARE complexes zipper in three distinct stages. Science. 2012;337:1340–3. https://doi.org/10.1126/science.1224492.
174. Zhang X, Rebane AA, Ma L, Li F, Jiao J, Qu H, et al. Stability, folding dynamics, and long-range conformational transition of the synaptic t-SNARE complex. Proc Natl Acad Sci U S A. 2016;113:E8031–40. https://doi.org/10.1073/pnas.1605748113.
175. Ma L, Rebane AA, Yang G, Xi Z, Kang Y, Gao Y, et al. Munc18-1-regulated stage-wise SNARE assembly underlying synaptic exocytosis. elife. 2015;4:e09580. https://doi.org/10.7554/eLife.09580.
176. Liu Y, Wan C, Rathore SS, Stowell MHB, Yu H, Shen J. SNARE zippering is suppressed by a conformational constraint that is removed by v-SNARE splitting. Cell Rep. 2021;34:108611. https://doi.org/10.1016/j.celrep.2020.108611.
177. Zhang Y. Energetics, kinetics, and pathway of SNARE folding and assembly revealed by optical tweezers: energetics, kinetics and pathway of SNARE assembly. Protein Sci. 2017;26:1252–65. https://doi.org/10.1002/pro.3116.
178. Fiebig KM, Rice LM, Pollock E, Brunger AT. Folding intermediates of SNARE complex assembly. Nat Struct Biol. 1999;6:117–23. https://doi.org/10.1038/5803.
179. Pobbati AV, Stein A, Fasshauer D. N- to C-terminal SNARE complex assembly promotes rapid membrane fusion. Science. 2006;313:673–6. https://doi.org/10.1126/science.1129486.
180. Melia TJ, Weber T, McNew JA, Fisher LE, Johnston RJ, Parlati F, et al. Regulation of membrane fusion by the membrane-proximal coil of the t-SNARE during zippering of SNAREpins. J Cell Biol. 2002;158:929–40. https://doi.org/10.1083/jcb.200112081.
181. Fasshauer D, Margittai M. A transient N-terminal interaction of SNAP-25 and syntaxin nucleates SNARE assembly. J Biol Chem. 2004;279:7613–21. https://doi.org/10.1074/jbc.M312064200.

182. Li F, Kümmel D, Coleman J, Reinisch KM, Rothman JE, Pincet F. A half-zippered SNARE complex represents a functional intermediate in membrane fusion. J Am Chem Soc. 2014;136:3456–64. https://doi.org/10.1021/ja410690m.
183. Poirier MA, Hao JC, Malkus PN, Chan C, Moore MF, King DS, et al. Protease resistance of syntaxin.SNAP-25.VAMP complexes. Implications for assembly and structure. J Biol Chem. 1998;273:11370–7. https://doi.org/10.1074/jbc.273.18.11370.
184. Han X, Jackson MB. Structural transitions in the synaptic SNARE complex during Ca^{2+}-triggered exocytosis. J Cell Biol. 2006;172:281–93. https://doi.org/10.1083/jcb.200510012.
185. Lou X, Shin Y-K. SNARE zippering. Biosci Rep. 2016;36:e00327. https://doi.org/10.1042/BSR20160004.
186. Zhao C, Slevin JT, Whiteheart SW. Cellular functions of NSF: not just SNAPs and SNAREs. FEBS Lett. 2007;581:2140–9. https://doi.org/10.1016/j.febslet.2007.03.032.
187. White KI, Zhao M, Choi UB, Pfuetzner RA, Brunger AT. Structural principles of SNARE complex recognition by the AAA+ protein NSF. elife. 2018;7:e38888. https://doi.org/10.7554/eLife.38888.
188. Khan YA, White KI, Brunger AT. The AAA+ superfamily: a review of the structural and mechanistic principles of these molecular machines. Crit Rev Biochem Mol Biol. 2022;57:156–87. https://doi.org/10.1080/10409238.2021.1979460.
189. Zhao M, Brunger AT. Recent advances in deciphering the structure and molecular mechanism of the AAA+ ATPase N-Ethylmaleimide-Sensitive Factor (NSF). J Mol Biol. 2016;428:1912–26. https://doi.org/10.1016/j.jmb.2015.10.026.
190. Zhao M, Wu S, Zhou Q, Vivona S, Cipriano DJ, Cheng Y, et al. Mechanistic insights into the recycling machine of the SNARE complex. Nature. 2015;518:61–7. https://doi.org/10.1038/nature14148.
191. Whiteheart SW, Matveeva EA. Multiple binding proteins suggest diverse functions for the N-ethylmaleimide sensitive factor. J Struct Biol. 2004;146:32–43. https://doi.org/10.1016/j.jsb.2003.09.015.
192. Burgalossi A, Jung S, Meyer G, Jockusch WJ, Jahn O, Taschenberger H, et al. SNARE protein recycling by αSNAP and βSNAP supports synaptic vesicle priming. Neuron. 2010;68:473–87. https://doi.org/10.1016/j.neuron.2010.09.019.
193. Xu J, Xu Y, Ellis-Davies GCR, Augustine GJ, Tse FW. Differential regulation of exocytosis by α- and β-SNAPs. J Neurosci. 2002;22:53–61. https://doi.org/10.1523/JNEUROSCI.22-01-00053.2002.
194. Sudlow AW, McFerran BW, Bodill H, Barnard RJO, Morgan A, Burgoyne RD. Similar effects of α- and β-SNAP on Ca^{2+}-regulated exocytosis. FEBS Lett. 1996;393:185–8. https://doi.org/10.1016/0014-5793(96)00880-0.
195. Inoue H, Matsuzaki Y, Tanaka A, Hosoi K, Ichimura K, Arasaki K, et al. γ-SNAP stimulates disassembly of endosomal SNARE complexes and regulates endocytic trafficking pathways. J Cell Sci. 2015;128:2781–94. https://doi.org/10.1242/jcs.158634.
196. Marz KE, Lauer JM, Hanson PI. Defining the SNARE complex binding surface of alpha-SNAP: implications for SNARE complex disassembly. J Biol Chem. 2003;278:27000–8. https://doi.org/10.1074/jbc.M302003200.
197. Scales SJ, Yoo BY, Scheller RH. The ionic layer is required for efficient dissociation of the SNARE complex by alpha-SNAP and NSF. Proc Natl Acad Sci U S A. 2001;98:14262–7. https://doi.org/10.1073/pnas.251547598.
198. Lauer JM, Dalal S, Marz KE, Nonet ML, Hanson PI. SNARE complex zero layer residues are not critical for N-ethylmaleimide-sensitive factor-mediated disassembly. J Biol Chem. 2006;281:14823–32. https://doi.org/10.1074/jbc.M512706200.
199. Huang X, Sun S, Wang X, Fan F, Zhou Q, Lu S, et al. Mechanistic insights into the SNARE complex disassembly. Sci Adv. 2019;5:eaau8164. https://doi.org/10.1126/sciadv.aau8164.
200. Prinslow EA, Stepien KP, Pan Y-Z, Xu J, Rizo J. Multiple factors maintain assembled *trans*-SNARE complexes in the presence of NSF and αSNAP. elife. 2019;8:e38880. https://doi.org/10.7554/eLife.38880.

201. Choi UB, Zhao M, White KI, Pfuetzner RA, Esquivies L, Zhou Q, et al. NSF-mediated disassembly of on- and off-pathway SNARE complexes and inhibition by complexin. elife. 2018;7:e36497. https://doi.org/10.7554/eLife.36497.
202. Xu Y, Zhu L, Wang S, Ma C. Munc18 − Munc13-dependent pathway of SNARE complex assembly is resistant to NSF and α-SNAP. FEBS J. 2022;289:6367–84. https://doi.org/10.1111/febs.16528.
203. Klassen MP, Wu YE, Maeder CI, Nakae I, Cueva JG, Lehrman EK, et al. An Arf-like small G protein, ARL-8, promotes the axonal transport of presynaptic cargoes by suppressing vesicle aggregation. Neuron. 2010;66:710–23. https://doi.org/10.1016/j.neuron.2010.04.033.
204. Niwa S, Tao L, Lu SY, Liew GM, Feng W, Nachury MV, et al. BORC regulates the axonal transport of synaptic vesicle precursors by activating ARL-8. Curr Biol. 2017;27:2569–78.e4. https://doi.org/10.1016/j.cub.2017.07.013.
205. Pu J, Schindler C, Jia R, Jarnik M, Backlund P, Bonifacino JS. BORC, a multisubunit complex that regulates lysosome positioning. Dev Cell. 2015;33:176–88. https://doi.org/10.1016/j.devcel.2015.02.011.
206. Vukoja A, Rey U, Petzoldt AG, Ott C, Vollweiter D, Quentin C, et al. Presynaptic biogenesis requires axonal transport of lysosome-related vesicles. Neuron. 2018;99:1216–32.e7. https://doi.org/10.1016/j.neuron.2018.08.004.
207. Wu Ye E, Huo L, Maeder Celine I, Feng W, Shen K. The balance between capture and dissociation of presynaptic proteins controls the spatial distribution of synapses. Neuron. 2013;78:994–1011. https://doi.org/10.1016/j.neuron.2013.04.035.
208. Goldstein AYN, Wang X, Schwarz TL. Axonal transport and the delivery of presynaptic components. Curr Opin Neurobiol. 2008;18:495–503. https://doi.org/10.1016/j.conb.2008.10.003.
209. Li J, Edelmann L, Jahn R, Dahlstrom A. Axonal transport and distribution of synaptobrevin I and II in the rat peripheral nervous system. J Neurosci. 1996;16:137–47. https://doi.org/10.1523/JNEUROSCI.16-01-00137.1996.
210. Hummel JJA, Hoogenraad CC. Specific KIF1A–adaptor interactions control selective cargo recognition. J Cell Biol. 2021;220:e202105011. https://doi.org/10.1083/jcb.202105011.
211. Okada Y, Yamazaki H, Sekine-Aizawa Y, Hirokawa N. The neuron-specific kinesin superfamily protein KIF1A is a uniqye monomeric motor for anterograde axonal transport of synaptic vesicle precursors. Cell. 1995;81:769–80. https://doi.org/10.1016/0092-8674(95)90538-3.
212. Mundigl O, Matteoli M, Daniell L, Thomas-Reetz A, Metcalf A, Jahn R, et al. Synaptic vesicle proteins and early endosomes in cultured hippocampal neurons: differential effects of Brefeldin A in axon and dendrites. J Cell Biol. 1993;122:1207–21. https://doi.org/10.1083/jcb.122.6.1207.
213. Hall DH, Hedgecock EM. Kinesin-related gene *unc-104* is required for axonal transport of synaptic vesicles in *C. elegans*. Cell. 1991;65:837–47. https://doi.org/10.1016/0092-8674(91)90391-B.
214. Chua JJE, Butkevich E, Worseck JM, Kittelmann M, Grønborg M, Behrmann E, et al. Phosphorylation-regulated axonal dependent transport of syntaxin 1 is mediated by a Kinesin-1 adapter. Proc Natl Acad Sci U S A. 2012;109:5862–7. https://doi.org/10.1073/pnas.1113819109.
215. Gonzalo S, Linder ME. SNAP-25 palmitoylation and plasma membrane targeting require a functional secretory pathway. Mol Biol Cell. 1998;9:585–97. https://doi.org/10.1091/mbc.9.3.585.
216. Gonzalo S, Greentree WK, Linder ME. SNAP-25 is targeted to the plasma membrane through a novel membrane-binding Domain. J Biol Chem. 1999;274:21313–8. https://doi.org/10.1074/jbc.274.30.21313.
217. Salaün C, James DJ, Greaves J, Chamberlain LH. Plasma membrane targeting of exocytic SNARE proteins. Biochim Biophys Acta (BBA) Mol Cell Res. 2004;1693:81–9. https://doi.org/10.1016/j.bbamcr.2004.05.008.

218. Morton AM, Cunningham AL, Diefenbach RJ. Kinesin-1 plays a role in transport of SNAP-25 to the plasma membrane. Biochem Biophys Res Commun. 2010;391:388–93. https://doi.org/10.1016/j.bbrc.2009.11.068.
219. Bar-On D, Wolter S, van de Linde S, Heilemann M, Nudelman G, Nachliel E, et al. Super-resolution imaging reveals the internal architecture of nano-sized syntaxin clusters. J Biol Chem. 2012;287:27158–67. https://doi.org/10.1074/jbc.M112.353250.
220. Koh S, Yamamoto A, Inoue A, Inoue Y, Akagawa K, Kawamura Y, et al. Immunoelectron microscopic localization of the HPC-1 antigen in rat cerebellum. J Neurocytol. 1993;22:995–1005. https://doi.org/10.1007/BF01218356.
221. Sieber JJ, Willig KI, Kutzner C, Gerding-Reimers C, Harke B, Donnert G, et al. Anatomy and dynamics of a supramolecular membrane protein cluster. Science. 2007;317:1072–6. https://doi.org/10.1126/science.1141727.
222. Chamberlain LH, Gould GW. The vesicle- and target-SNARE proteins that mediate Glut4 vesicle fusion are localized in detergent-insoluble lipid rafts present on distinct intracellular membranes. J Biol Chem. 2002;277:49750–4. https://doi.org/10.1074/jbc.M206936200.
223. Cotrufo T, Perez-Branguli F, Muhaisen A, Ros O, Andres R, Baeriswyl T, et al. A signaling mechanism coupling Netrin-1/deleted in colorectal cancer chemoattraction to SNARE-mediated exocytosis in axonal growth cones. J Neurosci. 2011;31:14463–80. https://doi.org/10.1523/JNEUROSCI.3018-11.2011.
224. Zhai RG, Vardinon-Friedman H, Cases-Langhoff C, Becker B, Gundelfinger ED, Ziv NE, et al. Assembling the presynaptic active zone. Neuron. 2001;29:131–43. https://doi.org/10.1016/S0896-6273(01)00185-4.
225. Lai Y, Choi UB, Leitz J, Rhee HJ, Lee C, Altas B, et al. Molecular mechanisms of synaptic vesicle priming by Munc13 and Munc18. Neuron. 2017;95:591–607. e10. https://doi.org/10.1016/j.neuron.2017.07.004.
226. Yang B, Gonzalez L Jr, Prekeris R, Steegmaier M, Advani RJ, Scheller RH. SNARE interactions are not selective. Implications for membrane fusion specificity. J Biol Chem. 1999;274:5649–53. https://doi.org/10.1074/jbc.274.9.5649.
227. Tsui MM, Banfield DK. Yeast Golgi SNARE interactions are promiscuous. J Cell Sci. 2000;113:145–52. https://doi.org/10.1242/jcs.113.1.145.
228. Weninger K, Bowen ME, Chu S, Brunger AT. Single-molecule studies of SNARE complex assembly reveal parallel and antiparallel configurations. Proc Natl Acad Sci U S A. 2003;100:14800–5. https://doi.org/10.1073/pnas.2036428100.
229. Bajohrs M, Darios F, Peak-Chew SY, Davletov B. Promiscuous interaction of SNAP-25 with all plasma membrane syntaxins in a neuroendocrine cell. Biochem J. 2005;392:283–9. https://doi.org/10.1042/BJ20050583.
230. Jahn R, Scheller RH. SNAREs--engines for membrane fusion. Nat Rev Mol Cell Biol. 2006;7:631–43. https://doi.org/10.1038/nature05387.
231. Hata Y, Slaughter CA, Südhof TC. Synaptic vesicle fusion complex contains *unc-18* homologue bound to syntaxin. Nature. 1993;366:347–51. https://doi.org/10.1038/366347a0.
232. Rowe J, Calegari F, Taverna E, Longhi R, Rosa P. Syntaxin 1A is delivered to the apical and basolateral domains of epithelial cells: the role of munc-18 proteins. J Cell Sci. 2001;114:3323–32. https://doi.org/10.1242/jcs.114.18.3323.
233. Arunachalam L, Han L, Tassew NG, He Y, Wang L, Xie L, et al. Munc18-1 is critical for plasma membrane localization of syntaxin1 but not of SNAP-25 in PC12 cells. Mol Biol Cell. 2008;19:722–34. https://doi.org/10.1091/mbc.e07-07-0662.
234. Han L, Jiang T, Han GA, Malintan NT, Xie L, Wang L, et al. Rescue of Munc18-1 and −2 double knockdown reveals the essential functions of interaction between Munc18 and closed syntaxin in PC12 cells. Mol Biol Cell. 2009;20:4962–75. https://doi.org/10.1091/mbc.e09-08-0712.
235. Medine CN, Rickman C, Chamberlain LH, Duncan RR. Munc18-1 prevents the formation of ectopic SNARE complexes in living cells. J Cell Sci. 2007;120:4407–15. https://doi.org/10.1242/jcs.020230.

236. Rickman C, Medine CN, Bergmann A, Duncan RR. Functionally and spatially distinct modes of MUNC18-syntaxin 1 interaction. J Biol Chem. 2007;282:12097–103. https://doi.org/10.1074/jbc.M700227200.
237. Pevsner J, Hsu SC, Scheller RH. n-Sec1: a neural-specific syntaxin-binding protein. Proc Natl Acad Sci U S A. 1994;91:1445–9. https://doi.org/10.1073/pnas.91.4.1445.
238. Sitarska E, Xu J, Park S, Liu X, Quade B, Stepien K, et al. Autoinhibition of Munc18-1 modulates synaptobrevin binding and helps to enable Munc13-dependent regulation of membrane fusion. elife. 2017;6:e24278. https://doi.org/10.7554/eLife.24278.
239. Khvotchev M, Dulubova I, Sun J, Dai H, Rizo J, Südhof TC. Dual modes of Munc18-1/SNARE interactions are coupled by functionally critical binding to syntaxin-1 N terminus. J Neurosci. 2007;27:12147–55. https://doi.org/10.1523/JNEUROSCI.3655-07.2007.
240. Wu MN, Littleton JT, Bhat MA, Prokop A, Bellen HJ. ROP, the *Drosophila* Sec1 homolog, interacts with syntaxin and regulates neurotransmitter release in a dosage-dependent manner. EMBO J. 1998;17:127–39. https://doi.org/10.1093/emboj/17.1.127.
241. Nicholson KL, Munson M, Miller RB, Filip TJ, Fairman R, Hughson FM. Regulation of SNARE complex assembly by an N-terminal domain of the t-SNARE Sso1p. Nat Struct Biol. 1998;5:793–802. https://doi.org/10.1038/1834.
242. Dresbach T, Burns ME, O'Connor V, DeBello WM, Betz H, Augustine GJ. A neuronal Sec1 homolog regulates neurotransmitter release at the squid giant synapse. J Neurosci. 1998;18:2923–32. https://doi.org/10.1523/JNEUROSCI.18-08-02923.1998.
243. Carr CM, Grote E, Munson M, Hughson FM, Novick PJ. Sec1p binds to SNARE complexes and concentrates at sites of secretion. J Cell Biol. 1999;146:333–44. https://doi.org/10.1083/jcb.146.2.333.
244. Dulubova I, Yamaguchi T, Gao Y, Min SW, Huryeva I, Südhof TC, et al. How Tlg2p/syntaxin 16 'snares' Vps45. EMBO J. 2002;21:3620–31. https://doi.org/10.1093/emboj/cdf381.
245. Yamaguchi T, Dulubova I, Min SW, Chen X, Rizo J, Südhof TC. Sly1 binds to Golgi and ER syntaxins via a conserved N-terminal peptide motif. Dev Cell. 2002;2:295–305. https://doi.org/10.1016/S1534-5807(02)00125-9.
246. McEwen JM, Kaplan JM. UNC-18 promotes both the anterograde trafficking and synaptic function of syntaxin. Mol Biol Cell. 2008;19:3836–46. https://doi.org/10.1091/mbc.e08-02-0160.
247. Fan J, Yang X, Lu J, Chen L, Xu P. Role of H(abc) domain in membrane trafficking and targeting of syntaxin 1A. Biochem Biophys Res Commun. 2007;359:245–50. https://doi.org/10.1016/j.bbrc.2007.05.065.
248. Yang X, Xu P, Xiao Y, Xiong X, Xu T. Domain requirement for the membrane trafficking and targeting of syntaxin 1A. J Biol Chem. 2006;281:15457–63. https://doi.org/10.1074/jbc.M513246200.
249. Demircioglu FE, Burkhardt P, Fasshauer D. The SM protein Sly1 accelerates assembly of the ER–Golgi SNARE complex. Proc Natl Acad Sci U S A. 2014;111:13828–33. https://doi.org/10.1073/pnas.1408254111.
250. Kosodo Y, Noda Y, Adachi H, Yoda K. Binding of Sly1 to Sed5 enhances formation of the yeast early Golgi SNARE complex. J Cell Sci. 2002;115:3683–91. https://doi.org/10.1242/jcs.00027.
251. Mueller BD, Merrill SA, Watanabe S, Liu P, Singh A, Maldonado-Catala P, et al. CaV1 and CaV2 calcium channels mediate the release of distinct pools of synaptic vesicles. bioRxiv. 2022:490438. https://doi.org/10.1101/2022.05.03.490438.
252. Dittman JS. Unc13: a multifunctional synaptic marvel. Curr Opin Neurobiol. 2019;57:17–25. https://doi.org/10.1016/j.conb.2018.12.011.
253. Piao C, Sigrist SJ. (M)Unc13s in active zone diversity: a *Drosophila* perspective. Front Synaptic Neurosci. 2022;13:798204. https://doi.org/10.3389/fnsyn.2021.798204.
254. Basu J, Shen N, Dulubova I, Lu J, Guan R, Guryev O, et al. A minimal domain responsible for Munc13 activity. Nat Struct Mol Biol. 2005;12:1017–8. https://doi.org/10.1038/nsmb1001.

255. Wang S, Li Y, Gong J, Ye S, Yang X, Zhang R, et al. Munc18 and Munc13 serve as a functional template to orchestrate neuronal SNARE complex assembly. Nat Commun. 2019;10:69. https://doi.org/10.1038/s41467-018-08028-6.
256. Grushin K, Kalyana Sundaram RV, Sindelar CV, Rothman JE. Munc13 structural transitions and oligomers that may choreograph successive stages in vesicle priming for neurotransmitter release. Proc Natl Acad Sci U S A. 2022;119:e2121259119. https://doi.org/10.1073/pnas.2121259119.
257. Li F, Kalyana Sundaram RV, Gatta AT, Coleman J, Ramakrishnan S, Krishnakumar SS, et al. Vesicle capture by membrane-bound Munc13-1 requires self-assembly into discrete clusters. FEBS Lett. 2021;595:2185–96. https://doi.org/10.1002/1873-3468.14157.
258. Chicka Michael C, Ren Q, Richards D, Hellman Lance M, Zhang J, Fried Michael G, et al. Role of Munc13-4 as a Ca^{2+}-dependent tether during platelet secretion. Biochem J. 2016;473:627–39. https://doi.org/10.1042/BJ20151150.
259. Deng L, Kaeser PS, Xu W, Südhof TC. RIM proteins activate vesicle priming by reversing autoinhibitory homodimerization of Munc13. Neuron. 2011;69:317–31. https://doi.org/10.1016/j.neuron.2011.01.005.
260. Camacho M, Basu J, Trimbuch T, Chang S, Pulido-Lozano C, Chang S-S, et al. Heterodimerization of Munc13 C2A domain with RIM regulates synaptic vesicle docking and priming. Nat Commun. 2017;8:15293. https://doi.org/10.1038/ncomms15293.
261. Brockmann MM, Zarebidaki F, Camacho M, Grauel MK, Trimbuch T, Südhof TC, et al. A trio of active zone proteins comprised of RIM-BPs, RIMs, and Munc13s governs neurotransmitter release. Cell Rep. 2020;32:107960. https://doi.org/10.1016/j.celrep.2020.107960.
262. Kaeser PS, Südhof TC. RIM function in short- and long-term synaptic plasticity. Biochem Soc Trans. 2005;33:1345. https://doi.org/10.1042/BST20051345.
263. Wang X, Gong J, Zhu L, Wang S, Yang X, Xu Y, et al. Munc13 activates the Munc18-1/syntaxin-1 complex and enables Munc18-1 to prime SNARE assembly. EMBO J. 2020;39:e103631. https://doi.org/10.15252/embj.2019103631.
264. Wang S, Choi UB, Gong J, Yang X, Li Y, Wang AL, et al. Conformational change of syntaxin linker region induced by Munc13s initiates SNARE complex formation in synaptic exocytosis. EMBO J. 2017;36:816–29. https://doi.org/10.15252/embj.201695775.
265. Aravamudan B, Fergestad T, Davis WS, Rodesch CK, Broadie K. *Drosophila* UNC-13 is essential for synaptic transmission. Nat Neurosci. 1999;2:965–71. https://doi.org/10.1038/14764.
266. Augustin I, Rosenmund C, Südhof TC, Brose N. Munc13-1 is essential for fusion competence of glutamatergic synaptic vesicles. Nature. 1999;400:457–61. https://doi.org/10.1038/22768.
267. Richmond JE, Davis WS, Jorgensen EM. UNC-13 is required for synaptic vesicle fusion in *C. elegans*. Nat Neurosci. 1999;2:959–64. https://doi.org/10.1038/14755.
268. Varoqueaux F, Sigler A, Rhee JS, Brose N, Enk C, Reim K, et al. Total arrest of spontaneous and evoked synaptic transmission but normal synaptogenesis in the absence of Munc13-mediated vesicle priming. Proc Natl Acad Sci U S A. 2002;99:9037–42. https://doi.org/10.1073/pnas.122623799.
269. Tien C-W, Yu B, Huang M, Stepien KP, Sugita K, Xie X, et al. Open syntaxin overcomes exocytosis defects of diverse mutants in *C elegans*. Nat Commun. 2020;11:5516. https://doi.org/10.1038/s41467-020-19178-x.
270. Christie MP, Whitten AE, King GJ, Hu SH, Jarrott RJ, Chen KE, et al. Low-resolution solution structures of Munc18:Syntaxin protein complexes indicate an open binding mode driven by the Syntaxin N-peptide. Proc Natl Acad Sci U S A. 2012;109:9816–21. https://doi.org/10.1073/pnas.1116975109.
271. Jiao J, He M, Port SA, Baker RW, Xu Y, Qu H, et al. Munc18-1 catalyzes neuronal SNARE assembly by templating SNARE association. elife. 2018;7:e41771. https://doi.org/10.7554/eLife.41771.
272. Meijer M, Burkhardt P, de Wit H, Toonen RF, Fasshauer D, Verhage M. Munc18-1 mutations that strongly impair SNARE-complex binding support normal synaptic transmission. EMBO J. 2012;31:2156–68. https://doi.org/10.1038/emboj.2012.72.

273. Park S, Bin N-R, Michael Rajah M, Kim B, Chou T-C, Kang S-YA, et al. Conformational states of syntaxin-1 govern the necessity of N-peptide binding in exocytosis of PC12 cells and *Caenorhabditis elegans*. Mol Biol Cell. 2016;27:669–85. https://doi.org/10.1091/mbc.E15-09-0638.
274. Hu SH, Latham CF, Gee CL, James DE, Martin JL. Structure of the Munc18c/Syntaxin4 N-peptide complex defines universal features of the N-peptide binding mode of Sec1/Munc18 proteins. Proc Natl Acad Sci U S A. 2007;104:8773–8. https://doi.org/10.1073/pnas.0701124104.
275. Shen J, Rathore SS, Khandan L, Rothman JE. SNARE bundle and syntaxin N-peptide constitute a minimal complement for Munc18-1 activation of membrane fusion. J Cell Biol. 2010;190:55–63. https://doi.org/10.1083/jcb.201003148.
276. Shen C, Liu Y, Yu H, Gulbranson DR, Kogut I, Bilousova G, et al. The N-peptide–binding mode is critical to Munc18-1 function in synaptic exocytosis. J Biol Chem. 2018;293:18309–17. https://doi.org/10.1074/jbc.RA118.005254.
277. Dulubova I, Yamaguchi T, Araç D, Li H, Huryeva I, Min SW, et al. Convergence and divergence in the mechanism of SNARE binding by Sec1/Munc18-like proteins. Proc Natl Acad Sci U S A. 2003;100:32–7. https://doi.org/10.1073/pnas.232701299.
278. Colgren J, Burkhardt P. The premetazoan ancestry of the synaptic toolkit and appearance of first neurons. Essays Biochem. 2022;66:781–95. https://doi.org/10.1042/ebc20220042.
279. Peng R, Gallwitz D. Sly1 protein bound to Golgi syntaxin Sed5p allows assembly and contributes to specificity of SNARE fusion complexes. J Cell Biol. 2002;157:645–55. https://doi.org/10.1083/jcb.200202006.
280. Peng R, Gallwitz D. Multiple SNARE interactions of an SM protein: Sed5p/Sly1p binding is dispensable for transport. EMBO J. 2004;23:3939–49. https://doi.org/10.1038/sj.emboj.7600410.
281. Shen J, Tareste DC, Paumet F, Rothman JE, Melia TJ. Selective activation of cognate SNAREpins by Sec1/Munc18 proteins. Cell. 2007;128:183–95. https://doi.org/10.1016/j.cell.2006.12.016.
282. André T, Classen J, Brenner P, Betts MJ, Dörr B, Kreye S, et al. The interaction of Munc18-1 helix 11 and 12 with the central region of the VAMP2 SNARE motif is essential for SNARE templating and synaptic transmission. eNeuro. 2020;7:ENEURO.0278-20.2020. https://doi.org/10.1523/ENEURO.0278-20.2020.
283. Ma C, Su L, Seven AB, Xu Y, Rizo J. Reconstitution of the vital functions of Munc18 and Munc13 in neurotransmitter release. Science. 2013;339:421–5. https://doi.org/10.1126/science.1230473.
284. Cijsouw T, Weber JP, Broeke JH, Broek JAC, Schut D, Kroon T, et al. Munc18-1 redistributes in nerve terminals in an activity- and PKC-dependent manner. J Cell Biol. 2014;204:759–75. https://doi.org/10.1083/jcb.201308026.
285. Stepien KP, Xu J, Zhang X, Bai X-C, Rizo J. SNARE assembly enlightened by cryo-EM structures of a synaptobrevin–Munc18-1–syntaxin-1 complex. Sci Adv. 2022;8:eabo5272. https://doi.org/10.1126/sciadv.abo5272.
286. Yang J, Jin H, Liu Y, Guo Y, Zhang Y. A dynamic template complex mediates Munc18-chaperoned SNARE assembly. Proc Natl Acad Sci U S A. 2022;119:e2215124119. https://doi.org/10.1073/pnas.2215124119.
287. Li F, Tiwari N, Rothman JE, Pincet F. Kinetic barriers to SNAREpin assembly in the regulation of membrane docking/priming and fusion. Proc Natl Acad Sci U S A. 2016;113:10536–41. https://doi.org/10.1073/pnas.1604000113.
288. Liu T, Tucker WC, Bhalla A, Chapman ER, Weisshaar JC. SNARE-driven, 25-millisecond vesicle fusion *in vitro*. Biophys J. 2005;89:2458–72. https://doi.org/10.1529/biophysj.105.062539.
289. Kyoung M, Srivastava A, Zhang Y, Diao J, Vrljic M, Grob P, et al. *In vitro* system capable of differentiating fast Ca^{2+}-triggered content mixing from lipid exchange for mechanistic stud-

ies of neurotransmitter release. Proc Natl Acad Sci U S A. 2011;108:E304–13. https://doi.org/10.1073/pnas.1107900108.
290. Kreutzberger Alex JB, Liang B, Kiessling V, Tamm LK. Assembly and comparison of plasma membrane SNARE acceptor complexes. Biophys J. 2016;110:2147–50. https://doi.org/10.1016/j.bpj.2016.04.011.
291. Liu W, Stout RF, Parpura V. Ternary SNARE complexes in parallel versus anti-parallel orientation: examination of their disassembly using single-molecule force spectroscopy. Cell Calcium. 2012;52:241–9. https://doi.org/10.1016/j.ceca.2012.03.008.
292. Xiao W, Poirier MA, Bennett MK, Shin YK. The neuronal t-SNARE complex is a parallel four-helix bundle. Nat Struct Biol. 2001;8:308–11. https://doi.org/10.1038/86174.
293. Zhang F, Chen Y, Kweon DH, Kim CS, Shin YK. The four-helix bundle of the neuronal target membrane SNARE complex is neither disordered in the middle nor uncoiled at the C-terminal region. J Biol Chem. 2002;277:24294–8. https://doi.org/10.1074/jbc.M201200200.
294. Hatsuzawa K, Lang T, Fasshauer D, Bruns D, Jahn R. The R-SNARE motif of tomosyn forms SNARE core complexes with syntaxin 1 and SNAP-25 and down-regulates exocytosis. J Biol Chem. 2003;278:31159–66. https://doi.org/10.1074/jbc.M305500200.
295. Lehman K, Rossi G, Adamo JE, Brennwald P. Yeast homologues of tomosyn and lethal giant larvae function in exocytosis and are associated with the plasma membrane SNARE, Sec9. J Cell Biol. 1999;146:125–40. https://doi.org/10.1083/jcb.146.1.125.
296. Sakisaka T, Yamamoto Y, Mochida S, Nakamura M, Nishikawa K, Ishizaki H, et al. Dual inhibition of SNARE complex formation by tomosyn ensures controlled neurotransmitter release. J Cell Biol. 2008;183:323–37. https://doi.org/10.1083/jcb.200805150.
297. Widberg CH, Bryant NJ, Girotti M, Rea S, James DE. Tomosyn interacts with the t-SNAREs syntaxin4 and SNAP23 and plays a role in insulin-stimulated GLUT4 translocation. J Biol Chem. 2003;278:35093–101. https://doi.org/10.1074/jbc.M304261200.
298. Williams AL, Bielopolski N, Meroz D, Lam AD, Passmore DR, Ben-Tal N, et al. Structural and functional analysis of tomosyn identifies domains important in exocytotic regulation. J Biol Chem. 2011;286:14542–53. https://doi.org/10.1074/jbc.M110.215624.
299. McEwen JM, Madison JM, Dybbs M, Kaplan JM. Antagonistic regulation of synaptic vesicle priming by tomosyn and UNC-13. Neuron. 2006;51:303–15. https://doi.org/10.1016/j.neuron.2006.06.025.
300. Gracheva EO, Burdina AO, Holgado AM, Berthelot-Grosjean M, Ackley BD, Hadwiger G, et al. Tomosyn inhibits synaptic vesicle priming in *Caenorhabditis elegans*. PLoS Biol. 2006;4:e261. https://doi.org/10.1371/journal.pbio.0040261.
301. Pobbati AV, Razeto A, Boddener M, Becker S, Fasshauer D. Structural basis for the inhibitory role of tomosyn in exocytosis. J Biol Chem. 2004;279:47192–200. https://doi.org/10.1074/jbc.M408767200.
302. Sauvola CW, Akbergenova Y, Cunningham KL, Aponte-Santiago NA, Littleton JT. The decoy SNARE Tomosyn sets tonic versus phasic release properties and is required for homeostatic synaptic plasticity. elife. 2021;10:e72841. https://doi.org/10.7554/eLife.72841.
303. Collins KM, Thorngren NL, Fratti RA, Wickner WT. Sec17p and HOPS, in distinct SNARE complexes, mediate SNARE complex disruption or assembly for fusion. EMBO J. 2005;24:1775–86. https://doi.org/10.1038/sj.emboj.7600658.
304. Starai VJ, Hickey CM, Wickner W. HOPS proofreads the *trans*-SNARE complex for yeast vacuole fusion. Mol Biol Cell. 2008;19:2500–8. https://doi.org/10.1091/mbc.e08-01-0077.
305. Lee S, Shin J, Jung Y, Son H, Shin J, Jeong C, et al. Munc18-1 induces conformational changes of syntaxin-1 in multiple intermediates for SNARE assembly. Sci Rep. 2020;10:11623. https://doi.org/10.1038/s41598-020-68476-3.
306. Jakhanwal S, Lee CT, Urlaub H, Jahn R. An activated Q-SNARE SM protein complex as a possible intermediate in SNARE assembly. EMBO J. 2017;36:1788–802. https://doi.org/10.15252/embj.201696270.

307. Kalyana Sundaram RV, Jin H, Li F, Shu T, Coleman J, Yang J, et al. Munc13 binds and recruits SNAP25 to chaperone SNARE complex assembly. FEBS Lett. 2021;595:297–309. https://doi.org/10.1002/1873-3468.14006.
308. Shu T, Jin H, Rothman JE, Zhang Y. Munc13-1 MUN domain and Munc18-1 cooperatively chaperone SNARE assembly through a tetrameric complex. Proc Natl Acad Sci U S A. 2020;117:1036–41. https://doi.org/10.1073/pnas.1914361117.
309. Wang S, Ma C. Neuronal SNARE complex assembly guided by Munc18-1 and Munc13-1. FEBS Open Bio. 2022;12:1939–57. https://doi.org/10.1002/2211-5463.13394.
310. Shin J, Lou X, Kweon D-H, Shin Y-K. Multiple conformations of a single SNAREpin between two nanodisc membranes reveal diverse pre-fusion states. Biochem J. 2014;459:95–102. https://doi.org/10.1042/BJ20131668.
311. Xue R, Meng H, Yin J, Xia J, Hu Z, Liu H. The role of calmodulin vs. synaptotagmin in exocytosis. Front Mol Neurosci. 2021;14:691363. https://doi.org/10.3389/fnmol.2021.691363.
312. Starai VJ, Thorngren N, Fratti RA, Wickner W. Ion regulation of homotypic vacuole fusion in *Saccharomyces cerevisiae*. J Biol Chem. 2005;280:16754–62. https://doi.org/10.1074/jbc.M500421200.
313. Flanagan JJ, Barlowe C. Cysteine-disulfide cross-linking to monitor SNARE complex assembly during endoplasmic reticulum-Golgi transport. J Biol Chem. 2006;281:2281–8. https://doi.org/10.1074/jbc.M511695200.
314. Allolio C, Harries D. Calcium ions promote membrane fusion by forming negative-curvature inducing clusters on specific anionic lipids. ACS Nano. 2021;15:12880–7. https://doi.org/10.1021/acsnano.0c08614.
315. Melcrová A, Pokorna S, Pullanchery S, Kohagen M, Jurkiewicz P, Hof M, et al. The complex nature of calcium cation interactions with phospholipid bilayers. Sci Rep. 2016;6:38035. https://doi.org/10.1038/srep38035.
316. Bilkova E, Pleskot R, Rissanen S, Sun S, Czogalla A, Cwiklik L, et al. Calcium directly regulates phosphatidylinositol 4,5-bisphosphate headgroup conformation and recognition. J Am Chem Soc. 2017;139:4019–24. https://doi.org/10.1021/jacs.6b11760.
317. Witkowska A, Heinz LP, Grubmüller H, Jahn R. Tight docking of membranes before fusion represents a metastable state with unique properties. Nat Commun. 2021;12:3606. https://doi.org/10.1038/s41467-021-23722-8.
318. Weber AM, Wong FK, Tufford AR, Schlichter LC, Matveev V, Stanley EF. N-type Ca^{2+} channels carry the largest current: implications for nanodomains and transmitter release. Nat Neurosci. 2010;13:1348–50. https://doi.org/10.1038/nn.2657.
319. Sabatini BL, Regehr WG. Timing of neurotransmission at fast synapses in the mammalian brain. Nature. 1996;384:170–2. https://doi.org/10.1038/384170a0.
320. Giraudo CG, Eng WS, Melia TJ, Rothman JE. A clamping mechanism involved in SNARE-dependent exocytosis. Science. 2006;313:676–80. https://doi.org/10.1126/science.1129450.
321. Melia TJ. Putting the clamps on membrane fusion: how complexin sets the stage for calcium-mediated exocytosis. FEBS Lett. 2007;581:2131–9. https://doi.org/10.1016/j.febslet.2007.02.066.
322. Yin L, Kim J, Shin Y-K. Complexin splits the membrane-proximal region of a single SNAREpin. Biochem J. 2016;473:2219–24. https://doi.org/10.1042/BCJ20160339.
323. Brunger AT, Leitz J, Zhou Q, Choi UB, Lai Y. Ca^{2+}-triggered synaptic vesicle fusion initiated by release of inhibition. Trends Cell Biol. 2018;28:631–45. https://doi.org/10.1016/j.tcb.2018.03.004.
324. Bai J, Chapman ER. The C2 domains of synaptotagmin--partners in exocytosis. Trends Biochem Sci. 2004;29:143–51. https://doi.org/10.1016/j.tibs.2004.01.008.
325. Davis AF, Bai J, Fasshauer D, Wolowick MJ, Lewis JL, Chapman ER. Kinetics of synaptotagmin responses to Ca^{2+} and assembly with the core SNARE complex onto membranes. Neuron. 1999;24:363–76. https://doi.org/10.1016/S0896-6273(00)80850-8.
326. Brose N, Petrenko AG, Südhof TC, Jahn R. Synaptotagmin: a calcium sensor on the synaptic vesicle surface. Science. 1992;256:1021–5. https://doi.org/10.1126/science.1589771.

327. Geppert M, Goda Y, Hammer RE, Li C, Rosahl TW, Stevens CF, et al. Synaptotagmin I: a major Ca^{2+} sensor for transmitter release at a central synapse. Cell. 1994;79:717–27. https://doi.org/10.1016/0092-8674(94)90556-8.
328. Fernandez-Chacon R, Konigstorfer A, Gerber SH, Garcia J, Matos MF, Stevens CF, et al. Synaptotagmin I functions as a calcium regulator of release probability. Nature. 2001;410:41–9. https://doi.org/10.1038/35065004.
329. Littleton JT, Stern M, Schulze K, Perin M, Bellen HJ. Mutational analysis of *Drosophila* synaptotagmin demonstrates its essential role in Ca^{2+}-activated neurotransmitter release. Cell. 1993;74:1125–34. https://doi.org/10.1016/0092-8674(93)90733-7.
330. Rhee JS, Li LY, Shin OH, Rah JC, Rizo J, Südhof TC, et al. Augmenting neurotransmitter release by enhancing the apparent Ca^{2+} affinity of synaptotagmin 1. Proc Natl Acad Sci U S A. 2005;102:18664–9. https://doi.org/10.1073/pnas.0509153102.
331. Schneggenburger R, Neher E. Intracellular calcium dependence of transmitter release rates at a fast central synapse. Nature. 2000;406:889–93. https://doi.org/10.1038/35022702.
332. Shao X, Li C, Fernandez I, Zhang X, Südhof TC, Rizo J. Synaptotagmin-syntaxin interaction: the C2 domain as a Ca^{2+}-dependent electrostatic switch. Neuron. 1997;18:133–42. https://doi.org/10.1016/S0896-6273(01)80052-0.
333. Zhang X, Rizo J, Südhof TC. Mechanism of Phospholipid Binding by the C2A-Domain of Synaptotagmin I. Biochemistry. 1998;37:12395–403. https://doi.org/10.1021/bi9807512.
334. Chapman ER, Davis AF. Direct interaction of a Ca^{2+}-binding loop of synaptotagmin with lipid bilayers. J Biol Chem. 1998;273:13995–4001. https://doi.org/10.1074/jbc.273.22.13995.
335. Wu Z, Ma L, Courtney NA, Zhu J, Landajuela A, Zhang Y, et al. Polybasic patches in both C2 domains of synaptotagmin-1 are required for evoked neurotransmitter release. J Neurosci. 2022;42:5816–29. https://doi.org/10.1523/JNEUROSCI.1385-21.2022.
336. Bai J, Earles CA, Lewis JL, Chapman ER. Membrane-embedded synaptotagmin penetrates *cis* or *trans* target membranes and clusters via a novel mechanism. J Biol Chem. 2000;275:25427–35. https://doi.org/10.1074/jbc.M906729199.
337. Littleton JT, Bai J, Vyas B, Desai R, Baltus AE, Garment MB, et al. Synaptotagmin mutants reveal essential functions for the C2B domain in Ca^{2+}-triggered fusion and recycling of synaptic vesicles *in vivo*. J Neurosci. 2001;21:1421–33. https://doi.org/10.1523/JNEUROSCI.21-05-01421.2001.
338. Shin OH, Rhee JS, Tang J, Sugita S, Rosenmund C, Südhof TC. Sr^{2+} binding to the Ca^{2+} binding site of the synaptotagmin 1 C2B domain triggers fast exocytosis without stimulating SNARE interactions. Neuron. 2003;37:99–108. https://doi.org/10.1016/S0896-6273(02)01145-5.
339. Li L, Liu H, Wang W, Chandra M, Collins BM, Hu Z. SNT-1 functions as the Ca^{2+} sensor for tonic and evoked neurotransmitter release in *Caenorhabditis elegans*. J Neurosci. 2018;38:5313–24. https://doi.org/10.1523/JNEUROSCI.3097-17.2018.
340. Gruget C, Bello O, Coleman J, Krishnakumar SS, Perez E, Rothman JE, et al. Synaptotagmin-1 membrane binding is driven by the C2B domain and assisted cooperatively by the C2A domain. Sci Rep. 2020;10:18011. https://doi.org/10.1038/s41598-020-74923-y.
341. Nyenhuis SB, Thapa A, Cafiso DS. Phosphatidylinositol 4,5 bisphosphate controls the *cis* and *trans* interactions of synaptotagmin-1. Biophys J. 2019;117:247–57. https://doi.org/10.1016/j.bpj.2019.06.016.
342. Bai H, Xue R, Bao H, Zhang L, Yethiraj A, Cui Q, et al. Different states of synaptotagmin regulate evoked versus spontaneous release. Nat Commun. 2016;7:10971. https://doi.org/10.1038/ncomms10971.
343. Araç D, Chen X, Khant HA, Ubach J, Ludtke SJ, Kikkawa M, et al. Close membrane-membrane proximity induced by Ca^{2+}-dependent multivalent binding of synaptotagmin-1 to phospholipids. Nat Struct Mol Biol. 2006;13:209–17. https://doi.org/10.1038/nsmb1056.
344. Bai J, Tucker WC, Chapman ER. PIP_2 increases the speed of response of synaptotagmin and steers its membrane-penetration activity toward the plasma membrane. Nat Struct Mol Biol. 2004;11:36–44. https://doi.org/10.1016/S0896-6273(04)00117-5.

345. Xue M, Ma C, Craig TK, Rosenmund C, Rizo J. The Janus-faced nature of the C2B domain is fundamental for synaptotagmin-1 function. Nat Struct Mol Biol. 2008;15:1160–8. https://doi.org/10.1038/nsmb.1508.
346. Rufener E, Frazier AA, Wieser CM, Hinderliter A, Cafiso DS. Membrane-bound orientation and position of the synaptotagmin C2B domain determined by site-directed spin labeling. Biochemistry. 2005;44:18–28. https://doi.org/10.1021/bi048370d.
347. Fernandez I, Araç D, Ubach J, Gerber SH, Shin O, Gao Y, et al. Three-dimensional structure of the synaptotagmin 1 C2B-domain: synaptotagmin 1 as a phospholipid binding machine. Neuron. 2001;32:1057–69. https://doi.org/10.1016/S0896-6273(01)00548-7.
348. Zhou Q, Lai Y, Bacaj T, Zhao M, Lyubimov AY, Uervirojnangkoorn M, et al. Architecture of the synaptotagmin–SNARE machinery for neuronal exocytosis. Nature. 2015;525:62–7. https://doi.org/10.1038/nature14975.
349. Voleti R, Jaczynska K, Rizo J. Ca^{2+}-dependent release of synaptotagmin-1 from the SNARE complex on phosphatidylinositol 4,5-bisphosphate-containing membranes. elife. 2020;9:e57154. https://doi.org/10.7554/eLife.57154.
350. Gipson P, Fukuda Y, Danev R, Lai Y, Chen D-H, Baumeister W, et al. Morphologies of synaptic protein membrane fusion interfaces. Proc Natl Acad Sci U S A. 2017;114:9110–5. https://doi.org/10.1073/pnas.1708492114.
351. Tucker WC, Weber T, Chapman ER. Reconstitution of Ca^{2+}-regulated membrane fusion by synaptotagmin and SNAREs. Science. 2004;304:435–8. https://doi.org/10.1126/science.1097196.
352. Chicka MC, Hui E, Liu H, Chapman ER. Synaptotagmin arrests the SNARE complex before triggering fast, efficient membrane fusion in response to Ca^{2+}. Nat Struct Mol Biol. 2008;15:827. https://doi.org/10.1038/nsmb.1463.
353. Schiavo G, Stenbeck G, Rothman JE, Söllner TH. Binding of the synaptic vesicle v-SNARE, synaptotagmin, to the plasma membrane t-SNARE, SNAP-25, can explain docked vesicles at neurotoxin-treated synapses. Proc Natl Acad Sci U S A. 1997;94:997–1001. https://doi.org/10.1073/pnas.94.3.997.
354. Chang S, Trimbuch T, Rosenmund C. Synaptotagmin-1 drives synchronous Ca^{2+}-triggered fusion by C2B-domain-mediated synaptic-vesicle-membrane attachment. Nat Neurosci. 2018;21:33–40. https://doi.org/10.1038/s41593-017-0037-5.
355. Schupp M, Malsam J, Ruiter M, Scheutzow A, Wierda KDB, Söllner TH, et al. Interactions between SNAP-25 and synaptotagmin-1 are involved in vesicle priming, clamping spontaneous and stimulating evoked neurotransmission. J Neurosci. 2016;36:11865–80. https://doi.org/10.1523/JNEUROSCI.1011-16.2016.
356. Brewer KD, Bacaj T, Cavalli A, Camilloni C, Swarbrick JD, Liu J, et al. Dynamic binding mode of a Synaptotagmin-1–SNARE complex in solution. Nat Struct Mol Biol. 2015;22:555–64. https://doi.org/10.1038/nsmb.3035.
357. Bai J, Wang P, Chapman ER. C2A activates a cryptic Ca^{2+}-triggered membrane penetration activity within the C2B domain of synaptotagmin I. Proc Natl Acad Sci U S A. 2002;99:1665–70. https://doi.org/10.1073/pnas.032541099.
358. Kiessling V, Kreutzberger AJB, Liang B, Nyenhuis SB, Seelheim P, Castle JD, et al. A molecular mechanism for calcium-mediated synaptotagmin-triggered exocytosis. Nat Struct Mol Biol. 2018;25:911–7. https://doi.org/10.1038/s41594-018-0130-9.
359. Gong J, Lai Y, Li X, Wang M, Leitz J, Hu Y, et al. C-terminal domain of mammalian complexin-1 localizes to highly curved membranes. Proc Natl Acad Sci U S A. 2016;113:E7590–9. https://doi.org/10.1073/pnas.1609917113.
360. Lottermoser JA, Dittman JS. Complexin membrane interactions: implications for synapse evolution and function. J Mol Biol. 2023;435:167774. https://doi.org/10.1016/j.jmb.2022.167774.
361. Pabst S, Hazzard JW, Antonin W, Südhof TC, Jahn R, Rizo J, et al. Selective interaction of complexin with the neuronal SNARE complex. J Biol Chem. 2000;275:19808–18. https://doi.org/10.1074/jbc.M002571200.

362. Wragg RT, Parisotto DA, Li Z, Terakawa MS, Snead D, Basu I, et al. Evolutionary divergence of the C-terminal domain of complexin accounts for functional disparities between vertebrate and invertebrate complexins. Front Mol Neurosci. 2017;10:146. https://doi.org/10.3389/fnmol.2017.00146.
363. McMahon HT, Missler M, Li C, Südhof TC. Complexins: cytosolic proteins that regulate SNAP receptor function. Cell. 1995;83:111–9. https://doi.org/10.1016/0092-8674(95)90239-2.
364. Chen X, Tomchick DR, Kovrigin E, Araç D, Machius M, Südhof TC, et al. Three-dimensional structure of the complexin/SNARE complex. Neuron. 2002;33:397–409. https://doi.org/10.1016/S0896-6273(02)00583-4.
365. Trimbuch T, Xu J, Flaherty D, Tomchick DR, Rizo J, Rosenmund C. Re-examining how complexin inhibits neurotransmitter release. elife. 2014;3:e02391. https://doi.org/10.7554/eLife.02391.
366. Radoff DT, Dong Y, Snead D, Bai J, Eliezer D, Dittman JS. The accessory helix of complexin functions by stabilizing central helix secondary structure. elife. 2014;3:e04553. https://doi.org/10.7554/eLife.04553.
367. Rizo J, Sari L, Qi Y, Im W, Lin MM. All-atom molecular dynamics simulations of Synaptotagmin-SNARE-complexin complexes bridging a vesicle and a flat lipid bilayer. elife. 2022;11:e76356. https://doi.org/10.7554/eLife.76356.
368. Malsam J, Bärfuss S, Trimbuch T, Zarebidaki F, Sonnen AFP, Wild K, et al. Complexin suppresses spontaneous exocytosis by capturing the membrane-proximal regions of VAMP2 and SNAP25. Cell Rep. 2020;32:107926. https://doi.org/10.1016/j.celrep.2020.107926.
369. Reim K, Mansour M, Varoqueaux F, McMahon HT, Südhof TC, Brose N, et al. Complexins regulate a late step in Ca^{2+}-dependent neurotransmitter release. Cell. 2001;104:71–81. https://doi.org/10.1016/S0092-8674(01)00192-1.
370. Xue M, Stradomska A, Chen H, Brose N, Zhang W, Rosenmund C, et al. Complexins facilitate neurotransmitter release at excitatory and inhibitory synapses in mammalian central nervous system. Proc Natl Acad Sci U S A. 2008;105:7875–80. https://doi.org/10.1073/pnas.0803012105.
371. Courtney NA, Bao H, Briguglio JS, Chapman ER. Synaptotagmin 1 clamps synaptic vesicle fusion in mammalian neurons independent of complexin. Nat Commun. 2019;10:4076. https://doi.org/10.1038/s41467-019-12015-w.
372. Jorquera RA, Huntwork-Rodriguez S, Akbergenova Y, Cho RW, Littleton JT. Complexin controls spontaneous and evoked neurotransmitter release by regulating the timing and properties of synaptotagmin activity. J Neurosci. 2012;32:18234–45. https://doi.org/10.1523/JNEUROSCI.3212-12.2012.
373. Hobson RJ, Liu Q, Watanabe S, Jorgensen EM. Complexin maintains vesicles in the primed state in *C. elegans*. Curr Biol. 2011;21:106–13. https://doi.org/10.1016/j.cub.2010.12.015.
374. Martin JA, Hu Z, Fenz KM, Fernandez J, Dittman JS. Complexin has opposite effects on two modes of synaptic vesicle fusion. Curr Biol. 2011;21:97–105. https://doi.org/10.1016/j.cub.2010.12.014.
375. Xue M, Reim K, Chen X, Chao HT, Deng H, Rizo J, et al. Distinct domains of complexin I differentially regulate neurotransmitter release. Nat Struct Mol Biol. 2007;14:949–58. https://doi.org/10.1038/nsmb1292.
376. Xue M, Lin YQ, Pan H, Reim K, Deng H, Bellen HJ, et al. Tilting the balance between facilitatory and inhibitory functions of mammalian and *Drosophila* complexins orchestrates synaptic vesicle exocytosis. Neuron. 2009;64:367–80. https://doi.org/10.1016/j.neuron.2009.09.043.
377. Yang X, Pei J, Kaeser-Woo YJ, Bacaj T, Grishin NV, Südhof TC. Evolutionary conservation of complexins: from choanoflagellates to mice. EMBO Rep. 2015;16:1308–17. https://doi.org/10.15252/embr.201540305.
378. Diao J, Cipriano DJ, Zhao M, Zhang Y, Shah S, Padolina MS, et al. Complexin-1 enhances the on-rate of vesicle docking via simultaneous SNARE and membrane interactions. J Am Chem Soc. 2013;135:15274–7. https://doi.org/10.1021/ja407392n.

379. Arthur CP, Dean C, Pagratis M, Chapman ER, Stowell MHB. Loss of synaptotagmin IV results in a reduction in synaptic vesicles and a distortion of the Golgi structure in cultured hippocampal neurons. Neuroscience. 2010;167:135–42. https://doi.org/10.1016/j.neuroscience.2010.01.056.
380. Zhu J, McDargh ZA, Li F, Krishnakumar SS, Rothman JE, O'Shaughnessy B. Synaptotagmin rings as high-sensitivity regulators of synaptic vesicle docking and fusion. Proc Natl Acad Sci U S A. 2022;119:e2208337119. https://doi.org/10.1073/pnas.2208337119.
381. Huntwork S, Littleton JT. A complexin fusion clamp regulates spontaneous neurotransmitter release and synaptic growth. Nat Neurosci. 2007;10:1235–7. https://doi.org/10.1038/nn1980.
382. Brunger AT, Leitz J. The core complex of the Ca^{2+}-triggered presynaptic fusion machinery. J Mol Biol. 2022;435:167853. https://doi.org/10.1016/j.jmb.2022.167853.
383. Rizo J. Molecular mechanisms underlying neurotransmitter release. Annu Rev Biophys. 2022;51:377–408. https://doi.org/10.1146/annurev-biophys-111821-104732.
384. Maximov A, Tang J, Yang X, Pang ZP, Südhof TC. Complexin controls the force transfer from SNARE complexes to membranes in fusion. Science. 2009;323:516–21. https://doi.org/10.1126/science.1166505.
385. Cao P, Yang X, Südhof TC. Complexin activates exocytosis of distinct secretory vesicles controlled by different synaptotagmins. J Neurosci. 2013;33:1714–27. https://doi.org/10.1523/JNEUROSCI.4087-12.2013.
386. Kaeser-Woo YJ, Yang X, Südhof TC. C-terminal complexin sequence is selectively required for clamping and priming but not for Ca^{2+} triggering of synaptic exocytosis. J Neurosci. 2012;32:2877–85. https://doi.org/10.1523/JNEUROSCI.3360-11.2012.
387. Yang X, Kaeser-Woo YJ, Pang ZP, Xu W, Südhof TC. Complexin clamps asynchronous release by blocking a secondary Ca^{2+} sensor via its accessory α helix. Neuron. 2010;68:907–20. https://doi.org/10.1016/j.neuron.2010.11.001.
388. Xue M, Craig TK, Xu J, Chao H-T, Rizo J, Rosenmund C. Binding of the complexin N terminus to the SNARE complex potentiates synaptic-vesicle fusogenicity. Nat Struct Mol Biol. 2010;17:568–75. https://doi.org/10.1038/nsmb.1791.
389. Chang S, Reim K, Pedersen M, Neher E, Brose N, Taschenberger H. Complexin stabilizes newly primed synaptic vesicles and prevents their premature fusion at the mouse calyx of held synapse. J Neurosci. 2015;35:8272–90. https://doi.org/10.1523/JNEUROSCI.4841-14.2015.
390. Neher E, Brose N. Dynamically primed synaptic vesicle states: key to understand synaptic short-term plasticity. Neuron. 2018;100:1283–91. https://doi.org/10.1016/j.neuron.2018.11.024.
391. Lee JS, Ho W-K, Neher E, Lee S-H. Superpriming of synaptic vesicles after their recruitment to the readily releasable pool. Proc Natl Acad Sci U S A. 2013;110:15079–84. https://doi.org/10.1073/pnas.1314427110.
392. Palfreyman MT, Jorgensen EM. Unc13 aligns SNAREs and superprimes synaptic vesicles. Neuron. 2017;95:473–5. https://doi.org/10.1016/j.neuron.2017.07.017.
393. Ishiyama S, Schmidt H, Cooper BH, Brose N, Eilers J. Munc13-3 superprimes synaptic vesicles at granule cell-to-basket cell synapses in the mouse cerebellum. J Neurosci. 2014;34:14687–96. https://doi.org/10.1523/JNEUROSCI.2060-14.2014.
394. Schlüter OM, Basu J, Südhof TC, Rosenmund C. Rab3 superprimes synaptic vesicles for release: implications for short-term synaptic plasticity. J Neurosci. 2006;26:1239–46. https://doi.org/10.1523/jneurosci.3553-05.2006.
395. Michelassi F, Liu H, Hu Z, Dittman JS. A C1-C2 module in Munc13 inhibits calcium-dependent neurotransmitter release. Neuron. 2017;95:577–90.e5. https://doi.org/10.1016/j.neuron.2017.07.015.
396. Taschenberger H, Woehler A, Neher E. Superpriming of synaptic vesicles as a common basis for intersynapse variability and modulation of synaptic strength. Proc Natl Acad Sci U S A. 2016;113:E4548–57. https://doi.org/10.1073/pnas.1606383113.

397. Murray DH, Jahnel M, Lauer J, Avellaneda MJ, Brouilly N, Cezanne A, et al. An endosomal tether undergoes an entropic collapse to bring vesicles together. Nature. 2016;537:107–11. https://doi.org/10.1038/nature19326.
398. Chernomordik LV, Kozlov MM. Mechanics of membrane fusion. Nat Struct Mol Biol. 2008;15:675–83. https://doi.org/10.1038/nsmb.1463.
399. Kozlov MM, McMahon HT, Chernomordik LV. Protein-driven membrane stresses in fusion and fission. Trends Biochem Sci. 2010;35:699–706. https://doi.org/10.1016/j.tibs.2010.06.003.
400. Kozlov MM, Markin VS. Possible mechanism of membrane fusion. Biofizika. 1983;28:242–7.
401. Markin VS, Kozlov MM, Borovjagin VL. On the theory of membrane fusion. The stalk mechanism. Gen Physiol Biophys. 1984;3:361–77.
402. Efrat A, Chernomordik LV, Kozlov MM. Point-like protrusion as a prestalk intermediate in membrane fusion pathway. Biophys J. 2007;92:L61–3. https://doi.org/10.1529/biophysj.106.103341.
403. Smirnova YG, Marrink S-J, Lipowsky R, Knecht V. Solvent-exposed tails as prestalk transition states for membrane fusion at low hydration. J Am Chem Soc. 2010;132:6710–8. https://doi.org/10.1021/ja910050x.
404. Yang L, Huang HW. Observation of a membrane fusion intermediate structure. Science. 2002;297:1877–9. https://doi.org/10.1126/science.1074354.
405. Wong JL, Koppel DE, Cowan AE, Wessel GM. Membrane hemifusion is a stable intermediate of exocytosis. Dev Cell. 2007;12:653–9. https://doi.org/10.1016/j.devcel.2007.02.007.
406. Reese C, Heise F, Mayer A. *Trans*-SNARE pairing can precede a hemifusion intermediate in intracellular membrane fusion. Nature. 2005;436:410–4. https://doi.org/10.1083/jcb.200502115.
407. Jun Y, Wickner W. Assays of vacuole fusion resolve the stages of docking, lipid mixing, and content mixing. Proc Natl Acad Sci U S A. 2007;104:13010–5. https://doi.org/10.1073/pnas.0700970104.
408. Kemble GW, Danieli T, White JM. Lipid-anchored influenza hemagglutinin promotes hemifusion, not complete fusion. Cell. 1994;76:383–91. https://doi.org/10.1016/0092-8674(94)90344-1.
409. Lu X, Zhang F, McNew JA, Shin YK. Membrane fusion induced by neuronal SNAREs transits through hemifusion. J Biol Chem. 2005;280:30538–41. https://doi.org/10.1074/jbc.M506862200.
410. Yoon TY, Okumus B, Zhang F, Shin YK, Ha T. Multiple intermediates in SNARE-induced membrane fusion. Proc Natl Acad Sci U S A. 2006;103:19731–6. https://doi.org/10.1073/pnas.0606032103.
411. Diao J, Grob P, Cipriano DJ, Kyoung M, Zhang Y, Shah S, et al. Synaptic proteins promote calcium-triggered fast transition from point contact to full fusion. elife. 2012:e00109. https://doi.org/10.7554/eLife.00109.
412. Oelkers M, Witt H, Halder P, Jahn R, Janshoff A. SNARE-mediated membrane fusion trajectories derived from force-clamp experiments. Proc Natl Acad Sci U S A. 2016;113:13051–6. https://doi.org/10.1073/pnas.1615885113.
413. Risselada HJ, Bubnis G, Grubmüller H. Expansion of the fusion stalk and its implication for biological membrane fusion. Proc Natl Acad Sci U S A. 2014;111:11043–8. https://doi.org/10.1073/pnas.1323221111.
414. Palfreyman MT, Jorgensen EM. *In Vivo* analysis of membrane fusion. In: John W, Sons L, editors. Encyclopedia of life sciences (ELS); 2015. p. 1–21. https://doi.org/10.1002/9780470015902.a0020891.pub2Wiley.
415. Podbilewicz B. Virus and cell fusion mechanisms. Annu Rev Cell Dev Biol. 2014;30:111–39. https://doi.org/10.1146/annurev-cellbio-101512-122422.
416. Joardar A, Pattnaik GP, Chakraborty H. Mechanism of membrane fusion: interplay of lipid and peptide. J Membr Biol. 2022;255:211–24. https://doi.org/10.1007/s00232-022-00233-1.

417. Poirier MA, Xiao W, Macosko JC, Chan C, Shin YK, Bennett MK. The synaptic SNARE complex is a parallel four-stranded helical bundle. Nat Struct Biol. 1998;5:765–9. https://doi.org/10.1038/1799.
418. Langosch D, Hofmann M, Ungermann C. The role of transmembrane domains in membrane fusion. Cell Mol Life Sci. 2007;64:850–64. https://doi.org/10.1007/s00018-007-6439-x.
419. Hu Y, Zhu L, Ma C. Structural roles for the juxtamembrane linker region and transmembrane region of synaptobrevin 2 in membrane fusion. Front Cell Dev Biol. 2021;8:609708. https://doi.org/10.3389/fcell.2020.609708.
420. Borisovska M, Schwarz YN, Dhara M, Yarzagaray A, Hugo S, Narzi D, et al. Membrane-proximal tryptophans of synaptobrevin II stabilize priming of secretory vesicles. J Neurosci. 2012;32:15983–97. https://doi.org/10.1523/JNEUROSCI.6282-11.2012.
421. James DJ, Khodthong C, Kowalchyk JA, Martin TF. Phosphatidylinositol 4,5-bisphosphate regulates SNARE-dependent membrane fusion. J Cell Biol. 2008;182:355–66. https://doi.org/10.1083/jcb.200801056.
422. Lam AD, Tryoen-Toth P, Tsai B, Vitale N, Stuenkel EL. SNARE-catalyzed fusion events are regulated by Syntaxin1A lipid interactions. Mol Biol Cell. 2008;19:485–97. https://doi.org/10.1091/mbc.e07-02-0148.
423. Vardar G, Salazar-Lázaro A, Zobel S, Trimbuch T, Rosenmund C. Syntaxin-1A modulates vesicle fusion in mammalian neurons via juxtamembrane domain dependent palmitoylation of its transmembrane domain. elife. 2022;11:e78182. https://doi.org/10.7554/eLife.78182.
424. Van Komen JS, Bai X, Rodkey TL, Schaub J, McNew JA. The polybasic juxtamembrane region of Sso1p is required for SNARE function *in vivo*. Eukaryot Cell. 2005;4:2017–28. https://doi.org/10.1128/EC.4.12.2017-2028.2005.
425. Kesavan J, Borisovska M, Bruns D. v-SNARE actions during Ca^{2+}-triggered exocytosis. Cell. 2007;131:351–63. https://doi.org/10.1016/j.cell.2007.09.025.
426. Kiessling V, Tamm LK. Measuring distances in supported bilayers by fluorescence interference-contrast microscopy: polymer supports and SNARE proteins. Biophys J. 2003;84:408–18. https://doi.org/10.1016/S0006-3495(03)74861-9.
427. Stein A, Weber G, Wahl MC, Jahn R. Helical extension of the neuronal SNARE complex into the membrane. Nature. 2009;460:525–8. https://doi.org/10.1038/nature08156.
428. Knecht V, Grubmüller H. Mechanical coupling via the membrane fusion SNARE protein syntaxin 1A: a molecular dynamics study. Biophys J. 2003;84:1527–47. https://doi.org/10.1016/S0006-3495(03)74965-0.
429. Hernandez JM, Kreutzberger AJ, Kiessling V, Tamm LK, Jahn R. Variable cooperativity in SNARE-mediated membrane fusion. Proc Natl Acad Sci U S A. 2014;111:12037–42. https://doi.org/10.1073/pnas.1407435111.
430. Van Den Bogaart G, Holt MG, Bunt G, Riedel D, Wouters FS, Jahn R. One SNARE complex is sufficient for membrane fusion. Nat Struct Mol Biol. 2010;17:358–64. https://doi.org/10.1038/nsmb.1748.
431. Shi L, Shen QT, Kiel A, Wang J, Wang HW, Melia TJ, et al. SNARE proteins: one to fuse and three to keep the nascent fusion pore open. Science. 2012;335:1355–9. https://doi.org/10.1126/science.1214984.
432. Li F, Pincet F, Perez E, Eng WS, Melia TJ, Rothman JE, et al. Energetics and dynamics of SNAREpin folding across lipid bilayers. Nat Struct Mol Biol. 2007;14:890–6. https://doi.org/10.1038/nsmb1310.
433. Rickman C, Hu K, Carroll J, Davletov B. Self-assembly of SNARE fusion proteins into star-shaped oligomers. Biochem J. 2005;388:75–9. https://doi.org/10.1042/BJ20041818.
434. Li X, Radhakrishnan A, Grushin K, Kasula R, Chaudhuri A, Gomathinayagam S, et al. Symmetrical organization of proteins under docked synaptic vesicles. FEBS Lett. 2019;593:144–53. https://doi.org/10.1002/1873-3468.13316.
435. Radhakrishnan A, Li X, Grushin K, Krishnakumar SS, Liu J, Rothman JE. Symmetrical arrangement of proteins under release-ready vesicles in presynaptic terminals. Proc Natl Acad Sci U S A. 2021;118:e2024029118. https://doi.org/10.1073/pnas.2024029118.

436. Manca F, Pincet F, Truskinovsky L, Rothman JE, Foret L, Caruel M. SNARE machinery is optimized for ultrafast fusion. Proc Natl Acad Sci U S A. 2019;116:2435–42. https://doi.org/10.1073/pnas.1820394116.
437. Bowen ME, Engelman DM, Brunger AT. Mutational analysis of synaptobrevin transmembrane domain oligomerization. Biochemistry. 2002;41:15861–6. https://doi.org/10.1021/bi0269411.
438. Roy R, Peplowska K, Rohde J, Ungermann C, Langosch D. Role of the Vam3p transmembrane segment in homodimerization and SNARE complex formation. Biochemistry. 2006;45:7654–60. https://doi.org/10.1021/bi052620o.
439. Laage R, Rohde J, Brosig B, Langosch D. A conserved membrane-spanning amino acid motif drives homomeric and supports heteromeric assembly of presynaptic SNARE proteins. J Biol Chem. 2000;275:17481–7. https://doi.org/10.1074/jbc.M910092199.
440. Margittai M, Otto H, Jahn R. A stable interaction between syntaxin 1a and synaptobrevin 2 mediated by their transmembrane domains. FEBS Lett. 1999;446:40–4. https://doi.org/10.1016/S0014-5793(99)00028-9.
441. Montecucco C, Schiavo G, Pantano S. SNARE complexes and neuroexocytosis: how many, how close? Trends Biochem Sci. 2005;30:367–72. https://doi.org/10.1016/j.tibs.2005.05.002.
442. Raciborska DA, Trimble WS, Charlton MP. Presynaptic protein interactions *in vivo*: evidence from botulinum A, C, D and E action at frog neuromuscular junction. Eur J Neurosci. 1998;10:2617–28. https://doi.org/10.1046/j.1460-9568.1998.00270.x.
443. Stewart BA, Mohtashami M, Trimble WS, Boulianne GL. SNARE proteins contribute to calcium cooperativity of synaptic transmission. Proc Natl Acad Sci U S A. 2000;97:13955–60. https://doi.org/10.1073/pnas.250491397.
444. Hua Y, Scheller RH. Three SNARE complexes cooperate to mediate membrane fusion. Proc Natl Acad Sci U S A. 2001;98:8065–70. https://doi.org/10.1073/pnas.131214798.
445. Mohrmann R, de Wit H, Verhage M, Neher E, Sørensen JB. Fast vesicle fusion in living cells requires at least three SNARE complexes. Science. 2010;330:502–5. https://doi.org/10.1126/science.1193134.
446. Mohrmann R, Sørensen JB. SNARE requirements en route to exocytosis: from many to few. J Mol Neurosci. 2012;48:387–94. https://doi.org/10.1007/s12031-012-9744-2.
447. Sinha R, Ahmed S, Jahn R, Klingauf J. Two synaptobrevin molecules are sufficient for vesicle fusion in central nervous system synapses. Proc Natl Acad Sci U S A. 2011;108:14318–23. https://doi.org/10.1073/pnas.1101818108.
448. Dodge FA, Rahamimoff R. Co-operative action of calcium ions in transmitter release at the neuromuscular junction. J Physiol. 1967;193:419–32. https://doi.org/10.1113/jphysiol.1967.sp008367.
449. Littleton JT, Barnard RJ, Titus SA, Slind J, Chapman ER, Ganetzky B. SNARE-complex disassembly by NSF follows synaptic-vesicle fusion. Proc Natl Acad Sci U S A. 2001;98:12233–8. https://doi.org/10.1073/pnas.221450198.
450. Koo Seong J, Kochlamazashvili G, Rost B, Puchkov D, Gimber N, Lehmann M, et al. Vesicular Synaptobrevin/VAMP2 Levels Guarded by AP180 Control Efficient Neurotransmission. Neuron. 2015;88:330–44. https://doi.org/10.1016/j.neuron.2015.08.034.
451. Okamoto M, Schoch S, Südhof TC. EHSH1/Intersectin, a protein that contains EH and SH3 domains and binds to dynamin and SNAP-25. J Biol Chem. 1999;274:18446–54. https://doi.org/10.1074/jbc.274.26.18446.
452. Jäpel M, Gerth F, Sakaba T, Bacetic J, Yao L, Koo S-J, et al. Intersectin-mediated clearance of SNARE complexes is required for fast neurotransmission. Cell Rep. 2020;30:409–20.e6. https://doi.org/10.1016/j.celrep.2019.12.035.
453. Watanabe S, Trimbuch T, Camacho-Pérez M, Rost BR, Brokowski B, Söhl-Kielczynski B, et al. Clathrin regenerates synaptic vesicles from endosomes. Nature. 2014;515:228–33. https://doi.org/10.1038/nature13846.
454. Rothman JE. The principle of membrane fusion in the cell (Nobel lecture). Angew Chem. 2014;53:12676–94. https://doi.org/10.1002/anie.201402380.
455. Südhof TC. The molecular machinery of neurotransmitter release (Nobel lecture). Angew Chem. 2014;53:12696–717. https://doi.org/10.1002/anie.201406359.

456. Bracher A, Kadlec J, Betz H, Weissenhorn W. X-ray structure of a neuronal complexin-SNARE complex from squid. J Biol Chem. 2002;277:26517–23. https://doi.org/10.1074/jbc.M203460200.
457. Waterhouse A, Bertoni M, Bienert S, Studer G, Tauriello G, Gumienny R, et al. SWISS-MODEL: homology modelling of protein structures and complexes. Nucleic Acids Res. 2018;46:W296–303. https://doi.org/10.1093/nar/gky427.
458. Pettersen EF, Goddard TD, Huang CC, Meng EC, Couch GS, Croll TI, et al. UCSF ChimeraX: structure visualization for researchers, educators, and developers. Protein Sci. 2021;30:70–82. https://doi.org/10.1002/pro.3943.

Calcium Sensors of Neurotransmitter Release

Qiangjun Zhou

Abstract Calcium (Ca^{2+}) plays a critical role in triggering all three primary modes of neurotransmitter release (synchronous, asynchronous, and spontaneous). Synaptotagmin1, a protein with two C2 domains, is the first isoform of the synaptotagmin family that was identified and demonstrated as the primary Ca^{2+} sensor for synchronous neurotransmitter release. Other isoforms of the synaptotagmin family as well as other C2 proteins such as the double C2 domain protein family were found to act as Ca^{2+} sensors for different modes of neurotransmitter release. Major recent advances and previous data suggest a new model, release-of-inhibition, for the initiation of Ca^{2+}-triggered synchronous neurotransmitter release. Synaptotagmin1 binds Ca^{2+} via its two C2 domains and relieves a primed pre-fusion machinery. Before Ca^{2+} triggering, synaptotagmin1 interacts Ca^{2+} independently with partially zippered SNARE complexes, the plasma membrane, phospholipids, and other components to form a primed pre-fusion state that is ready for fast release. However, membrane fusion is inhibited until the arrival of Ca^{2+} reorients the Ca^{2+}-binding loops of the C2 domain to perturb the lipid bilayers, help bridge the membranes, and/or induce membrane curvatures, which serves as a power stroke to activate fusion. This chapter reviews the evidence supporting these models and discusses the molecular interactions that may underlie these abilities.

Keywords Synaptotagmin · Synchronous release · Asynchronous release · Spontaneous release · SNARE complex · Complexin · Vesicle fusion

Q. Zhou (✉)
Department of Cell and Developmental Biology, Vanderbilt Brain Institute, Vanderbilt University, Nashville, TN, USA
e-mail: qiangjun.zhou@vanderbilt.edu

Z.-W. Wang (ed.), *Molecular Mechanisms of Neurotransmitter Release*,
Advances in Neurobiology 33, https://doi.org/10.1007/978-3-031-34229-5_5

Ca^{2+} in the presynaptic terminal triggers synaptic vesicle exocytosis, thereby releasing the neurotransmitters contained in synaptic vesicles during synaptic transmission. As described in previous chapters, the formation of a SNARE (*s*oluble *N*-ethylmaleimide-sensitive factor *a*ttachment *re*ceptor) complex is an essential step in synaptic vesicle fusion. While SNARE complex formation is Ca^{2+}-independent, other factors introduce the Ca^{2+} sensitivity that is required for synaptic vesicle fusion. As we will describe in this chapter, the extraordinary speed, complexity, and precision of Ca^{2+}-triggered neurotransmitter release are mediated, at least in part, by the Ca^{2+} sensor synaptotagmins (Syts) and its cofactor complexins.

In the 1980s, several synaptic Ca^{2+}-binding proteins, including the C2 domain protein Syt, were proposed as potential Ca^{2+} sensors. The first isoform of the synaptotagmin family, Syt1, is a synaptic vesicle protein that was initially identified as p65 in a monoclonal antibody screen for active zone proteins [1]. Subsequent studies from the Südhof laboratory established and confirmed that Syt1 acts as the primary Ca^{2+} sensor for membrane fusion [2–7]. This was also confirmed by studies in many species, including mouse [8], *Drosophila melanogaster* [9], zebrafish [10], as well as *Caenorhabditis elegans* [10–12] .

1 Structure and Biochemical Properties of Synaptotagmins and Other Ca^{2+} Sensors

Synaptotagmins constitute an evolutionarily conserved family of proteins, which contain a short luminal/extracellular domain, a single transmembrane domain (or residues that allow membrane association in the case of Syt16 and 17), a variable juxta-membrane linker, and two cytoplasmic calcium-binding C2 domains termed C2A and C2B (Fig. 1). Seventeen genes encoding canonical Syts exist in mammals with differential expression patterns across tissues and cell types [13]. All seventeen Syts are expressed in the brain, and eight of them (Syt1, 2, 3, 5, 6, 7, 9 and 10) bind Ca^{2+} and regulate vesicle fusion. Syts are evolutionarily conserved, with multiple orthologs of mammalian Syts found in invertebrates. The diversity of Syts is further amplified by alternative splicing, posttranslational modifications, and homo/heterodimerization (Fig. 1). Moreover, Syts showed distinct regional distribution in different organs, cell types and subcellular sites, as well as developmental changes or switch in gene expression [13]. In addition, proteins of the double C2 domain (Doc2) family, Doc2A and Doc2B, have been implicated in synaptic transmission as Ca^{2+} sensors [14–16].

The C2 domain, a sequence motif that was first identified in protein kinase C, is a region containing about 130 residues [17]. Normally C2 domains are found in proteins that bind phospholipids for cell membrane targeting. Their function as autonomously folded Ca^{2+}-binding domains was first discovered with Syt1 [3]. The atomic structure of Syt1's C2 domain was determined by X-ray crystallography and nuclear magnetic resonance (NMR) [18–22]. These structural studies revealed that

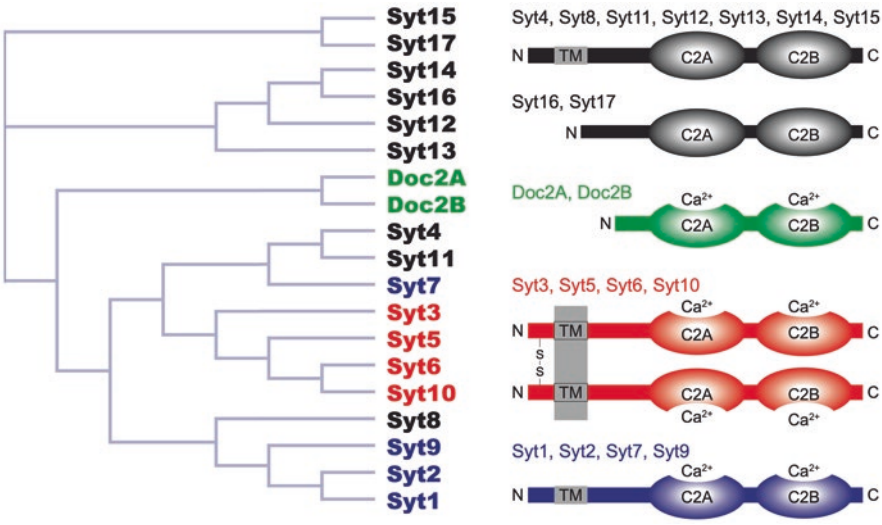

Fig. 1 Conservation, canonical domain structures, and classification of synaptotagmins and Doc2s. Left: Human synaptotagmins and human Doc2s amino acid similarity. The phylogenetic tree of Syt1 homologs represents the amino acid sequence similarities, not evolutionary backgrounds. FASTA sequences were taken from Uniprot.org and analyzed via Clustal Omega (https://www.ebi.ac.uk/Tools/msa/clustalo/). Note that some Syts have alternative gene names (e.g., human Syt9 refers to Uniprot ID O00445, human Syt5 refers to Uniprot ID Q86SS6). Right: Canonical domain structures and classification of synaptotagmins and Doc2s. Eight synaptotagmins bind Ca^{2+} (Syt1, 2, 3, 5, 6, 7, 9, and 10; colored in blue and red); the remaining Syts do not (colored in black). The eight Ca^{2+}-binding synaptotagmins fall into two broad classes that differ in the absence (Syt1, 2, 7, and 9; colored in blue) or presence (Syt3, 5, 6, and 10; colored in red) of disulfide-bonded cysteine residues in their N-terminal sequences

C2 domains are composed of a stable, eight-stranded β-sandwich with flexible loops emerging from the top and bottom (Fig. 2). Ca^{2+} binds exclusively to the top loops of the β-sandwich, which form a cuplike binding site for two to three Ca^{2+} ions in close vicinity. The bound Ca^{2+} ions are coordinated by five highly conserved aspartate residues and other residues located in these two flexible loops (Fig. 2). Although all C2 domains contain the same Ca^{2+} binding site architecture, some lack the canonical aspartate residues to ligate Ca^{2+} and are thus thought to be Ca^{2+} independent (e.g., in Syt4, 8, 11, and 15; Fig. 1).

In addition to the Ca^{2+}-binding motifs in the C2 domains, Syts contain a polylysine motif in the fourth β-strand of the C2 domain (Fig. 2). This motif supplies a patch of positively charged residues on the side of the C2 domain, near the Ca^{2+}-binding motif. Syts also contain another highly basic region (R398/399 region in Syt1 C2B domain) at the bottom of the C2B domain. These motifs are highly conserved and have been implicated in interactions with the SNARE complex and membrane binding [23–26]. C2 domains are now generally recognized as Ca^{2+}-dependent or -independent membrane-targeting modules, which are found in over 100 different proteins with functions ranging from signal transduction to membrane trafficking.

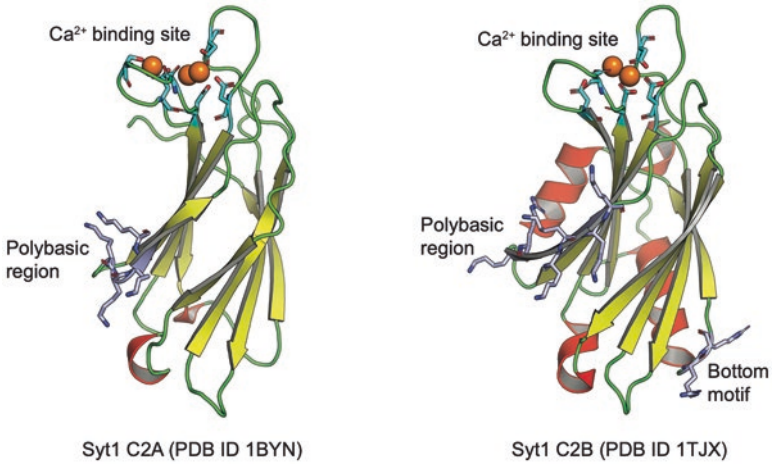

Fig. 2 Ribbon diagrams of the atomic resolution structures of the Ca^{2+}-bound C2A and C2B domains of Syt1. In the diagrams of the C2A and C2B domains, selected residues of the polybasic regions and bottom motif are represented by the stick mode

2 Ca^{2+} Sensors and Neurotransmitter Release

Neural information encoded by action potentials is passed through chemical synapses in the anterograde direction by release of neurotransmitters, neuropeptides, and other factors from the presynaptic terminal. There are three primary modes of neurotransmitter release: synchronous, asynchronous, and spontaneous. Most neuronal communication relies on synchronous release, which occurs within a few milliseconds after an action potential reaches a presynaptic bouton. However, also important are the influences of asynchronous release, which occurs with a longer and variable delay, and persists from tens of milliseconds to tens of seconds after the arrival of an action potential. Briefly, both synchronous and asynchronous release requires Ca^{2+} influx through voltage-gated Ca^{2+} channels and the presence of Ca^{2+} sensors [27]. Spontaneous release occurs in the absence of an action potential, but most studies support that spontaneous release is also Ca^{2+} sensitive and proportional to intracellular Ca^{2+} level [27, 28].

2.1 Synaptotagmins as Ca^{2+} Sensors for Evoked Release

Knockout (KO) studies of Syt1 showed that Syt1 deletion selectively abolished or severely decreased synchronous release (Fig. 3), suggesting that Syt1 is the Ca^{2+} sensor for fast, synchronous release of neurotransmitter [4]. Strikingly, Syt1 KO neurons still retained a delayed asynchronous form of release that may be dramatically enhanced by sustained moderate- to high-frequency stimulus train [29]. At most synapses, almost all (>90%) release at low-frequency stimulation is

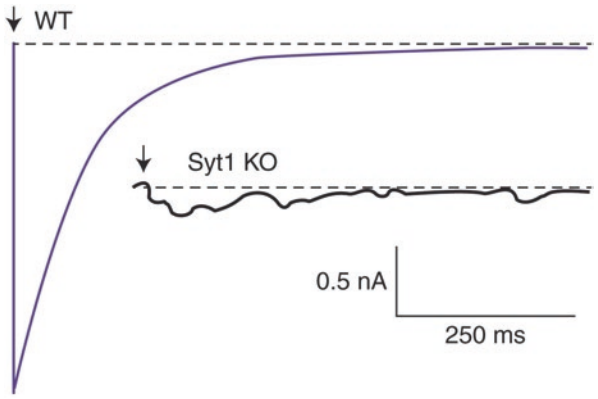

Fig. 3 Syt1 functions as synaptic Ca^{2+} sensors for neurotransmitter release. Deletion of Syt1 in cortical neurons blocks fast synchronous neurotransmitter release. Panels depict representative inhibitory postsynaptic currents (IPSCs) monitored in cortical neurons cultured from littermate wild-type (WT) and Syt1 knockout (Syt1 KO) neurons (arrow = action potential). (Modified from Xu et al. [39])

synchronous [30–33]. However, at some specialized synapses, such as those from deep cerebellar nuclei (DCN) to the inferior olive (IO), and from cholecystokinin (CCK)-containing interneurons to the dentate granule cells in hippocampus, asynchronous release is common [34–37]. These findings indicate that the asynchronous release is likely mediated by another Ca^{2+} sensor.

The fact that synchronous release occurs within tens to hundreds of milliseconds after the stimulus indicates that a fast and low-affinity Ca^{2+} sensor responds rapidly to a localized high concentration of Ca^{2+}. A systematic survey of Ca^{2+}-binding Syts demonstrated that those with the lowest Ca^{2+} affinity (EC50 = 10–20 μM), including Syt1, Syt2, and Syt9 (also known as Syt5), are the fast Ca^{2+} sensors mediating synchronous release [38]. These three Syts trigger synchronous release with quite distinct kinetics, which fits well with their differential expression patterns (Syt9 is primarily expressed in the limbic system, while Syt2 is primarily expressed in auditory system and the neuromuscular junction) [39]. While asynchronous release also requires Ca^{2+}, the mechanism and Ca^{2+} source are different from those of synchronous release. Intracellular addition of high concentrations of the slow Ca^{2+} chelator EGTA blocked delayed asynchronous release, but had minimal effects on synchronous release [40–42]. This suggests that high-affinity Ca^{2+} sensors specifically regulate asynchronous release, responding to bulk cytosolic Ca^{2+} fluctuations rather than to highly localized Ca^{2+} microdomains. Syt7 showed tenfold higher Ca^{2+} affinity (EC_{50} = 1–2 μM) and slower kinetics compared with Syt1, which led to the hypothesis that Syt7 mediates asynchronous release [38]. This hypothesis was supported by studies showing that knockdown of Syt7 selectively reduced asynchronous release [10, 43]. However, despite growing data supporting the notion that Syt7 mediates asynchronous release as a Ca^{2+} sensor, the presynaptic mechanisms underlying asynchronous synaptic vesicle fusion are still not well understood. It is also unclear if other Ca^{2+} sensors (e.g., Doc2) mediate asynchronous release.

2.2 Ca^{2+} Sensors for Spontaneous Release

Spontaneous release events were initially viewed as random events independent of action potentials and were described as biological noise in the synapse [44]. However, a number of functional roles for spontaneous neurotransmission, including maintaining synaptic dynamics in several organisms as well as regulating synapse and circuit development, have been proposed [45–47]. Moreover, most recent findings suggest that aberrant spontaneous neurotransmission might cause neurological disease in humans [48, 49]. Whether spontaneous release is Ca^{2+}-dependent remains controversial but current studies indicate that spontaneous release has a significant Ca^{2+}-dependent component at many synapses, albeit with a weaker concentration dependence than evoked release [50–53]. There are several possible Ca^{2+} sensors for regulating spontaneous release, including the same fast Ca^{2+} sensors that mediate evoked release and the specialized cytoplasmic Ca^{2+} sensors of the Doc2 protein family [15, 51, 54, 55]. Loss of Syt1 or Syt2 increases spontaneous release, indicating that the fast Ca^{2+} sensors may help regulate spontaneous release [4, 8, 29, 56–58].

Doc2 proteins are cytosolic proteins that contain two C2 domains and share many structural and functional properties with Syts but have a higher Ca^{2+} sensitivity [59, 60]. Doc2 proteins promote membrane fusion in response to exceptionally low increases in Ca^{2+}, half-maximal membrane binding occurs at 175 nm calcium for Doc2B, at 450 nm calcium for DocA [15, 55, 61]. Knockout or shRNA-mediated knockdown of Doc2 proteins caused more than 50% reduction in spontaneous release while evoked neurotransmission was essentially normal, confirming the differential nature of spontaneous and evoked release [15, 55]. A recent study showed a divergence in the regulation of excitatory and inhibitory spontaneous signaling by different Doc2 isoforms and Syt1. Specially, Doc2A mediates glutamatergic spontaneous release whereas Doc2B and Syt1 both regulate GABAergic spontaneous release [14]. These findings are evidence of complexity in the mechanisms of these Ca^{2+} sensors in synaptic vesicle exocytosis, implying that spontaneous release and action potential-dependent evoked release may be regulated independently in neurons and be controlled by different release machineries.

3 Binding Partners of Ca^{2+} Sensors

Ca^{2+} sensors must couple Ca^{2+} influx to synaptic vesicle fusion for neurotransmitter release. However, Ca^{2+} binding to Ca^{2+} sensors including Syt1 and Doc2 proteins does not cause a major conformational change, but instead dramatically changes the C2 domain's electrostatic potential [19, 22, 62]. Therefore, it is likely that Ca^{2+} binding to the negative charges in the Ca^{2+}-binding sites of Ca^{2+} sensors acts as an "electrostatic switch" or mediates electrostatic interactions with membrane phospholipids to regulate the interactions of Ca^{2+} sensors with presynaptic components [2, 63, 64]. Thus, it is important to investigate the binding partners of Ca^{2+} sensors

and understand how Ca^{2+} affects these interactions. The next section reviews what is currently known regarding the Ca^{2+}-independent and -dependent partners of Ca^{2+} sensors in the context of how these interactions may mediate synaptic vesicle fusion.

3.1 Phospholipids

Syt1 was first proposed to function as a Ca^{2+} sensor for synaptic transmission when it was found to bind Ca^{2+} at physiological levels in a complex with anionic membranes [2]. Further studies demonstrated that Ca^{2+} binding to phospholipids is key to synaptic vesicle fusion. Indeed, Ca^{2+}-dependent membrane binding is a highly conserved property of C2 domains [65]. Numerous biochemical studies have confirmed that Ca^{2+}-dependent as well as Ca^{2+}-independent interactions occur between Syts and anionic phospholipids and membranes, including phosphatidylinositol-4,5-bisphophate (PIP2)-containing membranes [2, 3, 23, 25, 26, 63, 66–73].

3.1.1 Ca^{2+}-Dependent Membrane Binding

High-resolution structures of Syt and Doc2 proteins showed that Ca^{2+}-binding residues in the C2 domain only partially coordinate the Ca^{2+} ions [68, 74]. The Ca^{2+}-binding affinity increases in the presence of a negatively charged phospholipid membrane because the negatively charged phospholipid headgroups complement the coordination sphere for Ca^{2+} ions in the C2 domain [2, 22, 68, 75]. It has been proposed that the C2 domain partially penetrates membranes that contain anionic phospholipids upon binding Ca^{2+} [20, 63, 76–79]. In addition to the Ca^{2+}-mediated electrostatic interaction, Syts binding to membranes may be mostly mediated by hydrophobic interactions [80]. Two highly conserved hydrophobic residues of the penetration loops are exposed on the tips of the Ca^{2+}-binding site in each C2A/B domain. In vitro studies have demonstrated that these hydrophobic resides in each C2A/B domain penetrate into the plasma membrane in the presence of Ca^{2+} [63, 77–79, 81–84]. When these hydrophobic residues are made more hydrophobic by mutation to tryptophan, the apparent Ca^{2+}-binding affinity for negatively charged phospholipids increases [85]. More interestingly, the penetration loops of different Ca^{2+} sensors differ in their degrees of hydrophobicity and penetration, which may determine the distinct contributions of different Ca^{2+} sensors to membrane bending and Ca^{2+} triggering.

3.1.2 Ca^{2+}-Independent Membrane Binding

The C2 domains of Syts and Doc2s can bind to the plasma membrane in not only a Ca^{2+}-dependent manner but also a Ca^{2+}-independent manner due to the presence of multiple basic sequences including the polybasic region and bottom motif on the

exposed surface (Fig. 2). Among the basic sequences, two regions are particularly important for synaptic vesicle fusion. In vitro studies implicated the motif of R398 and R399 at the bottom of the Syt1 C2B domain in membrane bridging [86, 87]. This polybasic motif of the Syt1 and Doc2 C2B domains has been found to bind to PIP2-containing membranes in the absence of Ca^{2+} [66, 88–92]. The C2A domain also has a highly conserved polybasic motif located on the side of the protein (Fig. 2), and contributes to Ca^{2+}-independent membrane binding in the same way as the C2B domain. Both the C2A and C2B polybasic motifs of Syt1 are required for synchronization of neurotransmitter release [90, 93–96]. In general, these motifs for Ca^{2+}-independent membrane binding are essential for efficient Ca^{2+}-independent docking and/or priming of synaptic vesicles, and probably also required for Ca^{2+} triggered vesicle fusion.

3.2 SNARE Proteins and Complexin

Syt1 has been reported to interact with both the SNARE complex and individual SNAREs including syntaxin-1 and SNAP-25 [97, 98]. However, it has been difficult to tell whether these interactions are biologically relevant or result from dynamic and non-specific interactions under specific experimental conditions. Additionally, the small soluble protein complexin also tightly binds to the SNARE complex (Fig. 4a) and plays a critical role in regulating vesicle fusion [99–101]. Functional studies and characterization of all these factors raises many mechanistic questions: How do these proteins (SNAREs, Syts, and complexins) achieve fusion in less than a millisecond upon Ca^{2+} triggering; how do they localize in the specific narrow space between the plasma membrane and synaptic vesicles; and how is the process regulated? Recent structural studies using X-ray crystallography and NMR spectroscopy have revealed three different binding interfaces among neuronal SNARE complex, complexin-1, and Syt1. These findings allow a better understanding about the behaviors and molecular mechanisms of action of these proteins in synaptic vesicle fusion.

High-resolution crystal structures of the SNARE complex and Syt1 revealed binding of the Syt1 C2B domain to the SNARE complex through a primary interface involving two regions of the C2B domain, including region I comprised of E295, K297, N336, and Y338, and region II comprised of R281, K288, and the bottom basic motif of R398 and R399 (Fig. 4c). The primary SNARE-Syt1 interface is structurally preserved in multiple different crystal packing environments and under different experimental conditions, suggesting that it is a genuine and specific interface [26, 102]. Disruption of the primary SNARE-Syt1 complex interface by mutations abolished fast synchronous release in cultured neurons and greatly reduced the efficiency of Ca^{2+}-triggered fusion of single vesicles reconstituted with neuronal SNAREs, Syt1, and complexin-1 [26]. The second interface formed between the

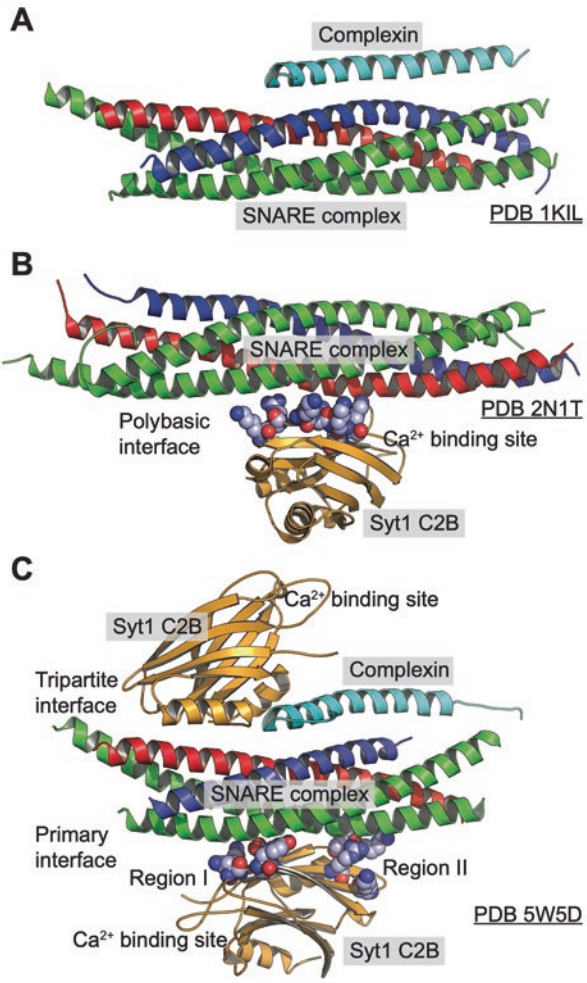

Fig. 4 Three interfaces of the SNARE complex, complexin, and Syt1 C2B domain have been revealed by X-ray crystallography and NMR spectroscopy. (**a**) Ribbon diagram of the crystal structure of the SNARE complex bound to a complexin-1 fragment. (**b**) Ribbon diagram of a representative conformer of the ensemble of NMR structures of the synaptotagmin-1 C2B domain bound to the SNARE complex via the polybasic region. (**c**) Ribbon diagram of the crystal structure of Syt1 C2B bound to a complexin-1–SNARE subcomplex through the primary interface and the tripartite interface. Synaptobrevin is in blue, syntaxin-1 is in red, SNAP25 is in green, the complexin-1 fragment is in cyan, and Syt1 C2B domain is in gold. Selected residues in Syt1 C2B domain involved in the polybasic interface and the primary interface are represented by the sphere mode. The C2A domain is not shown

polybasic region of the C2B domain and the SNARE complex is also reported recently (Fig. 4b) [23]. Further studies confirmed that Syt1 binds to the SNARE complex through the primary interface, and to PIP2-containing membranes through the polybasic regions before Ca^{2+} influx [24, 25, 78]. Recent results also suggest that the very tight interaction of C2 domains with phosphatidylserine (PS)- and PIP2-contanining membranes as well as membrane penetration induced by Ca^{2+} might lead to membrane fusion [24].

Primary sequence alignment indicates that the critical amino acid residues of the SNARE-Syt1 primary interface are only conserved among the fast Ca^{2+} sensors Sty1, Syt2, and Syt9. Based on a fragment of SNAP-25 that participates in the interface as observed in the crystal structure of the SNARE-Syt1 complex, a hydrocarbon-stapled peptide has been designed to specifically inhibit Ca^{2+}-triggered fusion of vesicles reconstituted with either neuronal SNAREs and Syt1 or airway SNAREs and Syt2 [26, 102–104]. This engineered stapled peptide enters airway epithelial cells to inhibit fusion of the secretory granule with the cell membrane and block mucin secretion in IL-13-primed airway epithelial cells in vitro and in vivo in mice. These results reinforce the notion that the primary interface is a universal binding site of fast Ca^{2+} sensors for SNARE complexes.

The third binding interface (called tripartite interface) was formed between Syt1 C2B domain and SNARE/Complexin subcomplex via interactions with both the SNARE and complexin components, as revealed by X-ray crystallography (Fig. 4c). However, the binding of the C2B domain to the SNARE/Complexin subcomplex through the tripartite interface has not been detected in solution by NMR spectroscopy [24]. This tripartite interface might be formed only in a specific membrane environment, as shown by one possible arrangement in Fig. 5. Further evidence is needed to support the physiological importance of this interface.

The Ca^{2+} sensors including Syt1, Syt7, and Doc2s also function in other steps of the synaptic vesicle cycle, including docking, priming, fusion pore expansion, and endocytosis [61, 94, 98, 105–111]. As PIP2 is located predominantly in the plasma membrane, where t-SNAREs are also located, it has been proposed that the Ca^{2+}-independent interaction of Syt1 with PIP2, t-SNAREs, or partially-zipped SNARE complexes may mediate synaptic vesicle docking and priming [26, 89, 90, 102, 112, 113].

So far, there is no direct evidence that the C2A domain interacts with the SNARE complex or complexin. It might be the case that the C2A domain of Syt1 is important but not essential, consistent with the difference in physiological importance of the C2A and C2B domains. Mutating one area of the Syt1 C2B Ca^{2+}-binding site completely abolishes evoked release in vivo, whereas a similar mutation in the Syt1 C2A Ca^{2+}-binding site causes less severe phenotypes [96, 114–117]. Nevertheless, recent studies show that the Syt1 C2A domain can also bind to the membrane in the absence of Ca^{2+} [111], and insert into the membrane upon Ca^{2+} triggering [78] to modulate Syt1 function [118–120] acting as a facilitator.

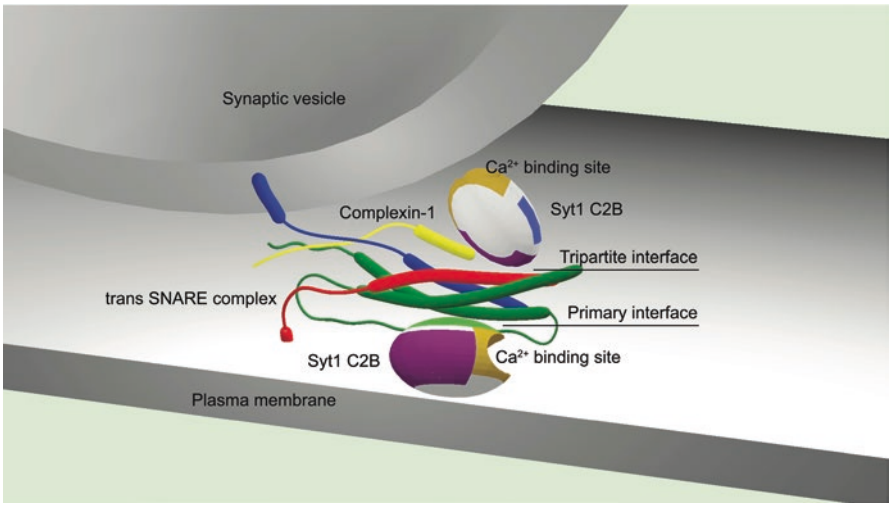

Fig. 5 Schema of the trans SNARE complex interacting with two Syt1 C2B domains and the central α-helix of complexin-1 in the core quaternary arrangement. The trans SNARE complex consists of synaptobrevin-2 (blue), syntaxin-1A (red), and SNAP-25A (green). The trans SNARE complex forms two interfaces (referred to as primary and tripartite interfaces) with two Syt1 C2B domains (represented as multicolored ellipsoids), one of which also involves the central α-helix of complexin-1 (yellow). The colors of the C2B ellipsoid indicate the loops involved in Ca^{2+} binding (gold), the primary SNARE–Syt1 interface (green), the tripartite SNARE–complexin-1–Syt1 interface (purple), and the polybasic region (blue). For clarity, the rest of Syt1, including the C2A domain and the transmembrane domain, has been omitted. For the trans SNARE complex, the primary interface mainly involves SNAP-25A, while the tripartite interface involves synaptobrevin-2, syntaxin-1A, and complexin-1 (yellow)

3.3 Supramolecular Arrangements

Multiple SNARE complexes are probably involved in Ca^{2+}-triggered fusion [121–124]. It may be possible to form supramolecular organization of the fusion machinery at least including SNAREs and Ca^{2+} sensors to achieve the rapid (~100 ms) and Ca^{2+}-synchronized vesicle fusion for neurotransmitter release. In addition to interacting with SNAREs and membranes, Syts are capable of forming oligomeric rings on membranes containing acidic lipids and in solution [78, 125–127]. Moreover, the formation of cooperative supra-molecular assembly of multiple SNARE complexes and their binding partners has also been supported by the observation of six protein densities at the release site of the primed synaptic vesicles in tomographic images of cultured primary hippocampal neurons [128]. Undoubtedly, further research will be required to establish whether the higher order organization of the fusion machinery is necessary and sufficient to facilitate neurotransmitter release.

4 Synaptotagmin-Associated Diseases

Recent advances in genetic technology are advancing our understanding of genetic disorders of synaptic proteins, including Syt1 [129–131] and Syt2 [132–137].

4.1 Syt1 Baker-Gordon Syndrome

Heterozygous mutations in Syt1 are associated with a neurodevelopmental disorder known as Baker-Gordon syndrome (or *SYT1*-associated neurodevelopmental disorder, OMIM 618218). Patients display neurodevelopmental impairments and symptoms including delayed developmental milestones, profound intellectual disability, infantile hypotonia, movement disorders, sleep disturbances, and episodic agitation. Fifteen de novo variants in SYT1 were identified in 22 individuals. All identified C2B missense variants are located in the region surrounding the Ca^{2+}-binding site (M303V/K, D304G, S309P, Y365C, D366E, K367dup, I368T, G369D, N371K) with one exception, N341S, which is located in the primary interface with the SNARE complex [130, 131, 138]. Four variants were identified in regions of undetermined function outside of the Ca^{2+}-binding site in the Syt1 C2A domain, which is congruent with the dominant negative effect of the Syt1 C2A mutants in the Ca^{2+}-binding site. All individuals with the C2A variants displayed either mild or moderate clinical phenotypes. However, the variants linked to the most severe clinical phenotypes are all located in the C2B domain. The differential effects of C2A and C2B mutations on clinical severity are consistent with the theory that the two C2 domains may play different roles in Syt1 functions [120, 139]. Moreover, these four C2A substitutions provide the first indication of the importance of previously unrecognized residues and regions in Syt1 C2A domain.

4.2 Syt2 Congenital Myasthenic Syndrome

Both dominant and recessive missense variants in *SYT2* have been reported to cause a presynaptic congenital myasthenic syndrome (CMS7, OMIM 616040), which is in agreement with Syt2 being the major isoform expressed at the neuromuscular junction [132, 133, 135–137, 140]. Similar to Syt1, all heterozygous missense mutations (S306L, D307A, P308L, and I371K) in Syt2 situate around the Ca^{2+}-binding site of the C2B domain [134, 136, 137]. In addition, the recently identified homozygous Syt2 variants also include nonsense, deletion, and frameshift mutations [132, 133, 135].

Acknowledgments I thank Dr. Zhao-Wen Wang, Dr. Natalí L. Chanaday Ricagni, Dr. Rong Sun, Elena D Bagatelas, and Liana Wilson for comments on the manuscript. This work was supported by National Institutes of Health (NIH) grant R00MH113764.

References

1. Matthew WD, Tsavaler L, Reichardt LF. Identification of a synaptic vesicle-specific membrane protein with a wide distribution in neuronal and neurosecretory tissue. J Cell Biol. 1981;91:257–69. https://doi.org/10.1083/jcb.91.1.257.
2. Brose N, Petrenko AG, Sudhof TC, Jahn R. Synaptotagmin: a calcium sensor on the synaptic vesicle surface. Science. 1992;256:1021–5. https://doi.org/10.1126/science.1589771.
3. Davletov BA, Sudhof TC. A single C2 domain from synaptotagmin I is sufficient for high affinity Ca2+/phospholipid binding. J Biol Chem. 1993;268:26386–90. https://doi.org/10.1016/s0021-9258(19)74326-9.
4. Geppert M, Goda Y, Hammer RE, Li C, Rosahl TW, Stevens CF, et al. Synaptotagmin I: a major Ca2+ sensor for transmitter release at a central synapse. Cell. 1994;79:717–27. https://doi.org/10.1016/0092-8674(94)90556-8.
5. Perin MS, Brose N, Jahn R, Sudhof TC. Domain structure of synaptotagmin (p65). J Biol Chem. 1991;266:623–9. https://doi.org/10.1016/s0021-9258(18)52480-7.
6. Perin MS, Fried VA, Mignery GA, Jahn R, Südhof TC. Phospholipid binding by a synaptic vesicle protein homologous to the regulatory region of protein kinase C. Nature. 1990;345:260–3. https://doi.org/10.1038/345260a0.
7. Perin MS, Johnston PA, Ozcelik T, Jahn R, Francke U, Sudhof TC. Structural and functional conservation of synaptotagmin (p65) in Drosophila and humans. J Biol Chem. 1991;266:615–22. https://doi.org/10.1016/s0021-9258(18)52479-0.
8. Nishiki TI, Augustine GJ. Dual roles of the C2B domain of synaptotagmin I in synchronizing Ca2+-dependent neurotransmitter release. J Neurosci. 2004;24:8542–50. https://doi.org/10.1523/JNEUROSCI.2545-04.2004.
9. Lee J, Guan Z, Akbergenova Y, Troy Littleton J. Genetic analysis of synaptotagmin C2 domain specificity in regulating spontaneous and evoked neurotransmitter release. J Neurosci. 2013;33:187–200. https://doi.org/10.1523/JNEUROSCI.3214-12.2013.
10. Wen H, Linhoff MW, McGinley MJ, Li GL, Corson GM, Mandel G, et al. Distinct roles for two synaptotagmin isoforms in synchronous and asynchronous transmitter release at zebrafish neuromuscular junction. Proc Natl Acad Sci U S A. 2010;107:13906–11. https://doi.org/10.1073/pnas.1008598107.
11. Li L, Liu H, Krout M, Richmond JE, Wang Y, Bai J, et al. A novel dual Ca2+ sensor system regulates Ca2+-dependent neurotransmitter release. J Cell Biol. 2021;220:e202008121. https://doi.org/10.1083/JCB.202008121.
12. Li L, Liu H, Wang W, Chandra M, Collins BM, Hu Z. SNT-1 functions as the Ca2+ sensor for tonic and evoked neurotransmitter release in caenorhabditis elegans. J Neurosci. 2018;38:5313–24. https://doi.org/10.1523/JNEUROSCI.3097-17.2018.
13. Wolfes AC, Dean C. The diversity of synaptotagmin isoforms. Curr Opin Neurobiol. 2020;63:198–209. https://doi.org/10.1016/j.conb.2020.04.006.
14. Courtney NA, Briguglio JS, Bradberry MM, Greer C, Chapman ER. Excitatory and inhibitory neurons utilize different Ca2+ sensors and sources to regulate spontaneous release. Neuron. 2018;98:977–91.e5. https://doi.org/10.1016/j.neuron.2018.04.022.
15. Pang ZP, Bacaj T, Yang X, Zhou P, Xu W, Südhof TC. Doc2 supports spontaneous synaptic transmission by a Ca2+-independent mechanism. Neuron. 2011;70:244–51. https://doi.org/10.1016/j.neuron.2011.03.011.
16. Yao J, Gaffaney JD, Kwon SE, Chapman ER. Doc2 is a Ca2+ sensor required for asynchronous neurotransmitter release. Cell. 2011;147:666–77. https://doi.org/10.1016/j.cell.2011.09.046.
17. Coussens L, Parker PJ, Rhee L, Yang-Feng TL, Chen E, Waterfield MD, et al. Multiple, distinct forms of bovine and human protein kinase C suggest diversity in cellular signaling pathways. Science. 1986;233:859–66. https://doi.org/10.1126/science.3755548.
18. Fernandez I, Araç D, Ubach J, Gerber SH, Shin O, Gao Y, et al. Three-dimensional structure of the synaptotagmin 1 C2B-domain: synaptotagmin 1 as a phospholipid binding machine. Neuron. 2001;32:1057–69. https://doi.org/10.1016/S0896-6273(01)00548-7.

19. Shao X, Fernandez I, Südhof TC, Rizo J. Solution structures of the Ca2+-free and Ca2+-bound C2A domain of synaptotagmin I: does Ca2+ induce a conformational change? Biochemistry. 1998;37:16106–15. https://doi.org/10.1021/bi981789h.
20. Sutton RB, Davletov BA, Berghuis AM, Sudhof TC, Sprang SR. Structure of the first C2 domain of synaptotagmin I: a novel Ca2+/phospholipid-binding fold. Cell. 1995;80:929–38. https://doi.org/10.1016/0092-8674(95)90296-1.
21. Sutton RB, Ernst JA, Brunger AT. Crystal structure of the cytosolic C2A-C2B domains of synaptotagmin III: implications for Ca+2-independent SNARE complex interaction. J Cell Biol. 1999;147:589–98. https://doi.org/10.1083/jcb.147.3.589.
22. Ubach J, Zhang X, Shao X, Südhof TC, Rizo J. Ca2+ binding to synaptotagmin: how many Ca2+ ions bind to the tip of a C2-domain? EMBO J. 1998;17:3921–30. https://doi.org/10.1093/emboj/17.14.3921.
23. Brewer KD, Bacaj T, Cavalli A, Camilloni C, Swarbrick JD, Liu J, et al. Dynamic binding mode of a Synaptotagmin-1-SNARE complex in solution. Nat Struct Mol Biol. 2015;22:555–64. https://doi.org/10.1038/nsmb.3035.
24. Voleti R, Jaczynska K, Rizo J. Ca2+-dependent release of synaptotagmin-1 from the snare complex on phosphatidylinositol 4,5-bisphosphate-containing membranes. elife. 2020;9:1–95. https://doi.org/10.7554/ELIFE.57154.
25. Wang S, Li Y, Ma C. Synaptotagmin-1 C2B domain interacts simultaneously with SNAREs and membranes to promote membrane fusion. elife. 2016;5:209–17. https://doi.org/10.7554/eLife.14211.
26. Zhou Q, Lai Y, Bacaj T, Zhao M, Lyubimov AY, Uervirojnangkoorn M, et al. Architecture of the synaptotagmin-SNARE machinery for neuronal exocytosis. Nature. 2015;525:62–7. https://doi.org/10.1038/nature14975.
27. Kaeser PS, Regehr WG. Molecular mechanisms for synchronous, asynchronous, and spontaneous neurotransmitter release. Annu Rev Physiol. 2014;76:333–63. https://doi.org/10.1146/annurev-physiol-021113-170338.
28. Kavalali ET. The mechanisms and functions of spontaneous neurotransmitter release. Nat Rev Neurosci. 2015;16:5–16. https://doi.org/10.1038/nrn3875.
29. Maximov A, Südhof TC. Autonomous function of synaptotagmin 1 in triggering synchronous release independent of asynchronous release. Neuron. 2005;48:547–54. https://doi.org/10.1016/j.neuron.2005.09.006.
30. Atluri PP, Regehr WG. Delayed release of neurotransmitter from cerebellar granule cells. J Neurosci. 1998;18:8214–27. https://doi.org/10.1523/jneurosci.18-20-08214.1998.
31. Barrett EF, Stevens CF. The kinetics of transmitter release at the frog neuromuscular junction. J Physiol. 1972;227:691–708. https://doi.org/10.1113/jphysiol.1972.sp010054.
32. Goda Y, Stevens CF. Two components of transmitter release at a central synapse. Proc Natl Acad Sci U S A. 1994;91:12942–6. https://doi.org/10.1073/pnas.91.26.12942.
33. Zengel JE, Magleby KL. Differential effects of Ba2+, Sr2+, and Ca2+ on stimulation-induced changes in transmitter release at the frog neuromuscular junction. J Gen Physiol. 1980;76:175–211. https://doi.org/10.1085/jgp.76.2.175.
34. Best AR, Regehr WG. Inhibitory regulation of electrically coupled neurons in the inferior olive is mediated by asynchronous release of GABA. Neuron. 2009;62:555–65. https://doi.org/10.1016/j.neuron.2009.04.018.
35. Daw MI, Tricoire L, Erdelyi F, Szabo G, McBain CJ. Asynchronous transmitter release from cholecystokinin-containing inhibitory interneurons is widespread and target-cell independent. J Neurosci. 2009;29:11112–22. https://doi.org/10.1523/JNEUROSCI.5760-08.2009.
36. Iremonger KJ, Bains JS. Integration of asynchronously released quanta prolongs the postsynaptic spike window. J Neurosci. 2007;27:6684–91. https://doi.org/10.1523/JNEUROSCI.0934-07.2007.
37. Labrakakis C, Lorenzo LE, Bories C, Ribeiro-da-Silva A, De Koninck Y. Inhibitory coupling between inhibitory interneurons in the spinal cord dorsal horn. Mol Pain. 2009;5:1744–8069. https://doi.org/10.1186/1744-8069-5-24.

38. Sugita S, Shin OH, Han W, Lao Y, Südhof TC. Synaptotagmins form a hierarchy of exocytotic Ca2+ sensors with distinct Ca2+ affinities. EMBO J. 2002;21:270–80. https://doi.org/10.1093/emboj/21.3.270.
39. Xu J, Mashimo T, Südhof TC. Synaptotagmin-1, -2, and -9: Ca2+ sensors for fast release that specify distinct presynaptic properties in subsets of neurons. Neuron. 2007;54:567–81. https://doi.org/10.1016/j.neuron.2007.05.004.
40. Hagler DJ, Goda Y. Properties of synchronous and asynchronous release during pulse train depression in cultured hippocampal neurons. J Neurophysiol. 2001;85:2324–34. https://doi.org/10.1152/jn.2001.85.6.2324.
41. Otsu Y, Shahrezaei V, Li B, Raymond LA, Delaney KR, Murphy TH. Competition between phasic and asynchronous release for recovered synaptic vesicles at developing hippocampal autaptic synapses. J Neurosci. 2004;24:420–33. https://doi.org/10.1523/JNEUROSCI.4452-03.2004.
42. Yang H, Xu-Friedman MA. Developmental mechanisms for suppressing the effects of delayed release at the endbulb of held. J Neurosci. 2010;30:11466–75. https://doi.org/10.1523/JNEUROSCI.2300-10.2010.
43. Bacaj T, Wu D, Yang X, Morishita W, Zhou P, Xu W, et al. Synaptotagmin-1 and synaptotagmin-7 trigger synchronous and asynchronous phases of neurotransmitter release. Neuron. 2013;80:947–59. https://doi.org/10.1016/j.neuron.2013.10.026.
44. Fatt P, Katz B. Some observations on biological noise. Nature. 1950;166:597–8. https://doi.org/10.1038/166597a0.
45. Andreae LC, Burrone J. Spontaneous neurotransmitter release shapes dendritic arbors via long-range activation of NMDA receptors. Cell Rep. 2015;10:873–82. https://doi.org/10.1016/j.celrep.2015.01.032.
46. Banerjee S, Vernon S, Jiao W, Choi BJ, Ruchti E, Asadzadeh J, et al. Miniature neurotransmission is required to maintain Drosophila synaptic structures during ageing. Nat Commun. 2021;12:1–12. https://doi.org/10.1038/s41467-021-24490-1.
47. Huntwork S, Littleton JT. A complexin fusion clamp regulates spontaneous neurotransmitter release and synaptic growth. Nat Neurosci. 2007;10:1235–7. https://doi.org/10.1038/nn1980.
48. Alten B, Zhou Q, Shin O-H, Esquivies L, Lin P-Y, White KI, et al. Role of aberrant spontaneous neurotransmission in SNAP25-associated encephalopathies. Neuron. 2020;109:59–72. https://doi.org/10.1016/j.neuron.2020.10.012.
49. Autry AE, Adachi M, Nosyreva E, Na ES, Los MF, Cheng PF, et al. NMDA receptor blockade at rest triggers rapid behavioural antidepressant responses. Nature. 2011;475:91–6. https://doi.org/10.1038/nature10130.
50. Goswami SP, Bucurenciu I, Jonas P. Miniature IPSCs in hippocampal granule cells are triggered by voltage-gated Ca2+ channels via microdomain coupling. J Neurosci. 2012;32:14294–304. https://doi.org/10.1523/JNEUROSCI.6104-11.2012.
51. Liu Q, Chen B, Yankova M, Morest DK, Maryon E, Hand AR, et al. Presynaptic ryanodine receptors are required for normal quantal size at the Caenorhabditis elegans neuromuscular junction. J Neurosci. 2005;25:6745–54. https://doi.org/10.1523/JNEUROSCI.1730-05.2005.
52. Williams C, Chen W, Lee CH, Yaeger D, Vyleta NP, Smith SM. Coactivation of multiple tightly coupled calcium channels triggers spontaneous release of GABA. Nat Neurosci. 2012;15:1195–7. https://doi.org/10.1038/nn.3162.
53. Xu J, Pang ZP, Shin O-H, Südhof TC. Synaptotagmin-1 functions as a Ca2+ sensor for spontaneous release. Nat Neurosci. 2009;12:759–66. https://doi.org/10.1038/nn.2320.
54. Chanaday NL, Nosyreva E, Shin OH, Zhang H, Aklan I, Atasoy D, et al. Presynaptic store-operated Ca2+ entry drives excitatory spontaneous neurotransmission and augments endoplasmic reticulum stress. Neuron. 2021;109:1314–32.e5. https://doi.org/10.1016/j.neuron.2021.02.023.
55. Groffen AJ, Martens S, Arazola RD, Cornelisse LN, Lozovaya N, De Jong APH, et al. Doc2b is a high-affinity Ca2+sensor for spontaneous neurotransmitter release. Science. 2010;327:1614–8. https://doi.org/10.1126/science.1183765.

56. Liu H, Dean C, Arthur CP, Dong M, Chapman ER. Autapses and networks of hippocampal neurons exhibit distinct synaptic transmission phenotypes in the absence of synaptotagmin I. J Neurosci. 2009;29:7395–403. https://doi.org/10.1523/JNEUROSCI.1341-09.2009.
57. Sun J, Pang ZP, Qin D, Fahim AT, Adachi R, Südhof TC. A dual-Ca2+-sensor model for neurotransmitter release in a central synapse. Nature. 2007;450:676–82. https://doi.org/10.1038/nature06308.
58. Wierda KDB, Sørensen JB. Innervation by a GABAergic neuron depresses spontaneous release in glutamatergic neurons and unveils the clamping phenotype of synaptotagmin-1. J Neurosci. 2014;34:2100–10. https://doi.org/10.1523/JNEUROSCI.3934-13.2014.
59. Orita S, Sasaki T, Naito A, Komuro R, Ohtsuka T, Maeda M, et al. Doc2: a novel brain protein having two repeated C2-like domains. Biochem Biophys Res Commun. 1995;206:439–48. https://doi.org/10.1006/bbrc.1995.1062.
60. Verhage M, De Vries KJ, Røshol H, Burbach JPH, Gispen WH, Südhof TC. DOC2 proteins in rat brain: complementary distribution and proposed function as vesicular adapter proteins in early stages of secretion. Neuron. 1997;18:453–61. https://doi.org/10.1016/S0896-6273(00)81245-3.
61. Groffen AJA, Friedrich R, Brian EC, Ashery U, Verhage M. DOC2A and DOC2B are sensors for neuronal activity with unique calcium-dependent and kinetic properties. J Neurochem. 2006;97:818–33. https://doi.org/10.1111/j.1471-4159.2006.03755.x.
62. Davletov B, Perisic O, Williams RL. Calcium-dependent membrane penetration is a hallmark of the C2 domain of cytosolic phospholipase A2 whereas the C2A domain of synaptotagmin binds membranes electrostatically. J Biol Chem. 1998;273:19093–6. https://doi.org/10.1074/jbc.273.30.19093.
63. Chapman ER, Davis AF. Direct interaction of a Ca2+-binding loop of synaptotagmin with lipid bilayers. J Biol Chem. 1998;273:13995–4001. https://doi.org/10.1074/jbc.273.22.13995.
64. Shao X, Li C, Fernandez I, Zhang X, Südhof TC, Rizo J. Synaptotagmin-syntaxin interaction: the C2 domain as a Ca2+-dependent electrostatic switch. Neuron. 1997;18:133–42. https://doi.org/10.1016/S0896-6273(01)80052-0.
65. Rizo J, Sudhof TC. C2-domains, structure and function of a universal Ca2+-binding domain. J Biol Chem (Elsevier). 1998;273:15879–82.
66. Bai J, Tucker WC, Chapman ER. PIP2 increases the speed of response of synaptotagmin and steers its membrane-penetration activity toward the plasma membrane. Nat Struct Mol Biol. 2004;11:36–44. https://doi.org/10.1038/nsmb709.
67. Choi UB, Strop P, Vrljic M, Chu S, Brunger AT, Weninger KR. Single-molecule FRET-derived model of the synaptotagmin 1-SNARE fusion complex. Nat Struct Mol Biol. 2010;17:318–24. https://doi.org/10.1038/nsmb.1763.
68. Fernández-Chacón R, Königstorfer A, Gerber SH, García J, Matos MF, Stevens CF, et al. Synaptotagmin I functions as a calcium regulator of release probability. Nature. 2001;410:41–9. https://doi.org/10.1038/35065004.
69. Hui E, Bai J, Wang P, Sugimori M, Llinas RR, Chapman ER. Three distinct kinetic groupings of the synaptotagmin family: candidate sensors for rapid and delayed exocytosis. Proc Natl Acad Sci U S A. 2005;102:5210–4. https://doi.org/10.1073/pnas.0500941102.
70. Kochubey O, Schneggenburger R. Synaptotagmin increases the dynamic range of synapses by driving Ca^2+-evoked release and by clamping a near-linear remaining Ca^2+ sensor. Neuron. 2011;69:736–48. https://doi.org/10.1016/J.NEURON.2011.01.013.
71. Kuo W, Herrick DZ, Ellena JF, Cafiso DS. The calcium-dependent and calcium-independent membrane binding of synaptotagmin 1: two modes of C2B binding. J Mol Biol. 2009;387:284. https://doi.org/10.1016/J.JMB.2009.01.064.
72. Pérez-Lara Á, Thapa A, Nyenhuis SB, Nyenhuis DA, Halder P, Tietzel M, et al. PtdInsP2 and PtdSer cooperate to trap synaptotagmin-1 to the plasma membrane in the presence of calcium. elife. 2016;5:115–8. https://doi.org/10.7554/eLife.15886.

73. Vrljic M, Strop P, Hill RC, Hansen KC, Chu S, Brunger AT. Post-translational modifications and lipid binding profile of insect cell-expressed full-length mammalian synaptotagmin 1. Biochemistry. 2011;50:9998–10012. https://doi.org/10.1021/bi200998y.
74. Giladi M, Michaeli L, Almagor L, Bar-On D, Buki T, Ashery U, et al. The C2B domain is the primary Ca2+ sensor in DOC2B: a structural and functional analysis. J Mol Biol. 2013;425:4629–41. https://doi.org/10.1016/j.jmb.2013.08.017.
75. Zhang X, Rizo J, Südhof TC. Mechanism of phospholipid binding by the C2A-domain of synaptotagmin I. Biochemistry. 1998;37:12395–403. https://doi.org/10.1021/bi9807512.
76. Bai J, Earles CA, Lewis JL, Chapman ER. Membrane-embedded synaptotagmin penetrates cis or trans target membranes and clusters via a novel mechanism. J Biol Chem. 2000;275:25427–35. https://doi.org/10.1074/jbc.M906729199.
77. Davis AF, Bai J, Fasshauer D, Wolowick MJ, Lewis JL, Chapman ER. Kinetics of synaptotagmin responses to CA2+ and assembly with the core SNARE complex onto membranes. Neuron. 1999;24:363–76. https://doi.org/10.1016/S0896-6273(00)80850-8.
78. Grushin K, Wang J, Coleman J, Rothman JE, Sindelar CV, Krishnakumar SS. Structural basis for the clamping and Ca2+ activation of SNARE-mediated fusion by synaptotagmin. Nat Commun. 2019;10:2413. https://doi.org/10.1038/s41467-019-10391-x.
79. Hui E, Bai J, Chapman ER. Ca2+-triggered simultaneous membrane penetration of the tandem C2-domains of synaptotagmin I. Biophys J. 2006;91:1767–77. https://doi.org/10.1529/biophysj.105.080325.
80. Gerber SH, Rizo J, Südhof TC. Role of electrostatic and hydrophobic interactions in Ca2+-dependent phospholipid binding by the C2A-domain from synaptotagmin I. Diabetes. 2002;51:S12–S8. https://doi.org/10.2337/diabetes.51.2007.s12.
81. Bai J, Wang P, Chapman ER. C2A activates a cryptic Ca2+-triggered membrane penetration activity within the C2B domain of synaptotagmin I. Proc Natl Acad Sci U S A. 2002;99:1665–70. https://doi.org/10.1073/pnas.032541099.
82. Chae YK, Abildgaard F, Chapman ER, Markley JL. Lipid binding ridge on loops 2 and 3 of the C2A domain of synaptotagmin I as revealed by NMR spectroscopy. J Biol Chem. 1998;273:25659–63. https://doi.org/10.1074/jbc.273.40.25659.
83. Herrick DZ, Sterbling S, Rasch KA, Hinderliter A, Cafiso DS. Position of synaptotagmin I at the membrane interface: cooperative interactions of tandem C2 domains. Biochemistry. 2006;45:9668–74. https://doi.org/10.1021/bi060874j.
84. Rufener E, Frazier AA, Wieser CM, Hinderliter A, Cafiso DS. Membrane-bound orientation and position of the synaptotagmin C2B domain determined by site-directed spin labeling. Biochemistry. 2005;44:18–28. https://doi.org/10.1021/bi048370d.
85. Rhee JS, Li LY, Shin OH, Rah JC, Rizo J, Südhof TC, et al. Augmenting neurotransmitter release by enhancing the apparent Ca2+ affinity of synaptotagmin 1. Proc Natl Acad Sci U S A. 2005;102:18664–9. https://doi.org/10.1073/pnas.0509153102.
86. Araç D, Chen X, Khant HA, Ubach J, Ludtke SJ, Kikkawa M, et al. Close membrane-membrane proximity induced by Ca2+-dependent multivalent binding of synaptotagmin-1 to phospholipids. Nat Struct Mol Biol. 2006;13:209–17. https://doi.org/10.1038/nsmb1056.
87. Xue M, Ma C, Craig TK, Rosenmund C, Rizo J. The Janus-faced nature of the C(2)B domain is fundamental for synaptotagmin-1 function. Nat Struct Mol Biol. 2008;15:1160–8. https://doi.org/10.1038/nsmb.1508.
88. Bradberry MM, Bao H, Lou X, Chapman ER. Phosphatidylinositol 4,5-bisphosphate drives Ca2-independent membrane penetration by the tandem C2 domain proteins synaptotagmin-1 and Doc2. J Biol Chem. 2019;294:10942–53. https://doi.org/10.1074/jbc.RA119.007929.
89. Lai Y, Lou X, Diao J, Shin YK. Molecular origins of synaptotagmin 1 activities on vesicle docking and fusion pore opening. Sci Rep. 2015;5:1–7. https://doi.org/10.1038/srep09267.
90. Loewen CA, Lee SM, Shin YK, Reist NE. C2B polylysine motif of synaptotagmin facilitates a Ca2+-independent stage of synaptic vesicle priming in vivo. Mol Biol Cell. 2006;17:5211–26. https://doi.org/10.1091/mbc.E06-07-0622.

91. Park Y, Seo JB, Fraind A, Pérez-Lara A, Yavuz H, Han K, et al. Synaptotagmin-1 binds to PIP 2 -containing membrane but not to SNAREs at physiological ionic strength. Nat Struct Mol Biol. 2015;22:815–23. https://doi.org/10.1038/nsmb.3097.
92. Van Bogaart GD, Meyenberg K, Diederichsen U, Jahn R. Phosphatidylinositol 4,5-bisphosphate increases Ca2+ affinity of synaptotagmin-1 by 40-fold. J Biol Chem. 2012;287:16447–53. https://doi.org/10.1074/jbc.M112.343418.
93. Borden CR, Stevens CF, Sullivan JM, Zhu Y. Synaptotagmin mutants Y311N and K326/327A alter the calcium dependence of neurotransmission. Mol Cell Neurosci. 2005;29:462–70. https://doi.org/10.1016/j.mcn.2005.03.015.
94. Chang S, Trimbuch T, Rosenmund C. Synaptotagmin-1 drives synchronous Ca2+-triggered fusion by C2B-domain-mediated synaptic-vesicle-membrane attachment. Nat Neurosci. 2018;21:33–42. https://doi.org/10.1038/s41593-017-0037-5.
95. Liu PW, Hosokawa T, Hayashi Y. Regulation of synaptic nanodomain by liquid–liquid phase separation: a novel mechanism of synaptic plasticity. Curr Opin Neurobiol. 2021;69:84–92. https://doi.org/10.1016/j.conb.2021.02.004.
96. Mackler JM, Drummond JA, Loewen CA, Robinson IM, Reist NE. The C2B Ca2+-binding motif of synaptotagmin is required for synaptic transmission in vivo. Nature. 2002;418:340–4. https://doi.org/10.1038/nature00846.
97. Chapman ER. How does synaptotagmin trigger neurotransmitter release? Annu Rev Biochem. 2008;77:615–41. https://doi.org/10.1146/annurev.biochem.77.062005.101135.
98. Littleton JT, Bai J, Vyas B, Desai R, Baltus AE, Garment MB, et al. Synaptotagmin mutants reveal essential functions for the C2B domain in Ca2+-triggered fusion and recycling of synaptic vesicles in vivo. J Neurosci. 2001;21:1421–33.
99. Chen X, Tomchick DR, Kovrigin E, Arac D, Machius M, Sudhof TC, et al. Three-dimensional structure of the complexin/SNARE complex. Neuron. 2002;33:397–409.
100. Maximov A, Tang J, Yang X, Pang ZP, Südhof TC. Complexin controls the force transfer from SNARE complexes to membranes in fusion. Science. 2009;323:516–21. https://doi.org/10.1126/science.1166505.
101. McMahon HT, Missler M, Li C, Südhof TC. Complexins: cytosolic proteins that regulate SNAP receptor function. Cell. 1995;83:111–9. https://doi.org/10.1016/0092-8674(95)90239-2.
102. Zhou Q, Zhou P, Wang AL, Wu D, Zhao M, Südhof TC, et al. The primed SNARE-complexin-synaptotagmin complex for neuronal exocytosis. Nature. 2017;548:420–5. https://doi.org/10.1038/nature23484.
103. Lai Y, Fois G, Flores JR, Tuvim MJ, Zhou Q, Yang K, et al. Inhibition of calcium-triggered secretion by hydrocarbon-stapled peptides. Nature. 2022;603:949–56. https://doi.org/10.1038/s41586-022-04543-1.
104. Lai Y, Tuvim MJ, Leitz J, Peters J, Pfuetzner RA, Esquivies L, et al. Screening of hydrocarbon-stapled peptides for inhibition of calcium-triggered exocytosis. Front Pharmacol. 2022;13:2022.03.21.484632. https://doi.org/10.3389/fphar.2022.891041.
105. Chen C, Satterfield R, Young SM, Jonas P. Triple function of synaptotagmin 7 ensures efficiency of high-frequency transmission at central GABAergic synapses. Cell Rep. 2017;21:2082–9. https://doi.org/10.1016/j.celrep.2017.10.122.
106. Li YC, Chanaday NL, Xu W, Kavalali ET. Synaptotagmin-1- and synaptotagmin-7-dependent fusion mechanisms target synaptic vesicles to kinetically distinct endocytic pathways. Neuron. 2017;93:616–31.e3. https://doi.org/10.1016/j.neuron.2016.12.010.
107. Nyenhuis SB, Karandikar N, Kiessling V, Kreutzberger AJB, Thapa A, Liang B, et al. Conserved arginine residues in synaptotagmin 1 regulate fusion pore expansion through membrane contact. Nat Commun. 2021;12:1–13. https://doi.org/10.1038/s41467-021-21090-x.
108. Poskanzer KE, Marek KW, Sweeney ST, Davis GW. Synaptotagmin I is necessary for compensatory synaptic vesicle endocytosis in vivo. Nature. 2003;426:559–63. https://doi.org/10.1038/nature02184.

109. Segovia M, Alés E, Montes AM, Bonifas I, Jemal I, Lindau M, et al. Push-and-pull regulation of the fusion pore by synaptotagmin-7. Proc Natl Acad Sci U S A. 2010;107:19032–7. https://doi.org/10.1073/pnas.1014070107.
110. Vevea JD, Kusick GF, Courtney KC, Chen E, Watanabe S, Chapman ER. Synaptotagmin 7 is targeted to the axonal plasma membrane through g-secretase processing to promote synaptic vesicle docking in mouse hippocampal neurons. elife. 2021;10:e67261. https://doi.org/10.7554/eLife.67261.
111. Wu Z, Dharan N, McDargh ZA, Thiyagarajan S, O'shaughnessy B, Karatekin E. The neuronal calcium sensor synaptotagmin-1 and snare proteins cooperate to dilate fusion pores. elife. 2021;10:e68215. https://doi.org/10.7554/eLife.68215.
112. Chen Y, Wang YH, Zheng Y, Li M, Wang B, Wang QW, et al. Synaptotagmin-1 interacts with PI(4,5)P2 to initiate synaptic vesicle docking in hippocampal neurons. Cell Rep. 2021;34:108842. https://doi.org/10.1016/j.celrep.2021.108842.
113. Schiavo G, Stenbeck G, Rothman JE, Söllner TH. Binding of the synaptic vesicle v-SNARE, synaptotagmin, to the plasma membrane t-SNARE, SNAP-25, can explain docked vesicles at neurotoxin-treated synapses. Proc Natl Acad Sci U S A. 1997;94:997–1001. https://doi.org/10.1073/pnas.94.3.997.
114. Fernández-Chacón R, Shin O-H, Königstorfer A, Matos MF, Meyer AC, Garcia J, et al. Structure/function analysis of Ca2+ binding to the C2A domain of synaptotagmin 1. J Neurosci. 2002;22:8438–46. 22/19/8438 [pii].
115. Paddock BE, Wang Z, Biela LM, Chen K, Getzy MD, Striegel A, et al. Membrane penetration by synaptotagmin is required for coupling calcium binding to vesicle fusion in vivo. J Neurosci. 2011;31:2248–57. https://doi.org/10.1523/JNEUROSCI.3153-09.2011.
116. Robinson IM, Ranjan R, Schwarz TL. Synaptotagmins I and IV promote transmitter release independently of Ca(2+) binding in the C(2)A domain. Nature. 2002;418:336–40. https://doi.org/10.1038/nature00915.
117. Stevens CF, Sullivan JM. The synaptotagmin C2A domain is part of the calcium sensor controlling fast synaptic transmission. Neuron. 2003;39:299–308.
118. Bai H, Xue R, Bao H, Zhang L, Yethiraj A, Cui Q, et al. Different states of synaptotagmin regulate evoked versus spontaneous release. Nat Commun. 2016;7:10971. https://doi.org/10.1038/ncomms10971.
119. Striegel AR, Biela LM, Evans CS, Wang Z, Delehoy JB, Sutton RB, et al. Calcium binding by synaptotagmin's C2A domain is an essential element of the electrostatic switch that triggers synchronous synaptic transmission. J Neurosci. 2012;32:1253–60. https://doi.org/10.1523/JNEUROSCI.4652-11.2012.
120. Yoshihara M, Guan Z, Littleton JT. Differential regulation of synchronous versus asynchronous neurotransmitter release by the C2 domains of synaptotagmin 1. Proc Natl Acad Sci U S A. 2010;107:14869–74. https://doi.org/10.1073/pnas.1000606107.
121. Mohrmann R, De Wit H, Verhage M, Neher E, Sørensen JB. Fast vesicle fusion in living cells requires at least three SNARE complexes. Science. 2010;330:502–5. https://doi.org/10.1126/science.1193134.
122. Shi L, Shen QT, Kiel A, Wang J, Wang HW, Melia TJ, et al. SNARE proteins: one to fuse and three to keep the nascent fusion pore open. Science. 2012;335:1355–9. https://doi.org/10.1126/science.1214984.
123. Sinha R, Ahmed S, Jahn R, Klingauf J. Two synaptobrevin molecules are sufficient for vesicle fusion in central nervous system synapses. Proc Natl Acad Sci U S A. 2011;108:14318–23. https://doi.org/10.1073/pnas.1101818108.
124. Van Den Bogaart G, Jahn R. Counting the SNAREs needed for membrane fusion. J Mol Cell Biol. 2011;3:204–5. https://doi.org/10.1093/jmcb/mjr004.
125. Wang J, Bello O, Auclair SM, Coleman J, Pincet F, Krishnakumar SS, et al. Calcium sensitive ring-like oligomers formed by synaptotagmin. Proc Natl Acad Sci U S A. 2014;111:13966–71. https://doi.org/10.1073/pnas.1415849111.

126. Wang J, Li F, Bello OD, Sindelar CV, Pincet F, Krishnakumar SS, et al. Circular oligomerization is an intrinsic property of synaptotagmin. elife. 2017;6:e27441. https://doi.org/10.7554/eLife.27441.
127. Zanetti MN, Bello OD, Wang J, Coleman J, Cai Y, Sindelar CV, et al. Ring-like oligomers of synaptotagmins and related C2 domain proteins. elife. 2016;5:e17262. https://doi.org/10.7554/eLife.17262.
128. Radhakrishnan A, Li X, Grushin K, Krishnakumar SS, Liu J, Rothman JE. Symmetrical arrangement of proteins under release-ready vesicles in presynaptic terminals. Proc Natl Acad Sci USA. 2021;118:e2024029118. https://doi.org/10.1073/pnas.2024029118.
129. Baker K, Gordon SL, Grozeva D, Van Kogelenberg M, Roberts NY, Pike M, et al. Identification of a human synaptotagmin-1 mutation that perturbs synaptic vesicle cycling. J Clin Investig. 2015;125:1670–8. https://doi.org/10.1172/JCI79765.
130. Bradberry MM, Courtney NA, Dominguez MJ, Lofquist SM, Knox AT, Sutton RB, et al. Molecular basis for synaptotagmin-1-associated neurodevelopmental disorder. Neuron. 2020;107:52–64.e7. https://doi.org/10.1016/j.neuron.2020.04.003.
131. Melland H, Bumbak F, Kolesnik-Taylor A, Ng-Cordell E, John A, Constantinou P, et al. Expanding the genotype and phenotype spectrum of SYT1-associated neurodevelopmental disorder. Genet Med. 2022;24:880–93. https://doi.org/10.1016/j.gim.2021.12.002.
132. Bauché S, Sureau A, Sternberg D, Rendu J, Buon C, Messéant J, et al. New recessive mutations in SYT2 causing severe presynaptic congenital myasthenic syndromes. Neurology. Genetics. 2020;6:e534. https://doi.org/10.1212/NXG.0000000000000534.
133. Donkervoort S, Mohassel P, Laugwitz L, Zaki MS, Kamsteeg EJ, Maroofian R, et al. Biallelic loss of function variants in SYT2 cause a treatable congenital onset presynaptic myasthenic syndrome. Am J Med Genet A. 2020;182:2272–83. https://doi.org/10.1002/ajmg.a.61765.
134. Herrmann DN, Horvath R, Sowden JE, Gonzalez M, Gonzales M, Sanchez-Mejias A, et al. Synaptotagmin 2 mutations cause an autosomal-dominant form of lambert-eaton myasthenic syndrome and nonprogressive motor neuropathy. Am J Hum Genet. 2014;95:332–9. https://doi.org/10.1016/j.ajhg.2014.08.007.
135. Maselli RA, van der Linden H, Ferns M. Recessive congenital myasthenic syndrome caused by a homozygous mutation in SYT2 altering a highly conserved C-terminal amino acid sequence. Am J Med Genet A. 2020;182:1744–9. https://doi.org/10.1002/ajmg.a.61579.
136. Mironovich O, Dadali E, Malmberg S, Markova T, Ryzhkova O, Poliakov A. Identification of a novel de novo variant in the syt2 gene causing a rare type of distal hereditary motor neuropathy. Genes. 2020;11:1–8. https://doi.org/10.3390/genes11111238.
137. Montes-Chinea NI, Guan Z, Coutts M, Vidal C, Courel S, Rebelo AP, et al. Identification of a new SYT2 variant validates an unusual distal motor neuropathy phenotype. Neurol Genet. 2018;4:282. https://doi.org/10.1212/NXG.0000000000000282.
138. Baker K, Gordon SL, Melland H, Bumbak F, Scott DJ, Jiang TJ, et al. SYT1-associated neurodevelopmental disorder: a case series. Brain. 2018;141:2576–91. https://doi.org/10.1093/brain/awy209.
139. Shin OH, Xu J, Rizo J, Südhof TC. Differential but convergent functions of Ca2+ binding to synaptotagmin-1 C2 domains mediate neurotransmitter release. Proc Natl Acad Sci U S A. 2009;106:16469–74. https://doi.org/10.1073/pnas.0908798106.
140. Maselli RA, Wei DT, Hodgson TS, Sampson JB, Vazquez J, Smith HL, et al. Dominant and recessive congenital myasthenic syndromes caused by SYT2 mutations. Muscle Nerve. 2021;64:219–24. https://doi.org/10.1002/mus.27332.

Roles and Sources of Calcium in Synaptic Exocytosis

Zhao-Wen Wang, Sadaf Riaz, and Longgang Niu

Abstract Calcium ions (Ca^{2+}) play a critical role in triggering neurotransmitter release. The rate of release is directly related to the concentration of Ca^{2+} at the presynaptic site, with a supralinear relationship. There are two main sources of Ca^{2+} that trigger synaptic vesicle fusion: influx through voltage-gated Ca^{2+} channels in the plasma membrane and release from the endoplasmic reticulum via ryanodine receptors. This chapter will cover the sources of Ca^{2+} at the presynaptic nerve terminal, the relationship between neurotransmitter release rate and Ca^{2+} concentration, and the mechanisms that achieve the necessary Ca^{2+} concentrations for triggering synaptic exocytosis at the presynaptic site.

Keywords calcium · exocytosis · neurotransmitter release · calcium channel · ryanodine receptor · mitochondrion

1 Introduction

Calcium ions (Ca^{2+}) are involved in various biological functions. One of the most well-known functions is their role in triggering neurotransmitter release at the presynaptic nerve terminal. Over a century ago, Locke discovered that the transmission between nerves and muscles is significantly affected by the presence of Ca^{2+} in the surrounding medium [1]. Later research conducted by many others demonstrated that extracellular Ca^{2+} is crucial for evoked neurotransmitter release and that its concentration influences the amplitude of end-plate potentials recorded from muscle cells [2–5].

Z.-W. Wang (✉) · S. Riaz · L. Niu
Department of Neuroscience, University of Connecticut School of Medicine, Farmington, CT, USA
e-mail: zwwang@uchc.edu

Z.-W. Wang (ed.), *Molecular Mechanisms of Neurotransmitter Release*, Advances in Neurobiology 33, https://doi.org/10.1007/978-3-031-34229-5_6

Neurotransmitters can be released spontaneously or in response to action potentials. In general, spontaneous release occurs when individual synaptic vesicles undergo exocytosis, while action potential-evoked release reflects synchronized exocytosis of multiple synaptic vesicles. The role of Ca^{2+} in action potential-evoked release is well established. When an action potential reaches the nerve terminal, depolarization opens voltage-gated Ca^{2+} channels (VGCCs) in the plasma membrane, resulting in an influx of Ca^{2+}. Ca^{2+} can also originate from the endoplasmic reticulum (ER) through a coupling between VGCCs in the plasma membrane and ryanodine receptors (RyRs) in the ER membrane [6, 7]. Ca^{2+} then binds to Ca^{2+}-sensing proteins to trigger synaptic exocytosis (see Chapter "Calcium Sensors of Neurotransmitter Release"). The released neurotransmitters act on specific postsynaptic receptors, resulting in either excitatory or inhibitory currents in the postsynaptic cell, depending on the types of neurotransmitter and postsynaptic receptor, as well as physiological or experimental conditions. The temporal relationships among the presynaptic action potential, presynaptic Ca^{2+} current, and excitatory postsynaptic current (EPSC) are depicted in Fig. 1. Ca^{2+} release from the ER is not included in this figure because its kinetics are not well defined. As illustrated in the figure, Ca^{2+} influx begins around the peak of the action potential and ends before the nerve terminal is fully repolarized. Neurotransmitter release, as reflected by the postsynaptic currents, occurs with a further delay.

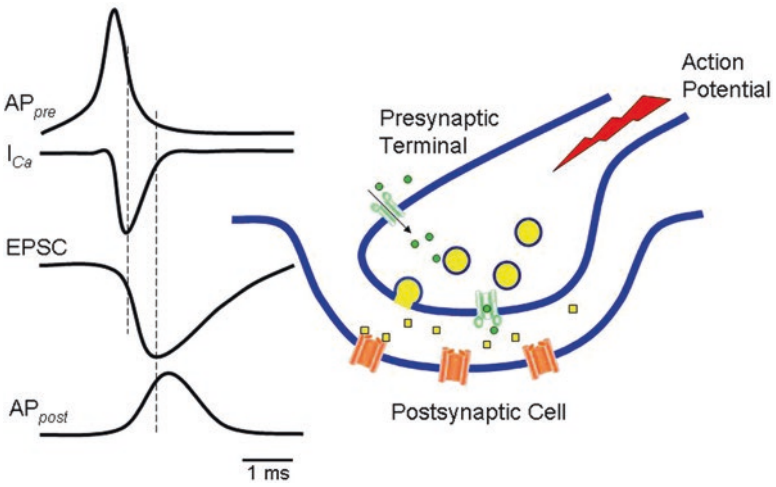

Fig. 1 Pre- and postsynaptic events in response to a presynaptic action potential. Depolarization of the presynaptic terminal by the action potential (AP_{pre}) causes Ca^{2+} influx (I_{Ca}) through voltage-gated Ca^{2+} channels in the plasma membrane. Ca^{2+} triggers the release of a neurotransmitter, which causes excitatory postsynaptic current (EPSC) by activating ionotropic postsynaptic receptors. An action potential may occur in the postsynaptic cell (AP_{post}) if the cell is depolarized beyond a threshold by the EPSC. (This schematic figure is based on published data [194, 195])

2 Neurotransmitter Release Rate Is Supralinearly Related to Ca^{2+} Concentration

The rate of neurotransmitter release is quantitatively related to the concentration of Ca^{2+} ($[Ca^{2+}]$). Dodge and Rahamimoff [4] demonstrated that at the frog neuromuscular junction (NMJ), the rate of neurotransmitter release increases with elevated extracellular $[Ca^{2+}]$ ($[Ca^{2+}]_o$). However, the relationship is not linear. When $[Ca^{2+}]_o$ is relatively low, a small change in concentration results in a large change in neurotransmitter release, as reflected by the amplitude of end-plate potentials. Plotting the results in double-logarithmic coordinates yields a straight line with a slope of approximately 4, leading to the conclusion that the rate of neurotransmitter release is proportional to $[Ca^{2+}]_o$ raised to the fourth power (Release rate $\propto [Ca^{2+}]_o^4$).

The work of Dodge and Rahamimoff showed the quantitative relationship between neurotransmitter release rate and $[Ca^{2+}]_o$. However, the Ca^{2+} sensor of the synaptic release machinery is located inside the presynaptic nerve terminal. Thus, intracellular rather than extracellular Ca^{2+} triggers neurotransmitter release. What would be the relationship between neurotransmitter release rate and cytoplasmic $[Ca^{2+}]$ ($[Ca^{2+}]_i$)? This relationship has been analyzed with a technique called Ca^{2+}-uncaging. In this technique, a photolysable Ca^{2+}-chelator such as DM-nitrophen is introduced into the presynaptic nerve terminal through a whole-cell patch-clamp glass pipette. Ca^{2+} is released from the photolysable Ca^{2+}-chelator upon flash of an ultraviolet light, resulting in a rapid and uniform increase of $[Ca^{2+}]_i$ at the presynaptic nerve terminal. The level of $[Ca^{2+}]_i$ at the presynaptic nerve terminal may be controlled by varying the light intensity and measured by imaging with a low-affinity fluorescent Ca^{2+} indictor. The rate of neurotransmitter release is evaluated by measuring either membrane capacitance of the presynaptic terminal, which increases when the plasma membrane area enlarges with synaptic vesicle fusion, or the amplitude of excitatory postsynaptic potentials or currents, which reflect postsynaptic responses to the released neurotransmitter. This Ca^{2+}-uncaging technique is apparently suitable for analyzing the relationship between release rate and $[Ca^{2+}]_i$ because it triggers release of the same pool of synaptic vesicles as do action potentials [8]. Analyses of several nerve terminals, including the goldfish retinal bipolar cell synaptic terminal [9] (Fig. 2), crayfish motor neuron terminal [10], and rat calyx of Held presynaptic terminal [8, 11] (Fig. 2), have revealed a non-linear dependence of the release rate on $[Ca^{2+}]_i$ with a slope of approximately 3–4 in plots with double-logarithmic coordinates, which resembles the relationship between the release rate and $[Ca^{2+}]_o$ [4].

The reason why neurotransmitter release rate is supralinearly related to $[Ca^{2+}]_i$ is not entirely clear. Several mechanisms have been suggested to explain the apparent Ca^{2+} cooperativity. One possible explanation is that the Ca^{2+} binding properties of synaptotagmin could be responsible for the cooperativity [12]. A minimal kinetic model, based on flash-photolysis data from the calyx of Held synapse, indicates that five identical Ca^{2+}-binding steps are required before synaptic vesicle fusion [8, 11]. The total number of Ca^{2+} binding sites in synaptotagmin I matches the number of

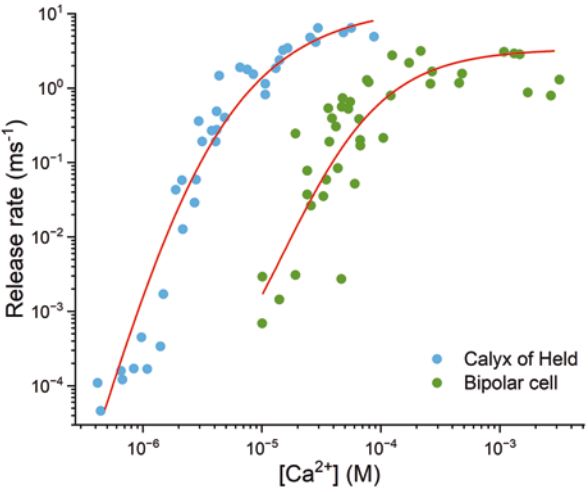

Fig. 2 Relationship between Ca^{2+} concentration and neurotransmitter release rate in the calyx of Held and goldfish retinal bipolar cell presynaptic terminals. The graph shows that the rate of neurotransmitter release is proportional to the fourth power of Ca^{2+} concentration and that the sensitivity to Ca^{2+} differs by approximately one order of magnitude between the two synapses. (The graph was generated from published figs [9, 11] using the Digitizer tool of Origin Pro software (OriginLab Corporation))

Ca^{2+} binding steps in this proposed Ca^{2+} binding kinetic model [12]. Additionally, Ca^{2+} cooperativity for the fast synchronous release component is eliminated in *Drosophila* synaptotagmin null or C2B domain-deletion mutants [13, 14]. Another explanation is that the apparent Ca^{2+} cooperativity may reflect the mean number of SNARE complexes that mediate a vesicle fusion, since SNARE complexes can form oligomers of 3–4 [15]. Another possibility is that SNARE proteins might be responsible for Ca^{2+} cooperativity, as mutations of either syntaxin 1A or synaptobrevin reduces Ca^{2+} cooperativity at the *Drosophila* NMJ [16]. It is also possible that the overlapping of Ca^{2+} micro- or nanodomains at the active zone might contribute to the Ca^{2+} cooperativity [17], or that the saturation of cytoplasmic Ca^{2+} buffer(s) might contribute to the supralinearity [18]. Moreover, the function of presynaptic BK channels might affect the apparent Ca^{2+} cooperativity, as seen in analyses of neuromuscular transmission in wild-type and *slo-1* (BK channel) mutants of *Caenorhabditis elegans*. In the *slo-1* loss-of-function (*lf*) mutant, the apparent Ca^{2+} cooperativity is decreased because SLO-1 dysfunction increases neurotransmitter release at low but not high $[Ca^{2+}]_o$ [19]. These proposed models suggest that the molecular basis of Ca^{2+} cooperativity is still poorly understood and may be attributable to more than one mechanism.

The relationship between $[Ca^{2+}]_i$ and neurotransmitter release rate can vary between different synapses, as illustrated by several examples. At some synapses, such as the squid giant synapse [17] and chick ciliary ganglion synapse [20], the apparent Ca^{2+} cooperativity is approximately 1, indicating a linear relationship between $[Ca^{2+}]_i$ and release rate. At other synapses, including the excitatory synapse

between sensory afferent fibers and motoneurons in rat lumbar spinal cord [21] and the synapse between mossy fiber boutons and granule cells in rat cerebellum [22], the apparent Ca^{2+} cooperativity ranges from 1.2 to 1.6. In other cases, such as the rat calyx of Held synapse, activation of protein kinase C can change the apparent Ca^{2+} cooperativity from ~4 of the control level to ~3 [23]. The apparent Ca^{2+} cooperativity derived from evoked postsynaptic currents at the *C. elegans* NMJ is 2.1, which is reduced to 1.3 when the *slo-1* BK channel is mutated (Fig. 3) [19]. Therefore, the relationship between $[Ca^{2+}]_i$ and neurotransmitter release rate can be complex and vary between different synapses and between different experimental conditions.

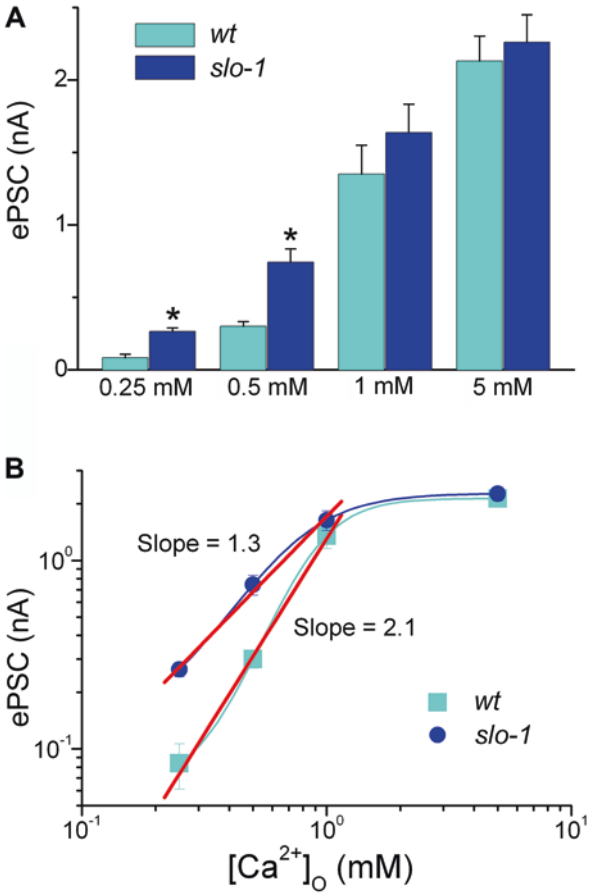

Fig. 3 The apparent Ca^{2+} cooperativity is decreased in *C. elegans slo-1* (BK channel) mutants. (**a**) The amplitude of evoked postsynaptic currents (ePSC) was significantly increased at the *C. elegans* neuromuscular junction in a *slo-1* null mutant at 250 or 500 μM but not 1 or 5 mM $[Ca^{2+}]_o$. The asterisk indicates a statistically significant difference compared with the wild-type (WT). This figure was adapted from reference [19]. (**b**) The same data as in (**a**) but plotted using logarithmic coordinates, showing that the apparent Ca^{2+} cooperativity, as indicated by the slope factor from a linear fit, was decreased in the *slo-1* mutant. These findings suggest that SLO-1 plays a role in the regulation of synaptic transmission

Another divalent cation that has been implicated in controlling neurotransmitter release under experimental conditions is Mg^{2+}. However, unlike Ca^{2+}, Mg^{2+} inhibits release. An increase in $[Mg^{2+}]$ reduces the Ca^{2+} sensitivity of neurotransmitter release [4]. It has been suggested that Mg^{2+} antagonizes the function of Ca^{2+} through competitive effects [21, 24], although the exact mechanism is unclear. One possibility is that Mg^{2+} blocks Ca^{2+} entry through membrane Ca^{2+} channels [25, 26]. In addition, Mg^{2+} has been shown to activate the BK channel when applied to the cytoplasmic side in inside-out membrane patches [27–29]. Because the BK channel is an important negative regulator of neurotransmitter release [30, 31] (also see Chapter "Regulation of Neurotransmitter Release by K+ Channels"), an increase in $[Mg^{2+}]$ could potentially downregulate neurotransmitter release via the BK channel. However, it should be noted that a relatively high $[Mg^{2+}]_i$ is needed to activate the BK channel [28, 29], making it questionable whether $[Mg^{2+}]_i$ can reach sufficiently high levels to regulate the function of presynaptic BK channels in neurons.

3 Ca^{2+} Concentrations Required for Neurotransmitter Release Vary from Synapse to Synapse

The fast phase of action potential-induced neurotransmitter release requires relatively high concentrations of Ca^{2+}. For example, at the squid giant synapse terminal, studies on the effects of intraterminally injected Ca^{2+} chelators with different affinities suggest that several hundred micromolar $[Ca^{2+}]$ may be necessary to trigger neurotransmitter release [32]. Similarly, at the goldfish retinal bipolar neuron synaptic terminal, Ca^{2+}-uncaging experiments indicate that a minimum of ~10 μM $[Ca^{2+}]$ is required to initiate neurotransmitter release, and ~200 μM $[Ca^{2+}]$ is needed to achieve release at half maximal rate [9]. In permeabilized synaptosomes prepared from rat cerebral cortex, glutamate release has a threshold of ~50 μM $[Ca^{2+}]$, with half-maximal and maximal release occurring at 200–300 μM and 1 mM $[Ca^{2+}]$, respectively [33]. These findings suggest that action potential-evoked neurotransmitter release at these synapses may require hundreds of micromolar $[Ca^{2+}]$. However, at the calyx of Held glutamatergic terminal, Ca^{2+}-uncaging experiments suggest that 10–25 μM $[Ca^{2+}]$ is sufficient to induce the peak release rate [34] or to mimic the release caused by action potentials [8, 11]. Thus, the concentration of Ca^{2+} required for fast neurotransmitter release can vary as much as one order of magnitude among different synapses (Fig. 2).

4 Ca^{2+} Forms High Concentration Domains at the Presynaptic Terminal

The increase in presynaptic $[Ca^{2+}]_i$ following an action potential is typically small compared to the concentration required for fast neurotransmitter release, as evidenced by studies at the squid giant synapse, where presynaptic $[Ca^{2+}]_i$ increases by

5 nM from a resting level of approximately 50–100 nM [17]. Therefore, the spatially averaged $[Ca^{2+}]_i$ following an action potential is much lower than that required for fast neurotransmitter release. Mathematical modeling from the 1980s suggests that $[Ca^{2+}]_i$ does not change uniformly in response to action potentials but forms hemispheric high-concentration domains (<50 nm in radius) around the open Ca^{2+} channels [35–37]. These domains, resulting from the entry of Ca^{2+} through single channels, are known as Ca^{2+} nanodomains [35, 38] (Fig. 4) and typically peak within 1 ms of channel opening, with $[Ca^{2+}]$ as high as a few hundred micromolar at the center of the domain but dropping rapidly with distance from the channel [37, 38]. Clustering of Ca^{2+} channels can lead to the formation of larger Ca^{2+} microdomains [35, 38] (Fig. 4). However, the terms "nanodomain" and "microdomain" are not always consistently defined. For example, Neher and colleagues use the term "nanodomain" to refer to elevated $[Ca^{2+}]_i$ in the immediate vicinity (10–100 nm) of a few Ca^{2+} channels, and "microdomain" to refer to elevated $[Ca^{2+}]_i$ within 1 μm of active zones [39].

The concentration of Ca^{2+} in Ca^{2+} microdomains has been assessed by analyzing "hot spots," which are putative Ca^{2+} microdomains, in Ca^{2+} imaging experiments. At the presynaptic terminal of the squid giant synapse, $[Ca^{2+}]$ in the Ca^{2+} microdomain is 200–300 μM [40], which is consistent with estimates made by analyzing the inhibitory effects of different Ca^{2+}-chelating agents on neurotransmitter release [32]. In contrast, at the presynaptic terminal of goldfish retinal bipolar cells, the Ca^{2+} microdomain has an average concentration of ~2 μM and a peak concentration of ~7 μM at its center [41]. In addition to Ca^{2+} imaging techniques, presynaptic BK channel activity has been used to measure local $[Ca^{2+}]$ resulting from Ca^{2+} entry through VGCCs. This approach takes advantage of the Ca^{2+}-dependent property of the BK channel and the physical colocalization of the BK channel with VGCCs at the presynaptic terminal. Analyses have shown that local $[Ca^{2+}]$ can exceed 100 μM at the presynaptic terminal of cultured *Xenopus* NMJ preparation [42]. The Ca^{2+} concentrations determined using the Ca^{2+} imaging and BK channel sensor approaches are consistent with those required to trigger fast neurotransmitter release at these synapses.

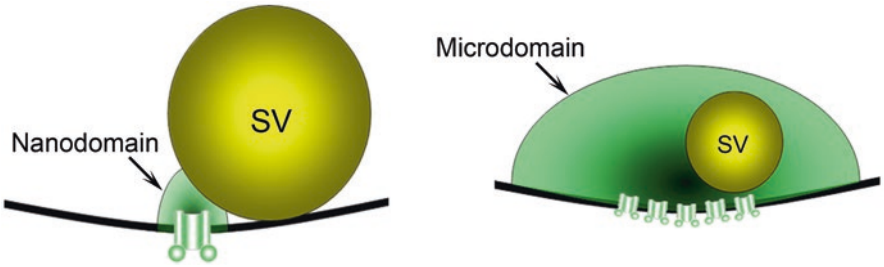

Fig. 4 Ca^{2+} accumulates at the inner mouth of voltage-sensitive Ca^{2+} channels to form Ca^{2+} nanodomains and microdomains. A Ca^{2+} nanodomain results from the opening of one Ca^{2+} channel, whereas a Ca^{2+} microdomain results from the opening of a cluster of Ca^{2+} channels [35, 196]

The properties of Ca^{2+} microdomains at presynaptic terminals have been analyzed using various imaging techniques. At the presynaptic terminal of the squid giant synapse, *n*-aequorin-J imaging reveals that a stable set of quantum emission domains (QEDs) develop in response to sustained 10 Hz stimulation. These QEDs are 0.25 to 0.6 μm^2 in size and have an average lifetime of 200 ms [40]. However, the measured lifetime of QEDs is longer than expected for the transient Ca^{2+} signal in the microdomain. This is likely due to technical limitations [40].

At the presynaptic terminal of a cultured frog NMJ preparation, low-affinity Ca^{2+} indicator Oregon Green 488 confocal imaging shows that action potentials induce spot-like fluorescent transients. The fluorescent spot peaks within ~1 ms, decays with one rapid ($\tau 1$ = 1.7 ms) and two slow components ($\tau 2$ = 16 ms, $\tau 3$ = 78 ms), and is 0.6–3.0 μm in full width at maximum [43]. Total internal reflection fluorescence microscopy (TIRFM) has also been adapted to measure Ca^{2+} signals in Ca^{2+} nano- or microdomains. This technique provides excellent spatial and temporal resolutions as fluorescent excitation is restricted to a thin (~100 nm) layer at the refractive boundary between the microscope cover glass and the cell [44]. Using TIRFM, fluorescent "hot spots" are observed near the plasma membrane at the presynaptic terminal of goldfish bipolar neurons in response to membrane depolarization [45]. The fluorescent hot spot has two components, including a fast component that rises and declines abruptly with membrane depolarization and repolarization, and a slow component that rises steadily during depolarization and declines rather slowly after repolarization. Interestingly, the slow component is also observed outside of the fluorescent hot spots, suggesting that it likely reflects global cytoplasmic [Ca^{2+}] changes that are also observed using standard fluorescence microscopy [46–48]. Another study using TIRFM shows that depolarization generates Ca^{2+} microdomains that appear within 20–40 ms and disappear within 20–40 ms in goldfish retinal bipolar cells [41].

The distance between Ca^{2+} nano- or microdomains and the Ca^{2+} sensor for synaptic vesicle exocytosis is a topic of interest in neuroscience research. Electron microscopy tomography of frog NMJs has revealed that VGCCs are located only 10–20 nm away from synaptic vesicles [49]. Mathematical modeling of the calyx of Held presynaptic site has suggested that the distance between synaptic vesicles and clusters of VGCCs ranges from 30 to 300 nm, with an average of about 100 nm [50].

To estimate the distance between Ca^{2+} channels and the Ca^{2+} sensor for exocytosis, researchers often compare the inhibitory effects of the Ca^{2+}-chelating agents BAPTA and EGTA on neurotransmitter release. Although BAPTA and EGTA have similar equilibrium affinities for Ca^{2+}, BAPTA binds Ca^{2+} several hundred times faster than EGTA because EGTA, but not BAPTA, is protonated at physiological pH, and the bound protons must dissociate from EGTA prior to Ca^{2+} binding [51]. If the Ca^{2+} domain is hundreds of nanometers away from the Ca^{2+} sensor, both BAPTA and EGTA would inhibit neurotransmitter release. However, if the Ca^{2+} domain is tens of nanometers away from the Ca^{2+} sensor, only BAPTA would inhibit release [52].

There are two primary methods for determining whether the release of synaptic vesicles is regulated by Ca^{2+} nano- or microdomains. The first method involves

analyzing the effects of BAPTA and EGTA on neurotransmitter release [35]. If only BAPTA can inhibit the release, it is likely that the release is controlled by Ca^{2+} nanodomains. If both BAPTA and EGTA can inhibit the release, it is likely that the release is controlled by Ca^{2+} microdomains. This analysis has suggested that the release at squid giant synapse [53], goldfish retinal bipolar synapse [54, 55], and mature calyx of Held synapses [56] is controlled by Ca^{2+} nanodomains. In contrast, the release at immature calyx of Held synapses [56, 57], cortical pyramidal neurons [58, 59], and cerebellar parallel fiber-Purkinje cell synapse [60] is controlled by Ca^{2+} microdomains.

The second approach involves analyzing the relationship between the release rate and the number of functional Ca^{2+} channels or Ca^{2+} influx [38, 61]. If there is a linear relationship between the two, it suggests that the release is triggered by Ca^{2+} nanodomains. If there is a supralinear relationship, it suggests that the release is triggered by Ca^{2+} microdomains. Using this method, it has been suggested that the release at the squid giant synapse and chick ciliary synapse is mediated by Ca^{2+} nanodomains, while the release at the calyx of Held synapse is triggered by Ca^{2+} microdomains [61]. Growing evidence suggests that nanodomain coupling may be more prevalent than microdomain coupling in mammalian central neurons [52, 62–64]. Nanodomain coupling can improve the accuracy of synaptic transmission [52, 62]. For more information on nanodomain coupling, two excellent review articles are available [38, 52].

5 Voltage-Gated Ca^{2+} Channels Are the Primary Source of Ca^{2+} for Neurotransmitter Release

Neuronal VGCCs generally consist of four subunits: α_1, β, α_2, and δ [65]. The α_2 and δ subunits are also collectively called the $\alpha_2\delta$ subunit because they are formed from cleavage of a single translational product. The α_1 subunit is a large (190–250 kDa) transmembrane protein consisting of four repeat domains. The membrane topology of each repeat domain resembles that of the α subunit of a typical voltage-gated K^+ channel, with six membrane-spanning segments (S1–S6), a P (pore) loop between S5 and S6, cytoplasmic amino and carboxyl terminals, and positively charged residues in the S4 segment. The δ subunit is also a membrane-associated protein with a single membrane-spanning domain. The β and α_2 subunits have no integral membrane spanning domains. The β subunit interacts with the intracellular loop between the first and second repeat domain of the α_1 subunit, whereas the α_2 subunit associates with the δ subunit on the extracellular side through a disulfide linkage. In skeletal muscle and some other tissues, VGCCs may include an additional γ subunit, which is an integral membrane protein with four membrane-spanning domains. The structures of $Ca_V1.1$, $Ca_V2.2$, and $Ca_V3.1$ channels have been determined by single-particle cryo-electron microscopy (cryo-EM) [66–71], which provide major insights into the molecular architecture underlying their biophysical properties. A schematic diagram of one α_1 with various auxiliary subunits is shown in Fig. 5.

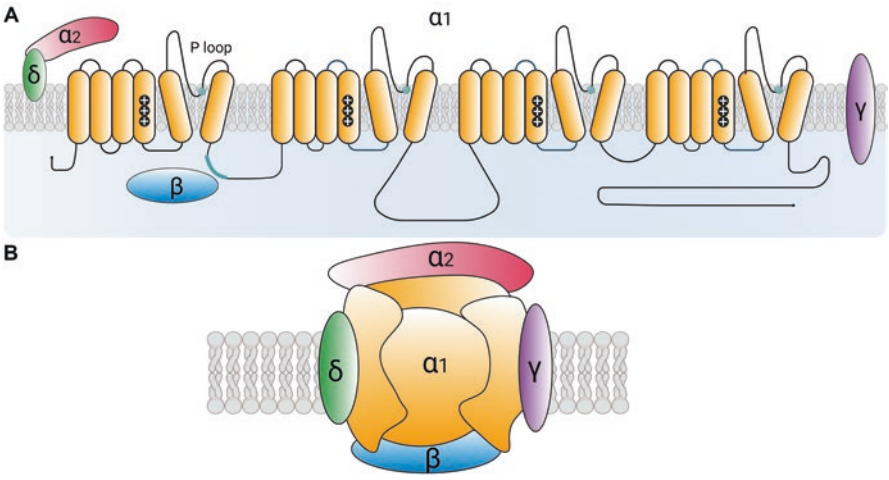

Fig. 5 Schematic diagrams showing the membrane topology and organization of voltage-gated Ca^{2+} channel (VGCC) subunits. (**a**) Membrane topology of Ca^{2+} channel subunits. The α_1 subunit consists of four repeat domains (I, II, III, and IV). Each repeat domain has six membrane-spanning segments (S1–S6) with a P (pore) loop between S5 and S6. The β subunit interacts with the α_1 subunit at the intracellular loop between the first and second repeating domains. The δ subunit has a single membrane-spanning segment. The α_2 subunit associates with the δ subunit through a disulfide linkage on the extracellular side. The γ subunit has four putative membrane-spanning segments. (**b**) Overall structure of a VGCC, which includes the α_1, β, δ, and α_2 subunits. (Created with BioRender.com)

Ca^{2+} channels are encoded by multiple genes and have diverse functional and pharmacological properties. Several methods have been used to classify Ca^{2+} channels. They are classified into high voltage-activated (HVA) and low voltage-activated (LVA) channels according to the degree of membrane depolarization needed for activation. LVA channels activate at a threshold of approximately −70 mV, whereas HVA channels activate at a threshold of approximately −20 mV [65].

Ca^{2+} channels are classified into L-, N-, P/Q-, R-, and T-types according to biophysical/pharmacological properties and tissue distribution. The L-type channel was named for its relatively large single channel conductance and long open duration (slow inactivation). The T-type channel was named for its tiny conductance and transient opening. The N-type channel was named because it was first identified in neurons. The P-type was first described in Purkinje cells. The Q-type was named because it was blocked by the same toxin that blocks the P-type (omega-agatoxin IVA) but with a lower sensitivity to the toxin and distinct inactivation kinetics, and because the letter "Q" follows "P" in the English alphabet. P- and Q-type channels are often collectively called the P/Q-type. The R-type was named for being resistant to organic calcium channel antagonists available at the time [65, 72, 73].

With the molecular cloning of the different subunits of Ca^{2+} channels, a nomenclature system based on compositions of the α_1 subunit was introduced in 1994 [74]. The α_1 subunit of skeletal muscle Ca^{2+} channels was named as α_{1S}, and subsequently

cloned α_1 subunits as α_{1A} through α_{1E}. However, this nomenclature system cannot conveniently accommodate newly identified Ca^{2+} channels and does not reflect the evolutionary relationship among the different α_1 subunits. As a result, a new nomenclature system based on amino acid sequence was adopted in 2000 [75]. Ca^{2+} channels are named $Ca_V x.y$, where Ca indicates the principal permeating ion, v indicates the principal physiological regulator (voltage), and x is a numerical identifier of the α_1 subunit subfamily, and y is a number indicating the order of discovery of the α_1 subunit within that subfamily. In this new nomenclature system, primary sequences of α_1 subunits are greater than 70% identical within the same subfamily, but less than 40% between different subfamilies. It is worth noting that the α_1 subunits of P- and Q-type channels are encoded by the same gene. The distinct biophysical and pharmacological properties of P- and Q-type channels are caused by different splice forms of the α_1 subunit and different β subunits [72]. Table 1 shows the relationships among the different nomenclatures, and commonly used blockers specific to the Ca^{2+} channels.

Many studies have been conducted to identify Ca^{2+} channels that trigger neurotransmitter release at presynaptic nerve terminals. They are generally identified by analyzing the effects of specific Ca^{2+} channel blockers on the amplitude of evoked postsynaptic currents or potentials, or on the amplitude or slope of field excitatory postsynaptic potentials. These analyses have revealed that $Ca_V2.1$ (P/Q--type) and $Ca_V2.2$ (N-type) channels play prominent roles in neurotransmitter release at many synapses, such as excitatory synapses in the hippocampus [76–79], inhibitory synapses in the cerebellum and spinal cord [78], and dopaminergic synapses in the striatum [80]. At some synapses, only one type of channel appears to be responsible for Ca^{2+} influx at the presynaptic terminal. For example, neurotransmitter

Table 1 Classification of voltage-gated Ca^{2+} channels (VGCCs)

Activation voltage	Pharmacological and biophysical properties	α_1 Subunit composition	α_1 Subunit sequence	Most commonly used blockers
HVA	L-type	α1S	$Ca_V1.1$	Dihydropyridine antagonists
		α1C	$Ca_V1.2$	
		α1D	$Ca_V1.3$	
		α1F	$Ca_V1.4$	
	P/Q-type	α1A	$Ca_V2.1$	ω-Agatoxin IVA
	N-type	α1B	$Ca_V2.2$	ω-Conotoxin GVIA
	R-type	α1E	$Ca_V2.3$	SNX-482
LVA	T-type	α1G	$Ca_V3.1$	Mibefradil
		α1H	$Ca_V3.2$	
		α1I	$Ca_V3.3$	

This table was based on papers by Lacinova [65] and Catteralls et al. [72]
VGCCs are classified into high voltage-activated (HVA) and low voltage-activated (LVA) channels according to the degree of membrane depolarization needed for activation, into L-, P/Q-, N-, R-, and T-type channels according to biophysical and pharmacological properties, and tissue distribution, into α_{1S}, $\alpha_{1A\text{-}I}$ channels according to the α_1 subunit composition, and into $Ca_V1.1$–1.4, $Ca_V2.1$–2.3, and $Ca_V3.1$–3.3 according to the primary sequence of the α_1 subunit

release at mature NMJs is triggered by Ca^{2+} influx through $Ca_V2.1$ alone [81–85]. At other synapses, such as the glutamatergic synapse between hippocampal CA1 and CA3 neurons, neurotransmitter release is triggered by Ca^{2+} influx through both $Ca_V2.1$ and $Ca_V2.2$ [76]. At still other synapses, such as the calyx of Held synapse, $Ca_V2.3$ (R-type) as well as $Ca_V2.1$ and $Ca_V2.2$ channels contribute to the release [86]. Thus, members of the Ca_V2 subfamily play important roles in triggering neurotransmitter release, but their relative contributions may vary from synapse to synapse.

Ca_V1 (L-type) and Ca_V3 (T-type) channels are generally not involved in Ca^{2+} influx at the presynaptic nerve terminal, although some unusual examples have been reported. For instance, at the presynaptic terminal of rat retinal bipolar cells, both Ca_V1 and Ca_V3 channels contribute to neurotransmitter release [87]. At the presynaptic terminal of goldfish retinal bipolar cells, Ca_V1 appears to be exclusively responsible for mediating neurotransmitter release [88]. It is still unclear why Ca_V2 channels are more suited to control neurotransmitter release than Ca_V1 and Ca_V3 channels. One clue comes from analyses of the effects of exogenously introduced α1 subunits in the superior cervical ganglion (SCG). In SCG neurons, acetylcholine release is typically mediated by $Ca_V2.2$. However, when different α1 subunits were expressed in these neurons, $Ca_V2.1$ and $Ca_V2.3$ were localized to nerve terminals and could mediate synaptic transmission, whereas $Ca_V1.2$ showed no presynaptic localization and no effect on synaptic transmission [89]. Similarly, *C. elegans* cholinergic motor neurons expresses both UNC-2 (Ca_V2) and EGL-19(Ca_V1), which are located at the center and lateral areas of presynaptic sites, respectively [90]. Only UNC-2 is required for evoked neurotransmitter release although both channels contribute to minis [90, 91]. These results suggest that trafficking and localization to proper sites in nerve terminals may be a factor in determining whether a particular Ca^{2+} channel can contribute to neurotransmitter release.

The types of Ca^{2+} channels that facilitate neurotransmitter release at the presynaptic terminal are regulated during development and can change when the predominant channel is mutated. For instance, at thalamic and cerebellar inhibitory synapses, immature neurons predominantly use $Ca_V2.2$ for neurotransmitter release, whereas mature neurons use $Ca_V2.1$ [92]. At the rat calyx of Held synapse, neurotransmitter release is triggered by Ca^{2+} influx through $Ca_V2.1$, $Ca_V2.2$, and $Ca_V2.3$ during postnatal day 4–9 [86, 93]. However, contributions from $Ca_V2.2$ and $Ca_V2.3$ gradually decrease after postnatal day 7, and by postnatal day 10, $Ca_V2.1$ almost exclusively mediates the release [93]. Wild-type mouse NMJ primarily relies on $Ca_V2.1$ for neurotransmitter release [94]. However, in $Ca_V2.1$ knockout mice, $Ca_V2.2$ and $Ca_V2.3$ are involved in mediating neurotransmitter release at the NMJ [94]. Similarly, at the NMJ of tottering mice, which carry a mutation in the α1 subunit of $Ca_V2.1$, the predominant Ca^{2+} channels that mediate neurotransmitter release are $Ca_V2.2$ and/or $Ca_V2.3$ [95, 96].

The developmental switch from $Ca_V2.2$ to $Ca_V2.1$ is potentially of physiological significance. In $Ca_V2.1$ knockout mice, paired-pulse facilitation, which is typically observed in wild-type synapses, is often absent at the calyx of Held synapse [97] and NMJ [94]. Moreover, synaptic depression in response to high-frequency

(100 Hz) stimulation is more severe in the knockout mice than in the wild-type [98]. Therefore, the developmental switch from $Ca_V2.2$ to $Ca_V2.1$ could enhance synaptic efficacy.

6 Ryanodine Receptor-Mediated Ca^{2+} Release Contributes to Neurotransmitter Release

The ER is a complex network that extends throughout the neuron, including the soma, dendrites, axons, and presynaptic terminals [90, 99–106]. Due to the vast amount of ER present in neurons, it has been suggested that the ER functions as a neuron-within-a-neuron [7]. The ER is a crucial intracellular Ca^{2+} store, and Ca^{2+} release from the ER is facilitated by two types of ionotropic receptors on the ER membrane: inositol 1,4,5-triphosphate receptor ($InsP_3R$) and ryanodine receptor (RyR). The ER Ca^{2+} store is refilled by sarco(endo)plasmic reticulum Ca^{2+} ATPase (SERCA) pumps [6]. Although the ER contains a significant amount of Ca^{2+}, the concentration of free Ca^{2+} is maintained within the range of 100–500 μM due to buffering by Ca^{2+}-binding proteins [107]. Ca^{2+} release from the ER plays an essential role in presynaptic functions, particularly in the process of neurotransmitter release. In this subsection, the focus is on the role of RyRs in neurotransmitter release.

The RyR channel plays a critical role in mediating intracellular Ca^{2+} release. Structurally, the channel is composed of four subunits, each of which contains multiple transmembrane domains that interact with the ER membrane. The amino-terminal domain of the RyR protein is particularly large and interacts with various regulators, including Ca^{2+}, ATP, caffeine, calstabin1 (FKBP12), calstabin2 (FKBP12.6), calmodulin, and VGCCs. Cryo-EM studies have revealed the binding sites for some of these regulators [108–121], shedding light on the molecular mechanisms of RyR gating. There are three isoforms of the RyR protein (RyR1, RyR2, and RyR3) encoded by separate genes, with each isoform exhibiting distinct expression patterns in different cell types. Dysregulation of RyR activity has been linked to numerous pathologies, including cardiac arrhythmias, malignant hyperthermia, and neurodegenerative diseases.

The RyR channel can be activated by two different mechanisms: Ca^{2+}-induced Ca^{2+} release (CICR) and depolarization-induced Ca^{2+} release (DICR) (Fig. 6a). In skeletal and cardiac muscles, RyR1 and RyR2 are the predominant isoforms, respectively. Skeletal muscle cells contain RyR1 in the sarcoplasmic reticulum (SR) membrane, which interacts with the plasma membrane's dihydropyridine receptor (DHPR), $Ca_V1.1$, at the location of transverse tubules. Specifically, one RyR1 channel's cytosolic domain interacts with four DHPRs (a tetrad) (Fig. 6b). In contrast, RyR2 in the heart is activated by CICR, which depends on Ca^{2+} influx through $Ca_V1.2$. Skeletal muscles also express RyR3 at a lower level, which is also activated by CICR. The physical interactions occur specifically between $Ca_V1.1$ and RyR1

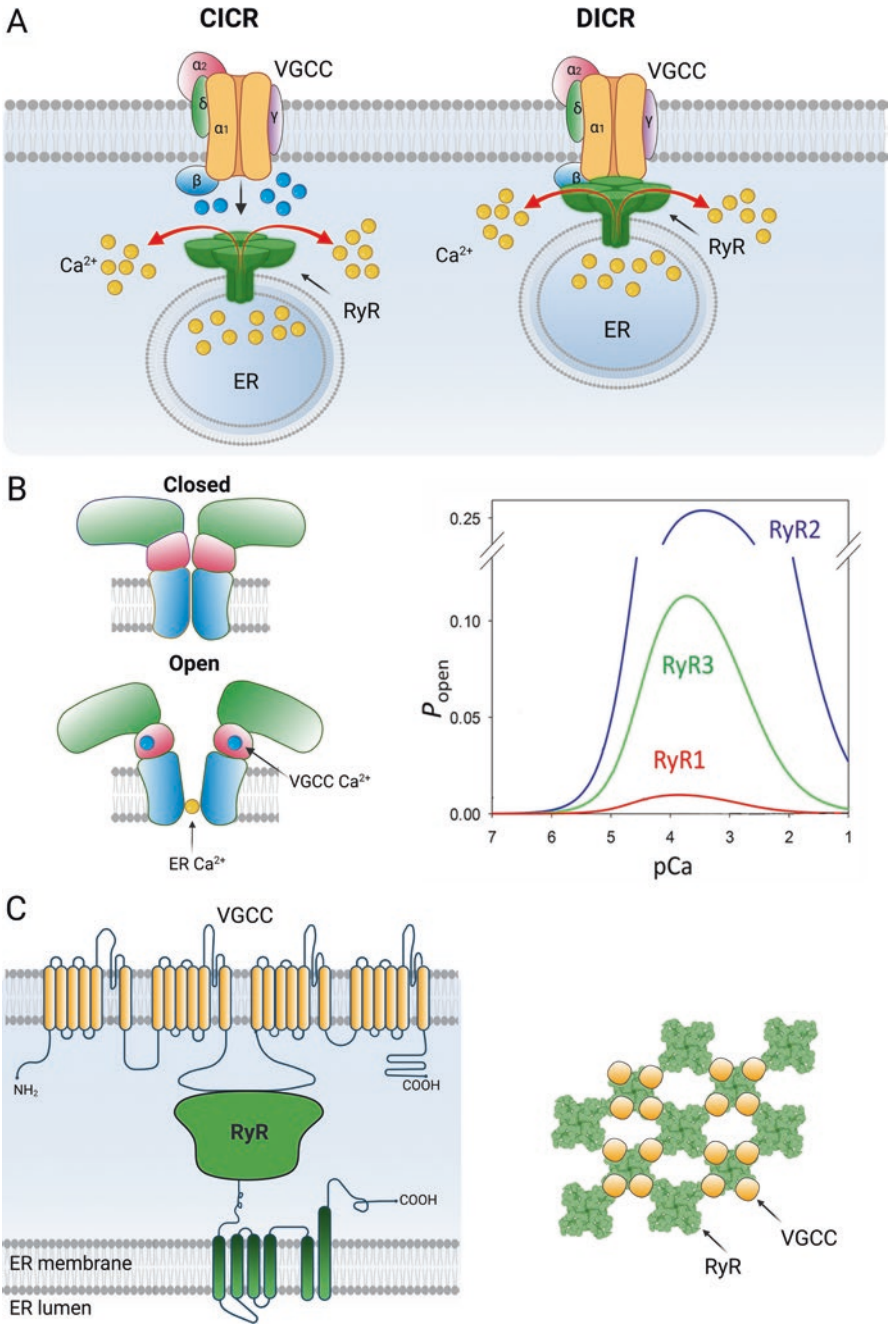

Fig. 6 Ryanodine receptors (RyRs) may be activated by two different mechanisms: Ca^{2+}-induced Ca^{2+} release (CICR) and depolarization-induced Ca^{2+} release (DICR). (**a**) Diagram depicting CICR and DICR. (**b**) In CICR, Ca^{2+} entering the cell through voltage-gated Ca^{2+} channels (VGCCs)

[121–126]. The interactions are mediated by $Ca_V1.1$'s intracellular loop between the III and IV repeat domains and RyR1 cytosolic "feet" [121–126] (Fig. 6b). The activation of RyR1 is coupled to the depolarization-induced conformational changes of DHPRs rather than DHPR-mediated Ca^{2+} influx.

RyR channels, regardless of their isoform, can be activated by Ca^{2+}-induced Ca^{2+} release (CICR) but their sensitivities to Ca^{2+} can vary. The effects of Ca^{2+} on RyR activity depend on its concentration, as it can either activate or inhibit the channels. RyRs are typically activated by lower concentrations of Ca^{2+}, while higher concentrations tend to inhibit their activity. This is likely due to Ca^{2+} binding to different sites with varying affinities within the channels (Fig. 6b). Further detailed explanations of the theories behind CICR and DICR are available in a review article by Eduardo Rios [127].

All three RyR isoforms are expressed in mammalian brains. Analysis of RyR expression in brain tissues from several mammalian species indicates that (1) RyRs are expressed in neurons throughout the brain; (2) the three different RyR isoforms are differentially expressed in brain tissues; (3) a specific brain area often expresses more than one RyR isoform; and (4) RyR2 is the predominant isoform in most brain areas [128–135] (see also https://mouse.brain-map.org/). For example, mRNAs of all three RyR isoforms are detected in the mouse hippocampus, with RyR2 being the most abundant [129, 135, 136].

Only a limited number of studies have examined the molecular mechanisms underlying RyR activation in neurons. While it is widely accepted that neuronal RyRs are activated via CICR [7, 137], there is also evidence to support the occurrence of DICR in neurons. For example, depolarization of mouse hypothalamic magnocellular neurons has been shown to increase the frequency of RyR-mediated Ca^{2+} syntillas (brief focal Ca^{2+} transients) at presynaptic terminals where RyR1 expression is detected, even in the absence of extracellular Ca^{2+}. This effect can be blocked by nifedipine, a DHPR antagonist, indicating that membrane depolarization may trigger RyR-mediated Ca^{2+} release from the ER through coupling between a VGCC and RyR1 [138]. Similarly, in the hypothalamic neurohypophysial system, depolarization has been found to induce ER Ca^{2+} release and neuropeptide secretion even in the absence of extracellular Ca^{2+}, and these effects can be antagonized by nifedipine, ryanodine, or BAPTA-AM, suggesting that direct coupling between Ca_V1 and RyRs can trigger ER Ca^{2+} release [139]. In the rat hippocampus, $Ca_V1.3$ and RyR2 colocalize and physically interact. Acute depolarization of hippocampal neurons by a high $[K^+]_o$ (60 mM) led to RyR-dependent Ca^{2+} release even in the absence of Ca^{2+} in the extracellular solution [140]. Taken together, these findings

Fig. 6 (continued) activate the RyR by binding to an activation module of the receptor. Adapted from reference [116]. The open probability (P_{open}) of RyRs consisting of RyR1, RyR2, or RyR3 all exhibit bidirectional responses to elevating Ca^{2+} concentrations but differ in their Ca^{2+} sensitivity. (**c**) In DICR, depolarization-induced conformational changes of VGCCs activate the RyR through physical interactions with the receptor. The intracellular loop between the II and III repeat domains of a VGCC physically interacts with the cytosolic domain of a RyR, and each RyR channel interacts with 4 VGCCs. (Created with BioRender.com except the right panel in (**b**), which was adapted from reference [127])

suggest that both DICR and CICR may occur in neurons, and that DICR is not exclusively mediated by coupling between $Ca_V1.1$ and RyR1, as concluded from studies with skeletal and cardiac muscles.

Presynaptic RyRs have been shown to play a role in regulating the frequency and amplitude of miniature postsynaptic currents (minis). For example, in the rat cerebellum, the frequency of inhibitory minis recorded from Purkinje cells was increased by 10 μM ryanodine but decreased by 100 μM ryanodine. The higher concentration of ryanodine also reduced the proportion of large-amplitude minis whereas the lower concentration of ryanodine showed no effect on the amplitude [141]. These opposite effects were attributed to activation and blockade of RyRs, respectively [141], because ryanodine can lock RyR in a sub-conductance state at submicromolar or low micromolar concentrations but block it at high micromolar concentrations [142]. In the rat hippocampus, nicotine increased the frequency of glutamatergic minis and the fraction of large-amplitude events. These effects were mimicked by the RyR activator caffeine but blocked by 100 μM ryanodine [143]. At the *C. elegans* NMJ, presynaptic RyRs were found to be important for the occurrence of minis. Null mutants of *unc-68*, which encodes the only RyR of *C. elegans*, showed greatly reduced mini frequency and essentially no large-amplitude events, while postsynaptic receptor sensitivities to acetylcholine and GABA remained normal [144]. A more recent study suggested that minis at the *C. elegans* NMJ depend on two different VGCCs, UNC-2 (a Ca_V2) and EGL-19 (a Ca_V1), and that EGL-19 functions through UNC-68 [90]. Taken together, these findings indicate that presynaptic RyRs can increase the frequency of minis and promote the occurrence of large-amplitude events.

Minis are generally thought to result from sporadic exocytosis of individual synaptic vesicles. The amplitude of minis could potentially be affected by a variety of factors. How might presynaptic RyRs increase the occurrence of large-amplitude minis? One hypothesis is that presynaptic RyRs may promote synchronized multivesicular exocytosis. This hypothesis was mainly based on the results of two studies. In one study [141], large-amplitude minis were thought to be due to multivesicular release because their proportion could be reduced by prolonged exposure to a Ca^{2+}-free extracellular solution. In the other study [143], a similar conclusion was reached because a positive correlation was observed between the rise time and mean amplitude of minis. It was reasoned that when multiple synaptic vesicles exocytose at the same time, a lack of absolute synchrony would result in an increased rise time. An alternative hypothesis is that presynaptic RyRs may increase the quantal size (the amount of neurotransmitter released from a vesicle in a single exocytotic event). This hypothesis was mainly based on analyses of synaptic transmission at the *C. elegans* NMJ, where large-amplitude minis are essentially eliminated by null mutations of the RyR gene *unc-68* [144]. Several lines of evidence suggest that RyR-dependent large-amplitude minis at the *C. elegans* NMJ were not due to multivesicular release [144]. First, the proportion of large-amplitude events did not decrease in syntaxin or SNAP25 mutants, which are severely defective in synchronizing synaptic vesicle exocytosis. Second, the rise time of minis was constant regardless of the amplitude. Third, the proportion of large-amplitude events did not

decrease when $[Ca^{2+}]_o$ was changed from 5 mM to zero [144]. Given the existence of these two competing hypotheses, further studies are needed to determine whether RyR-mediated large-amplitude minis are mono- or multiquantal, and whether this property varies from synapse to synapse.

Presynaptic RyRs are important for evoked neurotransmitter release and synaptic plasticity. At the *C. elegans* NMJ, the amplitude of evoked postsynaptic currents decreased by 40–50% in *unc-68* null mutants compared to wild-type, and this defect was rescued by expressing a wild-type *unc-68* transgene in neurons but not muscle cells [144, 145]. At inhibitory synapses between cerebellar basket and Purkinje neurons, the mean amplitude of evoked inhibitory postsynaptic currents decreased by ~30% when RyRs were blocked with ryanodine, and this effect appeared to be presynaptic because ryanodine also increased the paired-pulse ratio of the evoked responses [146]. In the presynaptic terminal of hippocampal pyramidal neurons, blocking RyRs with ryanodine inhibited paired-pulse facilitation of evoked EPSCs, suggesting a role for presynaptic RyRs in short-term synaptic plasticity [147]. At mossy fiber terminals in the hippocampus, blocking RyRs with the ryanodine receptor blocker TMB-8 reduced presynaptic Ca^{2+} accumulation and short-term synaptic depression caused by repetitive nerve stimuli. Immunohistochemistry showed that RyR2 is preferentially localized to the axons of hippocampal mossy fibers. These findings suggest that axonal RyR2 enables use-dependent Ca^{2+} release to facilitate presynaptic forms of synaptic plasticity at the mossy fiber-CA3 synapse [148]. At excitatory synapses between hippocampal CA3 neurons, blocking RyRs with ryanodine during the induction period but not afterward abolished NMDA receptor-dependent long-term depression (LTD), suggesting that presynaptic RyR-sensitive stores are required for LTD induction but not expression [149]. At frog motor terminals, conditioning nerve stimulation (10–20 Hz for 2–10 min) enhanced the amplitude and quantal content of end-plate potentials, and this effect of stimulation can be prevented by blocking RyRs with ryanodine [150].

The function of RyRs in regulating presynaptic Ca^{2+} signaling has been investigated through Ca^{2+} imaging in several studies. Using two-photon laser scanning fluorescence microscopy with Oregon Green-1, it was found that ryanodine (100 μM) inhibited AP-evoked Ca^{2+} transients by approximately 50% at the presynaptic terminal of rat cerebellar basket cells [141]. Confocal laser scanning microscopy with Oregon Green 488 BAPTA-1 demonstrated that ryanodine (20 μM) inhibited paired-pulse facilitation of Ca^{2+} transients at presynaptic boutons of hippocampal CA3 neurons [147]. Ca^{2+} imaging using fluo-3 and a signal mass approach showed that 10 μM ryanodine increased the frequency of syntillas, while 100 μM ryanodine decreased it at isolated mouse hypothalamic magnocellular nerve terminals [151]. Additionally, Ca^{2+} imaging by expressing GCaMP6 in *C. elegans* motor neurons showed that knockdown of the RyR gene *unc-68* reduced the frequency of Ca^{2+} transients [145]. These findings support the notion that presynaptic RyRs play a critical role in mobilizing Ca^{2+}.

The importance of RyRs in regulating neurotransmitter release is also demonstrated by the effects of mutations of proteins that regulate RyR function or expression. In mice, the conditional double knockout (cDKO) of presenilin 1 and presenilin

2, which are γ-secretases implicated in the generation of amyloid β peptides from an amyloid precursor protein, in presynaptic (CA3) but not postsynaptic (CA1) neurons in the hippocampal Schaeffer collateral pathway inhibits short-term synaptic facilitation and glutamate release. Blockade of RyRs with ryanodine (100 μM) mimics the defect of presynaptic cDKO in synaptic facilitation [152]. The presynaptic effects of cDKO are mainly due to reduced RyR protein expression [135]. Additionally, conditional knockout of ATG5, a protein essential to autophagy, augments evoked field excitatory postsynaptic potentials, caffeine-induced elevation of $[Ca^{2+}]_i$ in axons and presynapses, an action potential train-induced exocytosis, and RyR protein level in hippocampal neurons. The effects of ATG5 knockout on exocytosis can be eliminated by either dantrolene (an RyR antagonist) or RyR knockdown. These results suggest that knockout of ATG5 augments neurotransmitter release by increasing RyR expression [153]. In *C. elegans*, a hypomorphic mutation of *aipr-1*, which encodes an ortholog of human aryl hydrocarbon receptor-interacting protein (AIP), causes great increases in the frequency and amplitude of minis and in the amplitude of evoked postsynaptic currents at the NMJ. The effects of the *aipr-1* mutation may be eliminated by targeted expression of wild-type AIPR-1 in neurons but not muscle cells and occluded by a null mutation of the RyR gene *unc-68*. These findings suggest that a physiological function of AIPR-1 is to restrict RyR-mediated Ca^{2+} release from the ER [145].

Despite the evidence presented above, the role of presynaptic RyRs in controlling neurotransmitter release remains unclear for several reasons. Firstly, certain studies have demonstrated that the blockage of RyRs has little to no impact on synaptic transmission [154–157]. Secondly, the effect of ryanodine on neurotransmitter release often exhibits high variability even in studies claiming that presynaptic RyRs play a role in spontaneous or evoked release. For instance, in a study involving the application of ryanodine (10 μM), the frequency of inhibitory minis increased in only 4 out of 10 rat cerebellar Purkinje neurons [141] and 4 out of 12 mouse cerebellar Purkinje neurons [154]. Additionally, ryanodine (100 μM) showed a highly variable and often weak effect on evoked neurotransmitter release from rat cerebellar basket cell terminals [146]. Thirdly, while the use of 100 μM ryanodine to inhibit RyRs reduced the proportion of large-amplitude minis at cerebellar inhibitory synapses, the use of 10 μM ryanodine to activate RyRs did not demonstrate an opposite effect [141]. Finally, ryanodine has been used as a key pharmacological tool in the majority of previous studies. However, ryanodine is a bidirectional modulator of RyRs with poorly defined concentration boundaries for activation and inhibition. For instance, 10–20 μM ryanodine has been used either to activate [141, 143, 154] or to block [147, 150, 155, 158] RyRs. Thus, additional analyses involving more specific pharmacological agents or RyR mutants are necessary to better understand the function of presynaptic RyRs in neurotransmitter release.

The function of presynaptic inositol 1,4,5-trisphosphate receptors ($InsP_3Rs$) in neurotransmitter release is much less understood. The $InsP_3R$ is activated by InsP3, and its sensitivity to InsP3 is enhanced by Ca^{2+} [7]. In the rat barrel cortex, blockage of $InsP_3Rs$ using 2-aminoethoxydiphenylborane resulted in a reduced frequency of

minis recorded from layer II pyramidal neurons [158]. However, at the *C. elegans* NMJ, synaptic transmission appeared normal in a hypomorphic mutant of *itr-1*, which encodes the only $InsP_3R$ of *C. elegans* [144].

7 Presynaptic Mitochondria May Play a Role in Sustained Neurotransmitter Release

Mitochondria are highly concentrated at the presynaptic nerve terminal and serve at least two critical functions. First, they provide the energy needed by the presynaptic nerve terminal, which may account for up to 10% of the total energy required for neuronal signaling [159]. Second, they may regulate neurotransmitter release by modulating $[Ca^{2+}]_i$ at the presynaptic nerve terminal.

The interior of the mitochondrion is approximately 200 mV more negative than the exterior, creating a significant driving force for Ca^{2+} influx. Ca^{2+} may enter the mitochondrion through undefined uniporters in the inner membrane and exit through Na^+/Ca^{2+} and H^+/Ca^{2+} antiporters [160]. During sustained high-frequency nerve stimulation, the concentration of Ca^{2+} inside the mitochondrion ($[Ca^{2+}]_m$) increases due to enhanced uptake activity. There is ongoing debate about the levels that $[Ca^{2+}]_m$ can rise to, with estimates ranging from as low as a few micromolar to several hundred micromolar [160]. Ca^{2+} uptake into the mitochondria may occur even when the cytoplasmic $[Ca^{2+}]$ is as low as a few hundred nanomolar [161, 162].

The role of presynaptic mitochondria in neurotransmitter release has been examined in various synapses using pharmacological agents that depolarize the mitochondrial membrane or inhibit the uniporter. These analyses suggest that presynaptic mitochondria serve several functions in synaptic transmission. Firstly, they may accelerate recovery from short-term presynaptic depression. At the rat calyx of Held synapse, a train of stimuli at 200 Hz leads to synaptic depression, indicated by diminishing amplitudes of EPSCs. Following a resting period of 500 ms, the amplitude of EPSCs in response to a single stimulus recovered to ~80% of the first EPSC in the train. However, pharmacological agents that depolarize the mitochondria or inhibit the uniporter resulted in reduced EPSC amplitude recovery due to deficient mitochondrial Ca^{2+} sequestration [163]. Secondly, presynaptic mitochondria may alleviate synaptic depression in response to sustained nerve stimulation. At the lizard NMJ, the amplitude of end-plate potentials gradually decreases in response to a train of 500 stimuli at 50 Hz. Treatments that depolarize the mitochondria aggravated synaptic depression [164]. Thirdly, mitochondria may contribute to post-tetanic potentiation. At the crayfish NMJ, tetanus stimulation of the motor axon for 7–10 min at 20–33 Hz potentiated subsequent responses to nerve stimulation, which were blocked by pharmacological perturbation of mitochondrial Ca^{2+} handling [165]. These observations suggest that the regulation of Ca^{2+} by mitochondria may be essential in controlling neurotransmitter release during sustained nerve stimulation.

8 Are Minis Ca^{2+}-Dependent?

Traditionally, minis were considered as elementary events of action potential-evoked neurotransmitter release with no physiological significance, resulting from the full-collapse fusion of individual synaptic vesicles. However, over the past two decades, our understanding of minis has significantly progressed with several notable advances. First, minis may also occur through kiss-and-run exocytosis, where the release of neurotransmitters in the synaptic vesicle may be partial (Chapter "Multiple modes of fusion and retrieval at the calyx of Held synapse"). Second, minis may be essential for several important physiological functions, such as postsynaptic receptor clustering [166], modulation of NMDA receptor subunit composition during development [167], regulation of dendritic protein synthesis [168, 169], maintenance of dendritic spines [170], and action potential firing [143, 171]. Third, minis appear to be different from evoked responses in various ways: minis and evoked responses could result from the release of distinct populations of synaptic vesicles [172]; they could depend on the function of different synaptotagmins, with synaptotagmins 1 and 2 being important for evoked neurotransmitter release [12, 173, 174], and synaptotagmin 12, which does not bind Ca^{2+}, being important for minis [175]; minis and evoked responses might be mediated by different Ca^{2+} channels in the plasma membrane [176–178]; and they are differentially affected by mutations of synaptobrevin [179], SNAP25 [144, 180], and synaptotagmins [173, 174, 181]. At the *C. elegans* NMJ, with respect of VGCCs, evoked neurotransmitter release is mediated by Ca^{2+} entry through UNC-2, a Cav2 channel, while minis depend on Ca^{2+} entry through both UNC-2 and EGL-19, a Cav1 channel [91]. Time-resolved "flash-and-freeze" electron microscopy, fluorescence microscopy, and electrophysiology analyses indicate that UNC-2 and EGL-19 act on two spatially distinct pools of synaptic vesicles, including a central pool dependent on UNC-2 and a lateral pool dependent on EGL-19 and RyRs [90].

Despite the physiological significance of minis and their utility in analyzing synaptic transmission, it remains unclear whether the occurrence of minis is dependent on Ca^{2+}. Scientific literature often refers to minis as "Ca^{2+}-independent" events because they can occur in the presence of Ca^{2+}-free or nominally Ca^{2+}-free extracellular solutions. However, it is important to note that a significant amount of Ca^{2+} may be present in the water used to create nominally Ca^{2+}-free solutions, and RyR-mediated Ca^{2+} release from the ER may contribute to the generation of minis. Therefore, the term "Ca^{2+}-independence" may be not an accurate description of minis. In fact, there is no compelling evidence to suggest that minis can occur in the complete absence of Ca^{2+}, with the possible exceptions of minis induced by hypertonic solutions [182] and α-latrotoxin [183, 184].

The roles of extracellular Ca^{2+} and RyRs in minis have been examined in several previous studies. Extracellular Ca^{2+} appears to play a varying role in minis across different synapses. For instance, reducing $[Ca^{2+}]_o$ from 5 mM to zero in the presence of 5 mM EGTA resulted in an approximate 80% decrease in the frequency of minis at the *C. elegans* NMJ [144, 185]. Conversely, the application of ionomycin, a Ca^{2+}

ionophore, increased the frequencies of both excitatory and inhibitory minis in hippocampal brain slices [184]. These observations suggest that Ca^{2+} influx may induce minis. However, in several synapses investigated, the application of the Ca^{2+} channel blocker cadmium or a Ca^{2+}-free solution did not affect the frequency of minis [186–190], indicating that Ca^{2+} influx may not trigger minis. At the frog NMJ, changing $[Ca^{2+}]_o$ showed varying effects on the frequency of minis [191].

Similarly, manipulating the function of RyRs produced varying effects on minis. Blocking RyRs with ryanodine (20–100 μM) decreased the frequency of minis recorded from rat barrel cortex layer II pyramidal neurons [158], cerebellar Purkinje neurons [141], and hippocampal CA3 neurons [143]. On the other hand, activating RyRs with caffeine or ryanodine (10 μM) increased the frequency of minis recorded from pyramidal [158] and Purkinje [141] neurons. These observations suggest that RyR-mediated Ca^{2+} release from the ER is significant to minis. However, blocking RyRs with ryanodine (30 or 100 μM) did not exhibit a significant effect on the frequencies of glycinergic minis in rat auditory brainstem nuclei [156] and GABAergic minis in rat hippocampus [157], indicating that RyRs do not mediate minis at these synapses.

It is not clear why manipulations of $[Ca^{2+}]_o$ and RyR function have different effects on minis at different synapses. The results presented above do not provide enough evidence to tell whether Ca^{2+} is necessary for minis because some minis persisted when either $[Ca^{2+}]_o$ or RyR function was removed or blocked. One study has investigated the combined effects of a Ca^{2+}-free extracellular solution and RyR dysfunction on synaptic transmission in *C. elegans*. The study found that a null mutation of the RyR gene *unc-68* decreased the frequency of minis by more than 75% at the NMJ in the presence of 5 mM $[Ca^{2+}]_o$, and applying a Ca^{2+}-free extracellular solution almost completely eliminated the remaining minis [144]. Another study showed that minis at the *C. elegans* NMJ are essentially abolished by combined deficiencies of UNC-2 (Ca_V2) and EGL-19 (Ca_V1) even in the presence of extracellular Ca^{2+} (0.5 mM) [90]. These results suggest that Ca^{2+} may be necessary for minis, and that Ca^{2+} influx and RyR-mediated Ca^{2+} release are the only sources of Ca^{2+} that trigger synaptic exocytosis at the *C. elegans* NMJ.

If it is true that Ca^{2+} is required for the occurrence of minis, then the application of fast Ca^{2+} chelators such as BAPTA-AM might be able to eliminate all minis. However, in previous studies, BAPTA-AM had no effect on the frequency of minis at inhibitory synapses in rat auditory brainstem nuclei [156], excitatory synapses in cultured rat hippocampal neurons [192], and dorsolateral periaqueductal gray neurons of rats [193]. At other synapses, such as the mouse calyx of Held synapse and NMJ and rat barrel cortex layer II pyramidal neurons, a Ca^{2+}-free extracellular solution containing BAPTA-AM was able to significantly reduce the frequency of minis but not eliminate them [158, 174]. These observations suggest that either Ca^{2+} is not essential to minis at these synapses or that a very tight functional coupling exists between Ca^{2+} channels or RyRs and the Ca^{2+} sensor of synaptic exocytosis. Therefore, it may be useful to investigate the combined effects of a Ca^{2+}-free extracellular solution and RyR mutation on the frequency of minis in other systems to determine whether the findings from *C. elegans* are applicable to other synapses.

Acknowledgment This study was supported by the US National Institute of Health grants R01MN085927 (ZWW) and R01NS109388 (ZWW).

References

1. Locke FS. Notiz uber den einfluss physiologischer kochsalz-losung auf die elektrische erregbarkeit von muskel und nerv. Zbl Physiol. 1894;8:166–7.
2. Harvey AM, Macintosh FC. Calcium and synaptic transmission in a sympathetic ganglion. J Physiol. 1940;97:408–16. https://doi.org/10.1113/jphysiol.1940.sp003818.
3. Del Castillo J, Stark L. The effect of calcium ions on the motor end-plate potentials. J Physiol. 1952;116:507–15. https://doi.org/10.1113/jphysiol.1952.sp004720.
4. Dodge FA Jr, Rahamimoff R. Co-operative action a calcium ions in transmitter release at the neuromuscular junction. J Physiol. 1967;193:419–32. https://doi.org/10.1113/jphysiol.1967.sp008367.
5. Katz B, Miledi R. The effect of calcium on acetylcholine release from motor nerve terminals. Proc R Soc Lond B Biol Sci. 1965;161:496–503. https://doi.org/10.1098/rspb.1965.0017.
6. Verkhratsky A. The endoplasmic reticulum and neuronal calcium signalling. Cell Calcium. 2002;32:393–404. https://doi.org/10.1016/s0143416002001896.
7. Berridge MJ. Neuronal calcium signaling. Neuron. 1998;21:13–26. https://doi.org/10.1016/s0896-6273(00)80510-3.
8. Schneggenburger R, Neher E. Intracellular calcium dependence of transmitter release rates at a fast central synapse. Nature. 2000;406:889–93. https://doi.org/10.1038/35022702.
9. Heidelberger R, Heinemann C, Neher E, Matthews G. Calcium dependence of the rate of exocytosis in a synaptic terminal. Nature. 1994;371:513–5. https://doi.org/10.1038/371513a0.
10. Lando L, Zucker RS. Ca2+ cooperativity in neurosecretion measured using photolabile Ca2+ chelators. J Neurophysiol. 1994;72:825–30. https://doi.org/10.1152/jn.1994.72.2.825.
11. Bollmann JH, Sakmann B, Borst JG. Calcium sensitivity of glutamate release in a calyx-type terminal. Science. 2000;289:953–7. https://doi.org/10.1126/science.289.5481.953.
12. Fernandez-Chacon R, Konigstorfer A, Gerber SH, Garcia J, Matos MF, Stevens CF, et al. Synaptotagmin I functions as a calcium regulator of release probability. Nature. 2001;410:41–9. https://doi.org/10.1038/35065004.
13. Yoshihara M, Littleton JT. Synaptotagmin I functions as a calcium sensor to synchronize neurotransmitter release. Neuron. 2002;36:897–908. https://doi.org/10.1016/s0896-6273(02)01065-6.
14. Broadie K, Bellen HJ, DiAntonio A, Littleton JT, Schwarz TL. Absence of synaptotagmin disrupts excitation-secretion coupling during synaptic transmission. Proc Natl Acad Sci U S A. 1994;91:10727–31. https://doi.org/10.1073/pnas.91.22.10727.
15. Rickman C, Hu K, Carroll J, Davletov B. Self-assembly of SNARE fusion proteins into star-shaped oligomers. Biochem J. 2005;388:75–9. https://doi.org/10.1042/BJ20041818.
16. Stewart BA, Mohtashami M, Trimble WS, Boulianne GL. SNARE proteins contribute to calcium cooperativity of synaptic transmission. Proc Natl Acad Sci U S A. 2000;97:13955–60. https://doi.org/10.1073/pnas.250491397.
17. Augustine GJ, Adler EM, Charlton MP. The calcium signal for transmitter secretion from presynaptic nerve terminals. Ann N Y Acad Sci. 1991;635:365–81. https://doi.org/10.1111/j.1749-6632.1991.tb36505.x.
18. Felmy F, Neher E, Schneggenburger R. Probing the intracellular calcium sensitivity of transmitter release during synaptic facilitation. Neuron. 2003;37:801–11. https://doi.org/10.1016/s0896-6273(03)00085-0.
19. Liu Q, Chen B, Ge Q, Wang ZW. Presynaptic Ca^{2+}/calmodulin-dependent protein kinase II modulates neurotransmitter release by activating BK channels at *Caenorhabditis ele-*

gans neuromuscular junction. J Neurosci. 2007;27:10404–13. https://doi.org/10.1523/JNEUROSCI.5634-06.2007.
20. Gentile L, Stanley EF. A unified model of presynaptic release site gating by calcium channel domains. Eur J Neurosci. 2005;21:278–82. https://doi.org/10.1111/j.1460-9568.2004.03841.x.
21. Kuno M, Takahashi T. Effects of calcium and magnesium on transmitter release at Ia synapses of rat spinal motoneurones in vitro. J Physiol. 1986;376:543–53. https://doi.org/10.1113/jphysiol.1986.sp016169.
22. Eshra A, Schmidt H, Eilers J, Hallermann S. Calcium dependence of neurotransmitter release at a high fidelity synapse. elife. 2021;10 https://doi.org/10.7554/eLife.70408.
23. Lou X, Scheuss V, Schneggenburger R. Allosteric modulation of the presynaptic Ca2+ sensor for vesicle fusion. Nature. 2005;435:497–501. https://doi.org/10.1038/nature03568.
24. Hubbard JI, Jones SF, Landau EM. On the mechanism by which calcium and magnesium affect the release of transmitter by nerve impulses. J Physiol. 1968;196:75–86. https://doi.org/10.1113/jphysiol.1968.sp008495.
25. Shimosawa T, Takano K, Ando K, Fujita T. Magnesium inhibits norepinephrine release by blocking N-type calcium channels at peripheral sympathetic nerve endings. Hypertension. 2004;44:897–902. https://doi.org/10.1161/01.HYP.0000146536.68208.84.
26. Zhang A, Fan SH, Cheng TP, Altura BT, Wong RK, Altura BM. Extracellular Mg2+ modulates intracellular Ca2+ in acutely isolated hippocampal CA1 pyramidal cells of the Guinea-pig. Brain Res. 1996;728:204–8. https://doi.org/10.1016/0006-8993(96)00401-5.
27. Shi J, Krishnamoorthy G, Yang Y, Hu L, Chaturvedi N, Harilal D, et al. Mechanism of magnesium activation of calcium-activated potassium channels. Nature. 2002;418:876–80. https://doi.org/10.1038/nature00941.
28. Shi J, Cui J. Intracellular Mg(2+) enhances the function of BK-type Ca(2+)-activated K(+) channels. J Gen Physiol. 2001;118:589–606. https://doi.org/10.1085/jgp.118.5.589.
29. Zhang X, Solaro CR, Lingle CJ. Allosteric regulation of BK channel gating by Ca(2+) and Mg(2+) through a nonselective, low affinity divalent cation site. J Gen Physiol. 2001;118:607–36. https://doi.org/10.1085/jgp.118.5.607.
30. Robitaille R, Garcia ML, Kaczorowski GJ, Charlton MP. Functional colocalization of calcium and calcium-gated potassium channels in control of transmitter release. Neuron. 1993;11:645–55. https://doi.org/10.1016/0896-6273(93)90076-4.
31. Wang ZW, Saifee O, Nonet ML, Salkoff L. SLO-1 potassium channels control quantal content of neurotransmitter release at the *C. elegans* neuromuscular junction. Neuron. 2001;32:867–81. https://doi.org/10.1016/s0896-6273(01)00522-0.
32. Adler EM, Augustine GJ, Duffy SN, Charlton MP. Alien intracellular calcium chelators attenuate neurotransmitter release at the squid giant synapse. J Neurosci. 1991;11:1496–507. https://doi.org/10.1523/JNEUROSCI.11-06-01496.1991.
33. Tandon A, Bannykh S, Kowalchyk JA, Banerjee A, Martin TF, Balch WE. Differential regulation of exocytosis by calcium and CAPS in semi-intact synaptosomes. Neuron. 1998;21:147–54. https://doi.org/10.1016/s0896-6273(00)80522-x.
34. Wolfel M, Schneggenburger R. Presynaptic capacitance measurements and Ca2+ uncaging reveal submillisecond exocytosis kinetics and characterize the Ca2+ sensitivity of vesicle pool depletion at a fast CNS synapse. J Neurosci. 2003;23:7059–68. https://doi.org/10.1523/JNEUROSCI.23-18-07059.2003.
35. Augustine GJ, Santamaria F, Tanaka K. Local calcium signaling in neurons. Neuron. 2003;40:331–46. https://doi.org/10.1016/s0896-6273(03)00639-1.
36. Fogelson AL, Zucker RS. Presynaptic calcium diffusion from various arrays of single channels. Implications for transmitter release and synaptic facilitation. Biophys J. 1985;48:1003–17. https://doi.org/10.1016/S0006-3495(85)83863-7.
37. Simon SM, Llinas RR. Compartmentalization of the submembrane calcium activity during calcium influx and its significance in transmitter release. Biophys J. 1985;48:485–98. https://doi.org/10.1016/S0006-3495(85)83804-2.

38. Wang LY, Augustine GJ. Presynaptic nanodomains: a tale of two synapses. Front Cell Neurosci. 2014;8:455. https://doi.org/10.3389/fncel.2014.00455.
39. Neher E, Sakaba T. Multiple roles of calcium ions in the regulation of neurotransmitter release. Neuron. 2008;59:861–72. https://doi.org/10.1016/j.neuron.2008.08.019.
40. Llinas R, Sugimori M, Silver RB. Microdomains of high calcium concentration in a presynaptic terminal. Science. 1992;256:677–9. https://doi.org/10.1126/science.1350109.
41. Beaumont V, Llobet A, Lagnado L. Expansion of calcium microdomains regulates fast exocytosis at a ribbon synapse. Proc Natl Acad Sci U S A. 2005;102:10700–5. https://doi.org/10.1073/pnas.0501961102.
42. Yazejian B, Sun XP, Grinnell AD. Tracking presynaptic Ca^{2+} dynamics during neurotransmitter release with Ca^{2+}-activated K^+ channels. Nat Neurosci. 2000;3:566–71. https://doi.org/10.1038/75737.
43. DiGregorio DA, Peskoff A, Vergara JL. Measurement of action potential-induced presynaptic calcium domains at a cultured neuromuscular junction. J Neurosci. 1999;19:7846–59. https://doi.org/10.1523/JNEUROSCI.19-18-07846.1999.
44. Demuro A, Parker I. Imaging single-channel calcium microdomains. Cell Calcium. 2006;40:413–22. https://doi.org/10.1016/j.ceca.2006.08.006.
45. Zenisek D, Davila V, Wan L, Almers W. Imaging calcium entry sites and ribbon structures in two presynaptic cells. J Neurosci. 2003;23:2538–48. https://doi.org/10.1523/JNEUROSCI.23-07-02538.2003.
46. Heidelberger R, Matthews G. Calcium influx and calcium current in single synaptic terminals of goldfish retinal bipolar neurons. J Physiol. 1992;447:235–56. https://doi.org/10.1113/jphysiol.1992.sp019000.
47. Neves G, Lagnado L. The kinetics of exocytosis and endocytosis in the synaptic terminal of goldfish retinal bipolar cells. J Physiol. 1999;515(Pt 1):181–202. https://doi.org/10.1111/j.1469-7793.1999.181ad.x.
48. Zenisek D, Matthews G. The role of mitochondria in presynaptic calcium handling at a ribbon synapse. Neuron. 2000;25:229–37. https://doi.org/10.1016/s0896-6273(00)80885-5.
49. Harlow ML, Ress D, Stoschek A, Marshall RM, McMahan UJ. The architecture of active zone material at the frog's neuromuscular junction. Nature. 2001;409:479–84. https://doi.org/10.1038/35054000.
50. Meinrenken CJ, Borst JG, Sakmann B. Calcium secretion coupling at calyx of Held governed by nonuniform channel-vesicle topography. J Neurosci. 2002;22:1648–67. https://doi.org/10.1523/JNEUROSCI.22-05-01648.2002.
51. Tsien RY. New calcium indicators and buffers with high selectivity against magnesium and protons: design, synthesis, and properties of prototype structures. Biochemistry. 1980;19:2396–404. https://doi.org/10.1021/bi00552a018.
52. Eggermann E, Bucurenciu I, Goswami SP, Jonas P. Nanodomain coupling between Ca(2)(+) channels and sensors of exocytosis at fast mammalian synapses. Nat Rev Neurosci. 2011;13:7–21. https://doi.org/10.1038/nrn3125.
53. Swandulla D, Hans M, Zipser K, Augustine GJ. Role of residual calcium in synaptic depression and posttetanic potentiation: fast and slow calcium signaling in nerve terminals. Neuron. 1991;7:915–26. https://doi.org/10.1016/0896-6273(91)90337-y.
54. Burrone J, Neves G, Gomis A, Cooke A, Lagnado L. Endogenous calcium buffers regulate fast exocytosis in the synaptic terminal of retinal bipolar cells. Neuron. 2002;33:101–12. https://doi.org/10.1016/s0896-6273(01)00565-7.
55. von Gersdorff H, Matthews G. Dynamics of synaptic vesicle fusion and membrane retrieval in synaptic terminals. Nature. 1994;367:735–9. https://doi.org/10.1038/367735a0.
56. Fedchyshyn MJ, Wang LY. Developmental transformation of the release modality at the calyx of Held synapse. J Neurosci. 2005;25:4131–40. https://doi.org/10.1523/JNEUROSCI.0350-05.2005.
57. Borst JG, Sakmann B. Calcium influx and transmitter release in a fast CNS synapse. Nature. 1996;383:431–4. https://doi.org/10.1038/383431a0.

58. Ohana O, Sakmann B. Transmitter release modulation in nerve terminals of rat neocortical pyramidal cells by intracellular calcium buffers. J Physiol. 1998;513(Pt 1):135–48. https://doi.org/10.1111/j.1469-7793.1998.135by.x.
59. Rozov A, Burnashev N, Sakmann B, Neher E. Transmitter release modulation by intracellular Ca2+ buffers in facilitating and depressing nerve terminals of pyramidal cells in layer 2/3 of the rat neocortex indicates a target cell-specific difference in presynaptic calcium dynamics. J Physiol. 2001;531:807–26. https://doi.org/10.1111/j.1469-7793.2001.0807h.x.
60. Mintz IM, Sabatini BL, Regehr WG. Calcium control of transmitter release at a cerebellar synapse. Neuron. 1995;15:675–88. https://doi.org/10.1016/0896-6273(95)90155-8.
61. Schneggenburger R, Neher E. Presynaptic calcium and control of vesicle fusion. Curr Opin Neurobiol. 2005;15:266–74. https://doi.org/10.1016/j.conb.2005.05.006.
62. Bucurenciu I, Kulik A, Schwaller B, Frotscher M, Jonas P. Nanodomain coupling between Ca2+ channels and Ca2+ sensors promotes fast and efficient transmitter release at a cortical GABAergic synapse. Neuron. 2008;57:536–45. https://doi.org/10.1016/j.neuron.2007.12.026.
63. Schmidt H, Brachtendorf S, Arendt O, Hallermann S, Ishiyama S, Bornschein G, et al. Nanodomain coupling at an excitatory cortical synapse. Curr Biol. 2013;23:244–9. https://doi.org/10.1016/j.cub.2012.12.007.
64. Arai I, Jonas P. Nanodomain coupling explains Ca(2)(+) independence of transmitter release time course at a fast central synapse. elife. 2014;3 https://doi.org/10.7554/eLife.04057.
65. Lacinova L. Voltage-dependent calcium channels. Gen Physiol Biophys. 2005;24(Suppl 1):1–78.
66. Gao S, Yao X, Yan N. Structure of human Ca(v)2.2 channel blocked by the painkiller ziconotide. Nature. 2021;596:143–7. https://doi.org/10.1038/s41586-021-03699-6.
67. Zhao Y, Huang G, Wu Q, Wu K, Li R, Lei J, et al. Cryo-EM structures of apo and antagonist-bound human Ca(v)3.1. Nature. 2019;576:492–7. https://doi.org/10.1038/s41586-019-1801-3.
68. Wu J, Yan Z, Li Z, Yan C, Lu S, Dong M, et al. Structure of the voltage-gated calcium channel Cav1.1 complex. Science. 2015;350:aad2395. https://doi.org/10.1126/science.aad2395.
69. Gao S, Yan N. Structural basis of the modulation of the voltage-gated calcium ion channel Ca(v) 1.1 by Dihydropyridine compounds*. Angew Chem Int Ed Engl. 2021;60:3131–7. https://doi.org/10.1002/anie.202011793.
70. Zhao Y, Huang G, Wu J, Wu Q, Gao S, Yan Z, et al. Molecular basis for ligand modulation of a mammalian voltage-gated Ca(2+) channel. Cell. 2019;177:1495–506 e12. https://doi.org/10.1016/j.cell.2019.04.043.
71. Wu J, Yan Z, Li Z, Qian X, Lu S, Dong M, et al. Structure of the voltage-gated calcium channel Ca(v)1.1 at 3.6 A resolution. Nature. 2016;537:191–6. https://doi.org/10.1038/nature19321.
72. Catterall WA, Perez-Reyes E, Snutch TP, Striessnig J, International Union of Pharmacology. XLVIII. Nomenclature and structure-function relationships of voltage-gated calcium channels. Pharmacol Rev. 2005;57:411–25. https://doi.org/10.1124/pr.57.4.5.
73. Randall A, Tsien RW. Pharmacological dissection of multiple types of Ca2+ channel currents in rat cerebellar granule neurons. J Neurosci. 1995;15:2995–3012. https://doi.org/10.1523/JNEUROSCI.15-04-02995.1995.
74. Birnbaumer L, Campbell KP, Catterall WA, Harpold MM, Hofmann F, Horne WA, et al. The naming of voltage-gated calcium channels. Neuron. 1994;13:505–6. https://doi.org/10.1016/0896-6273(94)90021-3.
75. Ertel EA, Campbell KP, Harpold MM, Hofmann F, Mori Y, Perez-Reyes E, et al. Nomenclature of voltage-gated calcium channels. Neuron. 2000;25:533–5. https://doi.org/10.1016/s0896-6273(00)81057-0.
76. Wheeler DB, Randall A, Tsien RW. Roles of N-type and Q-type Ca2+ channels in supporting hippocampal synaptic transmission. Science. 1994;264:107–11. https://doi.org/10.1126/science.7832825.

77. Wu LG, Saggau P. Pharmacological identification of two types of presynaptic voltage-dependent calcium channels at CA3-CA1 synapses of the hippocampus. J Neurosci. 1994;14:5613–22. https://doi.org/10.1523/JNEUROSCI.14-09-05613.1994.
78. Takahashi T, Momiyama A. Different types of calcium channels mediate central synaptic transmission. Nature. 1993;366:156–8. https://doi.org/10.1038/366156a0.
79. Luebke JI, Dunlap K, Turner TJ. Multiple calcium channel types control glutamatergic synaptic transmission in the hippocampus. Neuron. 1993;11:895–902. https://doi.org/10.1016/0896-6273(93)90119-c.
80. Turner TJ, Adams ME, Dunlap K. Multiple Ca2+ channel types coexist to regulate synaptosomal neurotransmitter release. Proc Natl Acad Sci U S A. 1993;90:9518–22. https://doi.org/10.1073/pnas.90.20.9518.
81. Uchitel OD, Protti DA, Sanchez V, Cherksey BD, Sugimori M, Llinas R. P-type voltage-dependent calcium channel mediates presynaptic calcium influx and transmitter release in mammalian synapses. Proc Natl Acad Sci U S A. 1992;89:3330–3. https://doi.org/10.1073/pnas.89.8.3330.
82. Protti DA, Reisin R, Mackinley TA, Uchitel OD. Calcium channel blockers and transmitter release at the normal human neuromuscular junction. Neurology. 1996;46:1391–6. https://doi.org/10.1212/wnl.46.5.1391.
83. Protti DA, Sanchez VA, Cherksey BD, Sugimori M, Llinas R, Uchitel OD. Mammalian neuromuscular transmission blocked by funnel web toxin. Ann N Y Acad Sci. 1993;681:405–7. https://doi.org/10.1111/j.1749-6632.1993.tb22921.x.
84. Bowersox SS, Miljanich GP, Sugiura Y, Li C, Nadasdi L, Hoffman BB, et al. Differential blockade of voltage-sensitive calcium channels at the mouse neuromuscular junction by novel omega-conopeptides and omega-agatoxin-IVA. J Pharmacol Exp Ther. 1995;273:248–56.
85. Araque A, Clarac F, Buno W. P-type Ca2+ channels mediate excitatory and inhibitory synaptic transmitter release in crayfish muscle. Proc Natl Acad Sci U S A. 1994;91:4224–8. https://doi.org/10.1073/pnas.91.10.4224.
86. Wu LG, Westenbroek RE, Borst JG, Catterall WA, Sakmann B. Calcium channel types with distinct presynaptic localization couple differentially to transmitter release in single calyx-type synapses. J Neurosci. 1999;19:726–36. https://doi.org/10.1523/JNEUROSCI.19-02-00726.1999.
87. Pan ZH, Hu HJ, Perring P, Andrade R. T-type Ca(2+) channels mediate neurotransmitter release in retinal bipolar cells. Neuron. 2001;32:89–98. https://doi.org/10.1016/s0896-6273(01)00454-8.
88. Tachibana M, Okada T, Arimura T, Kobayashi K, Piccolino M. Dihydropyridine-sensitive calcium current mediates neurotransmitter release from bipolar cells of the goldfish retina. J Neurosci. 1993;13:2898–909. https://doi.org/10.1523/JNEUROSCI.13-07-02898.1993.
89. Mochida S, Westenbroek RE, Yokoyama CT, Itoh K, Catterall WA. Subtype-selective reconstitution of synaptic transmission in sympathetic ganglion neurons by expression of exogenous calcium channels. Proc Natl Acad Sci U S A. 2003;100:2813–8. https://doi.org/10.1073/pnas.262787299.
90. Mueller BD, Merrill SA, Watanabe S, Liu P, Niu LG, Singh A, et al. CaV1 and CaV2 calcium channels mediate the release of distinct pools of synaptic vesicles. elife. 2023;12 https://doi.org/10.7554/eLife.81407.
91. Tong XJ, Lopez-Soto EJ, Li L, Liu H, Nedelcu D, Lipscombe D, et al. Retrograde synaptic inhibition is mediated by alpha-Neurexin binding to the alpha2delta subunits of N-type calcium channels. Neuron. 2017;95:326–40 e5. https://doi.org/10.1016/j.neuron.2017.06.018.
92. Iwasaki S, Momiyama A, Uchitel OD, Takahashi T. Developmental changes in calcium channel types mediating central synaptic transmission. J Neurosci. 2000;20:59–65. https://doi.org/10.1523/JNEUROSCI.20-01-00059.2000.
93. Iwasaki S, Takahashi T. Developmental changes in calcium channel types mediating synaptic transmission in rat auditory brainstem. J Physiol. 1998;509(Pt 2):419–23. https://doi.org/10.1111/j.1469-7793.1998.419bn.x.

94. Urbano FJ, Piedras-Renteria ES, Jun K, Shin HS, Uchitel OD, Tsien RW. Altered properties of quantal neurotransmitter release at endplates of mice lacking P/Q-type Ca2+ channels. Proc Natl Acad Sci U S A. 2003;100:3491–6. https://doi.org/10.1073/pnas.0437991100.
95. Pardo NE, Hajela RK, Atchison WD. Acetylcholine release at neuromuscular junctions of adult tottering mice is controlled by N-(cav2.2) and R-type (cav2.3) but not L-type (cav1.2) Ca2+ channels. J Pharmacol Exp Ther. 2006;319:1009–20. https://doi.org/10.1124/jpet.106.108670.
96. Kaja S, Van de Ven RC, Ferrari MD, Frants RR, Van den Maagdenberg AM, Plomp JJ. Compensatory contribution of Cav2.3 channels to acetylcholine release at the neuromuscular junction of tottering mice. J Neurophysiol. 2006;95:2698–704. https://doi.org/10.1152/jn.01221.2005.
97. Inchauspe CG, Martini FJ, Forsythe ID, Uchitel OD. Functional compensation of P/Q by N-type channels blocks short-term plasticity at the calyx of Held presynaptic terminal. J Neurosci. 2004;24:10379–83. https://doi.org/10.1523/JNEUROSCI.2104-04.2004.
98. Ishikawa T, Kaneko M, Shin HS, Takahashi T. Presynaptic N-type and P/Q-type Ca2+ channels mediating synaptic transmission at the calyx of Held of mice. J Physiol. 2005;568:199–209. https://doi.org/10.1113/jphysiol.2005.089912.
99. Tsukita S, Ishikawa H. Three-dimensional distribution of smooth endoplasmic reticulum in myelinated axons. J Electron Microsc. 1976;25:141–9.
100. Hartter DE, Burton PR, Laveri LA. Distribution and calcium-sequestering ability of smooth endoplasmic reticulum in olfactory axon terminals of frog brain. Neuroscience. 1987;23:371–86. https://doi.org/10.1016/0306-4522(87)90297-1.
101. Lindsey JD, Ellisman MH. The neuronal endomembrane system. I. Direct links between rough endoplasmic reticulum and the cis element of the Golgi apparatus. J Neurosci. 1985;5:3111–23. https://doi.org/10.1523/JNEUROSCI.05-12-03111.1985.
102. McGraw CF, Somlyo AV, Blaustein MP. Localization of calcium in presynaptic nerve terminals. An ultrastructural and electron microprobe analysis. J Cell Biol. 1980;85:228–41. https://doi.org/10.1083/jcb.85.2.228.
103. Singh N, Bartol T, Levine H, Sejnowski T, Nadkarni S. Presynaptic endoplasmic reticulum regulates short-term plasticity in hippocampal synapses. Commun Biol. 2021;4:241. https://doi.org/10.1038/s42003-021-01761-7.
104. Yalcin B, Zhao L, Stofanko M, O'Sullivan NC, Kang ZH, Roost A, et al. Modeling of axonal endoplasmic reticulum network by spastic paraplegia proteins. elife. 2017;6 https://doi.org/10.7554/eLife.23882.
105. Villegas R, Martinez NW, Lillo J, Pihan P, Hernandez D, Twiss JL, et al. Calcium release from intra-axonal endoplasmic reticulum leads to axon degeneration through mitochondrial dysfunction. J Neurosci. 2014;34:7179–89. https://doi.org/10.1523/JNEUROSCI.4784-13.2014.
106. Bouchard R, Pattarini R, Geiger JD. Presence and functional significance of presynaptic ryanodine receptors. Prog Neurobiol. 2003;69:391–418. https://doi.org/10.1016/s0301-0082(03)00053-4.
107. Berridge MJ. The endoplasmic reticulum: a multifunctional signaling organelle. Cell Calcium. 2002;32:235–49. https://doi.org/10.1016/s0143416002001823.
108. Chi X, Gong D, Ren K, Zhou G, Huang G, Lei J, et al. Molecular basis for allosteric regulation of the type 2 ryanodine receptor channel gating by key modulators. Proc Natl Acad Sci U S A. 2019;116:25575–82. https://doi.org/10.1073/pnas.1914451116.
109. Melville Z, Kim K, Clarke OB, Marks AR. High-resolution structure of the membrane-embedded skeletal muscle ryanodine receptor. Structure. 2022;30:172–80 e3. https://doi.org/10.1016/j.str.2021.08.001.
110. Woll KA, Haji-Ghassemi O, Van Petegem F. Pathological conformations of disease mutant Ryanodine Receptors revealed by cryo-EM. Nat Commun. 2021;12:807. https://doi.org/10.1038/s41467-021-21141-3.
111. Yan Z, Bai X, Yan C, Wu J, Li Z, Xie T, et al. Structure of the rabbit ryanodine receptor RyR1 at near-atomic resolution. Nature. 2015;517:50–5. https://doi.org/10.1038/nature14063.

112. Zalk R, Clarke OB, des Georges A, Grassucci RA, Reiken S, Mancia F, et al. Structure of a mammalian ryanodine receptor. Nature. 2015;517:44–9. https://doi.org/10.1038/nature13950.
113. Bai XC, Yan Z, Wu J, Li Z, Yan N. The Central domain of RyR1 is the transducer for long-range allosteric gating of channel opening. Cell Res. 2016;26:995–1006. https://doi.org/10.1038/cr.2016.89.
114. Chirasani VR, Pasek DA, Meissner G. Structural and functional interactions between the Ca(2+)-, ATP-, and caffeine-binding sites of skeletal muscle ryanodine receptor (RyR1). J Biol Chem. 2021;297:101040. https://doi.org/10.1016/j.jbc.2021.101040.
115. Peng W, Shen H, Wu J, Guo W, Pan X, Wang R, et al. Structural basis for the gating mechanism of the type 2 ryanodine receptor RyR2. Science. 2016;354:aah5324. https://doi.org/10.1126/science.aah5324.
116. des Georges A, Clarke OB, Zalk R, Yuan Q, Condon KJ, Grassucci RA, et al. Structural basis for gating and activation of RyR1. Cell. 2016;167:145–57 e17. https://doi.org/10.1016/j.cell.2016.08.075.
117. Samso M, Shen X, Allen PD. Structural characterization of the RyR1-FKBP12 interaction. J Mol Biol. 2006;356:917–27. https://doi.org/10.1016/j.jmb.2005.12.023.
118. Samso M, Wagenknecht T, Allen PD. Internal structure and visualization of transmembrane domains of the RyR1 calcium release channel by cryo-EM. Nat Struct Mol Biol. 2005;12:539–44. https://doi.org/10.1038/nsmb938.
119. Efremov RG, Leitner A, Aebersold R, Raunser S. Architecture and conformational switch mechanism of the ryanodine receptor. Nature. 2015;517:39–43. https://doi.org/10.1038/nature13916.
120. Gong D, Chi X, Wei J, Zhou G, Huang G, Zhang L, et al. Modulation of cardiac ryanodine receptor 2 by calmodulin. Nature. 2019;572:347–51. https://doi.org/10.1038/s41586-019-1377-y.
121. Ogawa H, Kurebayashi N, Yamazawa T, Murayama T. Regulatory mechanisms of ryanodine receptor/Ca(2+) release channel revealed by recent advancements in structural studies. J Muscle Res Cell Motil. 2021;42:291–304. https://doi.org/10.1007/s10974-020-09575-6.
122. Kugler G, Weiss RG, Flucher BE, Grabner M. Structural requirements of the dihydropyridine receptor alpha1S II-III loop for skeletal-type excitation-contraction coupling. J Biol Chem. 2004;279:4721–8. https://doi.org/10.1074/jbc.M307538200.
123. Nakai J, Tanabe T, Konno T, Adams B, Beam KG. Localization in the II-III loop of the dihydropyridine receptor of a sequence critical for excitation-contraction coupling. J Biol Chem. 1998;273:24983–6. https://doi.org/10.1074/jbc.273.39.24983.
124. Takekura H, Paolini C, Franzini-Armstrong C, Kugler G, Grabner M, Flucher BE. Differential contribution of skeletal and cardiac II-III loop sequences to the assembly of dihydropyridine-receptor arrays in skeletal muscle. Mol Biol Cell. 2004;15:5408–19. https://doi.org/10.1091/mbc.e04-05-0414.
125. Protasi F, Takekura H, Wang Y, Chen SR, Meissner G, Allen PD, et al. RYR1 and RYR3 have different roles in the assembly of calcium release units of skeletal muscle. Biophys J. 2000;79:2494–508. https://doi.org/10.1016/S0006-3495(00)76491-5.
126. Yamazawa T, Takeshima H, Sakurai T, Endo M, Iino M. Subtype specificity of the ryanodine receptor for Ca2+ signal amplification in excitation-contraction coupling. EMBO J. 1996;15:6172–7.
127. Rios E. Calcium-induced release of calcium in muscle: 50 years of work and the emerging consensus. J Gen Physiol. 2018;150:521–37. https://doi.org/10.1085/jgp.201711959.
128. Furuichi T, Furutama D, Hakamata Y, Nakai J, Takeshima H, Mikoshiba K. Multiple types of ryanodine receptor/Ca^{2+} release channels are differentially expressed in rabbit brain. J Neurosci. 1994;14:4794–805. https://doi.org/10.1523/JNEUROSCI.14-08-04794.1994.
129. Mori F, Fukaya M, Abe H, Wakabayashi K, Watanabe M. Developmental changes in expression of the three ryanodine receptor mRNAs in the mouse brain. Neurosci Lett. 2000;285:57–60. https://doi.org/10.1016/s0304-3940(00)01046-6.

130. Giannini G, Conti A, Mammarella S, Scrobogna M, Sorrentino V. The ryanodine receptor/calcium channel genes are widely and differentially expressed in murine brain and peripheral tissues. J Cell Biol. 1995;128:893–904. https://doi.org/10.1083/jcb.128.5.893.
131. Nakanishi S, Kuwajima G, Mikoshiba K. Immunohistochemical localization of ryanodine receptors in mouse central nervous system. Neurosci Res. 1992;15:130–42. https://doi.org/10.1016/0168-0102(92)90026-9.
132. Hakamata Y, Nakai J, Takeshima H, Imoto K. Primary structure and distribution of a novel ryanodine receptor/calcium release channel from rabbit brain. FEBS Lett. 1992;312:229–35. https://doi.org/10.1016/0014-5793(92)80941-9.
133. Murayama T, Ogawa Y. Properties of Ryr3 ryanodine receptor isoform in mammalian brain. J Biol Chem. 1996;271:5079–84. https://doi.org/10.1074/jbc.271.9.5079.
134. Lai FA, Dent M, Wickenden C, Xu L, Kumari G, Misra M, et al. Expression of a cardiac Ca(2+)-release channel isoform in mammalian brain. Biochem J. 1992;288(Pt 2):553–64. https://doi.org/10.1042/bj2880553.
135. Wu B, Yamaguchi H, Lai FA, Shen J. Presenilins regulate calcium homeostasis and presynaptic function via ryanodine receptors in hippocampal neurons. Proc Natl Acad Sci U S A. 2013;110:15091–6. https://doi.org/10.1073/pnas.1304171110.
136. Adasme T, Haeger P, Paula-Lima AC, Espinoza I, Casas-Alarcon MM, Carrasco MA, et al. Involvement of ryanodine receptors in neurotrophin-induced hippocampal synaptic plasticity and spatial memory formation. Proc Natl Acad Sci U S A. 2011;108:3029–34. https://doi.org/10.1073/pnas.1013580108.
137. Del Prete D, Checler F, Chami M. Ryanodine receptors: physiological function and deregulation in Alzheimer disease. Mol Neurodegener. 2014;9:21. https://doi.org/10.1186/1750-1326-9-21.
138. De Crescenzo V, Fogarty KE, Zhuge R, Tuft RA, Lifshitz LM, Carmichael J, et al. Dihydropyridine receptors and type 1 ryanodine receptors constitute the molecular machinery for voltage-induced Ca^{2+} release in nerve terminals. J Neurosci. 2006;26:7565–74. https://doi.org/10.1523/JNEUROSCI.1512-06.2006.
139. Velazquez-Marrero C, Custer EE, Marrero H, Ortiz-Miranda S, Lemos JR. Voltage-induced Ca(2+) release by ryanodine receptors causes neuropeptide secretion from nerve terminals. J Neuroendocrinol. 2020;32:e12840. https://doi.org/10.1111/jne.12840.
140. Kim S, Yun HM, Baik JH, Chung KC, Nah SY, Rhim H. Functional interaction of neuronal Cav1.3 L-type calcium channel with ryanodine receptor type 2 in the rat hippocampus. J Biol Chem. 2007;282:32877–89. https://doi.org/10.1074/jbc.M701418200.
141. Llano I, Gonzalez J, Caputo C, Lai FA, Blayney LM, Tan YP, et al. Presynaptic calcium stores underlie large-amplitude miniature IPSCs and spontaneous calcium transients. Nat Neurosci. 2000;3:1256–65. https://doi.org/10.1038/81781.
142. Sutko JL, Airey JA, Welch W, Ruest L. The pharmacology of ryanodine and related compounds. Pharmacol Rev. 1997;49:53–98.
143. Sharma G, Vijayaraghavan S. Modulation of presynaptic store calcium induces release of glutamate and postsynaptic firing. Neuron. 2003;38:929–39. https://doi.org/10.1016/s0896-6273(03)00322-2.
144. Liu Q, Chen B, Yankova M, Morest DK, Maryon E, Hand AR, et al. Presynaptic ryanodine receptors are required for normal quantal size at the *Caenorhabditis elegans* neuromuscular junction. J Neurosci. 2005;25:6745–54. https://doi.org/10.1523/JNEUROSCI.1730-05.2005.
145. Chen B, Liu P, Hujber EJ, Li Y, Jorgensen EM, Wang ZW. AIP limits neurotransmitter release by inhibiting calcium bursts from the ryanodine receptor. Nat Commun. 2017;8:1380. https://doi.org/10.1038/s41467-017-01704-z.
146. Galante M, Marty A. Presynaptic ryanodine-sensitive calcium stores contribute to evoked neurotransmitter release at the basket cell-Purkinje cell synapse. J Neurosci. 2003;23:11229–34. https://doi.org/10.1523/JNEUROSCI.23-35-11229.2003.

147. Emptage NJ, Reid CA, Fine A. Calcium stores in hippocampal synaptic boutons mediate short-term plasticity, store-operated Ca^{2+} entry, and spontaneous transmitter release. Neuron. 2001;29:197–208. https://doi.org/10.1016/s0896-6273(01)00190-8.
148. Shimizu H, Fukaya M, Yamasaki M, Watanabe M, Manabe T, Kamiya H. Use-dependent amplification of presynaptic Ca2+ signaling by axonal ryanodine receptors at the hippocampal mossy fiber synapse. Proc Natl Acad Sci U S A. 2008;105:11998–2003. https://doi.org/10.1073/pnas.0802175105.
149. Unni VK, Zakharenko SS, Zablow L, DeCostanzo AJ, Siegelbaum SA. Calcium release from presynaptic ryanodine-sensitive stores is required for long-term depression at hippocampal CA3-CA3 pyramidal neuron synapses. J Neurosci. 2004;24:9612–22. https://doi.org/10.1523/JNEUROSCI.5583-03.2004.
150. Narita K, Akita T, Hachisuka J, Huang S, Ochi K, Kuba K. Functional coupling of Ca(2+) channels to ryanodine receptors at presynaptic terminals. Amplification of exocytosis and plasticity. J Gen Physiol. 2000;115:519–32. https://doi.org/10.1085/jgp.115.4.519.
151. De Crescenzo V, ZhuGe R, Velazquez-Marrero C, Lifshitz LM, Custer E, Carmichael J, et al. Ca2+ syntillas, miniature Ca2+ release events in terminals of hypothalamic neurons, are increased in frequency by depolarization in the absence of Ca2+ influx. J Neurosci. 2004;24:1226–35. https://doi.org/10.1523/JNEUROSCI.4286-03.2004.
152. Zhang C, Wu B, Beglopoulos V, Wines-Samuelson M, Zhang D, Dragatsis I, et al. Presenilins are essential for regulating neurotransmitter release. Nature. 2009;460:632–6. https://doi.org/10.1038/nature08177.
153. Kuijpers M, Kochlamazashvili G, Stumpf A, Puchkov D, Swaminathan A, Lucht MT, et al. Neuronal autophagy regulates presynaptic neurotransmission by controlling the axonal endoplasmic reticulum. Neuron. 2021;109:299–313 e9. https://doi.org/10.1016/j.neuron.2020.10.005.
154. Bardo S, Robertson B, Stephens GJ. Presynaptic internal Ca2+ stores contribute to inhibitory neurotransmitter release onto mouse cerebellar Purkinje cells. Br J Pharmacol. 2002;137:529–37. https://doi.org/10.1038/sj.bjp.0704901.
155. Carter AG, Vogt KE, Foster KA, Regehr WG. Assessing the role of calcium-induced calcium release in short-term presynaptic plasticity at excitatory central synapses. J Neurosci. 2002;22:21–8. https://doi.org/10.1523/JNEUROSCI.22-01-00021.2002.
156. Lim R, Oleskevich S, Few AP, Leao RN, Walmsley B. Glycinergic mIPSCs in mouse and rat brainstem auditory nuclei: modulation by ruthenium red and the role of calcium stores. J Physiol. 2003;546:691–9. https://doi.org/10.1113/jphysiol.2002.035071.
157. Savic N, Sciancalepore M. Intracellular calcium stores modulate miniature GABA-mediated synaptic currents in neonatal rat hippocampal neurons. Eur J Neurosci. 1998;10:3379–86. https://doi.org/10.1046/j.1460-9568.1998.00342.x.
158. Simkus CR, Stricker C. The contribution of intracellular calcium stores to mEPSCs recorded in layer II neurones of rat barrel cortex. J Physiol. 2002;545:521–35. https://doi.org/10.1113/jphysiol.2002.022103.
159. Laughlin SB. Energy as a constraint on the coding and processing of sensory information. Curr Opin Neurobiol. 2001;11:475–80. https://doi.org/10.1016/s0959-4388(00)00237-3.
160. Rizzuto R, Duchen MR, Pozzan T. Flirting in little space: the ER/mitochondria Ca2+ liaison. Sci STKE. 2004;2004:re1. https://doi.org/10.1126/stke.2152004re1.
161. Colegrove SL, Albrecht MA, Friel DD. Dissection of mitochondrial Ca2+ uptake and release fluxes in situ after depolarization-evoked [Ca2+](i) elevations in sympathetic neurons. J Gen Physiol. 2000;115:351–70. https://doi.org/10.1085/jgp.115.3.351.
162. David G, Barrett JN, Barrett EF. Evidence that mitochondria buffer physiological Ca2+ loads in lizard motor nerve terminals. J Physiol. 1998;509(Pt 1):59–65. https://doi.org/10.1111/j.1469-7793.1998.059bo.x.
163. Billups B, Forsythe ID. Presynaptic mitochondrial calcium sequestration influences transmission at mammalian central synapses. J Neurosci. 2002;22:5840–7. https://doi.org/10.1523/JNEUROSCI.22-14-05840.2002.

164. Talbot JD, David G, Barrett EF. Inhibition of mitochondrial Ca2+ uptake affects phasic release from motor terminals differently depending on external [Ca2+]. J Neurophysiol. 2003;90:491–502. https://doi.org/10.1152/jn.00012.2003.
165. Tang Y, Zucker RS. Mitochondrial involvement in post-tetanic potentiation of synaptic transmission. Neuron. 1997;18:483–91. https://doi.org/10.1016/s0896-6273(00)81248-9.
166. Saitoe M, Schwarz TL, Umbach JA, Gundersen CB, Kidokoro Y. Absence of junctional glutamate receptor clusters in *Drosophila* mutants lacking spontaneous transmitter release. Science. 2001;293:514–7. https://doi.org/10.1126/science.1061270.
167. Barria A, Malinow R. Subunit-specific NMDA receptor trafficking to synapses. Neuron. 2002;35:345–53. https://doi.org/10.1016/s0896-6273(02)00776-6.
168. Sutton MA, Wall NR, Aakalu GN, Schuman EM. Regulation of dendritic protein synthesis by miniature synaptic events. Science. 2004;304:1979–83. https://doi.org/10.1126/science.1096202.
169. Sutton MA, Ito HT, Cressy P, Kempf C, Woo JC, Schuman EM. Miniature neurotransmission stabilizes synaptic function via tonic suppression of local dendritic protein synthesis. Cell. 2006;125:785–99. https://doi.org/10.1016/j.cell.2006.03.040.
170. McKinney RA, Capogna M, Durr R, Gahwiler BH, Thompson SM. Miniature synaptic events maintain dendritic spines via AMPA receptor activation. Nat Neurosci. 1999;2:44–9. https://doi.org/10.1038/4548.
171. Carter AG, Regehr WG. Quantal events shape cerebellar interneuron firing. Nat Neurosci. 2002;5:1309–18. https://doi.org/10.1038/nn970.
172. Sara Y, Virmani T, Deak F, Liu X, Kavalali ET. An isolated pool of vesicles recycles at rest and drives spontaneous neurotransmission. Neuron. 2005;45:563–73. https://doi.org/10.1016/j.neuron.2004.12.056.
173. Geppert M, Goda Y, Hammer RE, Li C, Rosahl TW, Stevens CF, et al. Synaptotagmin I: a major Ca^{2+} sensor for transmitter release at a central synapse. Cell. 1994;79:717–27. https://doi.org/10.1016/0092-8674(94)90556-8.
174. Pang ZP, Sun J, Rizo J, Maximov A, Sudhof TC. Genetic analysis of synaptotagmin 2 in spontaneous and Ca2+−triggered neurotransmitter release. EMBO J. 2006;25:2039–50. https://doi.org/10.1038/sj.emboj.7601103.
175. Maximov A, Shin OH, Liu X, Sudhof TC. Synaptotagmin-12, a synaptic vesicle phosphoprotein that modulates spontaneous neurotransmitter release. J Cell Biol. 2007;176:113–24. https://doi.org/10.1083/jcb.200607021.
176. Katz E, Ferro PA, Cherksey BD, Sugimori M, Llinas R, Uchitel OD. Effects of Ca^{2+} channel blockers on transmitter release and presynaptic currents at the frog neuromuscular junction. J Physiol. 1995;486(Pt 3):695–706. https://doi.org/10.1113/jphysiol.1995.sp020845.
177. Bao J, Li JJ, Perl ER. Differences in Ca2+ channels governing generation of miniature and evoked excitatory synaptic currents in spinal laminae I and II. J Neurosci. 1998;18:8740–50. https://doi.org/10.1523/JNEUROSCI.18-21-08740.1998.
178. Losavio A, Muchnik S. Spontaneous acetylcholine release in mammalian neuromuscular junctions. Am J Phys. 1997;273:C1835–41. https://doi.org/10.1152/ajpcell.1997.273.6.C1835.
179. Schoch S, Deak F, Konigstorfer A, Mozhayeva M, Sara Y, Sudhof TC, et al. SNARE function analyzed in synaptobrevin/VAMP knockout mice. Science. 2001;294:1117–22. https://doi.org/10.1126/science.1064335.
180. Washbourne P, Thompson PM, Carta M, Costa ET, Mathews JR, Lopez-Bendito G, et al. Genetic ablation of the t-SNARE SNAP-25 distinguishes mechanisms of neuroexocytosis. Nat Neurosci. 2002;5:19–26. https://doi.org/10.1038/nn783.
181. Littleton JT, Stern M, Schulze K, Perin M, Bellen HJ. Mutational analysis of Drosophila synaptotagmin demonstrates its essential role in Ca(2+)-activated neurotransmitter release. Cell. 1993;74:1125–34. https://doi.org/10.1016/0092-8674(93)90733-7.
182. Rosenmund C, Stevens CF. Definition of the readily releasable pool of vesicles at hippocampal synapses. Neuron. 1996;16:1197–207. https://doi.org/10.1016/s0896-6273(00)80146-4.

183. Sudhof TC. The synaptic vesicle cycle: a cascade of protein-protein interactions. Nature. 1995;375:645–53. https://doi.org/10.1038/375645a0.
184. Capogna M, Gahwiler BH, Thompson SM. Presynaptic inhibition of calcium-dependent and -independent release elicited with ionomycin, gadolinium, and alpha-latrotoxin in the hippocampus. J Neurophysiol. 1996;75:2017–28. https://doi.org/10.1152/jn.1996.75.5.2017.
185. Richmond JE, Davis WS, Jorgensen EM. UNC-13 is required for synaptic vesicle fusion in *C. elegans*. Nat Neurosci. 1999;2:959–64. https://doi.org/10.1038/14755.
186. Han MH, Kawasaki A, Wei JY, Barnstable CJ. Miniature postsynaptic currents depend on Ca2+ released from internal stores via PLC/IP3 pathway. Neuroreport. 2001;12:2203–7. https://doi.org/10.1097/00001756-200107200-00032.
187. Hajos N, Katona I, Naiem SS, MacKie K, Ledent C, Mody I, et al. Cannabinoids inhibit hippocampal GABAergic transmission and network oscillations. Eur J Neurosci. 2000;12:3239–49. https://doi.org/10.1046/j.1460-9568.2000.00217.x.
188. Silinsky EM. On the mechanism by which adenosine receptor activation inhibits the release of acetylcholine from motor nerve endings. J Physiol. 1984;346:243–56. https://doi.org/10.1113/jphysiol.1984.sp015019.
189. Scanziani M, Capogna M, Gahwiler BH, Thompson SM. Presynaptic inhibition of miniature excitatory synaptic currents by baclofen and adenosine in the hippocampus. Neuron. 1992;9:919–27. https://doi.org/10.1016/0896-6273(92)90244-8.
190. Scholz KP, Miller RJ. Inhibition of quantal transmitter release in the absence of calcium influx by a G protein-linked adenosine receptor at hippocampal synapses. Neuron. 1992;8:1139–50. https://doi.org/10.1016/0896-6273(92)90134-y.
191. Fatt P, Katz B. Spontaneous subthreshold activity at motor nerve endings. J Physiol. 1952;117:109–28.
192. Abenavoli A, Forti L, Bossi M, Bergamaschi A, Villa A, Malgaroli A. Multimodal quantal release at individual hippocampal synapses: evidence for no lateral inhibition. J Neurosci. 2002;22:6336–46. https://doi.org/10.1523/JNEUROSCI.22-15-06336.2002.
193. Yang YM, Chung JM, Rhim H. Cellular action of cholecystokinin-8S-mediated excitatory effects in the rat periaqueductal gray. Life Sci. 2006;79:1702–11. https://doi.org/10.1016/j.lfs.2006.05.027.
194. Meinrenken CJ, Borst JG, Sakmann B. Local routes revisited: the space and time dependence of the Ca2+ signal for phasic transmitter release at the rat calyx of Held. J Physiol. 2003;547:665–89. https://doi.org/10.1113/jphysiol.2002.032714.
195. Xu J, Wu LG. The decrease in the presynaptic calcium current is a major cause of short-term depression at a calyx-type synapse. Neuron. 2005;46:633–45. https://doi.org/10.1016/j.neuron.2005.03.024.
196. Augustine GJ. How does calcium trigger neurotransmitter release? Curr Opin Neurobiol. 2001;11:320–6. https://doi.org/10.1016/s0959-4388(00)00214-2.

Regulation of Presynaptic Calcium Channels

Pengyu Zong and Lixia Yue

Abstract Voltage-gated calcium channels (VGCCs), especially $Ca_v2.1$ and $Ca_v2.2$, are the major mediators of Ca^{2+} influx at the presynaptic membrane in response to neuron excitation, thereby exerting a predominant control on synaptic transmission. To guarantee the timely and precise release of neurotransmitters at synapses, the activity of presynaptic VGCCs is tightly regulated by a variety of factors, including auxiliary subunits, membrane potential, G protein-coupled receptors (GPCRs), calmodulin (CaM), Ca^{2+}-binding proteins (CaBP), protein kinases, various interacting proteins, alternative splicing events, and genetic variations.

Keywords Voltage-gated Ca^{2+} channel · Calmodulin · G protein-coupled receptor · GPCR · Phosphatidylinositol 4,5-bisphosphate · PIP_2 · Ca^{2+}-binding protein · CaBP · Protein kinase · Alternative splicing · Channelopathy

1 Introduction

Ca^{2+} influx through the presynaptic membrane is required for neurotransmitter release [1] and critical for strengthening presynaptic plasticity [2]. A variety of Ca^{2+}-permeable ion channels have been identified in the presynaptic plasma membrane, including N-methyl-D-aspartate (NMDA) glutamate receptors [3], kainate glutamate receptors [4], transient receptor potential (TRP) channels [5], and voltage-gated Ca^{2+} channels (VGCCs) [6]. Interestingly, in some primitive invertebrates, apparent sodium channels at presynaptic sites are actually permeable to Ca^{2+} [7]. Among all these Ca^{2+}-permeable channels, Ca^{2+} influx mediated by VGCCs is indispensable for the most fundamental and important function of the presynaptic

P. Zong · L. Yue (✉)
Department of Cell Biology, Calhoun Cardiology Center, University of Connecticut School of Medicine, Farmington, CT, USA
e-mail: lyue@uchc.edu

Z.-W. Wang (ed.), *Molecular Mechanisms of Neurotransmitter Release*,
Advances in Neurobiology 33, https://doi.org/10.1007/978-3-031-34229-5_7

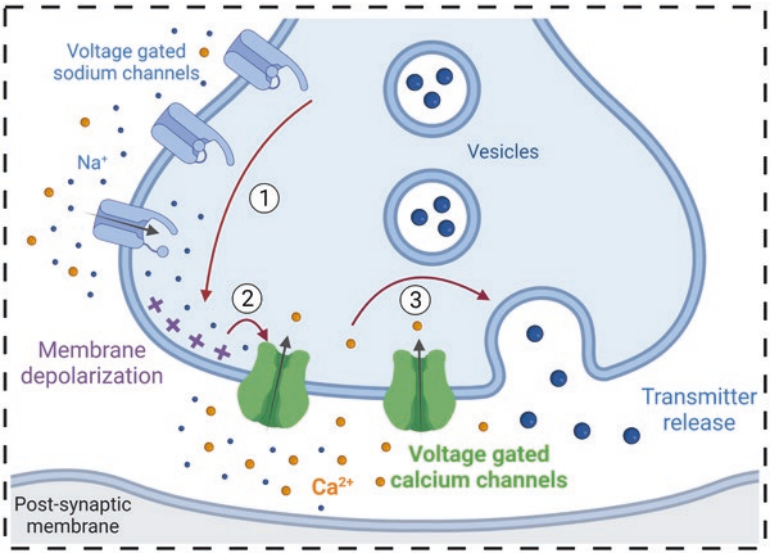

Fig. 1 VGCCs and synaptic transmission. There are three key steps for neurotransmitter release at presynaptic membrane. *Step 1*: The action potential following neuron excitation is transmitted to the presynaptic membrane by voltage-gate sodium channels. *Step 2*: The sodium influx depolarizes the presynaptic membrane, which leads to the activation of VGCCs and subsequent Ca^{2+} influx into the axon terminal. *Step 3*: Increase of intracellular Ca^{2+} triggers neurotransmitter release from the vesicles

membrane: release of neurotransmitters [1] (Fig. 1). The regulation of VGCCs at presynaptic membranes has been extensively studied. In this chapter, we focus on reviewing and discussing studies on the regulation of presynaptic VGCCs.

2 The Discovery History of VGCCs

The physiological function of Ca^{2+} was first discovered in 1883 by Ringer, who found that the Ca^{2+} ion in the blood was indispensable for cardiac contraction [8]. The crucial role of Ca^{2+} in mediating neurotransmitter release in the nervous system was first documented by Katz and Miledi [9] in 1967. In the same year, Reuter recorded Ca^{2+} currents in Purkinje cells from the heart [10]. The study of Ca^{2+} channels got a boost in 1970s thanks to the discovery and development of various Ca^{2+} channel blockers, most notably dihydropyridines (DHPs). In 1982, one century after the first discovery of the physiological role of Ca^{2+} in cellular functions, Fenwick succeeded in recording single-channel Ca^{2+} currents in bovine chromaffin cells, confirming the presence of Ca^{2+} channels [11]. The neuronal Ca^{2+} channels were demonstrated in 1984 when Carbone recorded low voltage-activated Ca^{2+} currents in the dorsal root ganglion cells (DRGs) of rats and chickens [12]. Ca^{2+} currents

recorded in DRGs were later classified into several types based on their biophysical and pharmacological characteristics.

In 1985, Fedulova found that there are two different types of Ca^{2+} currents in neonatal rat DRGs, one is large and long-lasting activated by strong depolarization and the other is tiny and transient activated by weak depolarization [13]. Thus, the former was named the L-type Ca^{2+} channel and the latter was named the T-type Ca^{2+} channel. In the same year, Nowycky demonstrated a third type of Ca^{2+} current in chicken DRGs, characterized by relief of inactivation at a lower (more negative) membrane potential compared to the L-type, but with activation by stronger depolarization compared to the T-type [14, 15]. The distinctive properties of this third type of Ca^{2+} channel led to the name of the N-type (neither L nor T) [14]. The N-type Ca^{2+} channel appears to be predominately expressed in neuronal cells (N) [16]. In 1987, ω-conotoxin GVIA, a toxin from the marine snail *Conus geographus*, was identified as a specific blocker for N-type Ca^{2+} channels [16, 17]. In 1989, Llinas observed a new type of Ca^{2+} current in cerebellar Purkinje cells, which could not be blocked by either DHPs or ω-conotoxin GVIA and was named the P-type because of its first discovery in the Purkinje cells. In 1992, a toxin from the American funnel web spider, ω-agatoxin IVA, was found to specifically block the P-type Ca^{2+} current [18]. In 1995, Pearson and Randfall observed another type of Ca^{2+} current in rat cerebellar granule cells, which could be inhibited by the P-type current blocker ω-agatoxin IVA, but its kinetics was different from that of the P-type [19, 20]. This new current was named the Q-type, although it was later found that the P-type and the Q-type are from two different isoforms of the same channel ($Ca_v2.2$) [21]. In the same study, Randfall also identified a novel type of Ca^{2+} current resistant to all the available Ca^{2+} channel blockers at that time, which was named the R-type [20]. Later, a toxin from the hair spider *Hysterocrates gigas*, SNX-482, was found to be a selective inhibitor of the R-type Ca^{2+} channel [22].

Based on the membrane potentials required for their activation, VGCCs are divided into two classes, high-voltage activated (HVA) and low-voltage activated (LVA) [23] channels (Fig. 2a). HVA channels, including the L-type, N-type, P/Q--type, and R-type, require strong depolarization for activation, whereas LVA channels, including only the T-type, can be activated at less depolarized membrane voltages [23]. The LVA channels typically have a small single-channel conductance (8–12 pS) [24, 25], whereas the HVA channels generally display larger single-channel conductance (15–25 pS) [26, 27]. In 2000, a nomenclature system for VGCCs was introduced based on the discovery times of the pore-forming subunit genes and sequence homology (see details below) [28]. The L-type VGCCs were named Ca_v1, the T-type VGCCs Ca_v3, and the non-L- and non-T-type VGCCs Ca_v2 (Fig. 2a) [29].

L-type Ca^{2+} channels are well known for their roles in regulating muscle (skeletal, smooth, and cardiac) contraction, gene expression, and hormone secretion [30]. Some members of the L-type Ca^{2+} channels are also involved in tonic and slow neurotransmitter release from presynaptic sites in the auditory [31] and visual systems [32] and the release of catecholamine from chromaffin cells [33]. N-type and P/Q-type Ca^{2+} channels are critical to fast synaptic transmission and presynaptic

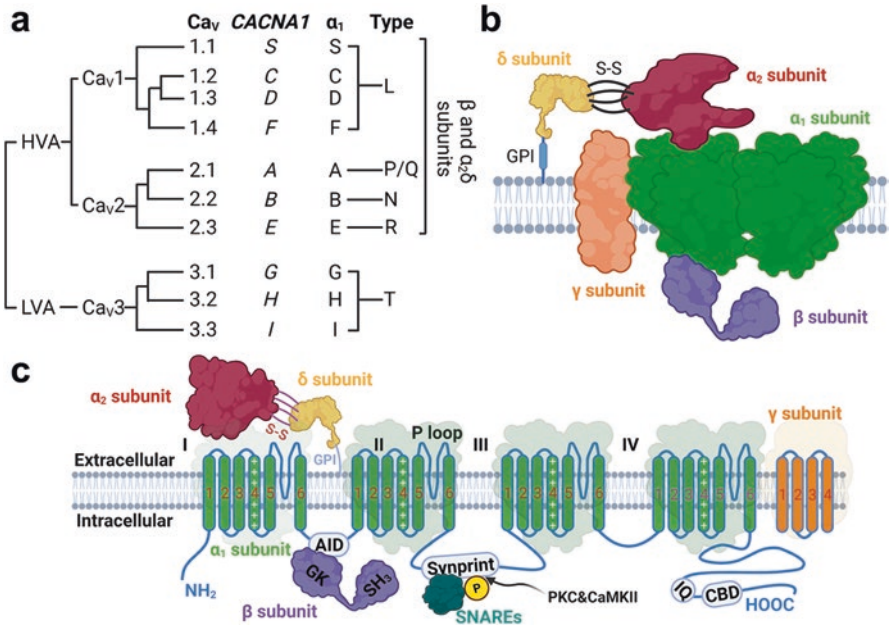

Fig. 2 Classification and compositions of VGCCs. (**a**) Classification and dendrogram of VGCCs based on the α_1 subunits. VGCCs are divided into high-voltage activated (HVA) and low-voltage activated (LVA) groups. The former is further divided into two families (Ca_v1 and Ca_v2), whereas the latter has only one family (Ca_v3). The VGCCs were also given other names based on either their biophysical and pharmacological properties (L-type, P/Q-type, N-type, R-type, and T-type) or the tissues where they were first identified (S/skeletal; C/cardiac) and the order of their discoveries (A, B, D, E, F, G, H, I). (**b**) Diagram of VGCC subunit compositions. (**c**) Diagram of membrane topologies of VGCC subunits and interacting proteins. The α_1 subunit consists of four repeat domains (I–IV) with each having six transmembrane helices (TM1–6). It contains several functionally important domains and motifs, including an alpha interaction domain (AID) that binds to the guanylate kinase (GK) and Src homology 3 (SH3) domains of the β subunit, a synprint motif that may bind to a variety of active zone proteins and allow phosphorylation by protein kinas C (PKC) and Ca^{2+}/calmodulin-dependent protein kinase II (CaMKII), an IQ motif and a CBD motif that bind to calmodulin. The δ subunit is anchored to the cell membrane by a glycosylphosphatidylinositol (GPI), whereas the α_2 subunit associates with the membrane through four disulfate bonds with the δ subunit. The transmembrane γ subunit has four transmembrane helices and interacts with domain IV of the α_1 subunit of the $Ca_v1.1$ family

plasticity in the nervous system [34]. T-type Ca^{2+} channels regulate neuronal excitability and are required for oscillatory activities in excitable cells, including neurons regulating the sleep cycle and cardiac cells serving as pacemakers [35]. Interestingly, some T-type Ca^{2+} channels are also critical to catecholamine release from chromaffin cells [36] and neurotransmitter release from some specific cells in the retina [37], olfactory bulb [38], DRG, and hippocampus [39, 40].

3 Classification of VGCCs

VGCCs translate membrane depolarization into Ca^{2+} entry, thereby influencing virtually almost all aspects of cellular functions, including determining cellular excitability and coupling cellular electrical activities to various fundamental cellular functions such as muscle contractions, neurotransmitter release and hormone secretion, intracellular signaling pathways (e.g., the CaMKII signaling pathway), and gene expression regulation [41]. VGCCs play a critical role in the evolution of organisms [42]. There are 10 VGCCs in mammals, which form a structurally related ion channel superfamily (Fig. 2a). The pore-forming α1 subunits of VGCCs are composed of four homologous but non-identical repeating units (repeats I–IV) (Fig. 2b, c). Each unit resembles the subunit of a typical voltage-gated potassium channel, containing six transmembrane domains (S1–S6) with a P-loop, which contains the selectivity filter between S5 and S6 [23]. An ancestral VGCC might have evolved from two rounds of duplication of either a voltage-gated potassium channel subunit [43, 44] or a bacterial voltage-gated sodium channel subunit [45], which resembles the subunits of mammalian voltage-gated potassium channels in membrane topology, and function as tetramers. The α1 subunits are the primary determinants of different types of VGCCs, and the ten different α1 subunits, including four L-type, three T-type, one P/Q-type, and one R-type [42], can be divided into three structurally and functionally related subfamilies (Fig. 2a).

The three subfamilies designated based on the gene-based novel nomenclature of VGCCs (e.g., $Ca_v1.1$, $Ca_v2.2$, $Ca_v3.3$) depict the discovery history of VGCCs. The purification of DHP binding receptors in the skeletal muscle in 1987 led to the discoveries of several VGCC subunits [46]: α_1, α_2, β, γ, and δ, which were named based on their decreasing size in the PAGE gel. The α_1 subunit was proposed to be the pore-forming subunit as it showed direct binding to DHPs, and the others were proposed to be auxiliary subunits [46]. In 1988, the mRNA of the α_1 subunit of the skeletal L-type VGCC (α_1S) [47] was identified, which was followed by discoveries of the genes encoding the α_1 subunits of the cardiac L-type VGCC (α_1C) in 1989 [48], the P/Q-type VGCC (α_1A) in 1990, the N-type VGCC (α_1B) in 1991, and the R-type (α_1E) VGCC in 1993. In 1992 and 1998, two new L-type VGCCs genes were identified in the brain and named α_1D [49] and α_1F [50, 51]. Finally, the genes for three T-type VGCCs genes were cloned in 1998 and 1999 and named α_1G [24], α_1H [24, 52], and α_1I [53] (Fig. 2a). Thus, except for the first two genes α_1S and α_1C, which were designated based on the organs where they were originally identified, the nomenclature of the other pore-forming α_1 subunits was based on the time order of their discoveries.

In 2000, a new nomenclature system for VGCCs was introduced [28]. Because the gene encoding the skeletal muscle L-type VGCC, α_1S, was first identified (1988) and the VGCCs encoded by α_1C, α_1D, and α_1F share similar biophysical properties with α_1S, L-type VGCCs were named the Ca_v1 family. Based on their discovery sequence, α_1S, α_1C, α_1D, and α_1F were named $Ca_v1.1$, $Ca_v1.2$, $Ca_v1.3$, and $Ca_v1.4$, respectively. Because the P/Q-type, N-type, and R-type VGCCs exhibit similar

biophysical properties, and their genes were found secondary to the L-type, they were named the Ca_v2 family, with α_1A, α_1B, and α_1C named $Ca_v2.1$, $Ca_v2.2$, and $Ca_v2.3$, respectively. The genes for the T-type VGCCs were last identified ($Ca_v3.1$ in 1998) and were given the name the Ca_v3 family, with α_1G, α_1H, and α_1I called $Ca_v3.1$, $Ca_v3.2$, and $Ca_v3.3$, respectively (Fig. 2a).

The phylogenetic tree of Ca^{2+} channels in vertebrates is not well understood as those of voltage-gated potassium channels and sodium channels [43]. The divisions of VGCCs into three families must be very ancient events because orthologs of Cav1, Cav2, and Cav3 genes also exist in the nematode *Caenorhabditis elegans*. Amino acid sequences of vertebrate VGCCs share greater than 70% similarities within each family but less than 40% similarities between families [28] (Fig. 2a). This can explain the distinct similarities and differences in biophysical properties among the VGCCs of the different families. Moreover, Ca_v1 and Ca_v2 share more similarities with each other than with Ca_v3, which has led to the hypothesis that Ca_v1 and Ca_v2 may have evolved from a common ancestral HVA Ca^{2+} channel.

In neurons, Ca_v1 channels are mainly expressed at cell bodies and dendrites, and their activation is required for activity-induced gene expression, which is critical to many brain functions, including learning and memory [30, 54]. $Ca_v1.3$ and $Ca_v1.4$ are also expressed in the presynaptic membrane of cochlear hair cells and photoreceptor cells, respectively, where they support the tonic release of transmitters [31, 32]. Ca_v2 channels are mainly expressed at the presynaptic membrane and regulate synaptic transmission and presynaptic plasticity [34]. Ca_v3 channels are generally expressed at cell bodies and dendrites, although $Ca_v3.2$ and $Ca_v3.3$ may also regulate presynaptic transmitter release [36–40, 55]. Due to their unique LVA property, presynaptic Ca_v3 might serve to regulate neuronal excitability and oscillatory activities [35].

4 Molecular Structure of VGCCs

4.1 Pore-Forming Subunit

VGCCs, voltage-gated Na^+ channels, and voltage-gated K^+ channels share a largely conserved pore domain, which determines ion selectivity. Compared to K^+ channels, the prominent feature of voltage-gated Na^+ channels and VGCCs is a single 190 kDa α_1 pore-forming subunit containing four homologous repeat domains (I–IV), and each domain has six transmembrane helices (S1–S6) [56] (Fig. 2b, c). In contrast, voltage-gated K^+ channels have four separate pore-forming α subunits, and each subunit has six transmembrane helices [42]. The S4 helix is highly positively charged by lysine (K) and arginine (R) residues in typical voltage-gated ion channels [56]. When the positive charges beneath the cell membrane increase (usually caused by sodium influx), the S4 helix in all the four domains will be lifted, which leads to the opening of the channel pore [57]. The four P-loops between S5 and S6 of VGCCs contain the selectivity filter for Ca^{2+} ions (Fig. 2b, c). The central

component of the selectivity filter for Ca^{2+} is four negatively charged amino acid residues (glutamate/E or aspartate/D) [7]. The four residues for Ca_v1 and Ca_v2 are EEEE, while those for Ca_v3 are EEDD. In comparison, the most common selectivity motifs for K^+ and Na^+ channels are GYGD [58] (G/glycine, Y/tyrosine) and DEKA [59] (A/alanine), respectively. The C-tail of VGCCs is located intracellularly and is exceptionally long (>600 amino acid residues) [56], making it an ideal binding target for a variety of interacting proteins including CaM (Fig. 2b, c).

The transmembrane domain is highly conserved between Ca_v1, Ca_v2, and Ca_v3, while the intracellular cytoplasmic linkers and the carboxyl tail exhibit remarkable diversity [23]. There are significant structural differences between HVA (Ca_v1 and Ca_v2) and LVA (Ca_v3) channels. Firstly, the domain I–II linker of HVA channels bears an alpha interaction domain (AID), which is required for the association with the β subunit [56, 57] (Fig. 2b, c), whereas the domain I–II linker of LVA channels does not have it [7]. Secondly, the C-terminal tail of HVA channels has isoleucine-glutamate (IQ) and calmodulin (CaM) binding (CBD) motifs. Both IQ and CBD motifs are required for the regulation by CaM, but they are absent in LVA channels [60] (Fig. 2b, c).

4.2 Auxiliary Subunits

Besides the pore-forming α_1 subunit, VGCCs also have four classical auxiliary subunits, including a 170 kDa extracellular $\alpha_2\delta$ subunit, a 55 kDa intracellular β subunit, and a 33 kDa transmembrane γ subunit [46] (Fig. 2b, c). The $\alpha_2\delta$ and β subunits are encoded by four genes, and there are eight genes (γ1–8) encoding γ subunit-like proteins [61]. Interestingly, only one of the γ subunit-like proteins, the γ1 subunit, associates with a specific VGCC, the $Ca_v1.1$ in skeletal muscle [46, 62–65]. In contrast, CaM binds to all the members in Ca_v1 and Ca_v2 subfamilies, making it a factual fifth subunit [60, 61, 66–68].

The α_2 and δ subunits are encoded by the same gene. They are translated as a single polypeptide and undergo a posttranslational cleavage. The two cleaved polypeptides α_2 and δ connect to each other by four disulfide bonds to form the $\alpha_2\delta$ subunit [69, 70]. A von Willebrand factor domain A (VWA) and two cache domains in $\alpha_2\delta$ associate with extracellular loops of the domain I of the α_1 subunit [56]. Moreover, the δ subunit is tethered to the cell membrane by a glycophosphatidylinositol (GPI) anchor [57]. Interestingly, gabapentin, an agonist originally designed for the GABA receptor, can serve as a specific ligand for the $\alpha_2\delta$ subunit in VGCCs [71] (Fig. 2b, c).

The β subunit contains two major structural domains, a Src homology 3 (SH3) domain and a guanylate kinase (GK) domain [62] (Fig. 2c). Kinase function of the GK domain is lost due to several mutations in the catalytic motif, but the GK domain directly interacts with the AID domain in the domain I–II linker of the α_1 subunit, which is also in the vicinity of the S4 helix of domain II in the α_1 subunit [56]. The γ subunit contains four transmembrane helices and binds to the S4 helix of domain IV in the α_1 subunit [56] (Fig. 2b, c).

5 Regulation of Presynaptic VGCCs

The main presynaptic Ca_v channels involved in transmitter release in the central and peripheral nervous systems are $Ca_v2.1$, $Ca_v2.2$, and $Ca_v2.3$, whereas $Ca_v1.3$ and $Ca_v1.4$ are key to the functioning of the specialized ribbon synapses of the cochlea and retina. T-type VGCCs including $Ca_v3.2$ and $Ca_v3.3$ were also found to be present at the presynaptic sites in entorhinal cortical layer III neurons [40] and mitral cells [55]. To fulfill the remarkably diverse functions of synapses, the activity of presynaptic VGCCs is precisely controlled by a wide range of regulators (Fig. 4).

5.1 Voltage-Dependent Activation and Voltage-Dependent Inactivation (VDI)

Because VGCCs are voltage-gated channels, any factor influencing either the resting membrane potential or membrane depolarization (e.g., sodium channels, potassium channels) may alter their activities (Fig. 3a, b). Compared to those of the HVA group, VGCCs of the LVA group (Ca_v3) are more prone to be influenced by changes in the resting membrane potential because they are easier to be activated or inactivated by small changes in the resting membrane potential [72]. The hyperpolarization-activated cyclic nucleotide-gated (HCN) channels were found to colocalize with the $Ca_v3.2$ channel in pyramidal neurons and inhibit the activation of $Ca_v3.2$, thereby suppressing neurotransmitter release [40]. This inhibitory effect is likely caused by HCN-induced hyperpolarization. Moreover, in mitral cells, $Ca_v3.3$ was also shown to be important for maintaining the basal intracellular Ca^{2+} concentration at the presynaptic membrane, which is important for the asynchronous transmitter release required for smelling [55].

Ca^{2+} is an important intracellular signaling molecule and can be cytotoxic if intracellular Ca^{2+} concentration is too high [41]. Therefore, timely tight control of Ca^{2+} influx is critical for the precise regulation of signaling activation and prevention of Ca^{2+} overload. Similar to some voltage-gated Na^+ and K^+ channels, VGCCs undergo inactivation following their activation by membrane depolarization [34]. This phenomenon is referred to as voltage-dependent inactivation (VDI) (Fig. 3a, b). VDI is an intrinsic property of all the ten α_1 subunits, although different α_1 subunits exhibit different inactivation kinetics. The "ball and chain" and "hinged-lid" mechanisms have been confirmed to underlie the VDI of voltage-gated Na^+ channels [73, 74], while the mechanisms causing VDI of VGCCs are not well understood.

Inhibition of VDI was observed in $Ca_v2.1$ with the mutation of a $G_{\beta\gamma}$ binding site from QXXER to QXXEE [75] ("X" stands for any residue), $Ca_v2.1$ with either V714A or I1819A mutation [76], $Ca_v2.3$ with R378Q mutation [77], and $Ca_v1.2$ with substitution of Ile 829 to a residue with a hydrophobic side chain (e.g., I829A, I829G, or I829V) [78, 79]. Enhanced VDI was demonstrated in $Ca_v2.1$ with T666M mutation [76], $Ca_v1.2$ with substitution of position 823 to residues with smaller side

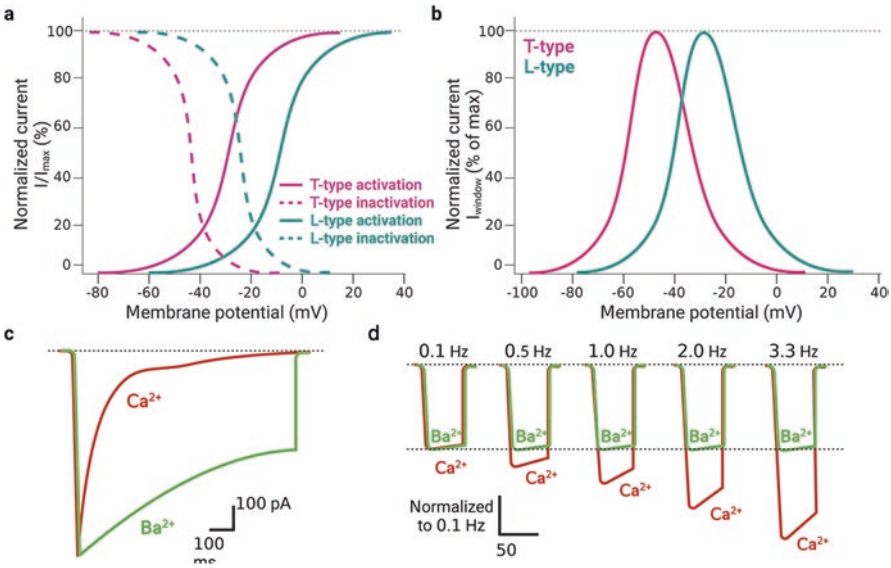

Fig. 3 Voltage-dependent activation and inactivation (VDA/VDI) and Ca^{2+}-dependent inactivation and facilitation (CDI/CDF). (**a**) Voltage-dependent activation (VDA, solid line) and voltage-dependent inactivation (VDI, dash line) of L-type (green) and T-type (pink) Ca_v channels. (**b**) Window currents shown in (**a**) at each voltage were replotted as percentage of mamimal window currents. The window current of VGCC originates from the region of overlap between the activation and inactivation curves [221]. (**c**) Ca^{2+}-dependent inactivation of Ca_v channels. Note the much faster time-dependent inactivation of Ca_v channel when the permeate cations are Ca^{2+} ions in comparison with Ba^{2+} ions. (**d**). Ca^{2+}-dependent facilitation. At higher frequency, Ca^{2+} currents are noticablely bigger than Ba^{2+} currents. ((**a**, **b**) were adapted from Dolphin [72] and (**c**, **d**) were adapted from Zühlke et al. [83])

chains (e.g., F829A, F829F, or F829V) [78], and substitution of $Ca_v1.2$ sequence in domain II or III with that of $Ca_v2.3$ [79–81]. It is noticeable that all these mutations or substitutions are located in either the S6 transmembrane domain or the domain I–II linker region, highlighting the importance of these two areas in mediating the VDI of VGCCs. It has been proposed that membrane depolarization changes the S6 conformation and exposes a docking site for the I–II linker, leading to subsequent docking of the I–II linker onto the bottom of the channel pore, thereby causing the VDI of VGCCs [34].

5.2 *Ca^{2+}-Dependent Inactivation (CDI) and Ca^{2+}-Dependent Facilitation (CDF)*

Besides the precise and rapid regulation of Ca^{2+} influx by VDI, VGCCs are also subjected to Ca^{2+}-dependent inactivation (CDI), another important negative feedback mechanism for controlling Ca^{2+} influx (Fig. 3c). CDI of VGCCs is mediated

by association with calmodulin (CaM) [82, 83]. Adding a competitive inhibitor-like distal carboxyl tail to $Ca_v1.3$ and $Ca_v1.4$ prevents the binding of CaM, thereby inhibiting CDI [84]. The CDI of different α_1 subunits shows different inhibitory kinetics, which may result from different CaM binding affinities caused by their structural differences [60]. As mentioned earlier, the binding of CaM to VGCCs requires both the IQ and CBD motifs in the C-tail of the α_1 subunit, which are absent in the T-type VGCCs [68, 84]. Thus, CDI is an inactivation mechanism for Ca_v1 and Ca_v2 [34].

The CDI in Ca_v1 and Ca_v2 is different in kinetics and requirement of Ca^{2+}. A local increase of Ca^{2+} near the channel pore is enough to trigger a rapid CDI of Ca_v1 [60, 85], whereas the CDI of Ca_v2 is slow and requires a global increase of intracellular Ca^{2+} [86, 87]. This can be explained by a different involvement of high-affinity or low-affinity lobes of CaM. The N-lobe of CaM has low Ca^{2+} affinity, whereas the C-lobe of CaM has high Ca^{2+} affinity [60, 88, 89]. Both the N- and C-lobes are involved in the modulation of fast CDI of Ca_v1. However, only N-lobe is involved in CDI in $Ca_v2.2$ and $Ca_v2.3$, whereas the C-lobe causes rapid facilitation in Ca2.1, which counteracts the CDI induced by the N-lobe [34, 60].

The presence of the CaM binding domain in VGCCs does not guarantee the CDI. $Ca_v1.3$ and $Ca_v1.4$ are not regulated by CDI, albeit they have the CaM binding domain [90, 91]. The CDI of $Ca_v1.3$ was observed in in vitro overexpression systems but not detected in the native auditory hair cells [91] due to the presence of endogenous Ca^{2+}-binding protein 4 (CaBP4), a CaM analog that can compete with CaM in binding to the IQ and CBD motifs [91–93]. The lack of CDI in $Ca_v1.4$ is caused by an autoinhibitory domain [94, 95] in the distal portion of the C-tail, which competes with CaM for the binding to CBD [84]. The attenuation of self-activation by CDI may be necessary for the tonic transmitter release in photoreceptor cells and hair cells [95].

Ca^{2+}-dependent facilitation (CDF) observed in native $Ca_v2.1$ [83, 96] refers to a phenomenon that an increase of intracellular Ca^{2+} enhances the activation and accelerates the recovery of VGCCs (Fig. 3d) [82]. Mutation of the first two residues of the IQ motif in $Ca_v2.1$ to alanine abolishes the CaM-dependent CDF without influencing the CDI, indicating the importance of the IQ motif for CDF [82]. Substitution of the only isoleucine in the IQ motif of Ca_v1 eliminates the CDI but induces the CDF [83]. Unlike CDI, which only needs Ca^{2+} binding to the N-lobe [82], the CaM-dependent CDF requires Ca^{2+} binding to both the N- and C-lobes. It is interesting that CaM can have opposite effects on the same molecule. The likely explanation for this compulsive phenomenon is that Ca^{2+} binds to the N-lobe and the C-lobe of pre-associated CaM sequentially. Since the IQ-interacting C-lobe has a higher affinity to Ca^{2+}, it can respond to the initial local influx of Ca^{2+} to trigger the CDF. With a global rise of cytosolic Ca^{2+}, the CBD-interacting low-affinity N-lobe will begin to induce the CDI [82].

5.3 Regulation by Auxiliary Subunits

5.3.1 $Ca_v\beta$

The auxiliary β subunits are required for plasma membrane expression and proper gating of Ca_v1 and Ca_v2 channels [97] and are crucial for the modulation of HVA channels by various regulators such as G-proteins, kinases, and Ras-related RGK GTPases [98]. All the transcripts of the four β subunits undergo alternative splicing [99]. Different β subunits and even different alternative splicing isoforms of the same subunit could differ substantially in regulatory efficiency [99]. Moreover, posttranslational modifications, such as palmitoylation, can influence the effects of β subunits on the kinetics of VDI [100, 101]. Therefore, the regulation of VGCCs by β subunits exhibits significant diversity [99]. The binding of the GK domain in the β subunits to the AID domain in the α_1 subunits not only changes their gating properties (e.g., negatively shifted voltage-dependent activation, increased rates of VDI and CDI) but also increases their surface expression [102]. This β subunit-induced enhance of HVA surface expression results from increased channel folding and reduced proteolytic degradation as well as masking of an ER retention signal [103–105].

5.3.2 $Ca_v\alpha_2\delta$

The four different $\alpha_2\delta$ subunits ($\alpha_2\delta$-1-4) are all abundantly expressed in the brain, and $\alpha_2\delta$-4 has the highest expression level in the retina [106]. Similar to the β subunits, different $\alpha_2\delta$ subunits have different regulatory efficacy, which is also influenced by alternative splicing [62]. Inside the VWA domain of the α_2 subunit exists a metal-ion-dependent adhesion site (MIDAS), and the regulation of $\alpha_2\delta$ subunits on the α_1 subunits depends on the binding of Ca^{2+} to the MIDAS [56, 107]. By binding to the extracellular loop of domain I in the α_1 subunits, $\alpha_2\delta$ subunits significantly enhance the surface expression of HVA channels [56, 62]. Compared to the β subunits, the influence of $\alpha_2\delta$ subunits on gating properties is much smaller, although the coexpression of $\alpha_2\delta$ subunits with β subunits can produce an additional increase in current intensity [62, 108]. Interestingly, $\alpha_2\delta$ subunits are not considered auxiliary subunits for $Ca_v3.1$, but the coexpression of $\alpha_2\delta$ subunits with α_1G markedly enhances the current density and increases the surface expression of α_1G [109–111]. Moreover, $\alpha_2\delta$ subunits may serve as receptors for thrombospondin, an extracellular protein, and may play an important role in synaptogenesis [112].

5.3.3 $Ca_v\gamma$

As described previously, γ subunits only associate with the $Ca_v1.1$ in the skeletal muscle. Although some γ subunit-like proteins show regulation on current gating properties in in vitro overexpression systems [113], and many isoforms of γ

subunit-like proteins are present in the brain, none of them shows association with VGCCs [61, 63–65]. Therefore, nowadays γ subunits tend to be excluded from the auxiliary subunits of VGCCs. Interestingly, the γ2 subunit may associate with the AMPA glutamate receptor and regulate its gating properties and surface trafficking [114, 115].

5.4 Regulation by G Protein-Coupled Receptors (GPCRs)

VGCCs can be regulated directly by GPCRs or indirectly by various factors that influence the activation of GPCRs. In this session, we mainly focus on the direct regulation of presynaptic VGCCs by GPCRs.

5.4.1 Voltage-Dependent Regulation

Inhibition of Ca_v2 by GPCRs (G_o/G_i), such as GABA-B receptor, opioid receptor, (endocannabinoid-1) CB1 receptor, dopamine receptor, and metabotropic glutamate receptors [116–121], is a critical negative regulatory mechanism of neurotransmitter release. Since this inhibition can be completely reversed by depolarization, it is referred to as the voltage-dependent regulation by GPCRs [23]. Injection of purified $G_{\beta\gamma}$ subunit into presynaptic SCG neurons reduces synaptic transmission, whereas injection of G_α transducin, which may sequester endogenous free $G_{\beta\gamma}$, inhibits the GPCR-induced transmission suppression [122, 123]. When activated, the $G_{\beta\gamma}$ subunit released by G_o/G_i can directly bind to Ca_v2 and inhibit its activation, thereby suppressing synaptic transmission. The GPCRs need to be colocalized with Ca_v2 to allow a rapid binding of the released $G_{\beta\gamma}$ subunit to Ca_v2 [124].

All the three subtypes in the Ca_v2 family can be inhibited by $G_{\beta\gamma}$, although the inhibitory efficacy is not the same due to the different binding affinity with $G_{\beta\gamma}$ [125]. The binding of $G_{\beta\gamma}$ to Ca_v2 did not change their single-channel conductance, but positively shifted the activation curve and slowed down the activation rate [126–128]. Interestingly, $G_{\beta\gamma}$ binding causes a significant change in the gating current, indicating that the voltage-sensing of Ca_v2 is also influenced [129, 130]. $G_{\beta\gamma}$ mainly binds to the QXXER motif of the α_1 subunit, which is located in the AID domain, the same interacting area for the β subunit [131]. As a result, $G_{\beta\gamma}$-mediated inhibition is strongly influenced by β subunits, and the reversal of $G_{\beta\gamma}$-mediated inhibition by depolarization depends on the binding of β subunit to the AID domain [132, 133]. The molecular mechanism of $G_{\beta\gamma}$-induced Ca_v2 inhibition at structural level, however, remains unclear [125].

5.4.2 Voltage-Independent Regulation

GPCRs can also regulate VGCCs by directly associating with VGCCs or indirectly activating intracellular signaling cascades, which is called the voltage-independent regulation of GPCRs [23]. Compared to the instantaneous voltage-dependent regulation, this regulation is slower and cannot be reversed by depolarization.

Regulation by Physical Interaction with GPCRs

Metabotropic glutamate receptors were the first GPCR shown to physically associate with Ca_v2 [134]. Nociception receptor (NOP) was also found to bind to $Ca_v2.2$ and to regulate channel function in the absence of ligands. Although the underlying mechanisms were unclear at the time, it was the first study reporting the regulation of VGCCs by GPCRs through direct physical interaction [135]. Similar regulation was also discovered with several opioid receptors [136, 137]. NOP was later found to promote the internalization of $Ca_v2.2$ through direct physical association [138, 139]. Similarly, the D1 and D2 dopamine receptors may influence the surface trafficking and internalization of $Ca_v2.2$ [121, 140].

Regulation by Presynaptic Phosphatidylinositol 4,5-Bisphosphate (PIP_2)

PIP_2, a phospholipid in the inner leaflet of the plasma membrane, is critical for maintaining the opening state of many channels, including Ca_v2 [141–143]. Interestingly, PIP_2 has dual regulatory effects on Ca_v2. The regulation of Ca_v2 by PIP_2 was first confirmed by the observation that a rundown of $Ca_v2.1$ and $Ca_v2.2$ activities in excised patches was reversed by the application of PIP_2 and was accelerated by a PIP_2 antibody [144, 145]. Interestingly, PIP_2 also inhibits the activation of Ca_v2 in a voltage-dependent manner, and this inhibition can be prevented by PKA-mediated phosphorylation of Ca_v2 [144]. The underlying mechanisms for the dual regulation of PIP_2 on Ca_v2 remain elusive, but the physiological significance of the positive regulation has been observed in several studies. Activation of muscarinic M_1 receptor, a G_q-coupled GPCR, inhibits the activation of $Ca_v2.1$ in neostriatal projection neurons, and this effect can be reversed by inhibition of phospholipase C (PLC) or supplement of PIP_2 intracellularly [146]. It was later shown that G_q-coupled GPCRs facilitate $Ca_v2.1$ inactivation in neurons by PLC-mediated PIP_2 hydrolysis [145]. The regulation of Ca_v2 by PIP_2 suggests that PIP_2 may influence synaptic transmission. A recent study showed that generation of PIP_2 in chromaffin cells by photo-uncaging promoted exocytosis [147], whereas depletion of PIP_2 at the presynaptic membrane by intraterminal loading of anti-PIP_2 antibody suppressed neurotransmitter release from presynaptic terminals at the calyx of Held synapse [148].

5.5 Regulation by Kinases

VGCCs, especially presynaptic Ca_v2, can be phosphorylated by many kinases, including protein kinase C (PKC), Ca^{2+}/calmodulin-dependent protein kinase (CaMKII), and cyclin-dependent-like kinase 5 (CDK5).

PKC phosphorylates Ca_v2 at multiple sites, including the $G_{\beta\gamma}$ binding site in the I–II linker and the SNAP receptor (SNARE) protein binding site in the II–III linker [149–151]. This phosphorylation can prevent the bindings of $G_{\beta\gamma}$ and SNARE proteins to Ca_v2, thereby abolishing their regulation on Ca_v2. PKC activator can suppress the $G_{\beta\gamma}$-mediated inhibition of $Ca_v2.2$ in cultured sympathetic neurons, leading to facilitation of synaptic transmission [152, 153]. SNARE proteins bind to the II–III linker (also known as the "synprint site") and inhibit Ca_v2 activation (see details below). Thus, the inhibition of SNARE proteins on Ca_v2 can be prevented by PKC phosphorylation [149].

CaMKII plays a critical role in regulating gene expression in neurons in response to increased postsynaptic activities [154]. Whether presynaptic CaMKII can induce gene expression in either nuclei or mitochondria remains unclear due to difficulties in distinguishing between presynaptic and postsynaptic CaMKII-induced responses. Similar to PKC, CaMKII is also expressed at the presynaptic plasma membrane and can phosphorylate the synprint site on Ca_v2, which prevents SNARE proteins from binding to the synprint site and relieves their inhibition on Ca_v2 [149, 155, 156].

In comparison to PKC and CaMKII, the regulatory effects of CDK5 on Ca_v2 are controversial. CDK5 can phosphorylate the synprint site in the II–III linker of Ca_v2 and prevent the binding of SNARE proteins [157, 158]. Inhibition of CDK5 using a dominant-negative CDK5 construct enhances $Ca_v2.2$ currents and facilitates synaptic transmission [159]. However, roscovitine, an inhibitor of CDK5, inhibits $Ca_v2.1$ currents and neurotransmitter release [158], which might be due to a non-specific antagonizing effect of roscovitine on $Ca_v2.1$ [158]. Furthermore, another study showed that CDK5 inhibits the presynaptic $Ca_v2.2$ activation and suppresses the vesicular release [160].

5.6 Regulation by Ca^{2+}-Binding Proteins (CaBPs)

As described earlier, CaM binds to the IQ and CBD motifs in Ca_v2 and induces CDI and CDF. Besides CaM, presynaptic VGCCs are also regulated by many other Ca^{2+}-binding proteins (CaBPs), and their regulation on VGCCs is Ca^{2+} dependent [161]. Like CaM, CaBPs have four EF-hands [162]. There are eight members in the CaBP family (CaBP1-8) [162], among which CaBP1, CaBP4, and CaBP5 have been shown to regulate VGCCs. Moreover, bioinformatic analyses have uncovered many CaBP variants, which can further diversify their regulatory effects on VGCCs [163].

CaBP1 is widely expressed in the central nervous system, including the retina and inner ear [164]. A direct binding of CaBP1 to the CBD of $Ca_v2.1$ not only

inhibits channel activation but also prevents the CaM-mediated CDF [165]. Different from the inhibitory effects on $Ca_v2.1$, CaBP1 can produce a positive regulatory effect on $Ca_v1.3$ and $Ca_v1.4$, which could be important for their tonic activation at presynaptic membrane. CaBP1 is densely expressed in the hair cells (presynaptic) of the ribbon synapses in the ear and can counteract the CaM-meditated inhibition on $Ca_v1.3$ [91, 166]. Similarly, CaBP1 was found to be critical for $Ca_v1.4$-mediated presynaptic transmitter release in the retina [167]. Visinin-like protein 2 (VILIP-2), a CaBP1-related protein, binds to both the IQ and CBD motifs in $Ca_v2.1$ [168], producing an opposite effect compared to CaBP1, which is characterized by inhibited channel inactivation [168].

Similar to CaBP1, CaBP4 binds to the CBD and inhibits the CDI of presynaptic $Ca_v1.3$ in hair cells, although this regulation is much weaker than that of CaBP1 [166]. CaBP4 is also expressed at the presynaptic terminal of photoreceptor cells and is required for the development of synapses in the retina [167, 169]. By binding to the CBD of $Ca_v1.4$, CaBP4 negatively shifts the activation curve to promote channel activation, and this effect may be further enhanced by PKC phosphorylation of CaBP4 [167, 169]. CaBP4 also colocalizes with $Ca_v1.2$ in the retina and suppresses its CDI. Moreover, knockout of CaBP5 results in reduced synaptic transmission in the retina [170]. Thus, different CaBPs can have different regulatory effects on VGCCs.

5.7 Regulation by Active Zone Proteins

In the active zone where neurotransmitters are released, the presynaptic VGCCs $Ca_v2.1$, $Ca_v2.2$, and $Ca_v2.3$ form signaling complexes with various proteins to trigger transmitter release upon neuronal firing.

5.7.1 Presynaptic Ca^{2+} Signaling Complex

$Ca_v2.1$ and $Ca_v2.2$ physically interact with SNARE proteins and synaptotagmin, which is required for an almost instantaneous (<200 μs) release of neurotransmitters in response to Ca^{2+} influx at the presynaptic membrane [171]. Syntaxin-1A, SNAP-25, and synaptotagmin can all bind to the synprint site in the domain I–II linker in the α_1 subunits of different Ca_v2 isoforms but with varied affinities [155, 172–176]. The binding of different proteins to the synprint site is regulated by kinases and Ca^{2+} concentrations. The binding of syntaxin-1A and SNAP-25 to the synprint site of VGCCs can be inhibited by PKC or CaMKII phosphorylation of the synprint site [149–151]. While Ca^{2+}-dependent binding of syntaxin-1A to Ca_v2 is maximal at 20 μM Ca^{2+} with decreased binding at both lower and higher Ca^{2+} concentrations [177], the binding of synaptotagmin to the synprint site increases with increasing Ca^{2+} concentrations. Therefore, syntaxin-1A and synaptotagmin compete for the synprint binding site in such a dynamic way that higher Ca^{2+}

concentrations favors the binding of synaptotagmin, whereas lower Ca^{2+} concentrations favors the binding of syntaxin-1A [177].

Not only the association of SNARE proteins with Ca_v2 channels is regulated by Ca^{2+} concentrations, the interacting SNARE proteins can also in turn directly regulate the function of Ca_v2 [6]. Coexpression of syntaxin-1A or SNAP-25 with Ca_v2 inhibits channel activity and enhances the channel's VDI [178–180]. The inhibitory effects of syntaxin-1A and SNAP-25 on Ca_v2 can be abolished by coexpressing SNAP-25 and synaptotagmin in Xenopus oocytes, suggesting that assembly of the SNARE complex might inhibit the binding of syntaxin-1A and SNAP-25 to Ca_v2 [178–180]. This negative regulatory effects of SNARE proteins on Ca_v2 could be an important negative feedback mechanism to ensure precise control of neurotransmitter release [6].

5.7.2 Other Presynaptic Proteins

The unique long and coiled C-tail of the α_1 subunit can interact with many proteins, as indicated by proteomic screening [181]. Rab-interacting molecule (RIM), a presynaptic protein important for exocytosis, was shown to interact with the synprint site [182]. In contrast to the inhibitory effects of SNARE proteins and synaptotagmin, an association of RIM with Ca_v2 increases the channel activity and promotes synaptic transmission [183]. Moreover, RIM can bind to the β subunit and enhance its positive regulation of the channel function [184]. Different from RIM, the binding of another active zone protein, CAST/ERC2, to Ca_v2 serves to inhibit channel function [185]. Moreover, Mint-1 and CASK form a tri-complex with Ca_v2, which increases its surface trafficking, thereby enhancing exocytosis [186].

CaMKII is one of the proteins that can physically associate with the C-tail of α_1 subunits. Interaction of CaMKII with Ca_v2 results in increased channel activities, which is a function independent of its kinase activity [156]. In addition, as described earlier, phosphorylation of the synprint site at the domain II–III linker by CaMKII inhibits the binding of SNARE proteins to Ca_v2, which prevents the inhibition of Ca_v2 by SNARE proteins. Thus, CaMKII can regulate Ca_v2-mediated transmitter release by at least two different mechanisms.

Munc13 is a presynaptic protein that interacts with several active zone proteins, including Ca_v2 [187]. Loss of Munc13 results in reduced presynaptic Ca^{2+} influx [187]. The physical association between Munc13 and Ca_v2 is essential to the proper physiological function of Ca_v2 in transmitter release [187]. Another presynaptic Ca_v2 associating protein is collapsin response mediator protein-2 (CRMP-2), an adopter protein, which is important in neuronal development [188]. The physical association of CRMP-2 with Ca_v2 potentiates Ca_v2 activity and transmitter release [189, 190], whereas disrupting the Ca_v2-CRMP-2 interaction in vivo by a disrupting peptide inhibits the enhanced pathological neurotransmitter release during chronic pain [191].

5.8 *Regulation of Presynaptic VGCCs by Alternative Splicing and RNA Editing*

5.8.1 Regulation by Alternative Splicing

Alternative splicing occurs to both the α_1 and β subunits of VGCCs, which confer VGCCs with diverse functional properties [192]. Therefore, the expression of various splicing isoforms needs to be precisely regulated to furnish VGCCs with proper functional properties at both the temporal and spatial (cell-specific) levels [193]. The alternative splicing of VGCC gene transcripts enables extraordinarily precise control over Ca^{2+} influx at the presynaptic membrane. Here we mainly focus on the alternative splicing of $Ca_v1.3$, $Ca_v1.4$, $Ca_v2.1$, and $Ca_v2.2$, as the role of the Ca_v3 family in presynaptic Ca^{2+} influx is not well understood, and it is difficult to selectively determine the expression of Ca_v3 variants at presynaptic membrane due to its predominant expression at cell bodies and dendrites.

The alternative splicing variants of $Ca_v1.3$ produced by removal of a distal and a proximal regulatory domain in the C-tail exhibit a negative shift of the activation curve and an enhanced CDI [194], whereas the splicing variant with removal of the distal regulatory domain alone shows enhanced channel activity but with a less pronounced effect on CDI [194]. The human retina expresses at least 19 splicing variants of $Ca_v1.4$ [195], and one variant with a C-tail deletion exhibits increased channel activity but enhanced CDI [195].

The Ca_v2 subfamily undergoes more extensive splicing in comparison with Ca_v1. Strikingly, in brain tissue from mouse, rat, and human, alternative splicing of $Ca_v2.1$ occurs in an age- and sex-dependent manner [196]. Insertion of several residues into the domain I–II linker and the C-tail of $Ca_v2.1$ results in an inhibition of the VDI [197]. In another study, a splicing variant produced by combined inclusion and exclusion of exons 43 and 44 in $Ca_v2.1$ exhibits an enhanced CDI [198]. CDF of $Ca_v2.1$ can also be significantly influenced by concerted splicing at an EF-hand-like domain at the C-tail [199]. Some $Ca_v2.1$ splicing variants with changes in the synprint site are no longer sensitive to regulation by SNARE proteins [200]. Moreover, the binding affinity of Ca_v2 for the β subunit can be influenced by alternative splicing in the domain I–II linker [201]. In $Ca_v2.2$, alternative splicing in the S3-S4 regions of domains III and IV not only influences channel properties but also determines the tissue-specific distribution of $Ca_v2.2$ due to tissue-specific alternative splicing patterns [202, 203]. As expected, alternative splicing in the domain II–III linker influences the regulation of $Ca_v2.2$ by SNARE proteins as it contains the synprint site [204, 205]. Furthermore, the splicing of exon 37 can produce a series of effects on $Ca_v2.2$, including changing channel gating properties and altering channel regulation by GPCR [193]. With the advancement of next-generation sequencing technology, many new splicing variants will likely be identified in the future.

5.8.2 Regulation by RNA Editing

Different from alternative splicing, RNA editing does not delete or insert nucleotides in the mRNA. It usually causes changes in a single nucleotide. The mRNA of $Ca_v1.3$ is edited by adenosine deaminase, leading to a modification of the IQ motif, which consequently enhances the CDI and inhibits channel function in neurons of the suprachiasmatic nucleus [206, 207]. Since studies of VGCC RNA editing are still in their infancy, future investigations may provide more insights into RNA editing-related regulations on VGCCs.

5.9 Presynaptic VGCCs Channelopathies

Dysregulation of presynaptic VGCCs caused by genetic variations is associated with a variety of neuronal disorders in humans. Gain-of-function mutations of $Ca_v2.1$, R192Q, and S218L are associated with familial hemiplegic migraine type I (FHM1). The R192Q and S218L mutations cause an increase in the open probability of $Ca_v2.1$ and a negative shift in the voltage-dependent activation [208]. Knock-in mice carrying these mutations exhibit increased Ca^{2+} influx during action potential, leading to enhanced glutamate release at cortical pyramidal neuron synapses. Interestingly, at the calyx Held, S218L-knockin mice show reduced Ca^{2+} influx during action potential due to the reduced peak current of $Ca_v2.1$, but increased Ca^{2+} influx at resting membrane potential caused by a negative shift (~10 mV) of the half-maximal activation voltage [209–211]. These gain-of-function mutations also increase the susceptibility of cortical neurons to the spreading of depolarizations and seizures in mice subjected to traumatic brain injuries [212].

A large genome-wide analysis of schizophrenia has identified that genes encoding α1C, α1I, β2, and Ca_v-interacting proteins such as RIMs are among the disease-associated loci [213]. However, it remains to be determined whether mutations of these genes are related to neuropsychiatric disorders. Moreover, two mutations of the Rab3-interacting molecule 3 (RIM3) gene identified in autism patients, E176A and M259V, partially cancel the suppressing effect of RIM3 on VDI of $Ca_v2.1$ in transfected HEK293 cells [214]. At ribbon synapses in the retina, a mutation of the interacting protein CaBP4 (R216X) makes the protein less effective in enhancing the VDA of long $Ca_v1.4$ variants [167, 215], resulting in stationary night blindness type-2-related visual impairment [216]. Similarly, a loss-of-function mutation of CaBP2 (F164X) results in dysfunction of $Ca_v1.3$, thereby causing an autosomal recessive hearing impairment [217]. Future studies on genetic variations caused dysregulation of VGCCs will further shed light on the link between presynaptic Ca_v channels and nervous system disorders in humans.

6 Perspective

Since the first single-channel current of VGCCs was recorded 40 years ago, our knowledge on the regulation of VGCCs has advanced extensively. Auxiliary subunits, membrane potentials, CaM, GPCRs, protein kinases, active zone proteins, and alternative splicing all contribute to the precise and tight regulation of presynaptic VGCCs (as summarized in Fig. 4). Recently developed techniques and technologies have allowed us to embrace the new knowledge such as the atomic structure of VGCCs including $Ca_v1.1$ and $Ca_v3.1$ [56, 57, 218] obtained by cyro-EM, the

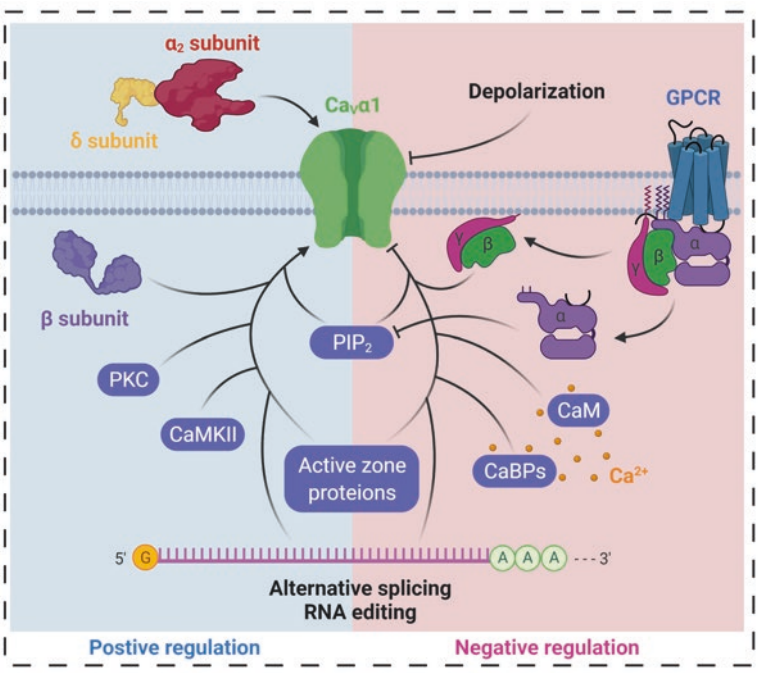

Fig. 4 Summary of regulators for presynaptic VGCCs. All the regulators can be divided into two groups based on their either positive (blue/left side) or negative (red/right side) effects on channel functions. GPCR can have dual regulatory effects. Gi/o activation leads to the release of $G_{\beta\gamma}$ subunit, which can directly inhibit channel activation. Gq activation further activates phospholipase C, which hydrolyzes the phosphatidylinositol 4,5-bisphosphate (PIP_2). PIP_2 is needed for channel opening, but can also inhibit channel activation after membrane depolarization. Some active zone proteins can enhance the activation and surface expression of VGCCs, while other active zone proteins can produce an opposite effect. Some alternative splicing variants of VGCCs exhibit enhanced channel function, while some other variants have reduced function. Membrane depolarization can directly activate VGCCs, but can also cause VDI. CaM binding inactivates VGCCs, which is the major mechanism of CDI. Generally, most of CaBPs inhibit channel function. PKC and CaMKII phosphorylate the binding site on VGCCs for SNARE proteins and prevent their binding, thereby indirectly promoting channel activation. $\alpha_2\delta$ and β subunits not only enhance channel activation but also markedly increase the surface expression of VGCCs

cell-type specific targeting of GPCRs by DART (drugs acutely restricted tethering) [219], and spatial mapping of multiplexed proteins by immune-SABER (immunostaining with signal amplification by exchange reaction) [220]. These advanced techniques and the continuously evolving new technologies will further shape our understanding and shed light on critical questions such as how the organization and regulation of Ca_v channels impact synaptic plasticity in healthy and diseased states.

References

1. Sudhof TC. Calcium control of neurotransmitter release. Cold Spring Harb Perspect Biol. 2012;4:a011353. https://doi.org/10.1101/cshperspect.a011353.
2. Catterall WA, Few AP. Calcium channel regulation and presynaptic plasticity. Neuron. 2008;59:882–901. https://doi.org/10.1016/j.neuron.2008.09.005.
3. Abrahamsson T, Chou CYC, Li SY, Mancino A, Costa RP, Brock JA, et al. Differential regulation of evoked and spontaneous release by presynaptic NMDA receptors. Neuron. 2017;96:839–55.e5. https://doi.org/10.1016/j.neuron.2017.09.030.
4. Lerma J. Roles and rules of kainate receptors in synaptic transmission. Nat Rev Neurosci. 2003;4:481–95. https://doi.org/10.1038/nrn1118.
5. Wu SW, Fenwick AJ, Peters JH. Channeling satiation: a primer on the role of TRP channels in the control of glutamate release from vagal afferent neurons. Physiol Behav. 2014;136:179–84. https://doi.org/10.1016/j.physbeh.2014.09.003.
6. Catterall WA. Structure and regulation of voltage-gated Ca2+ channels. Annu Rev Cell Dev Biol. 2000;16:521–55. https://doi.org/10.1146/annurev.cellbio.16.1.521.
7. Senatore A, Raiss H, Le P. Physiology and evolution of voltage-gated calcium channels in early diverging animal phyla: Cnidaria, Placozoa, Porifera and Ctenophora. Front Physiol. 2016;7:481. https://doi.org/10.3389/fphys.2016.00481.
8. Ringer S. A further contribution regarding the influence of the different constituents of the blood on the contraction of the heart. J Physiol. 1883;4:29–42.3. https://doi.org/10.1113/jphysiol.1883.sp000120.
9. Katz B, Miledi R. A study of synaptic transmission in the absence of nerve impulses. J Physiol. 1967;192:407–36. https://doi.org/10.1113/jphysiol.1967.sp008307.
10. Reuter H. The dependence of slow inward current in Purkinje fibres on the extracellular calcium-concentration. J Physiol. 1967;192:479–92. https://doi.org/10.1113/jphysiol.1967.sp008310.
11. Fenwick EM, Marty A, Neher E. Sodium and calcium channels in bovine chromaffin cells. J Physiol. 1982;331:599–635.
12. Carbone E, Lux HD. A low voltage-activated, fully inactivating Ca channel in vertebrate sensory neurones. Nature. 1984;310:501–2. https://doi.org/10.1038/310501a0.
13. Fedulova SA, Kostyuk PG, Veselovsky NS. Two types of calcium channels in the somatic membrane of new-born rat dorsal root ganglion neurones. J Physiol. 1985;359:431–46. https://doi.org/10.1113/jphysiol.1985.sp015594.
14. Nowycky MC, Fox AP, Tsien RW. Three types of neuronal calcium channel with different calcium agonist sensitivity. Nature. 1985;316:440–3. https://doi.org/10.1038/316440a0.
15. Fox AP, Nowycky MC, Tsien RW. Single-channel recordings of three types of calcium channels in chick sensory neurones. J Physiol. 1987;394:173–200. https://doi.org/10.1113/jphysiol.1987.sp016865.
16. McCleskey EW, Fox AP, Feldman DH, Cruz LJ, Olivera BM, Tsien RW, et al. Omega-conotoxin: direct and persistent blockade of specific types of calcium channels in neurons

but not muscle. Proc Natl Acad Sci U S A. 1987;84:4327–31. https://doi.org/10.1073/pnas.84.12.4327.
17. Hoehn K, Watson TW, MacVicar BA. Multiple types of calcium channels in acutely isolated rat neostriatal neurons. J Neurosci. 1993;13:1244–57. https://doi.org/10.1523/JNEUROSCI.13-03-01244.1993.
18. Mintz IM, Venema VJ, Swiderek KM, Lee TD, Bean BP, Adams ME. P-type calcium channels blocked by the spider toxin omega-Aga-IVA. Nature. 1992;355:827–9. https://doi.org/10.1038/355827a0.
19. Pearson HA, Sutton KG, Scott RH, Dolphin AC. Characterization of Ca2+ channel currents in cultured rat cerebellar granule neurones. J Physiol. 1995;482(Pt 3):493–509. https://doi.org/10.1113/jphysiol.1995.sp020535.
20. Randall A, Tsien RW. Pharmacological dissection of multiple types of Ca2+ channel currents in rat cerebellar granule neurons. J Neurosci. 1995;15:2995–3012. https://doi.org/10.1523/JNEUROSCI.15-04-02995.1995.
21. Richards MW, Leroy J, Pratt WS, Dolphin AC. The HOOK-domain between the SH3 and the GK domains of Cavbeta subunits contains key determinants controlling calcium channel inactivation. Channels (Austin). 2007;1:92–101. https://doi.org/10.4161/chan.4145.
22. Newcomb R, Szoke B, Palma A, Wang G, Chen X, Hopkins W, et al. Selective peptide antagonist of the class E calcium channel from the venom of the tarantula Hysterocrates gigas. Biochemistry. 1998;37:15353–62. https://doi.org/10.1021/bi981255g.
23. Catterall WA. Voltage-gated calcium channels. Cold Spring Harb Perspect Biol. 2011;3:a003947. https://doi.org/10.1101/cshperspect.a003947. cshperspect.a003947 [pii].
24. Lee JH, Daud AN, Cribbs LL, Lacerda AE, Pereverzev A, Klockner U, et al. Cloning and expression of a novel member of the low voltage-activated T-type calcium channel family. J Neurosci. 1999;19:1912–21. https://doi.org/10.1523/JNEUROSCI.19-06-01912.1999.
25. Snutch TP, Peloquin J, Mathews E, McRory JE. Molecular properties of voltage-gated calcium channels. In: Madame Curie Bioscience Database [Internet]. Austin: Landes Bioscience; 2013.
26. Horne WA, Ellinor PT, Inman I, Zhou M, Tsien RW, Schwarz TL. Molecular diversity of Ca2+ channel alpha 1 subunits from the marine ray Discopyge ommata. Proc Natl Acad Sci U S A. 1993;90:3787–91. https://doi.org/10.1073/pnas.90.9.3787.
27. Handrock R, Schroder F, Hirt S, Haverich A, Mittmann C, Herzig S. Single-channel properties of L-type calcium channels from failing human ventricle. Cardiovasc Res. 1998;37:445–55. https://doi.org/10.1016/s0008-6363(97)00257-5.
28. Ertel EA, Campbell KP, Harpold MM, Hofmann F, Mori Y, Perez-Reyes E, et al. Nomenclature of voltage-gated calcium channels. Neuron. 2000;25:533–5. https://doi.org/10.1016/s0896-6273(00)81057-0.
29. Dolphin AC. Voltage-gated calcium channels: their discovery, function and importance as drug targets. Brain Neurosci Adv. 2018;2. https://doi.org/10.1177/2398212818794805.
30. Lipscombe D, Helton TD, Xu W. L-type calcium channels: the low down. J Neurophysiol. 2004;92:2633–41. https://doi.org/10.1152/jn.00486.2004.
31. Striessnig J. Lonely but diverse: Cav1.3 L-type Ca(2+) channels in cochlear inner hair cells. Channels (Austin). 2013;7:133–4. https://doi.org/10.4161/chan.24457.
32. Waldner DM, Bech-Hansen NT, Stell WK. Channeling vision: CaV1.4-A critical link in retinal signal transmission. Biomed Res Int. 2018;2018:7272630. https://doi.org/10.1155/2018/7272630.
33. Vandael DH, Mahapatra S, Calorio C, Marcantoni A, Carbone E. Cav1.3 and Cav1.2 channels of adrenal chromaffin cells: emerging views on cAMP/cGMP-mediated phosphorylation and role in pacemaking. Biochim Biophys Acta. 2013;1828:1608–18. https://doi.org/10.1016/j.bbamem.2012.11.013.
34. Simms BA, Zamponi GW. Neuronal voltage-gated calcium channels: structure, function, and dysfunction. Neuron. 2014;82:24–45. https://doi.org/10.1016/j.neuron.2014.03.016.

35. Perez-Reyes E. Molecular physiology of low-voltage-activated t-type calcium channels. Physiol Rev. 2003;83:117–61. https://doi.org/10.1152/physrev.00018.2002.
36. Carabelli V, Marcantoni A, Comunanza V, Carbone E. Fast exocytosis mediated by T- and L-type channels in chromaffin cells: distinct voltage-dependence but similar Ca2+ -dependence. Eur Biophys J. 2007;36:753–62. https://doi.org/10.1007/s00249-007-0138-2.
37. Hamby AM, Rosa JM, Hsu CH, Feller MB. CaV3.2 KO mice have altered retinal waves but normal direction selectivity. Vis Neurosci. 2015;32:E003. https://doi.org/10.1017/S0952523814000364.
38. Egger V, Svoboda K, Mainen ZF. Dendrodendritic synaptic signals in olfactory bulb granule cells: local spine boost and global low-threshold spike. J Neurosci. 2005;25:3521–30. https://doi.org/10.1523/JNEUROSCI.4746-04.2005.
39. Jacus MO, Uebele VN, Renger JJ, Todorovic SM. Presynaptic Cav3.2 channels regulate excitatory neurotransmission in nociceptive dorsal horn neurons. J Neurosci. 2012;32:9374–82. https://doi.org/10.1523/JNEUROSCI.0068-12.2012.
40. Huang Z, Lujan R, Kadurin I, Uebele VN, Renger JJ, Dolphin AC, et al. Presynaptic HCN1 channels regulate Cav3.2 activity and neurotransmission at select cortical synapses. Nat Neurosci. 2011;14:478–86. https://doi.org/10.1038/nn.2757.
41. Clapham DE. Calcium signaling. Cell. 2007;131:1047–58. https://doi.org/10.1016/j.cell.2007.11.028.
42. Moran Y, Barzilai MG, Liebeskind BJ, Zakon HH. Evolution of voltage-gated ion channels at the emergence of Metazoa. J Exp Biol. 2015;218:515–25. https://doi.org/10.1242/jeb.110270.
43. Strong M, Chandy KG, Gutman GA. Molecular evolution of voltage-sensitive ion channel genes: on the origins of electrical excitability. Mol Biol Evol. 1993;10:221–42. https://doi.org/10.1093/oxfordjournals.molbev.a039986.
44. Ren D, Yue L, Navarro B, Ramos A, Clapham D. The cation selectivity filter of the one-repeat voltage-gated sodium channel, NaChBac. Biophys J, Biophysical Society, Bethesda. 2003:24A-A.
45. Yu FH, Yarov-Yarovoy V, Gutman GA, Catterall WA. Overview of molecular relationships in the voltage-gated ion channel superfamily. Pharmacol Rev. 2005;57:387–95. https://doi.org/10.1124/pr.57.4.13.
46. Takahashi M, Seagar MJ, Jones JF, Reber BF, Catterall WA. Subunit structure of dihydropyridine-sensitive calcium channels from skeletal muscle. Proc Natl Acad Sci U S A. 1987;84:5478–82. https://doi.org/10.1073/pnas.84.15.5478.
47. Tanabe T, Takeshima H, Mikami A, Flockerzi V, Takahashi H, Kangawa K, et al. Primary structure of the receptor for calcium channel blockers from skeletal muscle. Nature. 1987;328:313–8. https://doi.org/10.1038/328313a0.
48. Mikami A, Imoto K, Tanabe T, Niidome T, Mori Y, Takeshima H, et al. Primary structure and functional expression of the cardiac dihydropyridine-sensitive calcium channel. Nature. 1989;340:230–3. https://doi.org/10.1038/340230a0.
49. Williams ME, Brust PF, Feldman DH, Patthi S, Simerson S, Maroufi A, et al. Structure and functional expression of an omega-conotoxin-sensitive human N-type calcium channel. Science. 1992;257:389–95. https://doi.org/10.1126/science.1321501.
50. Bech-Hansen NT, Naylor MJ, Maybaum TA, Pearce WG, Koop B, Fishman GA, et al. Loss-of-function mutations in a calcium-channel alpha1-subunit gene in Xp11.23 cause incomplete X-linked congenital stationary night blindness. Nat Genet. 1998;19:264–7. https://doi.org/10.1038/947.
51. Strom TM, Nyakatura G, Apfelstedt-Sylla E, Hellebrand H, Lorenz B, Weber BH, et al. An L-type calcium-channel gene mutated in incomplete X-linked congenital stationary night blindness. Nat Genet. 1998;19:260–3. https://doi.org/10.1038/940.
52. Cribbs LL, Lee JH, Yang J, Satin J, Zhang Y, Daud A, et al. Cloning and characterization of alpha1H from human heart, a member of the T-type Ca2+ channel gene family. Circ Res. 1998;83:103–9. https://doi.org/10.1161/01.res.83.1.103.

53. Yamada T, Kawahara K, Kosugi T, Tanaka M. Nitric oxide produced during sublethal ischemia is crucial for the preconditioning-induced down-regulation of glutamate transporter GLT-1 in neuron/astrocyte co-cultures. Neurochem Res. 2006;31:49–56. https://doi.org/10.1007/s11064-005-9077-4.
54. Li B, Tadross MR, Tsien RW. Sequential ionic and conformational signaling by calcium channels drives neuronal gene expression. Science. 2016;351:863–7. https://doi.org/10.1126/science.aad3647.
55. Fekete A, Johnston J, Delaney KR. Presynaptic T-type Ca2+ channels modulate dendrodendritic mitral-mitral and mitral-periglomerular connections in mouse olfactory bulb. J Neurosci. 2014;34:14032–45. https://doi.org/10.1523/JNEUROSCI.0905-14.2014.
56. Wu J, Yan Z, Li Z, Qian X, Lu S, Dong M, et al. Structure of the voltage-gated calcium channel Ca(v)1.1 at 3.6 A resolution. Nature. 2016;537:191–6. https://doi.org/10.1038/nature19321.
57. Wu J, Yan Z, Li Z, Yan C, Lu S, Dong M, et al. Structure of the voltage-gated calcium channel Cav1.1 complex. Science. 2015;350:aad2395. https://doi.org/10.1126/science.aad2395.
58. Maser P, Hosoo Y, Goshima S, Horie T, Eckelman B, Yamada K, et al. Glycine residues in potassium channel-like selectivity filters determine potassium selectivity in four-loop-per-subunit HKT transporters from plants. Proc Natl Acad Sci U S A. 2002;99:6428–33. https://doi.org/10.1073/pnas.082123799.
59. Jiang D, Shi H, Tonggu L, Gamal El-Din TM, Lenaeus MJ, Zhao Y, et al. Structure of the cardiac sodium channel. Cell. 2020;180:122–34.e10. https://doi.org/10.1016/j.cell.2019.11.041.
60. Ben-Johny M, Yue DT. Calmodulin regulation (calmodulation) of voltage-gated calcium channels. J Gen Physiol. 2014;143:679–92. https://doi.org/10.1085/jgp.201311153.
61. Dolphin AC, Lee A. Presynaptic calcium channels: specialized control of synaptic neurotransmitter release. Nat Rev Neurosci. 2020;21:213–29. https://doi.org/10.1038/s41583-020-0278-2.
62. Dolphin AC. Voltage-gated calcium channels and their auxiliary subunits: physiology and pathophysiology and pharmacology. J Physiol. 2016;594:5369–90. https://doi.org/10.1113/JP272262.
63. Moss FJ, Viard P, Davies A, Bertaso F, Page KM, Graham A, et al. The novel product of a five-exon stargazin-related gene abolishes Ca(V)2.2 calcium channel expression. EMBO J. 2002;21:1514–23. https://doi.org/10.1093/emboj/21.7.1514.
64. Walsh CP, Davies A, Butcher AJ, Dolphin AC, Kitmitto A. Three-dimensional structure of CaV3.1: comparison with the cardiac L-type voltage-gated calcium channel monomer architecture. J Biol Chem. 2009;284:22310–21. https://doi.org/10.1074/jbc.M109.017152.
65. Muller CS, Haupt A, Bildl W, Schindler J, Knaus HG, Meissner M, et al. Quantitative proteomics of the Cav2 channel nano-environments in the mammalian brain. Proc Natl Acad Sci U S A. 2010;107:14950–7. https://doi.org/10.1073/pnas.1005940107.
66. Mori MX, Vander Kooi CW, Leahy DJ, Yue DT. Crystal structure of the CaV2 IQ domain in complex with Ca2+/calmodulin: high-resolution mechanistic implications for channel regulation by Ca2+. Structure. 2008;16:607–20. https://doi.org/10.1016/j.str.2008.01.011.
67. Kim EY, Rumpf CH, Van Petegem F, Arant RJ, Findeisen F, Cooley ES, et al. Multiple C-terminal tail Ca(2+)/CaMs regulate Ca(V)1.2 function but do not mediate channel dimerization. EMBO J. 2010;29:3924–38. https://doi.org/10.1038/emboj.2010.260.
68. Ben Johny M, Yang PS, Bazzazi H, Yue DT. Dynamic switching of calmodulin interactions underlies Ca2+ regulation of CaV1.3 channels. Nat Commun. 2013;4:1717. https://doi.org/10.1038/ncomms2727.
69. Jay SD, Sharp AH, Kahl SD, Vedvick TS, Harpold MM, Campbell KP. Structural characterization of the dihydropyridine-sensitive calcium channel alpha 2-subunit and the associated delta peptides. J Biol Chem. 1991;266:3287–93. https://doi.org/10.1016/S0021-9258(18)49986-3.
70. De Jongh KS, Warner C, Catterall WA. Subunits of purified calcium channels. Alpha 2 and delta are encoded by the same gene. J Biol Chem. 1990;265:14738–41. https://doi.org/10.1016/S0021-9258(18)77174-3.

71. Hendrich J, Van Minh AT, Heblich F, Nieto-Rostro M, Watschinger K, Striessnig J, et al. Pharmacological disruption of calcium channel trafficking by the alpha2delta ligand gabapentin. Proc Natl Acad Sci U S A. 2008;105:3628–33. https://doi.org/10.1073/pnas.0708930105.
72. Dolphin AC. Functions of presynaptic voltage-gated calcium channels. Function (Oxf). 2021;2:zqaa027. https://doi.org/10.1093/function/zqaa027.
73. Hoshi T, Zagotta WN, Aldrich RW. Biophysical and molecular mechanisms of Shaker potassium channel inactivation. Science. 1990;250:533–8. https://doi.org/10.1126/science.2122519.
74. West JW, Patton DE, Scheuer T, Wang Y, Goldin AL, Catterall WA. A cluster of hydrophobic amino acid residues required for fast Na(+)-channel inactivation. Proc Natl Acad Sci U S A. 1992;89:10910–4. https://doi.org/10.1073/pnas.89.22.10910.
75. Herlitze S, Hockerman GH, Scheuer T, Catterall WA. Molecular determinants of inactivation and G protein modulation in the intracellular loop connecting domains I and II of the calcium channel alpha1A subunit. Proc Natl Acad Sci U S A. 1997;94:1512–6. https://doi.org/10.1073/pnas.94.4.1512.
76. Kraus RL, Sinnegger MJ, Glossmann H, Hering S, Striessnig J. Familial hemiplegic migraine mutations change alpha1A Ca2+ channel kinetics. J Biol Chem. 1998;273:5586–90. https://doi.org/10.1074/jbc.273.10.5586.
77. Berrou L, Bernatchez G, Parent L. Molecular determinants of inactivation within the I–II linker of alpha1E (CaV2.3) calcium channels. Biophys J. 2001;80:215–28. https://doi.org/10.1016/S0006-3495(01)76008-0.
78. Stotz SC, Zamponi GW. Identification of inactivation determinants in the domain IIS6 region of high voltage-activated calcium channels. J Biol Chem. 2001;276:33001–10. https://doi.org/10.1074/jbc.M104387200.
79. Stotz SC, Zamponi GW. Structural determinants of fast inactivation of high voltage-activated Ca(2+) channels. Trends Neurosci. 2001;24:176–81. https://doi.org/10.1016/s0166-2236(00)01738-0.
80. Spaetgens RL, Zamponi GW. Multiple structural domains contribute to voltage-dependent inactivation of rat brain alpha(1E) calcium channels. J Biol Chem. 1999;274:22428–36. https://doi.org/10.1074/jbc.274.32.22428.
81. Stotz SC, Hamid J, Spaetgens RL, Jarvis SE, Zamponi GW. Fast inactivation of voltage-dependent calcium channels. A hinged-lid mechanism? J Biol Chem. 2000;275:24575–82. https://doi.org/10.1074/jbc.M000399200.
82. Lee A, Wong ST, Gallagher D, Li B, Storm DR, Scheuer T, et al. Ca2+/calmodulin binds to and modulates P/Q-type calcium channels. Nature. 1999;399:155–9. https://doi.org/10.1038/20194.
83. Zuhlke RD, Pitt GS, Deisseroth K, Tsien RW, Reuter H. Calmodulin supports both inactivation and facilitation of L-type calcium channels. Nature. 1999;399:159–62. https://doi.org/10.1038/20200.
84. Liu X, Yang PS, Yang W, Yue DT. Enzyme-inhibitor-like tuning of Ca(2+) channel connectivity with calmodulin. Nature. 2010;463:968–72. https://doi.org/10.1038/nature08766.
85. Zamponi GW. Calmodulin lobotomized: novel insights into calcium regulation of voltage-gated calcium channels. Neuron. 2003;39:879–81. https://doi.org/10.1016/s0896-6273(03)00564-6.
86. Tadross MR, Dick IE, Yue DT. Mechanism of local and global Ca2+ sensing by calmodulin in complex with a Ca2+ channel. Cell. 2008;133:1228–40. https://doi.org/10.1016/j.cell.2008.05.025.
87. Dick IE, Tadross MR, Liang H, Tay LH, Yang W, Yue DT. A modular switch for spatial Ca2+ selectivity in the calmodulin regulation of CaV channels. Nature. 2008;451:830–4. https://doi.org/10.1038/nature06529.
88. Kuboniwa H, Tjandra N, Grzesiek S, Ren H, Klee CB, Bax A. Solution structure of calcium-free calmodulin. Nat Struct Biol. 1995;2:768–76. https://doi.org/10.1038/nsb0995-768.

89. Kretsinger RH, Rudnick SE, Weissman LJ. Crystal structure of calmodulin. J Inorg Biochem. 1986;28:289–302. https://doi.org/10.1016/0162-0134(86)80093-9.
90. McRory JE, Hamid J, Doering CJ, Garcia E, Parker R, Hamming K, et al. The CACNA1F gene encodes an L-type calcium channel with unique biophysical properties and tissue distribution. J Neurosci. 2004;24:1707–18. https://doi.org/10.1523/JNEUROSCI.4846-03.2004.
91. Yang PS, Alseikhan BA, Hiel H, Grant L, Mori MX, Yang W, et al. Switching of Ca2+-dependent inactivation of Ca(v)1.3 channels by calcium binding proteins of auditory hair cells. J Neurosci. 2006;26:10677–89. https://doi.org/10.1523/JNEUROSCI.3236-06.2006.
92. Findeisen F, Rumpf CH, Minor DL Jr. Apo states of calmodulin and CaBP1 control CaV1 voltage-gated calcium channel function through direct competition for the IQ domain. J Mol Biol. 2013;425:3217–34. https://doi.org/10.1016/j.jmb.2013.06.024.
93. Oz S, Benmocha A, Sasson Y, Sachyani D, Almagor L, Lee A, et al. Competitive and non-competitive regulation of calcium-dependent inactivation in CaV1.2 L-type Ca2+ channels by calmodulin and Ca2+-binding protein 1. J Biol Chem. 2013;288:12680–91. https://doi.org/10.1074/jbc.M113.460949.
94. Singh A, Hamedinger D, Hoda JC, Gebhart M, Koschak A, Romanin C, et al. C-terminal modulator controls Ca2+-dependent gating of Ca(v)1.4 L-type Ca2+ channels. Nat Neurosci. 2006;9:1108–16. https://doi.org/10.1038/nn1751.
95. Wahl-Schott C, Baumann L, Cuny H, Eckert C, Griessmeier K, Biel M. Switching off calcium-dependent inactivation in L-type calcium channels by an autoinhibitory domain. Proc Natl Acad Sci U S A. 2006;103:15657–62. https://doi.org/10.1073/pnas.0604621103.
96. Lee A, Zhou H, Scheuer T, Catterall WA. Molecular determinants of Ca(2+)/calmodulin-dependent regulation of Ca(v)2.1 channels. Proc Natl Acad Sci U S A. 2003;100:16059–64. https://doi.org/10.1073/pnas.2237000100.
97. Lacerda AE, Kim HS, Ruth P, Perez-Reyes E, Flockerzi V, Hofmann F, et al. Normalization of current kinetics by interaction between the alpha 1 and beta subunits of the skeletal muscle dihydropyridine-sensitive Ca2+ channel. Nature. 1991;352:527–30. https://doi.org/10.1038/352527a0.
98. Buraei Z, Yang J. Structure and function of the beta subunit of voltage-gated Ca(2)(+) channels. Biochim Biophys Acta. 1828;2013:1530–40. https://doi.org/10.1016/j.bbamem.2012.08.028.
99. Buraei Z, Yang J. The ss subunit of voltage-gated Ca2+ channels. Physiol Rev. 2010;90:1461–506. https://doi.org/10.1152/physrev.00057.2009.
100. Qin N, Platano D, Olcese R, Costantin JL, Stefani E, Birnbaumer L. Unique regulatory properties of the type 2a Ca2+ channel beta subunit caused by palmitoylation. Proc Natl Acad Sci U S A. 1998;95:4690–5. https://doi.org/10.1073/pnas.95.8.4690.
101. Hurley JH, Cahill AL, Currie KP, Fox AP. The role of dynamic palmitoylation in Ca2+ channel inactivation. Proc Natl Acad Sci U S A. 2000;97:9293–8. https://doi.org/10.1073/pnas.160589697.
102. Brice NL, Dolphin AC. Differential plasma membrane targeting of voltage-dependent calcium channel subunits expressed in a polarized epithelial cell line. J Physiol. 1999;515(Pt 3):685–94. https://doi.org/10.1111/j.1469-7793.1999.685ab.x.
103. Altier C, Garcia-Caballero A, Simms B, You H, Chen L, Walcher J, et al. The Cavbeta subunit prevents RFP2-mediated ubiquitination and proteasomal degradation of L-type channels. Nat Neurosci. 2011;14:173–80. https://doi.org/10.1038/nn.2712.
104. Bichet D, Cornet V, Geib S, Carlier E, Volsen S, Hoshi T, et al. The I–II loop of the Ca2+ channel alpha1 subunit contains an endoplasmic reticulum retention signal antagonized by the beta subunit. Neuron. 2000;25:177–90. https://doi.org/10.1016/s0896-6273(00)80881-8.
105. Waithe D, Ferron L, Page KM, Chaggar K, Dolphin AC. Beta-subunits promote the expression of Ca(V)2.2 channels by reducing their proteasomal degradation. J Biol Chem. 2011;286:9598–611. https://doi.org/10.1074/jbc.M110.195909.
106. Qin N, Yagel S, Momplaisir ML, Codd EE, D'Andrea MR. Molecular cloning and characterization of the human voltage-gated calcium channel alpha(2)delta-4 subunit. Mol Pharmacol. 2002;62:485–96. https://doi.org/10.1124/mol.62.3.485.

107. Canti C, Nieto-Rostro M, Foucault I, Heblich F, Wratten J, Richards MW, et al. The metal-ion-dependent adhesion site in the Von Willebrand factor-A domain of alpha2delta subunits is key to trafficking voltage-gated Ca2+ channels. Proc Natl Acad Sci U S A. 2005;102:11230–5. https://doi.org/10.1073/pnas.0504183102.
108. Yasuda T, Chen L, Barr W, McRory JE, Lewis RJ, Adams DJ, et al. Auxiliary subunit regulation of high-voltage activated calcium channels expressed in mammalian cells. Eur J Neurosci. 2004;20:1–13. https://doi.org/10.1111/j.1460-9568.2004.03434.x.
109. Dolphin AC, Wyatt CN, Richards J, Beattie RE, Craig P, Lee JH, et al. The effect of alpha2-delta and other accessory subunits on expression and properties of the calcium channel alpha1G. J Physiol. 1999;519(Pt 1):35–45. https://doi.org/10.1111/j.1469-7793.1999.0035o.x.
110. Gao B, Sekido Y, Maximov A, Saad M, Forgacs E, Latif F, et al. Functional properties of a new voltage-dependent calcium channel alpha(2)delta auxiliary subunit gene (CACNA2D2). J Biol Chem. 2000;275:12237–42. https://doi.org/10.1074/jbc.275.16.12237.
111. Dubel SJ, Altier C, Chaumont S, Lory P, Bourinet E, Nargeot J. Plasma membrane expression of T-type calcium channel alpha(1) subunits is modulated by high voltage-activated auxiliary subunits. J Biol Chem. 2004;279:29263–9. https://doi.org/10.1074/jbc.M313450200.
112. Eroglu C, Allen NJ, Susman MW, O'Rourke NA, Park CY, Ozkan E, et al. Gabapentin receptor alpha2delta-1 is a neuronal thrombospondin receptor responsible for excitatory CNS synaptogenesis. Cell. 2009;139:380–92. https://doi.org/10.1016/j.cell.2009.09.025.
113. Rousset M, Cens T, Restituito S, Barrere C, Black JL 3rd, McEnery MW, et al. Functional roles of gamma2, gamma3 and gamma4, three new Ca2+ channel subunits, in P/Q-type Ca2+ channel expressed in Xenopus oocytes. J Physiol. 2001;532:583–93. https://doi.org/10.1111/j.1469-7793.2001.0583e.x.
114. Tomita S, Adesnik H, Sekiguchi M, Zhang W, Wada K, Howe JR, et al. Stargazin modulates AMPA receptor gating and trafficking by distinct domains. Nature. 2005;435:1052–8. https://doi.org/10.1038/nature03624.
115. Matsuda S, Kakegawa W, Budisantoso T, Nomura T, Kohda K, Yuzaki M. Stargazin regulates AMPA receptor trafficking through adaptor protein complexes during long-term depression. Nat Commun. 2013;4:2759. https://doi.org/10.1038/ncomms3759.
116. Holz GG, Rane SG, Dunlap K. GTP-binding proteins mediate transmitter inhibition of voltage-dependent calcium channels. Nature. 1986;319:670–2. https://doi.org/10.1038/319670a0.
117. Scott RH, Dolphin AC. Regulation of calcium currents by a GTP analogue: potentiation of (-)-baclofen-mediated inhibition. Neurosci Lett. 1986;69:59–64. https://doi.org/10.1016/0304-3940(86)90414-3.
118. Herlitze S, Garcia DE, Mackie K, Hille B, Scheuer T, Catterall WA. Modulation of Ca2+ channels by G-protein beta gamma subunits. Nature. 1996;380:258–62. https://doi.org/10.1038/380258a0.
119. Takahashi T, Forsythe ID, Tsujimoto T, Barnes-Davies M, Onodera K. Presynaptic calcium current modulation by a metabotropic glutamate receptor. Science. 1996;274:594–7. https://doi.org/10.1126/science.274.5287.594.
120. Brown SP, Safo PK, Regehr WG. Endocannabinoids inhibit transmission at granule cell to Purkinje cell synapses by modulating three types of presynaptic calcium channels. J Neurosci. 2004;24:5623–31. https://doi.org/10.1523/JNEUROSCI.0918-04.2004.
121. Kisilevsky AE, Mulligan SJ, Altier C, Iftinca MC, Varela D, Tai C, et al. D1 receptors physically interact with N-type calcium channels to regulate channel distribution and dendritic calcium entry. Neuron. 2008;58:557–70. https://doi.org/10.1016/j.neuron.2008.03.002.
122. Stephens GJ, Mochida S. G protein {beta}{gamma} subunits mediate presynaptic inhibition of transmitter release from rat superior cervical ganglion neurones in culture. J Physiol. 2005;563:765–76. https://doi.org/10.1113/jphysiol.2004.080192.
123. Bucci G, Mochida S, Stephens GJ. Inhibition of synaptic transmission and G protein modulation by synthetic CaV2.2 Ca(2)+ channel peptides. J Physiol. 2011;589:3085–101. https://doi.org/10.1113/jphysiol.2010.204735.

124. Dolphin AC. G protein modulation of voltage-gated calcium channels. Pharmacol Rev. 2003;55:607–27. https://doi.org/10.1124/pr.55.4.3.
125. Zamponi GW, Currie KP. Regulation of Ca(V)2 calcium channels by G protein coupled receptors. Biochim Biophys Acta. 1828;2013:1629–43. https://doi.org/10.1016/j.bbamem.2012.10.004.
126. Bean BP. Neurotransmitter inhibition of neuronal calcium currents by changes in channel voltage dependence. Nature. 1989;340:153–6. https://doi.org/10.1038/340153a0.
127. Carabelli V, Lovallo M, Magnelli V, Zucker H, Carbone E. Voltage-dependent modulation of single N-Type Ca2+ channel kinetics by receptor agonists in IMR32 cells. Biophys J. 1996;70:2144–54. https://doi.org/10.1016/S0006-3495(96)79780-1.
128. Dolphin AC, Wootton JF, Scott RH, Trentham DR. Photoactivation of intracellular guanosine triphosphate analogues reduces the amplitude and slows the kinetics of voltage-activated calcium channel currents in sensory neurones. Pflugers Arch. 1988;411:628–36. https://doi.org/10.1007/BF00580858.
129. Hernandez-Ochoa EO, Garcia-Ferreiro RE, Garcia DE. G protein activation inhibits gating charge movement in rat sympathetic neurons. Am J Physiol Cell Physiol. 2007;292:C2226–38. https://doi.org/10.1152/ajpcell.00540.2006.
130. Rebolledo-Antunez S, Farias JM, Arenas I, Garcia DE. Gating charges per channel of Ca(V)2.2 channels are modified by G protein activation in rat sympathetic neurons. Arch Biochem Biophys. 2009;486:51–7. https://doi.org/10.1016/j.abb.2009.04.002.
131. Van Petegem F, Clark KA, Chatelain FC, Minor DL Jr. Structure of a complex between a voltage-gated calcium channel beta-subunit and an alpha-subunit domain. Nature. 2004;429:671–5. https://doi.org/10.1038/nature02588.
132. Dresviannikov AV, Page KM, Leroy J, Pratt WS, Dolphin AC. Determinants of the voltage dependence of G protein modulation within calcium channel beta subunits. Pflugers Arch. 2009;457:743–56. https://doi.org/10.1007/s00424-008-0549-7.
133. Mochida S. Presynaptic calcium channels. Int J Mol Sci. 2019;20:10.3390/ijms20092217.
134. Kitano J, Nishida M, Itsukaichi Y, Minami I, Ogawa M, Hirano T, et al. Direct interaction and functional coupling between metabotropic glutamate receptor subtype 1 and voltage-sensitive Cav2.1 Ca2+ channel. J Biol Chem. 2003;278:25101–8. https://doi.org/10.1074/jbc.M303266200.
135. Beedle AM, McRory JE, Poirot O, Doering CJ, Altier C, Barrere C, et al. Agonist-independent modulation of N-type calcium channels by ORL1 receptors. Nat Neurosci. 2004;7:118–25. https://doi.org/10.1038/nn1180.
136. Chee MJ, Morl K, Lindner D, Merten N, Zamponi GW, Light PE, et al. The third intracellular loop stabilizes the inactive state of the neuropeptide Y1 receptor. J Biol Chem. 2008;283:33337–46. https://doi.org/10.1074/jbc.M804671200.
137. Evans RM, You H, Hameed S, Altier C, Mezghrani A, Bourinet E, et al. Heterodimerization of ORL1 and opioid receptors and its consequences for N-type calcium channel regulation. J Biol Chem. 2010;285:1032–40. https://doi.org/10.1074/jbc.M109.040634.
138. Altier C, Khosravani H, Evans RM, Hameed S, Peloquin JB, Vartian BA, et al. ORL1 receptor-mediated internalization of N-type calcium channels. Nat Neurosci. 2006;9:31–40. https://doi.org/10.1038/nn1605.
139. Murali SS, Napier IA, Rycroft BK, Christie MJ. Opioid-related (ORL1) receptors are enriched in a subpopulation of sensory neurons and prolonged activation produces no functional loss of surface N-type calcium channels. J Physiol. 2012;590:1655–67. https://doi.org/10.1113/jphysiol.2012.228429.
140. Kisilevsky AE, Zamponi GW. D2 dopamine receptors interact directly with N-type calcium channels and regulate channel surface expression levels. Channels (Austin). 2008;2:269–77. https://doi.org/10.4161/chan.2.4.6402.
141. Suh BC, Hille B. PIP2 is a necessary cofactor for ion channel function: how and why? Annu Rev Biophys. 2008;37:175–95. https://doi.org/10.1146/annurev.biophys.37.032807.125859.

142. Delmas P, Coste B, Gamper N, Shapiro MS. Phosphoinositide lipid second messengers: new paradigms for calcium channel modulation. Neuron. 2005;47:179–82. https://doi.org/10.1016/j.neuron.2005.07.001. S0896-6273(05)00562-3 [pii].
143. Suh BC, Leal K, Hille B. Modulation of high-voltage activated Ca(2+) channels by membrane phosphatidylinositol 4,5-bisphosphate. Neuron. 2010;67:224–38. https://doi.org/10.1016/j.neuron.2010.07.001. S0896-6273(10)00521-0 [pii].
144. Wu L, Bauer CS, Zhen XG, Xie C, Yang J. Dual regulation of voltage-gated calcium channels by PtdIns(4,5)P2. Nature. 2002;419:947–52. https://doi.org/10.1038/nature01118. nature01118 [pii].
145. Gamper N, Reznikov V, Yamada Y, Yang J, Shapiro MS. Phosphatidylinositol [correction] 4,5-bisphosphate signals underlie receptor-specific Gq/11-mediated modulation of N-type Ca2+ channels. J Neurosci. 2004;24:10980–92. https://doi.org/10.1523/JNEUROSCI.3869-04.2004. 24/48/10980 [pii].
146. Rodriguez-Menchaca AA, Adney SK, Zhou L, Logothetis DE. Dual regulation of voltage-sensitive ion channels by PIP(2). Front Pharmacol. 2012;3:170. https://doi.org/10.3389/fphar.2012.00170.
147. Walter AM, Muller R, Tawfik B, Wierda KD, Pinheiro PS, Nadler A, et al. Phosphatidylinositol 4,5-bisphosphate optical uncaging potentiates exocytosis. Elife. 2017;6:10.7554/eLife.30203.
148. Taoufiq Z, Eguchi K, Takahashi T. Rho-kinase accelerates synaptic vesicle endocytosis by linking cyclic GMP-dependent protein kinase activity to phosphatidylinositol-4,5-bisphosphate synthesis. J Neurosci. 2013;33:12099–104. https://doi.org/10.1523/JNEUROSCI.0730-13.2013.
149. Yokoyama CT, Sheng ZH, Catterall WA. Phosphorylation of the synaptic protein interaction site on N-type calcium channels inhibits interactions with SNARE proteins. J Neurosci. 1997;17:6929–38. https://doi.org/10.1523/JNEUROSCI.17-18-06929.1997.
150. Hamid J, Nelson D, Spaetgens R, Dubel SJ, Snutch TP, Zamponi GW. Identification of an integration center for cross-talk between protein kinase C and G protein modulation of N-type calcium channels. J Biol Chem. 1999;274:6195–202. https://doi.org/10.1074/jbc.274.10.6195.
151. Wu X, Kushwaha N, Albert PR, Penington NJ. A critical protein kinase C phosphorylation site on the 5-HT(1A) receptor controlling coupling to N-type calcium channels. J Physiol. 2002;538:41–51. https://doi.org/10.1113/jphysiol.2001.012668.
152. Zhu Y, Ikeda SR. Modulation of Ca(2+)-channel currents by protein kinase C in adult rat sympathetic neurons. J Neurophysiol. 1994;72:1549–60. https://doi.org/10.1152/jn.1994.72.4.1549.
153. Martin R, Bartolome-Martin D, Torres M, Sanchez-Prieto J. Non-additive potentiation of glutamate release by phorbol esters and metabotropic mGlu7 receptor in cerebrocortical nerve terminals. J Neurochem. 2011;116:476–85. https://doi.org/10.1111/j.1471-4159.2010.07134.x.
154. Bayer KU, Schulman H. CaM kinase: still inspiring at 40. Neuron. 2019;103:380–94. https://doi.org/10.1016/j.neuron.2019.05.033.
155. Yokoyama CT, Myers SJ, Fu J, Mockus SM, Scheuer T, Catterall WA. Mechanism of SNARE protein binding and regulation of Cav2 channels by phosphorylation of the synaptic protein interaction site. Mol Cell Neurosci. 2005;28:1–17. https://doi.org/10.1016/j.mcn.2004.08.019.
156. Jiang X, Lautermilch NJ, Watari H, Westenbroek RE, Scheuer T, Catterall WA. Modulation of CaV2.1 channels by Ca2+/calmodulin-dependent protein kinase II bound to the C-terminal domain. Proc Natl Acad Sci U S A. 2008;105:341–6. https://doi.org/10.1073/pnas.0710213105.
157. Tomizawa K, Ohta J, Matsushita M, Moriwaki A, Li ST, Takei K, et al. Cdk5/p35 regulates neurotransmitter release through phosphorylation and downregulation of P/Q-type voltage-dependent calcium channel activity. J Neurosci. 2002;22:2590–7. https://doi.org/10.1523/JNEUROSCI.22-07-02590.2002.

158. Yan Z, Chi P, Bibb JA, Ryan TA, Greengard P. Roscovitine: a novel regulator of P/Q-type calcium channels and transmitter release in central neurons. J Physiol. 2002;540:761–70. https://doi.org/10.1113/jphysiol.2001.013376.
159. Su SC, Seo J, Pan JQ, Samuels BA, Rudenko A, Ericsson M, et al. Regulation of N-type voltage-gated calcium channels and presynaptic function by cyclin-dependent kinase 5. Neuron. 2012;75:675–87. https://doi.org/10.1016/j.neuron.2012.06.023.
160. Kim SH, Ryan TA. Balance of calcineurin Aalpha and CDK5 activities sets release probability at nerve terminals. J Neurosci. 2013;33:8937–50. https://doi.org/10.1523/JNEUROSCI.4288-12.2013.
161. Nejatbakhsh N, Feng ZP. Calcium binding protein-mediated regulation of voltage-gated calcium channels linked to human diseases. Acta Pharmacol Sin. 2011;32:741–8. https://doi.org/10.1038/aps.2011.64.
162. Haeseleer F, Palczewski K. Calmodulin and Ca2+-binding proteins (CaBPs): variations on a theme. Adv Exp Med Biol. 2002;514:303–17. https://doi.org/10.1007/978-1-4615-0121-3_18.
163. McCue HV, Haynes LP, Burgoyne RD. Bioinformatic analysis of CaBP/calneuron proteins reveals a family of highly conserved vertebrate Ca2+-binding proteins. BMC Res Notes. 2010;3:118. https://doi.org/10.1186/1756-0500-3-118.
164. Haeseleer F, Sokal I, Verlinde CL, Erdjument-Bromage H, Tempst P, Pronin AN, et al. Five members of a novel Ca(2+)-binding protein (CABP) subfamily with similarity to calmodulin. J Biol Chem. 2000;275:1247–60. https://doi.org/10.1074/jbc.275.2.1247.
165. Lee A, Westenbroek RE, Haeseleer F, Palczewski K, Scheuer T, Catterall WA. Differential modulation of Ca(v)2.1 channels by calmodulin and Ca2+-binding protein 1. Nat Neurosci. 2002;5:210–7. https://doi.org/10.1038/nn805.
166. Cui G, Meyer AC, Calin-Jageman I, Neef J, Haeseleer F, Moser T, et al. Ca2+-binding proteins tune Ca2+-feedback to Cav1.3 channels in mouse auditory hair cells. J Physiol. 2007;585:791–803. https://doi.org/10.1113/jphysiol.2007.142307.
167. Haeseleer F, Imanishi Y, Maeda T, Possin DE, Maeda A, Lee A, et al. Essential role of Ca2+-binding protein 4, a Cav1.4 channel regulator, in photoreceptor synaptic function. Nat Neurosci. 2004;7:1079–87. https://doi.org/10.1038/nn1320.
168. Lautermilch NJ, Few AP, Scheuer T, Catterall WA. Modulation of CaV2.1 channels by the neuronal calcium-binding protein visinin-like protein-2. J Neurosci. 2005;25:7062–70. https://doi.org/10.1523/JNEUROSCI.0447-05.2005.
169. Lee A, Jimenez A, Cui G, Haeseleer F. Phosphorylation of the Ca2+-binding protein CaBP4 by protein kinase C zeta in photoreceptors. J Neurosci. 2007;27:12743–54. https://doi.org/10.1523/JNEUROSCI.4264-07.2007.
170. Rieke F, Lee A, Haeseleer F. Characterization of Ca2+-binding protein 5 knockout mouse retina. Invest Ophthalmol Vis Sci. 2008;49:5126–35. https://doi.org/10.1167/iovs.08-2236.
171. Schneggenburger R, Neher E. Presynaptic calcium and control of vesicle fusion. Curr Opin Neurobiol. 2005;15:266–74. https://doi.org/10.1016/j.conb.2005.05.006.
172. Sheng ZH, Rettig J, Takahashi M, Catterall WA. Identification of a syntaxin-binding site on N-type calcium channels. Neuron. 1994;13:1303–13. https://doi.org/10.1016/0896-6273(94)90417-0.
173. Sheng ZH, Yokoyama CT, Catterall WA. Interaction of the synprint site of N-type Ca2+ channels with the C2B domain of synaptotagmin I. Proc Natl Acad Sci U S A. 1997;94:5405–10. https://doi.org/10.1073/pnas.94.10.5405.
174. Kim DK, Catterall WA. Ca2+-dependent and -independent interactions of the isoforms of the alpha1A subunit of brain Ca2+ channels with presynaptic SNARE proteins. Proc Natl Acad Sci U S A. 1997;94:14782–6. https://doi.org/10.1073/pnas.94.26.14782.
175. Rettig J, Sheng ZH, Kim DK, Hodson CD, Snutch TP, Catterall WA. Isoform-specific interaction of the alpha1A subunits of brain Ca2+ channels with the presynaptic proteins syntaxin and SNAP-25. Proc Natl Acad Sci U S A. 1996;93:7363–8. https://doi.org/10.1073/pnas.93.14.7363.

176. Li Q, Lau A, Morris TJ, Guo L, Fordyce CB, Stanley EF. A syntaxin 1, Galpha(o), and N-type calcium channel complex at a presynaptic nerve terminal: analysis by quantitative immunocolocalization. J Neurosci. 2004;24:4070–81. https://doi.org/10.1523/JNEUROSCI.0346-04.2004.
177. Sheng ZH, Rettig J, Cook T, Catterall WA. Calcium-dependent interaction of N-type calcium channels with the synaptic core complex. Nature. 1996;379:451–4. https://doi.org/10.1038/379451a0.
178. Bezprozvanny I, Scheller RH, Tsien RW. Functional impact of syntaxin on gating of N-type and Q-type calcium channels. Nature. 1995;378:623–6. https://doi.org/10.1038/378623a0.
179. Wiser O, Bennett MK, Atlas D. Functional interaction of syntaxin and SNAP-25 with voltage-sensitive L- and N-type Ca2+ channels. EMBO J. 1996;15:4100–10. https://doi.org/10.1002/j.1460-2075.1996.tb00785.x.
180. Zhong H, Yokoyama CT, Scheuer T, Catterall WA. Reciprocal regulation of P/Q-type Ca2+ channels by SNAP-25, syntaxin and synaptotagmin. Nat Neurosci. 1999;2:939–41. https://doi.org/10.1038/14721.
181. Khanna R, Zougman A, Stanley EF. A proteomic screen for presynaptic terminal N-type calcium channel (CaV2.2) binding partners. J Biochem Mol Biol. 2007;40:302–14. https://doi.org/10.5483/bmbrep.2007.40.3.302.
182. Coppola T, Magnin-Luthi S, Perret-Menoud V, Gattesco S, Schiavo G, Regazzi R. Direct interaction of the Rab3 effector RIM with Ca2+ channels, SNAP-25, and synaptotagmin. J Biol Chem. 2001;276:32756–62. https://doi.org/10.1074/jbc.M100929200.
183. Hibino H, Pironkova R, Onwumere O, Vologodskaia M, Hudspeth AJ, Lesage F. RIM binding proteins (RBPs) couple Rab3-interacting molecules (RIMs) to voltage-gated Ca(2+) channels. Neuron. 2002;34:411–23. https://doi.org/10.1016/s0896-6273(02)00667-0.
184. Kiyonaka S, Wakamori M, Miki T, Uriu Y, Nonaka M, Bito H, et al. RIM1 confers sustained activity and neurotransmitter vesicle anchoring to presynaptic Ca2+ channels. Nat Neurosci. 2007;10:691–701. https://doi.org/10.1038/nn1904.
185. Kiyonaka S, Nakajima H, Takada Y, Hida Y, Yoshioka T, Hagiwara A, et al. Physical and functional interaction of the active zone protein CAST/ERC2 and the beta-subunit of the voltage-dependent Ca(2+) channel. J Biochem. 2012;152:149–59. https://doi.org/10.1093/jb/mvs054.
186. Maximov A, Bezprozvanny I. Synaptic targeting of N-type calcium channels in hippocampal neurons. J Neurosci. 2002;22:6939–52. https://doi.org/10.1523/JNEUROSCI.22-16-06939.2002.
187. Calloway N, Gouzer G, Xue M, Ryan TA. The active-zone protein Munc13 controls the use-dependence of presynaptic voltage-gated calcium channels. Elife. 2015;4. https://doi.org/10.7554/eLife.07728.
188. Chew LA, Khanna R. CRMP2 and voltage-gated ion channels: potential roles in neuropathic pain. Neuronal Signal. 2018;2. https://doi.org/10.1042/NS20170220.
189. Chi XX, Schmutzler BS, Brittain JM, Wang Y, Hingtgen CM, Nicol GD, et al. Regulation of N-type voltage-gated calcium channels (Cav2.2) and transmitter release by collapsin response mediator protein-2 (CRMP-2) in sensory neurons. J Cell Sci. 2009;122:4351–62. https://doi.org/10.1242/jcs.053280.
190. Brittain JM, Piekarz AD, Wang Y, Kondo T, Cummins TR, Khanna R. An atypical role for collapsin response mediator protein 2 (CRMP-2) in neurotransmitter release via interaction with presynaptic voltage-gated calcium channels. J Biol Chem. 2009;284:31375–90. https://doi.org/10.1074/jbc.M109.009951.
191. Brittain JM, Duarte DB, Wilson SM, Zhu W, Ballard C, Johnson PL, et al. Suppression of inflammatory and neuropathic pain by uncoupling CRMP-2 from the presynaptic Ca(2)(+) channel complex. Nat Med. 2011;17:822–9. https://doi.org/10.1038/nm.2345.
192. Lipscombe D, Andrade A, Allen SE. Alternative splicing: functional diversity among voltage-gated calcium channels and behavioral consequences. Biochim Biophys Acta. 1828;2013:1522–9. https://doi.org/10.1016/j.bbamem.2012.09.018.

193. Zamponi GW, Striessnig J, Koschak A, Dolphin AC. The physiology, pathology, and pharmacology of voltage-gated calcium channels and their future therapeutic potential. Pharmacol Rev. 2015;67:821–70. https://doi.org/10.1124/pr.114.009654.
194. Bock G, Gebhart M, Scharinger A, Jangsangthong W, Busquet P, Poggiani C, et al. Functional properties of a newly identified C-terminal splice variant of Cav1.3 L-type Ca2+ channels. J Biol Chem. 2011;286:42736–48. https://doi.org/10.1074/jbc.M111.269951.
195. Tan GM, Yu D, Wang J, Soong TW. Alternative splicing at C terminus of Ca(V)1.4 calcium channel modulates calcium-dependent inactivation, activation potential, and current density. J Biol Chem. 2012;287:832–47. https://doi.org/10.1074/jbc.M111.268722.
196. Chang SY, Yong TF, Yu CY, Liang MC, Pletnikova O, Troncoso J, et al. Age and gender-dependent alternative splicing of P/Q-type calcium channel EF-hand. Neuroscience. 2007;145:1026–36. https://doi.org/10.1016/j.neuroscience.2006.12.054.
197. Bourinet E, Soong TW, Sutton K, Slaymaker S, Mathews E, Monteil A, et al. Splicing of alpha 1A subunit gene generates phenotypic variants of P- and Q-type calcium channels. Nat Neurosci. 1999;2:407–15. https://doi.org/10.1038/8070.
198. Soong TW, DeMaria CD, Alvania RS, Zweifel LS, Liang MC, Mittman S, et al. Systematic identification of splice variants in human P/Q-type channel alpha1(2.1) subunits: implications for current density and Ca2+-dependent inactivation. J Neurosci. 2002;22:10142–52. https://doi.org/10.1523/JNEUROSCI.22-23-10142.2002.
199. Chaudhuri D, Chang SY, DeMaria CD, Alvania RS, Soong TW, Yue DT. Alternative splicing as a molecular switch for Ca2+/calmodulin-dependent facilitation of P/Q-type Ca2+ channels. J Neurosci. 2004;24:6334–42. https://doi.org/10.1523/JNEUROSCI.1712-04.2004.
200. Rajapaksha WR, Wang D, Davies JN, Chen L, Zamponi GW, Fisher TE. Novel splice variants of rat CaV2.1 that lack much of the synaptic protein interaction site are expressed in neuroendocrine cells. J Biol Chem. 2008;283:15997–6003. https://doi.org/10.1074/jbc.M710544200.
201. Sandoz G, Bichet D, Cornet V, Mori Y, Felix R, De Waard M. Distinct properties and differential beta subunit regulation of two C-terminal isoforms of the P/Q-type Ca(2+)-channel alpha(1A) subunit. Eur J Neurosci. 2001;14:987–97. https://doi.org/10.1046/j.0953-816x.2001.01728.x.
202. Lin Z, Haus S, Edgerton J, Lipscombe D. Identification of functionally distinct isoforms of the N-type Ca2+ channel in rat sympathetic ganglia and brain. Neuron. 1997;18:153–66. https://doi.org/10.1016/s0896-6273(01)80054-4.
203. Lin Z, Lin Y, Schorge S, Pan JQ, Beierlein M, Lipscombe D. Alternative splicing of a short cassette exon in alpha1B generates functionally distinct N-type calcium channels in central and peripheral neurons. J Neurosci. 1999;19:5322–31. https://doi.org/10.1523/JNEUROSCI.19-13-05322.1999.
204. Kaneko S, Cooper CB, Nishioka N, Yamasaki H, Suzuki A, Jarvis SE, et al. Identification and characterization of novel human Ca(v)2.2 (alpha 1B) calcium channel variants lacking the synaptic protein interaction site. J Neurosci. 2002;22:82–92. https://doi.org/10.1523/JNEUROSCI.22-01-00082.2002.
205. Szabo Z, Obermair GJ, Cooper CB, Zamponi GW, Flucher BE. Role of the synprint site in presynaptic targeting of the calcium channel CaV2.2 in hippocampal neurons. Eur J Neurosci. 2006;24:709–18. https://doi.org/10.1111/j.1460-9568.2006.04947.x.
206. Huang H, Tan BZ, Shen Y, Tao J, Jiang F, Sung YY, et al. RNA editing of the IQ domain in Ca(v)1.3 channels modulates their Ca(2)(+)-dependent inactivation. Neuron. 2012;73:304–16. https://doi.org/10.1016/j.neuron.2011.11.022.
207. Bazzazi H, Ben Johny M, Adams PJ, Soong TW, Yue DT. Continuously tunable Ca(2+) regulation of RNA-edited CaV1.3 channels. Cell Rep. 2013;5:367–77. https://doi.org/10.1016/j.celrep.2013.09.006.
208. Pietrobon D. CaV2.1 channelopathies. Pflugers Arch. 2010;460:375–93. https://doi.org/10.1007/s00424-010-0802-8.
209. Vecchia D, Tottene A, van den Maagdenberg AM, Pietrobon D. Abnormal cortical synaptic transmission in CaV2.1 knockin mice with the S218L missense mutation which causes a

severe familial hemiplegic migraine syndrome in humans. Front Cell Neurosci. 2015;9:8. https://doi.org/10.3389/fncel.2015.00008.
210. Di Guilmi MN, Wang T, Inchauspe CG, Forsythe ID, Ferrari MD, van den Maagdenberg AM, et al. Synaptic gain-of-function effects of mutant Cav2.1 channels in a mouse model of familial hemiplegic migraine are due to increased basal [Ca2+]i. J Neurosci. 2014;34:7047–58. https://doi.org/10.1523/JNEUROSCI.2526-13.2014.
211. Tottene A, Conti R, Fabbro A, Vecchia D, Shapovalova M, Santello M, et al. Enhanced excitatory transmission at cortical synapses as the basis for facilitated spreading depression in Ca(v)2.1 knockin migraine mice. Neuron. 2009;61:762–73. https://doi.org/10.1016/j.neuron.2009.01.027.
212. Terpollili NA, Dolp R, Waehner K, Schwarzmaier SM, Rumbler E, Todorov B, et al. CaV2.1 channel mutations causing familial hemiplegic migraine type 1 increase the susceptibility for cortical spreading depolarizations and seizures and worsen outcome after experimental traumatic brain injury. Elife. 2022;11. https://doi.org/10.7554/eLife.74923.
213. Schizophrenia Working Group of the Psychiatric Genomics C. Biological insights from 108 schizophrenia-associated genetic loci. Nature. 2014;511:421–7. https://doi.org/10.1038/nature13595.
214. Takada Y, Hirano M, Kiyonaka S, Ueda Y, Yamaguchi K, Nakahara K, et al. Rab3 interacting molecule 3 mutations associated with autism alter regulation of voltage-dependent Ca(2)(+) channels. Cell Calcium. 2015;58:296–306. https://doi.org/10.1016/j.ceca.2015.06.007.
215. Shaltiel L, Paparizos C, Fenske S, Hassan S, Gruner C, Rotzer K, et al. Complex regulation of voltage-dependent activation and inactivation properties of retinal voltage-gated Cav1.4 L-type Ca2+ channels by Ca2+-binding protein 4 (CaBP4). J Biol Chem. 2012;287:36312–21. https://doi.org/10.1074/jbc.M112.392811.
216. Zeitz C, Kloeckener-Gruissem B, Forster U, Kohl S, Magyar I, Wissinger B, et al. Mutations in CABP4, the gene encoding the Ca2+-binding protein 4, cause autosomal recessive night blindness. Am J Hum Genet. 2006;79:657–67. https://doi.org/10.1086/508067.
217. Schrauwen I, Helfmann S, Inagaki A, Predoehl F, Tabatabaiefar MA, Picher MM, et al. A mutation in CABP2, expressed in cochlear hair cells, causes autosomal-recessive hearing impairment. Am J Hum Genet. 2012;91:636–45. https://doi.org/10.1016/j.ajhg.2012.08.018.
218. Zhao Y, Huang G, Wu Q, Wu K, Li R, Lei J, et al. Cryo-EM structures of apo and antagonist-bound human Cav3.1. Nature. 2019;576:492–7. https://doi.org/10.1038/s41586-019-1801-3.
219. Shields BC, Kahuno E, Kim C, Apostolides PF, Brown J, Lindo S, et al. Deconstructing behavioral neuropharmacology with cellular specificity. Science. 2017;356. https://doi.org/10.1126/science.aaj2161.
220. Saka SK, Wang Y, Kishi JY, Zhu A, Zeng Y, Xie W, et al. Immuno-SABER enables highly multiplexed and amplified protein imaging in tissues. Nat Biotechnol. 2019;37:1080–90. https://doi.org/10.1038/s41587-019-0207-y.
221. Crunelli V, Toth TI, Cope DW, Blethyn K, Hughes SW. The 'window' T-type calcium current in brain dynamics of different behavioural states. J Physiol. 2005;562:121–9. https://doi.org/10.1113/jphysiol.2004.076273.

Functional Roles of UNC-13/Munc13 and UNC-18/Munc18 in Neurotransmission

Frédéric A. Meunier and Zhitao Hu

Abstract Neurotransmitters are released from synaptic and secretory vesicles following calcium-triggered fusion with the plasma membrane. These exocytotic events are driven by assembly of a ternary SNARE complex between the vesicle SNARE synaptobrevin and the plasma membrane-associated SNAREs syntaxin and SNAP-25. Proteins that affect SNARE complex assembly are therefore important regulators of synaptic strength. In this chapter, we review our current understanding of the roles played by two SNARE interacting proteins: UNC-13/Munc13 and UNC-18/Munc18. We discuss results from both invertebrate and vertebrate model systems, highlighting recent advances, focusing on the current consensus on molecular mechanisms of action and nanoscale organization, and pointing out some unresolved aspects of their functions.

Keywords Munc13 · Munc18 · Exocytosis · Priming · Docking · SNARE complex · Syntaxin · SNAP-25 · Synaptobrevin · Synaptic transmission

1 Introduction

Neurotransmitter release from synaptic terminals is mediated by the fusion of neurotransmitter-filled vesicles with the plasma membrane [1, 2]. Synaptic vesicle fusion is triggered by depolarization-induced calcium influx on a microsecond

F. A. Meunier (✉)
Clem Jones Centre for Ageing Dementia Research (CJCADR), Queensland Brain Institute, The University of Queensland, Brisbane, QLD, Australia

School of Biomedical Sciences, The University of Queensland, Brisbane, QLD, Australia
e-mail: f.meunier@uq.edu.au

Z. Hu (✉)
Clem Jones Centre for Ageing Dementia Research (CJCADR), Queensland Brain Institute, The University of Queensland, Brisbane, QLD, Australia
e-mail: z.hu1@uq.edu.au

Z.-W. Wang (ed.), *Molecular Mechanisms of Neurotransmitter Release*, Advances in Neurobiology 33, https://doi.org/10.1007/978-3-031-34229-5_8

time-scale [3]. This rapidity suggests that a pool of synaptic vesicles is competent or "primed" to undergo membrane fusion immediately upon calcium entry. Vesicle priming and fusion require the function of members of the conserved SNARE (soluble NSF attachment protein receptor; NSF, *N*-ethylmaleimide-sensitive factor) protein superfamily (Fig. 1a) [4–8].

SNAREs are small membrane-associated proteins that contain a conserved SNARE domain (also known as SNARE motif) [9]. Syntaxin and SNAP-25 are plasma membrane-associated SNAREs (*t*-SNAREs, "*t*" for "target"), whereas synaptobrevin is a vesicle membrane-associated SNARE (*v*-SNARE, "*v*" for "vesicle"). *t*-SNAREs and *v*-SNAREs are also known as "Q-SNAREs" and "R-SNAREs", respectively, based on whether an amino acid residue at the center of the SNARE domain is glutamine or arginine (see chapter "SNARE Proteins in Synaptic Vesicle Fusion" for details). Single SNARE domains of syntaxin and synaptobrevin interact with two SNARE domains in SNAP-25 to form a parallel four alpha-helical bundle termed the SNARE complex. SNARE complexes may be assembled either *in trans* from *t*- and *v*-SNAREs located on different membranes (plasma membrane and vesicle membrane) or in *cis* from *t*- and *v*-SNAREs located on the same membrane. SNARE complex assembly in *trans* is predicted to bring the vesicle membrane into close apposition with the plasma membrane [6, 10, 11]—a prerequisite for membrane fusion. In fact, loss of syntaxin function results in a decrease in the number of synaptic vesicles contacting the plasma membrane near presynaptic dense

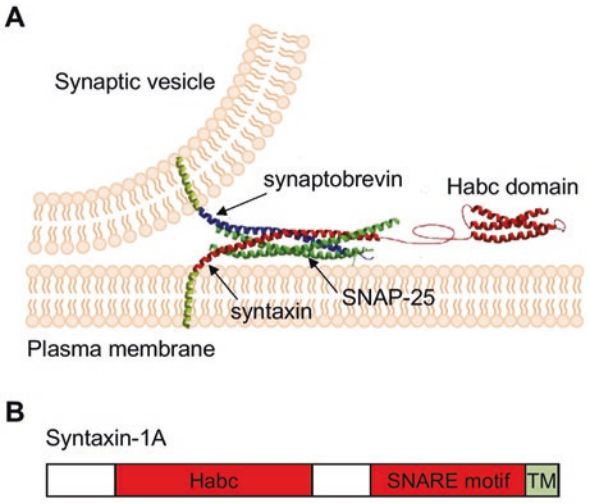

Fig. 1 SNARE complexes mediate synaptic vesicle priming and fusion. (**a**) Vesicle-associated SNARE synaptobrevin (blue), and plasma membrane-associated SNAREs syntaxin (red) and SNAP-25 (green) assemble into a four-helix bundle, which bridges the gap between the two membranes to promote priming and fusion. Syntaxin is in the open conformation where the Habc domain is not folded back against the SNARE domain. (**b**) Domain structure of syntaxin-1A. (Figure adapted from Sutton et al. [10])

projections [12, 13], suggesting that some of the synaptic vesicles represent the morphological equivalent of functionally primed vesicles [12, 14].

Syntaxin contains four α-helical domains, Ha, Hb, Hc, and H3 (Fig. 1b). The H3 domain is the SNARE domain that binds to the SNARE domains of synaptobrevin and SNAP-25. In solution, syntaxin adopts a default "closed" confirmation in which its N-terminus, containing the Habc alpha helices, folds over and occludes its C-terminal SNARE domain [15]. Syntaxin must adopt an "open" configuration to expose its SNARE domain in order for SNARE complex assembly to proceed (Fig. 1). Some proteins that bind syntaxin may therefore regulate vesicle priming by modulating SNARE interactions. Both UNC-13/Munc13 [16, 17] and UNC-18/Munc18 [18, 19] bind syntaxin and are implicated in the regulation of synaptic vesicle priming. Here we review the evidence implicating these proteins in vesicle priming and fusion, discuss the interaction between them and the SNAREs, and outline current models for how these proteins function in this critical process.

2 UNC-13/Munc13

2.1 Identification

The *unc-13* gene was first identified in 1974 in a genetic screen for *Caenorhabditis elegans* mutants showing uncoordinated (unc) movements by the Nobel Laureate Sydney Brenner, with the aim of identifying genes required for synaptic transmission at neuromuscular junctions (NMJs) [20]. Subsequently, homologous genes were identified in other species, including Munc13 in mammals and Dunc13 in *Drosophila*. It appears that UNC-13 homologs only exist in organisms that have nervous systems. UNC-13 and its homologs have multiple isoforms (Fig. 2). In both *C. elegans* and *Drosophila*, a single gene produces two different isoforms of proteins from alternative splicing [21, 22]. In mouse, four different genes (Munc13-1 to -4) give rise to five Munc13 isoforms, including Munc13-1, ubMunc13-2, bMunc13-2, Munc13-3, and Munc13-4 [23, 24].

2.2 Expression

All the UNC-13 isoforms in *C. elegans* and *Drosophila* are expressed pan-neuronally, and are highly enriched at presynaptic terminals but they show differential distributions at presynaptic sites. At the *C. elegans* NMJ, the long isoform UNC-13L exhibits colocalization with the active zone protein UNC-10/RIM, a Ca^{2+} channel recruiter, whereas the short isoform UNC-13S displays a relatively diffuse distribution and is located further away from the site of Ca^{2+} entry [25]. At the *Drosophila* NMJ, UNC13A is localized only 70 nm away from Ca^{2+} channels,

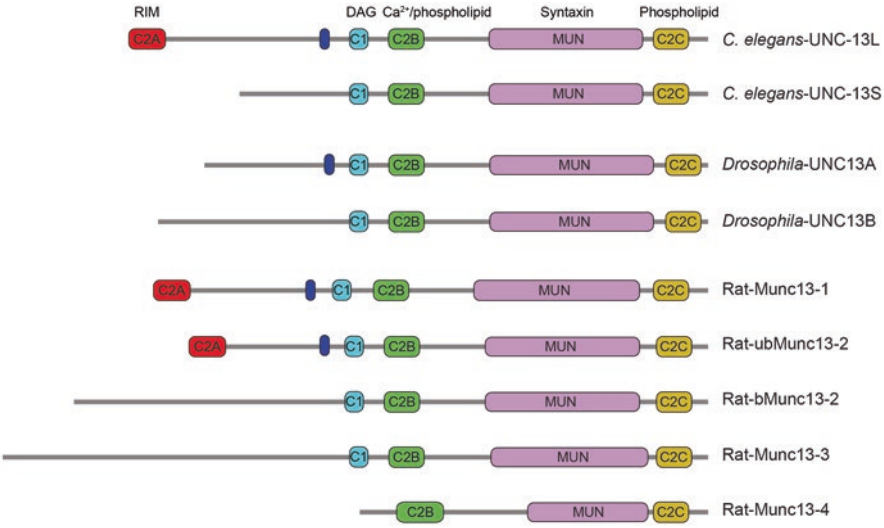

Fig. 2 UNC-13/Munc13 isoforms in different species. Domain structures of UNC-13/Munc13 from *C. elegans*, *Drosophila*, and rat are shown. The blue box represents the calmodulin-binding domain. The other major domains are identified by their binding partners indicated in *C. elegans*-UNC-13L. (Domain structure is predicted by Pfam.xfam.org)

whereas UNC13B is localized 120 nm away [26]. In rodent brains, Munc13-1, -2, and -3 are all expressed in the nervous system, but they exhibit tissue and temporal expression specificity [24, 27–29], with Munc13-1 being the prominent isoform in many central synapses and highly concentrated at active zones, bMunc13-2 having a lower expression level and displaying more diffuse expression relative to active zone proteins [30], and Munc13-3 being primarily expressed in the cerebellum [28, 29, 31]. Recent studies show that Munc13-3 is also expressed in perforant path terminals targeting the dendrites of granule cells in the hippocampus [32], and in calyx of Held synapses [30]. In contrast, Munc13-4 is barely detectable in brain tissues but broadly expressed in other tissues [33].

2.3 Structure

UNC-13/Munc13 are large (1500–2000 amino acid) multi-domain proteins. In general, UNC-13/Munc13 isoforms are grouped into two classes based on the presence or absence of an extended amino terminus (Fig. 2). In *C. elegans* and mouse, the N-termini of UNC-13L, Munc13-1, and ubMunc13-2 contain a C2A domain and a calmodulin-binding domain, whereas the other isoforms lack these domains. The C2A domain exhibits a highly conserved interaction with the active zone protein UNC-10/RIM, thereby localizing the proteins close to Ca^{2+} entry sites [34–37]. The Ntermini of the UNC-13/Munc13 isoforms without a C2A domain may also have

distinct binding partners. For example, the coiled-coil motif in the N-terminal of bMunc13-2 binds to the active zone protein ELKS1, and this interaction is critical for proper localization of bMunc13-2 [38]. In *Drosophila*, neither UNC13A nor UNC13B contains a C2A domain, but UNC13A possesses a calmodulin-binding domain in its N-terminus [39]. Despite the differences in their N-termini, all UNC-13/Munc13 isoforms have a highly conserved C-terminal region, consisting of a diacylglycerol (DAG)-binding C1 domain [40], a Ca^{2+} and phospholipid-binding C2B domain [41], a SNARE-binding MUN domain [17], and a phospholipid-binding C-terminus which includes a C2C domain [42, 43].

2.4 Function

2.4.1 Overall Function

The functional importance of UNC-13/Munc13 has been investigated in both vertebrates and invertebrates. Mutants lacking *unc-13* or its homologs exhibit a nearly complete loss of neurotransmitter release from presynaptic nerve terminals, as indicated by the absence of both spontaneous and evoked neurotransmitter release. This is associated with a severe reduction in the size of the readily releasable pool (RRP) of synaptic vesicles [39, 44, 45], demonstrating that UNC-13/Munc13 is required for vesicle priming. Consistent with this notion, overexpression of Munc13-1 in chromaffin cells increases the pool of readily releasable dense-core vesicles [46]. The priming function of UNC-13/Munc13 is also supported by its synaptic localization near electron-dense presynaptic specializations (termed dense projections) [14], which are thought to be presynaptic organizers for many of the proteins required for neurotransmitter release, such as voltage-gated calcium channels, liprin, bassoon, piccolo, CAST, and RIM [47]. UNC-13/Munc13 localization to sites near dense projections may ensure that vesicle priming occurs at appropriate sites near calcium channels [14]. Ultrastructural analysis of the synaptic morphology by high-pressure freezing electron microscopy has revealed that the number of plasma membrane-contacting vesicles is significantly reduced in *unc-13*/Munc13 knockout mutants, indicating that UNC-13/Munc13 is also required for vesicle docking [12, 13, 48]. Despite the striking phenotype in synaptic transmission, *unc-13*/Munc13 knockout mutants display normal nervous system architecture [44, 49].

2.4.2 Functions of UNC-13/Munc13 Isoforms

Multiple UNC-13/Munc13 isoforms coexist in many synapse types, such as NMJs in worms and flies, the calyx of Held synapse in the mouse auditory system, and the glutamatergic synapses in the mouse hippocampus. In general, the isoforms that localize close to Ca^{2+} entry sites (i.e., UNC-13L, UNC13A, and Munc13-1) play dominant roles in synaptic transmission, with knockout of these isoforms leading to

a ~90% reduction in evoked neurotransmitter release (Fig. 3) [25, 26, 49]. In contrast, knockout of the isoforms that are further away from Ca^{2+} entry sites (i.e., UNC-13S, UNC13B, and bMunc13-2) either does not produce any change or leads to only a minor decrease in evoked neurotransmitter release [25, 26, 49] (Fig. 3). In some synapse types, Munc13 isoforms appear to have redundant functions. For example, evoked GABA release is not affected by the knockout of either Munc13-1 or Munc13-2 in hippocampal GABAergic neurons, but is abolished in Munc13-1/2 double-knockout neurons [49]. Expression of either the C2A-containing or the C2A-lacking UNC-13/Munc13 isoforms in *unc-13*/Munc13 null mutants is sufficient to restore the RRP in worms and mice, suggesting that they are all able to prime synaptic vesicles [25, 49].

2.4.3 Functions in Release Kinetics

In addition to their roles in vesicle docking, priming, and fusion, UNC-13/Munc13 isoforms are also involved in regulating the kinetics of neurotransmitter release. At the *C. elegans* NMJ, evoked EPSCs in *unc-13* null mutants rescued by UNC-13L and UNC-13S independently exhibit significantly faster and slower kinetics,

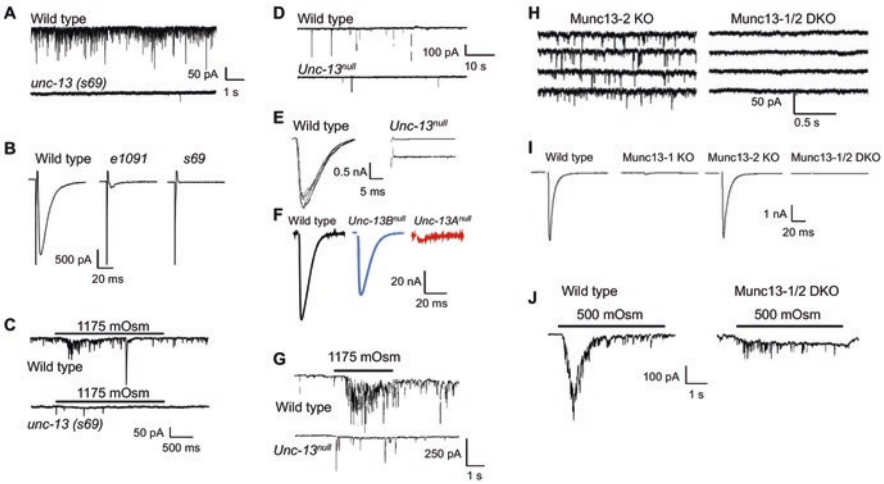

Fig. 3 The function of UNC-13/Munc13 in synaptic transmission in vertebrates and invertebrates. Miniature excitatory postsynaptic currents (mEPSCs), stimulus-evoked EPSCs, and hypertonic sucrose-evoked responses recorded at the *C. elegans* NMJ (**a**–**c**) and the *Drosophila* NMJ (**d**–**g**), and in cultured mouse hippocampal neurons (**h**–**j**). In *C. elegans*, both UNC-13 isoforms are eliminated in the *s69* null mutants, whereas only the long isoform (UNC-13L) is present in the *e1091* mutants. Synaptic transmission is nearly abolished in *unc-13*/Munc13 null mutants in all species. UNC-13L in worm, Unc13A in fly, and Munc13-1 in mice are the primary isoforms that account for the majority of neurotransmitter release in the indicated synapse types, whereas other isoforms play minor roles in those synapses. (This figure was adapted from Aravamudan et al. [39], Augustin et al. [45], Richmond et al. [44], Varoqueaux et al. [49], and Bohme et al. [26])

respectively, than those observed in wild type [25, 50] (Fig. 4a, b). Interestingly, UNC-13L colocalizes with UNC-10/RIM, which physically binds to voltage-gated Ca^{2+} channels [51], whereas UNC-13S has a more diffuse distribution and is located further away from UNC-10/RIM (Fig. 4c). The apparent inverse relationship between the effects of these two UNC-13 isoforms on the rise rate of evoked EPSCs, and their relative distances from UNC-13/RIM, suggests that the fast and slow kinetics of vesicle fusion are due to tight and loose couplings, respectively, between synaptic vesicles and the Ca^{2+} entry site. Studies in fly and mouse also show that distinct UNC13/Munc13 isoforms localize at different synaptic regions relative to Ca^{2+} entry, thereby triggering release with different kinetics, likely by mediating synaptic vesicles from different pools [26, 30].

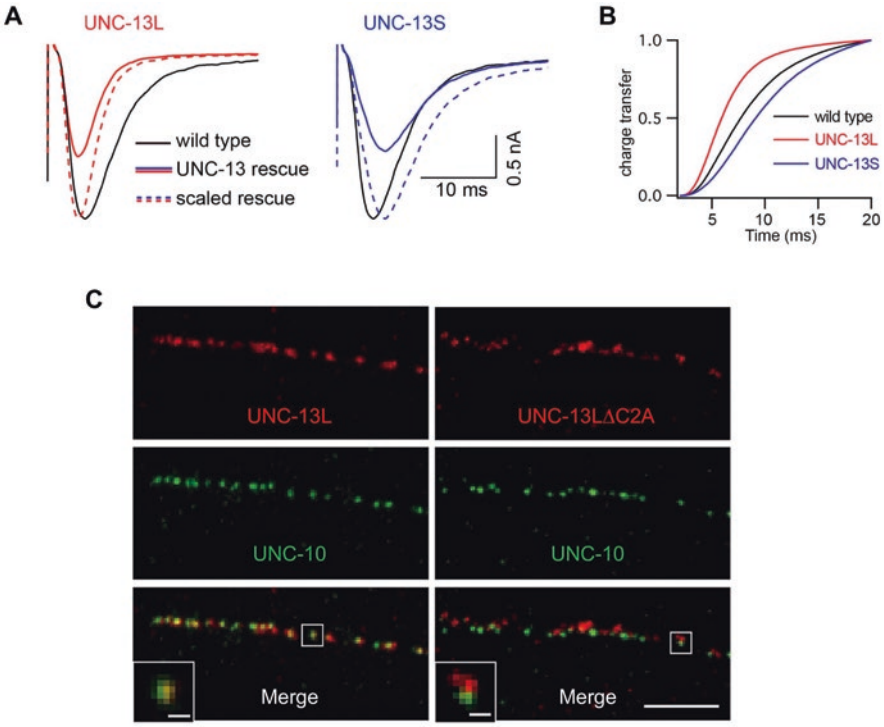

Fig. 4 Fast and slow neurotransmitter release at the *C. elegans* neuromuscular junction are mediated by UNC-13L and UNC-13S, respectively. (**a**) Stimulus-evoked excitatory postsynaptic currents were recorded from body wall muscle cells of wild-type worms and *unc-13(s69)* mutant worms rescued by either UNC-13L (red) or UNC-13S (blue). The dashed curves represent EPSCs normalized to wild-type EPSC amplitude. (**b**) The normalized cumulative charge transfer shows the overall release kinetics of the EPSCs. (**c**) Localization of UNC-13L and UNC-13LΔC2A relative to the active zone marker UNC-10/RIM. The C2A domain is critical to positioning UNC-13 at the release sites close to points of Ca^{2+} entry. (Figure adapted from Hu et al. [25] and Zhou et al. [50])

2.4.4 Functions of Different Domains

As a synaptic hub protein, the function of UNC-13/Munc13 is determined by its various functional domains, which have different binding partners. Although it is still unclear how different domains are coordinated, the function of each individual domain has been investigated in different model organisms.

The MUN Domain

To define the region of UNC-13/Munc13 required for vesicle priming, attempts to identify a minimal UNC-13/Munc13 rescuing fragment have been made in different species. In cultured neurons from Munc13-1/2 double-knockout mice, overexpression of the MUN domain (amino acids 859-1531) partially restores evoked glutamate and GABA release, accompanied by a partial recovery of the RRP in excitatory hippocampal neurons and a full recovery of the RRP in inhibitory hippocampal neurons [52], demonstrating the function of the MUN domain in vesicle priming. Consistent with this finding, studies in chromaffin cells and the *C. elegans* NMJ have revealed that MUNC2C is the minimal fragment required for priming, and any fragment lacking the MUN domain fails to restore the RRP [16, 53], highlighting the MUN domain of UNC-13/Munc13 as the primary regulator of priming activity.

A study using the C-terminal region of Munc13-1 (amino acids 1181-1736) as bait in a yeast two-hybrid screen identified syntaxin-1B as a binding partner [17]. The clones isolated in this screen encoded the first two alpha helices (Ha and Hb) of syntaxin, suggesting that the role of UNC-13/Munc13 in vesicle priming is through its interaction with the syntaxin N-terminus. This notion is supported by the observations that mutations disrupting syntaxin binding to the MUN domain abolish Munc13-1-dependent dense-core vesicle priming [53], and that mutations in the *C. elegans* UNC-13S MUN domain (K1000A/K1002A) that disrupt syntaxin binding also reduce evoked neurotransmitter release [16]. Recent crystal structure studies of the MUN domain have also identified two highly conserved residues that mediate the interaction of MUN and syntaxin (N1128 and F1131 in Munc13-1). Substitution of these two residues by alanine in Munc13-1 abolishes the stimulatory effect of the MUN domain on SNARE complex assembly, and mutations of the corresponding amino acid residues in *C. elegans* UNC-13S reduces synaptic transmission [54]. Together, these experiments indicate that UNC-13/Munc13 promotes synaptic vesicle priming and exocytosis through interacting with syntaxin.

The observed interaction between the MUN domain and syntaxin has led to the speculation that UNC-13/Munc13 may facilitate vesicle priming by promoting or stabilizing the open conformation of syntaxin [55]. In *C. elegans unc-13* mutants, introduction of a constitutively open UNC-64/syntaxin-1A (caused by L166A and E167A mutations), partially restored synaptic vesicle priming, suggesting that UNC-13 is involved in the transition of syntaxin from its closed to open configuration [16, 56]. This was further supported by NMR and fluorescence spectroscopy showing that the Munc13-1 MUN domain dramatically accelerates the transition of syntaxin-1 from being a molecular complex with Munc18-1, which keeps syntaxin in the closed state, to the assembled SNARE complex [57].

The incomplete rescuing effect of open UNC-64/syntaxin-1A on *unc-13* mutant synaptic phenotypes [56, 58] suggests that UNC-13 may play additional roles in exocytosis [58, 59]. Indeed, recent studies have revealed that the MUN domain also promotes the proper arrangement of the SNARE domains within the SNARE complex [60, 61]. In the SNARE complex, all the four α-helices are arranged with their amino and carboxyl terminal ends in the same direction [10]. When the ternary SNARE complex is assembled in vitro starting from a syntaxin/SNAP25 assembled docking platform, the MUN domain promotes the proper N- to C-terminal parallel configuration between syntaxin and synaptobrevin [60]. This function of the MUN domain significantly improves the efficiency of Ca^{2+}-triggered single-vesicle fusion, emphasizing its indirect role in Ca^{2+}-mediated vesicle fusion. In addition to this function, the MUN domain also cooperates with Munc18 to mediate the proper syntaxin and SNAP-25 configuration within the SNARE complex such that the two SNARE domains of SNAP-25 orient along syntaxin in the N to C direction. These recent findings have expanded our understanding that the MUN domain is not only required at the initial step but also throughout the process of SNARE assembly.

The C1 Domain

The C1 domain in UNC-13/Munc13 was originally found to bind to phorbol ester (PE) and diacylglycerol (DAG) [62], and this interaction promotes recruitment of Munc13 to the plasma membrane in human embryonic kidney cells (HEK293) [63]. In calyx of Held and hippocampal synapses, PE treatment strongly enhances synaptic potentiation, which is occluded by a point mutation in Munc-13-1 (H567K) that blocks C1 binding to PE [59, 64, 65]. Studies in *C. elegans* have shown that mutation of the corresponding amino acid residue (H173K) in UNC-13S eliminates a PE-induced hypersensitivity of animals to the acetylcholinesterase inhibitor aldicarb, which reflects enhanced cholinergic synaptic transmission [66]. In addition, the H567K mutation significantly increases synaptic transmission without altering the RRP, indicating a higher release probability. The mutation is therefore considered a gain-of-function mutation in UNC-13/Munc13. This notion is supported by the fact that synaptic transmission in Munc13-1^{H567K} synapses is similar to that in PE-potentiated wild-type synapses. These observations have led to the hypothesis that the C1 domain may serve as an autoinhibitory domain to inhibit UNC-13 function in neurotransmitter release [65, 67–69]. This hypothesis is supported by the recent observation that a complete deletion of the C1 domain enhances neurotransmitter release [70–72].

Recent studies in *Drosophila* have revealed that the UNC-13 C1 domain is also a target of ethanol. Flies with reduced activity of UNC13 exhibit significantly higher preference for ethanol in comparison to wild type [73], and this phenotype is rescued by expression of rat Munc13-1, demonstrating that Munc13-1 is a conserved presynaptic regulator of ethanol-related behaviors. The C1 domain of Munc13 appears to be the target site for ethanol binding in vitro because mutation of G582 within it reduces ethanol binding. The Munc13-1 C1 domain also shows higher conformational stability in the presence of ethanol [74]. Intoxicating levels of ethanol exposure do not impact either Ca^{2+} influx or membrane depolarization, but

dramatically inhibits synaptic vesicle fusion in fly olfactory sensory neurons [75]. Ethanol binding to the C1 domain at concentrations comparable with binge exposure reduces binding of DAG, which might reduce neuronal activity by interfering with DAG-mediated localization of Munc13 to the synaptic membrane [75]. These studies highlight the importance of the Munc-13 C1 domain in alcohol-induced changes in neuronal activity and cognitive functions.

The C2B Domain

The C2B domain of Munc13 is known as a Ca^{2+} and phospholipid-binding motif. The crystal structure of the C2B domain in the presence or absence of Ca^{2+} consists of a typical C2 domain β-sandwich fold with top loops containing Ca^{2+} binding sites [41, 76]. It should be noted that Ca^{2+}-dependent phospholipid binding of Munc13 C2B occurs at relatively high concentrations of phosphatidylinositol 4-phosphate (PIP) and phosphatidylinositol 4,5-bisphosphate (PIP_2) in comparison to other C2 domains (e.g., the C2B domain in synaptotagmin-1). This unusual biochemical property of the Munc13 C2B domain has been partially attributed to its Ca^{2+}-binding loop 3 which uniquely contains a protruding α-helix. A point mutation in loop 1 that renders the phospholipid-binding properties of the Munc13-2 C2B domain similar to those of synaptotagmin-1 significantly increases neurotransmitter release probability [41]. Replacement of two aspartate residues (D629 and D635) in loop 1 by asparagine abolishes Ca^{2+} binding and Ca^{2+}-dependent phospholipid binding to the C2B domain. This impairs synaptic facilitation induced by action potential trains but not evoked neurotransmitter release caused by single action potentials in mouse neuronal cultures, suggesting that the C2B domain acts as a Ca^{2+}-dependent regulator of short-term synaptic plasticity. A recent study showed that the binding of the Munc13-1 C2B domain to Ca^{2+} and phospholipid fine-tunes the rate of synaptic vesicle replenishment following a train stimulus [77].

In *C. elegans,* deleting the C2B domain in either UNC-13L or UNC-13S enhances Ca^{2+}-dependent neurotransmitter release and causes an increased sensitivity to aldicarb, which inhibits worm locomotion by inhibiting the breakdown of acetylcholine to cause sustained muscle contraction [78]. These results suggest that the C2B domain may have an autoinhibitory function in UNC-13, similar to that of the C1 domain [70–72]. The aldicarb hypersensitivity is not observed in worms expressing a mutated isoform of UNC-13L, in which its C2B domain is replaced by that of rat Munc13-1, suggesting that the function of the C2B domain is conserved. The similar autoinhibitory functions of the C1 and C2B domains suggest that they might function cooperatively as a module. Consistently, in the crystal structure of the C1C2BMUN fragment, the Ca^{2+}-binding loops of the C2B domain lie in close proximity to the DAG/PE-binding region of the C1 domain [67]. This arrangement is expected to promote cooperation between the C1 and C2B domains in membrane binding, providing a structural basis for synergy between increases in DAG and Ca^{2+} to enhance the release probability in response to repetitive stimulation. The inhibitory effects of C1 and C2B domains on spontaneous release are more robust in the absence of Ca^{2+} than in the presence of Ca^{2+}, suggesting that Ca^{2+} may antagonize the autoinhibitory effects [70,

71]. The Ca^{2+}-dependent disinhibition of UNC-13 allows synaptic vesicles to move into a superpriming state in which the vesicles are more fusogenic, likely resulting from function of the MUN domain. This notion is supported by the recent findings in *C. elegans* that deleting either the C1 and C2B domains in UNC-13S, or the C1, C2B, and the linker domain between C2A and C1 in UNC-13L (also called sUNC-13), produces hyperactive UNC-13 proteins that dramatically increase Ca^{2+} sensitivity and release probability but decrease synaptic depression [70, 71]. Moreover, the hypersecretion induced by sUNC-13 is partially due to a more efficient function of the MUN domain in promoting the open syntaxin conformation. These recent studies suggest that the C1 and C2B domains act in concert to stabilize an inactive state of UNC-13/Munc13 in the absence of membrane recruitment signals such as Ca^{2+}, PIPs, and DAG.

The C2C Domain

All UNC-13/Munc13 isoforms contain a highly conserved C-terminal sequence with a C2C domain. Several studies have shown that perturbing the C-terminal end of UNC-13/Munc13 has deleterious functional consequences at the synapse. UNC-13/Munc13 lacking the C-terminal region is unable to prime synaptic vesicles in *C. elegans* and hippocampal neurons [16, 43], and dense-core vesicles in chromaffin cells [53]. Studies in *C. elegans* have revealed that one or two alpha helices in the MUN domain that precedes the C2C domain and a predicted alpha helix of the last 60 residues (MCT) fold together into a stable membrane-binding protein domain in vitro [42]. Deletion of either C2C or MCT impairs synaptic transmission, decreases synaptic vesicle priming, and disrupts nervous system function [42], providing further evidence that the C-terminal sequence is indispensable for UNC-13/Munc13 function. Despite these advances, it remains unclear how the C-terminal region in UNC-13/Munc13 mediates vesicle priming and fusion due to a lack of structural information. In the crystal structure of the C1C2BMUN fragment, the MUN domain has a long rod-like shape with the C1 and C2B domains packed on one end [67] (Fig. 5a, b). This structure has led to a bridge model, in which the C1 and C2B domains bind to the plasma membrane, whereas the C-terminal region binds to synaptic vesicle membranes (Fig. 5c). Two experimental results support this model. First, mutations in C2C that disrupt liposome binding strongly impair in vitro liposome fusion as well as in vivo synaptic vesicle docking, priming, and fusion [43]. Second, a deficiency in aldicarb sensitivity, which reflects reduced synaptic transmission, caused by a loss of the C-terminal region is significantly restored by artificially tethering the UNC-13 C-terminus to synaptic vesicles but not the plasma membrane [42]. These findings indicate that the C-terminal region serves as an attachment site for synaptic vesicles, and that this association is required for efficient docking and priming.

The C2A Domain

The C2A domain, present in *C. elegans* UNC-13L as well as mammalian Munc13-1 and ubMunc13-2, was first found to bind to the zinc finger domain (ZF) of RIM to form a heterodimer [37]. Crystal structure of the C2A domain has revealed that the

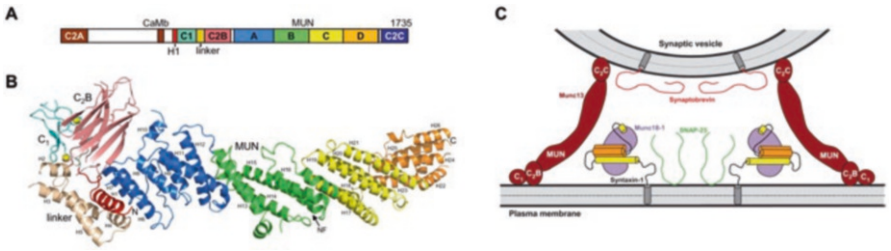

Fig. 5 Crystal structure of Munc13-1 C1C2BMUN domains and the model of UNC-13/Munc13 in promoting vesicle fusion. (**a**) Domain structure of rat Munc13-1. The major domains include C2A, CaMb (calmodulin-binding domain), C1, C2B, MUN (subdomains A–D), and C2C. (**b**) Structure of C1-C2B-MUN (color coded similar to panel A with helices labeled). Zn^{2+} bound to the C1 domain is shown as yellow spheres. (**c**) The bridge model of UNC-13/Munc13 function. In this model, the C1 and the C2B domains interact with the plasma membrane, and the C-terminal end sequence including the C2C domain binds to the vesicle membrane, allowing the MUN domain to promote the transition from the syntaxin-Munc18-1 complex to the SNARE complex. (Adapted from Xu et al. [67])

Munc13-1 C2A domain forms a tight homodimer, and that the configuration of the C2A/C2A homodimer competes with that of a C2A/RIM heterodimer [36, 79]. Studies have been conducted with mice and *C. elegans* to understand how interactions between Munc13-1 and RIM couples synaptic vesicle priming to presynaptic plasticity. In cultured hippocampal neurons, the Munc13-1 C2A/C2A homodimer locks Munc13-1 in an autoinhibitory state, which inhibits synaptic vesicle priming; formation of the C2A/ZF heterodimer between Munc13-1 and RIM switches on the priming function of Munc13-1 [35]. Ultrastructural analyses of synaptic morphology by electron microscopy indicate that the heterodimer of Munc13-1 C2A and RIM also regulates synaptic vesicle docking [48]. In *C. elegans*, UNC-13L can also form C2A/C2A homodimers and C2A/RIM heterodimers, demonstrating that the homo- and hetero-interactions are conserved across species. Disrupting UNC-13L homodimerization does not lead to changes in synaptic transmission, whereas blocking C2A/RIM heterodimerization decreases the probability of neurotransmitter release. It should be noted that the priming of synaptic vesicles in *C. elegans* requires neither the heterodimerization of UNC-13 C2A/RIM nor the C2A domain of UNC-13, as animals lacking the C2A domain of UNC-13L exhibit primed vesicle levels similar to those of wild-type animals [34]. Moreover, the monomeric C2A domain still supports tonic release, and evoked release still occurs albeit at a reduced level in the absence of C2A/RIM heterodimerization [34]. The different results from the mouse and worm studies suggest that the priming mechanism is not entirely identical between these two species.

Other N-Terminal Domains

Although some UNC-13/Munc13 isoforms do not have a C2A domain, their N-terminal sequences also play important regulatory roles in synaptic transmission. It has been shown that the coiled-coil motif in the N-terminus of bMunc13-2 binds to the active zone protein ELKS1, and this interaction is critical to the proper

localization of bMunc13-2 and is required for synaptic vesicle priming in hippocampal synapses [38]. At *Drosophila* olfactory synapses, UNC13A and UNC13B isoforms are clustered at different positions in the release site by the active zone protein Bruchpilot (Brp, mammalian ELKS1 ortholog) and Syd-1, respectively, likely through interactions with their N-terminal sequences [80]. At the *C. elegans* NMJ, an N-terminal M domain in UNC-13S (1-259aa) inhibits the probability of neurotransmitter release by interacting with the C1 and C2B domains. Moreover, the M domain may enhance the release probability when it is fused to the MUNC2C fragment, suggesting that this domain also has intrinsic facilitatory functions [70]. However, it remains to be determined whether the M domain is regulated by other proteins for its function. These studies reveal various mechanisms by which the N-terminal sequences in C2A-lacking UNC-13/Munc13s regulate protein localization and function.

The Calmodulin-Binding Domain

A calmodulin-binding domain (CaMb) exists in all C2A-containing UNC-13/Munc13 isoforms of *C. elegans* and mice, as well as in the UNC13A isoform of *Drosophila*. This domain consists of several amino acid residues that are highly conserved across species. Calmodulin binds to the CaMb domain in a Ca^{2+}-dependent manner [81, 82]. Unlike the Munc13 C2B domain, which is directly activated by Ca^{2+} influx during action potentials, the CaMb domain is stimulated only after the synthesis of PIPs in response to accumulating residual Ca^{2+}. In mice, arginine substitution of a conserved tryptophan residue in the CaM-binding motif of either Munc13-1(W464R) or ubMunc13-2(W387R) completely abolishes CaM binding [81]. In autaptic cultures of hippocampal neurons expressing these mutated Munc13 isoforms, evoked synaptic transmission and vesicle priming are normal, indicating that basal priming and release do not require CaM binding to Munc13. However, disruption of Munc13 binding to CaM causes great changes in synaptic plasticity. Specifically, a high-frequency stimulation-induced synaptic depression associated with wild-type Munc13-1 becomes more pronounced in the presence of Munc13-1(W464R), and the moderate augmentation normally observed following a stimulation train is reduced, suggesting a deficiency in refilling the primed pool of vesicles. Similarly, the calyx of Held synapse in Munc13-1(W464R) knockin mice exhibits a slower rate of synaptic vesicle replenishment, aberrant short-term depression, and reduced recovery from synaptic depression after high-frequency stimulation [69]. In *C. elegans*, rescue of an *unc-13* null mutant (*s69*) with a chimeric UNC-13 protein containing the predicted CaM-binding domain fused with the R domain (UNC-13 region containing the C1, C2B, MUN, and C2C domains) results in evoked responses with significantly faster activation kinetics and more EGTA-resistance than that with UNC13R [25]. This shows that the CaM-binding domain expedites release kinetics and reinforces Ca^{2+} coupling. These studies place Ca^{2+}-CaM-Munc13-1 as a core complex in facilitating short-term plasticity.

3 UNC-18/Munc18

3.1 Identification

Like UNC-13, UNC-18 was first implicated in the regulation of synaptic transmission as a result of forward genetic screens conducted by the Nobel Laureate Sydney Brenner [20]. Based on the premise that mutations disrupting genes required for synaptic transmission would result in locomotory defects in the soil nematode *C. elegans*, Brenner identified and named the 18th isolated uncoordinated mutant *unc-18*. Null mutations in the *unc-18* locus result in almost complete paralysis of *C. elegans*. UNC-18 is a ~67 kDa cytosolic protein [83], and is a member of a molecularly and structurally conserved protein family. Most organisms contain between 4 and 7 genes encoding UNC-18-related proteins (4 in yeast and flies, 6 in worms, and 7 in humans and mice). Although all of them perform conserved functions in vesicle trafficking and fusion, they may play such roles in different intracellular compartments (see review by Toonen and Verhage [84]). The closest homologs of UNC-18 are Sec1p in yeast [85], and Munc18-1/n-sec-1/rbsec1, Munc18-2, and Munc18c (encoded by three different genes) in mice [84, 86], which has led to the general name SM (Sec/Munc18) proteins for this family of proteins. In *Drosophila*, the homolog is Rop [87]. UNC-18, Munc18-1, and Rop are all enriched in neurons, whereas Munc18-2 is largely expressed in epithelial cells and Munc18c is ubiquitous.

3.2 Structure

UNC-18/Munc18 proteins contain three domains within the broadly conserved Sec1 homology region, named domains 1–3 (Fig. 6a). The crystal structure of rat Munc18-1 (also known as neuronal Sec1/nSec1) reveals a horseshoe-shaped molecule with a central cavity (~15 A wide) lined by amino residues of domains 1 and 3 [88] (Fig. 6b). Crystal structures solved for several other SM family members, including squid Sec-1 [89], yeast Sly1p [90], and mouse Munc18c [91], exhibit a similar horseshoe structure with conserved binding pockets (Fig. 6b), indicating that SM proteins have conserved structural features.

3.3 Function

Mutant analyses indicate that various SM proteins play a conserved role in membrane fusion by acting at distinct intracellular locations [84, 92–94]. For SM proteins acting at presynaptic sites, disruption of their functions invariably leads to severe release defects, as exemplified by *C. elegans unc-18* null mutants (Fig. 6c) [95]. In *Drosophila* Rop null mutants, which cannot be directly analyzed for

synaptic transmission at the NMJ due to an embryonic lethality phenotype, indirect assessment of neurotransmission in temperature-sensitive Rop mutants by electroretinogram suggests an absence of neurotransmission at non-permissive temperatures [87]. In neonates of Munc18-1 knockout mice, all synaptic activities are absent in spite of apparently normal synaptogenesis [96]. In chromaffin cells from the Munc18-1 null mice, the release of catecholamines is severely impaired [97]. These defects of synaptic transmission and chromaffin cell function have been attributed to a reduction in the readily releasable vesicle pool (RRP) based on a reduced number of synaptic vesicles contacting the presynaptic plasma membrane and reduced postsynaptic current response to hypertonic sucrose solutions (an assay for assessing the size of the RRP) in Munc18/*unc-18* mutant worms and mice [95, 97, 98] (Fig. 6c, d).

SM proteins are one of several protein classes implicated in vesicle docking. However, molecular events and functional consequences of the docking process are not fully understood, which is partly because docked vesicles are identified based on variable morphological criteria, and their numbers differ depending on the imaging techniques used [12, 14, 99, 100]. It is also likely that docking measured by stationary analysis (i.e., fixed tissues) does not capture the true vesicle docking status [101]. Live cell imaging by total internal reflection fluorescence microscopy (TIRFM) suggests that the Munc18-1-dependent docking defect represents changes in several kinetically distinct vesicle docking states. In wild-type chromaffin cells, vesicle docking can be described as three states based on the dwell time: transiently

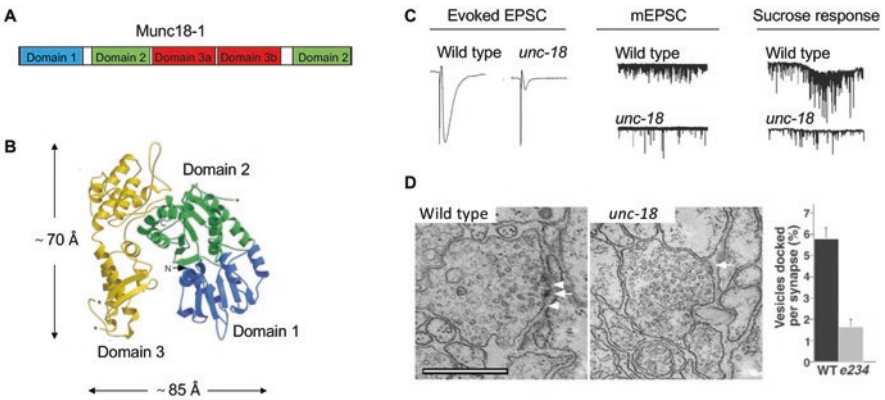

Fig. 6 The crystal structure and function of UNC-18/Munc18. (**a**) Domain architecture of nSec1/Munc18-1. (**b**) The crystal structure of rat Munc18-1 reveals that the Sec1 homology region forms a horseshoe-shaped topography with a central cavity lined by domains 1 and 3. (**c**) *unc-18(e234)* mutant of *C. elegans* exhibits dramatic decreases in the amplitude of evoked excitatory postsynaptic currents (EPSC), the frequency of miniature EPSC (mEPSC), and the postsynaptic currents induced by a hypertonic sucrose solution at the neuromuscular junction. (**d**) Consistent with a decrease in primed vesicles, fewer vesicles contact the plasma membrane at the NMJ in *unc-18* mutants than wild type. White arrowheads indicate docked SVs. (Figure adapted from Weimer et al. [95] and Misura et al. [88])

visiting (<1 s), short-retained (1–10 s), and long-retained (>10 s). Incidents of both visiting and long-retained events are significantly reduced in the Munc18-1 mutant compared with the wild type, which accounts for the reduced number of docked vesicles observed by conventional EM [102]. In the absence of Munc18-1, vesicle docking appears to be hindered by a thickening of the submembrane actin cytomatrix, as actin depolymerization by latrunculin restores morphological docking in Munc18-1 mutant cells. However, the docked vesicles restored by latrunculin treatment remain fusion-incompetent and exhibit weaker tethering forces than wild-type docked vesicles, as measured by an autocorrelation analysis [102]. These results suggest that strong vesicle tethering likely correlates with the primed state. Consistent with this notion, some vesicle-tethering events in wild-type chromaffin cells display unusually long dwell times under conditions that promote vesicle priming [101]. Because cleavage of either syntaxin-1A or SNAP-25 in chromaffin cells by clostridial neurotoxin C also reduces strong tethering of vesicles [102] and results in reduced morphological docking [103], it appears that strongly tethered docked vesicles represent the morphological correlates of functionally primed vesicles [101, 102]. Consistently, the number of docked vesicles in synapses of *C. elegans* prepared by high-pressure freezing fixation is greatly decreased in priming-defective *unc-64*/syntaxin-1A and *unc-13* mutants compared with wild type [12, 14]. This effect of *unc-64* and *unc-13* mutations on synaptic vesicle docking was not detected in previous studies using a conventional chemical fixation method [7, 44, 104–106], which exemplifies the well-known superiority of high-pressure freezing over conventional chemical fixation in preserving synaptic structures.

Together these observations indicate that Munc18-1 is required in at least two distinct processes: regulating submembrane actin cytomatrix to permit vesicle delivery to the plasma membrane, which is a prerequisite for weak tethering, and rendering vesicles strongly tethered and fusion-competent. Precise molecular mechanisms by which Munc18 performs these functions remain to be fully elucidated, but the similar phenotypes of Munc18-1 and syntaxin-1A mutants suggest that they may interact to promote fusion competence of vesicles.

3.4 Interaction with Syntaxin

Although all SM proteins interact with their cognate syntaxin partners, there is considerable heterogeneity in binding modes, which have thwarted efforts to identify a unifying mechanism of SM protein function [84, 92, 99]. These modes include SM interactions with closed syntaxin (Fig. 7a), with assembled *cis*- or *trans*-SNARE complex (Fig. 7b, c), and with an N-terminal syntaxin peptide (Fig. 7d).

The difficulty in assigning a conserved function to SM proteins partially stems from the existence of a neuron-specific and high-affinity interaction between Munc18-1 and monomeric syntaxin-1A, in which the cavity formed by the Munc18-1 horseshoe envelopes syntaxin, locking it in a closed configuration

incompatible with SNARE complex formation [15, 107]. This binding mode is thus predicted to negatively regulate exocytosis. This hypothesis is supported by impaired secretion observed upon overexpression of *Drosophila* Rop [108, 109] and squid Sec1 [110], but is disputed by enhanced release observed upon Munc18-1 overexpression in chromaffin cells [97] and mammalian neurons [98]. Heterologous expression studies suggest that complexes of Munc18-1 with closed syntaxin-1A are predominantly localized to intracellular compartments rather than the plasma membrane, leading to the speculation that Munc18-1 binding to closed syntaxin-1A may perform a chaperone function to prevent nonspecific SNARE complex assembly en route to the plasma membrane and/or stabilize syntaxin-1A during the transit [111]. This latter possibility is supported by observed reductions in syntaxin-1A levels in Munc18-1 and UNC-18 null mutants [95, 96]. The Munc-18 and closed syntaxin-1A interaction may also be important for vesicle docking because a mutated Munc18-1 with reduced affinity for closed syntaxin-1A cannot rescue vesicle docking in Munc18-1 null chromaffin cells as effectively as wild-type Munc-18 [112]. This docking defect may represent a specific loss in weakly tethered vesicles (discussed earlier) since vesicle priming is still well supported by this mutated form of Munc18-1. Thus, binding of Munc18-1 to closed syntaxin appears to stimulate a vesicle-tethering step that is distinct from the involvement of Munc18-1 in the priming process [112]. Munc18-2 can also support vesicle docking in Munc18-1 null mutants, but it is less effective in priming vesicles, likely because it is adapted to function with syntaxin-3. Interestingly, Munc18-2 can compete with wild-type Munc18-1 for binding to closed syntaxin-1A and inhibit progression to the priming step when it is overexpressed in chromaffin cells [112]. This experiment implies that there are two sequential binding modes between Munc18-1 and syntaxin-1A; a monomeric interaction between Munc18-1 and closed syntaxin-1A that is required for tethering, and a subsequent interacting mode that regulates vesicles priming.

The binding between Munc18-1 and the N-terminus of open syntaxin-1A may serve this priming function [111, 113]. This N-peptide binding mode is a feature

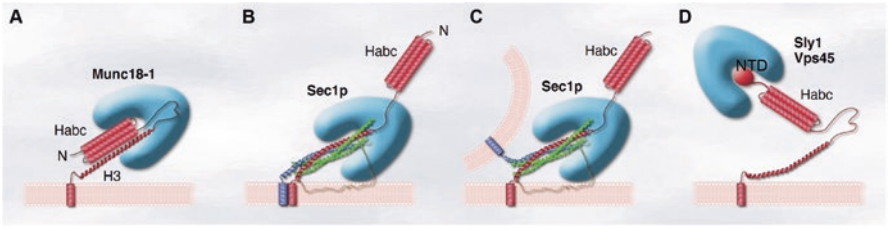

Fig. 7 The binding modes of SM proteins to syntaxin. Several configurations of SM protein interactions with syntaxin have been proposed, including SM interactions with closed syntaxin (**a**), with assembled *cis*-SNARE complex (**b**) or *trans*-SNARE complex (**c**), and with an N-terminal syntaxin peptide (**d**). The red-colored molecule represents syntaxin with several major domains, including an N-terminal domain (N), a Habc domain of 3 α-helices, a SNARE domain (H3), and a membrane spanning domain. The teal-colored molecules represent SM proteins from three different species, including Munc18-1 of mouse, Sec1p of yeast, and Sly1 of *Drosophila*. (Figure adapted from Toonen et al. [84])

confirmed with many SM proteins and syntaxin [90, 91, 114, 115], which requires a conserved short peptide sequence at the syntaxin N-terminus to fit into a conserved hydrophobic pocket on the external side of the SM horseshoe structure in domain 1 [90, 91]. Heterologous expression studies suggest that the binding between Munc18-1 and the syntaxin N-peptide occurs preferentially at the plasma membrane and appears to be important in promoting SNARE complex assembly once syntaxin has adopted its open conformation [111]. Specifically, heterodimers of open syntaxin and Munc18-1 can readily form complexes with SNAP-25 either alone or together with synaptobrevin, whereas open syntaxin lacking the N-peptide does not bind to Munc18-1 in vitro and cannot assemble into SNARE complexes [111]. These observations suggest that Munc18-1 can remain associated with syntaxin during sequential stages of SNARE complex formation [116]. This association is however unlikely to be physiologically relevant in neurosecretory cells [117] and neurons [118] because interfering with the hydrophobic pocket underpinning this association has no significant effect on neuroexocytosis in these two models. However, an inhibition of mast cell degranulation by mutations altering the hydrophobic pocket [119] suggests that this interaction could play a role in the immune system.

In recent years, the focus has shifted toward a major priming function of Munc18-1 domain 3a, which can transit to a conformation incompatible with binding to closed syntaxin-1 [120]. The hinge loop of domain 3a physically interacts with syntaxin-1 to promote its open conformation [121, 122]. Interestingly, the size of the hinge loop seems to matter more than its amino acid composition in the promoting effects of domain 3a on syntaxin-1 opening and subsequent SNARE complex formation. Either deletion [122] or insertion [121] in the hinge loop negatively impacts exocytosis and SNARE complex assembly. However, a mutation at the start of the loop (P335A) was found to facilitate the extended α-helical conformation (Fig. 8) and accelerate fusion in a liposome mixing assay [123] and in neurosecretory cells [124]. It has been proposed that domain 3a may serve as a molecular switch that can be turned on upon binding to VAMP2, and that the interaction between VAMP2 and Munc18-1 may play a key role in operating the switch. A mutation of residue A297 to bulky histidine in Munc18-1 prevents this interaction and blocks exocytosis, suggesting that interfering with VAMP2 binding can prevent domain 3a function in priming [125]. Domain 3a therefore holds the key to controlling the molecular switch that underpins vesicular priming, via opening of syntaxin-1 and ensuing SNARE complex assembly culminating in the fusion pore opening.

3.5 Nanoscale Environment

The cortical actin network plays a critical role in providing the nanoscale forces to move secretory vesicles to their docking sites at the plasma membrane in neurosecretory cells where they undergo priming and Ca^{2+}-dependent fusion [122, 126]. Specifically, Myosin VI recruits secretory vesicles to the plasma membrane, and

Myosin II promotes a relaxation of the cortical actin network leading to synchronized translocation of secretory vesicles to the plasma membrane [122, 127]. At the plasma membrane, Munc18-1 controls the docking and priming of vesicles. Munc18-1 molecules detected in the vicinity of the plasma membrane exist in two major states, mobile and immobile, based on their diffusion coefficients. An increase of the mobile population in neurosecretory cells in response to secretagogue stimulation suggests that Munc18-1 has to exit the confinement of the release sites to allow the occurrence of vesicle fusion [127, 128], and that this process is likely driven by a displacement of Munc18-1 from syntaxin-SNAP-25 dimers induced by synaptobrevin. This may promote SNARE complex assembly by generating a productive syntaxin-SNAP-25 acceptor complex for synaptobrevin [129]. αSNAP may also facilitate the switch of Munc18-1 function in controlling syntaxin opening thereby ensuring the fidelity of SNARE complex formation [130]. In vitro liposome fusion assays indicate that Munc18-1 facilitates vesicle fusion by promoting SNARE complex assembly via a syntaxin-1A N-peptide interaction. Furthermore, the ability of Munc18-1 to promote liposome fusion is successful only when cognate SNAREs are present [131]. This suggests that one of the functions of Munc18-1, and perhaps other SM proteins as well, is to ensure the specificity of the SNARE assembly reaction in each trafficking compartment.

Munc18-1 therefore participates in two distinct and sequential steps of the vesicle cycle. It first interacts with closed syntaxin-1A to promote syntaxin-1A trafficking to the plasma membrane, and then interacts with VAMP2 to promote syntaxin-1 opening to ensure the fidelity of SNARE complex assembly [111, 113, 131, 132]. The SM-SNARE complex binding mode has now been established for several SMs involved in various cellular trafficking events including regulated exocytosis

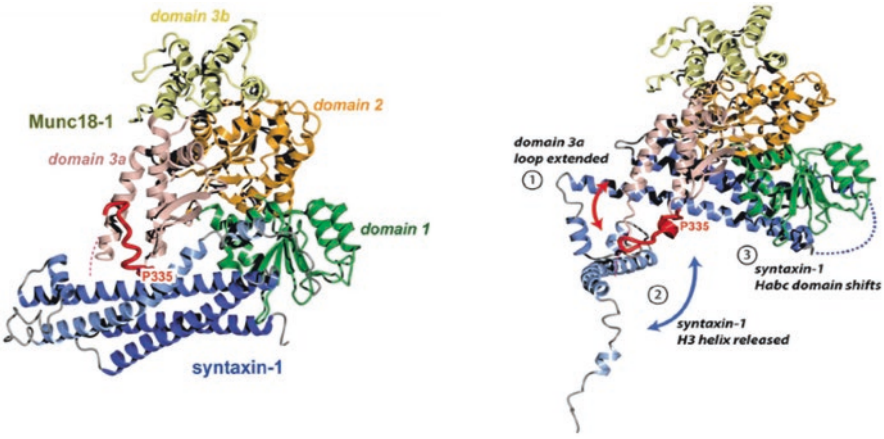

Fig. 8 Munc18-1 domain 3a structures. At least two different modes of interaction between Munc18-1 and syntaxin-1A have been identified. The left panel shows the closed structure of Munc18-1 in complex with the soluble region of syntaxin-1A, as solved by X-ray crystallography. The right panel shows the open conformation of Munc18-1. (Figure adapted from Hu et al. [120] and Burkhardt et al. [143])

(Munc18-1), constitutive secretion (Sec1p), endocytosis (Vps45), and ER to Golgi trafficking (Sly1p), suggesting that this interaction underlies a conserved vesicle trafficking function [133–137].

4 Interactions Between UNC-13/Munc13 and UNC-18/Munc18

The fact that *C. elegans unc-18* and *unc-13* mutants are similarly paralyzed with reduced evoked release and fewer docked/primed vesicles suggests that UNC-18 and UNC-13 likely act in the same pathway. This possibility is further supported by their mutual interactions with the N-terminus of syntaxin [17]. Furthermore, the observation that an UNC-13 protein fragment can interact directly with UNC-18 and displace UNC-18 from syntaxin in vitro suggests that the binding of UNC-18 and UNC-13 to syntaxin may be convergent or sequential events [18]. The notion that Munc13 and Munc18 act in the same process is further supported by the recent observation that DAG and phorbol ester-induced synaptic potentiation requires both Munc13-1 activation and PKC-dependent phosphorylation of Munc18-1 [138]. Specifically, binding of phorbol ester to the C1 domain of Munc13-1 potentiates release only if phorbol ester-mediated PKC-dependent phosphorylation of Munc18-1 precedes it [138, 139].

Mechanistically, it is still unclear what sequence of events underlies the actions of Munc13 and Munc18 in either basal or potentiated synaptic transmission. An essential role of UNC-13/Munc13 appears to be to promote the availability of open syntaxin, possibly through a direct interaction with the syntaxin N-terminus [12, 16, 53, 56, 59]. If this model is correct, at what point does UNC-18 become involved? Is Munc13 involved in promoting a change in Munc18-1 domain 3A conformation [122] leading to syntaxin-1A opening? Accumulating evidence indicates that all SM proteins may interact with assembled SNARE complexes [116, 117, 140], suggesting that this is the key event underlying their conserved permissive role. If so, UNC-18 binding to the SNARE complex must occur after UNC-13 has rendered the syntaxin SNARE domain accessible for SNARE complex assembly. There are results suggesting that the MUN domain of Munc13-1 works together with Munc18-1 to initiate SNARE assembly by stabilizing an intermediate complex containing Munc18-1, syntaxin-1A, and VAMP2 [132, 141]. Precisely how the interaction between Munc18-1 and the SNARE complex may promote fusion is yet to be determined.

This hypothetical model does not adequately address the fact that Munc18-1 also binds to the closed conformation of syntaxin-1A. One possibility is that the action of UNC-13/Munc13 in promoting the opening of syntaxin causes a conformational rearrangement that disrupts the high-affinity Munc18-1/syntaxin dimer to allow syntaxin to open. However, this model fails to incorporate other roles of UNC-13/Munc13-1 in the regulation of exocytosis that are independent of the MUN domain,

such as vesicle targeting via RIM/Rab interactions [14, 36], synaptic potentiation via the C1 and C2B domains, as well as regulations involving interactions with Doc2, a C2 domain protein that binds Ca^{2+} [142]. Furthermore, this model does not address other known roles of UNC-18/Munc18-1 in the transport or stabilization of syntaxin, vesicle delivery, and PKC-dependent synaptic potentiation. Both Munc13 and Munc18 are multi-domain proteins capable of interacting with several other proteins, which may provide mechanisms to regulate their central roles in exocytosis to meet various physiological demands.

5 Summary

The consensus from recent studies is that UNC-18/Munc18 and UNC-13/Munc13 act in concert to allow vesicle priming by promoting SNARE complex assembly. These events lead to the stable association of vesicles with the plasma membrane and drive the vesicles to acquire a fusion-competent state. However, many details remain to be elucidated regarding the temporal sequence, mechanics, and modulation by regulatory proteins in the execution of neurotransmission.

References

1. Heuser JE, Reese TS, Dennis MJ, Jan Y, Jan L, Evans L. Synaptic vesicle exocytosis captured by quick freezing and correlated with quantal transmitter release. J Cell Biol. 1979;81:275–300. https://doi.org/10.1083/jcb.81.2.275.
2. Ceccarelli B, Grohovaz F, Hurlbut WP. Freeze-fracture studies of frog neuromuscular junctions during intense release of neurotransmitter. I. Effects of black widow spider venom and Ca2+-free solutions on the structure of the active zone. J Cell Biol. 1979;81:163–77. https://doi.org/10.1083/jcb.81.1.163.
3. Sabatini BL, Regehr WG. Timing of neurotransmission at fast synapses in the mammalian brain. Nature. 1996;384:170–2. https://doi.org/10.1038/384170a0.
4. Chen YA, Scales SJ, Scheller RH. Sequential SNARE assembly underlies priming and triggering of exocytosis. Neuron. 2001;30:161–70. https://doi.org/10.1016/s0896-6273(01)00270-7.
5. Lonart G, Sudhof TC. Assembly of SNARE core complexes prior to neurotransmitter release sets the readily releasable pool of synaptic vesicles. J Biol Chem. 2000;275:27703–7. https://doi.org/10.1074/jbc.C000237200.
6. Hanson PI, Roth R, Morisaki H, Jahn R, Heuser JE. Structure and conformational changes in NSF and its membrane receptor complexes visualized by quick-freeze/deep-etch electron microscopy. Cell. 1997;90:523–35. https://doi.org/10.1016/s0092-8674(00)80512-7.
7. Broadie K, Prokop A, Bellen HJ, O'Kane CJ, Schulze KL, Sweeney ST. Syntaxin and synaptobrevin function downstream of vesicle docking in Drosophila. Neuron. 1995;15:663–73. https://doi.org/10.1016/0896-6273(95)90154-x.
8. Sollner T, Whiteheart SW, Brunner M, Erdjument-Bromage H, Geromanos S, Tempst P, et al. SNAP receptors implicated in vesicle targeting and fusion. Nature. 1993;362:318–24. https://doi.org/10.1038/362318a0.
9. Chen YA, Scheller RH. SNARE-mediated membrane fusion. Nat Rev Mol Cell Biol. 2001;2:98–106. https://doi.org/10.1038/35052017.

10. Sutton RB, Fasshauer D, Jahn R, Brunger AT. Crystal structure of a SNARE complex involved in synaptic exocytosis at 2.4 A resolution. Nature. 1998;395:347–53. https://doi.org/10.1038/26412.
11. Lin RC, Scheller RH. Structural organization of the synaptic exocytosis core complex. Neuron. 1997;19:1087–94. https://doi.org/10.1016/s0896-6273(00)80399-2.
12. Hammarlund M, Palfreyman MT, Watanabe S, Olsen S, Jorgensen EM. Open syntaxin docks synaptic vesicles. PLoS Biol. 2007;5:e198. https://doi.org/10.1371/journal.pbio.0050198.
13. Imig C, Min SW, Krinner S, Arancillo M, Rosenmund C, Sudhof TC, et al. The morphological and molecular nature of synaptic vesicle priming at presynaptic active zones. Neuron. 2014;84:416–31. https://doi.org/10.1016/j.neuron.2014.10.009.
14. Weimer RM, Gracheva EO, Meyrignac O, Miller KG, Richmond JE, Bessereau JL. UNC-13 and UNC-10/rim localize synaptic vesicles to specific membrane domains. J Neurosci. 2006;26:8040–7. https://doi.org/10.1523/JNEUROSCI.2350-06.2006.
15. Dulubova I, Sugita S, Hill S, Hosaka M, Fernandez I, Sudhof TC, et al. A conformational switch in syntaxin during exocytosis: role of munc18. EMBO J. 1999;18:4372–82. https://doi.org/10.1093/emboj/18.16.4372.
16. Madison JM, Nurrish S, Kaplan JM. UNC-13 interaction with syntaxin is required for synaptic transmission. Curr Biol. 2005;15:2236–42. https://doi.org/10.1016/j.cub.2005.10.049.
17. Betz A, Okamoto M, Benseler F, Brose N. Direct interaction of the rat unc-13 homologue Munc13-1 with the N terminus of syntaxin. J Biol Chem. 1997;272:2520–6. https://doi.org/10.1074/jbc.272.4.2520.
18. Sassa T, Harada S, Ogawa H, Rand JB, Maruyama IN, Hosono R. Regulation of the UNC-18-Caenorhabditis elegans syntaxin complex by UNC-13. J Neurosci. 1999;19:4772–7. https://doi.org/10.1523/JNEUROSCI.19-12-04772.1999.
19. Pevsner J, Hsu SC, Scheller RH. n-Sec1: a neural-specific syntaxin-binding protein. Proc Natl Acad Sci U S A. 1994;91:1445–9. https://doi.org/10.1073/pnas.91.4.1445.
20. Brenner S. The genetics of Caenorhabditis elegans. Genetics. 1974;77:71–94. https://doi.org/10.1093/genetics/77.1.71.
21. Kohn RE, Duerr JS, McManus JR, Duke A, Rakow TL, Maruyama H, et al. Expression of multiple UNC-13 proteins in the Caenorhabditis elegans nervous system. Mol Biol Cell. 2000;11:3441–52. https://doi.org/10.1091/mbc.11.10.3441.
22. Xu XZ, Wes PD, Chen H, Li HS, Yu M, Morgan S, et al. Retinal targets for calmodulin include proteins implicated in synaptic transmission. J Biol Chem. 1998;273:31297–307. https://doi.org/10.1074/jbc.273.47.31297.
23. Koch H, Hofmann K, Brose N. Definition of Munc13-homology-domains and characterization of a novel ubiquitously expressed Munc13 isoform. Biochem J. 2000;349:247–53. https://doi.org/10.1042/0264-6021:3490247.
24. Brose N, Hofmann K, Hata Y, Sudhof TC. Mammalian homologues of Caenorhabditis elegans unc-13 gene define novel family of C2-domain proteins. J Biol Chem. 1995;270:25273–80. https://doi.org/10.1074/jbc.270.42.25273.
25. Hu Z, Tong XJ, Kaplan JM. UNC-13L, UNC-13S, and Tomosyn form a protein code for fast and slow neurotransmitter release in Caenorhabditis elegans. Elife. 2013;2:e00967. https://doi.org/10.7554/eLife.00967.
26. Bohme MA, Beis C, Reddy-Alla S, Reynolds E, Mampell MM, Grasskamp AT, et al. Active zone scaffolds differentially accumulate Unc13 isoforms to tune Ca(2+) channel-vesicle coupling. Nat Neurosci. 2016;19:1311–20. https://doi.org/10.1038/nn.4364.
27. Yang CB, Zheng YT, Li GY, Mower GD. Identification of Munc13-3 as a candidate gene for critical-period neuroplasticity in visual cortex. J Neurosci. 2002;22:8614–8.
28. Augustin I, Korte S, Rickmann M, Kretzschmar HA, Sudhof TC, Herms JW, et al. The cerebellum-specific Munc13 isoform Munc13-3 regulates cerebellar synaptic transmission and motor learning in mice. J Neurosci. 2001;21:10–7. https://doi.org/10.1523/JNEUROSCI.21-01-00010.2001.

29. Augustin I, Betz A, Herrmann C, Jo T, Brose N. Differential expression of two novel Munc13 proteins in rat brain. Biochem J. 1999;337(Pt 3):363–71. https://doi.org/10.1042/bj3370363.
30. Chen Z, Cooper B, Kalla S, Varoqueaux F, Young SM Jr. The Munc13 proteins differentially regulate readily releasable pool dynamics and calcium-dependent recovery at a central synapse. J Neurosci. 2013;33:8336–51. https://doi.org/10.1523/JNEUROSCI.5128-12.2013.
31. Ishiyama S, Schmidt H, Cooper BH, Brose N, Eilers J. Munc13-3 superprimes synaptic vesicles at granule cell-to-basket cell synapses in the mouse cerebellum. J Neurosci. 2014;34:14687–96. https://doi.org/10.1523/JNEUROSCI.2060-14.2014.
32. Netrakanti PR, Cooper BH, Dere E, Poggi G, Winkler D, Brose N, et al. Fast cerebellar reflex circuitry requires synaptic vesicle priming by munc13-3. Cerebellum. 2015;14:264–83. https://doi.org/10.1007/s12311-015-0645-0.
33. Feldmann J, Callebaut I, Raposo G, Certain S, Bacq D, Dumont C, et al. Munc13-4 is essential for cytolytic granules fusion and is mutated in a form of familial hemophagocytic lymphohistiocytosis (FHL3). Cell. 2003;115:461–73. https://doi.org/10.1016/s0092-8674(03)00855-9.
34. Liu H, Li L, Nedelcu D, Hall Q, Zhou L, Wang W, et al. Heterodimerization of UNC-13/RIM regulates synaptic vesicle release probability but not priming in *C. elegans*. Elife. 2019;8. https://doi.org/10.7554/eLife.40585.
35. Deng L, Kaeser PS, Xu W, Sudhof TC. RIM proteins activate vesicle priming by reversing autoinhibitory homodimerization of Munc13. Neuron. 2011;69:317–31. https://doi.org/10.1016/j.neuron.2011.01.005.
36. Dulubova I, Lou X, Lu J, Huryeva I, Alam A, Schneggenburger R, et al. A Munc13/RIM/Rab3 tripartite complex: from priming to plasticity? EMBO J. 2005;24:2839–50. https://doi.org/10.1038/sj.emboj.7600753.
37. Betz A, Thakur P, Junge HJ, Ashery U, Rhee JS, Scheuss V, et al. Functional interaction of the active zone proteins Munc13-1 and RIM1 in synaptic vesicle priming. Neuron. 2001;30:183–96. https://doi.org/10.1016/s0896-6273(01)00272-0.
38. Kawabe H, Mitkovski M, Kaeser PS, Hirrlinger J, Opazo F, Nestvogel D, et al. ELKS1 localizes the synaptic vesicle priming protein bMunc13-2 to a specific subset of active zones. J Cell Biol. 2017;216:1143–61. https://doi.org/10.1083/jcb.201606086.
39. Aravamudan B, Fergestad T, Davis WS, Rodesch CK, Broadie K. Drosophila UNC-13 is essential for synaptic transmission. Nat Neurosci. 1999;2:965–71. https://doi.org/10.1038/14764.
40. Maruyama IN, Brenner S. A phorbol ester/diacylglycerol-binding protein encoded by the unc-13 gene of Caenorhabditis elegans. Proc Natl Acad Sci U S A. 1991;88:5729–33. https://doi.org/10.1073/pnas.88.13.5729.
41. Shin OH, Lu J, Rhee JS, Tomchick DR, Pang ZP, Wojcik SM, et al. Munc13 C2B domain is an activity-dependent Ca2+ regulator of synaptic exocytosis. Nat Struct Mol Biol. 2010;17:280–8. https://doi.org/10.1038/nsmb.1758.
42. Padmanarayana M, Liu H, Michelassi F, Li L, Betensky D, Dominguez MJ, et al. A unique C2 domain at the C terminus of Munc13 promotes synaptic vesicle priming. Proc Natl Acad Sci U S A. 2021;118. https://doi.org/10.1073/pnas.2016276118.
43. Quade B, Camacho M, Zhao X, Orlando M, Trimbuch T, Xu J, et al. Membrane bridging by Munc13-1 is crucial for neurotransmitter release. Elife. 2019;8. https://doi.org/10.7554/eLife.42806.
44. Richmond JE, Davis WS, Jorgensen EM. UNC-13 is required for synaptic vesicle fusion in *C. elegans*. Nat Neurosci. 1999;2:959–64. https://doi.org/10.1038/14755.
45. Augustin I, Rosenmund C, Sudhof TC, Brose N. Munc13-1 is essential for fusion competence of glutamatergic synaptic vesicles. Nature. 1999;400:457–61. https://doi.org/10.1038/22768.
46. Ashery U, Varoqueaux F, Voets T, Betz A, Thakur P, Koch H, et al. Munc13-1 acts as a priming factor for large dense-core vesicles in bovine chromaffin cells. EMBO J. 2000;19:3586–96. https://doi.org/10.1093/emboj/19.14.3586.
47. Zhen M, Jin Y. Presynaptic terminal differentiation: transport and assembly. Curr Opin Neurobiol. 2004;14:280–7. https://doi.org/10.1016/j.conb.2004.05.013.

48. Camacho M, Basu J, Trimbuch T, Chang S, Pulido-Lozano C, Chang SS, et al. Heterodimerization of Munc13 C2A domain with RIM regulates synaptic vesicle docking and priming. Nat Commun. 2017;8:15293. https://doi.org/10.1038/ncomms15293.
49. Varoqueaux F, Sigler A, Rhee JS, Brose N, Enk C, Reim K, et al. Total arrest of spontaneous and evoked synaptic transmission but normal synaptogenesis in the absence of Munc13-mediated vesicle priming. Proc Natl Acad Sci U S A. 2002;99:9037–42. https://doi.org/10.1073/pnas.122623799.
50. Zhou K, Stawicki TM, Goncharov A, Jin Y. Position of UNC-13 in the active zone regulates synaptic vesicle release probability and release kinetics. Elife. 2013;2:e01180. https://doi.org/10.7554/eLife.01180.
51. Kaeser PS, Deng L, Wang Y, Dulubova I, Liu X, Rizo J, et al. RIM proteins tether Ca2+ channels to presynaptic active zones via a direct PDZ-domain interaction. Cell. 2011;144:282–95. https://doi.org/10.1016/j.cell.2010.12.029.
52. Basu J, Shen N, Dulubova I, Lu J, Guan R, Guryev O, et al. A minimal domain responsible for Munc13 activity. Nat Struct Mol Biol. 2005;12:1017–8. https://doi.org/10.1038/nsmb1001.
53. Stevens DR, Wu ZX, Matti U, Junge HJ, Schirra C, Becherer U, et al. Identification of the minimal protein domain required for priming activity of Munc13-1. Curr Biol. 2005;15:2243–8. https://doi.org/10.1016/j.cub.2005.10.055.
54. Yang X, Wang S, Sheng Y, Zhang M, Zou W, Wu L, et al. Syntaxin opening by the MUN domain underlies the function of Munc13 in synaptic-vesicle priming. Nat Struct Mol Biol. 2015;22:547–54. https://doi.org/10.1038/nsmb.3038.
55. Brose N, Rosenmund C, Rettig J. Regulation of transmitter release by Unc-13 and its homologues. Curr Opin Neurobiol. 2000;10:303–11. https://doi.org/10.1016/s0959-4388(00)00105-7.
56. Richmond JE, Weimer RM, Jorgensen EM. An open form of syntaxin bypasses the requirement for UNC-13 in vesicle priming. Nature. 2001;412:338–41. https://doi.org/10.1038/35085583.
57. Ma C, Li W, Xu Y, Rizo J. Munc13 mediates the transition from the closed syntaxin-Munc18 complex to the SNARE complex. Nat Struct Mol Biol. 2011;18:542–9. https://doi.org/10.1038/nsmb.2047.
58. McEwen JM, Madison JM, Dybbs M, Kaplan JM. Antagonistic regulation of synaptic vesicle priming by Tomosyn and UNC-13. Neuron. 2006;51:303–15. https://doi.org/10.1016/j.neuron.2006.06.025.
59. Basu J, Betz A, Brose N, Rosenmund C. Munc13-1 C1 domain activation lowers the energy barrier for synaptic vesicle fusion. J Neurosci. 2007;27:1200–10. https://doi.org/10.1523/JNEUROSCI.4908-06.2007.
60. Lai Y, Choi UB, Leitz J, Rhee HJ, Lee C, Altas B, et al. Molecular mechanisms of synaptic vesicle priming by Munc13 and Munc18. Neuron. 2017;95:591–607.e10. https://doi.org/10.1016/j.neuron.2017.07.004.
61. Palfreyman MT, Jorgensen EM. Unc13 aligns SNAREs and superprimes synaptic vesicles. Neuron. 2017;95:473–5. https://doi.org/10.1016/j.neuron.2017.07.017.
62. Kazanietz MG, Lewin NE, Bruns JD, Blumberg PM. Characterization of the cysteine-rich region of the Caenorhabditis elegans protein Unc-13 as a high affinity phorbol ester receptor. Analysis of ligand-binding interactions, lipid cofactor requirements, and inhibitor sensitivity. J Biol Chem. 1995;270:10777–83. https://doi.org/10.1074/jbc.270.18.10777.
63. Betz A, Ashery U, Rickmann M, Augustin I, Neher E, Sudhof TC, et al. Munc13-1 is a presynaptic phorbol ester receptor that enhances neurotransmitter release. Neuron. 1998;21:123–36. https://doi.org/10.1016/s0896-6273(00)80520-6.
64. Lou X, Korogod N, Brose N, Schneggenburger R. Phorbol esters modulate spontaneous and Ca2+-evoked transmitter release via acting on both Munc13 and protein kinase C. J Neurosci. 2008;28:8257–67. https://doi.org/10.1523/JNEUROSCI.0550-08.2008.
65. Rhee JS, Betz A, Pyott S, Reim K, Varoqueaux F, Augustin I, et al. Beta phorbol ester- and diacylglycerol-induced augmentation of transmitter release is mediated by Munc13s and not by PKCs. Cell. 2002;108:121–33. https://doi.org/10.1016/s0092-8674(01)00635-3.

66. Lackner MR, Nurrish SJ, Kaplan JM. Facilitation of synaptic transmission by EGL-30 Gqalpha and EGL-8 PLCbeta: DAG binding to UNC-13 is required to stimulate acetylcholine release. Neuron. 1999;24:335–46. https://doi.org/10.1016/s0896-6273(00)80848-x.
67. Xu J, Camacho M, Xu Y, Esser V, Liu X, Trimbuch T, et al. Mechanistic insights into neurotransmitter release and presynaptic plasticity from the crystal structure of Munc13-1 C1C2BMUN. Elife. 2017;6. https://doi.org/10.7554/eLife.22567.
68. Liu X, Seven AB, Camacho M, Esser V, Xu J, Trimbuch T, et al. Functional synergy between the Munc13 C-terminal C1 and C2 domains. Elife. 2016;5. https://doi.org/10.7554/eLife.13696.
69. Lipstein N, Sakaba T, Cooper BH, Lin KH, Strenzke N, Ashery U, et al. Dynamic control of synaptic vesicle replenishment and short-term plasticity by Ca(2+)-calmodulin-Munc13-1 signaling. Neuron. 2013;79:82–96. https://doi.org/10.1016/j.neuron.2013.05.011.
70. Liu H, Li L, Sheoran S, Yu Y, Richmond JE, Xia J, et al. The M domain in UNC-13 regulates the probability of neurotransmitter release. Cell Rep. 2021;34:108828. https://doi.org/10.1016/j.celrep.2021.108828.
71. Li L, Liu H, Hall Q, Wang W, Yu Y, Kaplan JM, et al. A hyperactive form of unc-13 enhances Ca(2+) sensitivity and synaptic vesicle release probability in C. elegans. Cell Rep. 2019;28:2979–2995.e4. https://doi.org/10.1016/j.celrep.2019.08.018.
72. Michelassi F, Liu H, Hu Z, Dittman JS. A C1-C2 module in Munc13 inhibits calcium-dependent neurotransmitter release. Neuron. 2017;95:577–590.e5. https://doi.org/10.1016/j.neuron.2017.07.015.
73. Das J, Xu S, Pany S, Guillory A, Shah V, Roman GW. The pre-synaptic Munc13-1 binds alcohol and modulates alcohol self-administration in Drosophila. J Neurochem. 2013;126:715–26. https://doi.org/10.1111/jnc.12315.
74. You Y, Das J. Effect of ethanol on Munc13-1 C1 in membrane: a molecular dynamics simulation study. Alcohol Clin Exp Res. 2020;44:1344–55. https://doi.org/10.1111/acer.14363.
75. Xu S, Pany S, Benny K, Tarique K, Al-Hatem O, Gajewski K, et al. Ethanol regulates presynaptic activity and sedation through presynaptic Unc13 proteins in Drosophila. eNeuro. 2018;5. https://doi.org/10.1523/ENEURO.0125-18.2018.
76. Rizo J, Sudhof TC. C2-domains, structure and function of a universal Ca2+-binding domain. J Biol Chem. 1998;273:15879–82. https://doi.org/10.1074/jbc.273.26.15879.
77. Lipstein N, Chang S, Lin KH, Lopez-Murcia FJ, Neher E, Taschenberger H, et al. Munc13-1 is a Ca(2+)-phospholipid-dependent vesicle priming hub that shapes synaptic short-term plasticity and enables sustained neurotransmission. Neuron. 2021;109:3980–4000.e7. https://doi.org/10.1016/j.neuron.2021.09.054.
78. Mahoney TR, Luo S, Nonet ML. Analysis of synaptic transmission in Caenorhabditis elegans using an aldicarb-sensitivity assay. Nat Protoc. 2006;1:1772–7. https://doi.org/10.1038/nprot.2006.281.
79. Lu J, Machius M, Dulubova I, Dai H, Sudhof TC, Tomchick DR, et al. Structural basis for a Munc13-1 homodimer to Munc13-1/RIM heterodimer switch. PLoS Biol. 2006;4:e192. https://doi.org/10.1371/journal.pbio.0040192.
80. Fulterer A, Andlauer TFM, Ender A, Maglione M, Eyring K, Woitkuhn J, et al. Active zone scaffold protein ratios tune functional diversity across brain synapses. Cell Rep. 2018;23:1259–74. https://doi.org/10.1016/j.celrep.2018.03.126.
81. Junge HJ, Rhee JS, Jahn O, Varoqueaux F, Spiess J, Waxham MN, et al. Calmodulin and Munc13 form a Ca2+ sensor/effector complex that controls short-term synaptic plasticity. Cell. 2004;118:389–401. https://doi.org/10.1016/j.cell.2004.06.029.
82. Dimova K, Kawabe H, Betz A, Brose N, Jahn O. Characterization of the Munc13-calmodulin interaction by photoaffinity labeling. Biochim Biophys Acta. 2006;1763:1256–65. https://doi.org/10.1016/j.bbamcr.2006.09.017.
83. Saifee O, Wei L, Nonet ML. The *Caenorhabditis elegans unc-64* locus encodes a syntaxin that interacts genetically with synaptobrevin. Mol Biol Cell. 1998;9:1235–52. https://doi.org/10.1091/mbc.9.6.1235.

84. Toonen RF, Verhage M. Vesicle trafficking: pleasure and pain from SM genes. Trends Cell Biol. 2003;13:177–86. https://doi.org/10.1016/s0962-8924(03)00031-x.
85. Novick P, Schekman R. Secretion and cell-surface growth are blocked in a temperature-sensitive mutant of Saccharomyces cerevisiae. Proc Natl Acad Sci U S A. 1979;76:1858–62. https://doi.org/10.1073/pnas.76.4.1858.
86. Hata Y, Slaughter CA, Sudhof TC. Synaptic vesicle fusion complex contains unc-18 homologue bound to syntaxin. Nature. 1993;366:347–51. https://doi.org/10.1038/366347a0.
87. Harrison SD, Broadie K, van de Goor J, Rubin GM. Mutations in the *Drosophila Rop* gene suggest a function in general secretion and synaptic transmission. Neuron. 1994;13:555–66. https://doi.org/10.1016/0896-6273(94)90025-6.
88. Misura KM, Scheller RH, Weis WI. Three-dimensional structure of the neuronal-Sec1-syntaxin 1a complex. Nature. 2000;404:355–62. https://doi.org/10.1038/35006120.
89. Bracher A, Weissenhorn W. Crystal structures of neuronal squid Sec1 implicate inter-domain hinge movement in the release of t-SNAREs. J Mol Biol. 2001;306:7–13. https://doi.org/10.1006/jmbi.2000.4347.
90. Bracher A, Weissenhorn W. Structural basis for the Golgi membrane recruitment of Sly1p by Sed5p. EMBO J. 2002;21:6114–24. https://doi.org/10.1093/emboj/cdf608.
91. Hu SH, Latham CF, Gee CL, James DE, Martin JL. Structure of the Munc18c/Syntaxin4 N-peptide complex defines universal features of the N-peptide binding mode of Sec1/Munc18 proteins. Proc Natl Acad Sci U S A. 2007;104:8773–8. https://doi.org/10.1073/pnas.0701124104.
92. Gallwitz D, Jahn R. The riddle of the Sec1/Munc-18 proteins – new twists added to their interactions with SNAREs. Trends Biochem Sci. 2003;28:113–6. https://doi.org/10.1016/S0968-0004(03)00028-8.
93. Rizo J, Sudhof TC. Snares and Munc18 in synaptic vesicle fusion. Nat Rev Neurosci. 2002;3:641–53. https://doi.org/10.1038/nrn898.
94. Schekman R, Novick P. 23 genes, 23 years later. Cell. 2004;116:S13–5. https://doi.org/10.1016/s0092-8674(03)00972-3. 11 p following S19.
95. Weimer RM, Richmond JE, Davis WS, Hadwiger G, Nonet ML, Jorgensen EM. Defects in synaptic vesicle docking in *unc-18* mutants. Nat Neurosci. 2003;6:1023–30. https://doi.org/10.1038/nn1118.
96. Verhage M, Maia AS, Plomp JJ, Brussaard AB, Heeroma JH, Vermeer H, et al. Synaptic assembly of the brain in the absence of neurotransmitter secretion. Science. 2000;287:864–9. https://doi.org/10.1126/science.287.5454.864.
97. Voets T, Toonen RF, Brian EC, de Wit H, Moser T, Rettig J, et al. Munc18-1 promotes large dense-core vesicle docking. Neuron. 2001;31:581–91. https://doi.org/10.1016/s0896-6273(01)00391-9.
98. Toonen RF, Wierda K, Sons MS, de Wit H, Cornelisse LN, Brussaard A, et al. Munc18-1 expression levels control synapse recovery by regulating readily releasable pool size. Proc Natl Acad Sci U S A. 2006;103:18332–7. https://doi.org/10.1073/pnas.0608507103.
99. Wojcik SM, Brose N. Regulation of membrane fusion in synaptic excitation-secretion coupling: speed and accuracy matter. Neuron. 2007;55:11–24. https://doi.org/10.1016/j.neuron.2007.06.013.
100. Rostaing P, Real E, Siksou L, Lechaire JP, Boudier T, Boeckers TM, et al. Analysis of synaptic ultrastructure without fixative using high-pressure freezing and tomography. Eur J Neurosci. 2006;24:3463–74. https://doi.org/10.1111/j.1460-9568.2006.05234.x.
101. Nofal S, Becherer U, Hof D, Matti U, Rettig J. Primed vesicles can be distinguished from docked vesicles by analyzing their mobility. J Neurosci. 2007;27:1386–95. https://doi.org/10.1523/JNEUROSCI.4714-06.2007.
102. Toonen RF, Kochubey O, de Wit H, Gulyas-Kovacs A, Konijnenburg B, Sorensen JB, et al. Dissecting docking and tethering of secretory vesicles at the target membrane. EMBO J. 2006;25:3725–37. https://doi.org/10.1038/sj.emboj.7601256.

103. de Wit H, Cornelisse LN, Toonen RF, Verhage M. Docking of secretory vesicles is syntaxin dependent. PLoS One. 2006;1:e126. https://doi.org/10.1371/journal.pone.0000126.
104. Marsal J, Ruiz-Montasell B, Blasi J, Moreira JE, Contreras D, Sugimori M, et al. Block of transmitter release by botulinum C1 action on syntaxin at the squid giant synapse. Proc Natl Acad Sci U S A. 1997;94:14871–6. https://doi.org/10.1073/pnas.94.26.14871.
105. O'Connor V, Heuss C, De Bello WM, Dresbach T, Charlton MP, Hunt JH, et al. Disruption of syntaxin-mediated protein interactions blocks neurotransmitter secretion. Proc Natl Acad Sci U S A. 1997;94:12186–91. https://doi.org/10.1073/pnas.94.22.12186.
106. Kidokoro Y. Roles of SNARE proteins and synaptotagmin I in synaptic transmission: studies at the Drosophila neuromuscular synapse. Neurosignals. 2003;12:13–30. https://doi.org/10.1159/000068912.
107. Yang B, Steegmaier M, Gonzalez LC Jr, Scheller RH. nSec1 binds a closed conformation of syntaxin1A. J Cell Biol. 2000;148:247–52. https://doi.org/10.1083/jcb.148.2.247.
108. Wu MN, Littleton JT, Bhat MA, Prokop A, Bellen HJ. ROP, the Drosophila Sec1 homolog, interacts with syntaxin and regulates neurotransmitter release in a dosage-dependent manner. EMBO J. 1998;17:127–39. https://doi.org/10.1093/emboj/17.1.127.
109. Schulze KL, Littleton JT, Salzberg A, Halachmi N, Stern M, Lev Z, et al. Rop, a Drosophila homolog of yeast Sec1 and vertebrate n-Sec1/Munc-18 proteins, is a negative regulator of neurotransmitter release in vivo. Neuron. 1994;13:1099–108. https://doi.org/10.1016/0896-6273(94)90048-5.
110. Dresbach T, Burns ME, O'Connor V, DeBello WM, Betz H, Augustine GJ. A neuronal Sec1 homolog regulates neurotransmitter release at the squid giant synapse. J Neurosci. 1998;18:2923–32. https://doi.org/10.1523/JNEUROSCI.18-08-02923.1998.
111. Rickman C, Medine CN, Bergmann A, Duncan RR. Functionally and spatially distinct modes of munc18-syntaxin 1 interaction. J Biol Chem. 2007;282:12097–103. https://doi.org/10.1074/jbc.M700227200.
112. Gulyas-Kovacs A, de Wit H, Milosevic I, Kochubey O, Toonen R, Klingauf J, et al. Munc18-1: sequential interactions with the fusion machinery stimulate vesicle docking and priming. J Neurosci. 2007;27:8676–86. https://doi.org/10.1523/JNEUROSCI.0658-07.2007.
113. Dulubova I, Khvotchev M, Liu S, Huryeva I, Sudhof TC, Rizo J. Munc18-1 binds directly to the neuronal SNARE complex. Proc Natl Acad Sci U S A. 2007;104:2697–702. https://doi.org/10.1073/pnas.0611318104.
114. Dulubova I, Yamaguchi T, Gao Y, Min SW, Huryeva I, Sudhof TC, et al. How Tlg2p/syntaxin 16 'snares' Vps45. EMBO J. 2002;21:3620–31. https://doi.org/10.1093/emboj/cdf381.
115. Yamaguchi T, Dulubova I, Min SW, Chen X, Rizo J, Sudhof TC. Sly1 binds to Golgi and ER syntaxins via a conserved N-terminal peptide motif. Dev Cell. 2002;2:295–305. https://doi.org/10.1016/s1534-5807(02)00125-9.
116. Latham CF, Meunier FA. Munc18a: Munc-y business in mediating exocytosis. Int J Biochem Cell Biol. 2007;39:1576–81. https://doi.org/10.1016/j.biocel.2006.11.015.
117. Malintan NT, Nguyen TH, Han L, Latham CF, Osborne SL, Wen PJ, et al. Abrogating Munc18-1-SNARE complex interaction has limited impact on exocytosis in PC12 cells. J Biol Chem. 2009;284:21637–46. https://doi.org/10.1074/jbc.M109.013508.
118. Meijer M, Burkhardt P, de Wit H, Toonen RF, Fasshauer D, Verhage M. Munc18-1 mutations that strongly impair SNARE-complex binding support normal synaptic transmission. EMBO J. 2012;31:2156–68. https://doi.org/10.1038/emboj.2012.72.
119. Bin NR, Jung CH, Piggott C, Sugita S. Crucial role of the hydrophobic pocket region of Munc18 protein in mast cell degranulation. Proc Natl Acad Sci U S A. 2013;110:4610–5. https://doi.org/10.1073/pnas.1214887110.
120. Hu SH, Christie MP, Saez NJ, Latham CF, Jarrott R, Lua LH, et al. Possible roles for Munc18-1 domain 3a and Syntaxin1 N-peptide and C-terminal anchor in SNARE complex formation. Proc Natl Acad Sci U S A. 2011;108:1040–5. https://doi.org/10.1073/pnas.0914906108.
121. Han GA, Bin NR, Kang SY, Han L, Sugita S. Domain 3a of Munc18-1 plays a crucial role at the priming stage of exocytosis. J Cell Sci. 2013;126:2361–71. https://doi.org/10.1242/jcs.126862.

122. Martin S, Tomatis VM, Papadopulos A, Christie MP, Malintan NT, Gormal RS, et al. The Munc18-1 domain 3a loop is essential for neuroexocytosis but not for syntaxin-1A transport to the plasma membrane. J Cell Sci. 2013;126:2353–60. https://doi.org/10.1242/jcs.126813.
123. Parisotto D, Pfau M, Scheutzow A, Wild K, Mayer MP, Malsam J, et al. An extended helical conformation in domain 3a of Munc18-1 provides a template for SNARE (soluble N-ethylmaleimide-sensitive factor attachment protein receptor) complex assembly. J Biol Chem. 2014;289:9639–50. https://doi.org/10.1074/jbc.M113.514273.
124. Han GA, Park S, Bin NR, Jung CH, Kim B, Chandrasegaram P, et al. A pivotal role for pro-335 in balancing the dual functions of Munc18-1 domain-3a in regulated exocytosis. J Biol Chem. 2014;289:33617–28. https://doi.org/10.1074/jbc.M114.584805.
125. Kasula R, Blum A, Salla-Martret M, Chai YJ, Jiang A, et al. VAMP2 binding to Munc18-1 domain 3a controls the nanoscale reorganization of the plasma membrane and vesicle interface during vesicular priming. SSRN Electron J. 2019. https://doi.org/10.2139/ssrn.3362260.
126. Ahmad W. Dihydrolipoamide dehydrogenase suppression induces human tau phosphorylation by increasing whole body glucose levels in a C. elegans model of Alzheimer's disease. Exp Brain Res. 2018;236:2857–66. https://doi.org/10.1007/s00221-018-5341-0.
127. Kasula R, Chai YJ, Bademosi AT, Harper CB, Gormal RS, Morrow IC, et al. The Munc18-1 domain 3a hinge-loop controls syntaxin-1A nanodomain assembly and engagement with the SNARE complex during secretory vesicle priming. J Cell Biol. 2016;214:847–58. https://doi.org/10.1083/jcb.201508118.
128. Padmanabhan P, Bademosi AT, Kasula R, Lauwers E, Verstreken P, Meunier FA. Need for speed: super-resolving the dynamic nanoclustering of syntaxin-1 at exocytic fusion sites. Neuropharmacology. 2020;169:107554. https://doi.org/10.1016/j.neuropharm.2019.02.036.
129. Zilly FE, Sorensen JB, Jahn R, Lang T. Munc18-bound syntaxin readily forms SNARE complexes with synaptobrevin in native plasma membranes. PLoS Biol. 2006;4:e330. https://doi.org/10.1371/journal.pbio.0040330.
130. Stepien KP, Prinslow EA, Rizo J. Munc18-1 is crucial to overcome the inhibition of synaptic vesicle fusion by alphaSNAP. Nat Commun. 2019;10:4326. https://doi.org/10.1038/s41467-019-12188-4.
131. Shen J, Tareste DC, Paumet F, Rothman JE, Melia TJ. Selective activation of cognate SNAREpins by Sec1/Munc18 proteins. Cell. 2007;128:183–95. https://doi.org/10.1016/j.cell.2006.12.016.
132. Jiao J, He M, Port SA, Baker RW, Xu Y, Qu H, et al. Munc18-1 catalyzes neuronal SNARE assembly by templating SNARE association. Elife. 2018;7. https://doi.org/10.7554/eLife.41771.
133. Carpp LN, Ciufo LF, Shanks SG, Boyd A, Bryant NJ. The Sec1p/Munc18 protein Vps45p binds its cognate SNARE proteins via two distinct modes. J Cell Biol. 2006;173:927–36. https://doi.org/10.1083/jcb.200512024.
134. Carr CM, Grote E, Munson M, Hughson FM, Novick PJ. Sec1p binds to SNARE complexes and concentrates at sites of secretion. J Cell Biol. 1999;146:333–44. https://doi.org/10.1083/jcb.146.2.333.
135. Peng R, Gallwitz D. Multiple SNARE interactions of an SM protein: Sed5p/Sly1p binding is dispensable for transport. EMBO J. 2004;23:3939–49. https://doi.org/10.1038/sj.emboj.7600410.
136. Scott BL, Van Komen JS, Irshad H, Liu S, Wilson KA, McNew JA. Sec1p directly stimulates SNARE-mediated membrane fusion in vitro. J Cell Biol. 2004;167:75–85. https://doi.org/10.1083/jcb.200405018.
137. Togneri J, Cheng YS, Munson M, Hughson FM, Carr CM. Specific SNARE complex binding mode of the Sec1/Munc-18 protein, Sec1p. Proc Natl Acad Sci U S A. 2006;103:17730–5. https://doi.org/10.1073/pnas.0605448103.
138. Wierda KD, Toonen RF, de Wit H, Brussaard AB, Verhage M. Interdependence of PKC-dependent and PKC-independent pathways for presynaptic plasticity. Neuron. 2007;54:275–90. https://doi.org/10.1016/j.neuron.2007.04.001.

139. Palfreyman M, Jorgensen EM. PKC defends crown against Munc13. Neuron. 2007;54:179–80. https://doi.org/10.1016/j.neuron.2007.04.002.
140. Latham CF, Osborne SL, Cryle MJ, Meunier FA. Arachidonic acid potentiates exocytosis and allows neuronal SNARE complex to interact with Munc18a. J Neurochem. 2007;100:1543–54. https://doi.org/10.1111/j.1471-4159.2006.04286.x.
141. Wang S, Li Y, Gong J, Ye S, Yang X, Zhang R, et al. Munc18 and Munc13 serve as a functional template to orchestrate neuronal SNARE complex assembly. Nat Commun. 2019;10:69. https://doi.org/10.1038/s41467-018-08028-6.
142. Groffen AJ, Martens S, Diez Arazola R, Cornelisse LN, Lozovaya N, de Jong AP, et al. Doc2b is a high-affinity Ca2+ sensor for spontaneous neurotransmitter release. Science. 2010;327:1614–8. https://doi.org/10.1126/science.1183765.
143. Burkhardt P, Hattendorf DA, Weis WI, Fasshauer D. Munc18a controls SNARE assembly through its interaction with the syntaxin N-peptide. EMBO J. 2008;27:923–33. https://doi.org/10.1038/emboj.2008.37.

The Role of Tomosyn in the Regulation of Neurotransmitter Release

Chun Hin Chow, Mengjia Huang, and Shuzo Sugita

Abstract Soluble NSF attachment protein receptor (SNARE) proteins play a central role in synaptic vesicle (SV) exocytosis. These proteins include the vesicle-associated SNARE protein (v-SNARE) synaptobrevin and the target membrane-associated SNARE proteins (t-SNAREs) syntaxin and SNAP-25. Together, these proteins drive membrane fusion between synaptic vesicles (SV) and the presynaptic plasma membrane to generate SV exocytosis. In the presynaptic active zone, various proteins may either enhance or inhibit SV exocytosis by acting on the SNAREs. Among the inhibitory proteins, tomosyn, a syntaxin-binding protein, is of particular importance because it plays a critical and evolutionarily conserved role in controlling synaptic transmission. In this chapter, we describe how tomosyn was discovered, how it interacts with SNAREs and other presynaptic regulatory proteins to regulate SV exocytosis and synaptic plasticity, and how its various domains contribute to its synaptic functions.

Keywords Tomosyn · Exocytosis · Synaptic vesicles · SNARE proteins · UNC-18 · Munc18 · Syntaxin

1 Discovery

Tomosyn was first discovered as a syntaxin-1 binding protein. At that time, Munc18-1 was known as a protein associated with syntaxin-1 [1–3]. The binding of Munc18-1 to syntaxin-1 appeared to be dynamic rather than stable. However, it was unclear how Munc18-1 dissociates from syntaxin-1, which prompted efforts of

C. H. Chow · M. Huang · S. Sugita (✉)
Division of Experimental & Translational Neuroscience, Krembil Brain Institute, University Health Network, Toronto, ON, Canada

Faculty of Medicine, Department of Physiology, University of Toronto, Toronto, ON, Canada
e-mail: Shuzo.Sugita@uhnresearch.ca

Z.-W. Wang (ed.), *Molecular Mechanisms of Neurotransmitter Release*,
Advances in Neurobiology 33, https://doi.org/10.1007/978-3-031-34229-5_9

searching for a novel binding partner of either syntaxin-1 or Munc18-1 that regulates their interaction [4]. From extracted rat cerebral cytosol, a novel protein of 130 kDa coimmunoprecipitated with syntaxin-1A, and was named tomosyn, which was coined from "*tomo*" (meaning a friend in Japanese) and "*syn*" (a binding partner of syntaxin-1). The mammalian tomosyn identified is a protein of approximately 1000 amino acid residues in length (depending on species) and contains several identified domains (Fig. 1). Tomosyn binds to syntaxin-1 [4], but not syntaxin-2, 3, and 4. This property of tomosyn differs from those of the Munc18 isoforms, namely, Munc18-1, 2, and 3, which can bind to different syntaxin isoforms [5–10].

Interestingly, the binding location of tomosyn on syntaxin-1 largely overlaps with that of the v-SNARE synaptobrevin-2 (also called vesicle associated membrane protein 2, VAMP2) [4]. Since synaptobrevin plays a pivotal role in SV exocytosis, the binding of tomosyn to a similar region in syntaxin-1 provoked further research on tomosyn. Yeast two-hybrid assays indicated that a predicted coiled-coil domain in the C-terminus of tomosyn mediates its binding to syntaxin-1. The putative coiled-coil domain of tomosyn has high sequence homology with the SNARE motif (an amphipathic α-helix) of the v-SNARE proteins synaptobrevin-1, 2, and 4 [11]. Because the SNARE motif of v-SNAREs interacts with those of the t-SNAREs

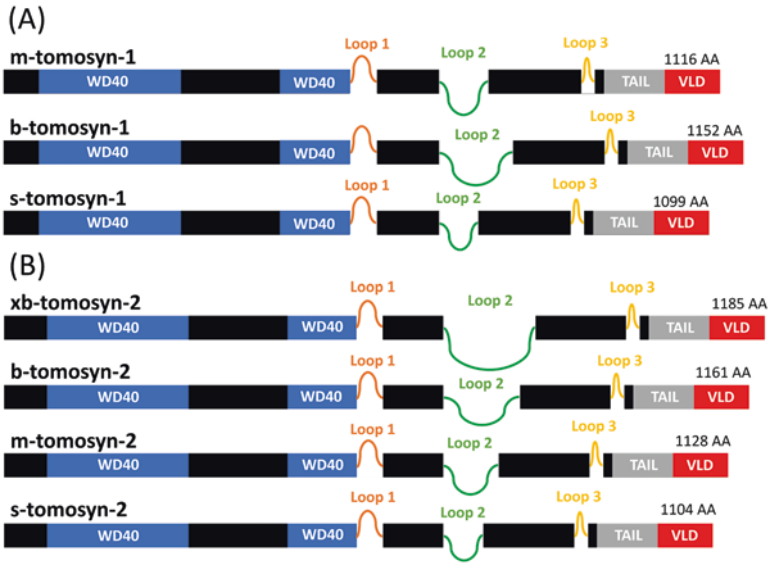

Fig. 1 Domain structure and alternative splicing of mouse tomosyn. (**a**) Tomosyn-1 contains an N-terminal WD40 repeat domain, 3 loops (loops 1–3), a tail domain, and a C-terminal VAMP-like domain (VLD). The alternatively spliced sites lie in the region of loop 2, which is also termed the highly variable region (HVR). There are three alternatively spliced isoforms of tomosyn-1: m-tomosyn-1 (1116 amino acids (AA)), b-tomosyn-1 (big) (1152 AA), and s-tomosyn-1 (small) (1099 AA). (**b**) Tomosyn-2 is highly similar to tomosyn-1, containing the WD40 domain, 3 loops, a tail domain, and the VLD. There are four alternatively spliced forms of tomosyn-2, and similar to tomosyn-1, loop2 is where the splice sites are located

(syntaxin and SNAP-25) to form the SNARE complex, the similar binding location of tomosyn and synaptobrevin-2 in syntaxin led to the speculation that tomosyn might be able to substitute synaptobrevin-2 in the SNARE complex. As expected, Fujita et al. demonstrated a novel complex formed by tomosyn, syntaxin-1, and SNAP-25 [4]. The binding of tomosyn to the t-SNAREs (syntaxin-1 and SNAP-25) can prevent synaptobrevin-2 from binding to the t-SNAREs, forming the tomosyn-SNARE complex [12].

Tomosyn's ability to block the synaptobrevin-SNARE formation led to the hypothesis that tomosyn inhibits vesicles exocytosis. This hypothesis subsequently gained support by evidence from multiple systems and organisms. For example, overexpression of tomosyn inhibits Ca^{2+}-dependent release of growth hormone from PC12 cells [4]. Tomosyn inhibits insulin secretion and glucose transporter type 4 (GLUT4) cell surface expression in pancreatic beta cells [13–15]. Knockout of tomosyn in *Caenorhabditis elegans*, *Drosophila*, and mice augments evoked excitatory postsynaptic currents [16–22]. To understand tomosyn's inhibitory roles in exocytosis, we begin by describing its biochemical and biophysical properties.

2 Structure and Domains

Since the discovery of tomosyn, a top priority was to characterize its structure. The first crystal structure of tomosyn was obtained with the yeast homolog of tomosyn, Sro7 [23]. This structure was later used as a template to build the structures of tomosyns in other species, including mice and *Drosophila* [18, 24]. Major structural domains of tomosyn include N-terminal WD40 repeats, a C-terminal VAMP-like domain (VLD), and a tail region before the VLD (Fig. 1).

Mammals have two isoforms of tomosyn encoded by two different genes, *tomosyn-1* and *tomosyn-2* [25] (Fig. 1). The two genes have very similar gene structures with conserved N-terminal WD40 and C-terminal VLD domains [25]. *Tomosyn-1* encodes three alternatively spliced isoforms that vary in the protein sequence length, including m-tomosyn-1 ("m" for "medium"), b-tomosyn-1 ("b" for "big," 36 amino acid residues longer than m-tomosyn-1), and s-tomosyn-1 ("s" for "small," 17 amino acid residues shorter than m-tomosyn-1) [4, 26]. The different splice isoforms display distinct expression patterns and syntaxin-binding specificities. m-tomosyn-1 and s-tomosyn-1 are specifically expressed in the brain and exclusively interact with syntaxin-1, whereas b-tomosyn-1 is expressed in various tissues, and can bind to both syntaxin-4 and syntaxin-1 [15, 26]. *Tomosyn-2* encodes four alternatively spliced isoforms [25] (Fig. 1). Tomosyn-2 expression is restricted to the brain, especially in the hippocampus and cerebellum [25]. The major structural difference between tomosyn-1 and tomosyn-2 lies within a highly variable region (HVR) where a loop structure of variable length exists [24, 25].

Mammalian tomosyns undergo various posttranslational modifications. For example, the HVR is a target for SUMOylation [24], which is a process of attaching the small ubiquitin-like modifier (SUMO) to a protein by the sequential actions of an E1 SUMO activating enzyme, an E2 SUMO conjugating enzyme, and a SUMO E3 ligase [27]. The C-terminal of tomosyn-1 is responsible for interacting with PIASγ, an E3 ligase used in the SUMOylation process [28]. In addition, tomosyn-1 is phosphorylated at multiple sites. Protein kinase A (PKA) phosphorylates Serine 724 located in the linker region between the WD40 domain and the VLD [29]. Tomosyn-1 is also a phosphorylation target of Cdk5 [22]. These posttranslational modifications may contribute to tomosyn's inhibitory effects on exocytosis and synaptic transmission.

2.1 Conservation of Tomosyn in Lower Organisms

Tomosyn is highly conserved across various species as a syntaxin interacting protein. As stated above, Sro7 is the yeast homolog of tomosyn. Structurally, Sro7 contains WD40 domains at the N-terminal and an alpha-helix at the C-terminal domain (CTD) [23]. The α-helical CTD domain of Sro7 enables its binding to both Sec9, a yeast homolog of SNAP-25, and Sso1, a yeast homolog of syntaxin [23, 30]. Sro7 interacts with Sec9 and Sso1 to inhibit SNARE complex formation and vesicle exocytosis [23]. Therefore, Sro7 CTD exhibits functional similarity to the VLD motif of tomosyn.

In other organisms including humans, mice, zebrafish, *Drosophila*, and *C. elegans*, the defining VLD motif of tomosyn is conserved [16, 18]. A highly conserved arginine (R) residue located in the center of the SNARE motif of synaptobrevin-2 plays a key role in the formation of the SNARE complex. It interacts with three glutamine (Q) residues located in the centers of the SNARE motifs of syntaxin-1 and SNAP-25 (Fig. 2a, b). This R residue as well as a glutamate (E) residue before it and an aspartate (D) residue following it are conserved in synaptobrevins of various species. Although the tomosyn VLD motif is highly similar to the synaptobrevin-2 SNARE domain, tomosyn often has a different amino acid at the third position and is variable across species [16, 18] (Fig. 2a). Despite the variation in the VLD sequence, the ability of tomosyn to bind to syntaxin in the lower organisms *C. elegans* and *Drosophila* is unaltered [16, 18]. Similar to mammalian tomosyn, alternative splicing of tomosyn occurs in the lower organisms. In *Drosophila*, tomosyn is encoded by one gene and alternatively spliced at exon 13, generating distinct isoforms with variations in the WD40 domain [18]. In *C. elegans*, tomosyn is encoded by the gene *tom-1*, and spliced into 3 isoforms, *tom-1A/B/C*. TOM-1B differs from the other two splice variants in that it is shorter and lacks the N-terminal WD40 domain [16]. In spite of some protein sequence differences among various tomosyn isoforms, the VLD domain is highly conserved, suggesting that it plays critical roles in tomosyn's functions.

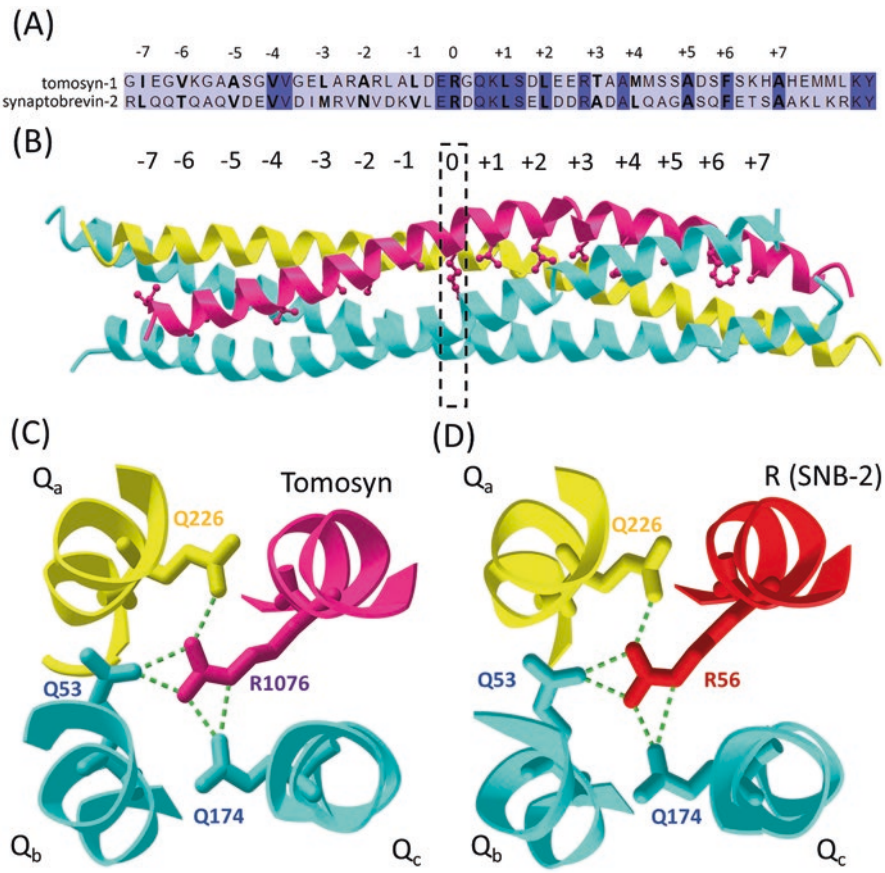

Fig. 2 Tomosyn VAMP-like domain (VLD). (**a**) Sequence alignment of the tomosyn-1-VLD at the C-terminal end and the synaptobervin-2 C-terminal SNARE domain of *Mus musculus* (mouse). The dark blue color represents sequence identity, and the light blue color represents similarity. (**b**) Structure of the rat tomosyn-SNARE. The quadrable α-helical structure is similar to the synaptobrevin-2-mediated SNARE complex. The arginine (R) of tomosyn (pink) interacting with syntaxin-1 (Q_a, yellow) and SNAP-25 (Q_{bc}, cyan) is highlighted in the box. (**c**) Interaction of R1076 of tomosyn with glutamine (Q) 226 of syntaxin-1, Q53 of SNAP25 Q_b and Q174 of SNAP25 Q_c. (**d**) Similar interaction of R56 of synaptobrevin-2 (R, SNB-2, red) with the Q-SNAREs. Hydrogen bonds are shown in green

2.2 *Biochemical Interactions*

Sequence alignment showed that the C-terminus of tomosyn is highly similar to the coiled-coil SNARE domain of synaptobrevin proteins, which is the region responsible for interacting with t-SNAREs [11, 18, 31, 32]. This suggests that the tomosyn C-terminal VLD is indispensable for tomosyn interaction with syntaxin. Multiple in vitro studies confirmed this notion by demonstrating that the tomosyn C-terminal

domain alone can bind to syntaxin-1 [12, 26, 33–35]. In addition, the C-terminal of tomosyn is solely capable of forming a heat-resistant complex with syntaxin-1 and SNAP-25 in a 1:1:1 ratio, termed the tomosyn-SNARE [12, 36]. The structure of the tomosyn-SNARE contains a quadruple α-helical structure. This structure is similar to the SNARE complex formed by synaptobrevin-2, syntaxin-1, and SNAP-25 [37] (Fig. 2b). The formation of the tomosyn-SNARE is likely initiated by a binary tomosyn-syntaxin-1 interaction since tomosyn cannot bind to SNAP25 directly [34]. Moreover, the dissociation of the tomosyn-SNARE utilizes a similar pathway to the synaptobrevin-2-SNARE complex. The synaptobrevin-2-SNARE complex is dissociated by α-NSF (N-ethylmaleimide-sensitive factor), SNAP (soluble NSF attachment protein), and ATP [38, 39]. Similarly, tomosyn-SNARE is dissociated by the same three components [12, 40]. In summary, the tomosyn's VLD domain makes it the ideal candidate to replace synaptobrevin-2 in t-SNAREs binding.

Beyond t-SNAREs, tomosyn interplays with other SNARE-mediated fusion regulatory proteins in the active zone. For example, the tomosyn N-terminal WD40 domain can interact with synaptotagmin-1 in a Ca^{2+}-dependent manner [41]. Synaptotagmin-1 is a Ca^{2+} sensor that promotes SNARE-mediated membrane fusion [42–45]. Upon Ca^{2+} entry, the tomosyn N-terminal WD40 domain binds to synaptotagmin-1 to inhibit the promoting effect of synaptotagmin-1 on SV fusion. The tomosyn-synatotagmin-1 interaction also promotes the formation of the inhibitory tomosyn-SNARE complex [41]. On the other hand, although tomosyn-SNARE and synaptobrevin-2-SNARE are similar in structure, they differ in interactions with complexin. Specifically, complexin binds to the latter but not the former [18, 37]. Complexin acts on the synaptobrevin-2-SNARE complex via a grappling mechanism to produce dual effects: promoting Ca^{2+}-dependent synchronized release and inhibiting spontaneous SV fusion [46]. The absence of an interaction between tomosyn-SNARE and complexin is in agreement with the notion of tomosyn being an inhibitor of SV fusion because the tomosyn-SNARE complex does not participate in SV exocytosis.

3 Inhibitory Roles of Tomosyn in Neurotransmitter Release

3.1 Tomosyn Presynaptic Localization

Given tomosyn's ability to form of the inhibitory tomosyn-SNARE complex, its primary function in neurons is blocking neurotransmitter release. Tomosyn is highly expressed in presynaptic neurons [4, 17, 19, 47]. In mice, tomosyn-1 was detected in various parts of the brain, including in the CA1, CA2, and CA3 regions, mossy fibers, and the dentate gyrus in the hippocampus [4, 20, 25, 47]. Double immunostaining using antibodies against tomosyn-1 and vesicular glutamate transporter 1 (VGLUT1) indicated that these two proteins colocalize at presynaptic sites in excitatory neurons. On the contrary, tomosyn-1 is not present in vesicular GABA transporter (VGAT) positive inhibitory neurons [47]. Therefore, tomosyn-1 localizes specifically to presynaptic excitatory neurons in mammals.

Tomosyn expression is mainly detected at presynaptic regions in neurons. Tomosyn-1 immunostaining revealed a punctate pattern in the mossy fiber stratum lucidum but weak staining in dendrites and cell bodies in the dentate gyrus region, which is consistent with the predominantly presynaptic expression of tomosyn-1 [47]. Moreover, live imaging of fluorescently tagged tomosyn-1 puncta and SVs in cultured mammalian hippocampal neurons demonstrated a direct association of tomosyn-1 with SVs [48]. Tomosyns of other species also showed predominantly presynaptic expression in neurons. For example, tomosyn displays a punctate expression pattern in the axons of *C. elegans* ventral nerve cord motor neurons, and the puncta of tomosyn colocalize with those of the presynaptic marker synaptobrevin (SNB-1) [16, 17, 49, 50]. Similarly, in *Drosophila*, tomosyn is localized at presynaptic sites in motor neurons [19]. Therefore, multiple lines of evidence indicated tomosyn's presynaptic localization, which is consistent with its role in regulating presynaptic release of excitatory neurotransmitters.

3.2 Inhibition on Basal Synaptic Transmission

Tomosyn's functional roles in neuronal transmission were studied through knockout (KO), knockdown (KD), and loss-of-function (*lf*) mutant models. In the tomosyn-1 global knockout mouse model, stimulation of the mossy fibers causes a larger evoked excitatory postsynaptic potential (EPSC) amplitude in postsynaptic neurons compared with the wild type, indicating that the absence of tomosyn-1 enhances synaptic transmission [20]. Moreover, in *Drosophila*, tomosyn KD and loss-of-function mutant models displayed enhanced evoked release amplitude and total charge transfer compared with the wild type, indicating potentiated synaptic transmission [18, 19].

The in vivo functions of tomosyn can be studied by using *tom-1* mutants of *C. elegans*. A commonly used method to assess neurotransmission in *C. elegans* is to quantify the percentage of worms paralyzed over time in the presence of aldicarb, which is a cholinesterase inhibitor. Application of aldicarb causes acetylcholine accumulation at the neuromuscular junction, which eventually leads to spastic paralysis of animals [51]. Therefore, mutant worms with enhanced acetylcholine release become paralyzed faster than wild-type worms, and vice versa. *tom-1(lf)* mutants become paralyzed faster than the wild type in the aldicarb sensitivity assay, suggesting that acetylcholine release might be increased in the mutants [16, 17, 49, 50].

Electrophysiological recordings show that the decay rate of EPSCs at the *C. elegans* neuromuscular junction is greatly slowed, which is associated with a much increased charge transfer (current integral) and often accompanied by an increased EPSC peak amplitude in *tom-1(lf)* mutants compared with wild type

[16, 17, 52, 53]. On the contrary, overexpressing tomosyn reduced evoked EPSC current integral [52]. The peak amplitude and decay rate of EPSCs reflect the fast synchronous component and the slow asynchronous component of EPSCs, respectively. To distinguish the contribution of tomosyn to the specific component, EGTA, a slow Ca^{2+} ion chelator, was used in *C. elegans* EPSC recording. EGTA addition rescued the long decay time of evoked EPSC in *tom-1(lf)* mutants back to the wild-type level [53]. Therefore, tomosyn appears to be important to regulating the slow asynchronous component of evoked EPSCs. Collectively, the behavioral and electrophysiological data as well as the presynaptic localization of tomosyn in neurons suggest that tomosyn plays an inhibitory role in neurotransmitter release.

There are various ways to modulate presynaptic neurotransmitter release, including changing the active zone arrangement and regulating the SV pool size. As demonstrated in the *C. elegans tom-1(lf)* mutant, there was no gross change in active zone protein arrangement [16, 17]. Hence, the augmented SV exocytosis in *tom-1(lf)* mutants is not due to altered presynaptic structures. In contrast, multiple lines of evidence pointed to tomosyn's function in regulating SV pool sizes [16, 17, 22, 54]. In cultured rodent hippocampal cultures, tomosyn-1 KD increases the sizes of the readily releasable pool (RRP) and the recycling pool (RP), whereas tomosyn-1overexpression tends to have opposite effects [22]. Phosphorylation of tomosyn-1 by Cdk5 enhances its ability to reduce the RRP and RP sizes, via interactions of tomosyn-1 with Rab3A and synapsin [22]. The size of the RRP is also increased in motor neurons of *C. elegans tom-1(lf)* mutants, as assessed by comparing postsynaptic currents evoked by a hyperosmotic sucrose solution between the mutants and wild type [16, 17]. Further analyses of the presynaptic function of tomosyn suggested that it also regulates SV trafficking. Electron microscopy of *C. elegans tom-1* mutants showed increased primed/docked, and tethered SVs in presynaptic neurons [16, 54]. Therefore, tomosyn, by inhibiting SV priming and docking, negatively regulates RRP size, ultimately causing a reduction in synaptic transmission.

In addition, tomosyn may regulate synaptic transmission in a retrograde pathway involving neurexin and neuroligin. In *C. elegans*, inactivation of a muscle microRNA, miR-1, leads to the creation of a retrograde signal that suppresses acetylcholine release. Neurexin and neuroligin act downstream of miR-1 to increase tomosyn presynaptic expression. Therefore, miR-1 retrogradely inhibits the evoked release by elevating the presynaptic tomosyn level [55].

3.3 Interaction with Munc18-1/UNC-18 and Munc13/UNC-13

Tomosyn functionally interacts with Munc13/UNC-13 and Munc18-1/UNC-18, which interact with SNAREs to promote SV fusion and regulate SV docking and priming [56–58]. In *C. elegans*, *unc-13(s69)*, a null mutant, has much fewer SVs in contact with the presynaptic plasma membrane than wild type, and essentially no

EPSCs and hyperosmotic sucrose-evoked postsynaptic currents at the NMJ [16, 17, 59]. Some of these phenotypes of the *unc-13* mutant are opposite to those of *tom-1(lf)* mutants and can be partially rescued by combing the mutant with *tom-1(ok285)*, a putative null mutant, suggesting that tomosyn works antagonistically with UNC-13 in vesicles priming [16, 17]. An early study suggested that UNC-13 plays a role in promoting the transition of syntaxin from a closed conformation to an open confirmation that is required for SNARE complex assembly [59]. However, knockin of open syntaxin (L166A/E167A) hardly rescued the *unc-13* null mutant, suggesting that UNC-13 plays a minor role in altering syntaxin conformation [60]. Hence, subsequent studies turned to investigating other functions of UNC-13 and potential interplays between UNC-13 and tomosyn.

UNC-13 has two isoforms: UNC-13L (long isoform) and UNC-13S (short isoform), which are responsible for the fast and slow components of evoked EPSCs, respectively [53]. In *C. elegans*, lack of tomosyn leads to the accumulation of UNC-13S (short isoform) at synapses [17]. To understand the interaction between tomosyn and UNC-13S, *unc-13(e51)* and *unc-13(e1091)*, which encode truncated forms of UNC-13L but intact UNC-13S, were studied alongside the *tom-1* mutant. In the double mutant *tom-1(ok285)unc-13(e1091 or e51)*, observed defects of *unc-13(e1091/e51)* in the evoked release, RRP, and locomotion are partially rescued. Moreover, inactivating tomosyn in animals expressing only UNC-13S significantly increases the quantal content of evoked EPSCs at the NMJ [53]. These results suggest that tomosyn specifically inhibits the UNC-13S-mediated slow component of evoked release. This conclusion is also in agreement with the aforementioned slow EPSC decay phenotype of *tom-1(lf)* mutants. Thus, tomosyn and UNC-13S appear to act together to regulate the slow component of evoked release. It has been shown that an M-domain of UNC-13S can inhibit the release probability of cholinergic neurons [61]. Although the specific molecular pathway involved in the synaptic functions of tomosyn and UNC-13 remains unclear, tomosyn and the M-domain of UNC-13 might interact to suppress presynaptic release.

Other functions of UNC-13 include chaperone activity for the SNARE complex and promotion of vesicle priming in coordination with UNC-18 [62–64]. Therefore, analyses of genetic interactions among *unc-13*, *unc-18*, and *tom-1* mutants may provide insights into tomosyn function (Fig. 3). UNC-18 and its mammalian homolog Munc18-1 regulate vesicles priming and serve as chaperones of syntaxin-1 to promote its trafficking [41, 66–69]. An UNC-18(P334A)/Munc18-1(P335A) mutation makes domain-3a of the protein to adopt an unfurled and extended conformation, which increases synaptic exocytosis [50, 70, 71]. Knockin of the UNC-18(P334A) mutation into the genetic background of *unc-13(s69)* causes slightly increases in motility and aldicarb sensitivity, which provide further evidence for the gain-of-function nature of the UNC-18(P334A) mutation. The rescuing effects of *unc-18(P334A)* and *tom-1(ok285)* on the neurotransmitter release defect of *unc-13(s69)* are comparable [50, 60]. A triple mutant of *tom-1(ok285)*, *unc-13(s69)*, and *unc-18(P334A)* has been generated and used to further understand the interplay among the three proteins. Compared with the *unc-13(s69)* mutant, the triple mutant is significantly improved in thrashing ability and restored to the

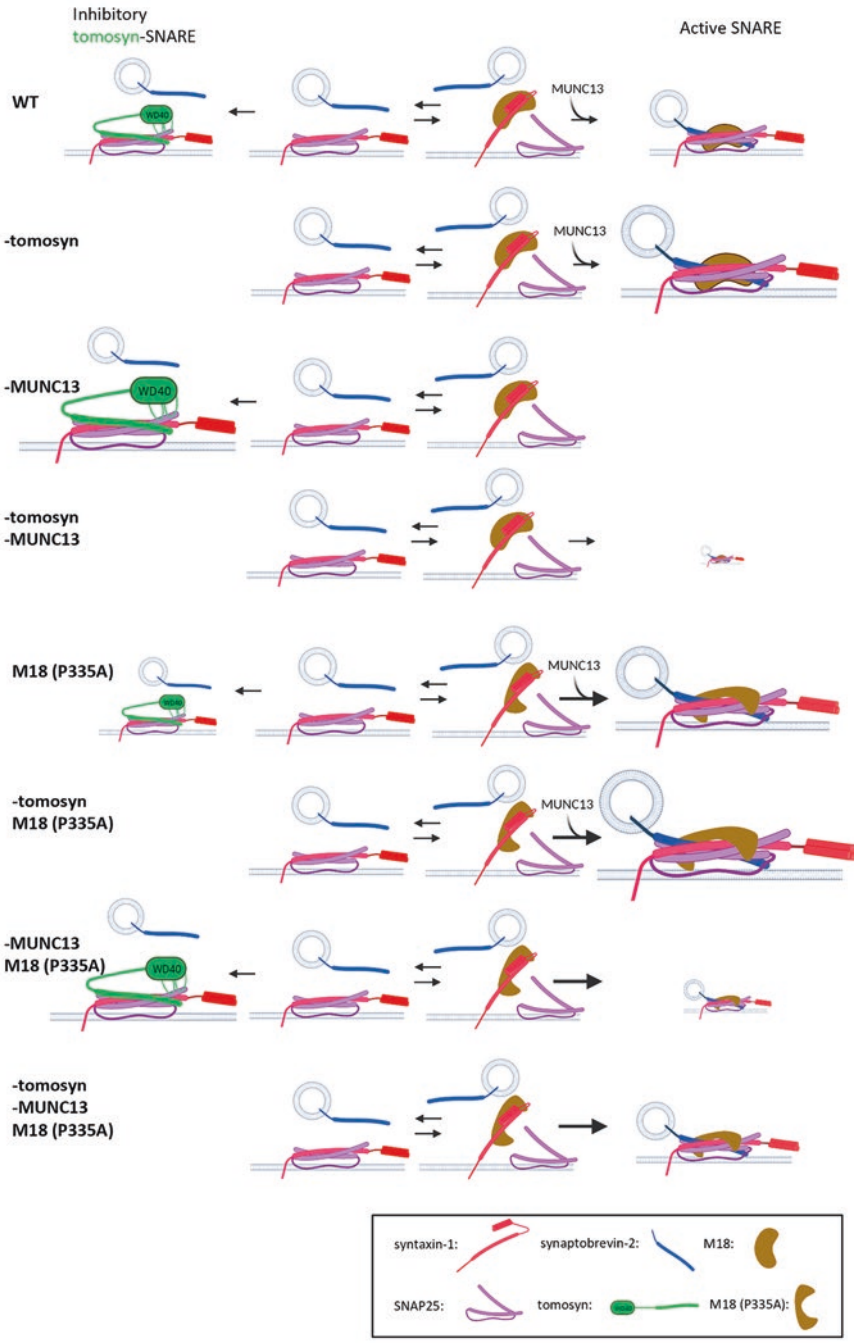

Fig. 3 Model of the interaction among tomosyn, UNC-18/Munc18, and UNC-13/Munc13 in regulating presynaptic synaptic vesicles (SV) release. In wild-type (WT) condition, when tomosyn

wild-type level in aldicarb sensitivity [50]. The synergistic effects of UNC-18 gain-of-function and tomosyn loss-of-function suggest that tomosyn and UNC-18 act downstream of UNC-13 to antagonistically control neurotransmitter release (Fig. 3). This model is consistent with the biochemical template model of Munc18/UNC-18 function in which Munc18/UNC-18 favors the formation of active SNARE complexes containing synaptobrevin over the inhibitory tomosyn-SNARE complex by simultaneously binding to syntaxin and synaptobrevin via domain 3 [72].

3.4 Synaptic Plasticity

Beyond its role in controlling neurotransmitter release, tomosyn contributes to various forms of synaptic plasticity. Several studies have used paired-pulse stimulation to demonstrate a role of tomosyn in short-term synaptic plasticity. In the mammalian hippocampus, tomosyn-1 KD or KO led to weaker paired-pulse facilitation (PPF) and enhanced paired-pulse depression (PPD) [20–22, 73]. Similarly, at the *Drosophila* NMJ, tomosyn KD increased PPD [19]. An increase in neurotransmitter release probability generally causes a larger initial peak response but a smaller second peak response in paired-pulse stimulation, both the weakened PPF and strengthened PPD indicate increased presynaptic release probability (Pr). Thus, a reduction of tomosyn's presynaptic function increases the release probability of the neurons. Tomosyn-1 global KO mice also show a higher susceptibility to dentate gyrus kindling stimulation than wild-type mice, suggesting enhanced glutamate release from the excitatory neurons [74].

The presence of tomosyn defines the overall Pr of motor neurons in *Drosophila*, which, in turn, modulate the synaptic plasticity [18]. There are two types of motor neurons in *Drosophila*. The first is Ib, which has tonic sustained release with low

Fig. 3 (continued) binds to syntaxin-1 and SNAP-25, it forms the inhibitory tomosyn-SNARE to inhibit SV fusion. In contrast, Munc18-1 displaces SNAP-25 to form the binary complex with syntaxin-1 in closed formation. With the aid of Munc13, it leads to SNARE complex formation and fusion of SV [65] (*WT*). When tomosyn is removed, inhibitory tomosyn-SNARE is absent, which favors active synaptobrevin-2-containing SNARE formation (shown by a larger size) (*-tomosyn*). However, without Munc13, the binary interaction formed by Munc18-1 and syntaxin-1 is not efficiently transitioned to active SNARE. Therefore, in the absence of Munc13, tomosyn-SNARE formation is favored, inhibiting neurotransmitter release (*-MUNC13*). When tomosyn is removed in the background of losing Munc13, the removal of inhibition by tomosyn again favors active SNARE formation, even without Munc13. Yet, this rescue in active SNARE formation is minimal (small size of active SNARE) (*-tomosyn*, *-MUNC13*). Munc18-1 (P335A) (UNC-18 (P334A)) is the unfurled form of Munc18-1, facilitating active SNARE complex formation (*M18 (P335A)*). In the absence of tomosyn, SV fusion is further enhanced (*-tomosyn, M18 (P335A)*). However, without Munc13, Munc18-1 (P335A) cannot efficiently promote the formation of active SNARE complex, hence favoring tomosyn-SNARE (*-MUNC13, M18 (P335A)*). Finally, Munc18-1 (P335A) can strongly rescue the deficit of Munc13 in the absence of inhibitory tomosyn. Neurotransmitter release is closed to wild-type level (*-tomosyn, -MUNC13, M18 (P335A)*)

release probability, and the other is Is, which has phasic rapid depression with high release probability. Tomosyn is highly expressed in Ib neurons but not expressed in Is neurons. Electrophysiological analyses of evoked release at the NMJ indicate that null mutation of the tomosyn gene enhances the Pr at Ib but not Is synapses, suggesting that tomosyn functions exclusively in Ib motor neurons to maintain a low Pr. The low Pr of Ib neurons is critical to the generation of presynaptic homeostatic potentiation (PHP), which is a compensation mechanism for postsynaptic deficits to maintain proper synaptic transmission. A loss of tomosyn at the Ib synapses would maximize the Pr (depleting the RRP), and prevent PHP generation [18]. Consequently, the regulation of Pr is key to tomosyn's role in controlling synaptic communication.

Furthermore, tomosyn contributes to the generation of long-term plasticity (LTP) primarily via a presynaptic mechanism. At hippocampal mossy fiber to CA3 pyramidal cell synapses, LTP induced by either tetanic stimulation or forskolin is weaker in tomosyn-1 KO and KD mice than wild type [20, 21]. Forskolin activates adenylyl cyclase to increase intracellular levels of cAMP, which, in turn, activates PKA to phosphorylate various proteins, including tomosyn-1 [29]. It has been shown that PKA phosphorylation of tomosyn promotes synchronous SV release, which might be the basis for tomosyn's roles in regulating LTP [29]. On the other hand, post-tetanic potentiation caused by mossy fiber stimulation is driven mainly by increased presynaptic release [75]. It is augmented in mice deficient in tomosyn-1 due to the increased presynaptic Pr [21]. Therefore, a physiological function of tomosyn appears to be modulating short-term and long-term plasticity by inhibiting the Pr.

Since tomosyn-1 plays a role in generating LTP, it is also important in learning and memory processes. The CA3 network in the mammalian hippocampus is important to spatial memories [76]. Mice overexpressing tomosyn-1 in the dentate gyrus (presynaptic neuron projecting the mossy fiber) show mild deficits and impaired learning in the Morris water maze test, which is used to assess spatial memory [73]. However, LTP at the mossy fibers and CA3 pyramidal neuron synapses are unchanged in these mice [20, 21, 73], suggesting that tomosyn-1 does not alter animals' spatial learning and memory via LTP modulation.

3.5 Potential Postsynaptic Functions

The above studies suggest that tomosyn is important to presynaptic function. However, tomosyn-1 is also detected at dendrites and somata of hippocampal neurons [47, 77, 78], and tomosyn-1 KD is associated with reduced dendritic complexity and spine density in hippocampal neurons [77, 78], suggesting that postsynaptic tomosyn-1 might regulate dendritic development. In addition, postsynaptic tomosyn-1 might regulate postsynaptic receptor expression, as suggested by a reduced frequency of AMPA receptor-mediated miniature excitatory postsynaptic currents (mEPSCs) accompanied by lower AMPA receptor

surface expression in tomosyn-1 KD mice [78]. However, the role of tomosyn in postsynaptic receptor surface expression remains uncertain because most studies with rat hippocampal neurons, *Drosophila*, and *C. elegans* have been unable to demonstrate an effect of tomosyn deficiency on the frequency of mEPSCs [17, 19, 22].

Efforts have been made to provide a mechanistic view of tomosyn-1 function in AMPA receptor trafficking. The prevailing model is that the WD40 domain of tomosyn promotes dendritic stability by inhibiting a RhoA signaling pathway, resulting in enhanced AMPA receptor insertion into the dendritic plasma membrane [78]. The tomosyn-1-RhoA pathway has also been implicated in regulating overall neurite outgrowth. Specifically, a Rho-associated serine/threonine kinase (ROCK) phosphorylates syntaxin-1 to promote tomosyn-SNARE formation, which inhibits vesicle transport that is necessary for neurite outgrowth [79]. On the contrary, another signaling pathway, involving the ubiquitination of tomosyn-1 by HRD1 (an E3 ligase), promotes tomosyn-1 degradation to facilitate dendritic development [77]. Thus, tomosyn-1 might play important roles in postsynaptic dendritic morphology and development.

3.6 Regulation on Dense-Core Vesicles Release

Along with regulating synaptic vesicle release, tomosyn takes part in regulating the release of dense-core vesicles (DCV), which contain a variety of neurotransmitters, including neuropeptides and biogenic amines [48, 80–82]. Mammalian tomosyn-1 associates with DCVs and inhibits Ca^{2+}-dependent DCV release of catecholamines [48, 82]. Gracheva et al. have studied the role of tomosyn in regulating DCV release in vivo by investigating genetic interactions between tomosyn and UNC-31 in *C. elegans* [80, 81]. UNC-31, an ortholog of mammalian Ca^{2+}-dependent activator protein for secretion (CAPS), mediates DCV tethering, docking, and priming for neuropeptide release [83]. *tom-1* loss-of-function mutants have a reduction of DCVs in ventral nerve cord motor neurons due to an increase in DCV exocytosis, while overexpression of tomosyn increased the number of DCVs at the synapses. These data highlight tomosyn's role in neuropeptide release inhibition [81]. *unc-31(lf)* mutants show defective locomotion, accumulation of DCVs in neurons, and reduced amplitude and charge transfer of evoked EPSCs, reflecting the consequences of DCV release impairment. In a double mutant of *tom-1(lf);unc-31(lf)*, all the above-mentioned defects of the *unc-31(lf)* are partially mitigated [81], tomosyn is proposed to inhibit UNC-31 dependent DCVs fusion in a similar manner to inhibiting SV fusion. By forming the tomosyn-SNARE, SNARE complex formation between v-SANRE on DCVs and t-SNAREs on the plasma membrane is blocked. Thus, tomosyn appears to control both the release of both SVs (small clear vesicles) containing fast neurotransmitters and DCVs containing neuropeptides.

3.7 Mammalian Tomosyn-2 Function

In contrast to tomosyn-1, the major expression sites for tomosyn-2 are the pyramidal cell layer of the hippocampal CA2 region and the cerebellum [25, 47]. Tomosyn-2 is mainly localized at dendrites and dendritic spines, suggesting that it might have a postsynaptic function [47]. Global knockout of tomosyn-2 in mice impairs sensorimotor and motor performances [84]. The tomosyn-2 KO mice display a higher frequency of spontaneous end-plate potentials, and a decrease of paired-pulse facilitation at the NMJ, suggesting that removing tomosyn-2 increases neurotransmitter Pr [84]. Therefore, although tomosyn-2 is localized at postsynaptic regions, it may inhibit presynaptic release retrogradely at the NMJ. Interestingly, tomosyn-2 global KO did not alter synaptic transmission in hippocampal neuronal cultures, despite its prominent and strong expression in the hippocampus [84]. Nevertheless, live imaging of EYFP-tagged tomosyn-2 shows co-migration with SVs and DCVs, similar to tomosyn-1 [48]. Additionally, tomosyn-1 and -2 are similar in their abilities to inhibit exocytosis in PC12 cells [85]. So far, the function of tomosyn-2 in the central nervous system remains unclear.

4 Functions of Tomosyn Domains

4.1 C-Terminal VAMP-Like Domain: Formation of Tomosyn-SNARE

The C-terminal VLD was first proposed as the major component accounting for the inhibitory function of tomosyn. Using the in vitro FRET liposome system, tomosyn VLD blocked the usual synaptobrevin-2 interaction with t-SNAREs for liposome fusion [40]. The VLD inhibits normal SNARE formation by accelerating the formation of a tomosyn-SNARE complex. Consistent with the inhibitory role of tomosyn, overexpression of the VLD motif alone inhibited Ca^{2+}-dependent evoked release of dopamine in a PC12 cell system [12]. Nevertheless, the VLD alone is significantly weaker than full-length tomosyn in binding with syntaxin-1 [26, 33]. Consistent with the weaker binding, overexpression of the tomosyn VLD motif in the more physiological adrenal chromaffin cell culture did not affect exocytosis of DCVs [33]. Additionally, in both *C. elegans* and *Drosophila*, the C-terminal VLD of tomosyn does not have the same ability of inhibiting neurotransmitter release as the full-length tomosyn [18, 52]. Hence, although the VLD of tomosyn is necessary for binding to syntaxin, other parts of tomosyn also contribute to the inhibitory function of tomosyn on SNARE complex formation.

Although tomosyn is generally regarded as an inhibitor in the SNARE complex formation, there is evidence suggesting that its VLD also has an additional function of accelerating the SNARE complex formation. Upon forming the tomosyn-SNARE complex, tomosyn VLD accelerates the fusion of the N-terminal of the t-SNARE

[36]. In other words, the tomosyn-SNARE may also promote membrane fusion by acting as a template for subsequent binding of synaptobrevin-2 to t-SANREs. Therefore, the pre-binding of t-SNARE with tomosyn's VLD may lower the energy barrier in SNARE complex formation.

4.2 N-Terminal WD40 Domain

The N-terminal of tomosyn contains WD-40 repeats, which are repeating units ending with tryptophan and aspartate (WD). The WD40 domain has a diverse set of functions, including signal transduction, gene regulation, and vesicle trafficking [86]. The N-terminal WD40 domain of tomosyn cannot interact with syntaxin-1 independently to form a complex with t-SNAREs [12]. Thus, the WD40 domain unlikely participates in syntaxin-1 binding directly. In adrenal chromaffin cell cultures, deletion of the N-terminus WD-40 domain eliminates the inhibitory effect of tomosyn on exocytosis. However, expression of the N-terminus domain alone does not affect exocytosis, indicating the N-terminal is necessary but not sufficient for release inhibition [33]. Interestingly, the WD-40 domain facilitates the oligomerization of SNAREs, which makes the SNAREs non-functional [20]. Moreover, in contrast to the results described above, it has been shown that fragments of the WD-40 domain can inhibit evoked excitatory postsynaptic potential (EPSP) to a similar level as VLD alone in cultured mouse superior cervical ganglion cells [20]. Thus, the N-terminal WD-40 domain could induce oligomerization of the SNARE proteins to inhibit SV fusion.

Besides the direct inhibitory effect on SNARE complex formation, the WD40 repeats can interact with Synaptotagmin-1 to control Ca^{2+}-dependent exocytosis [41]. For example, overexpression of tomosyn inhibits Ca^{2+}-dependent release of catecholamine from adrenal chromaffin cells and reduces Ca^{2+} sensitivity without changing the degree of Ca^{2+} cooperativity [12, 82]. However, in vivo data of *Drosophila* suggest that tomosyn inhibits SV exocytosis in a synaptotagmin-1-independent manner. Specifically, addition of a tomosyn *lf* mutation to a synaptotagmin-1 null mutant enhances evoked EPSC amplitude [18]. Therefore, the role of tomosyn in synaptotagmin-1-dependent exocytosis remains uncertain.

Another reported function of the WD40 domain is to localize tomosyn to synaptic vesicles. In a tomosyn *lf* mutant of *Drosophila*, expressing the tomosyn WD40 domain results in a similar degree of synaptic vesicle localization as expressing the full-length tomosyn [18]. This function of the WD40 domain appears to be conserved in mammals because deletion of the VLD domain does not impair tomosyn binding to SVs in cultured mammalian neurons [48]. Thus, it is the WD40 domain that mediates the localization of tomosyn to SVs. Notably, in both cell cultures and in vivo systems, neither the WD-40 domain, nor the VLD, nor a synthetic peptide of the WD-40 domain fused to the C-terminus can inhibit SV exocytosis to the same degree as the full-length tomosyn [18, 33, 52, 79], suggesting that other regions in tomosyn also contribute to tomosyn function.

4.3 Other Supporting Regions

As neither the N-terminal WD-40 domain nor the C-terminal VLD domain alone can fully recapitulate the inhibitory effect of the full-length tomosyn on SV exocytosis, the region between these two domains must have important functions. As shown in Fig. 1, a tail domain is located immediately upstream of the VLD domain in the C-terminal. In electrophysiological analyses of SGC neurons, a synthetic peptide containing both the tail domain and the VLD domain is significantly less effective in inhibiting evoked EPSCs than a peptide of the VLD domain alone [87], suggesting that the tail domain counteracts against VLD domain's inhibitory effect on neurotransmitter release. Similarly, in liposome fusion assays between t-SNARE vesicles and v-SNARE vesicles, application of both the tail domain and the VLD domain is less effective on vesicles fusion than application of only the VLD domain in inhibiting vesicle fusion [88]. Although it does not bind to syntaxin-1, the tail domain can directly interact with both the C-terminal domain and the WD-40 domain [87, 88]. When the tail domain binds to the WD-40 domain, the VLD can participate in the inhibition of active SNARE formation. On the contrary, when it interacts with the VLD, it frees the WD40 domain and inhibits VLD binding to t-SNAREs to form the tomosyn-SNARE [88]. Thus, the tail domain is thought to be an intramolecular switch in tomosyn function.

In addition to the aforementioned domains, mouse tomosyn-1 contains three loop structures, located between the N-terminal WD40 repeats and the tail domain [24]. Williams et al. express mouse tomosyn-1 in PC12 cells to study the loops' functions in high K^+-induced human growth hormone exocytosis [24]. Deletion of loop1 and loop3, but not loop2, causes a decreased inhibition of PC12 cell exocytosis. However, none of the deletions affect the ability of tomosyn to bind to syntaxin. Also, deletion of neither loop1 nor loop3 affects SV localization of tomosyn-1 [24, 34]. Therefore, loop1 and loop3 likely participate in the exocytosis inhibition, independent of syntaxin binding. Although loop1 and loop3 are not important to syntaxin binding, deleting either of them causes a significant reduction in the interaction of tomosyn with SNAP-25 in the tomosyn-SNARE complex [34]. Loop1 and loop3 therefore contribute to the overall inhibitory function by associating with SNAP25 in the tomosyn-SNARE. These loops might also explain why early studies expressing mammalian tomosyn VLD fragments did not reveal an inhibitory effect on exocytosis. Without the loops, the tomosyn VLD domain would not be able to form the tomosyn-SNARE complex efficiently, reducing its inhibitory activity.

5 Conclusion

Upon the first discovery of tomosyn as a syntaxin-binding protein, the "friend" of syntaxin is now regarded as one of the important inhibitors in neurotransmitter release. With its defining feature of the VLD domain, tomosyn inhibits active

SNARE complex formation. This domain is well conserved across many species, signifying the importance of tomosyn in regulating SNAREs interaction. With its ability to interact with t-SNAREs, tomosyn localizes in presynaptic neurons and associates with SVs and DCVs. When tomosyn binds to syntaxin, it leads to formation of the tomosyn-SNARE complex to inhibit SV fusion. At the synaptic level, tomosyn regulates vesicle pool size and, ultimately, SV release of neurotransmitters. Moreover, tomosyn's SNARE regulation allows its control over the docking of vesicles, therefore controlling the probability of release at the presynaptic sites. Hence, tomosyn is central to the regulation of synaptic plasticity and contributes to the generation of LTP. Although the functions of tomosyn at presynaptic sites are well documented by studies with mammals, *Drosophila*, and *C. elegans*, recent evidence from mammals suggests a potential postsynaptic role of tomosyn in regulating dendritic complexity. In conclusion, tomosyn, through its interaction with syntaxin, establishes itself as a critical regulator of neuronal communication.

Acknowledgments This work was supported by the Natural Sciences and Engineering Research Council of Canada (RGPIN-2020-07139), the Canadian Institute of Health Research (Project grant 165917), and the joint catalyst grant from the Rare Diseases: Models & Mechanisms Network and Dravet Canada. C.H.C and M.H. are supported by Vision Science Research Program from University Health Network. M.H. is a recipient of Ontario Graduate Scholarship. We thank Peter Argiropoulos for proofreading the manuscript.

References

1. Hata Y, Slaughter CA, Sudhof TC. Synaptic vesicle fusion complex contains unc-18 homologue bound to syntaxin. Nature. 1993;366:347–51. https://doi.org/10.1038/366347a0.
2. Pevsner J, Hsu SC, Scheller RH. n-Sec1: a neural-specific syntaxin-binding protein. Proc Natl Acad Sci U S A. 1994;91:1445–9. https://doi.org/10.1073/pnas.91.4.1445.
3. Garcia EP, Gatti E, Butler M, Burton J, De Camilli P. A rat brain Sec1 homologue related to Rop and UNC18 interacts with syntaxin. Proc Natl Acad Sci U S A. 1994;91:2003–7. https://doi.org/10.1073/pnas.91.6.2003.
4. Fujita Y, Shirataki H, Sakisaka T, Asakura T, Ohya T, Kotani H, et al. Tomosyn: a syntaxin-1-binding protein that forms a novel complex in the neurotransmitter release process. Neuron. 1998;20:905–15.
5. Riento K, Jantti J, Jansson S, Hielm S, Lehtonen E, Ehnholm C, et al. A sec1-related vesicle-transport protein that is expressed predominantly in epithelial cells. Eur J Biochem. 1996;239:638–46. https://doi.org/10.1111/j.1432-1033.1996.0638u.x.
6. Araki S, Tamori Y, Kawanishi M, Shinoda H, Masugi J, Mori H, et al. Inhibition of the binding of SNAP-23 to syntaxin 4 by Munc18c. Biochem Biophys Res Commun. 1997;234:257–62. https://doi.org/10.1006/bbrc.1997.6560.
7. Riento K, Galli T, Jansson S, Ehnholm C, Lehtonen E, Olkkonen VM. Interaction of Munc-18-2 with syntaxin 3 controls the association of apical SNAREs in epithelial cells. J Cell Sci. 1998;111(Pt 17):2681–8. https://doi.org/10.1242/jcs.111.17.2681.
8. Tamori Y, Kawanishi M, Niki T, Shinoda H, Araki S, Okazawa H, et al. Inhibition of insulin-induced GLUT4 translocation by Munc18c through interaction with syntaxin4 in 3T3-L1 adipocytes. J Biol Chem. 1998;273:19740–6. https://doi.org/10.1074/jbc.273.31.19740.

9. Hata Y, Sudhof TC. A novel ubiquitous form of Munc-18 interacts with multiple syntaxins. Use of the yeast two-hybrid system to study interactions between proteins involved in membrane traffic. J Biol Chem. 1995;270:13022–8. https://doi.org/10.1074/jbc.270.22.13022.
10. Bin NR, Jung CH, Kim B, Chandrasegram P, Turlova E, Zhu D, et al. Chaperoning of closed syntaxin-3 through Lys46 and Glu59 in domain 1 of Munc18 proteins is indispensable for mast cell exocytosis. J Cell Sci. 2015;128:1946–60. https://doi.org/10.1242/jcs.165662.
11. Masuda ES, Huang BC, Fisher JM, Luo Y, Scheller RH. Tomosyn binds t-SNARE proteins via a VAMP-like coiled coil. Neuron. 1998;21:479–80. https://doi.org/10.1016/s0896-6273(00)80559-0.
12. Hatsuzawa K, Lang T, Fasshauer D, Bruns D, Jahn R. The R-SNARE motif of tomosyn forms SNARE core complexes with syntaxin 1 and SNAP-25 and down-regulates exocytosis. J Biol Chem. 2003;278:31159–66. https://doi.org/10.1074/jbc.M305500200.
13. Zhang W, Lilja L, Mandic SA, Gromada J, Smidt K, Janson J, et al. Tomosyn is expressed in beta-cells and negatively regulates insulin exocytosis. Diabetes. 2006;55:574–81. https://doi.org/10.2337/diabetes.55.03.06.db05-0015.
14. Wang S, Liu Y, Crisman L, Wan C, Miller J, Yu H, et al. Genetic evidence for an inhibitory role of tomosyn in insulin-stimulated GLUT4 exocytosis. Traffic. 2020;21:636–46. https://doi.org/10.1111/tra.12760.
15. Widberg CH, Bryant NJ, Girotti M, Rea S, James DE. Tomosyn interacts with the t-SNAREs syntaxin4 and SNAP23 and plays a role in insulin-stimulated GLUT4 translocation. J Biol Chem. 2003;278:35093–101. https://doi.org/10.1074/jbc.M304261200.
16. Gracheva EO, Burdina AO, Holgado AM, Berthelot-Grosjean M, Ackley BD, Hadwiger G, et al. Tomosyn inhibits synaptic vesicle priming in Caenorhabditis elegans. PLoS Biol. 2006;4:e261.
17. McEwen JM, Madison JM, Dybbs M, Kaplan JM. Antagonistic regulation of synaptic vesicle priming by Tomosyn and UNC-13. Neuron. 2006;51:303–15.
18. Sauvola CW, Akbergenova Y, Cunningham KL, Aponte-Santiago NA, Littleton JT. The decoy SNARE Tomosyn sets tonic versus phasic release properties and is required for homeostatic synaptic plasticity. eLife. 2021;10:e72841. https://doi.org/10.7554/eLife.72841.
19. Chen K, Richlitzki A, Featherstone DE, Schwärzel M, Richmond JE. Tomosyn-dependent regulation of synaptic transmission is required for a late phase of associative odor memory. Proc Natl Acad Sci U S A. 2011;108:18482–7. https://doi.org/10.1073/pnas.1110184108.
20. Sakisaka T, Yamamoto Y, Mochida S, Nakamura M, Nishikawa K, Ishizaki H, et al. Dual inhibition of SNARE complex formation by tomosyn ensures controlled neurotransmitter release. J Cell Biol. 2008;183:323–37. https://doi.org/10.1083/jcb.200805150.
21. Ben-Simon Y, Rodenas-Ruano A, Alviña K, Lam AD, Stuenkel EL, Castillo PE, et al. A combined optogenetic-knockdown strategy reveals a major role of Tomosyn in mossy fiber synaptic plasticity. Cell Rep. 2015;12:396–404. https://doi.org/10.1016/j.celrep.2015.06.037.
22. Cazares VA, Njus MM, Manly A, Saldate JJ, Subramani A, Ben-Simon Y, et al. Dynamic partitioning of synaptic vesicle pools by the SNARE-binding protein Tomosyn. J Neurosci. 2016;36:11208–22. https://doi.org/10.1523/jneurosci.1297-16.2016.
23. Hattendorf DA, Andreeva A, Gangar A, Brennwald PJ, Weis WI. Structure of the yeast polarity protein Sro7 reveals a SNARE regulatory mechanism. Nature. 2007;446:567–71. https://doi.org/10.1038/nature05635.
24. Williams AL, Bielopolski N, Meroz D, Lam AD, Passmore DR, Ben-Tal N, et al. Structural and functional analysis of tomosyn identifies domains important in exocytotic regulation. J Biol Chem. 2011;286:14542–53. https://doi.org/10.1074/jbc.M110.215624.
25. Groffen AJ, Jacobsen L, Schut D, Verhage M. Two distinct genes drive expression of seven tomosyn isoforms in the mammalian brain, sharing a conserved structure with a unique variable domain. J Neurochem. 2005;92:554–68. https://doi.org/10.1111/j.1471-4159.2004.02890.x.
26. Yokoyama S, Shirataki H, Sakisaka T, Takai Y. Three splicing variants of tomosyn and identification of their syntaxin-binding region. Biochem Biophys Res Commun. 1999;256:218–22. https://doi.org/10.1006/bbrc.1999.0300.

27. Flotho A, Melchior F. Sumoylation: a regulatory protein modification in health and disease. Annu Rev Biochem. 2013;82:357–85. https://doi.org/10.1146/annurev-biochem-061909-093311.
28. Geerts CJ, Jacobsen L, van de Bospoort R, Verhage M, Groffen AJ. Tomosyn interacts with the SUMO E3 ligase PIASγ. PLoS One. 2014;9:e91697. https://doi.org/10.1371/journal.pone.0091697.
29. Baba T, Sakisaka T, Mochida S, Takai Y. PKA-catalyzed phosphorylation of tomosyn and its implication in Ca2+−dependent exocytosis of neurotransmitter. J Cell Biol. 2005;170:1113–25. https://doi.org/10.1083/jcb.200504055.
30. Lehman K, Rossi G, Adamo JE, Brennwald P. Yeast homologues of tomosyn and lethal giant larvae function in exocytosis and are associated with the plasma membrane SNARE, Sec9. J Cell Biol. 1999;146:125–40. https://doi.org/10.1083/jcb.146.1.125.
31. Sutton RB, Fasshauer D, Jahn R, Brunger AT. Crystal structure of a SNARE complex involved in synaptic exocytosis at 2.4 A resolution. Nature. 1998;395:347–53. https://doi.org/10.1038/26412.
32. Poirier MA, Xiao W, Macosko JC, Chan C, Shin YK, Bennett MK. The synaptic SNARE complex is a parallel four-stranded helical bundle. Nat Struct Biol. 1998;5:765–9. https://doi.org/10.1038/1799.
33. Yizhar O, Lipstein N, Gladycheva SE, Matti U, Ernst SA, Rettig J, et al. Multiple functional domains are involved in tomosyn regulation of exocytosis. J Neurochem. 2007;103:604–16. https://doi.org/10.1111/j.1471-4159.2007.04791.x.
34. Bielopolski N, Lam AD, Bar-On D, Sauer M, Stuenkel EL, Ashery U. Differential interaction of tomosyn with syntaxin and SNAP25 depends on domains in the WD40 β-propeller core and determines its inhibitory activity. J Biol Chem. 2014;289:17087–99. https://doi.org/10.1074/jbc.M113.515296.
35. Yu H, Rathore SS, Gulbranson DR, Shen J. The N- and C-terminal domains of tomosyn play distinct roles in soluble N-ethylmaleimide-sensitive factor attachment protein receptor binding and fusion regulation. J Biol Chem. 2014;289:25571–80. https://doi.org/10.1074/jbc.M114.591487.
36. Li F, Tiwari N, Rothman JE, Pincet F. Kinetic barriers to SNAREpin assembly in the regulation of membrane docking/priming and fusion. Proc Natl Acad Sci U S A. 2016;113:10536–41. https://doi.org/10.1073/pnas.1604000113.
37. Pobbati AV, Razeto A, Boddener M, Becker S, Fasshauer D. Structural basis for the inhibitory role of tomosyn in exocytosis. J Biol Chem. 2004;279:47192–200. https://doi.org/10.1074/jbc.M408767200.
38. Sollner T, Bennett MK, Whiteheart SW, Scheller RH, Rothman JE. A protein assembly-disassembly pathway in vitro that may correspond to sequential steps of synaptic vesicle docking, activation, and fusion. Cell. 1993;75:409–18. https://doi.org/10.1016/0092-8674(93)90376-2.
39. Prinslow EA, Stepien KP, Pan YZ, Xu J, Rizo J. Multiple factors maintain assembled trans-SNARE complexes in the presence of NSF and alphaSNAP. eLife. 2019;8:e38880. https://doi.org/10.7554/eLife.38880.
40. Li Y, Wang S, Li T, Zhu L, Ma C. Tomosyn guides SNARE complex formation in coordination with Munc18 and Munc13. FEBS Lett. 2018;592:1161–72. https://doi.org/10.1002/1873-3468.13018.
41. Yamamoto Y, Mochida S, Miyazaki N, Kawai K, Fujikura K, Kurooka T, et al. Tomosyn inhibits synaptotagmin-1-mediated step of Ca2+-dependent neurotransmitter release through its N-terminal WD40 repeats. J Biol Chem. 2010;285:40943–55. https://doi.org/10.1074/jbc.M110.156893.
42. Perin MS, Brose N, Jahn R, Sudhof TC. Domain structure of synaptotagmin (p65). J Biol Chem. 1991;266:623–9. https://doi.org/10.1016/S0021-9258(18)52480-7.
43. Brose N, Petrenko AG, Sudhof TC, Jahn R. Synaptotagmin: a calcium sensor on the synaptic vesicle surface. Science. 1992;256:1021–5. https://doi.org/10.1126/science.1589771.
44. Geppert M, Goda Y, Hammer RE, Li C, Rosahl TW, Stevens CF, et al. Synaptotagmin I: a major Ca^{2+} sensor for transmitter release at a central synapse. Cell. 1994;79:717–27.

45. Fernandez-Chacon R, Konigstorfer A, Gerber SH, Garcia J, Matos MF, Stevens CF, et al. Synaptotagmin I functions as a calcium regulator of release probability. Nature. 2001;410:41–9. https://doi.org/10.1038/35065004.
46. Sudhof TC, Rothman JE. Membrane fusion: grappling with SNARE and SM proteins. Science. 2009;323:474–7. https://doi.org/10.1126/science.1161748.
47. Barak B, Williams A, Bielopolski N, Gottfried I, Okun E, Brown MA, et al. Tomosyn expression pattern in the mouse hippocampus suggests both presynaptic and postsynaptic functions. Front Neuroanat. 2010;4:149. https://doi.org/10.3389/fnana.2010.00149.
48. Geerts CJ, Mancini R, Chen N, Koopmans FTW, Li KW, Smit AB, et al. Tomosyn associates with secretory vesicles in neurons through its N- and C-terminal domains. PLoS One. 2017;12:e0180912. https://doi.org/10.1371/journal.pone.0180912.
49. Dybbs M, Ngai J, Kaplan JM. Using microarrays to facilitate positional cloning: identification of tomosyn as an inhibitor of neurosecretion. PLoS Genet. 2005;1:6–16. https://doi.org/10.1371/journal.pgen.0010002.
50. Park S, Bin NR, Yu B, Wong R, Sitarska E, Sugita K, et al. UNC-18 and Tomosyn antagonistically control synaptic vesicle priming downstream of UNC-13 in Caenorhabditis elegans. J Neurosci. 2017;37:8797–815. https://doi.org/10.1523/JNEUROSCI.0338-17.2017.
51. Miller KG, Alfonso A, Nguyen M, Crowell JA, Johnson CD, Rand JB. A genetic selection for Caenorhabditis elegans synaptic transmission mutants. Proc Natl Acad Sci U S A. 1996;93:12593–8. https://doi.org/10.1073/pnas.93.22.12593.
52. Burdina AO, Klosterman SM, Shtessel L, Ahmed S, Richmond JE. In vivo analysis of conserved C. elegans tomosyn domains. PLoS One. 2011;6:e26185. https://doi.org/10.1371/journal.pone.0026185.
53. Hu Z, Tong XJ, Kaplan JM. UNC-13L, UNC-13S, and Tomosyn form a protein code for fast and slow neurotransmitter release in Caenorhabditis elegans. eLife. 2013;2:e00967. https://doi.org/10.7554/eLife.00967.
54. Gracheva EO, Maryon EB, Berthelot-Grosjean M, Richmond JE. Differential regulation of synaptic vesicle tethering and docking by UNC-18 and TOM-1. Front Synaptic Neurosci. 2010;2:141. https://doi.org/10.3389/fnsyn.2010.00141.
55. Hu Z, Hom S, Kudze T, Tong XJ, Choi S, Aramuni G, et al. Neurexin and neuroligin mediate retrograde synaptic inhibition in *C. elegans*. Science. 2012;337:980–4. https://doi.org/10.1126/science.1224896.
56. Richmond JE, Davis WS, Jorgensen EM. UNC-13 is required for synaptic vesicle fusion in *C. elegans*. Nat Neurosci. 1999;2:959–64.
57. Weimer RM, Richmond JE, Davis WS, Hadwiger G, Nonet ML, Jorgensen EM. Defects in synaptic vesicle docking in unc-18 mutants. Nat Neurosci. 2003;6:1023–30.
58. Gengyo-Ando K, Kitayama H, Mukaida M, Ikawa Y. A murine neural-specific homolog corrects cholinergic defects in Caenorhabditis elegans unc-18 mutants. J Neurosci. 1996;16:6695–702.
59. Richmond JE, Weimer RM, Jorgensen EM. An open form of syntaxin bypasses the requirement for UNC-13 in vesicle priming. Nature. 2001;412:338–41.
60. Tien CW, Yu B, Huang M, Stepien KP, Sugita K, Xie X, et al. Open syntaxin overcomes exocytosis defects of diverse mutants in C. elegans. Nat Commun. 2020;11:5516. https://doi.org/10.1038/s41467-020-19178-x.
61. Liu H, Li L, Sheoran S, Yu Y, Richmond JE, Xia J, et al. The M domain in UNC-13 regulates the probability of neurotransmitter release. Cell Rep. 2021;34:108828. https://doi.org/10.1016/j.celrep.2021.108828.
62. Lai Y, Choi UB, Leitz J, Rhee HJ, Lee C, Altas B, et al. Molecular mechanisms of synaptic vesicle priming by Munc13 and Munc18. Neuron. 2017;95:591–607.e510. https://doi.org/10.1016/j.neuron.2017.07.004.
63. Shu T, Jin H, Rothman JE, Zhang Y. Munc13-1 MUN domain and Munc18-1 cooperatively chaperone SNARE assembly through a tetrameric complex. Proc Natl Acad Sci U S A. 2020;117:1036–41. https://doi.org/10.1073/pnas.1914361117.

64. Wang X, Gong J, Zhu L, Wang S, Yang X, Xu Y, et al. Munc13 activates the Munc18-1/syntaxin-1 complex and enables Munc18-1 to prime SNARE assembly. EMBO J. 2020;39:e103631. https://doi.org/10.15252/embj.2019103631.
65. Ma C, Su L, Seven AB, Xu Y, Rizo J. Reconstitution of the vital functions of Munc18 and Munc13 in neurotransmitter release. Science. 2013;339:421–5. https://doi.org/10.1126/science.1230473.
66. Arunachalam L, Han L, Tassew NG, He Y, Wang L, Xie L, et al. Munc18-1 is critical for plasma membrane localization of syntaxin1 but not of SNAP-25 in PC12 cells. Mol Biol Cell. 2008;19:722–34. https://doi.org/10.1091/mbc.e07-07-0662.
67. Han L, Jiang T, Han GA, Malintan NT, Xie L, Wang L, et al. Rescue of Munc18-1 and -2 double knockdown reveals the essential functions of interaction between Munc18 and closed syntaxin in PC12 cells. Mol Biol Cell. 2009;20:4962–75. https://doi.org/10.1091/mbc.E09-08-0712.
68. Han GA, Malintan NT, Collins BM, Meunier FA, Sugita S. Munc18-1 as a key regulator of neurosecretion. J Neurochem. 2010;115:1–10. https://doi.org/10.1111/j.1471-4159.2010.06900.x.
69. Han GA, Malintan NT, Saw NM, Li L, Han L, Meunier FA, et al. Munc18-1 domain-1 controls vesicle docking and secretion by interacting with syntaxin-1 and chaperoning it to the plasma membrane. Mol Biol Cell. 2011;22:4134–49. https://doi.org/10.1091/mbc.E11-02-0135.
70. Parisotto D, Pfau M, Scheutzow A, Wild K, Mayer MP, Malsam J, et al. An extended helical conformation in domain 3a of Munc18-1 provides a template for SNARE (soluble N-ethylmaleimide-sensitive factor attachment protein receptor) complex assembly. J Biol Chem. 2014;289:9639–50. https://doi.org/10.1074/jbc.M113.514273.
71. Han GA, Park S, Bin NR, Jung CH, Kim B, Chandrasegaram P, et al. A pivotal role for pro-335 in balancing the dual functions of Munc18-1 domain-3a in regulated exocytosis. J Biol Chem. 2014;289:33617–28. https://doi.org/10.1074/jbc.M114.584805.
72. Baker RW, Jeffrey PD, Zick M, Phillips BP, Wickner WT, Hughson FM. A direct role for the Sec1/Munc18-family protein Vps33 as a template for SNARE assembly. Science. 2015;349:1111–4. https://doi.org/10.1126/science.aac7906.
73. Barak B, Okun E, Ben-Simon Y, Lavi A, Shapira R, Madar R, et al. Neuron-specific expression of tomosyn1 in the mouse hippocampal dentate gyrus impairs spatial learning and memory. NeuroMolecular Med. 2013;15:351–63. https://doi.org/10.1007/s12017-013-8223-4.
74. Batten SR, Matveeva EA, Whiteheart SW, Vanaman TC, Gerhardt GA, Slevin JT. Linking kindling to increased glutamate release in the dentate gyrus of the hippocampus through the STXBP5/tomosyn-1 gene. Brain Behav. 2017;7:e00795. https://doi.org/10.1002/brb3.795.
75. Nicoll RA, Schmitz D. Synaptic plasticity at hippocampal mossy fibre synapses. Nat Rev Neurosci. 2005;6:863–76. https://doi.org/10.1038/nrn1786.
76. Gilbert PE, Brushfield AM. The role of the CA3 hippocampal subregion in spatial memory: a process oriented behavioral assessment. Prog Neuro-Psychopharmacol Biol Psychiatry. 2009;33:774–81. https://doi.org/10.1016/j.pnpbp.2009.03.037.
77. Saldate JJ, Shiau J, Cazares VA, Stuenkel EL. The ubiquitin-proteasome system functionally links neuronal Tomosyn-1 to dendritic morphology. J Biol Chem. 2018;293:2232–46. https://doi.org/10.1074/jbc.M117.815514.
78. Shen W, Kilander MBC, Bridi MS, Frei JA, Niescier RF, Huang S, et al. Tomosyn regulates the small RhoA GTPase to control the dendritic stability of neurons and the surface expression of AMPA receptors. J Neurosci Res. 2020;98:1213–31. https://doi.org/10.1002/jnr.24608.
79. Sakisaka T, Baba T, Tanaka S, Izumi G, Yasumi M, Takai Y. Regulation of SNAREs by tomosyn and ROCK: implication in extension and retraction of neurites. J Cell Biol. 2004;166:17–25. https://doi.org/10.1083/jcb.200405002.
80. Gracheva EO, Burdina AO, Touroutine D, Berthelot-Grosjean M, Parekh H, Richmond JE. Tomosyn negatively regulates both synaptic transmitter and neuropeptide release at the C. elegans neuromuscular junction. J Physiol. 2007;585:705–9. https://doi.org/10.1113/jphysiol.2007.138321.

81. Gracheva EO, Burdina AO, Touroutine D, Berthelot-Grosjean M, Parekh H, Richmond JE. Tomosyn negatively regulates CAPS-dependent peptide release at Caenorhabditis elegans synapses. J Neurosci. 2007;27:10176–84.
82. Yizhar O, Matti U, Melamed R, Hagalili Y, Bruns D, Rettig J, et al. Tomosyn inhibits priming of large dense-core vesicles in a calcium-dependent manner. Proc Natl Acad Sci U S A. 2004;101:2578–83. https://doi.org/10.1073/pnas.0308700100.
83. Lin XG, Ming M, Chen MR, Niu WP, Zhang YD, Liu B, et al. UNC-31/CAPS docks and primes dense core vesicles in C. elegans neurons. Biochem Biophys Res Commun. 2010;397:526–31. https://doi.org/10.1016/j.bbrc.2010.05.148.
84. Geerts CJ, Plomp JJ, Koopmans B, Loos M, van der Pijl EM, van der Valk MA, et al. Tomosyn-2 is required for normal motor performance in mice and sustains neurotransmission at motor endplates. Brain Struct Funct. 2015;220:1971–82. https://doi.org/10.1007/s00429-014-0766-0.
85. Kumar R, Corbett MA, Smith NJ, Jolly LA, Tan C, Keating DJ, et al. Homozygous mutation of STXBP5L explains an autosomal recessive infantile-onset neurodegenerative disorder. Hum Mol Genet. 2015;24:2000–10. https://doi.org/10.1093/hmg/ddu614.
86. Neer EJ, Schmidt CJ, Nambudripad R, Smith TF. The ancient regulatory-protein family of WD-repeat proteins. Nature. 1994;371:297–300. https://doi.org/10.1038/371297a0.
87. Yamamoto Y, Mochida S, Kurooka T, Sakisaka T. Reciprocal intramolecular interactions of tomosyn control its inhibitory activity on SNARE complex formation. J Biol Chem. 2009;284:12480–90. https://doi.org/10.1074/jbc.M807182200.
88. Yamamoto Y, Fujikura K, Sakaue M, Okimura K, Kobayashi Y, Nakamura T, et al. The tail domain of tomosyn controls membrane fusion through tomosyn displacement by VAMP2. Biochem Biophys Res Commun. 2010;399:24–30. https://doi.org/10.1016/j.bbrc.2010.07.026.

Complexins: Ubiquitously Expressed Presynaptic Regulators of SNARE-Mediated Synaptic Vesicle Fusion

Francisco José López-Murcia, Kerstin Reim, and Holger Taschenberger

Abstract Neurotransmitter release is a spatially and temporally tightly regulated process, which requires assembly and disassembly of SNARE complexes to enable the exocytosis of transmitter-loaded synaptic vesicles (SVs) at presynaptic active zones (AZs). While the requirement for the core SNARE machinery is shared by most membrane fusion processes, SNARE-mediated fusion at AZs is uniquely regulated to allow very rapid Ca^{2+}-triggered SV exocytosis following action potential (AP) arrival. To enable a sub-millisecond time course of AP-triggered SV fusion, synapse-specific accessory SNARE-binding proteins are required in addition to the core fusion machinery. Among the known SNARE regulators specific for Ca^{2+}-triggered SV fusion are complexins, which are almost ubiquitously expressed in neurons. This chapter summarizes the structural features of complexins, models for their molecular interactions with SNAREs, and their roles in SV fusion.

Keywords Complexin · Neurotransmission · Presynapse · SNARE complex · Synaptic proteins

F. J. López-Murcia (✉)
Department of Pathology and Experimental Therapy, Institute of Neurosciences, University of Barcelona, L'Hospitalet de Llobregat, Barcelona, Spain

Bellvitge Biomedical Research Institute (IDIBELL), L'Hospitalet de Llobregat, Barcelona, Spain
e-mail: lopezmurcia@ub.edu

K. Reim (✉) · H. Taschenberger (✉)
Department of Molecular Neurobiology, Max Planck Institute for Multidisciplinary Sciences, Göttingen, Germany
e-mail: reim@mpinat.mpg.de; taschenberger@mpinat.mpg.de

Z.-W. Wang (ed.), *Molecular Mechanisms of Neurotransmitter Release*, Advances in Neurobiology 33, https://doi.org/10.1007/978-3-031-34229-5_10

Abbreviations

AA	Amino Acids
AH	Accessory Helix
AP	Action potential
AZ	Active zone
$[Ca^{2+}]$	Ca^{2+} concentration
CAPS	Calcium-dependent Activator Protein for Secretion
CH	Central Helix
CTD	C-Terminal Domain
CNS	Central nervous system
Cplx	Complexin protein
DKD	Double-knockdown
DKO	Double-knockout
dm	*Drosophila melanogaster*
eEPSC	Evoked excitatory postsynaptic current
eIPSC	Evoked inhibitory postsynaptic current
IPL	Inner plexiform layer
K_D	Equilibrium dissociation constant
KD	Knockdown
KO	Knockout
k_{off}	Dissociation rate constant
k_{on}	Association rate constant
mEPSC	Miniature excitatory postsynaptic current
MNTB	Medial Nucleus of the Trapezoid Body
MW	Molecular Weight
NTD	N-Terminal Domain
NMJ	Neuromuscular junction
OPL	Outer plexiform layer
PD	Parkinson's disease
RRP	Readily releasable pool
shRNA	Short hairpin RNA
SNAP25	Synaptosomal-associated protein, 25 kDa
SNARE	Soluble N-ethylmaleimide-sensitive factor attachment protein receptor
SNP	Single nucleotide polymorphism
Stx	Syntaxin
SV	Synaptic vesicle
Syb	Synaptobrevin
Syt	Synaptotagmin
TKO	Triple-knockout
UTR	Untranslated region
VAMP	Vesicle-Associated Membrane Protein

Exocytosis of synaptic vesicles (SVs) at presynaptic active zones (AZs) typically occurs within less than a millisecond after action potential (AP) arrival. To ensure such rapid exocytosis of SVs, they have to be in a fusion-ready state prior to AP arrival. This requires SVs to dock to the presynaptic membrane, which involves their translocation toward the AZ to be placed at molecularly defined release sites where the SV fusion apparatus is assembled [1, 2]. The core of the fusion apparatus is formed by the membrane-bridging SNARE complex consisting at central synapses of the three proteins syntaxin (Stx) 1, synaptobrevin (Syb) 2 (also referred to as VAMP2), and SNAP25 [3–6]. Stx and SNAP25 are anchored in the plasma membrane, while Syb is anchored in the SV membrane. This trimeric protein complex, known as the SNARE complex, forms a bundle of four α-helices (Stx and Syb each contribute one, and SNAP25 contributes two bundles), which brings SVs into close apposition with the presynaptic plasma membrane when the helices progressively associate with each other ("SNARE bundle zippering"). Assembly of the SNARE complex is an exoergic (energy-releasing) process, and the released energy is thought to overcome the energy barrier for membrane fusion. The function of the SNARE complex is controlled by a set of accessory proteins, some of which regulate its assembly, such as Munc18, Munc13, and CAPS [7–9], whereas others regulate the speed, temporal precision, and efficacy of the SNARE-mediated Ca^{2+}-dependent fusion process, such as the Ca^{2+} sensor protein synaptotagmin (Syt) [10, 11] and the regulatory protein complexin (Cplx) [12–14].

Docked SVs need to undergo a reversible priming process [15], likely by transitioning through several discriminable and molecularly defined states [16], to become fusion competent. For SVs in the fully primed and fusion-competent state, SNARE complexes are partially assembled. The "zippering-up" of the four-helix SNARE bundles pulls vesicle and plasma membranes together until opposing forces acting on the membrane anchors of Syb and Stx prevent further assembly. Alternatively or additionally, a complete assembly of the SNARE complex may be prevented by one or more regulatory factors acting as "fusion clamp" which lowers the probability of SV fusion with the plasma membrane at resting cytosolic Ca^{2+} concentration ($[Ca^{2+}]$). The putative "fusion clamp" is presumed to be released upon an increase in cytosolic $[Ca^{2+}]$ at the SV fusion site.

At most mammalian central nervous system (CNS) synapses, AZ proteins of the Munc13 and CAPS families mediate the SV priming reaction, most likely by regulating the conformation of Stx1 and its availability for SNARE complex formation [1, 17, 18]. It has been suggested that Cplxs operate at a post-priming step either by stabilizing SNARE complexes to maintain SVs in a highly fusogenic state [12, 19] or by acting as the proclaimed "fusion clamp" that arrests SNARE complex assembly to prevent premature fusion prior to the activation of Syt by Ca^{2+} [20–23]. Both of these postulated functions of Cplx are not necessarily mutually exclusive.

Cplxs are a family of evolutionarily conserved, small (MW = 15–18 kDa) cytosolic α-helical proteins consisting of 134 to 160 amino acid residues. Cplxs are highly charged (~40% charged residues) and bind tightly and in a 1:1 stoichiometry to assembled SNARE complexes [13, 24–26] (Fig. 1). Kinetic analyses show that Cplx1 and Cplx2 associate with SNARE complexes rapidly, within less than a

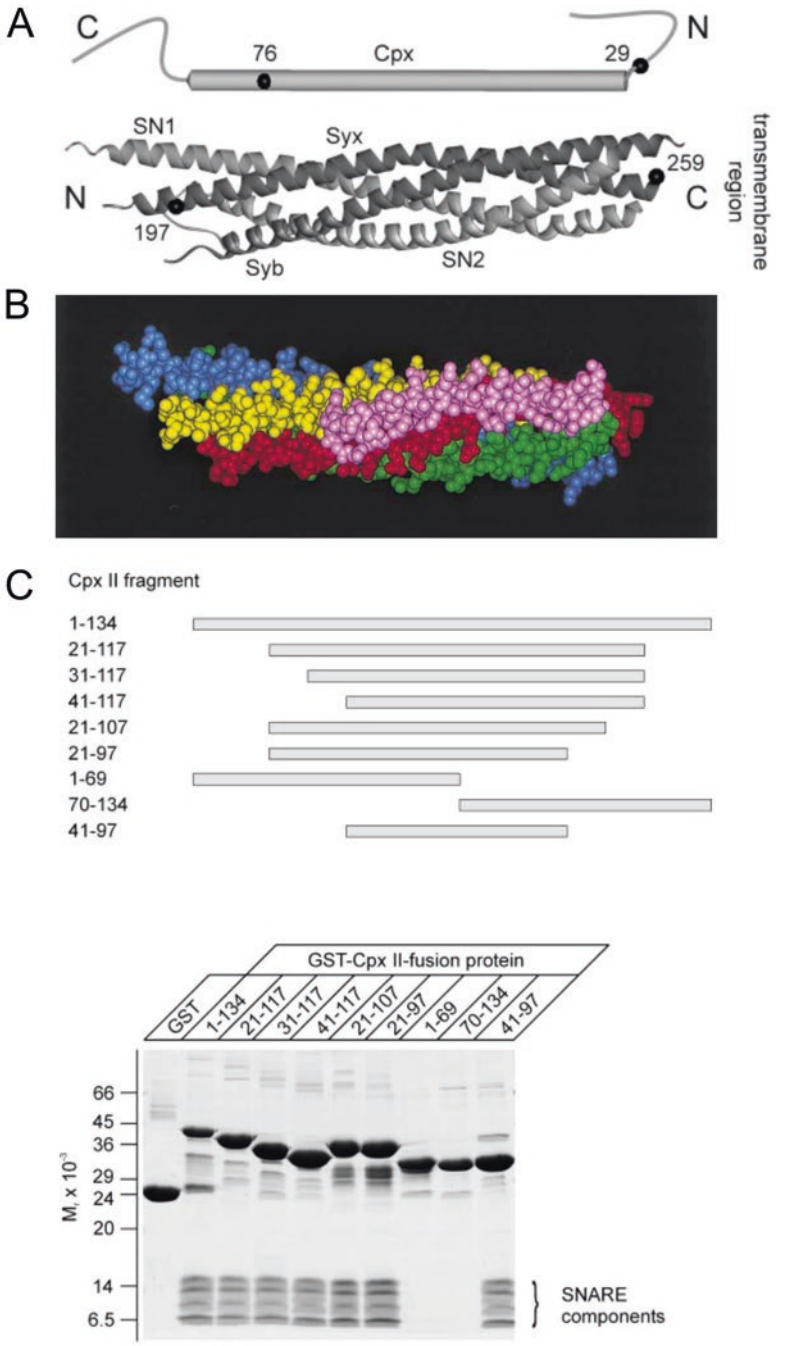

Fig. 1 Cplx binding to the synaptic SNARE complex. (**a**) FRET measurements indicate that Cplx is aligned antiparallel to the α-helices of the SNARE complex. Relative orientation of the labeling positions (black balls) for Stx and for Cplx as implied by the FRET measurements. The α-helical

Table 1 Four complexin paralogs encoded on different chromosomes are expressed in mammals

Protein name	Gene name	Chromosome location			Protein length (aa)
		Mouse	Rat	Human	
Complexin-1 (Synaphin-2)	Cplx1	5	14	4	134
Complexin-2 (Synaphin-1)	Cplx2	13	17	5	134
Complexin-3	Cplx3	9	8	15	158
Complexin-4	Cplx4	18	18	18	160

second, and with high affinity. Estimates for the association rate constant (k_{on}) and the steady-state affinity (K_D) range from 4×10^6 to 6×10^7 M^{-1} s^{-1} and from ten to several hundreds of nM, respectively. The estimated dissociation rate constant (k_{off}) is 0.3–0.4 s^{-1} [25]. These binding properties were obtained by experiments with full-length Cplx1 and Cplx2 in the presence of the transmembrane domains of Syb and Stx [25, 27–29]. The estimated half-life time for mammalian Cplx is about 2 to 5 days in cultured neurons [30–32] and about 10 days in vivo [33].

Four Cplxs paralogs (Cplx1, -2, -3, and -4) are encoded by four separate genes of the complexin/synaphin gene family in mammals (Table 1). Mammalian Cplx1 and Cplx2 are highly homologous (~80% amino acid identity) as are Cplx3 and Cplx4 (~60% amino acid identity), while homology between the two subfamilies (Cplx1/2 versus Cplx3/4) is limited (<30% amino acid identity) [34, 35]. Cplx2 is completely conserved across several mammalian species, and Cplx1 protein sequences differ only marginally between mice and humans (97% identity) [13, 34]. Cplx orthologs have been identified throughout the animal kingdom. For example, Cplx from *Nematostella vectensis*, a cnidarian sea anemone far separated from mammals in metazoan evolution, is able to functionally replace mouse Cplx in promoting Ca^{2+}-triggered exocytosis [36].

Cplx isoforms described for non-mammalian species, such as *Caenorhabditis elegans*, *Drosophila melanogaster* and *Xenopus laevis,* share a high level of amino acid sequence identity with mammalian Cplx1/2 [34]. *Drosophila melanogaster* Cplx (dmCplx) is encoded by a single gene on chromosome 3R with several isoforms generated by alternative splicing [37]. Some dmCplx isoforms contain C-terminal extensions with a CAAX box, which is a farnesylation consensus motif that is also found in mammalian Cplx3/4. The CAAX box may mediate membrane targeting [34, 38, 39]. Other dmCplx isoforms lack a C-terminal CAAX box, similar

Fig. 1 (continued) region of Cplx (residues 29–86) is drawn as a tube, the structure of the synaptic SNARE complex is depicted as a ribbon diagram. SN1, first helix of SNAP-25; SN2, second helix of SNAP-25; N, NH_2 terminus; C, COOH terminus. (**b**) Space filling model of the Cplx/SNARE complex. Coloring code: yellow, Stx; red, Syb; blue, SNAP-25 N-terminal SNARE motif; green, SNAP-25 C-terminal SNARE motif; pink, Cplx. (**c**) Mapping of the binding domain of Cplx by deletion mutagenesis. Truncated GST-Cplx2 fusion proteins were immobilized to glutathione-Sepharose beads and incubated with purified minimal core complex. After washing of the beads, bead-bound material was analyzed by SDS-PAGE and Coomassie Blue staining. All Cplx2 fragments bound to the minimal core complex except for the two fragments 1–69 and 70–134. (Modified from [24, 26])

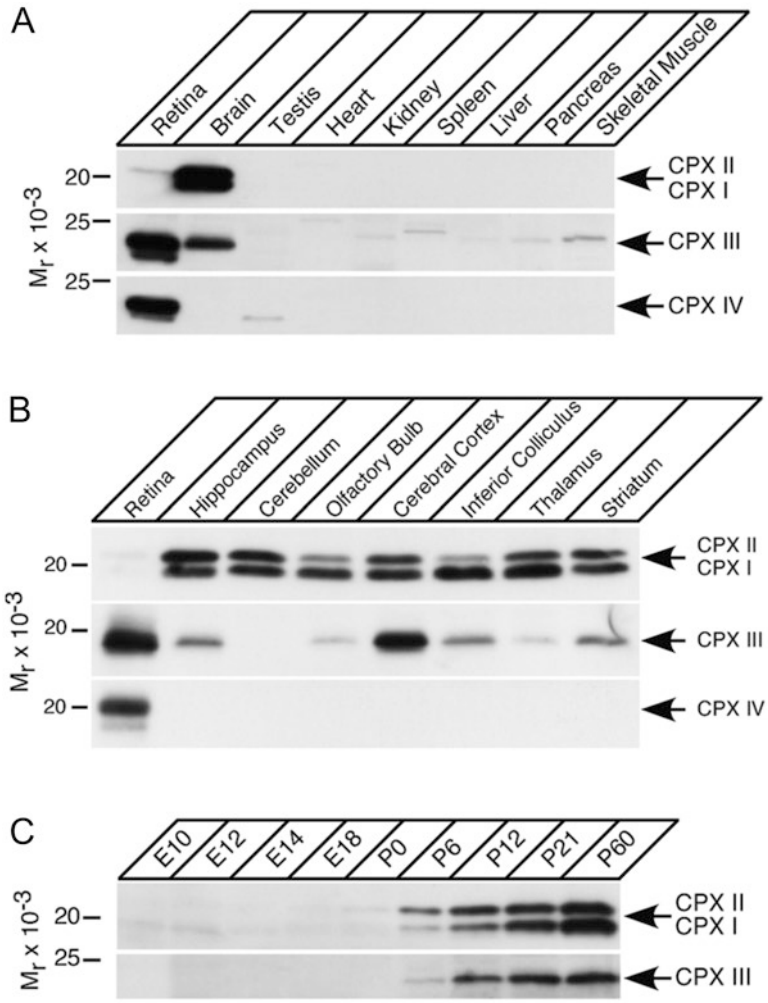

Fig. 2 Cplx expression in rat and mouse is restricted to brain and retina and developmentally regulated. (**a**, **b**) Homogenates from the indicated rat organs (**a**) or rat brain regions (**b**) were analyzed by Western blotting using specific antibodies to the indicated proteins (arrows). Cplx protein is highly and selectively expressed in retina and brain. Cplx1 and Cplx2 are co-expressed in many brain regions, while Cplx3 is predominantly and Cplx4 is exclusively expressed in retina. (**c**) Western blot analysis of brain homogenates from mice of different ages. Cplx1-, Cplx2-, and Cplx3-protein expression during mouse brain development is first detectable at P6 and increases to reach a plateau at around 20 days after birth. (Modified from [34])

to mammalian Cplx1/2. Thus, even though *Drosophila* dmCplxs are encoded by a single gene, alternative splicing generates functional protein variants that either contain or lack a CAAX box, similar to the mammalian Cplxs which, however, are encoded by four different genes [37].

1 Tissue Expression of Mammalian Complexins

In mammals, both Cplx1 and Cplx2 are expressed in the CNS, while Cplx2 mRNA and protein were also detected—at much lower level—in non-neuronal tissues [13] (Fig. 2a). Within the brain, Cplx1 and Cplx2 expression is not clearly segregated to particular neurotransmitter systems. In situ hybridization studies revealed that mRNA expression of Cplx1 overlaps with that of Cplx2 in many brain regions of mice which was confirmed by immunostaining [40] and Western blot analysis [34, 41, 42] (Fig. 2b). Many neuron types express both Cplx1 and Cplx 2, possibly at different levels, while some neurons express only one of them [12, 34, 40, 43–45].

Expression of Cplx protein in the mouse brain is developmentally regulated. It is first detectable at postnatal day 6 and increases to reach a plateau at around 20 days after birth [34] (Fig. 2c). Despite the fact that Cplx1 and Cplx2 were discovered more than two decades ago, their relative abundance, subcellular localization, respective synaptic functions, and developmental regulation in many neuronal populations are still unknown. Based on in situ hybridization, immunostaining, Western blot analysis, and functional assays, it is assumed that Cplx1 and Cplx2 are co-expressed in some cortical, hippocampal, and cerebellar synapses [12, 13, 35, 40–42, 46, 47]. In Cplx1/2 co-expressing synapses, genetic deletion of one of them does not cause obvious functional deficits, indicating redundancy in synaptic function [12, 47].

In contrast to Cplx1 and Cplx2, Cplx3 is only weakly expressed in some brain regions such as cerebral cortex and hippocampus, and Western blot analyses failed to detect Cplx4 in most brain regions. Instead, Cplx3 and Cplx4 were shown to be the predominant Cplx isoforms in the mammalian retina (Fig. 2b). While Cplx3 was found in several neuron types of the retina, Cplx4 is specifically expressed at retinal ribbon synapses [34, 48]. Cplx3 and Cplx4 are present in both synaptic layers of the retina, the outer plexiform layer (OPL) and the inner plexiform layer (IPL), where they colocalize with VGLUT1, the vesicular glutamate transporter. Cplx3/4 are differentially expressed in photoreceptors. Specifically, rod spherules contain only Cplx4, whereas cone pedicles contain both Cplx3 and Cplx4. In the IPL, Cplx3 is present in ribbon synapses of rod bipolar cell terminals as well as in conventional synapses of different neuron types (e.g., amacrine cell processes) [34, 49]. In contrast, Cplx4 is found exclusively in ribbon synapses of photoreceptors and bipolar cells of the retina. Interestingly, ribbon synapses of inner ear hair cells lack Cplx expression altogether [44, 50].

2 Domain Structure of Mammalian Complexins

Cplx proteins consist of four domains (Table 2). The functions of these domains have been studied in vitro, using reconstituted liposome fusion assays, and in situ, using neurons expressing truncated or mutated Cplx variants, or Cplx chimeras.

Table 2 Domain structure of murine Cplx1 and functional deficits observed after mutations

Domain	aa sequence	Impact of deletions	Impact of point mutations
N-terminal domain (NTD)	1–32	Spontaneous release ↓ [38, 64] Evoked release ↓ [19, 38, 52, 64]	Spontaneous release ↓ [19] Evoked release ↓ [52]
Accessory helix (AH)	33–48	Evoked release ↑ [38, 52]	Evoked release ↑ [38, 52] Evoked release ↓ [65] Evoked release — [53] Spontaneous release ↓ [65] Spontaneous release ↑ [53, 65]
Central helix (CH)	49–70		Complete loss of SNARE binding (loss of function) [24, 36, 52, 64]
C-terminal domain (CTD)	71–134	Spontaneous release ↑ [66] Spontaneous release — [67, 68] Evoked release ↓ [66, 68] Mislocalization of Cplx protein [67]	Spontaneous release ↑ [66]

The symbols ↓, ↑, and — indicate "decrease," "increase," and "no change," respectively

Despite low amino acid sequence identity between the members of the two subfamilies (Cplx1/2 and Cplx3/4), all Cplx isoforms share an evolutionarily highly conserved α-helix. This structure can be subdivided into two small α-helical subdomains: a central α-helix (CH) and an accessory α-helix (AH). The CH corresponds to the SNARE complex-binding domain and is required for all known Cplx functions. These two α-helices are flanked by the N- and C-terminal domains, which in mouse Cplx1/2 cover amino acid residues 1–32 (NTD) and 71–134 (CTD), respectively. Biochemical studies have shown that the CH binds to partially assembled SNARE complexes [24] and helps to assemble the trans-SNARE complex further. Crystal structures showed that Cplx binding occurs at the central polar layer of the ternary SNARE complex in an antiparallel fashion at the groove between Stx1 and Syb2 SNARE motifs [26, 51] (Fig. 1a, b). Cplx variants carrying CH point mutations or CH deletions are binding-deficient and no longer modify spontaneous or evoked fusion when expressed in Cplx-deficient neurons [52].

Cplx's AH is less conserved than its CH. The AH contains negatively charged amino acid residues, which presumably interact with the plasma membrane, without making contact with the SNARE complex [26, 51]. In structure-function studies using cultured neurons, increasing and decreasing negatively charged residues in the AH inhibited and stimulated release, respectively, suggesting the AH inhibits release through electrostatic repulsion by acting between the SV and plasma membranes [53]. During SNARE complex assembly, the AH replaces the C terminus of the Syb2 SNARE motif in the four-helix bundle, thereby preventing further C-terminal assembly of the SNARE bundles [52, 54]. Based on the impact of AH

mutations and chimeras on Cplx function in nematodes, an alternative model of AH function has been proposed. In this model, the AH operates by stabilizing the secondary structure of the CH rather than through protein or lipid interactions [55].

Cplx's N terminus can form an amphipathic α-helix to project toward the C terminus of the partially assembled trans-SNARE complex to facilitate SV fusion [19, 56]. The sequence in this region is relatively conserved across Cplx paralogs and orthologs, and the potential to form an amphipathic α-helix is conserved in all of them [19]. For mammalian synapses, binding of the Cplx N terminus might stabilize the SNARE complex C terminus, and promote full zippering of the SNARE bundle, which helps the SNAREs to exert mechanical force on the membranes to induce fusion. It may also help to remove the inhibition caused by the accessory α-helix [19]. At the nematode neuromuscular junction (NMJ), the Cplx N terminus appears to play an inhibitory role in neurotransmitter release because presynaptic expression of a Cplx variant with an N terminus deletion can enhance spontaneous and evoked release [57].

Cplx's C terminus is the least conserved domain of Cplx. The C termini of mammalian Cplx3 and Cplx4 contain CAAX motifs, a substrate for posttranslational modification by farnesylation [58], which targets Cplx3 and Cplx4 to membranes [34]. Both positive and negative roles of the CTD in membrane fusion have been observed depending on the preparation studied. For example, at the nematode NMJ, the C terminus is essential for Cplx's inhibitory function, and CTD-membrane interactions mediated by a helical conformation of a C-terminal motif were highly sensitive to membrane curvature. Mutations that disrupt helix formation without disrupting membrane binding compromise Cplx's inhibitory function in nematodes in vivo [59]. In reconstituted fusion assays, a stimulatory effect of mammalian Cpx1 on SNARE assembly and on fusion of high-curvature liposomes is lost when the C terminus is deleted or mutated [60]. Charged amino acid residues in the Cplx C terminus region bind to Syt1 which may help recruiting Syt1 to the SNARE complex [61]. Two serine residues of the mammalian Cplx2 C terminus may be phosphorylated in situ [62, 63] but functional consequences of Cplx2 phosphorylation are presently unknown.

3 Interaction of Complexin with the SNARE Complex

Mammalian Cplx1 and Cplx2 were discovered in a Stx co-immunoprecipitation assay of the synaptic SNARE complex using rat brain homogenate, and were shown to bind to the SNARE complex with nanomolar affinity [13]. Cplx does not bind Ca^{2+} and the Cplx-SNARE complex interaction is Ca^{2+}-independent. Further studies using proteoliposomes demonstrated that the central α-helix of Cplx1 and Cplx2 preferentially bind the central polar layer of preassembled ternary SNARE complexes with a stoichiometry of 1:1 without introducing major structural changes to the core SNARE complex [24, 26–28]. Using PC12 cells expressing Cplx and truncated versions of SNARE components, it was demonstrated that Cplx is able to bind to mutant versions of the SNARE complex mimicking partially assembled stages. The affinity of Cplx for the SNARE complex was positively correlated with the

extent of the SNARE complex preassembled. These results suggest that Cplx can bind to the SNARE complex before its complete formation [69]. At least four positively charged residues and one hydrophobic residue of the central α-helix of Cplx1 are essential to bind the SNARE complex at a groove formed by the SNARE motifs of Stx and Syb [24, 26, 52] (Fig. 1b).

The "fusion-clamp" model postulates that Cplx hinders SV fusion at resting conditions and Syt1 is required to relief the clamping activity during Ca^{2+}-triggered SV fusion [22]. This model is supported by two experimental findings: (1) Syt1 and Cplx compete for SNARE binding in in vitro experiments, in which Syt1 dislodged Cplx from SNARE complexes [22], and (2) increasing the local concentration of Cplx by expressing Cplx fused to Syb2 mimicked the loss-of-function phenotype of Syt1 KO neurons, suggesting that Syt1 can be displaced from the SNARE complex by an excess availability of Cplx [22]. However, several observations are inconsistent with a Cplx-Syt1-displacement model: Cplx and Syt1 have been demonstrated to concurrently bind SNAREs in vitro [70, 71] and Ca^{2+}-bound Syt1 does not appear to displace Cplx from SNARE complexes [71]. Furthermore, a more than tenfold overexpression of Cplx1 in wildtype neurons did not change synaptic function [52] suggesting that Cplx failed to compete with Syt1. Moreover, if Cplx1 acts as a "fusion clamp" that may be removed by Syt1, then SVs should be arrested and incapable of fusing in Syt1-lacking synapses. However, Syt1-deficient synapses actually show increased spontaneous in addition to diminished AP-evoked release [72, 73]. The C_2B domain of Syt1 has been postulated to function as a molecular clamp arresting SVs prior to Ca^{2+}-triggered fusion, and it was proposed that C_2B-mediated clamping of SV fusion operates independently of Cplx [74].

Even though Cplx1 and Syt1 do not seem to bind to SNARE complexes sequentially and do not compete for SNARE binding, this does not rule out a cooperative action of the two molecules. A revised model of Cplx interaction with the SNARE complex postulates that Cplx and Syt1 can bind in a coordinated fashion to the SNARE complex at the same time and thereby clamp fusion [75]. When cytosolic $[Ca^{2+}]$ rises, Ca^{2+} binds to the C_2B domain of Syt1 causing it to move closer to the SV membrane, while an inhibitory domain of Cplx is shifted away from the fusion pore, allowing Syt1 to bridge the two membranes without displacing Cplx from the SNARE complex [75]. Recently, crystal structures of a SNARE-Cplx-Syt1 complex were determined showing that Cpx and Syt1 bind to the SNARE complex at a shared interface to form a tripartite complex, suggesting Syt1 and Cplx may form a single regulatory unit. This tripartite complex has to be unlocked for Ca^{2+}-triggered fusion to start [70, 76].

4 The Role of Complexin in Neurotransmission

The role of Cplx in neurotransmission has been studied primarily in three model organisms—nematodes, fruit flies, and mice. Experimental approaches included antibody- and peptide-induced perturbations of Cplx function, overexpression of

Cplx, RNAi-mediated knockdown (KD) of Cplx expression, and genetic knockout (KO) of Cplx [77]. Supported by an overwhelming body of experimental evidence, there is a general consensus that Cplx promotes fast, synchronous AP-triggered transmitter release. Tampering with Cplx's function commonly weakens stimulus-evoked neurotransmission. On the other hand, despite more than two decades of intense research, the role of Cplx in spontaneous neurotransmitter release has remained surprisingly controversial, because, depending on the cell type, model organism or experimental approach used, Cplxs appear to exert either facilitatory or inhibitory effects on SV fusion [for review see 77–79].

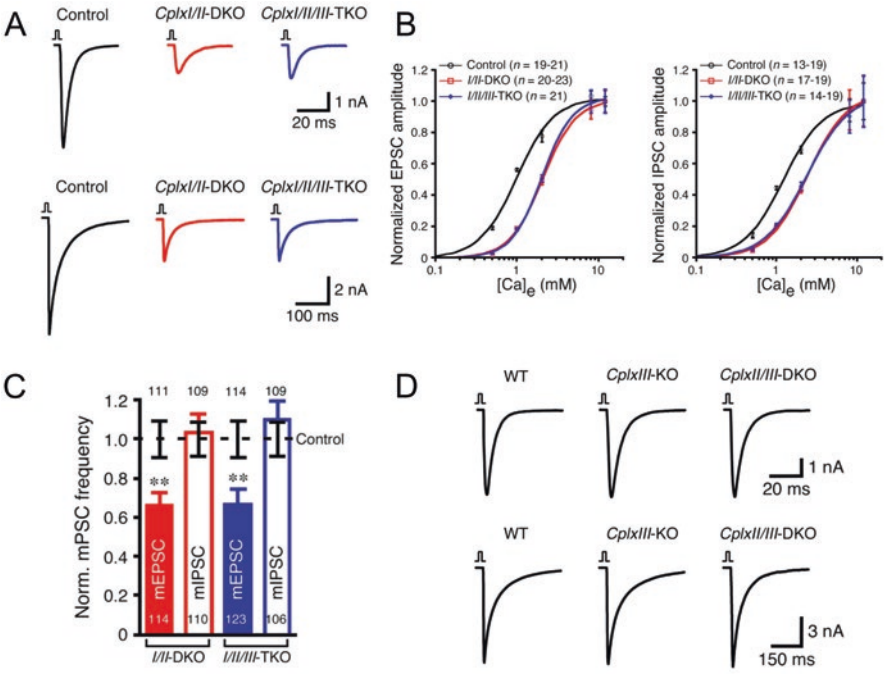

Fig. 3 Functional consequences of genetic Cplx removal in cultured synapses of the mouse brain. (**a**) AP-evoked synaptic transmission is strongly reduced in cultured murine Cplx1/2-DKO and Cplx1/2/3-TKO neurons. Representative traces of eEPSCs of cultured hippocampal glutamatergic synapses (top) and eIPSCs of cultured striatal GABAergic synapses (bottom). (**b**) Normalized amplitudes of eEPSCs (left) and eIPSCs (right) were plotted against external [Ca^{2+}] and fitted with a standard Hill equation. Genetic loss of Cplx results in a right-shifted dose-response curve indicating a lower apparent Ca^{2+}-sensitivity of evoked transmitter release. (**c**) Spontaneous neurotransmitter release in cultured murine Cplx1/2-DKO and Cplx1/2/3-TKO neurons. Normalized mEPSC frequencies are reduced, while normalized mIPSC frequencies are nearly unchanged. (**d**) AP-evoked synaptic transmission in cultured murine hippocampal (top) and striatal (bottom) Cplx3-KO and Cplx2/3-DKO neurons is unaltered. (Modified from [47])

4.1 Analysis of Complexin Function in Cultured Mammalian Synapses

The availability of mouse lines constitutively lacking expression of individual Cplx paralogs has greatly facilitated research on Cplx's function at mammalian synapses [12, 47, 48] (Fig. 3). More recently, conditional Cplx1 KO mice also became available [32]. RNA interference (RNAi)-mediated KD represents an alternative strategy employed in many studies in order to lower presynaptic Cplx expression levels [64, 65, 68, 70, 80]. In the following, experimental results obtained with both genetic strategies (KO and KD) will be compared and discussed.

Homozygous Cplx2 KO, Cplx3 KO and Cplx4 KO mice, and Cplx2/3 double-KO (DKO) mice are viable and fertile [12, 47, 48]. In contrast, Cplx1 KO mice show the earliest known onset of severe ataxia and tremor and eventually die at around 2–4 months of age [81, 82]. This indicates that some functions of Cplx1 cannot be taken over by its paralogs and/or that certain neuron populations, which regulate vital functions and are thus critical for survival, exclusively express Cplx1. Homozygous Cplx1/2 DKOs and Cplx1/2/3 triple-KO (TKO) mice die at birth [12, 47]. The perinatal lethality of mice lacking both Cplx1 and Cplx2 indicates that the remaining neurotransmitter release at Cplx1/2 DKO synapses is insufficient to sustain vital systemic functions. Morphological characterization of brains from homozygous adult Cplx1 KO and Cplx2 KO mice as well as newborn Cplx1/2 DKO mice did not reveal any alterations, and no changes in expression levels of presynaptic proteins were reported [12].

Because Cplx1 and Cplx2 are redundantly expressed in many brain regions and Cplx1/2 DKO and Cplx1/2/3 TKO mice die perinatally, Cplx's function at mammalian synapses has mainly been studied using neuronal culture systems. Among these, autaptic cultures (also called micro-island or microdot cultures) have been especially instrumental as they allow assaying functional properties of single neurons grown in isolation on a micro-island of an astrocytic feeder layer. These single neurons establish synaptic contacts with themselves thereby forming so-called autapses [83–85]. Cultured glutamatergic hippocampal and GABAergic striatal Cplx1/2 DKO autapses show normal synapse density, and electron micrographs illustrated that presynaptic morphological characteristics such as cytoplasmic SV density, number of docked SVs, and AZ lengths are unaltered [12]. Structural integrity of Cplx-lacking synapses was later confirmed also in electron micrographs obtained from organotypic hippocampal slice cultures established from postnatal day 0 Cplx1/2/3 TKO mouse pups and cultured for at least 3 weeks [86].

Cultured mammalian synapses lacking Cplx expression show dramatically altered synaptic function: In cultures prepared from Cplx1/2 DKO or Cplx1/2/3 TKO mice, AP-evoked excitatory and inhibitory postsynaptic currents (eEPSCs and eIPSCs) recorded at hippocampal and striatal autapses, respectively, were reduced by ≥65% compared to wildtype autapses (Fig. 3a). Further, the frequency of miniature EPSCs (mEPSCs), representing spontaneous SV fusion events in the absence of AP firing, was decreased by ≥40% without changes in mEPSC amplitude or

kinetics [12, 32, 47] (Fig. 3c). Finally, genetic Cplx loss shifted the balance between synchronous and delayed asynchronous transmitter release in cultured hippocampal autapses by attenuating the synchronous release component more strongly [12, 32].

Can reduced synaptic strength after genetic Cplx removal be caused by a decreased availability of primed and fusion-competent SVs forming the readily releasable pool (RRP)? In Cplx-lacking cultured autapses [12, 32, 47, 52], this does not seem to be the case because the responses to a brief hyperosmotic stimulus, which is often used to assess the size of the RRP, remain unaltered. Because of the absence of changes in the number of docked SVs at AZs in Cplx-lacking autapses and because of their generally similar RRP size, it was concluded that Cplxs operate at a post-priming step in SV fusion and their loss causes reduced release probability presumably by increasing the energy barrier for initiating membrane fusion [12, 87]. Consisted with this idea is the observation that normal synaptic strength can be restored in cultured Cplx-lacking synapses by increasing the extracellular Ca^{2+} concentration. In homozygous mutant Cplx1/2 DKO and Cplx1/2/3 TKO autapses, the dose-response relationship constructed from synaptic responses measured at various extracellular Ca^{2+} concentrations was shifted to the right, indicating that lack of Cplxs causes a reduced apparent Ca^{2+} sensitivity of the release machinery [12, 47] (Fig. 3b). A reduced fusogenicity of SVs in Cplx-lacking synapses is in line with a lower rate of spontaneous SV fusion events. Because none of the abovementioned functional deficits were observed in excitatory hippocampal and inhibitory striatal neurons prepared from homozygous Cplx1 single KO, Cplx2 single KO mice, or Cplx2/3 DKO mice, it can be concluded that expression of one of the two Cplx

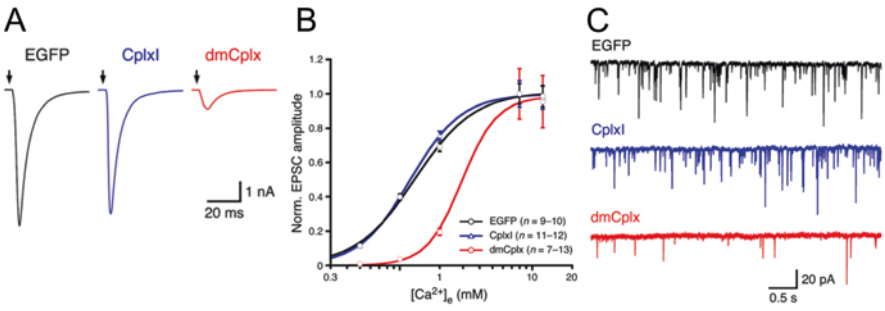

Fig. 4 Functional consequences of overexpression mouse and fly Cplx in hippocampal wildtype synapses of the mouse brain. Hippocampal wildtype neurons overexpressing mouse Cplx1 (blue) or dmCplx (red) together with EGFP were compared to wildtype neurons expressing EGFP alone (black). (**a**) AP-evoked synaptic transmission is virtually unaffected in autaptic murine hippocampal neurons overexpressing mouse Cplx1 but strongly reduced in neurons overexpressing dmCplx. The arrows represent stimulation onset. (**b**) Normalized amplitudes of synaptic responses were plotted against external $[Ca^{2+}]$ and fitted with a standard Hill equation. Overexpression of dmCplx results in a right-shifted dose-response curve indicating a lower apparent Ca^{2+}-sensitivity of evoked transmitter release. Overexpression of mouse Cplx1 does not alter the apparent Ca^{2+}-sensitivity. (**c**) Representative traces of mEPSCs. Spontaneous neurotransmitter release is unaltered in cultured neurons overexpressing mouse Cplx1. Overexpression of dmCplx results in a strong reduction in mEPSC frequencies. (Modified from [38])

paralogs Cplx1 and Cplx2 is sufficient to maintain normal synaptic function (Fig. 3d). Overexpression of Cplx1 in cultured hippocampal neurons prepared from wildtype mice did not noticeably change synaptic transmission (Fig. 4) [38].

Experiments analyzing the effects of short hairpin RNA (shRNA)-mediated KD on neurotransmitter release in high-density cultures of mammalian neurons have yielded results that are not in complete agreement with those from Cplx KO mouse neuron cultures. While KD studies generally support a facilitatory role of Cplx on AP-evoked synchronous neurotransmitter release, they, however, suggest that Cplxs inhibit rather than promote spontaneous SV fusion, lending support for a Cplx "fusion-clamp" model in mammalian neurons [64, 65, 80]. However, further analyses revealed that Cplx1/2 double knockdown (DKD)-mediated enhancement of the mEPSC rate occurs not only in Cplx1 expressing cortical and olfactory bulb synapses but also at synapses prepared from Cplx1/2 DKO mice, suggesting that the effect of Cplx1/2 DKD on mEPSC rate was independent of Cplx1 and Cplx2 [68]. Because DKD but not DKO of Cplx1 and Cplx2 was accompanied by upregulation of Cplx3 and Cplx4, it was suggested that a secondary effect of the Cplx3 and Cplx4 upregulation may have interfered with spontaneous release [for review see 78]. Consistently, overexpression of Cplx3 in cultured wildtype cortical neurons enhanced the mEPSC rate very similarly to shRNA-mediated Cplx1/2 DKD [68]. A recent study, which used a different shRNA sequence to achieve Cplx1/2 DKD in cultured cortical neurons, reported a reduction in AP-triggered eIPSCs amplitudes by half, whereas no significant effect was observed on the mIPSCs frequency [74]. In summary, similar consequences were observed in mammalian neurons after either Cplx KO or Cplx KD with respect to AP-evoked synchronous release. However, while Cplx KO generally decreases the rate of spontaneous release in cultured mammalian synapses, Cplx KD sometimes produced enhanced spontaneous released rates. That latter result may, however, be confounded by concomitant secondary effects of the KD strategy [78].

One possibility is that the reduced rate of spontaneous release observed in cultured neurons from constitutive Cplx KO mice might reflect a compensatory or homeostatic mechanism aimed at readjusting the balance between evoked and spontaneous neurotransmitter release. If this were true, one would expect to observe a transient upregulation of mEPSC frequencies following acute genetic Cplx removal due to the "unclamping" of spontaneous release. Such transient enhancement of spontaneous release would then be followed by a developmental downregulation. This possibility was addressed in autapses prepared from Cplx1^{floxed}-Cplx2/3 DKO mice [32] (Fig. 5). Cplx1-expressing hippocampal Cplx1^{floxed}-Cplx2/3 DKO

Fig. 5 (continued) represents the average Cre eEPSC superimposed onto the Ctrl eEPSCs for comparison. Right: The RRP size was probed by rapid application of hyperosmotic solution in the same Cre (red) and Ctrl (black) neurons as shown in the left panel. RRP size was unaltered after acute Cplx loss. (**e**) Summary data comparing release rate estimates for spontaneous, asynchronous, delayed, and evoked glutamate release in Ctrl (black) and Cre (red) neurons in hippocampal micro-island cultures. Cre neurons consistently showed lower release rates compared with Ctrl neurons under all experimental conditions. Fractions given in red represent $rate_{Cre}/rate_{Ctrl}$ ratios. (Modified from [32])

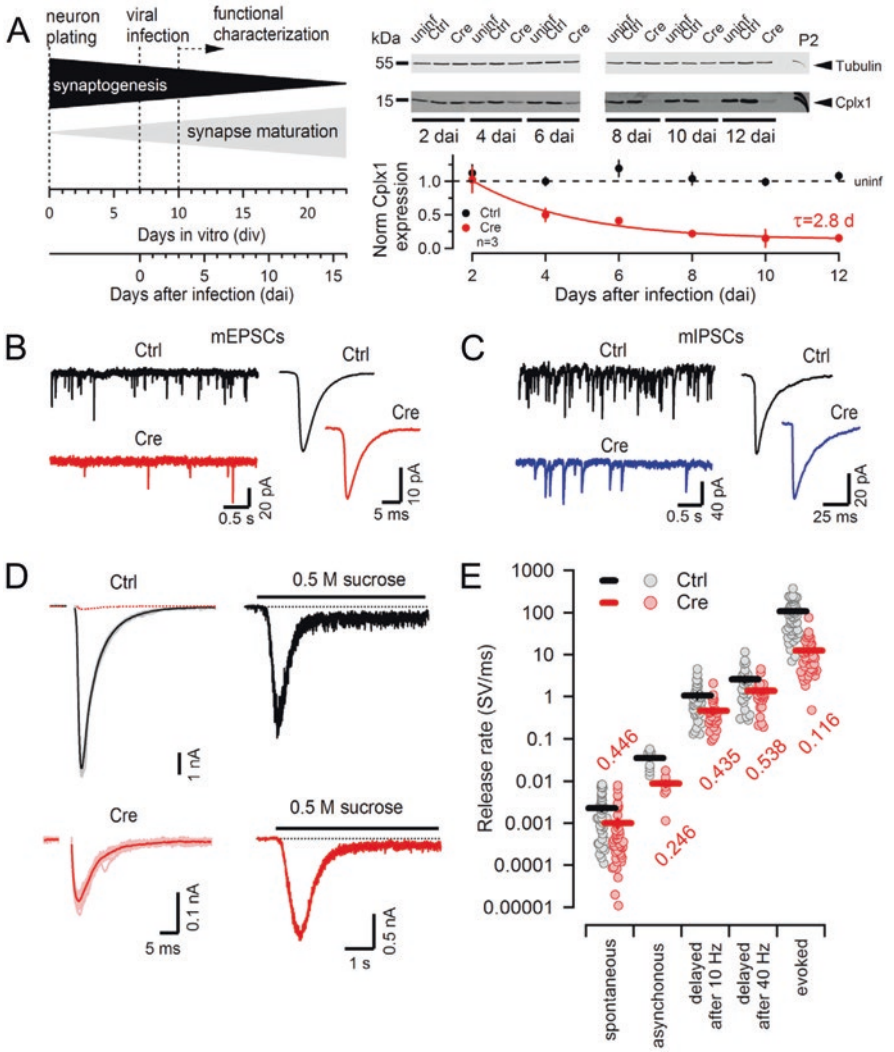

Fig. 5 Acute Cplx loss causes progressive attenuation of spontaneous, asynchronous, delayed, and AP-evoked transmitter release in cultured hippocampal synapses without affecting the readily releasable pool of SVs. (**a**) Experimental paradigm: P0–P1 hippocampal neurons from conditional Cplx TKO mice were maintained in culture and at div 7; the neurons were infected with either RFP (Ctrl) or Cre-RFP (Cre). Functional properties were assayed between day 3 and day 16 (left panel). Progressive loss of Cplx1 expression was assayed by Western blotting at various time points after infection. Virtually complete loss of Cplx1 protein in Cre-infected cultures was observed at day ≥8 (right panel). (**b**, **c**) Spontaneous release is reduced after acute Cplx loss. Sample traces and average waveforms of mEPSCs (B) and mIPSCs (C) recorded in a Ctrl (black) and a Cre (red and blue) neuron at day 10, when Cplx1 expression was completely abolished in Cre neurons. (**d**) Left: AP-evoked EPSCs in day 3–16 hippocampal autaptic neurons are strongly reduced in Cre neurons. Light-colored traces represent 15 consecutive eEPSCs recorded in a Ctrl (day 9, top) and a Cre (day 11, bottom) neuron. Average eEPSCs are superimposed in dark color. The dotted red trace

neurons were infected with Cre recombinase-encoding lentivirus at a time when most synapses had already been established. Viral infection led to progressive decline of Cplx expression (Fig. 5a) which eventually caused a reduction in AP-evoked release by ~90%, and a reduction in spontaneous glutamate release by over 60% (Fig. 5b, d). No transient upregulation of mEPSC frequency was observed in these experiments. In fact, for all modes of neurotransmitter release tested, including spontaneous release, asynchronous release, delayed release after 10-Hz and 40-Hz stimulus trains, and AP-evoked synchronous release, the release rate was consistently lower by at least a factor of about two in neurons infected with Cre recombinase-encoding lentivirus (Fig. 5e). These findings reinforce the notion that in mammalian synapses Cplx serves as a release promoting factor for both synchronous and asynchronous (spontaneous and delayed) release regardless of whether Cplx expression is removed constitutively or acutely.

4.2 Analysis of Complexin Function in Acute Brains Slices

In contrast to the wealth of data from cultured neurons, functional studies on the role of Cplx in neurotransmission in situ are sparse, which is largely due to the fact that many synapses of the mammalian brain co-express Cplx1 and Cplx2. In case of ablation of one of these Cplxs, the remaining Cplx isoform can at least partially compensate for the missing one as it was observed in experiments using Cplx1 and Cplx2 single KO mice. However, in constitutive Cplx1/2 DKO mice compensation is not possible, which consequently causes the death of such animals shortly after birth.

Intriguingly, some mammalian neurons only express a single Cplx paralog. For example, only Cplx1 is expressed at mature calyx [45] and endbulb of Held synapses [44], and the mouse NMJ [88]. Using constitutive Cplx1 KO mice [12], functional consequences of genetic Cplx ablation were studied in these solely Cplx1-expressing synapses in situ. Consistent with the earlier findings with cultured neurons, Cplx1-deficient synapses in these in situ preparations display strong decreases in the amplitude of AP-evoked synchronous neurotransmitter release and the rate of spontaneous SV release [44, 45, 88] (Fig. 6). Interestingly, immature mouse calyx of Held terminals contain both Cplx1 and Cplx2. The latter paralog is developmentally downregulated such that from about postnatal day 16 on, the calyx can essentially be regarded as an exclusively Cplx1-expressing terminal. During this period of postnatal development, functional deficits increasingly aggravated in Cplx1 KO calyx synapses. This is consistent with the idea that Cplx2 can functionally substitute for the missing Cplx1 at an early stage of synapse development. Later, when Cplx2 expression is absent or falls below a critical level, the functional deficits of Cplx1 KO become penetrant [45]. In addition, at both calyx of Held synapses and the NMJ of Cplx1 KO mice, wider eEPSCs were observed. Because the kinetics of mEPSCs remained essentially unchanged, the slower eEPSC time course indicates a tendency toward a desynchronization of AP-evoked transmitter release

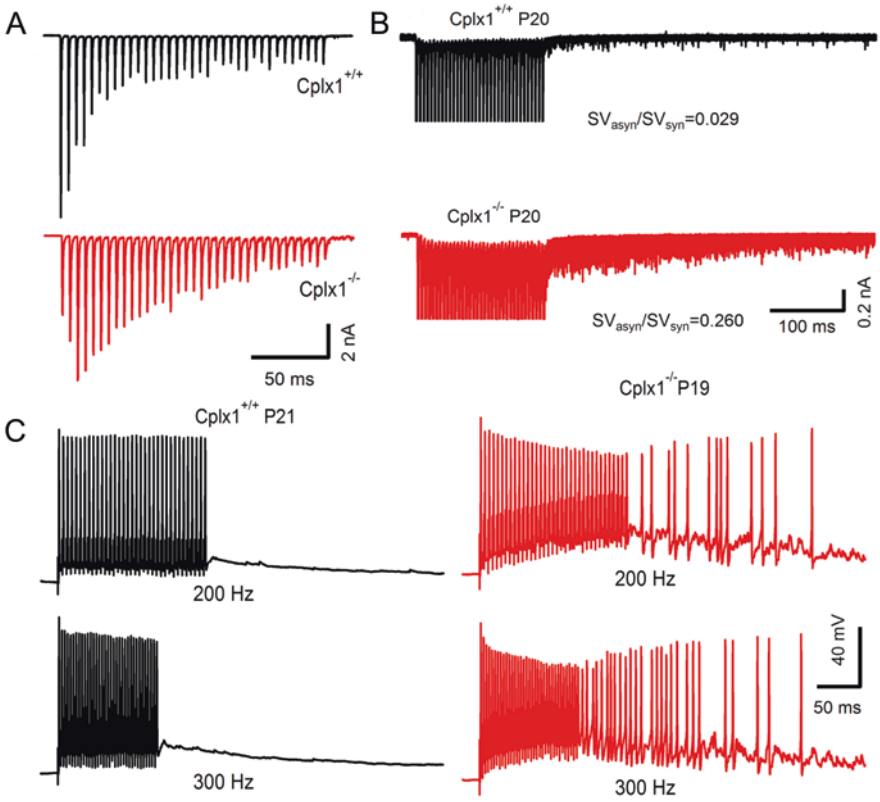

Fig. 6 Cplx-deficient mouse calyx of Held synapses show reduced synaptic strength, altered short-term plasticity and enhanced delayed release causing aberrant AP firing. (**a**) Representative 100 Hz trains consisting of 35 EPSCs evoked by afferent-fiber stimulation in a wildtype (black) and a Cplx1-deficient (red) calyx synapse. Lack of Cplx causes reduced initial eEPSC size and converts short-term depression typically observed at wildtype synapses to short-term facilitation. (**b**) Ten consecutive traces of 200 Hz trains consisting of 35 EPSCs evoked by afferent-fiber stimulation and recorded in a P20 wildtype (black) and a P20 Cplx-deficient (red) calyx synapse are shown superimposed. Amplitudes of AP-evoked synchronous EPSCs are truncated. Delayed asynchronous release is strongly enhanced during the first 500 ms following the stimulus trains in the Cplx-deficient synapse. (**c**) 200 Hz (top) and 300 Hz (bottom) postsynaptic AP trains elicited by afferent-fiber stimulation and recorded in current-clamp mode in postsynaptic MNTB principal neurons of a wildtype (black) and Cplx-deficient (red) calyx synapse. Whereas wildtype synapses follow presynaptic stimulation faithfully, Cplx-deficient neurons generate numerous aberrant spikes during and especially following the stimulus trains. (Modified from [45])

in synapses completely lacking Cplxs. This was also shown to occur in cultured hippocampal neurons, where wider eEPSCs were observed following genetic Cplx1 removal from Cplx2/3 DKO synapses [32]. Thus, in addition to promoting AP-evoked SV fusion, Cplx1 expression is also needed for synchronizing AP-triggered SV fusion, at least in some synapses.

As in cultured synapses lacking Cplx expression [12, 32, 47], short-term plasticity in situ in endbulb and calyx of Held synapses as well as in the NMJ of Cplx1 KO mice is characterized by smaller eEPSCs, attenuated eEPSCs depression and enhanced synaptic facilitation during AP trains, which is consistent with a reduced release probability. The decreased release probability lowers the consumption of SVs per AP and thereby reduces the relative synaptic depression at steady-state transmission during AP trains (Fig. 6a). At the mouse calyx of Held synapse, presynaptic AP waveforms and presynaptic Ca^{2+} currents are unchanged in Cplx1 KO mice [45]. This is in line with the notion that reduced release probability in Cplx-lacking terminals is caused by mechanisms downstream of Ca^{2+} influx, that is, by a lower apparent Ca^{2+}-sensitivity of SV fusion.

Intriguingly, Cplx-lacking calyx of Held synapses show very prominent delayed asynchronous release following high-frequency AP trains, which is in sharp contrast to only minimally occurring asynchronous release at wildtype calyces [45, 89] (Fig. 6b). Such elevated delayed release was also observed at endbulb of Held synapses of Cplx1 KO mice [44, 45]. In both calyx and endbulb Cplx1 KO synapses, the delayed transmitter release triggered numerous aberrant postsynaptic spikes, which distorted auditory information processing [44, 45] (Fig. 6c). It is tempting to speculate that a desynchronization of neurotransmitter release during and following repetitive AP firing may distort the temporal fidelity of information flow in neural circuits and contributes to the behavioral deficits described for Cplx1 KO mice.

Tonically operating ribbon synapses in the mouse retina and inner ear cochlea differ markedly from conventional synapses with respect to the role of Cplx for spontaneous release [90]. At synapses between rod bipolar and AII amacrine cells in the mouse retina, genetic removal of Cplx3 strongly attenuates fast, phasic neurotransmitter release in response to presynaptic depolarizations but augments spontaneous mEPSC frequencies. At light offset, the increased asynchronous release in the Cplx3 KO mice may distort light-dependent signaling at these synapses [91]. Besides expressing different Cplx paralogs, tonically operating retinal ribbon synapses might differ from conventional brain synapses in their resting values for cytosolic $[Ca^{2+}]$ at presynaptic endings. It is interesting to note in this context that mouse chromaffin cells of Cplx2 KO mice also show an enhanced tonic release which is evident only at elevated levels of cytosolic $[Ca^{2+}]$ ($\geq$500 nM) [92].

In mouse ribbon synapses, Cplx3/4 seem to play an additional role in organizing SVs around presynaptic ribbons. Cpx3 promotes SV tethering to ribbons of rod bipolar cells, as indicated by a reduced number of SVs around the ribbons in Cplx3 KO mice [93]. In photoreceptor ribbon synapses, the number of SVs associated with the ribbon base close to the plasma membrane is lower in light than in dark conditions in wildtype mice but remains unchanged in Cplx3/4 DKO mice [94]. In the retina of adult Cplx3/4 DKO mice, about 25% of photoreceptor terminals contain spherical free-floating ribbons, possibly representing breakdown products of anchored ribbons, which are rarely observed in wildtype retinae [48].

Molecular and physiological characterization of afferent inner hair cell synapses of the mouse cochlea indicates that they operate without Cplx [44, 50]. Since vesicular glutamate release rates at these sensory cells are tightly controlled even in the

absence of Cplx expression, a SV "fusion clamp" may not be required at inner hair cell synapses. Possibly, SV exocytosis at inner hair cell synapses is executed by mechanisms that differ from SNARE-mediated membrane fusion at conventional synapses or, alternatively, yet to be identified proteins act in the context of synaptic transmission at hair cell synapses. Both scenarios are conceivable and supported by the finding, that these synapses also lack neuronal SNAREs and Syt [90].

4.3 Analysis of Complexin Function in Invertebrate Synapses

Knowledge about invertebrate Cplxs has come mainly from studies of their functions at the NMJs of *Caenorhabditis elegans* and larvae of *Drosophila melanogaster*. Unlike mammals, these two invertebrate model organisms have only two or one Cplx-encoding gene(s): The two Cplx paralogs of *Caenorhabditis elegans* are encoded by two genes located on chromosome I (CPX-1) and chromosome X (CPX-2). CPX-1 and CPX-2 are differentially distributed, with a predominant expression of CPX-1 in all ventral cord motor neurons [57]. *Drosophila melanogaster*, on the other hand, has a single Cplx-encoding gene, which generates multiple dmCplx isoforms by alternative splicing [95]. The predominant dmCplx isoform dmCplx7A contains a CAAX box which is absent in dmCplx7B but also found in mammalian Cplx3 and Cplx4. Prenylation of dmCplx7A may tether it to membranes, increasing its local concentration at release sites and allowing it to bind to more SNARE complexes per SV. At the level of confocal microscopy, dmCplx7A, which contains the prenylation motif, and dmCplx7B, which lacks it, showed similar localization at the larval NMJ. This indicates that the dissimilar C-terminal sequences of dmCplx7A and dmCplx7B do not cause significant differences in trafficking to synapses [37].

The apparent effects of Cplx deficiencies on synaptic transmission differ between invertebrates (nematodes and flies) and mammals. While Cplx deficiencies in mammals inhibit both evoked synaptic responses and spontaneous SV fusion, Cplx loss in flies and nematodes causes a substantially increased spontaneous fusion rate but greatly decreases evoked responses [20, 38, 57, 93, 96, 97] (Fig. 7a). These experimental findings strongly support the notion that invertebrate Cplxs act as a "fusion clamp" for spontaneous SV fusion. In both nematodes and flies, the augmenting effect of Cplx deficiencies on spontaneous SV fusion may be observed whether or not the extracellular solution contains Ca^{2+} [20, 57].

Cplx-deficient fruit flies also exhibit a marked decrease in evoked EPSC amplitudes at their NMJs, as well as slowed eEPSC rise and decay times [95]. The impairment of evoked release likely reflects a true defect in SV exocytosis rather than a secondary effect of potential SV depletion resulting from the high rate of spontaneous fusion [38]. In addition, mutant flies have approximately 60% more AZs than wildtype at the NMJ, which is, however, insufficient to explain the >20-fold increase in spontaneous release. The morphological changes in Cplx-deficient fly NMJs may be a consequence of the dysregulated spontaneous SV fusion [20]. Fly NMJs of

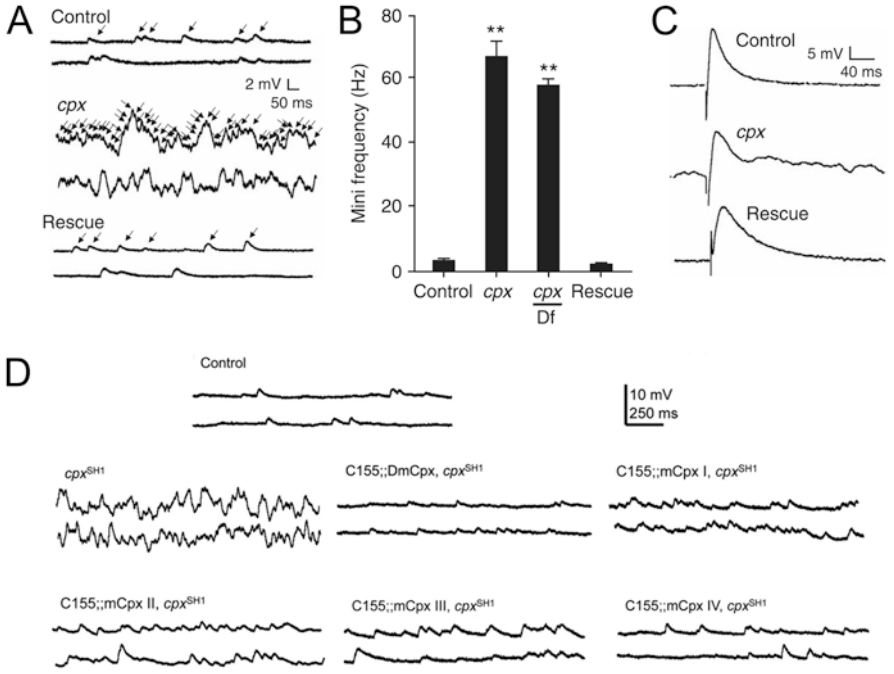

Fig. 7 CPX^{SH1} fly mutants show a marked increase in mEPSC frequency at larval NMJs which can be rescued by expression of fly or mouse Cplx protein. (**a**) Sample traces containing spontaneously occurring mEPSCs (arrows) in control, CPX^{SH1}, and rescue larvae. The CPX^{SH1} mutation results in a complete loss of Cplx protein expression and behaves like a Cplx null mutant. (**b**) Quantification of average mEPSC frequencies in control, CPX^{SH1}, CPX^{SH1} over CPX-deficient (Df), and rescue flies in 0.2 mM extracellular [Ca^{2+}]. The frequency of spontaneous release in CPX^{SH1} mutants remained strongly elevated even in 0 mM extracellular [Ca^{2+}]. (**c**) Sample traces of evoked responses in control, CPX^{SH1}, and rescue larvae at 0.2 mM extracellular [Ca^{2+}]. In high extracellular [Ca^{2+}], evoked responses in CPX^{SH1} mutants were significantly reduced compared with controls, whereas no difference was observed in low extracellular [Ca^{2+}]. (**d**) Sample traces containing mEPSC in control, CPX^{SH1}, and rescue fly strains expressing either dmCplx or the indicated mouse Cplx paralogs. The aberrant mEPSC frequency observed in CPX^{SH1} mutant fly larvae could be rescued fully by expression of dmCplx and partially by expression of either mouse Cplx1, Cplx2, Cplx3, or Cplx4. (Modified from [20, 39])

dmCplx mutants carrying a C-terminal truncation, which is predicted to disrupt prenylation and membrane targeting of dmCplx, exhibited normal evoked transmission but increased mEPSC frequency, suggesting that membrane interaction of dmCplx is required for regulating the spontaneous SV fusion rate but not evoked transmission [95].

Genetic removal of dmCplx does not change the number of SVs at AZs, indicating that dmCplx loss does not uncouple the processes required for morphological docking of SVs at AZs [96]. However, a more recent study reported fewer than normal tethered SVs when analyzing their number in concentric shells surrounding T-bars in dmCplx-deficient fly NMJs and concluded that dmCplx promotes SV

recruitment to the AZ [93]. That study identifies an interaction of dmCplx with the C-terminal region of Bruchpilot, an essential protein of the cytomatrix at the fly NMJ AZ. This interaction is lost in mutant dmCplx carrying a C-terminal truncation, which interferes with its synaptic localization and confers enhanced short-term depression during high-frequency stimulation of the fly NMJ [37, 93].

The seemingly opposite functional consequences of genetic Cplx removal on spontaneous SV fusion in fruit fly [20] and mouse [88] NMJs could be due to two possible causes. A first possibility is that fly and mouse Cplx orthologs inherently inhibit and promote the SV release machinery, respectively. A second possibility is that the actual functional consequences of Cplx deficiency are determined by the protein environment which likely differs between presynaptic endings of invertebrates and vertebrates [98]. To address this question, experiments were conducted in which murine Cplx was expressed in dmCplx null mutant fruit fly larvae. One study found that murine Cplx failed to reverse the increased spontaneous mEPSC rate at the dmCplx null mutant fly NMJ, suggesting that mouse and fly Cplx intrinsically differ in their functions [38]. However, another study reported that all four murine Cpx proteins function as "fusion clamps" when expressed in dmCplx null mutant flies, though their clamping abilities vary among isoforms [39] (Fig. 7d). In addition, expression of murine Cplx1, Cplx 2, or Cplx 3 enhanced evoked release even more strongly than expression of dmCplx in dmCplx null mutant flies [39]. In contrast, expression of dmCplx in cultured hippocampal neurons from Cplx1/2/3 TKO mice is unable to rescue AP-evoke release [38]. Moreover, overexpression of mammalian Cplx1 in cultured hippocampal neurons from wildtype mice did not interfere with AP-evoked synaptic transmission while that of dmCplx had a strong dominant negative effect [38] (Fig. 4). Thus, it remains controversial whether the differential effects of Cplx deficiencies on spontaneous and evoked SV fusion between fruit flies and mice are due to differences of Cplx intrinsic properties.

In nematodes, the rates of spontaneous SV fusion at the NMJ are similar between wildtype and Cplx mutant at extracellular $[Ca^{2+}] \geq 1$ mM. Lowering extracellular $[Ca^{2+}]$ strongly decreased the mEPSC frequency in wildtype synapses but did much less so in mutants. In addition, Cplx expression appeared to be necessary to maintain the pool of docked SVs since it was reduced by 70% in Cplx mutants [57]. Thus, Cplx may be required at the nematode NMJ to maintain a stable pool of docked SVs. In its absence, SVs may fuse or undock from the plasma membrane which largely accounts for the almost complete loss of evoked responses.

Cplx-deficient fruit flies and nematodes show different phenotypes at the behavioral level. The majority of Cplx mutant flies die before maturating to adulthood. The rare survivors are infertile, and show severe motor and visual defects [20, 37]. In contrast, both single and double mutants of *C. elegans cpx-1* and *cpx-2* are viable and can develop into fertile adults. Single mutants of *cpx-1* but not *cpx-2* show severe locomotion deficits. *cpx-1* mutants are also hypersensitive to aldicarb, an inhibitor of acetylcholinesterase. Inhibition of this enzyme results in a buildup of acetylcholine at the NMJ and other cholinergic synapses, resulting in spastic paralysis of the worm. Mutant animals secreting higher levels of acetylcholine become paralyzed faster than wildtype nematodes upon exposure to aldicarb [99, 100]. The

increased sensitivity of *cpx-1* mutant to aldicarb suggests increased acetylcholine release, which is consistent with the increased rate of mEPSC frequency described above.

5 Some Variants of the Human Cplx Gene Loci Are Disease-Associated

Synaptic function is sustained by repeated cycles of SV exo- and endocytosis, which requires a tightly regulated process of assembly and dissociation of the SNARE-mediated SV fusion machinery. Unsurprisingly, pathogenic variants in human gene loci encoding SNAREs and their regulatory and auxiliary proteins can result in a spectrum of clinically relevant deficits of brain function, leading to neurodevelopmental, neuromuscular, and neurodegenerative disorders which collectively have been termed SNAREopathies [101].

Cplx1 is prominently expressed in many brain regions including cortex, thalamus, hippocampus, and deep cerebellar nuclei, while Cplx2 is predominantly found in the cortex, basal ganglia, hippocampus, and cerebellar cortex. Altered expression of these two Cplx isoforms has been linked to several brain diseases [101–103]. Important neural circuits involved in social behavior are located in some of the Cplx-expressing brain regions, and both Cplx paralogs are dysregulated in some forms of neuropsychiatric disorders such as schizophrenia, major depression, and bipolar disorders [103].

Recent studies performing whole-exome sequencing (WES) to explore genetic backgrounds associated with intellectual disability (ID) identified various variants in genes encoding synaptic proteins. Among these were also homozygous mutations in the human gene for CPLX1 [104, 105]. Individuals carrying these pathologically relevant variants of the CPLX1 gene exhibited early infantile epileptic encephalopathy. Two affected siblings were reported to suffer from malignant migrating epilepsy and cortical atrophy. Magnetic resonance imaging (MRI) of one of the patients showed a small cleft in the cerebellum. Two other siblings showed severe epilepsy, global developmental delay, and intellectual disability. Finally, an individual with a missense mutation suffered from persistent generalized seizures and developmental delay. Interestingly, all of the identified mutations affected the C-terminal domain of Cplx1 which is thought to mediate membrane interactions [59] and/or to bind to Syt1 [61]. Because it is incompletely understood how the C terminus of mammalian Cplxs influences their function, the exact link between the identified gene defects and the observed brain disorders remains elusive.

Some of the human patients identified in the abovementioned studies exhibited severe motor problems, which are also characteristic for Cplx1-deficient mice. Motor coordination and locomotion deficits of Cplx1 KO mice include abnormal gait, inability to run or swim, impaired rotarod performance, dystonia, strong tremor, and sporadic seizures [81, 82]. The Cplx1 KO mouse line is of special

interest because some of its characteristic deficits, such as the strong cerebellar dysfunction, reduced novelty seeking, shuffled walking, dystonia as well as resting tremor [81], are similar to typical symptoms of human patients suffering from Parkinson's disease (PD). Genome-wide association studies (GWAS), which were conducted to search genetic variants predisposing to multifactorial PD, identified two loci on human chromosome 4 (CPLX1/GAK/TMEM175/DGKQ and SNCA) to be correlated with PD risk [106, 107]. A comprehensive sequence analysis identified two single nucleotide polymorphisms (SNPs) (rs76444973 and rs 34006598) within intron 1 of the human CPLX1 gene. Because the protein coding sequence starts in exon 2, the allelic variants are positioned upstream of the first ATG which makes a prediction about their effect on Cplx protein expression and/or function difficult. In a complementary approach, another SNP (rs10794536) associated with PD risk was found [108]. In contrast to the SNPs described earlier, this allelic variation is located in the 3′ untranslated region (UTR) of the CPLX1 gene, which might lead to the generation of Cplx1 mRNA with different stability. Altered Cplx1 levels in PD patients support this notion. Moreover, patients with α-synuclein gene duplication (PARK4 mutation) showed a downregulation of Cplx1 mRNA, which was experimentally confirmed to occur also in α-synuclein-overexpressing human neuroblastoma cells [108]. These findings are in line with a previously observed co-regulation of Cplx1 and α-synuclein protein expression in some mutant mice [108–111]. Although the molecular mechanisms mediating such an interplay are incompletely understood, these findings are significant because of two reasons: (i) They demonstrate that Cplx1 is a member of a larger group of presynaptic proteins which collectively and interdependently maintain and regulate SV fusion. Dysregulation of one or few individual constituents of this finely tuned molecular network may lead to synaptic dysfunction such as observed in PD pathology. (ii) In a number of studies, post-mortem tissue of PD patients and patients with other psychiatric and neurological diseases was used to estimate Cplx mRNA or protein levels. While it is disputable whether dysregulation of Cplxs can be reliably detected in such material, the use of CPLX1 mRNA levels in human blood probably as a potential disease biomarker holds promise [108].

SNP variants were found in the human genome not only for CPLX1 but also for CPLX2 [112]. Because changed expression levels of Cplx2 can be associated with cognitive deficits in schizophrenia and possibly also play a role in the development of other neuropsychiatric disorders, a phenotype-based genetic association study (PGAS) was initiated by the Göttingen Research Association for Schizophrenia (GRAS). Six cognition-relevant SNPs were identified to be distributed over the entire CPLX2 gene. All genetic variants reside outside of the protein coding region, but one of them, rs3822674, which is located in the 3'UTR of the human CPLX2 mRNA within a micro-RNA (has-miR-498) binding site, was of special interest. Expression studies in N2a cells showed, that this SNP potentially influences the posttranscriptional regulation of CPLX2 expression. Thus, the binding of a specific micro-RNA to the 3'UTR of CPLX2 mRNA may represent a mechanism to precisely regulate the Cplx2 expression level [112].

In summary, recent studies analyzing the disease relevance of both Cplx1 and Cplx2 provide evidence that not only expression per se but also tightly regulated levels of protein expression are required for normal neuronal function. While neurons obviously possess mechanisms to cope with temporary aberrations in presynaptic protein expression, persistent changes in Cplx expression, especially when occurring on the background of other molecular disturbances, may promote progressive functional decline. However, further research is necessary to clarify whether altered Cplx expression as it occurs in psychiatric and neurological disorders is disease cause or consequence [103].

6 Conclusions

Cplxs are regulatory proteins of the neurotransmitter release apparatus which, together with members of the Ca^{2+}-sensing Syt protein family, control Ca^{2+}-triggered SV fusion. It has been difficult to integrate experimental data on Cplx function into a coherent model. Hence, a consensus about the synaptic function of Cplxs has not been reached, which underscores the challenge in deriving models of molecular interactions based mainly on data obtained by perturbing synaptic proteins [113].

One undebated role of Cplxs is their function as facilitators of fast AP-evoked synchronous neurotransmitter release. This role of Cplxs appears to be evolutionarily conserved since elimination of Cplx expression greatly inhibits evoked transmitter release in all species examined, including *Caenorhabditis elegans*, *Drosophila melanogaster*, and mice. The notable exception of mammalian inner ear hair cell synapses, where Cplx KO does not alter evoked responses, presents no challenge because those cells do not express Cplx [44, 50].

A further consequence of genetic Cplx removal—primarily observed at invertebrate synapses but also at Cplx3/4-expressing ribbon synapses of the mammalian retina—is a prominent augmentation of asynchronous and spontaneous neurotransmitter release. The scientific literature is not unanimous regarding the mechanisms generating this enhancement and why it is seen at some but not at other Cplx-lacking synapses. It is attributed to an inhibitory and "fusion-clamp" like action exerted by Cplx in the absence of elevated cytosolic [Ca^{2+}]. The ability of Cplx to "clamp" asynchronous SV fusion may differ between different species [78]. In addition, other presynaptic proteins may assist Cplx in "clamping" asynchronous SV fusion in some synapses such that a loss of Cplx alone does not necessarily induce synaptic deficits.

Alternatively, Cplx may serve as an adaptor molecule governing the molecular composition of the SV fusion machinery [98]. Functional consequences of Cplx removal will then be determined by alternative SNARE-binding partners expressed in a given cell type, which may become part of an erroneously assembled fusion machinery in the absence of Cplx and which may confer anomalous functional properties to Cplx-lacking synapses. In such model, functional consequences of

substituting wildtype Cplx with a mutated variant will depend on how well the latter executes its role as an adaptor molecule.

Acknowledgments We would like to thank Dr. Noa Lipstein for insightful comments. F.J.L.-M. was a fellow of the Alexander von Humboldt Foundation and is supported by the Serra Húnter Programme and by the Spanish Ministry of Science and Innovation. K.R. acknowledges support by the German Research Foundation (DFG, grant RE 4382/2-1).

References

1. Wojcik SM, Brose N. Regulation of membrane fusion in synaptic excitation-secretion coupling: speed and accuracy matter. Neuron. 2007;55:11–24. https://doi.org/10.1016/j.neuron.2007.06.013.
2. Südhof TC. Neurotransmitter release: the last millisecond in the life of a synaptic vesicle. Neuron. 2013;80:675–90. https://doi.org/10.1016/j.neuron.2013.10.022.
3. Weber T, Zemelman BV, McNew JA, Westermann B, Gmachl M, Parlati F, et al. SNAREpins: minimal machinery for membrane fusion. Cell. 1998;92:759–72. https://doi.org/10.1016/s0092-8674(00)81404-x.
4. Rizo J, Xu J. The synaptic vesicle release machinery. Annu Rev Biophys. 2015;44:339–67. https://doi.org/10.1146/annurev-biophys-060414-034057.
5. Südhof TC, Rothman JE. Membrane fusion: grappling with SNARE and SM proteins. Science. 2009;323:474–7. https://doi.org/10.1126/science.1161748.
6. Jahn R, Fasshauer D. Molecular machines governing exocytosis of synaptic vesicles. Nature. 2012;490:201–7. https://doi.org/10.1038/nature11320.
7. Augustin I, Rosenmund C, Südhof TC, Brose N. Munc13-1 is essential for fusion competence of glutamatergic synaptic vesicles. Nature. 1999;400:457–61. https://doi.org/10.1038/22768.
8. Jockusch WJ, Speidel D, Sigler A, Sorensen JB, Varoqueaux F, Rhee JS, et al. CAPS-1 and CAPS-2 are essential synaptic vesicle priming proteins. Cell. 2007;131:796–808. https://doi.org/10.1016/j.cell.2007.11.002.
9. Verhage M, Maia AS, Plomp JJ, Brussaard AB, Heeroma JH, Vermeer H, et al. Synaptic assembly of the brain in the absence of neurotransmitter secretion. Science. 2000;287:864–9. https://doi.org/10.1126/science.287.5454.864.
10. Fernandez-Chacon R, Königstorfer A, Gerber SH, Garcia J, Matos MF, Stevens CF, et al. Synaptotagmin I functions as a calcium regulator of release probability. Nature. 2001;410:41–9. https://doi.org/10.1038/35065004.
11. Maximov A, Südhof TC. Autonomous function of synaptotagmin 1 in triggering synchronous release independent of asynchronous release. Neuron. 2005;48:547–54. https://doi.org/10.1016/j.neuron.2005.09.006.
12. Reim K, Mansour M, Varoqueaux F, McMahon HT, Südhof TC, Brose N, et al. Complexins regulate a late step in Ca^{2+}-dependent neurotransmitter release. Cell. 2001;104:71–81. https://doi.org/10.1016/s0092-8674(01)00192-1.
13. McMahon HT, Missler M, Li C, Südhof TC. Complexins: cytosolic proteins that regulate SNAP receptor function. Cell. 1995;83:111–9. https://doi.org/10.1016/0092-8674(95)90239-2.
14. Ishizuka T, Saisu H, Suzuki T, Kirino Y, Abe T. Molecular cloning of synaphins/complexins, cytosolic proteins involved in transmitter release, in the electric organ of an electric ray (Narke japonica). Neurosci Lett. 1997;232:107–10. https://doi.org/10.1016/s0304-3940(97)00586-7.
15. Kusick GF, Ogunmowo TH, Watanabe S. Transient docking of synaptic vesicles: implications and mechanisms. Curr Opin Neurobiol. 2022;74:102535. https://doi.org/10.1016/j.conb.2022.102535.

16. Neher E, Brose N. Dynamically primed synaptic vesicle states: key to understand synaptic short-term plasticity. Neuron. 2018;100:1283–91. https://doi.org/10.1016/j.neuron.2018.11.024.
17. Rosenmund C, Rettig J, Brose N. Molecular mechanisms of active zone function. Curr Opin Neurobiol. 2003;13:509–19. https://doi.org/10.1016/j.conb.2003.09.011.
18. Südhof TC. The molecular machinery of neurotransmitter release (Nobel lecture). Angew Chem Int Ed Engl. 2014;53:12696–717. https://doi.org/10.1002/anie.201406359.
19. Xue M, Craig TK, Xu J, Chao HT, Rizo J, Rosenmund C. Binding of the complexin N terminus to the SNARE complex potentiates synaptic-vesicle fusogenicity. Nat Struct Mol Biol. 2010;17:568–75. https://doi.org/10.1038/nsmb.1791.
20. Huntwork S, Littleton JT. A complexin fusion clamp regulates spontaneous neurotransmitter release and synaptic growth. Nat Neurosci. 2007;10:1235–7. https://doi.org/10.1038/nn1980.
21. Giraudo CG, Eng WS, Melia TJ, Rothman JE. A clamping mechanism involved in SNARE-dependent exocytosis. Science. 2006;313:676–80. https://doi.org/10.1126/science.1129450.
22. Tang J, Maximov A, Shin OH, Dai H, Rizo J, Südhof TC. A complexin/synaptotagmin 1 switch controls fast synaptic vesicle exocytosis. Cell. 2006;126:1175–87. https://doi.org/10.1016/j.cell.2006.08.030.
23. Schaub JR, Lu X, Doneske B, Shin YK, McNew JA. Hemifusion arrest by complexin is relieved by Ca^{2+}-synaptotagmin I. Nat Struct Mol Biol. 2006;13:748–50. https://doi.org/10.1038/nsmb1124.
24. Pabst S, Hazzard JW, Antonin W, Sudhof TC, Jahn R, Rizo J, et al. Selective interaction of complexin with the neuronal SNARE complex. Determination of the binding regions. J Biol Chem. 2000;275:19808–18. https://doi.org/10.1074/jbc.M002571200.
25. Pabst S, Margittai M, Vainius D, Langen R, Jahn R, Fasshauer D. Rapid and selective binding to the synaptic SNARE complex suggests a modulatory role of complexins in neuroexocytosis. J Biol Chem. 2002;277:7838–48. https://doi.org/10.1074/jbc.M109507200.
26. Chen X, Tomchick DR, Kovrigin E, Arac D, Machius M, Südhof TC, et al. Three-dimensional structure of the complexin/SNARE complex. Neuron. 2002;33:397–409. https://doi.org/10.1016/s0896-6273(02)00583-4.
27. Bowen ME, Weninger K, Ernst J, Chu S, Brunger AT. Single-molecule studies of synaptotagmin and complexin binding to the SNARE complex. Biophys J. 2005;89:690–702. https://doi.org/10.1529/biophysj.104.054064.
28. Li Y, Augustine GJ, Weninger K. Kinetics of complexin binding to the SNARE complex: correcting single molecule FRET measurements for hidden events. Biophys J. 2007;93:2178–87. https://doi.org/10.1529/biophysj.106.101220.
29. Krishnakumar SS, Li F, Coleman J, Schauder CM, Kummel D, Pincet F, et al. Re-visiting the trans insertion model for complexin clamping. elife. 2015;4 https://doi.org/10.7554/eLife.04463.
30. Heo S, Diering GH, Na CH, Nirujogi RS, Bachman JL, Pandey A, et al. Identification of long-lived synaptic proteins by proteomic analysis of synaptosome protein turnover. Proc Natl Acad Sci U S A. 2018;115:E3827–E36. https://doi.org/10.1073/pnas.1720956115.
31. Dörrbaum AR, Kochen L, Langer JD, Schuman EM. Local and global influences on protein turnover in neurons and glia. elife. 2018;7 https://doi.org/10.7554/eLife.34202.
32. Lopez-Murcia FJ, Reim K, Jahn O, Taschenberger H, Brose N. Acute Complexin knockout abates spontaneous and evoked transmitter release. Cell Rep. 2019;26:2521–30 e5. https://doi.org/10.1016/j.celrep.2019.02.030.
33. Fornasiero EF, Mandad S, Wildhagen H, Alevra M, Rammner B, Keihani S, et al. Precisely measured protein lifetimes in the mouse brain reveal differences across tissues and subcellular fractions. Nat Commun. 2018;9:4230. https://doi.org/10.1038/s41467-018-06519-0.
34. Reim K, Wegmeyer H, Brandstätter JH, Xue M, Rosenmund C, Dresbach T, et al. Structurally and functionally unique complexins at retinal ribbon synapses. J Cell Biol. 2005;169:669–80. https://doi.org/10.1083/jcb.200502115.

35. Takahashi S, Yamamoto H, Matsuda Z, Ogawa M, Yagyu K, Taniguchi T, et al. Identification of two highly homologous presynaptic proteins distinctly localized at the dendritic and somatic synapses. FEBS Lett. 1995;368:455–60. https://doi.org/10.1016/0014-5793(95)00713-j.
36. Yang X, Pei J, Kaeser-Woo YJ, Bacaj T, Grishin NV, Südhof TC. Evolutionary conservation of complexins: from choanoflagellates to mice. EMBO Rep. 2015;16:1308–17. https://doi.org/10.15252/embr.201540305.
37. Buhl LK, Jorquera RA, Akbergenova Y, Huntwork-Rodriguez S, Volfson D, Littleton JT. Differential regulation of evoked and spontaneous neurotransmitter release by C-terminal modifications of complexin. Mol Cell Neurosci. 2013;52:161–72. https://doi.org/10.1016/j.mcn.2012.11.009.
38. Xue M, Lin YQ, Pan H, Reim K, Deng H, Bellen HJ, et al. Tilting the balance between facilitatory and inhibitory functions of mammalian and Drosophila Complexins orchestrates synaptic vesicle exocytosis. Neuron. 2009;64:367–80. https://doi.org/10.1016/j.neuron.2009.09.043.
39. Cho RW, Song Y, Littleton JT. Comparative analysis of Drosophila and mammalian complexins as fusion clamps and facilitators of neurotransmitter release. Mol Cell Neurosci. 2010;45:389–97. https://doi.org/10.1016/j.mcn.2010.07.012.
40. Yamada M, Saisu H, Ishizuka T, Takahashi H, Abe T. Immunohistochemical distribution of the two isoforms of synaphin/complexin involved in neurotransmitter release: localization at the distinct central nervous system regions and synaptic types. Neuroscience. 1999;93:7–18. https://doi.org/10.1016/s0306-4522(99)00104-9.
41. Freeman W, Morton AJ. Differential messenger RNA expression of complexins in mouse brain. Brain Res Bull. 2004;63:33–44. https://doi.org/10.1016/j.brainresbull.2003.12.003.
42. Ishizuka T, Saisu H, Odani S, Kumanishi T, Abe T. Distinct regional distribution in the brain of messenger RNAs for the two isoforms of synaphin associated with the docking/fusion complex. Neuroscience. 1999;88:295–306. https://doi.org/10.1016/s0306-4522(98)00223-1.
43. Freeman W, Morton AJ. Regional and progressive changes in brain expression of complexin II in a mouse transgenic for the Huntington's disease mutation. Brain Res Bull. 2004;63:45–55. https://doi.org/10.1016/j.brainresbull.2003.12.004.
44. Strenzke N, Chanda S, Kopp-Scheinpflug C, Khimich D, Reim K, Bulankina AV, et al. Complexin-I is required for high-fidelity transmission at the endbulb of Held auditory synapse. J Neurosci. 2009;29:7991–8004. https://doi.org/10.1523/JNEUROSCI.0632-09.2009.
45. Chang S, Reim K, Pedersen M, Neher E, Brose N, Taschenberger H. Complexin stabilizes newly primed synaptic vesicles and prevents their premature fusion at the mouse calyx of held synapse. J Neurosci. 2015;35:8272–90. https://doi.org/10.1523/JNEUROSCI.4841-14.2015.
46. Ono S, Baux G, Sekiguchi M, Fossier P, Morel NF, Nihonmatsu I, et al. Regulatory roles of complexins in neurotransmitter release from mature presynaptic nerve terminals. Eur J Neurosci. 1998;10:2143–52. https://doi.org/10.1046/j.1460-9568.1998.00225.x.
47. Xue M, Stradomska A, Chen H, Brose N, Zhang W, Rosenmund C, et al. Complexins facilitate neurotransmitter release at excitatory and inhibitory synapses in mammalian central nervous system. Proc Natl Acad Sci U S A. 2008;105:7875–80. https://doi.org/10.1073/pnas.0803012105.
48. Reim K, Regus-Leidig H, Ammermuller J, El-Kordi A, Radyushkin K, Ehrenreich H, et al. Aberrant function and structure of retinal ribbon synapses in the absence of complexin 3 and complexin 4. J Cell Sci. 2009;122:1352–61. https://doi.org/10.1242/jcs.045401.
49. Landgraf I, Mühlhans J, Dedek K, Reim K, Brandstätter JH, Ammermüller J. The absence of Complexin 3 and Complexin 4 differentially impacts the ON and OFF pathways in mouse retina. Eur J Neurosci. 2012;36:2470–81. https://doi.org/10.1111/j.1460-9568.2012.08149.x.
50. Uthaiah RC, Hudspeth AJ. Molecular anatomy of the hair cell's ribbon synapse. J Neurosci. 2010;30:12387–99. https://doi.org/10.1523/JNEUROSCI.1014-10.2010.
51. Bracher A, Kadlec J, Betz H, Weissenhorn W. X-ray structure of a neuronal complexin-SNARE complex from squid. J Biol Chem. 2002;277:26517–23. https://doi.org/10.1074/jbc.M203460200.

52. Xue M, Reim K, Chen X, Chao HT, Deng H, Rizo J, et al. Distinct domains of complexin I differentially regulate neurotransmitter release. Nat Struct Mol Biol. 2007;14:949–58. https://doi.org/10.1038/nsmb1292.
53. Trimbuch T, Xu J, Flaherty D, Tomchick DR, Rizo J, Rosenmund C. Re-examining how complexin inhibits neurotransmitter release. elife. 2014;3:e02391. https://doi.org/10.7554/eLife.02391.
54. Giraudo CG, Garcia-Diaz A, Eng WS, Chen Y, Hendrickson WA, Melia TJ, et al. Alternative zippering as an on-off switch for SNARE-mediated fusion. Science. 2009;323:512–6. https://doi.org/10.1126/science.1166500.
55. Radoff DT, Dong Y, Snead D, Bai J, Eliezer D, Dittman JS. The accessory helix of complexin functions by stabilizing central helix secondary structure. elife. 2014;3 https://doi.org/10.7554/eLife.04553.
56. Lai Y, Choi UB, Zhang Y, Zhao M, Pfuetzner RA, Wang AL, et al. N-terminal domain of complexin independently activates calcium-triggered fusion. Proc Natl Acad Sci U S A. 2016;113:E4698–707. https://doi.org/10.1073/pnas.1604348113.
57. Hobson RJ, Liu Q, Watanabe S, Jorgensen EM. Complexin maintains vesicles in the primed state in C. elegans. Curr Biol. 2011;21:106–13. https://doi.org/10.1016/j.cub.2010.12.015.
58. Zhang FL, Casey PJ. Protein prenylation: molecular mechanisms and functional consequences. Annu Rev Biochem. 1996;65:241–69. https://doi.org/10.1146/annurev.bi.65.070196.001325.
59. Snead D, Wragg RT, Dittman JS, Eliezer D. Membrane curvature sensing by the C-terminal domain of complexin. Nat Commun. 2014;5:4955. https://doi.org/10.1038/ncomms5955.
60. Malsam J, Seiler F, Schollmeier Y, Rusu P, Krause JM, Söllner TH. The carboxy-terminal domain of complexin I stimulates liposome fusion. Proc Natl Acad Sci U S A. 2009;106:2001–6. https://doi.org/10.1073/pnas.0812813106.
61. Tokumaru H, Shimizu-Okabe C, Abe T. Direct interaction of SNARE complex binding protein synaphin/complexin with calcium sensor synaptotagmin 1. Brain Cell Biol. 2008;36:173–89. https://doi.org/10.1007/s11068-008-9032-9.
62. Shata A, Saisu H, Odani S, Abe T. Phosphorylated synaphin/complexin found in the brain exhibits enhanced SNARE complex binding. Biochem Biophys Res Commun. 2007;354:808–13. https://doi.org/10.1016/j.bbrc.2007.01.064.
63. Hill JJ, Callaghan DA, Ding W, Kelly JF, Chakravarthy BR. Identification of okadaic acid-induced phosphorylation events by a mass spectrometry approach. Biochem Biophys Res Commun. 2006;342:791–9. https://doi.org/10.1016/j.bbrc.2006.02.029.
64. Maximov A, Tang J, Yang X, Pang ZP, Südhof TC. Complexin controls the force transfer from SNARE complexes to membranes in fusion. Science. 2009;323:516–21. https://doi.org/10.1126/science.1166505.
65. Yang X, Kaeser-Woo YJ, Pang ZP, Xu W, Südhof TC. Complexin clamps asynchronous release by blocking a secondary Ca^{2+} sensor via its accessory alpha helix. Neuron. 2010;68:907–20. https://doi.org/10.1016/j.neuron.2010.11.001.
66. Kaeser-Woo YJ, Yang X, Südhof TC. C-terminal complexin sequence is selectively required for clamping and priming but not for Ca^{2+} triggering of synaptic exocytosis. J Neurosci. 2012;32:2877–85. https://doi.org/10.1523/JNEUROSCI.3360-11.2012.
67. Gong J, Lai Y, Li X, Wang M, Leitz J, Hu Y, et al. C-terminal domain of mammalian complexin-1 localizes to highly curved membranes. Proc Natl Acad Sci U S A. 2016;113:E7590–E9. https://doi.org/10.1073/pnas.1609917113.
68. Yang X, Cao P, Südhof TC. Deconstructing complexin function in activating and clamping Ca^{2+}-triggered exocytosis by comparing knockout and knockdown phenotypes. Proc Natl Acad Sci U S A. 2013;110:20777–82. https://doi.org/10.1073/pnas.1321367110.
69. Liu J, Guo T, Wei Y, Liu M, Sui SF. Complexin is able to bind to SNARE core complexes in different assembled states with distinct affinity. Biochem Biophys Res Commun. 2006;347:413–9. https://doi.org/10.1016/j.bbrc.2006.06.085.

70. Zhou Q, Zhou P, Wang AL, Wu D, Zhao M, Südhof TC, et al. The primed SNARE-complexin-synaptotagmin complex for neuronal exocytosis. Nature. 2017;548:420–5. https://doi.org/10.1038/nature23484.
71. Chicka MC, Chapman ER. Concurrent binding of complexin and synaptotagmin to liposome-embedded SNARE complexes. Biochemistry. 2009;48:657–9. https://doi.org/10.1021/bi801962d.
72. Xu J, Pang ZP, Shin OH, Südhof TC. Synaptotagmin-1 functions as a Ca2+ sensor for spontaneous release. Nat Neurosci. 2009;12:759–66. https://doi.org/10.1038/nn.2320.
73. Pang ZP, Melicoff E, Padgett D, Liu Y, Teich AF, Dickey BF, et al. Synaptotagmin-2 is essential for survival and contributes to Ca^{2+} triggering of neurotransmitter release in central and neuromuscular synapses. J Neurosci. 2006;26:13493–504. https://doi.org/10.1523/JNEUROSCI.3519-06.2006.
74. Courtney NA, Bao H, Briguglio JS, Chapman ER. Synaptotagmin 1 clamps synaptic vesicle fusion in mammalian neurons independent of complexin. Nat Commun. 2019;10:4076. https://doi.org/10.1038/s41467-019-12015-w.
75. Brewer KD, Bacaj T, Cavalli A, Camilloni C, Swarbrick JD, Liu J, et al. Dynamic binding mode of a Synaptotagmin-1-SNARE complex in solution. Nat Struct Mol Biol. 2015;22:555–64. https://doi.org/10.1038/nsmb.3035.
76. Sauvola CW, Littleton JT. SNARE regulatory proteins in synaptic vesicle fusion and recycling. Front Mol Neurosci. 2021;14:733138. https://doi.org/10.3389/fnmol.2021.733138.
77. Brose N. For better or for worse: complexins regulate SNARE function and vesicle fusion. Traffic. 2008;9:1403–13. https://doi.org/10.1111/j.1600-0854.2008.00758.x.
78. Trimbuch T, Rosenmund C. Should I stop or should I go? The role of complexin in neurotransmitter release. Nat Rev Neurosci. 2016;17:118–25. https://doi.org/10.1038/nrn.2015.16.
79. Mohrmann R, Dhara M, Bruns D. Complexins: small but capable. Cell Mol Life Sci. 2015;72:4221–35. https://doi.org/10.1007/s00018-015-1998-8.
80. Cao P, Yang X, Südhof TC. Complexin activates exocytosis of distinct secretory vesicles controlled by different synaptotagmins. J Neurosci. 2013;33:1714–27. https://doi.org/10.1523/JNEUROSCI.4087-12.2013.
81. Glynn D, Drew CJ, Reim K, Brose N, Morton AJ. Profound ataxia in complexin I knockout mice masks a complex phenotype that includes exploratory and habituation deficits. Hum Mol Genet. 2005;14:2369–85. https://doi.org/10.1093/hmg/ddi239.
82. Glynn D, Sizemore RJ, Morton AJ. Early motor development is abnormal in complexin 1 knockout mice. Neurobiol Dis. 2007;25:483–95. https://doi.org/10.1016/j.nbd.2006.10.011.
83. Bekkers JM, Stevens CF. Excitatory and inhibitory autaptic currents in isolated hippocampal neurons maintained in cell culture. Proc Natl Acad Sci U S A. 1991;88:7834–8.
84. Landis SC. Rat sympathetic neurons and cardiac myocytes developing in microcultures: correlation of the fine structure of endings with neurotransmitter function in single neurons. Proc Natl Acad Sci U S A. 1976;73:4220–4. https://doi.org/10.1073/pnas.73.11.4220.
85. Furshpan EJ, MacLeish PR, O'Lague PH, Potter DD. Chemical transmission between rat sympathetic neurons and cardiac myocytes developing in microcultures: evidence for cholinergic, adrenergic, and dual-function neurons. Proc Natl Acad Sci U S A. 1976;73:4225–9. https://doi.org/10.1073/pnas.73.11.4225.
86. Imig C, Min SW, Krinner S, Arancillo M, Rosenmund C, Südhof TC, et al. The morphological and molecular nature of synaptic vesicle priming at presynaptic active zones. Neuron. 2014;84:416–31. https://doi.org/10.1016/j.neuron.2014.10.009.
87. Schotten S, Meijer M, Walter AM, Huson V, Mamer L, Kalogreades L, et al. Additive effects on the energy barrier for synaptic vesicle fusion cause supralinear effects on the vesicle fusion rate. elife. 2015;4:e05531. https://doi.org/10.7554/eLife.05531.
88. Lin MY, Rohan JG, Cai H, Reim K, Ko CP, Chow RH. Complexin facilitates exocytosis and synchronizes vesicle release in two secretory model systems. J Physiol. 2013;591:2463–73. https://doi.org/10.1113/jphysiol.2012.244517.

89. Scheuss V, Taschenberger H, Neher E. Kinetics of both synchronous and asynchronous quantal release during trains of action potential-evoked EPSCs at the rat calyx of Held. J Physiol. 2007;585:361–81. https://doi.org/10.1113/jphysiol.2007.140988.
90. Moser T, Grabner CP, Schmitz F. Sensory processing at ribbon synapses in the retina and the Cochlea. Physiol Rev. 2020;100:103–44. https://doi.org/10.1152/physrev.00026.2018.
91. Mortensen LS, Park SJH, Ke JB, Cooper BH, Zhang L, Imig C, et al. Complexin 3 increases the fidelity of signaling in a retinal circuit by regulating exocytosis at ribbon synapses. Cell Rep. 2016;15:2239–50. https://doi.org/10.1016/j.celrep.2016.05.012.
92. Dhara M, Yarzagaray A, Schwarz Y, Dutta S, Grabner C, Moghadam PK, et al. Complexin synchronizes primed vesicle exocytosis and regulates fusion pore dynamics. J Cell Biol. 2014;204:1123–40. https://doi.org/10.1083/jcb.201311085.
93. Scholz N, Ehmann N, Sachidanandan D, Imig C, Cooper BH, Jahn O, et al. Complexin cooperates with Bruchpilot to tether synaptic vesicles to the active zone cytomatrix. J Cell Biol. 2019;218:1011–26. https://doi.org/10.1083/jcb.201806155.
94. Babai N, Sendelbeck A, Regus-Leidig H, Fuchs M, Mertins J, Reim K, et al. Functional roles of Complexin 3 and Complexin 4 at mouse photoreceptor ribbon synapses. J Neurosci. 2016;36:6651–67. https://doi.org/10.1523/JNEUROSCI.4335-15.2016.
95. Iyer J, Wahlmark CJ, Kuser-Ahnert GA, Kawasaki F. Molecular mechanisms of COMPLEXIN fusion clamp function in synaptic exocytosis revealed in a new Drosophila mutant. Mol Cell Neurosci. 2013;56:244–54. https://doi.org/10.1016/j.mcn.2013.06.002.
96. Jorquera RA, Huntwork-Rodriguez S, Akbergenova Y, Cho RW, Littleton JT. Complexin controls spontaneous and evoked neurotransmitter release by regulating the timing and properties of synaptotagmin activity. J Neurosci. 2012;32:18234–45. https://doi.org/10.1523/JNEUROSCI.3212-12.2012.
97. Martin JA, Hu Z, Fenz KM, Fernandez J, Dittman JS. Complexin has opposite effects on two modes of synaptic vesicle fusion. Curr Biol. 2011;21:97–105. https://doi.org/10.1016/j.cub.2010.12.014.
98. Neher E. Complexin: does it deserve its name? Neuron. 2010;68:803–6. https://doi.org/10.1016/j.neuron.2010.11.038.
99. Dittman JS, Kaplan JM. Behavioral impact of neurotransmitter-activated G-protein-coupled receptors: muscarinic and GABAB receptors regulate Caenorhabditis elegans locomotion. J Neurosci. 2008;28:7104–12. https://doi.org/10.1523/JNEUROSCI.0378-08.2008.
100. Miller KG, Alfonso A, Nguyen M, Crowell JA, Johnson CD, Rand JB. A genetic selection for Caenorhabditis elegans synaptic transmission mutants. Proc Natl Acad Sci U S A. 1996;93:12593–8. https://doi.org/10.1073/pnas.93.22.12593.
101. Verhage M, Sorensen JB. SNAREopathies: diversity in mechanisms and symptoms. Neuron. 2020;107:22–37. https://doi.org/10.1016/j.neuron.2020.05.036.
102. Melland H, Carr EM, Gordon SL. Disorders of synaptic vesicle fusion machinery. J Neurochem. 2021;157:130–64. https://doi.org/10.1111/jnc.15181.
103. Brose N. Altered complexin expression in psychiatric and neurological disorders: cause or consequence? Mol Cells. 2008;25:7–19.
104. Karaca E, Harel T, Pehlivan D, Jhangiani SN, Gambin T, Coban Akdemir Z, et al. Genes that affect brain structure and function identified by rare variant analyses of Mendelian neurologic disease. Neuron. 2015;88:499–513. https://doi.org/10.1016/j.neuron.2015.09.048.
105. Redler S, Strom TM, Wieland T, Cremer K, Engels H, Distelmaier F, et al. Variants in CPLX1 in two families with autosomal-recessive severe infantile myoclonic epilepsy and ID. Eur J Hum Genet. 2017;25:889–93. https://doi.org/10.1038/ejhg.2017.52.
106. Lill CM, Roehr JT, McQueen MB, Kavvoura FK, Bagade S, Schjeide BM, et al. Comprehensive research synopsis and systematic meta-analyses in Parkinson's disease genetics: the PDGene database. PLoS Genet. 2012;8:e1002548. https://doi.org/10.1371/journal.pgen.1002548.
107. Nalls MA, Pankratz N, Lill CM, Do CB, Hernandez DG, Saad M, et al. Large-scale meta-analysis of genome-wide association data identifies six new risk loci for Parkinson's disease. Nat Genet. 2014;46:989–93. https://doi.org/10.1038/ng.3043.

108. Lahut S, Gispert S, Omur O, Depboylu C, Seidel K, Dominguez-Bautista JA, et al. Blood RNA biomarkers in prodromal PARK4 and rapid eye movement sleep behavior disorder show role of complexin 1 loss for risk of Parkinson's disease. Dis Model Mech. 2017;10:619–31. https://doi.org/10.1242/dmm.028035.
109. Gispert S, Kurz A, Brehm N, Rau K, Walter M, Riess O, et al. Complexin-1 and Foxp1 expression changes are novel brain effects of alpha-Synuclein pathology. Mol Neurobiol. 2015;52:57–63. https://doi.org/10.1007/s12035-014-8844-0.
110. Chandra S, Fornai F, Kwon HB, Yazdani U, Atasoy D, Liu X, et al. Double-knockout mice for α- and β-synucleins: effect on synaptic functions. Proc Natl Acad Sci U S A. 2004;101:14966–71. https://doi.org/10.1073/pnas.0406283101.
111. Greten-Harrison B, Polydoro M, Morimoto-Tomita M, Diao L, Williams AM, Nie EH, et al. αβγ-Synuclein triple knockout mice reveal age-dependent neuronal dysfunction. Proc Natl Acad Sci U S A. 2010;107:19573–8. https://doi.org/10.1073/pnas.1005005107.
112. Begemann M, Grube S, Papiol S, Malzahn D, Krampe H, Ribbe K, et al. Modification of cognitive performance in schizophrenia by complexin 2 gene polymorphisms. Arch Gen Psychiatry. 2010;67:879–88. https://doi.org/10.1001/archgenpsychiatry.2010.107.
113. Stein A, Jahn R. Complexins living up to their name--new light on their role in exocytosis. Neuron. 2009;64:295–7. https://doi.org/10.1016/j.neuron.2009.10.026.

Regulation of Ryanodine Receptor-Dependent Neurotransmitter Release by AIP, Calstabins, and Presenilins

Zhao-Wen Wang, Longgang Niu, and Sadaf Riaz

Abstract Ryanodine receptors (RyRs) are Ca^{2+} release channels located in the endoplasmic reticulum membrane. Presynaptic RyRs play important roles in neurotransmitter release and synaptic plasticity. Recent studies suggest that the proper function of presynaptic RyRs relies on several regulatory proteins, including aryl hydrocarbon receptor-interacting protein, calstabins, and presenilins. Dysfunctions of these regulatory proteins can greatly impact neurotransmitter release and synaptic plasticity by altering the function or expression of RyRs. This chapter aims to describe the interaction between these proteins and RyRs, elucidating their crucial role in regulating synaptic function.

Keywords Ryanodine receptor · AIP · Aryl hydrocarbon receptor-interacting protein · AIPR-1 · Calstabin1 · Calstabin2 · FKBP12 · FKBP12.6 · Presenilin

Abbreviations

AD	Alzheimer's disease
AHR	Acryl hydrocarbon receptor
AIP	Aryl hydrocarbon receptor-interacting protein
APP	Amyloid precursor protein
Aβ	Amyloid β
cDKO	Conditional double knockout
ePSC	Evoked postsynaptic current

Z.-W. Wang (✉) · L. Niu · S. Riaz
Department of Neuroscience, University of Connecticut School of Medicine, Farmington, CT, USA
e-mail: zwwang@uchc.edu

Z.-W. Wang (ed.), *Molecular Mechanisms of Neurotransmitter Release*, Advances in Neurobiology 33, https://doi.org/10.1007/978-3-031-34229-5_11

ER	Endoplasmic reticulum
FIPA	Familial isolated pituitary adenoma
HSP	Heat shock protein
IP_3R	Inositol 1,4,5-trisphosphate receptor
NMJ	Neuromuscular junction
PPIase	Peptidylprolyl isomerase
PS1	Presenilin-1
PS2	Presenilin-2
RRP	Readily releasable pool
RyR	Ryanodine receptor
SERCA	Sarco(endo)plasmic reticulum Ca^{2+}-ATPase
TPR	Tetratricopeptide repeat
VGCC	Voltage-gated Ca^{2+} channel

1 Introduction

Ca^{2+} plays a critical role in both spontaneous and evoked neurotransmitter release (Chapter "Roles and Sources of Calcium in Synaptic Exocytosis"). It triggers synaptic vesicle exocytosis by binding to specific Ca^{2+} sensors located in the synaptic vesicle membrane (Chapter "Calcium Sensors of Neurotransmitter Release"). The sources of Ca^{2+} triggering synaptic vesicle exocytosis include Ca^{2+} influx through voltage-gated Ca^{2+} channels (VGCCs) in the presynaptic plasma membrane and ryanodine receptor (RyR)-mediated Ca^{2+} release from the endoplasmic reticulum (ER) (Chapter "Roles and Sources of Calcium in Synaptic Exocytosis"). Humans and mice each have three RyRs (RyR1, RyR2, and RyR3) encoded by three different genes. The expression of all three RyRs may be detected in the brain [1–9] (see also https://mouse.brain-map.org/). In contrast, the nematode *Caenorhabditis elegans* has only one gene encoding RyRs, *ryr-1* (also known as *unc-68*). The importance of RyR-mediated Ca^{2+} mobilization in neurotransmitter release has been demonstrated by many studies (Chapter "Roles and Sources of Calcium in Synaptic Exocytosis").

RyRs are activated by VGCCs in the plasma membrane, which perform this function either through physical interactions with RyRs or by Ca^{2+}-induced Ca^{2+} release, depending on the types of RYRs and VGCCs involved ([10] and Chapter "Roles and Sources of Calcium in Synaptic Exocytosis"). RyRs are also regulated by other proteins [11, 12]. In recent years, several proteins have emerged as potent regulators of synaptic transmission that act on RyRs, including aryl hydrocarbon receptor-interacting protein (AIP), calstabins, and presenilins. Deficiencies in these proteins can cause significant changes in neurotransmitter release and/or synaptic plasticity. In this chapter, we describe their roles in synaptic function and their mechanisms of action.

2 Regulation of Neurotransmitter Release by AIRP-1/AIP

2.1 Structure and Function of Human AIP

AIP is a member of the tetratricopeptide repeat (TPR) family of proteins. It contains a peptidylprolyl isomerase (PPIase)-like domain, a TPR domain, and a carboxyl (C)-terminus α-helix, also known as the α-7 helix [13] (Fig. 1a, b). PPIases are enzymes that catalyze the cis-trans isomerization of a peptide bond between a proline residue and a preceding amino acid residue in folded proteins, but the PPIase domain of AIP lacks this enzymatic activity [13, 14]. TPR domains are present in various proteins and typically contain three or more TPR motifs in tandem [15, 16]. Each TPR motif is a 34-amino acid peptide that exhibits strong conservation in amino acid size, hydrophobicity, spacing, and tertiary structure, despite variability in amino acid sequence [17]. The TPR domain of human AIP consists of three TPR motifs, with each TPR motif having a helix-loop-helix conformation and connecting to the next via a short loop. The α-7 helix is situated near the second α-helix of the third TPR motif, as depicted in the crystal structure of AIP [18] (Fig. 1b). This structure closely resembles that of AIP-like 1 in humans [19].

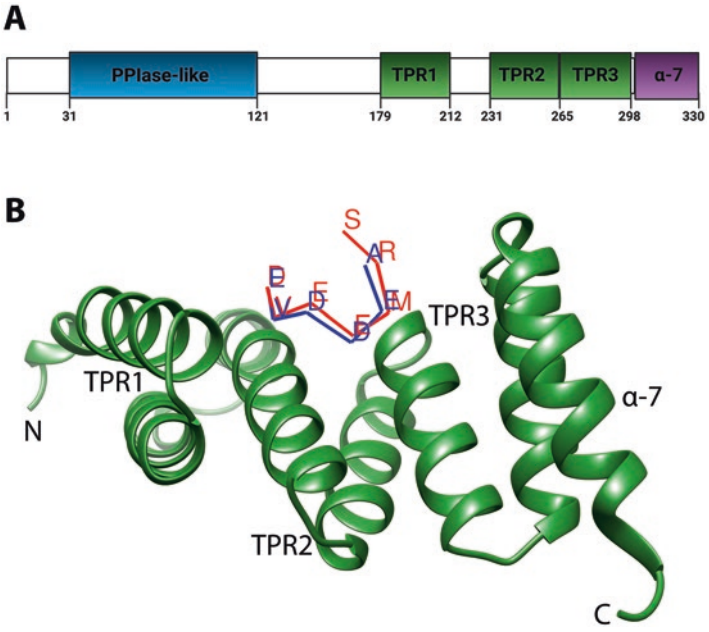

Fig. 1 Structures of human aryl hydrocarbon receptor-interacting protein (AIP). (**a**) Domain structure of AIP. (Adapted from Ref. [13]). (**b**) Ribbon diagram of the *t*etratrico*p*eptide *r*epeat (TPR) domain of AIP in complex with the carboxyl termini of HSP90 (PDB 4AIF, red) and TOMM20 (PDF 4APO, blue)

AIP is expressed widely throughout the human body, as noted on the NCBI Gene database (https://www.ncbi.nlm.nih.gov/gene/9049). In the brain, AIP is expressed in numerous regions, as reported on the Allen Brain Atlas website (https://mouse.brain-map.org/gene/show/11419). AIP is primarily known to interact with various molecular chaperones via its TPR domains to ensure proper folding of client (substrate) proteins [20]. Among the molecular chaperones that AIP may bind to are HSP90 (heat shock protein 90), HSP70, and TOMM20 [13]. While these proteins share a conserved motif at the extreme C-terminus (EEVD in HSP90 and HSP70, and DDVE in TOMM20), the amino acid sequence upstream of the conserved motif varies substantially among them, contributing to protein binding specificity [21]. It is worth noting that the EEVD and DDVE motifs are critical to TPR domain binding. Recent crystal structures of the TPR domain of human AIP in complex with a C-terminus peptide of HSP90 and TOMM20 have revealed that the conserved C-terminus motif EEVD or DDVE binds to a groove formed by the TPR domain (see Fig. 1b).

AIP also plays a crucial role in interacting with the aryl hydrocarbon receptor (AHR), a ligand-activated transcription factor, to regulate the transcription of xenobiotic metabolizing enzymes [22]. Some of the identified ligands of AHR include xenobiotics, which are foreign chemicals found within an organism (such as 2,3,7,8-tetrachlorodibenzo-p-dioxin/TCDD and polyaromatic hydrocarbons), as well as non-xenobiotic (endogenous) ligands, including indole derivatives, tryptophan metabolites, bilirubin, prostaglandin E2, and leukotriene B4 [22–24].

In humans, germline mutations of the AIP gene strongly predispose individuals to familial isolated pituitary adenomas (FIPA). Identified mutations in FIPA patients include nonsense and missense mutations, splice site mutations, insertion, and deletion. Although mutations may occur in various regions of AIP, the majority of them are located in the TPR domain [25]. FIPA patients are typically heterozygous for the mutation, but the tumor tissue may have a loss of heterozygosity due to a somatic mutation of the wild-type allele [26, 27]. Similarly, *AIP*$^{+/-}$ mice are susceptible to pituitary adenomas and exhibit a complete loss of AIP in the tumor tissue [28]. However, it remains unclear how AIP deficiency may promote tumorigenesis [25].

2.2 AIP Regulates Neurotransmitter Release by Acting on the RyR

The SLO-1 channel in *C. elegans* is a high-conductance K^+ channel gated by membrane voltage and cytosolic Ca^{2+}. Similar to the vertebrate Slo1 channel, SLO-1 downregulates neurotransmitter release at presynaptic sites [29–31] (Chapter "Regulation of Neurotransmitter Release by K^+Channels"). In *C. elegans*, *slo-1* loss-of-function and gain-of-function mutations increase and decrease neurotransmitter release, respectively, as evidenced by changes in the frequency of miniature postsynaptic currents (minis) and the amplitude of evoked postsynaptic currents (ePSCs) at the neuromuscular junction (NMJ) [32–39].

During a genetic screen for suppressors of a sluggish phenotype caused by a hyperactive SLO-1, we identified a mutant of the *aipr-1* gene, which is the *C. elegans* ortholog of human *AIP*. The *apir-1* mutant, *zw86*, exhibits large increases in the amplitudes of both minis and ePSCs, as well as the frequency of minis, compared to the wild type (Fig. 2a, b). These mutant phenotypes can be rescued by expressing wild-type AIPR-1 in neurons under the control of a panneuronal promoter, but not in muscle cells under the control of a muscle-specific promoter [40]. This suggests that the mutant phenotypes result from presynaptic deficiency of AIPR-1 and that a physiological function of AIPR-1 is to limit neurotransmitter release [40]. Consistent with this notion, AIPR-1 is enriched at presynaptic sites in *C. elegans* motor neurons [40].

In *apir-1(zw86)*, a single G-to-A nucleotide mutation at the splice acceptor site before the last exon, causes a frameshift of the coding sequence and disrupts the third TPR motif and the downstream α-7 helix of AIPR-1 [40]. It is presumably a hypomorphic mutant because its synaptic phenotypes can be rescued by expressing wild-type AIPR-1 in neurons, and null mutants of *aipr-1* arrest at early larval stages [40].

Remarkably, the *aipr-1(zw86)* mutant shows much stronger augmenting effects on synaptic transmission at the *C. elegans* NMJ than null mutations of any other known inhibitory regulators of presynaptic release, including tomosyn [41, 42] and complexins [43, 44]. Tomosyn inhibits neurotransmitter release by competing with synaptobrevin in binding to syntaxin and SNAP25 in the SNARE complex (Chapter "The Role of Tomosyn in the Regulation of Neurotransmitter Release"), which is a

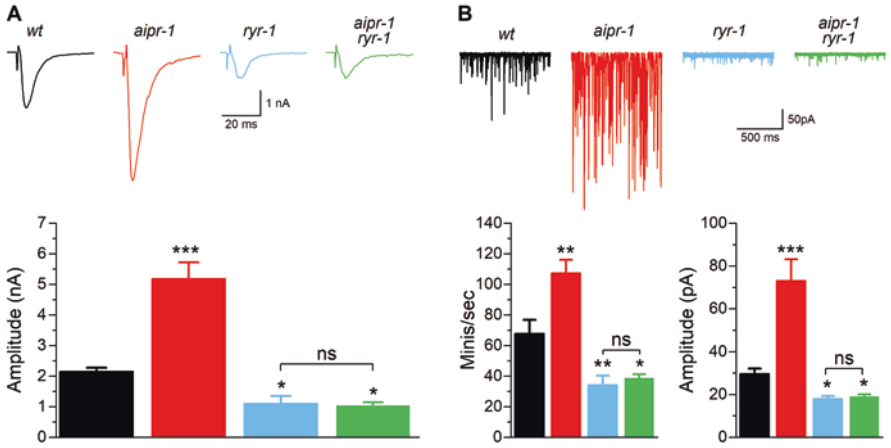

Fig. 2 AIPR-1 regulates synaptic transmission through ryanodine receptors at the *C. elegans* neuromuscular junction. (**a**) Sample traces and the amplitude of evoked postsynaptic currents (ePSCs). (**b**) Sample traces and the frequency and amplitude of miniature postsynaptic currents (minis). The mutants used were *aipr-1(zw86)* and *ryr-1(e540)*, a putative null. *ryr-1(e540)* occludes the augmenting effects of *aipr-1(zw86)* mutation on synaptic transmission. The asterisks indicate statistically significant differences (*$p < 0.05$, $p < 0.01$, and $p < 0.001$) compared with wild type (*wt*). (Adapted from Ref. [40])

four-α-helix bundle formed by the SNARE proteins synaptobrevin, syntaxin, and SNAP25 (Chapter "SNARE Proteins in Synaptic Vesicle Fusion"). Complexins interact with the SNARE proteins to clamp them in a half-zippered state (Chapters "SNARE Proteins in Synaptic Vesicle Fusion" and "Complexins: Ubiquitously Expressed Presynaptic Regulators of SNARE-Mediated Synaptic Vesicle Fusion"). Null mutations of *C. elegans* tomosyn gene *tom-1* cause a larger sucrose-evoked postsynaptic current, a slower decay time of ePSCs, and an increased number of docked synaptic vesicles at the NMJ compared with wild type but do not alter either the frequency and amplitude of minis or the amplitude of ePSCs [41, 42]. Null mutations of *C. elegans* complexin gene *cpx-1* increase the frequency of minis in a $[Ca^{2+}]_o$-dependent manner, essentially eliminate ePSCs, and reduce the numbers of total and docked synaptic vesicles at presynaptic sites of motor neurons [43, 44]. The much stronger augmenting effects of the *aipr-1* mutation on minis and ePSCs than those of *tom-1* and *cpx-1* mutations indicate that AIPR-1/AIP is an exceptionally powerful inhibitory regulator of neurotransmitter release.

How does AIPR-1 regulate the release of neurotransmitters? The PPIase-like domain of AIP/AIPR-1 resembles the domains found in FKBP-binding proteins, such as FKPB12 (calstabin1) and FKBP12.6 (calstabin2), although it lacks the PPIase activity associated with calstabins. Calstabins are known to inhibit the release of Ca^{2+} from the ER through RyRs [45–48]. A previous study by our group demonstrated that null mutations of the sole RyR-encoding gene, *ryr-1*, in *C. elegans* caused a significant reduction in the amplitudes of minis and ePSCs, as well as a great decrease in the frequency of minis at the NMJ when compared with wild type [49]. Interestingly, the phenotypes of *ryr-1* mutants were opposite to those of the *aipr-1* mutant. Given the inhibitory role of calstabins in RyR-mediated Ca^{2+} release from the ER and the opposite synaptic phenotypes of *aipr-1* and *ryr-1* mutants, we hypothesized that AIPR-1 might function through RyRs to restrict neurotransmitter release. To test this hypothesis, we compared minis and ePSCs between *ryr-1(e540)*, a putative null mutant resulting from a premature stop codon [50], and a *ryr-1(e540);aipr-1(zw86)* double mutant. As previously reported [49], the *ryr-1* single mutant showed significant decreases in the amplitude of ePSCs (Fig. 2a), as well as in the amplitude and frequency of minis (Fig. 2b). However, the *aipr-1;ryr-1* double mutant was indistinguishable from the *ryr-1* single mutant (Fig. 2a, b), suggesting that the augmenting effects of *aipr-1* mutation on minis and ePSCs are occluded by the *ryr-1* mutation [40]. These observations indicate that AIPR-1 might act like calstabins to restrict RyR-mediated Ca^{2+} release from the ER. Consistently, the genetically encoded Ca^{2+} sensor GCaMP6 showed that the knockdown of *aipr-1* specifically in motor neurons caused a significant increase in the frequency of Ca^{2+} transients in these neurons, whereas the knockdown of *ryr-1* had the opposite effect. Moreover, the augmenting effect of *aipr-1* knockdown on Ca^{2+} transients was occluded by the knockdown of *ryr-1* [40] (Fig. 3). Biomolecular fluorescence complementation assays confirmed that AIPR-1 and RYR-1 are physically very close in motor neurons in vivo [40]. Collectively, these results suggest that AIPR-1 acts on RyRs to restrict Ca^{2+} release from the ER.

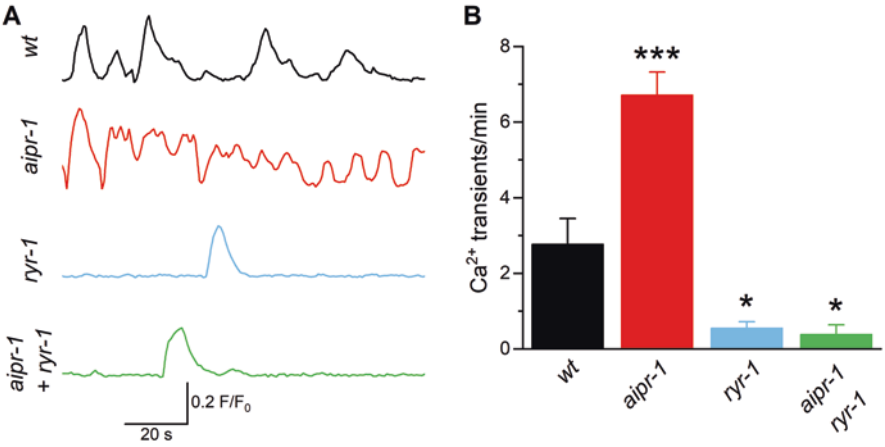

Fig. 3 AIPR-1 regulates Ca^{2+} bursts in motor neurons through ryanodine receptors. (**a**) Sample traces of Ca^{2+} transients of cholinergic motor neurons of wild type (*wt*), and *wt* worms with cholinergic motor neuron-targeted knockdown (RNAi) of either *aipr-1*, *ryr-1*, or both. (**b**) Comparison of the frequency of Ca^{2+} transients among the different groups. The augmenting effect of *aipr-1* RNAi is occluded by *ryr-1* RNAi in the double RNAi strain. The asterisks indicate statistically significant differences (*$p < 0.05$; ***$p < 0.001$) compared with *wt*. (Adapted from Ref. [40])

2.3 AIP Regulates RRP Size and Synaptic Vesicle Number Through a RyR-Independent Mechanism

The size of the readily releasable pool (RRP) of synaptic vesicles can be determined by measuring the integral of postsynaptic currents caused by a hypertonic sucrose solution, which induces the release of all primed synaptic vesicles in a Ca^{2+}-independent manner [51]. When a hypertonic sucrose solution was applied to the *C. elegans* ventral nerve cord containing motor neuron axons, *aipr-1(zw86)* showed a significantly larger postsynaptic current in the postsynaptic muscle cell than wild type [40] (Fig. 4a), indicating an increased RRP size. Furthermore, the number of synaptic vesicles in motor neurons was greater in *aipr-1(zw86)* than in wild type [40] (Fig. 4b). These findings suggest that AIPR-1 can modulate RRP size and synaptic vesicle number. However, even in the presence of a *ryr-1* null mutation, the effects of the *aipr-1* mutation on RRP size and synaptic vesicle number persisted (Fig. 4a, b), indicating that AIPR-1 regulates these processes through RyR-independent mechanisms. The enhanced sucrose response in the *aipr-1* mutant was completely abolished by a mutation of UNC-13/Munc-13 [40], a key player in synaptic vesicle priming [52, 53] (Chapter "Functional Roles of UNC-13/Munc13 and UNC-18/Munc18 in Neurotransmission"), suggesting that the increase in primed vesicles does not bypass the normal mechanisms for synaptic vesicle docking and priming.

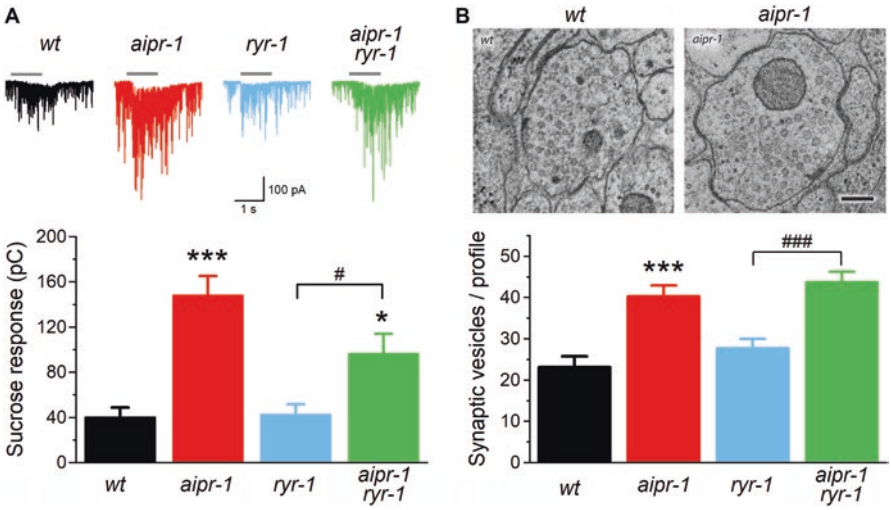

Fig. 4 AIPR-1 regulates the readily releasable pool (RRP) size and synaptic vesicle number through a ryanodine receptor-independent mechanism(s). (**a**) Sample traces and statistical comparison of postsynaptic currents (PSCs) in body-wall muscle cells evoked by a hyperosmotic solution. The horizontal gray lines above the sample traces mark the times of the hyperosmotic solution application. (**b**) Sample electron micrographs of the presynaptic site of *C. elegans* motor neurons and statistical comparison of synaptic vesicle numbers. *aipr-1(zw86)* but not *ryr-1(e540)* augments the evoked PSCs and synaptic vesicle number, and the effects of *aipr-1(zw86)* are not prevented by *ryr-1(e540)* in the double mutant. The asterisk (***$p < 0.001$) and pound symbols (#$p < 0.05$; ###$p < 0.001$) indicate significant differences compared with wild type (*wt*) and *ryr-1*, respectively. (Adapted from Ref. [40])

How might AIP regulate RRP size and synaptic vesicle number? As described earlier, AIP may serve as a co-chaperone for molecular chaperones such as HSP70, HSP90, and TOMM20, and function together with AHR. Because the molecular chaperones may perform quality control for many client proteins [54–56] and AHR may regulate the transcription of diverse target genes [57], AIP might function through one or more of the client proteins or target genes to regulate RRP size and synaptic vesicle number.

Although many AIP-interacting proteins had been identified [13, 25], RyRs were not among them and AIP had not been implicated in regulating neurotransmitter release prior to our study. The discovery of AIPR-1 as a potent inhibitory regulator of presynaptic release has raised some intriguing questions. For example, (1) Are the presynaptic functions of AIP conserved in mammals? (2) How are AIP's presynaptic functions regulated? (3) Are Ca^{2+} mishandling and abnormal neurotransmitter release involved in neurological disorders of individuals with AIP mutations?

Regarding question 1, we found that neuronal expression of human AIP in *C. elegans* can rescue the mini and ePSC phenotypes of *aipr-1(zw86)* [40], indicating that human AIP can substitute worm AIPR-1 in presynaptic functions. However, it remains to be determined whether mammalian AIP plays similar roles in native

neurons. With respect to question 2, it remains to be determined whether and how the presynaptic functions of AIP are regulated by synaptic activities and its presynaptic interacting partners. With respect to question 3, AIP mutations have not yet been linked to any neurological disorders in the Human Gene Mutation Database (https://www.hgmd.cf.ac.uk/ac/index.php). Because null mutations of AIP cause embryonic lethality in both mice [58] and worms [40], the vast majority of humans with AIP mutations are likely heterozygous. The lack of association between AIP mutations and human neurological disorders might be due to individuals with homozygous AIP mutations being unable to develop to a stage where neurological disorders are manifested, while those with heterozygous AIP mutations lack a detectable phenotype.

3 Regulation of Synaptic Transmission by Calstabins

FKBP12 and FKBP12.6 are members of the FK506-binding protein (FKBP) family, which are immunophilins that can bind to the immunosuppressant FK506 [59, 60]. These proteins are also known as calstabin1 and calstabin2, respectively, because they play a role in stabilizing the closed state of RyRs. Both human calstabins consist of 108 amino acids, with only 18 amino acid residues being different between them. Calstabins have a single domain, which is the FK506-binding domain and also serves as the PPIase domain [59, 60].

Calstabins bind to RyRs and regulate their function. Calstabins serve as stabilizers of RyR Ca^{2+} release channels by interacting with the cytosolic domain of RyR; reduced binding of calstabins causes leaky RyRs [61, 62]. Much of our current understanding of RyR regulation by calstabins has come from studies of skeletal and cardiac muscle cells. Calstabin1 and calstabin2 bind to RyR1 in skeletal muscle cells and RyR2 in cardiomyocytes, respectively, to modulate their functions [62–64].

Emerging evidence suggests that neuronal RyRs are regulated by calstabins. One study showed that chronic stress in mice can cause the dissociation of calstabin2 from the RyR2 channel complex through a signaling pathway that involves the stimulation of β-adrenergic receptors by catecholamine, activation of protein kinase A, and phosphorylation of RyR2 at serine 2808 by protein kinase A. The dissociation of calstabin2 from RyR2 leads to increased RyR single-channel open probability and calcium leakage in hippocampal neurons, increased latency in Morris Water Maze tests, and greatly subdued long-term potentiation in the hippocampal CA1 region [46]. These phenotypes caused by chronic stress can be prevented or rescued by either mutating serine 2808 to alanine in RyR2 or administering S107 orally, a compound that stabilizes the RyR2-calstabin2 interaction [46]. Another study showed that calstabin2 knockout in mice increases the firing rate of action potentials, augments ER Ca^{2+} release caused by caffeine (a RyR agonist), and suppresses long-term potentiation in hippocampal neurons [65]. However, neither of these studies investigated the specific function of presynaptic RyRs. Additionally, there are no other reports on presynaptic functions of calstabins to our knowledge. Since

presynaptic RyRs play crucial roles in both spontaneous and evoked neurotransmitter release (Chapter "Roles and Sources of Calcium in Synaptic Exocytosis"), it is conceivable that deficiencies of calstabins may cause increased neurotransmitter release. However, experiments are necessary to confirm this possibility.

4 Regulation of Neurotransmitter Release by Presenilins

Presenilins are a family of multi-pass transmembrane proteins, with two members in humans: presenilin-1 (PS1) and presenilin-2 (PS2). They are mainly known for their roles in the pathogenesis of Alzheimer's disease (AD). Approximately 90% of early-onset familial AD cases are linked to mutations of presenilins [66]. The accumulation of amyloid β (Aβ) plaques in brain tissues is one of the major pathological hallmarks and possibly a cause of AD [67]. Aβ is produced from an amyloid precursor protein (APP) through two sequential cleavage steps. APP is a single-pass transmembrane protein with a large extracellular domain. It is first cleaved by a β-secretase, BACE1 (beta-site APP cleaving enzyme 1), to remove its large extracellular domain, resulting in a membrane-bound C-terminal fragment (CTF) of 99 amino acid residues [68]. The CTF is then cleaved several times by a γ-secretase in a stepwise manner until free Aβ peptides of 37 to 43 amino acid residues are released from the membrane [69] (Fig. 5). Among the Aβ peptides, the larger ones, Aβ42 and Aβ43, are the pathogenic species in AD [69]. PS1 and PS2 serve as the catalytic subunit of the γ-secretase in a hetero-tetrameric protein complex that includes presenilin (PS1 or PS2), APH-1 (anterior pharynx defective-1), PEN-2 (presenilin enhancer 2), and nicastrin [69]. The γ-secretase complex containing PS1 is targeted to the plasma membrane, whereas that containing PS2 is targeted to the trans-Golgi network, endosomes, and lysosomes [70]. In a high-resolution cryo-electron microscopy structure of human PS1-containing γ-secretase in complex with an APP transmembrane fragment, the transmembrane domain of APP interacts with five surrounding transmembrane domains of PS1, with many of the mutations of APP and PS1 identified in AD patients mapped to the APP-PS1 interface [71]. Cleavage of the CTF by γ-secretase may produce Aβ of various lengths. Longer Aβ peptides, such as Aβ42 and Aβ43, which tend to self-aggregate, are strong predisposing factors for AD [69, 72–74], whereas shorter Aβ peptides, such as Aβ40, actually inhibit amyloid deposition [75]. However, an increased ratio of longer over shorter Aβ peptides (e.g., Aβ42/Aβ40) may be more important in the pathogenesis of AD than the absolute amount of longer Aβ peptides [76].

Presenilins, in addition to their function as γ-secretases, play a crucial role in maintaining Ca^{2+} homeostasis through various possible mechanisms. These include forming Ca^{2+} leak channels in the ER membrane [77, 78], regulating the activities of the sarco(endo)plasmic reticulum Ca^{2+}-ATPase (SERCA) in the ER membrane [79], VGCCs in the plasma membrane [80], capacitive Ca^{2+} entry through the plasma membrane [81, 82], and RyR- and inositol 1,4,5-trisphosphate receptor (IP_3R)-mediated Ca^{2+} release from the ER [8, 83–88]. Mutations in presenilins

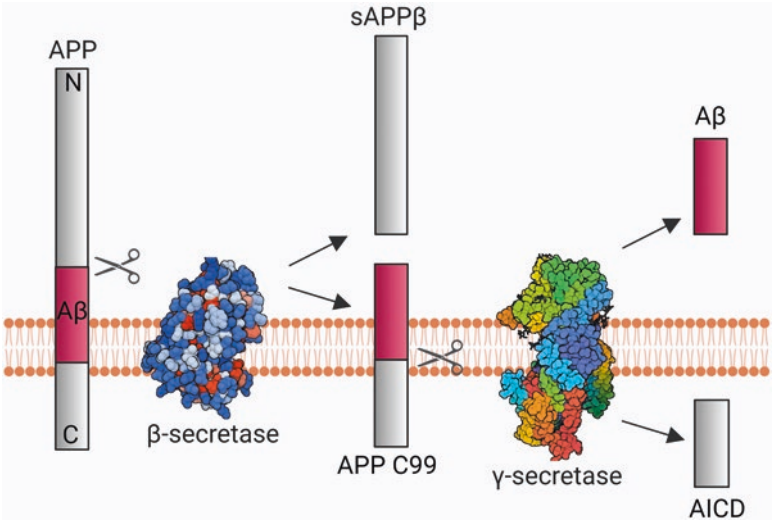

Fig. 5 Amyloidogenic pathway of amyloid precursor protein (APP). APP is cleaved sequentially by membrane-bound β-secretase (BACE1) and γ-secretase. BACE1 cleaves APP to generate a soluble APPβ (sAPPβ) and a membrane-bound APP C99 fragment. The C99 fragment is further cleaved by the γ-secretase to produce amyloid β peptides (Aβ). (Figure was created using BioRender (www.biorender.com))

causing Ca^{2+} dysregulation have been associated with Aβ generation and the pathogenesis of AD [66, 89, 90].

The interactions between presenilins and RyRs have been linked to synaptic function and neurotransmitter release. In the hippocampal Schaeffer-collateral pathway, conditional double knockout (cDKO) of PS1 and PS2 in CA3 neurons (presynaptic) but not CA1 neurons (postsynaptic) has been shown to inhibit paired-pulse facilitation, short-term synaptic facilitation, and theta burst-induced long-term potentiation [84] (Fig. 6a–c). Quantification of the decline rate of NMDAR-mediated excitatory postsynaptic currents resulting from low-frequency stimulation in the presence of the N-methyl-D-aspartate (NMDA) receptor open channel blocker MK-801 indicates a reduced glutamate release probability in the cDKO mice [84] (Fig. 6d). The inhibitory effect of the cDKO on short-term synaptic facilitation in hippocampal neurons can be mimicked and occluded by either depletion of ER Ca^{2+} stores using thapsigargin, an irreversible inhibitor of SERCA, or inhibition of RyR-mediated ER Ca^{2+} release with 100 μM ryanodine [84]. Additionally, depolarization-induced increases in cytosolic [Ca^{2+}] in cultured hippocampal neurons are blunted by inhibiting RyRs with ryanodine (100 μM), but not IP_3Rs with xestospongin C [84]. Taken together, the findings of this study indicate that cDKO of PS1 and PS2 reduces RyR-mediated Ca^{2+} release from the ER, leading to the inhibition of neurotransmitter release.

Presenilins are involved in increasing the level of RyR protein expression, which may be a physiological function of presenilins. The mRNAs of all three RyR

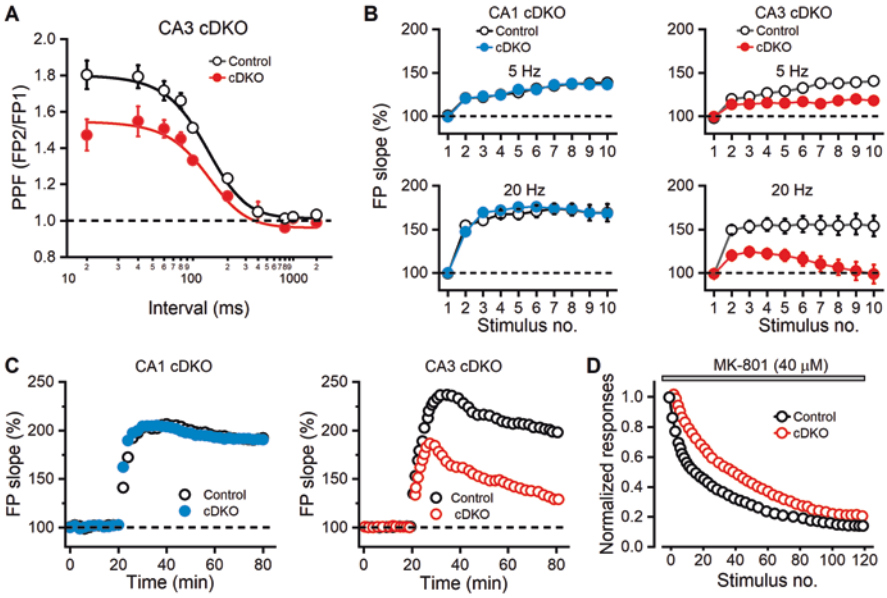

Fig. 6 Conditional double knockout (cDKO) of presynaptic presenilin-1 and presenilin-2 in mouse hippocampus impairs synaptic potentiation and reduces glutamate release. (**a**) Paired-pulse facilitation (PPF) is impaired in CA3 (presynaptic) cDKO mice compared with control mice. (**b**, **c**) Short- and long-synaptic potentiation is impaired in CA3 but not CA1 (postsynaptic) cDKO. (**d**) The decline rate of NMDAR-mediated excitatory postsynaptic currents evoked by low-frequency stimulation in the presence of MK-801 (NMDAR open channel blocker) is reduced in CA3 cDKO compared with the control. For simplicity, many data points in the original published figures are omitted in panels **c** and **d**. (Adapted from Ref. [84])

isoforms are expressed in the hippocampus, with RyR2 being the predominant isoform, and all three isoforms are expressed at similar levels in wild type and PS cDKO as indicated by quantitative RT-PCR [8]. However, western blots using a non-selective RyR antibody and a RyR2-specific antibody show that both total RyR proteins and specific RyR2 protein are reduced by more than 50% in the hippocampus of PS cDKO compared to wild type. In cultured hippocampal neurons of PS cDKO, Ca^{2+} release induced by caffeine is significantly reduced compared to wild type, and dantrolene, a specific RyR inhibitor, can inhibit caffeine-induced synaptic potentiation in hippocampal CA3 neurons of wild type but not PS cDKO [8]. These results suggest that presenilins play a regulatory role in increasing the level of RyR protein expression. However, it is still unknown whether the effect of presenilins on RyR protein level is due to increased translation or protein stability, and the mechanisms by which presenilins interact with other proteins to carry out this regulatory function are still not understood.

In addition to regulating RyR protein levels, presenilins may also play a role in regulating RyR function. Research has shown that the expression of an N-terminal fragment of PS1, but not PS2, in SH-SY5Y cells, a neuroblastoma cell line, can

inhibit RyR-mediated Ca^{2+} release. The effect of the N-terminal fragment depends on the presence of four cysteine residues [91].

In summary, emerging evidence suggests that AIP, calstabins, and presenilins may regulate RyR-mediated Ca^{2+} release from the ER, potentially impacting neurotransmitter release. However, there are still important questions to be answered. For instance, does AIP also regulate neurotransmitter release through RyRs in mammalian neurons? How does AIP regulate RRP size and synaptic vesicle number? Do deficiencies of presynaptic calstabins enhance neurotransmitter release? How do presenilins regulate RyR protein levels? Additionally, it is crucial to understand whether and how the functions of presynaptic AIP, calstabins, and presenilins are regulated by physiological conditions. Since RyR-mediated Ca^{2+} release plays a significant role in triggering synaptic vesicle exocytosis, answers to these questions could significantly advance our understanding of the regulatory mechanisms of neurotransmitter release.

Acknowledgment Supported by National Institute Health grants R01MH085927 and R01NS109388 to ZWW.

References

1. Furuichi T, Furutama D, Hakamata Y, Nakai J, Takeshima H, Mikoshiba K. Multiple types of ryanodine receptor/Ca^{2+} release channels are differentially expressed in rabbit brain. J Neurosci. 1994;14:4794–805. https://doi.org/10.1523/JNEUROSCI.14-08-04794.1994.
2. Hakamata Y, Nakai J, Takeshima H, Imoto K. Primary structure and distribution of a novel ryanodine receptor/calcium release channel from rabbit brain. FEBS Lett. 1992;312:229–35. https://doi.org/10.1016/0014-5793(92)80941-9.
3. Ottini L, Marziali G, Conti A, Charlesworth A, Sorrentino V. Alpha and beta isoforms of ryanodine receptor from chicken skeletal muscle are the homologues of mammalian RyR1 and RyR3. Biochem J. 1996;315(Pt 1):207–16. https://doi.org/10.1042/bj3150207.
4. Lai FA, Dent M, Wickenden C, Xu L, Kumari G, Misra M, et al. Expression of a cardiac Ca(2+)-release channel isoform in mammalian brain. Biochem J. 1992;288(Pt 2):553–64. https://doi.org/10.1042/bj2880553.
5. Nakanishi S, Kuwajima G, Mikoshiba K. Immunohistochemical localization of ryanodine receptors in mouse central nervous system. Neurosci Res. 1992;15:130–42. https://doi.org/10.1016/0168-0102(92)90026-9.
6. Sharp AH, McPherson PS, Dawson TM, Aoki C, Campbell KP, Snyder SH. Differential immunohistochemical localization of inositol 1,4,5-trisphosphate- and ryanodine-sensitive Ca2+ release channels in rat brain. J Neurosci. 1993;13:3051–63. https://doi.org/10.1523/JNEUROSCI.13-07-03051.1993.
7. Hiess F, Yao J, Song Z, Sun B, Zhang Z, Huang J, et al. Subcellular localization of hippocampal ryanodine receptor 2 and its role in neuronal excitability and memory. Commun Biol. 2022;5:183. https://doi.org/10.1038/s42003-022-03124-2.
8. Wu B, Yamaguchi H, Lai FA, Shen J. Presenilins regulate calcium homeostasis and presynaptic function via ryanodine receptors in hippocampal neurons. Proc Natl Acad Sci U S A. 2013;110:15091–6. https://doi.org/10.1073/pnas.1304171110.
9. Adasme T, Haeger P, Paula-Lima AC, Espinoza I, Casas-Alarcon MM, Carrasco MA, et al. Involvement of ryanodine receptors in neurotrophin-induced hippocampal synaptic plastic-

ity and spatial memory formation. Proc Natl Acad Sci U S A. 2011;108:3029–34. https://doi.org/10.1073/pnas.1013580108.
10. Lanner JT, Georgiou DK, Joshi AD, Hamilton SL. Ryanodine receptors: structure, expression, molecular details, and function in calcium release. Cold Spring Harb Perspect Biol. 2010;2:a003996. https://doi.org/10.1101/cshperspect.a003996.
11. Zalk R, Lehnart SE, Marks AR. Modulation of the ryanodine receptor and intracellular calcium. Annu Rev Biochem. 2007;76:367–85. https://doi.org/10.1146/annurev.biochem.76.053105.094237.
12. Del Prete D, Checler F, Chami M. Ryanodine receptors: physiological function and deregulation in Alzheimer disease. Mol Neurodegener. 2014;9:21. https://doi.org/10.1186/1750-1326-9-21.
13. Trivellin G, Korbonits M. AIP and its interacting partners. J Endocrinol. 2011;210:137–55. https://doi.org/10.1530/JOE-11-0054.
14. Fischer G, Aumuller T. Regulation of peptide bond cis/trans isomerization by enzyme catalysis and its implication in physiological processes. Rev Physiol Biochem Pharmacol. 2003;148:105–50. https://doi.org/10.1007/s10254-003-0011-3.
15. Das AK, Cohen PW, Barford D. The structure of the tetratricopeptide repeats of protein phosphatase 5: implications for TPR-mediated protein-protein interactions. EMBO J. 1998;17:1192–9. https://doi.org/10.1093/emboj/17.5.1192.
16. Perez-Riba A, Itzhaki LS. The tetratricopeptide-repeat motif is a versatile platform that enables diverse modes of molecular recognition. Curr Opin Struct Biol. 2019;54:43–9. https://doi.org/10.1016/j.sbi.2018.12.004.
17. Blatch GL, Lassle M. The tetratricopeptide repeat: a structural motif mediating protein-protein interactions. BioEssays. 1999;21:932–9. https://doi.org/10.1002/(SICI)1521-1878(199911)21:11<932::AID-BIES5>3.0.CO;2-N.
18. Morgan RM, Hernandez-Ramirez LC, Trivellin G, Zhou L, Roe SM, Korbonits M, et al. Structure of the TPR domain of AIP: lack of client protein interaction with the C-terminal alpha-7 helix of the TPR domain of AIP is sufficient for pituitary adenoma predisposition. PLoS One. 2012;7:e53339. https://doi.org/10.1371/journal.pone.0053339.
19. Yadav RP, Boyd K, Yu L, Artemyev NO. Interaction of the tetratricopeptide repeat domain of aryl hydrocarbon receptor-interacting protein-like 1 with the regulatory Pgamma subunit of phosphodiesterase 6. J Biol Chem. 2019;294:15795–807. https://doi.org/10.1074/jbc.RA119.010666.
20. Hartl FU, Bracher A, Hayer-Hartl M. Molecular chaperones in protein folding and proteostasis. Nature. 2011;475:324–32. https://doi.org/10.1038/nature10317.
21. Scheufler C, Brinker A, Bourenkov G, Pegoraro S, Moroder L, Bartunik H, et al. Structure of TPR domain-peptide complexes: critical elements in the assembly of the Hsp70-Hsp90 multichaperone machine. Cell. 2000;101:199–210. https://doi.org/10.1016/S0092-8674(00)80830-2.
22. Juricek L, Coumoul X. The aryl hydrocarbon receptor and the nervous system. Int J Mol Sci. 2018;19:2504. https://doi.org/10.3390/ijms19092504.
23. Rothhammer V, Quintana FJ. The aryl hydrocarbon receptor: an environmental sensor integrating immune responses in health and disease. Nat Rev Immunol. 2019;19:184–97. https://doi.org/10.1038/s41577-019-0125-8.
24. Barouki R, Aggerbeck M, Aggerbeck L, Coumoul X. The aryl hydrocarbon receptor system. Drug Metabol Drug Interact. 2012;27:3–8. https://doi.org/10.1515/dmdi-2011-0035.
25. Beckers A, Aaltonen LA, Daly AF, Karhu A. Familial isolated pituitary adenomas (FIPA) and the pituitary adenoma predisposition due to mutations in the aryl hydrocarbon receptor interacting protein (AIP) gene. Endocr Rev. 2013;34:239–77. https://doi.org/10.1210/er.2012-1013.
26. Vierimaa O, Georgitsi M, Lehtonen R, Vahteristo P, Kokko A, Raitila A, et al. Pituitary adenoma predisposition caused by germline mutations in the AIP gene. Science. 2006;312:1228–30. https://doi.org/10.1126/science.1126100.
27. Georgitsi M, De Menis E, Cannavo S, Makinen MJ, Tuppurainen K, Pauletto P, et al. Aryl hydrocarbon receptor interacting protein (AIP) gene mutation analysis in children and ado-

lescents with sporadic pituitary adenomas. Clin Endocrinol. 2008;69:621–7. https://doi.org/10.1111/j.1365-2265.2008.03266.x.
28. Raitila A, Lehtonen HJ, Arola J, Heliovaara E, Ahlsten M, Georgitsi M, et al. Mice with inactivation of aryl hydrocarbon receptor-interacting protein (Aip) display complete penetrance of pituitary adenomas with aberrant ARNT expression. Am J Pathol. 2010;177:1969–76. https://doi.org/10.2353/ajpath.2010.100138.
29. Robitaille R, Garcia ML, Kaczorowski GJ, Charlton MP. Functional colocalization of calcium and calcium-gated potassium channels in control of transmitter release. Neuron. 1993;11:645–55. https://doi.org/10.1016/0896-6273(93)90076-4.
30. Hu H, Shao LR, Chavoshy S, Gu N, Trieb M, Behrens R, et al. Presynaptic Ca^{2+}-activated K^+ channels in glutamatergic hippocampal terminals and their role in spike repolarization and regulation of transmitter release. J Neurosci. 2001;21:9585–97. https://doi.org/10.1523/JNEUROSCI.21-24-09585.2001.
31. Raffaelli G, Saviane C, Mohajerani MH, Pedarzani P, Cherubini E. BK potassium channels control transmitter release at CA3-CA3 synapses in the rat hippocampus. J Physiol. 2004;557:147–57. https://doi.org/10.1113/jphysiol.2004.062661.
32. Wang ZW, Saifee O, Nonet ML, Salkoff L. SLO-1 potassium channels control quantal content of neurotransmitter release at the *C. elegans* neuromuscular junction. Neuron. 2001;32:867–81. https://doi.org/10.1016/s0896-6273(01)00522-0.
33. Liu Q, Chen B, Ge Q, Wang ZW. Presynaptic Ca^{2+}/calmodulin-dependent protein kinase II modulates neurotransmitter release by activating BK channels at *Caenorhabditis elegans* neuromuscular junction. J Neurosci. 2007;27:10404–13. https://doi.org/10.1523/JNEUROSCI.5634-06.2007.
34. Chen B, Ge Q, Xia XM, Liu P, Wang SJ, Zhan H, et al. A novel auxiliary subunit critical to BK channel function in *Caenorhabditis elegans*. J Neurosci. 2010;30:16651–61. https://doi.org/10.1523/JNEUROSCI.3211-10.2010.
35. Chen B, Liu P, Zhan H, Wang ZW. Dystrobrevin controls neurotransmitter release and muscle Ca(2+) transients by localizing BK channels in Caenorhabditis elegans. J Neurosci. 2011;31:17338–47. https://doi.org/10.1523/JNEUROSCI.3638-11.2011.
36. Niu L, Li Y, Zong P, Liu P, Shui Y, Chen B, et al. Melatonin promotes sleep by activating the BK channel in *C. elegans*. Proc Natl Acad Sci U S A. 2020;117:25128–37. https://doi.org/10.1073/pnas.2010928117.
37. Abraham LS, Oh HJ, Sancar F, Richmond JE, Kim H. An alpha-catulin homologue controls neuromuscular function through localization of the dystrophin complex and BK channels in *Caenorhabditis elegans*. PLoS Genet. 2010;6:e1001077. https://doi.org/10.1371/journal.pgen.1001077.
38. Cheung TP, Choe JY, Richmond JE, Kim H. BK channel density is regulated by endoplasmic reticulum associated degradation and influenced by the SKN-1A/NRF1 transcription factor. PLoS Genet. 2020;16:e1008829. https://doi.org/10.1371/journal.pgen.1008829.
39. Oh KH, Haney JJ, Wang X, Chuang CF, Richmond JE, Kim H. ERG-28 controls BK channel trafficking in the ER to regulate synaptic function and alcohol response in C. elegans. elife. 2017;6:e24733. https://doi.org/10.7554/eLife.24733.
40. Chen B, Liu P, Hujber EJ, Li Y, Jorgensen EM, Wang ZW. AIP limits neurotransmitter release by inhibiting calcium bursts from the ryanodine receptor. Nat Commun. 2017;8:1380. https://doi.org/10.1038/s41467-017-01704-z.
41. Gracheva EO, Burdina AO, Holgado AM, Berthelot-Grosjean M, Ackley BD, Hadwiger G, et al. Tomosyn inhibits synaptic vesicle priming in Caenorhabditis elegans. PLoS Biol. 2006;4:e261. https://doi.org/10.1371/journal.pbio.0040261.
42. McEwen JM, Madison JM, Dybbs M, Kaplan JM. Antagonistic regulation of synaptic vesicle priming by Tomosyn and UNC-13. Neuron. 2006;51:303–15. https://doi.org/10.1016/j.neuron.2006.06.025.
43. Hobson RJ, Liu Q, Watanabe S, Jorgensen EM. Complexin maintains vesicles in the primed state in C. elegans. Curr Biol. 2011;21:106–13. https://doi.org/10.1016/j.cub.2010.12.015.

44. Martin JA, Hu Z, Fenz KM, Fernandez J, Dittman JS. Complexin has opposite effects on two modes of synaptic vesicle fusion. Curr Biol. 2011;21:97–105. https://doi.org/10.1016/j.cub.2010.12.014.
45. Wehrens XH, Lehnart SE, Huang F, Vest JA, Reiken SR, Mohler PJ, et al. FKBP12.6 deficiency and defective calcium release channel (ryanodine receptor) function linked to exercise-induced sudden cardiac death. Cell. 2003;113:829–40. https://doi.org/10.1016/s0092-8674(03)00434-3.
46. Liu X, Betzenhauser MJ, Reiken S, Meli AC, Xie W, Chen BX, et al. Role of leaky neuronal ryanodine receptors in stress-induced cognitive dysfunction. Cell. 2012;150:1055–67. https://doi.org/10.1016/j.cell.2012.06.052.
47. Shou W, Aghdasi B, Armstrong DL, Guo Q, Bao S, Charng MJ, et al. Cardiac defects and altered ryanodine receptor function in mice lacking FKBP12. Nature. 1998;391:489–92. https://doi.org/10.1038/35146.
48. Marx SO, Reiken S, Hisamatsu Y, Jayaraman T, Burkhoff D, Rosemblit N, et al. PKA phosphorylation dissociates FKBP12.6 from the calcium release channel (ryanodine receptor): defective regulation in failing hearts. Cell. 2000;101:365–76. https://doi.org/10.1016/s0092-8674(00)80847-8.
49. Liu Q, Chen B, Yankova M, Morest DK, Maryon E, Hand AR, et al. Presynaptic ryanodine receptors are required for normal quantal size at the *Caenorhabditis elegans* neuromuscular junction. J Neurosci. 2005;25:6745–54. https://doi.org/10.1523/JNEUROSCI.1730-05.2005.
50. Sakube Y, Ando H, Kagawa H. An abnormal ketamine response in mutants defective in the ryanodine receptor gene *ryr-1 (unc-68)* of *Caenorhabditis elegans*. J Mol Biol. 1997;267:849–64. https://doi.org/10.1006/jmbi.1997.0910.
51. Rosenmund C, Stevens CF. Definition of the readily releasable pool of vesicles at hippocampal synapses. Neuron. 1996;16:1197–207. https://doi.org/10.1016/s0896-6273(00)80146-4.
52. Augustin I, Rosenmund C, Sudhof TC, Brose N. Munc13-1 is essential for fusion competence of glutamatergic synaptic vesicles. Nature. 1999;400:457–61. https://doi.org/10.1038/22768.
53. Richmond JE, Davis WS, Jorgensen EM. UNC-13 is required for synaptic vesicle fusion in *C. elegans*. Nat Neurosci. 1999;2:959–64. https://doi.org/10.1038/14755.
54. Genest O, Wickner S, Doyle SM. Hsp90 and Hsp70 chaperones: collaborators in protein remodeling. J Biol Chem. 2019;294:2109–20. https://doi.org/10.1074/jbc.REV118.002806.
55. Rosenzweig R, Nillegoda NB, Mayer MP, Bukau B. The Hsp70 chaperone network. Nat Rev Mol Cell Biol. 2019;20:665–80. https://doi.org/10.1038/s41580-019-0133-3.
56. Taipale M, Jarosz DF, Lindquist S. HSP90 at the hub of protein homeostasis: emerging mechanistic insights. Nat Rev Mol Cell Biol. 2010;11:515–28. https://doi.org/10.1038/nrm2918.
57. Mulero-Navarro S, Fernandez-Salguero PM. New trends in aryl hydrocarbon receptor biology. Front Cell Dev Biol. 2016;4:45. https://doi.org/10.3389/fcell.2016.00045.
58. Lin BC, Sullivan R, Lee Y, Moran S, Glover E, Bradfield CA. Deletion of the aryl hydrocarbon receptor-associated protein 9 leads to cardiac malformation and embryonic lethality. J Biol Chem. 2007;282:35924–32. https://doi.org/10.1074/jbc.M705471200.
59. Chelu MG, Danila CI, Gilman CP, Hamilton SL. Regulation of ryanodine receptors by FK506 binding proteins. Trends Cardiovasc Med. 2004;14:227–34. https://doi.org/10.1016/j.tcm.2004.06.003.
60. Kang CB, Hong Y, Dhe-Paganon S, Yoon HS. FKBP family proteins: immunophilins with versatile biological functions. Neurosignals. 2008;16:318–25. https://doi.org/10.1159/000123041.
61. Lehnart SE, Mongillo M, Bellinger A, Lindegger N, Chen BX, Hsueh W, et al. Leaky Ca2+ release channel/ryanodine receptor 2 causes seizures and sudden cardiac death in mice. J Clin Invest. 2008;118:2230–45. https://doi.org/10.1172/JCI35346.
62. Lehnart SE, Wehrens XH, Marks AR. Calstabin deficiency, ryanodine receptors, and sudden cardiac death. Biochem Biophys Res Commun. 2004;322:1267–79. https://doi.org/10.1016/j.bbrc.2004.08.032.

63. Kaftan E, Marks AR, Ehrlich BE. Effects of rapamycin on ryanodine receptor/Ca(2+)-release channels from cardiac muscle. Circ Res. 1996;78:990–7. https://doi.org/10.1161/01.res.78.6.990.
64. Jayaraman T, Brillantes AM, Timerman AP, Fleischer S, Erdjument-Bromage H, Tempst P, et al. FK506 binding protein associated with the calcium release channel (ryanodine receptor). J Biol Chem. 1992;267:9474–7.
65. Yuan Q, Deng KY, Sun L, Chi S, Yang Z, Wang J, et al. Calstabin 2: an important regulator for learning and memory in mice. Sci Rep. 2016;6:21087. https://doi.org/10.1038/srep21087.
66. Ho A, Shen J. Presenilins in synaptic function and disease. Trends Mol Med. 2011;17:617–24. https://doi.org/10.1016/j.molmed.2011.06.002.
67. Hardy J, Selkoe DJ. The amyloid hypothesis of Alzheimer's disease: progress and problems on the road to therapeutics. Science. 2002;297:353–6. https://doi.org/10.1126/science.1072994.
68. Vassar R, Bennett BD, Babu-Khan S, Kahn S, Mendiaz EA, Denis P, et al. Beta-secretase cleavage of Alzheimer's amyloid precursor protein by the transmembrane aspartic protease BACE. Science. 1999;286:735–41. https://doi.org/10.1126/science.286.5440.735.
69. Guner G, Lichtenthaler SF. The substrate repertoire of gamma-secretase/presenilin. Semin Cell Dev Biol. 2020;105:27–42. https://doi.org/10.1016/j.semcdb.2020.05.019.
70. Meckler X, Checler F. Presenilin 1 and presenilin 2 target gamma-secretase complexes to distinct cellular compartments. J Biol Chem. 2016;291:12821–37. https://doi.org/10.1074/jbc.M115.708297.
71. Zhou R, Yang G, Guo X, Zhou Q, Lei J, Shi Y. Recognition of the amyloid precursor protein by human gamma-secretase. Science. 2019;363:eaaw0930. https://doi.org/10.1126/science.aaw0930.
72. Borchelt DR, Thinakaran G, Eckman CB, Lee MK, Davenport F, Ratovitsky T, et al. Familial Alzheimer's disease-linked presenilin 1 variants elevate Abeta1-42/1-40 ratio in vitro and in vivo. Neuron. 1996;17:1005–13. https://doi.org/10.1016/s0896-6273(00)80230-5.
73. Duff K, Eckman C, Zehr C, Yu X, Prada CM, Perez-tur J, et al. Increased amyloid-beta42(43) in brains of mice expressing mutant presenilin 1. Nature. 1996;383:710–3. https://doi.org/10.1038/383710a0.
74. Scheuner D, Eckman C, Jensen M, Song X, Citron M, Suzuki N, et al. Secreted amyloid beta-protein similar to that in the senile plaques of Alzheimer's disease is increased in vivo by the presenilin 1 and 2 and APP mutations linked to familial Alzheimer's disease. Nat Med. 1996;2:864–70. https://doi.org/10.1038/nm0896-864.
75. Kim J, Onstead L, Randle S, Price R, Smithson L, Zwizinski C, et al. Abeta40 inhibits amyloid deposition in vivo. J Neurosci. 2007;27:627–33. https://doi.org/10.1523/JNEUROSCI.4849-06.2007.
76. Sun L, Zhou R, Yang G, Shi Y. Analysis of 138 pathogenic mutations in presenilin-1 on the in vitro production of Abeta42 and Abeta40 peptides by gamma-secretase. Proc Natl Acad Sci U S A. 2017;114:E476–E85. https://doi.org/10.1073/pnas.1618657114.
77. Tu H, Nelson O, Bezprozvanny A, Wang Z, Lee SF, Hao YH, et al. Presenilins form ER Ca2+ leak channels, a function disrupted by familial Alzheimer's disease-linked mutations. Cell. 2006;126:981–93. https://doi.org/10.1016/j.cell.2006.06.059.
78. Zhang H, Sun S, Herreman A, De Strooper B, Bezprozvanny I. Role of presenilins in neuronal calcium homeostasis. J Neurosci. 2010;30:8566–80. https://doi.org/10.1523/JNEUROSCI.1554-10.2010.
79. Green KN, Demuro A, Akbari Y, Hitt BD, Smith IF, Parker I, et al. SERCA pump activity is physiologically regulated by presenilin and regulates amyloid beta production. J Cell Biol. 2008;181:1107–16. https://doi.org/10.1083/jcb.200706171.
80. Cook DG, Li X, Cherry SD, Cantrell AR. Presenilin 1 deficiency alters the activity of voltage-gated Ca2+ channels in cultured cortical neurons. J Neurophysiol. 2005;94:4421–9. https://doi.org/10.1152/jn.00745.2005.

81. Leissring MA, Akbari Y, Fanger CM, Cahalan MD, Mattson MP, LaFerla FM. Capacitative calcium entry deficits and elevated luminal calcium content in mutant presenilin-1 knockin mice. J Cell Biol. 2000;149:793–8. https://doi.org/10.1083/jcb.149.4.793.
82. Yoo AS, Cheng I, Chung S, Grenfell TZ, Lee H, Pack-Chung E, et al. Presenilin-mediated modulation of capacitative calcium entry. Neuron. 2000;27:561–72. https://doi.org/10.1016/s0896-6273(00)00066-0.
83. Chan SL, Mayne M, Holden CP, Geiger JD, Mattson MP. Presenilin-1 mutations increase levels of ryanodine receptors and calcium release in PC12 cells and cortical neurons. J Biol Chem. 2000;275:18195–200. https://doi.org/10.1074/jbc.M000040200.
84. Zhang C, Wu B, Beglopoulos V, Wines-Samuelson M, Zhang D, Dragatsis I, et al. Presenilins are essential for regulating neurotransmitter release. Nature. 2009;460:632–6. https://doi.org/10.1038/nature08177.
85. Cheung KH, Shineman D, Muller M, Cardenas C, Mei L, Yang J, et al. Mechanism of Ca2+ disruption in Alzheimer's disease by presenilin regulation of InsP3 receptor channel gating. Neuron. 2008;58:871–83. https://doi.org/10.1016/j.neuron.2008.04.015.
86. Stutzmann GE, Smith I, Caccamo A, Oddo S, Laferla FM, Parker I. Enhanced ryanodine receptor recruitment contributes to Ca2+ disruptions in young, adult, and aged Alzheimer's disease mice. J Neurosci. 2006;26:5180–9. https://doi.org/10.1523/JNEUROSCI.0739-06.2006.
87. Cheung KH, Mei L, Mak DO, Hayashi I, Iwatsubo T, Kang DE, et al. Gain-of-function enhancement of IP3 receptor modal gating by familial Alzheimer's disease-linked presenilin mutants in human cells and mouse neurons. Sci Signal. 2010;3:ra22. https://doi.org/10.1126/scisignal.2000818.
88. Stutzmann GE, Caccamo A, LaFerla FM, Parker I. Dysregulated IP3 signaling in cortical neurons of knock-in mice expressing an Alzheimer's-linked mutation in presenilin1 results in exaggerated Ca2+ signals and altered membrane excitability. J Neurosci. 2004;24:508–13. https://doi.org/10.1523/JNEUROSCI.4386-03.2004.
89. Green KN, LaFerla FM. Linking calcium to Abeta and Alzheimer's disease. Neuron. 2008;59:190–4. https://doi.org/10.1016/j.neuron.2008.07.013.
90. Honarnejad K, Herms J. Presenilins: role in calcium homeostasis. Int J Biochem Cell Biol. 2012;44:1983–6. https://doi.org/10.1016/j.biocel.2012.07.019.
91. Payne AJ, Gerdes BC, Naumchuk Y, McCalley AE, Kaja S, Koulen P. Presenilins regulate the cellular activity of ryanodine receptors differentially through isotype-specific N-terminal cysteines. Exp Neurol. 2013;250:143–50. https://doi.org/10.1016/j.expneurol.2013.09.001.

Regulation of Neurotransmitter Release by K^+ Channels

Zhao-Wen Wang, Laurence O. Trussell, and Kiranmayi Vedantham

Abstract K^+ channels play potent roles in the process of neurotransmitter release by influencing the action potential waveform and modulating neuronal excitability and release probability. These diverse effects of K^+ channel activation are ensured by the wide variety of K^+ channel genes and their differential expression in different cell types. Accordingly, a variety of K^+ channels have been implicated in regulating neurotransmitter release, including the Ca^{2+}- and voltage-gated K^+ channel Slo1 (also known as BK channel), voltage-gated K^+ channels of the Kv3 (Shaw-type), Kv1 (Shaker-type), and Kv7 (KCNQ) families, G-protein-gated inwardly rectifying K^+ (GIRK) channels, and SLO-2 (a Ca^{2+}-. Cl^-, and voltage-gated K^+ channel in *C. elegans*). These channels vary in their expression patterns, subcellular localization, and biophysical properties. Their roles in neurotransmitter release may also vary depending on the synapse and physiological or experimental conditions. This chapter summarizes key findings about the roles of K^+ channels in regulating neurotransmitter release.

Keywords Neurotransmitter release · Slo1 · SLO-1 · BK channel · Kv3 · Kv1 · Kv7 · KCNQ · GIRK · SLO-2 · G-protein-gated inwardly rectifying K^+ channel

Z.-W. Wang (✉) · K. Vedantham
Department of Neuroscience, University of Connecticut School of Medicine, Farmington, CT, USA
e-mail: zwwang@uchc.edu

L. O. Trussell
Oregon Hearing Research Center & Vollum Institute, Oregon Health and Science University, Portland, OR, USA

Z.-W. Wang (ed.), *Molecular Mechanisms of Neurotransmitter Release*, Advances in Neurobiology 33, https://doi.org/10.1007/978-3-031-34229-5_12

Abbreviations

4-AP	4-Aminopyridine
AP	Action potential
BDS-I	Blood-depressing substance-I
EPSC	Excitatory postsynaptic current
EPSP	Excitatory postsynaptic potential
IPSC	Inhibitory postsynaptic current
NMJ	Neuromuscular junction
PPR	Paired-pulse ratio
TEA	Tetraethylammonium
VGCC	Voltage-gated Ca^{2+} channel

1 Introduction

Ca^{2+} entry into presynaptic nerve terminals via voltage-gated Ca^{2+} channels is required for exocytosis of neurotransmitter [1–4]. Because both Ca^{2+}-channel gating and Ca^{2+} influx are voltage-dependent, the size and shape of presynaptic action potentials (APs) can control the level of transmitter release. In this chapter, we show that K^+ channels play a key role in this process in multiple ways. For example, K^+ current provides the repolarizing drive that sets the duration of the AP in nerve terminals. Thus, when K^+ channel activation is delayed or diminished, APs are broadened, and Ca^{2+} entry is thereby extended [5–8]. However, beyond spike shape, K^+ channels contribute to the resting potential, and changes in resting potential can impact the probability of transmitter release [9, 10]. These effects depend on the biophysical properties of K^+ channels, such as their sensitivity to membrane potential or to intracellular ligands that activate the channel, properties that vary widely depending on channel subunits. The human and mouse genomes contain approximately 80 genes each for the pore-forming subunits of K^+ channels, and the K^+ channels formed by the diverse subunits differ in structural and functional properties [11–15]. Moreover, the subtypes of K^+ channels that regulate neurotransmitter release can vary from neuron to neuron, from synapse to synapse, or vary in subcellular location. Valuable mechanistic insight into the dynamics of neural processing can come from an understanding of how these channels are activated during transmitter release and how they are regulated in health and disease.

A variety of electrophysiological, optical, genetic, and immunohistological/ultrastructural methods are required to reveal the role of K^+ channels in synaptic transmission. Electrophysiological or optical measurement of transmitter release in animals with genetic knockout or mutation of specific K^+ channels is a powerful approach, as is the assessment of release before and after pharmacological block of specific K^+ channels. It should be appreciated that while these approaches can reveal the importance of a given K^+ channel subtype, they do not speak to the location of

such channels. "Presynaptic" as an anatomical term may refer to a location within a nerve terminal or *en passant* bouton. However, because the voltage changes that drive release arise both in the presynaptic structure and in the adjoining axonal membrane, "presynaptic K^+ channels" could from the standpoint of function also refer to axonal ion channels. Besides the spatial distribution of channels, the time dependence of K^+ channel activation and inactivation and its interaction with short-term plasticity of exocytosis (which is also time-dependent) have important implications for experimental design and interpretation. Such plasticity is often assayed by using two sequential presynaptic stimuli, measuring the change in the amplitude of the second response relative to the first. This paired-pulse ratio (PPR) changes inversely with release probability, and thus AP broadening following K^+ channel inhibition would be expected to elevate presynaptic Ca^{2+} and decrease PPR. Interestingly, as PPR depends on the inter-spike interval, regulation of K^+ channels that determine AP frequency during endogenous activity in neurons may affect the degree of short-term plasticity. Thus, even non-presynaptic K^+ channels can impact the strength of synaptic transmission! This chapter, however, will focus mainly on the diversity of K^+ channels that are found at or near nerve terminals and how their particular properties are important determinants of synaptic function.

2 Slo1 (BK Channel)

Slo1, also known as the BK channel, is a member of the Slo family of K^+ channels, which consists of four members in mammals: Slo1, Slo2.1 (Slick), Slo2.2 (Slack), and Slo3. Slo1 was the first member of this family discovered, and was initially named Slo because it is encoded by the *Drosophila* slowpoke locus [16–18]. The name Slo1 was later adopted following the identification of other Slo-like channels. All members of the Slo family share a similar structure, consisting of an amino terminal region with membrane-spanning domains and the channel pore domain, and a large carboxyl terminal region that forms a gating ring [19–24]. Each channel is a tetramer made up of four Slo subunits. The various Slo channels share the functional property of having large single-channel conductance (60–270 pS) and being gated by both membrane voltage and specific cytosolic ions (Ca^{2+} for Slo1, Na^+ and Cl^- for Slo2, and pH/H^+ for Slo3) [19].

The central components of a Slo1 channel consist of four α-subunits, each of which is comprised of the core and tail domains. The core consists of seven transmembrane segments with a pore domain, while the tail has two RCK (regulator of conductance of K^+) domains (Fig. 1a). Slo1 is activated by both membrane depolarization and Ca^{2+} binding on the cytosolic side (Fig. 1b, c), with the core and tail domains conferring voltage and Ca^{2+} sensitivity, respectively [22, 23, 25, 26]. Auxiliary subunits, such as β-subunits, γ-subunits, and BKIP-1, can also associate with Slo1 and modulate its properties, including Ca^{2+} sensitivity [27–29], activation and inactivation rates [29–32], and surface expression [29] (reviews [33, 34]). Cryogenic electron microscopy has been used to resolve the 3-D structures of

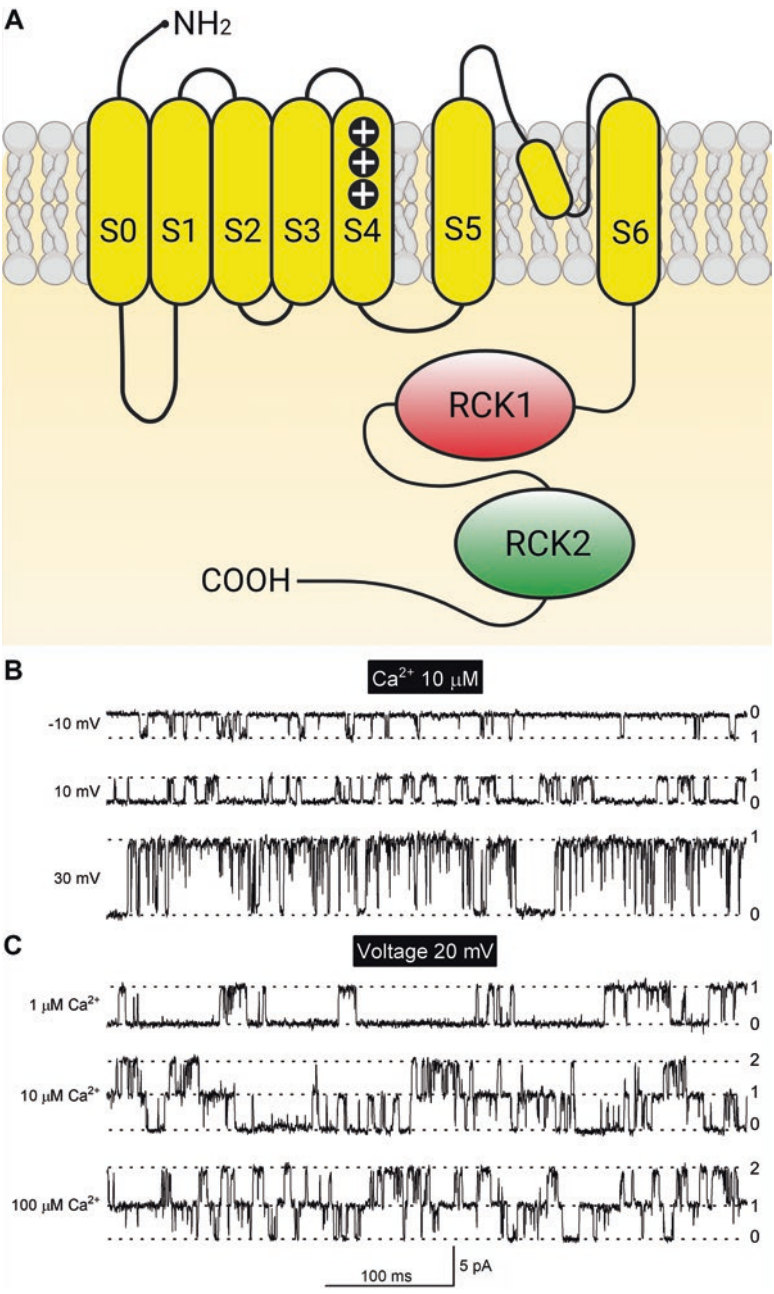

Fig. 1 Slo1 is activated by membrane depolarization and cytosolic Ca^{2+}. (**a**) Schematic diagram of a Slo1 α-subunit. (Created with BioRender.com). (**b**) Single-channel activities of an inside-out patch containing one Slo1 channel at three different membrane voltages in the presence of a constant Ca^{2+} concentration. (**c**) Single-channel activities of an inside-out patch containing two Slo1 channels at three different Ca^{2+} concentrations and a constant holding voltage. The inside-out patches were obtained from *Xenopus* oocytes that expressed mouse Slo1, and recorded in the presence of symmetric $[K^+]$. The Arabic numerals mark the closed (0) and open (1 or 2 channels) states

Aplysia californica Slo1 [23, 35] and human Slo1 [24, 36], providing insights into important biophysical properties of the channel, such as its dependence on Ca^{2+} and membrane voltage, large single-channel conductance, and the interference of scorpion toxin binding to the channel by β-subunits.

Slo1 is widely expressed in the brain and is particularly enriched at the presynaptic terminals of neurons [37]. Electrophysiological analyses have identified Slo1 currents at motor nerve terminals of mice [38], frogs [39–41], lizards [42, 43], and crayfish [44], at cochlear efferent nerve terminals of gerbils [45], at the calyx of Held presynaptic terminals of rats [46] and mice [47], at glutamatergic terminals in rat hippocampi [7, 48], at calyceal nerve terminals in chick ciliary ganglia [49], and in a rat synaptosomal preparation [50].

The use of double-label immunogold electron microscopy and double-label immunocytochemistry and immunohistochemistry techniques has provided further insights into the localization of Slo1 at presynaptic sites in various species. For instance, the use of antibodies against Slo1 and NMDA receptors showed that Slo1 is localized to the presynaptic membrane facing postsynaptic NMDA receptors in the rat hippocampus [48]. Antibodies against Slo1 and a presynaptic marker (synapsin I or vGlut1/vesicular glutamate transporter 1) revealed that Slo1 is localized at presynaptic sites in cultured mouse and rat hippocampal pyramidal neurons [51, 52] and at mouse calyx of Held presynaptic terminals [47].

At the frog neuromuscular junction (NMJ), biotin-conjugated charybdotoxin (a Slo1 blocker) labeling showed a banding pattern of Slo1 distribution that mirrored the distribution pattern of α-bungarotoxin-labeled postsynaptic acetylcholine receptors, and disappearance of the Slo1 banding pattern after denervation [53]. Immunohistochemistry at the *Drosophila* NMJ showed that Slo1 colocalizes with 14–3-3, a protein highly enriched in synaptic boutons [54]. At the *C. elegans* NMJ, GFP-tagged SLO-1 colocalizes with fRFP-tagged ELKS-1 and mCherry-tagged RAB-3, which are active zone and synaptic vesicle markers, respectively [55, 56]. Taken together, these findings provide compelling evidence of Slo1's presynaptic localization.

Slo1 is known to colocalize and associate with voltage-gated Ca^{2+} channels (VGCCs) in neurons. At the frog NMJ, Slo1 (labeled by charybdotoxin-biotin) was observed in the area of the nerve terminal that faces clusters of postsynaptic acetylcholine receptors (labeled by α-bungarotoxin-BODIPY), suggesting its colocalization with VGCCs at the active zone [53]. At the *C. elegans* NMJ, mStrawberry-tagged SLO-1 colocalized with GFP-tagged UNC-2 [57], a presynaptic Ca_V2 channel that plays a crucial role in neurotransmitter release [58, 59]. In nerve-muscle preparations of frogs and rats, the activity of presynaptic Slo1 was dependent on VGCCs [60, 61], suggesting their close apposition. In plasma membrane-enriched protein fractions prepared from rat brains, Slo1 was found with $Ca_V1.2$ (L-type), $Ca_V2.1$ (P/Q-type), and $Ca_V2.2$ (N-type) in macromolecular complexes, with $Ca_V2.1$ being the most abundant [62]. In frog saccular hair cells, Slo1 currents were detected at fluorescence hotspots of fluo3 (an intracellular Ca^{2+} indicator) during depolarization [63]. Electrophysiological recordings and ensemble-variance analyses of current fluctuations suggested that on average, each hair cell has about 20 clusters of

VGCCs and Ca^{2+}-activated K^+ channels, with each cluster containing approximately 90 VGCCs and 40 Ca^{2+}-activated K^+ channels [64]. The colocalization and association of Slo1 with VGCCs enables its activation by Ca^{2+} microdomains or nanodomains resulting from Ca^{2+} entry via neighboring VGCCs. Slo1 activity has been used to assess Ca^{2+} concentration at presynaptic terminals during AP activity [60, 64, 65].

Slo1's voltage- and Ca^{2+}-sensitivity, coupled with its proximity to presynaptic VGCCs, makes it an excellent candidate for limiting the magnitude and duration of neurotransmitter release, and this role is strongly supported by experimental evidence. For example, inhibition of Slo1 using iberiotoxin or charybdotoxin at the frog NMJ resulted in increased amplitudes of muscle end-plate potentials, which are equivalent to excitatory postsynaptic potentials (EPSPs) in neurons [53]. Similarly, in organotypic rat hippocampal slice culture, iberiotoxin enhanced the amplitude of the first excitatory postsynaptic current (EPSC) while reducing the PPR of EPSCs at synapses between CA3 pyramidal neurons [66]. At the *C. elegans* NMJ, loss-of-function mutations of *slo-1* led to an increase in evoked postsynaptic current amplitude and mini frequency when compared to wild-type, while gain-of-function mutations of *slo-1* had the opposite effect [29, 57, 67–70] (Fig. 2a, b). Furthermore, the amplitude of exogenous neurotransmitter-induced muscle whole-cell current and the mean amplitude of minis were unaffected by *slo-1* mutations (Fig. 2a, c), suggesting that the sensitivity of postsynaptic membrane to neurotransmitter remain unchanged in *slo-1* mutants [57, 70]. Interestingly, although the *C. elegans* genome harbors at least 80 K^+ channel genes [71, 72], *slo-1* was the only K^+ channel gene with mutants obtained in an unbiased genetic screen aimed at identifying inhibitory regulators of neurotransmitter release [67]. This observation implies that SLO-1 is a particularly important, if not unique, inhibitory regulator of neurotransmitter release in *C. elegans*.

In layer 5 pyramidal neurons, a single spike-evoked rise in Ca^{2+} resulted in the shortening of the duration of a second subsequent spike. When Slo1 is blocked with iberiotoxin, the second spike was widened to a larger degree than the first, and the amplitude of the EPSP evoked by the second spike was increased [73]. These findings suggest that during repetitive firing, Ca^{2+}-dependent activation of Slo1 by preceding spikes can fine-tune neurotransmitter release by limiting excessive spike broadening.

However, at other synapses, the exact role of Slo1 in regulating neurotransmitter release is not clear. For instance, in acute brain slices of rats, iberiotoxin increased the amplitude of the first EPSC and decreased the PPR of EPSCs at synapses between Schafer collaterals and CA1 pyramidal neurons only in the presence of 4-aminopyridine, which blocks various voltage-gated K^+ channels but not Slo1 [48]. This finding suggested that Slo1 may not have a significant role in regulating neurotransmitter release in these synapses [48]. Moreover, in acute hippocampal slices of rats, under basal conditions, Slo1 at mossy fiber synaptic boutons did not activate in response to presynaptic APs, and only after blockade of Kv3 channels did the blockade of Slo1 prolong the duration of mossy fiber bouton APs [7]. Additionally, at the calyx of Held presynaptic terminal in rats, depolarization voltage steps may

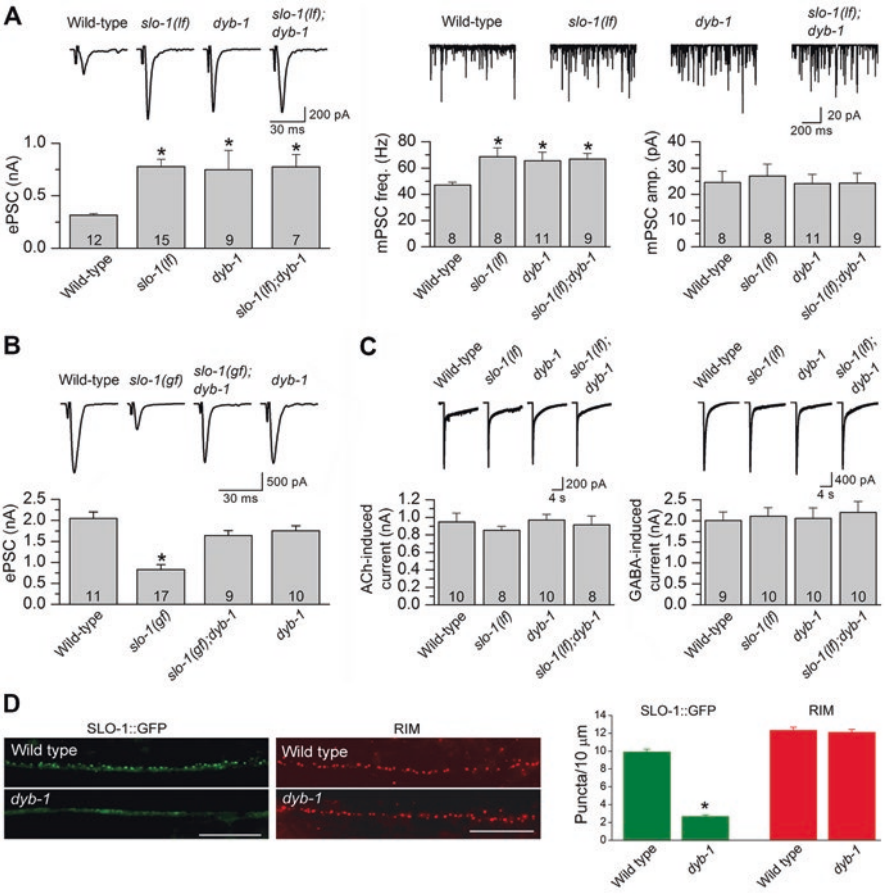

Fig. 2 Inhibitory effects of SLO-1 on neurotransmitter release the *C. elegans* neuromuscular junction depend on presynaptic localization by dystrobrevin (DYB-1). (**a**) Loss-of-function (*lf*) mutations of *slo-1* and *dyb-1* augment the amplitude of evoked postsynaptic current (EPSC) and the frequency of miniature postsynaptic current (mPSC), and the mutant effects are non-additive in *slo-1(lf);dyb-1(lf)* double mutant. $[Ca^{2+}]_o$ was 0.5 mM. (**b**) The amplitude of EPSC is greatly decreased in a strain expressing SLO-1(E350Q), a gain-of-function (*gf*) isoform, in neurons and muscle cells, and this phenotype is suppressed by *dyb-1(lf)*. $[Ca^{2+}]_o$ was 5.0 mM. (**c**) Muscle responses to exogenous acetylcholine (ACh, 100 µM) and γ-aminobutyric acid (GABA, 100 µM) are normal in *slo-1(lf)* and *dyb-1(lf)*. (**d**) The density of GFP-tagged SLO-1 (SLO-1::GFP) but not RIM (a presynaptic protein) in the dorsal nerve cord is significantly decreased in *dyb-1(lf)* compared with wild type. The asterisk (*) indicates a statistically significant difference ($p < 0.05$). The mutant strains used were *slo-1(md1745)* and *dyb-1(zw11)*. (Adapted from Ref. [57])

evoke an iberiotoxin-sensitive outward current, but this current constitutes only a small fraction (~12% at +20 mV) of the total terminal K^+ current [46]. These studies suggest either that Slo1 channels are expressed but perhaps not at sufficiently high numbers to impact exocytosis, or that they are recruited under as-yet-unknown physiological conditions.

Paradoxical effects of Slo1 inhibition have also been reported. For example, a *Drosophila Slo1* mutation reportedly led to a puzzling decrease in neurotransmitter release at the NMJ [74]. Additionally, the blockade of Slo1 reduced the amplitude of EPSCs evoked by light at salamander rod photoreceptor synapses [75] and by direct nerve stimulation in frog nerve-muscle coculture [76]. These results suggest that presynaptic Slo1 may facilitate neurotransmitter release, perhaps due to some unusual synaptic properties. The rod photoreceptor synapse of salamander may have special structural properties to allow Slo1 to enhance Ca^{2+} entry and neurotransmitter release by increasing extracellular K^+ concentration in the synaptic cleft, as speculated by the authors [75]. Additionally, it was suggested that in the cultured frog NMJ, when Slo1 is blocked, the resulting broadened presynaptic AP reduces the driving force for Ca^2, leading to reduced Ca^{2+} and exocytosis [76].

The mechanisms and significance of Slo1 presynaptic localization are becoming better understood. In rats, a conditional knockout of RIM-binding proteins (RBPs) 1 and 2 in presynaptic neurons at the calyx of Held synapse led to reduced Slo1 currents and expression at the terminal. The RBPs bind to Slo1 and presynaptic proteins (RIMs and VGCCs) through their FN3 and SH3 domains, respectively, to facilitate Slo1 presynaptic localization [47]. In *C. elegans*, SLO-1 presynaptic localization relies on both dystrobrevin (DYB-1) and α-catulin (CTN-1). Mutations in either *dyb-1* (Fig. 2d) or *ctn-1* disrupt SLO-1 presynaptic localization and produce synaptic phenotypes similar to those of *slo-1* mutants [57, 77] (Fig. 2a). It has been suggested that a hierarchical organization of α-catulin and dystrobrevin is necessary for SLO-1 presynaptic localization [56]. Although mammalian dystrobrevin and α-catulin also interact physically [78], their roles in the presynaptic localization of Slo1 are not known.

3 Kv3 Channels

The Kv3 family of voltage-gated K^+ channels comprises four members: Kv3.1, Kv3.2, Kv3.3, and Kv3.4. Like most other K^+ channels, Kv3 channels are tetramers that can be either homomeric or heteromeric. They are primarily found in fast-spiking neurons and have unusually fast activation and deactivation kinetics, allowing them to rapidly repolarize APs during high-frequency activity. In contrast to Kv1 channels, Kv3 channels are "high-threshold" voltage-gated K^+ channels (i.e., activated at membrane potentials more positive than ~ −10 mV) [79–81].

In heterologous expression systems, homomeric Kv3.1 or Kv3.2 channels exhibit minimal inactivation when subjected to depolarizing voltage steps of less than 1 second, while Kv3.3 or Kv3.4 channels display rapid inactivation (Fig. 3a). The inactivation of Kv3 channels occurs through a ball-and-chain mechanism, which involves charged amino acid residues in the amino termini of Kv3.3 and Kv3.4 [80, 81]. Despite the significant differences in inactivation rate among Kv3 channels, their normalized conductance versus voltage relationships remain quite similar (Fig. 3b).

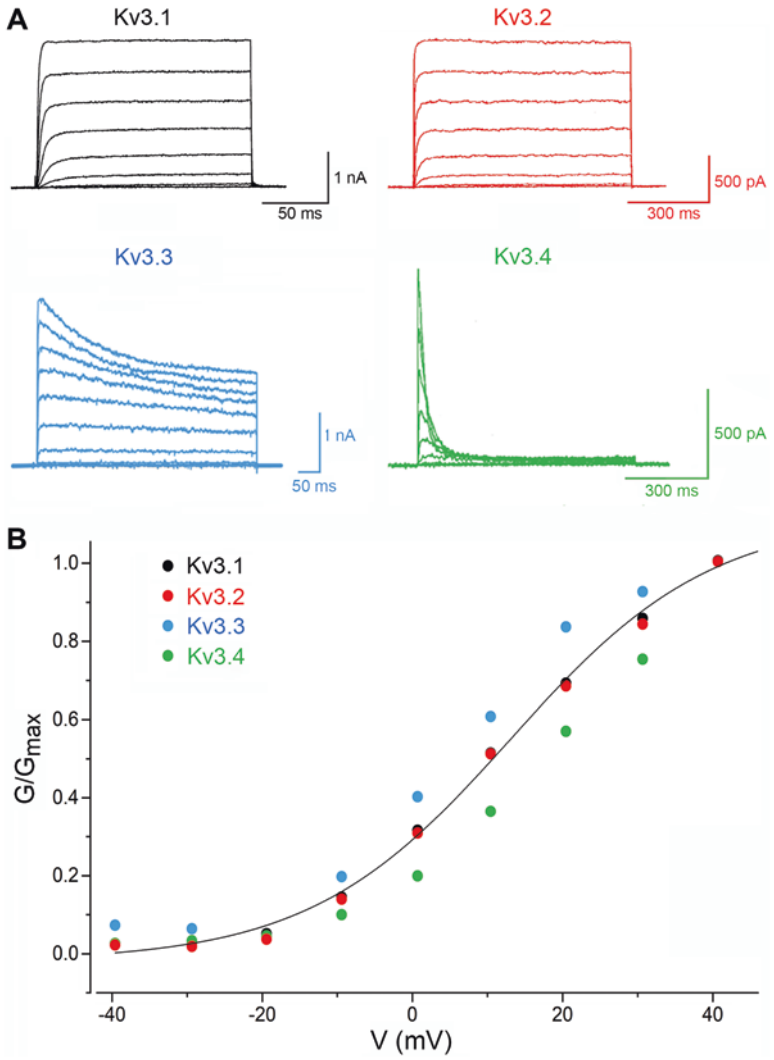

Fig. 3 Biophysical properties of Kv3 channels. (**a**) Typical current traces of Kv3 channels heterologously expressed in Chinese hamster ovary cells. (**b**) Normalized conductance (*g*) and voltage (*V*) relationships of different Kv3 channels. (Adapted from Refs. [80, 81])

Kv3 channels are broadly expressed in the brain, as described in [81] and evident in the Allen Brain Atlas (https://mouse.brain-map.org/). Neuronal Kv3 expression is observed in the soma, axon, and presynaptic terminals. Immunohistochemistry and immunoelectron microscopy studies show that all four Kv3 channels can be detected in presynaptic terminals to varying degrees [46, 82–84]. Given the localization of Kv3 channels to presynaptic boutons and their unusual biophysical properties, they are well-suited for modulating presynaptic APs and neurotransmitter release. In

rodent brain slice preparations, specific K^+ channel blockers such as blood-depressing substance-I (BDS-I), tetraethylammonium (TEA), and 4-aminopyridine (4-AP) have revealed the important role of Kv3 channels in regulating neurotransmitter release. BDS-I, a toxin from sea anemones, slows Kv3 channel activation kinetics and shifts the voltage range for channel activation to more positive voltages [85, 86]. TEA and 4-AP are capable of blocking both Kv3 and Kv1 channels, but at low concentrations, TEA preferentially blocks Kv3 channels due to its much lower half-maximal inhibitory concentration (IC_{50}) for Kv3 channels (0.1–0.2 mM) compared to Kv1 channels (0.5 – >10 mM) [87].

In the rat calyx of Held nerve terminal, TEA (1 mM) inhibited the outward K^+ current, prolonged the duration of presynaptic APs, and increased the amplitude of EPSCs. The TEA-sensitive outward current had fast activation kinetics and required a high voltage for activation [46], consistent with Kv3. Similarly, at the mouse calyx of Held synapse, TEA (1 mM) inhibited a high voltage-activated outward current, prolonged APs at the calyceal terminal (Fig. 4a, b), and augmented the amplitude of EPSCs. Knockout of Kv3.3, but not Kv3.1, produced similar effects and occluded the augmenting effect of TEA on EPSC amplitude (Fig. 4c, d) [83]. These results indicate that the physiological function of Kv3 channels at calyceal terminals is to

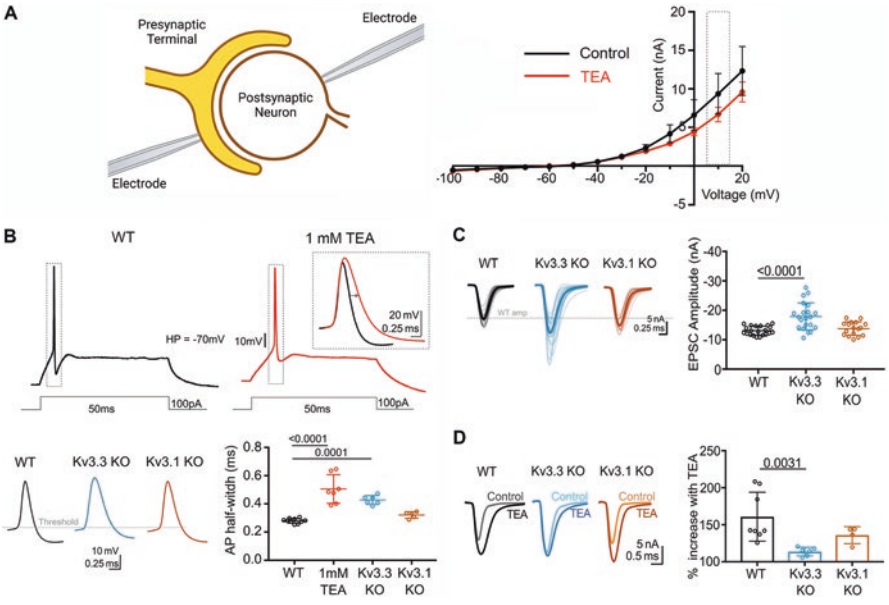

Fig. 4 Kv3 current facilitates AP repolarization in the presynaptic terminal and inhibits excitatory postsynaptic current (EPSC) at the calyx of Held synapse. (**a**) A diagram showing voltage-clamp recording of the calyceal terminal. (Created with BioRender.com) and a plot of the current and voltage relationship of wild-type (WT) mouse calyceal terminal in the absence and presence of 1 mM tetraethylammonium (TEA). (**b**, **c**) Effects of TEA, Kv3.3 knockout (KO), and Kv3.1 KO on AP half-width and EPSC amplitude. (**d**) Effect of TEA on EPSC amplitude in WT and knockout mice. (Adapted from Ref. [83])

restrict neurotransmitter release by accelerating AP repolarization. This conclusion is supported by the presence of Kv3.3 in mouse calyceal presynaptic terminals [83] and Kv3.1b and Kv3.4 in rat calyceal presynaptic terminals [46, 82].

In the mouse barrel cortex, which is a region of the primary somatosensory cortex, TEA (1 mM) has been shown to have effects on inhibitory neurotransmission [88]. Specifically, it increased the amplitude and reduced the PPR of evoked inhibitory postsynaptic current (IPSC) in synapses between fast-spiking neurons. TEA also enhanced AP-evoked Ca^{2+} transients in synaptic terminals of these neurons. Notably, the effect of TEA on evoked IPSC amplitude was not present in Kv3.1/Kv3.2 double knockout mice, suggesting that Kv3 channels are responsible for this effect. These findings suggest that Kv3 channels at presynaptic terminals of fast-spiking neurons inhibit neurotransmitter release by limiting Ca^{2+} influx. This conclusion is consistent with the reported expression of Kv3.1 and Kv3.2 in fast-spiking GABAergic interneurons, and their prominent localization in presynaptic terminals [84, 89].

In the hippocampus of rats, BDS-I has been shown to inhibit outward current and prolong the duration of APs at mossy fiber boutons. Additionally, the application of 4-AP was found to increase the amplitude but reduce the PPR of EPSCs recorded from CA3 pyramidal neurons in the hippocampus, indicating enhanced glutamate release from mossy fibers [7]. These results suggest that Kv3 channels at mossy fiber boutons play a physiological role in limiting neurotransmitter release.

In mouse cerebellar stellate cells, which are GABAergic inhibitory neurons, BDS-I or TEA (500 μM) increased the duration of presynaptic bouton APs (imaged by a voltage-sensitive dye) and increased the amplitude of evoked IPSCs. The blockade of Kv3 with BDS-I also prolonged the duration of APs at presynaptic boutons but not at the axon initial segment (AIS) or axon shaft [6, 90]. These results suggest that the physiological function of Kv3 is to inhibit neurotransmitter release by accelerating AP repolarization at presynaptic boutons. Interestingly, the width of APs varied between presynaptic boutons in the same axonal branch of stellate cells, and this difference was eliminated by TEA (500 μM). Furthermore, bouton-targeted two-photon laser uncaging of RuBi-4AP, a photolyzable 4-AP, could either prolong the duration of APs or have no effect in different boutons of the same axon branch, and the effect of RuBi-4AP uncaging on bouton AP duration was occluded by TEA but not the Kv1 blocker dendrotoxin-I [6]. These results suggest that the variability of spike duration between presynaptic boutons was mainly due to differences in Kv3 function, and that the effect of RuBi-4AP uncaging on AP width resulted from Kv3 blockade but not Kv1 blockade. In a more recent study, it was found that subthreshold somatic depolarization increased the width of bouton APs and the amplitude of evoked autaptic IPSCs but decreased the PPR of evoked IPSCs in stellate cells. Knockout of Kv3.4 but not Kv3.1 slowed the inactivation rate of K^+ currents in presynaptic boutons and eliminated the effects of somatic subthreshold depolarization on IPSC amplitude and PPR [91]. These results suggest that subthreshold depolarization may alter IPSC amplitude and PPR by inactivating channels containing Kv3.4.

4 Kv1 Channels

The family of Kv1 voltage-gated K^+ channels consists of seven members: Kv1.1 through Kv1.7 [92]. These channels, like Kv3 channels, are homomeric or heteromeric tetramers. However, they differ from Kv3 channels in that they begin to activate at membrane voltages near the resting membrane potential. This feature makes them low-threshold voltage-gated K^+ channels.

Kv1 channels are expressed in various brain regions and detected in neuronal somata, dendrites, axons, and nerve terminals [93–98]. Several toxins that specifically block Kv1 channels are often used to study the physiological functions of Kv1, including α-dendrotoxin (Kv1.1, Kv1.2, Kv1.6), dendrotoxin-I (Kv1.1 and Kv1.2), dendrotoxin-K (Kv1.1) [99], tityustoxin-Kα (kv1.2) [100], and margatoxin (Kv1.3, Kv1.2, and Kv1.1) [101]. Although 4-AP is also used to block Kv1 channels, it blocks Kv3 channels as well [87]. Kv1 channels are involved in regulating AP firing rate [46, 97, 102, 103] and repolarizing presynaptic APs [46]. They have also been implicated in regulating neurotransmitter release.

At the calyx of Held synapse in rats, Kv1.1 and Kv1.2 are located approximately 20 μm away from the terminal but are excluded from it, while Kv3.1 is localized at the presynaptic terminal [103]. Both low-threshold K^+ current, which is sensitive to margatoxin, dendrotoxin-I, and tityustoxin-Kα, and high-threshold K^+ current, which is sensitive to 1 mM TEA, are detected at the calyceal terminal (Fig. 5a–c). The high-threshold K^+ current activates faster than the low-threshold K^+ current, suggesting that they result from the functions of Kv3 and Kv1 channels, respectively. Treatment with TEA (1 mM) alone prolonged presynaptic APs and increased the amplitude of EPSCs at this synapse. In contrast, margatoxin may produce such effects only in the presence of TEA (Fig. 5d). The differential effects of TEA and margatoxin are thought to be due to the different activation kinetics of Kv1 and Kv3 channels. Under basal conditions, Kv3 channels can facilitate the repolarization of presynaptic APs due to their fast activation kinetics, while Kv1 channels can only do so under conditions with longer AP durations because of their slower activation kinetics [46]. An alternative interpretation is that Kv3 may exceed Kv1 in current amplitude, and thus more potently determine the decay of fast spikes [104].

Basket cells in the cerebellum are the primary source of inhibitory synaptic inputs to Purkinje cells, and they innervate these cells through a unique nerve terminal structure called the pinceaux [105]. Immunohistochemistry studies have shown that Kv1.1 and Kv1.2 are expressed in the basket cell pinceaux [93, 106, 107]. Patch-clamp recordings of basket cell nerve terminals have revealed an α-dendrotoxin-sensitive low-threshold K^+ current, in addition to an α-dendrotoxin-insensitive but TEA (1 mM)-sensitive high-threshold K^+ current [108]. Treatment with α-dendrotoxin has been shown to increase the frequency and amplitude of spontaneous IPSCs recorded from Purkinje cells [109]. These findings collectively suggest that Kv1 channels regulate neurotransmitter release at basket cell terminals, although it is not clear in those studies if the effects of α-dendrotoxin reflected block of K^+ channels in the pinceaux or the axon.

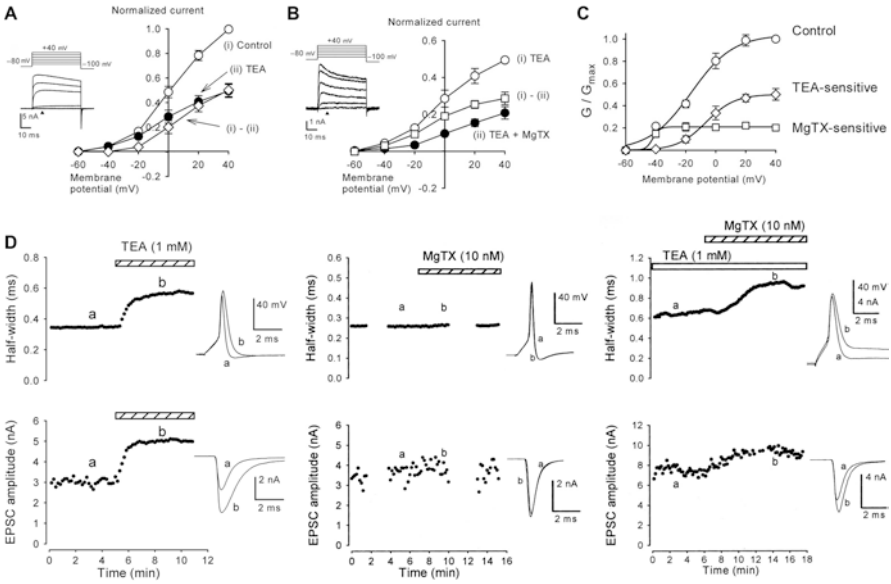

Fig. 5 Margatoxin (MgTX) increases the duration of presynaptic terminal APs and the amplitude of excitatory postsynaptic current (EPSC) at the rat calyx of Held synapse in the presence but not absence of tetraethylammonium (TEA). (**a**) Sample traces of TEA (1 mM)-sensitive K^+ current and current-voltage relationships of the indicated conditions. (**b**) Sample traces of MgTX (10 nM)-sensitive K^+ current and current-voltage relationships for the indicated conditions. (**c**) Conductance (G)–voltage relationships derived from the total K^+ current, TEA-sensitive K^+ current, and MgTX-sensitive K^+ current in the calyceal terminal. (**d**) Effects of TEA, MgTX alone, and MgTX in the presence of TEA on the half-width of presynaptic APs and the amplitude of EPSCs. (Adapted from Ref. [46])

In rat cortical layer 5 pyramidal neurons, Kv1 channels are enriched at the axon initial segment, where dendrotoxin-I can prolong the AP duration. Paired recordings between synaptically connected layer 5 pyramidal neurons have shown that subthreshold depolarization of the presynaptic neuron increases the amplitude but reduces the PPR of EPSPs [110]. The effect of presynaptic subthreshold depolarization on EPSP amplitude was eliminated by dendrotoxin-I. The interpretation was that subthreshold depolarization caused inactivation of axonal Kv1 channels, and APs driven during the period of depolarization were therefore broadened. These findings suggest that one physiological function of the Kv1 channels is to mediate regulation of neurotransmitter release by subthreshold signaling in axons [110].

Optical recording of APs using a voltage-sensitive dye in cerebellar SC interneurons has shown that dendrotoxin-I prolongs AP duration at the axon initial segment but not at presynaptic boutons, whereas BDS-I prolongs AP duration at presynaptic boutons but not at the axon initial segment. Consistent with these findings, TEA enhances AP-evoked IPSCs, but dendrotoxin-I does not have such an effect. Taken together, these results suggest that, unlike the situation in cortical pyramidal cells,

Kv1 channels in cerebellar SC interneurons do not impact presynaptic AP repolarization and neurotransmitter release [90].

In the rat brain, nitric oxide facilitates the release of GABA from neurons in the paraventricular nucleus [111]. Conversely, a μ-opioid receptor agonist inhibits GABA release from neurons in the basolateral amygdala [112]. The facilitatory effect of nitric oxide and the inhibitory effect of μ-opioid receptor activation on GABA release can both be prevented by inhibitors of Kv1.1 and Kv1.2 channels, such as 4-AP, α-dendrotoxin, dendrotoxin-K, and tityustoxin-Kα, indicating that these channels play a role in modulating GABA release [111, 112].

5 KCNQ Channels

The KCNQ family of voltage-gated K^+ channels consists of five members, KCNQ1/Kv7.1 through KCNQ5/Kv7.5, all of which are expressed in the mammalian nervous system. KCNQ channels exist as homomeric or heteromeric tetramers. The typical activation threshold for KCNQ channels is positive to −60 mV [113–115]. KCNQ channels are localized to axon initial segments where they effectively temper excitability; accordingly pharmacological blockade of KCNQ leads to hyperexcitability, and mutations in KCNQ subunits lead to epileptic seizure [116].

The KCNQ family of voltage-gated K^+ channels can have diverse effects on neurotransmitter release, depending on the synapse. At the presynaptic terminal of the rat calyx of Held, KCNQ channels are active at or near the resting membrane potential, as evidenced by the sensitivity of the resting membrane potential to pharmacological modulators. Prior research showed that small changes in resting potential modulate the probability of transmitter release at the calyx terminal by regulation of VGCC [10]. Given the role of KCNQ channels in determining resting potential, these channels could therefore play a role in controlling synaptic strength [117].

To explore this possibility further, presynaptic KCNQ was activated by slow voltage ramps applied to the presynaptic terminal; the resulting current was substantially inhibited by the KCNQ blockers XE991 (Fig. 6a) or linopirdine, while the KCNQ openers flupirtine and retigabine enhanced the current. Consistently, XE991-sensitive current at the calyceal terminal started to activate when the membrane potential reaches approximately −85 mV (Fig. 6b), which is significantly more hyperpolarized than the typical voltage threshold for KCNQ current activation (approximately −60 mV). During paired presynaptic stimulus experiments, XE991 increased the amplitude of the first EPSC but reduced the PPR (Fig. 6c), while flupirtine produced opposite effects. Furthermore, immunohistochemical experiments showed KCNQ5, but not KCNQ2, KCNQ3, or KCNQ4, in the calyceal terminal. The collective results suggest that KCNQ channels, likely KCNQ5, downregulate neurotransmitter release by modulating the resting membrane potential at the calyx of Held synapse [117]. Interestingly, the expression of KCNQ5 at this and related auditory nerve terminals was dependent on the presence of auditory signaling, as manipulations that lead to deafness eliminated KCNQ5 labeling [118].

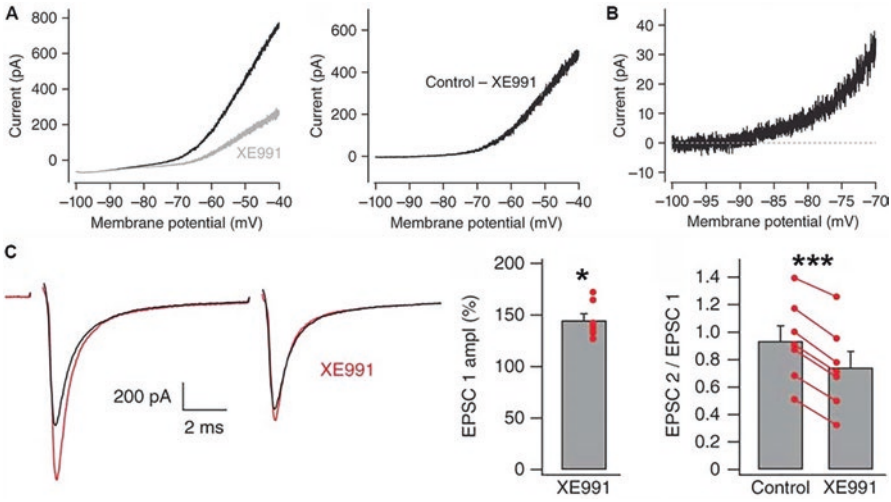

Fig. 6 XE991-sensitive current in the rat calyx of Held terminal regulates the amplitude and paired-pulse ratio of excitatory postsynaptic current (EPSC). (**a**) Outward current in response to a slow voltage ramp is greatly inhibited by the KCNQ channel blocker XE991 (10 μM). *Left*, Current in the absence and presence of XE991. *Right*, XE99-sensitive current obtained by subtracting the gray trace from the black trace in the left panel. (**b**) The initial portion of the XE991-sensitive current in the middle panel displayed at expanded scales. (**c**) EPSCs evoked by paired-pulse stimuli at 20-ms interval. Shown are sample traces of control and XE991 (*left*), EPSC1 amplitude in the presence of XE991 normalized by that of the control (*middle*), and comparison of the paired-pulse ration between Control and XE991 (*right*). $*p < 0.05$; $***p < 0.001$. (Adapted from Ref. [117])

A recent related study has shown that blockade of KCNQ channels in the rat calyceal terminal disrupts the homeostasis of AP amplitude and waveform during high-frequency stimulation. Normally, the AP waveform is stable during trains of high-frequency stimulation, but becomes increasingly small and wider in the presence of XE991. This suggests that KCNQ channels may accumulate in an open state during high-frequency spiking activity to facilitate reliable synaptic signaling [119].

In the rat hippocampal CA1 region, both KCNQ2 and KCNQ3 are expressed. The KCNQ blocker XE991 reduced the amplitude of presynaptic compound APs, whereas the KCNQ opener retigabine increased it, at 11.5 mM but not 2.5 mM $[K^+]_o$. At the higher $[K^+]_o$, XE991 also reduced the slope of evoked field EPSPs and the amplitude of evoked EPSPs, whereas retigabine had the opposite effects. Somatic recordings with hippocampal CA3 pyramidal neurons revealed that the resting membrane potential depolarized by approximately 15 mV when $[K^+]_o$ increased from 3.5 to 11.5 mM. Based on these results and computational modeling, it was suggested that M-current mediated by KCNQ channels enhance neurotransmitter release by reducing Na^+ channel inactivation [120]. However, this effect of KCNQ channels arises only in the context of a prior depolarization by elevated $[K^+]_o$, such as it may occur under conditions of enhanced electrical activity.

6 GIRK Channels

Inwardly rectifying K^+ (Kir) channels preferentially conduct inward K^+ current over outward K^+ current. Each channel is made up of four subunits, each with two transmembrane domains and a pore domain in between. Kir channels are classified into seven subfamilies (Kir1 through Kir7), with one or more members in each subfamily. Kir2 is the classic Kir channel subfamily, Kir3 is the subfamily of G protein-gated channels (also known as GIRK channels), Kir6 is the subfamily of ATP-sensitive channels, and the remaining subfamilies (Kir1, 4, 5, and 7) are K^+ transporters. There are four GIRK channels found in humans: GIRK1/Kir3.1, GIRK2/Kir3.2, GIRK3/Kir3.3, and GIRK4/Kir3.4. The activation of GIRK channels is mediated by the Gβγ subunit that is released from G proteins upon agonist binding to specific G protein-coupled receptors. Emerging evidence suggests that GIRK channels may have a role in regulating neurotransmitter release.

In the frog NMJ, inhibiting GIRK channels with nanomolar tertiapin-Q has been shown to cause significant decreases in the frequency of miniature end-plate potentials, the quantal content of end-plate potentials, and the magnitude of presynaptic Ca^{2+} transients. Blocking L-type, but not N- or P/Q-type, VGCCs may prevent the inhibitory effect of tertiapin-Q on end-plate potentials. These observations led to the suggestion that one physiological function of GIRK channels at motor neuron terminals is to enhance synaptic vesicle exocytosis by enhancing L-type VGCCs; the authors suggest that either GIRK-mediated hyperpolarization re-primes VGCC or there may be a direct coupling between the two channels [121].

In the rat striatum, which is innervated by histaminergic fibers and expresses histamine H3 receptors (H_3R), activation of the H_3R by the agonist immepip reduces the amplitude of EPSCs but increases PPR. This indicates decreased neurotransmitter release. The effects of immepip are prevented by the GIRK channel blocker tertiapin-Q, suggesting that immepip reduces neurotransmitter release by activating presynaptic Kir3 channels. Kir3 channels have been found in corticostriatal terminals, which is consistent with these findings [122].

7 Slo2 K^+ Channels

The Slo2 subfamily of K^+ channels in mammals includes Slo2.1/Slick (sequence resembling an intermediate conductance K^+ channel) and Slo2.2/Slack (sequence resembling a calcium-activated K^+ channel). These high-conductance K^+ channels are activated by both membrane voltage and cytosolic Na^+ and Cl^- [19, 123, 124]. They are expressed in various brain regions [125, 126]. Slo2.2 is a significant contributor to delayed outward currents in many types of neurons [127–129]. Mutations in *Kcnt1*, which encodes Slo2.2, have a strong association with epileptic disorders and intellectual disability [130–134]. Knockout of *Kcnt1* in mice results in neuronal hyperexcitability, heightened pain and itch responses, and cognitive impairment

[129]. However, it is unclear whether Slo2 channels modulate neurotransmitter release in mammalian neurons.

C. elegans has only one Slo2 gene, *slo-2*. Like mammalian Slo2, *C. elegans* SLO-2 is gated by voltage, cytosolic Cl^-, and a cytosolic cation [135]. However, in contrast to mammals, SLO-2 is activated by Ca^{2+} instead of Na^+ in *C. elegans*. This difference in cation dependence may have arisen due to the distinct roles of Na^+ and Ca^{2+} in neuronal activation. While voltage-gated Na^+ channels play a crucial role in neuronal functions in mammals, *C. elegans* lacks an obvious gene encoding voltage-gated Na^+ channels and relies on Ca^{2+} to mediate membrane depolarization [72, 136–139]. Although a small number of *C. elegans* neurons can fire APs [137, 139], the majority of them, including motor neurons [140], generate graded membrane voltage changes to perform their physiological functions. These "graded" neurons control postsynaptic cells by producing bursts of postsynaptic currents (PSC bursts) [141, 142], allowing for the assessment of neurotransmitter release by analyzing PSC burst properties. In *C. elegans* motor neurons, SLO-2 is the main conductor of delayed outward currents, and its function is coupled to Ca^{2+} entry through EGL-19, a Ca_V1 (L-type) VGCC. In *slo-2(lf)* mutants, the resting membrane potential of motor neurons is highly depolarized, and the duration and charge transfer rate of PSC bursts at the NMJ are significantly increased compared with wild type (Fig. 7a), while muscle cell responses to exogenous neurotransmitters (acetylcholine and GABA) remain normal (Fig. 7b, c). This suggests that one of the physiological functions of SLO-2 is to limit neurotransmitter release [143].

8 Summary

In this chapter, we have provided an overview of the K^+ channels that have been implicated in regulating neurotransmitter release. However, the number of K^+ channels and the variety of synapses that have been analyzed to date are limited. Only a small number of K^+ channels have been implicated, with relatively stronger evidence supporting the roles of Slo1 and Kv3 channels. Since K^+ channels are diverse in terms of their biophysical properties, expression patterns, and subcellular localizations, the identities of K^+ channels involved in regulating neurotransmitter release may differ significantly from synapse to synapse. Additionally, there may be other K^+ channels with unrecognized roles in regulating neurotransmitter release.

To evaluate the roles of K^+ channels in neurotransmitter release regulation, most previous studies have relied on analyzing the effects of channel blockers on EPSCs evoked by single or paired pulses. However, the significance of a K^+ channel in regulating neurotransmitter release may vary under different physiological conditions, and the results with blockers may be complicated by their non-specific effects. For instance, increased presynaptic firing can alter the activities of Slo1 and voltage-gated K^+ channels due to Ca^{2+} accumulation and channel inactivation, respectively. Moreover, some K^+ channel blockers used in prior studies also have blocking effects

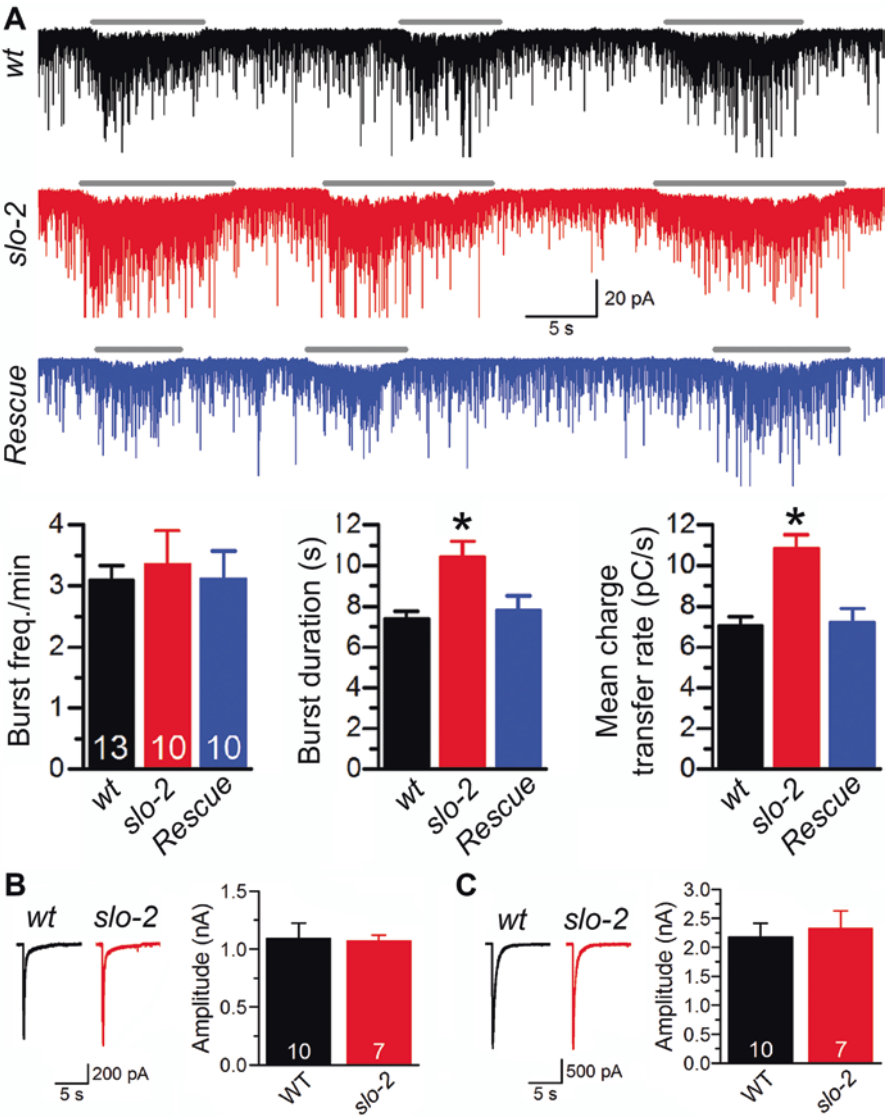

Fig. 7 Loss-of-function mutation of *slo-2* augments postsynaptic current (PSC) bursts without altering muscle cell responses to neurotransmitters at the *C. elegans* neuromuscular junction. (**a**) Sample traces of spontaneous postsynaptic currents showing PSC bursts (marked by horizontal lines) of wild type (*wt*), *slo-2(nf101)*, *slo-2(nf101)* expressing GFP-tagged wild-type SLO-2 pan-neuronally using *rab-3* promoter (*Rescue*), and comparisons of PSC burst frequency, duration, and mean charge transfer rate. $*p < 0.05$. (**b**, **c**) Sample traces and amplitudes of body-wall muscle whole-cell current induced by puffing 100 μM exogenous acetylcholine (**b**) or GABA (**c**)

on other channels, such as dendrotoxin-I on Slo1 [144], BDS-I on voltage-gated Na^+ channels [145], and δ-dendrotoxin on Kir1.1a (ROMK1) [146]. Thus, a more comprehensive understanding of neurotransmitter release regulation by K^+ channels can

be achieved by analyzing additional synapses, employing diverse experimental conditions, and utilizing a combination of genetic (e.g., knockout or knockdown) and pharmacological approaches.

Acknowledgment Supported by NIH grants R01MH085927 and R01NS109388 to ZWW, and R01DC004450 and R35NS116798 to LOT.

References

1. Schneggenburger R, Neher E. Intracellular calcium dependence of transmitter release rates at a fast central synapse. Nature. 2000;406:889–93. https://doi.org/10.1038/35022702.
2. Heidelberger R, Heinemann C, Neher E, Matthews G. Calcium dependence of the rate of exocytosis in a synaptic terminal. Nature. 1994;371:513–5. https://doi.org/10.1038/371513a0.
3. Lando L, Zucker RS. Ca2+ cooperativity in neurosecretion measured using photolabile Ca2+ chelators. J Neurophysiol. 1994;72:825–30. https://doi.org/10.1152/jn.1994.72.2.825.
4. Bollmann JH, Sakmann B, Borst JG. Calcium sensitivity of glutamate release in a calyx-type terminal. Science. 2000;289:953–7. https://doi.org/10.1126/science.289.5481.953.
5. Dodson PD, Forsythe ID. Presynaptic K^+ channels: electrifying regulators of synaptic terminal excitability. Trends Neurosci. 2004;27:210–7. https://doi.org/10.1016/j.tins.2004.02.012.
6. Rowan MJ, DelCanto G, Yu JJ, Kamasawa N, Christie JM. Synapse-level determination of action potential duration by K^+ channel clustering in axons. Neuron. 2016;91:370–83. https://doi.org/10.1016/j.neuron.2016.05.035.
7. Alle H, Kubota H, Geiger JR. Sparse but highly efficient Kv3 outpace BKCa channels in action potential repolarization at hippocampal mossy fiber boutons. J Neurosci. 2011;31:8001–12. https://doi.org/10.1523/JNEUROSCI.0972-11.2011.
8. Yang YM, Wang LY. Amplitude and kinetics of action potential-evoked Ca2+ current and its efficacy in triggering transmitter release at the developing calyx of Held synapse. J Neurosci. 2006;26:5698–708. https://doi.org/10.1523/JNEUROSCI.4889-05.2006.
9. Wang LY, Kaczmarek LK. High-frequency firing helps replenish the readily releasable pool of synaptic vesicles. Nature. 1998;394:384–8. https://doi.org/10.1038/28645.
10. Awatramani GB, Price GD, Trussell LO. Modulation of transmitter release by presynaptic resting potential and background calcium levels. Neuron. 2005;48:109–21. https://doi.org/10.1016/j.neuron.2005.08.038.
11. Gutman GA, Chandy KG, Grissmer S, Lazdunski M, McKinnon D, Pardo LA, et al. International Union of Pharmacology. LIII. Nomenclature and molecular relationships of voltage-gated potassium channels. Pharmacol Rev. 2005;57:473–508. https://doi.org/10.1124/pr.57.4.10.
12. Kubo Y, Adelman JP, Clapham DE, Jan LY, Karschin A, Kurachi Y, et al. International Union of Pharmacology. LIV. Nomenclature and molecular relationships of inwardly rectifying potassium channels. Pharmacol Rev. 2005;57:509–26. https://doi.org/10.1124/pr.57.4.11.
13. Goldstein SA, Bayliss DA, Kim D, Lesage F, Plant LD, Rajan S. International Union of Pharmacology. LV. Nomenclature and molecular relationships of two-P potassium channels. Pharmacol Rev. 2005;57:527–40. https://doi.org/10.1124/pr.57.4.12.
14. Kaczmarek LK, Aldrich RW, Chandy KG, Grissmer S, Wei AD, Wulff H. International Union of Basic and Clinical Pharmacology. C. Nomenclature and properties of calcium-activated and sodium-activated potassium channels. Pharmacol Rev. 2017;69:1–11. https://doi.org/10.1124/pr.116.012864.
15. Hofmann F, Biel M, Kaupp UB. International Union of Pharmacology. LI. Nomenclature and structure-function relationships of cyclic nucleotide-regulated channels. Pharmacol Rev. 2005;57:455–62. https://doi.org/10.1124/pr.57.4.8.

16. Elkins T, Ganetzky B, Wu CF. A *Drosophila* mutation that eliminates a calcium-dependent potassium current. Proc Natl Acad Sci U S A. 1986;83:8415–9. https://doi.org/10.1073/pnas.83.21.8415.
17. Atkinson NS, Robertson GA, Ganetzky B. A component of calcium-activated potassium channels encoded by the *Drosophila* slo locus. Science. 1991;253:551–5. https://doi.org/10.1126/science.1857984.
18. Adelman JP, Shen KZ, Kavanaugh MP, Warren RA, Wu YN, Lagrutta A, et al. Calcium-activated potassium channels expressed from cloned complementary DNAs. Neuron. 1992;9:209–16. https://doi.org/10.1016/0896-6273(92)90160-f.
19. Salkoff L, Butler A, Ferreira G, Santi C, Wei A. High-conductance potassium channels of the SLO family. Nat Rev Neurosci. 2006;7:921–31. https://doi.org/10.1038/nrn1992.
20. Hite RK, Yuan P, Li Z, Hsuing Y, Walz T, MacKinnon R. Cryo-electron microscopy structure of the Slo2.2 Na^+-activated K^+ channel. Nature. 2015;527:198–203. https://doi.org/10.1038/nature14958.
21. Wu Y, Yang Y, Ye S, Jiang Y. Structure of the gating ring from the human large-conductance Ca^{2+}-gated K^+ channel. Nature. 2010;466:393–7. https://doi.org/10.1038/nature09252.
22. Yuan P, Leonetti MD, Pico AR, Hsiung Y, MacKinnon R. Structure of the human BK channel Ca^{2+}-activation apparatus at 3.0 A resolution. Science. 2010;329:182–6. https://doi.org/10.1126/science.1190414.
23. Tao X, Hite RK, MacKinnon R. Cryo-EM structure of the open high-conductance Ca^{2+}-activated K^+ channel. Nature. 2017;541:46–51. https://doi.org/10.1038/nature20608.
24. Tao X, MacKinnon R. Molecular structures of the human Slo1 K^+ channel in complex with beta4. elife. 2019;8:e51409. https://doi.org/10.7554/eLife.51409.
25. Budelli G, Geng Y, Butler A, Magleby KL, Salkoff L. Properties of Slo1 K+ channels with and without the gating ring. Proc Natl Acad Sci U S A. 2013;110:16657–62. https://doi.org/10.1073/pnas.1313433110.
26. Xia XM, Zeng X, Lingle CJ. Multiple regulatory sites in large-conductance calcium-activated potassium channels. Nature. 2002;418:880–4. https://doi.org/10.1038/nature00956.
27. Brenner R, Jegla TJ, Wickenden A, Liu Y, Aldrich RW. Cloning and functional characterization of novel large conductance calcium-activated potassium channel beta subunits, hKCNMB3 and hKCNMB4. J Biol Chem. 2000;275:6453–61. https://doi.org/10.1074/jbc.275.9.6453.
28. McManus OB, Helms LM, Pallanck L, Ganetzky B, Swanson R, Leonard RJ. Functional role of the beta subunit of high conductance calcium-activated potassium channels. Neuron. 1995;14:645–50. https://doi.org/10.1016/0896-6273(95)90321-6.
29. Chen B, Ge Q, Xia XM, Liu P, Wang SJ, Zhan H, et al. A novel auxiliary subunit critical to BK channel function in *Caenorhabditis elegans*. J Neurosci. 2010;30:16651–61. https://doi.org/10.1523/JNEUROSCI.3211-10.2010.
30. Uebele VN, Lagrutta A, Wade T, Figueroa DJ, Liu Y, McKenna E, et al. Cloning and functional expression of two families of beta-subunits of the large conductance calcium-activated K^+ channel. J Biol Chem. 2000;275:23211–8. https://doi.org/10.1074/jbc.M910187199.
31. Xia XM, Ding JP, Lingle CJ. Molecular basis for the inactivation of Ca^{2+}- and voltage-dependent BK channels in adrenal chromaffin cells and rat insulinoma tumor cells. J Neurosci. 1999;19:5255–64. https://doi.org/10.1523/JNEUROSCI.19-13-05255.1999.
32. Xia XM, Ding JP, Zeng XH, Duan KL, Lingle CJ. Rectification and rapid activation at low Ca^{2+} of Ca^{2+}-activated, voltage-dependent BK currents: consequences of rapid inactivation by a novel beta subunit. J Neurosci. 2000;20:4890–903. https://doi.org/10.1523/JNEUROSCI.20-13-04890.2000.
33. Li Q, Yan J. Modulation of BK channel function by auxiliary beta and gamma subunits. Int Rev Neurobiol. 2016;128:51–90. https://doi.org/10.1016/bs.irn.2016.03.015.
34. Gonzalez-Perez V, Lingle CJ. Regulation of BK channels by beta and gamma subunits. Annu Rev Physiol. 2019;81:113–37. https://doi.org/10.1146/annurev-physiol-022516-034038.

35. Hite RK, Tao X, MacKinnon R. Structural basis for gating the high-conductance Ca^{2+}-activated K^+ channel. Nature. 2017;541:52–7. https://doi.org/10.1038/nature20775.
36. Tonggu L, Wang L. Structure of the human BK ion channel in lipid environment. Membranes (Basel). 2022;12:758. https://doi.org/10.3390/membranes12080758.
37. Knaus HG, Schwarzer C, Koch RO, Eberhart A, Kaczorowski GJ, Glossmann H, et al. Distribution of high-conductance Ca(2+)-activated K+ channels in rat brain: targeting to axons and nerve terminals. J Neurosci. 1996;16:955–63. https://doi.org/10.1523/JNEUROSCI.16-03-00955.1996.
38. Tabti N, Bourret C, Mallart A. Three potassium currents in mouse motor nerve terminals. Pflugers Arch. 1989;413:395–400. https://doi.org/10.1007/BF00584489.
39. Katz E, Ferro PA, Cherksey BD, Sugimori M, Llinas R, Uchitel OD. Effects of Ca^{2+} channel blockers on transmitter release and presynaptic currents at the frog neuromuscular junction. J Physiol. 1995;486(Pt 3):695–706. https://doi.org/10.1113/jphysiol.1995.sp020845.
40. Yazejian B, DiGregorio DA, Vergara JL, Poage RE, Meriney SD, Grinnell AD. Direct measurements of presynaptic calcium and calcium-activated potassium currents regulating neurotransmitter release at cultured Xenopus nerve-muscle synapses. J Neurosci. 1997;17:2990–3001. https://doi.org/10.1523/JNEUROSCI.17-09-02990.1997.
41. Sun XP, Yazejian B, Grinnell AD. Electrophysiological properties of BK channels in Xenopus motor nerve terminals. J Physiol. 2004;557:207–28. https://doi.org/10.1113/jphysiol.2003.060509.
42. Lindgren CA, Moore JW. Identification of ionic currents at presynaptic nerve endings of the lizard. J Physiol. 1989;414:201–22. https://doi.org/10.1113/jphysiol.1989.sp017684.
43. Morita K, Barrett EF. Evidence for two calcium-dependent potassium conductances in lizard motor nerve terminals. J Neurosci. 1990;10:2614–25. https://doi.org/10.1523/JNEUROSCI.10-08-02614.1990.
44. Sivaramakrishnan S, Bittner GD, Brodwick MS. Calcium-activated potassium conductance in presynaptic terminals at the crayfish neuromuscular junction. J Gen Physiol. 1991;98:1161–79. https://doi.org/10.1085/jgp.98.6.1161.
45. Wangemann P, Takeuchi S. Maxi-K^+ channel in single isolated cochlear efferent nerve terminals. Hear Res. 1993;66:123–9. https://doi.org/10.1016/0378-5955(93)90133-l.
46. Ishikawa T, Nakamura Y, Saitoh N, Li WB, Iwasaki S, Takahashi T. Distinct roles of Kv1 and Kv3 potassium channels at the calyx of Held presynaptic terminal. J Neurosci. 2003;23:10445–53. https://doi.org/10.1523/JNEUROSCI.23-32-10445.2003.
47. Sclip A, Acuna C, Luo F, Sudhof TC. RIM-binding proteins recruit BK-channels to presynaptic release sites adjacent to voltage-gated Ca(2+)-channels. EMBO J. 2018;37:e98637. https://doi.org/10.15252/embj.201798637.
48. Hu H, Shao LR, Chavoshy S, Gu N, Trieb M, Behrens R, et al. Presynaptic Ca^{2+}-activated K^+ channels in glutamatergic hippocampal terminals and their role in spike repolarization and regulation of transmitter release. J Neurosci. 2001;21:9585–97. https://doi.org/10.1523/JNEUROSCI.21-24-09585.2001.
49. Sun XP, Schlichter LC, Stanley EF. Single-channel properties of BK-type calcium-activated potassium channels at a cholinergic presynaptic nerve terminal. J Physiol. 1999;518(Pt 3):639–51. https://doi.org/10.1111/j.1469-7793.1999.0639p.x.
50. Farley J, Rudy B. Multiple types of voltage-dependent Ca^{2+}-activated K^+ channels of large conductance in rat brain synaptosomal membranes. Biophys J. 1988;53:919–34. https://doi.org/10.1016/S0006-3495(88)83173-4.
51. Sailer CA, Kaufmann WA, Kogler M, Chen L, Sausbier U, Ottersen OP, et al. Immunolocalization of BK channels in hippocampal pyramidal neurons. Eur J Neurosci. 2006;24:442–54. https://doi.org/10.1111/j.1460-9568.2006.04936.x.
52. Misonou H, Menegola M, Buchwalder L, Park EW, Meredith A, Rhodes KJ, et al. Immunolocalization of the Ca^{2+}-activated K^+ channel Slo1 in axons and nerve terminals of mammalian brain and cultured neurons. J Comp Neurol. 2006;496:289–302. https://doi.org/10.1002/cne.20931.

53. Robitaille R, Garcia ML, Kaczorowski GJ, Charlton MP. Functional colocalization of calcium and calcium-gated potassium channels in control of transmitter release. Neuron. 1993;11:645–55. https://doi.org/10.1016/0896-6273(93)90076-4.
54. Zhou Y, Schopperle WM, Murrey H, Jaramillo A, Dagan D, Griffith LC, et al. A dynamically regulated 14-3-3, Slob, and Slowpoke potassium channel complex in *Drosophila* presynaptic nerve terminals. Neuron. 1999;22:809–18. https://doi.org/10.1016/s0896-6273(00)80739-4.
55. Oh KH, Haney JJ, Wang X, Chuang CF, Richmond JE, Kim H. ERG-28 controls BK channel trafficking in the ER to regulate synaptic function and alcohol response in C. elegans. elife. 2017;6:e24733. https://doi.org/10.7554/eLife.24733.
56. Oh KH, Abraham LS, Gegg C, Silvestri C, Huang YC, Alkema MJ, et al. Presynaptic BK channel localization is dependent on the hierarchical organization of alpha-catulin and dystrobrevin and fine-tuned by CaV2 calcium channels. BMC Neurosci. 2015;16:26. https://doi.org/10.1186/s12868-015-0166-2.
57. Chen B, Liu P, Zhan H, Wang ZW. Dystrobrevin controls neurotransmitter release and muscle Ca(2+) transients by localizing BK channels in Caenorhabditis elegans. J Neurosci. 2011;31:17338–47. https://doi.org/10.1523/JNEUROSCI.3638-11.2011.
58. Saheki Y, Bargmann CI. Presynaptic CaV2 calcium channel traffic requires CALF-1 and the alpha(2)delta subunit UNC-36. Nat Neurosci. 2009;12:1257–65. https://doi.org/10.1038/nn.2383.
59. Richmond JE, Weimer RM, Jorgensen EM. An open form of syntaxin bypasses the requirement for UNC-13 in vesicle priming. Nature. 2001;412:338–41. https://doi.org/10.1038/35085583.
60. Yazejian B, Sun XP, Grinnell AD. Tracking presynaptic Ca^{2+} dynamics during neurotransmitter release with Ca^{2+}-activated K^+ channels. Nat Neurosci. 2000;3:566–71. https://doi.org/10.1038/75737.
61. Protti DA, Uchitel OD. P/Q-type calcium channels activate neighboring calcium-dependent potassium channels in mouse motor nerve terminals. Pflugers Arch. 1997;434:406–12. https://doi.org/10.1007/s004240050414.
62. Berkefeld H, Sailer CA, Bildl W, Rohde V, Thumfart JO, Eble S, et al. BK_{Ca}-Cav channel complexes mediate rapid and localized Ca^{2+}-activated K^+ signaling. Science. 2006;314:615–20. https://doi.org/10.1126/science.1132915.
63. Issa NP, Hudspeth AJ. Clustering of Ca2+ channels and Ca(2+)-activated K+ channels at fluorescently labeled presynaptic active zones of hair cells. Proc Natl Acad Sci U S A. 1994;91:7578–82. https://doi.org/10.1073/pnas.91.16.7578.
64. Roberts WM, Jacobs RA, Hudspeth AJ. Colocalization of ion channels involved in frequency selectivity and synaptic transmission at presynaptic active zones of hair cells. J Neurosci. 1990;10:3664–84. https://doi.org/10.1523/JNEUROSCI.10-11-03664.1990.
65. Sakaba T, Ishikane H, Tachibana M. Ca2+ -activated K+ current at presynaptic terminals of goldfish retinal bipolar cells. Neurosci Res. 1997;27:219–28. https://doi.org/10.1016/s0168-0102(97)01155-3.
66. Raffaelli G, Saviane C, Mohajerani MH, Pedarzani P, Cherubini E. BK potassium channels control transmitter release at CA3-CA3 synapses in the rat hippocampus. J Physiol. 2004;557:147–57. https://doi.org/10.1113/jphysiol.2004.062661.
67. Wang ZW, Saifee O, Nonet ML, Salkoff L. SLO-1 potassium channels control quantal content of neurotransmitter release at the *C. elegans* neuromuscular junction. Neuron. 2001;32:867–81. https://doi.org/10.1016/s0896-6273(01)00522-0.
68. Liu Q, Chen B, Ge Q, Wang ZW. Presynaptic Ca^{2+}/calmodulin-dependent protein kinase II modulates neurotransmitter release by activating BK channels at *Caenorhabditis elegans* neuromuscular junction. J Neurosci. 2007;27:10404–13. https://doi.org/10.1523/JNEUROSCI.5634-06.2007.
69. Niu L, Li Y, Zong P, Liu P, Shui Y, Chen B, et al. Melatonin promotes sleep by activating the BK channel in *C. elegans*. Proc Natl Acad Sci U S A. 2020;117:25128–37. https://doi.org/10.1073/pnas.2010928117.

70. Chen B, Liu P, Hujber EJ, Li Y, Jorgensen EM, Wang ZW. AIP limits neurotransmitter release by inhibiting calcium bursts from the ryanodine receptor. Nat Commun. 2017;8:1380. https://doi.org/10.1038/s41467-017-01704-z.
71. Salkoff L, Wei AD, Baban B, Butler A, Fawcett G, Ferreira G, et al. Potassium channels in *C. elegans*. In: The*Celegans*ResearchCommunity, editors. Wormbook; 2005. https://doi.org/10.1895/wormbook.1.42.1., http://www.wormbook.org.
72. Bargmann CI. Neurobiology of the *Caenorhabditis elegans* genome. Science. 1998;282:2028–33. https://doi.org/10.1126/science.282.5396.2028.
73. Roshchin MV, Matlashov ME, Ierusalimsky VN, Balaban PM, Belousov VV, Kemenes G, et al. A BK channel-mediated feedback pathway links single-synapse activity with action potential sharpening in repetitive firing. Sci Adv. 2018;4:eaat1357. https://doi.org/10.1126/sciadv.aat1357.
74. Warbington L, Hillman T, Adams C, Stern M. Reduced transmitter release conferred by mutations in the slowpoke-encoded Ca2(+)-activated K+ channel gene of Drosophila. Invertebr Neurosci. 1996;2:51–60. https://doi.org/10.1007/BF02336660.
75. Xu JW, Slaughter MM. Large-conductance calcium-activated potassium channels facilitate transmitter release in salamander rod synapse. J Neurosci. 2005;25:7660–8. https://doi.org/10.1523/JNEUROSCI.1572-05.2005.
76. Pattillo JM, Yazejian B, DiGregorio DA, Vergara JL, Grinnell AD, Meriney SD. Contribution of presynaptic calcium-activated potassium currents to transmitter release regulation in cultured *Xenopus* nerve-muscle synapses. Neuroscience. 2001;102:229–40. https://doi.org/10.1016/s0306-4522(00)00453-x.
77. Abraham LS, Oh HJ, Sancar F, Richmond JE, Kim H. An alpha-catulin homologue controls neuromuscular function through localization of the dystrophin complex and BK channels in *Caenorhabditis elegans*. PLoS Genet. 2010;6:e1001077. https://doi.org/10.1371/journal.pgen.1001077.
78. Lyssand JS, Whiting JL, Lee KS, Kastl R, Wacker JL, Bruchas MR, et al. Alpha-dystrobrevin-1 recruits alpha-catulin to the alpha1D-adrenergic receptor/dystrophin-associated protein complex signalosome. Proc Natl Acad Sci U S A. 2010;107:21854–9. https://doi.org/10.1073/pnas.1010819107.
79. Baranauskas G, Tkatch T, Nagata K, Yeh JZ, Surmeier DJ. Kv3.4 subunits enhance the repolarizing efficiency of Kv3.1 channels in fast-spiking neurons. Nat Neurosci. 2003;6:258–66. https://doi.org/10.1038/nn1019.
80. Rudy B, McBain CJ. Kv3 channels: voltage-gated K+ channels designed for high-frequency repetitive firing. Trends Neurosci. 2001;24:517–26. https://doi.org/10.1016/s0166-2236(00)01892-0.
81. Kaczmarek LK, Zhang Y. Kv3 channels: enablers of rapid firing, neurotransmitter release, and neuronal endurance. Physiol Rev. 2017;97:1431–68. https://doi.org/10.1152/physrev.00002.2017.
82. Elezgarai I, Diez J, Puente N, Azkue JJ, Benitez R, Bilbao A, et al. Subcellular localization of the voltage-dependent potassium channel Kv3.1b in postnatal and adult rat medial nucleus of the trapezoid body. Neuroscience. 2003;118:889–98. https://doi.org/10.1016/s0306-4522(03)00068-x.
83. Richardson A, Ciampani V, Stancu M, Bondarenko K, Newton S, Steinert JR, et al. Kv3.3 subunits control presynaptic action potential waveform and neurotransmitter release at a central excitatory synapse. elife. 2022;11:e75219. https://doi.org/10.7554/eLife.75219.
84. Chow A, Erisir A, Farb C, Nadal MS, Ozaita A, Lau D, et al. K(+) channel expression distinguishes subpopulations of parvalbumin- and somatostatin-containing neocortical interneurons. J Neurosci. 1999;19:9332–45. https://doi.org/10.1523/JNEUROSCI.19-21-09332.1999.
85. Yeung SY, Thompson D, Wang Z, Fedida D, Robertson B. Modulation of Kv3 subfamily potassium currents by the sea anemone toxin BDS: significance for CNS and biophysical studies. J Neurosci. 2005;25:8735–45. https://doi.org/10.1523/JNEUROSCI.2119-05.2005.

86. Martina M, Metz AE, Bean BP. Voltage-dependent potassium currents during fast spikes of rat cerebellar Purkinje neurons: inhibition by BDS-I toxin. J Neurophysiol. 2007;97:563–71. https://doi.org/10.1152/jn.00269.2006.
87. Coetzee WA, Amarillo Y, Chiu J, Chow A, Lau D, McCormack T, et al. Molecular diversity of K+ channels. Ann N Y Acad Sci. 1999;868:233–85. https://doi.org/10.1111/j.1749-6632.1999.tb11293.x.
88. Goldberg EM, Watanabe S, Chang SY, Joho RH, Huang ZJ, Leonard CS, et al. Specific functions of synaptically localized potassium channels in synaptic transmission at the neocortical GABAergic fast-spiking cell synapse. J Neurosci. 2005;25:5230–5. https://doi.org/10.1523/JNEUROSCI.0722-05.2005.
89. Sekirnjak C, Martone ME, Weiser M, Deerinck T, Bueno E, Rudy B, et al. Subcellular localization of the K+ channel subunit Kv3.1b in selected rat CNS neurons. Brain Res. 1997;766:173–87. https://doi.org/10.1016/s0006-8993(97)00527-1.
90. Rowan MJ, Tranquil E, Christie JM. Distinct Kv channel subtypes contribute to differences in spike signaling properties in the axon initial segment and presynaptic boutons of cerebellar interneurons. J Neurosci. 2014;34:6611–23. https://doi.org/10.1523/JNEUROSCI.4208-13.2014.
91. Rowan MJM, Christie JM. Rapid state-dependent alteration in K(v)3 channel availability drives flexible synaptic signaling dependent on somatic subthreshold depolarization. Cell Rep. 2017;18:2018–29. https://doi.org/10.1016/j.celrep.2017.01.068.
92. Trussell LO, Roberts MT. The role of potassium channels in the regulation of neurotransmitter release. In: Wang ZW, editor. Molecular mechanisms of neurotransmitter release. Totowa: Humana Press; 2008. p. 171–85.
93. Wang H, Kunkel DD, Schwartzkroin PA, Tempel BL. Localization of Kv1.1 and Kv1.2, two K channel proteins, to synaptic terminals, somata, and dendrites in the mouse brain. J Neurosci. 1994;14:4588–99. https://doi.org/10.1523/JNEUROSCI.14-08-04588.1994.
94. Sheng M, Tsaur ML, Jan YN, Jan LY. Subcellular segregation of two A-type K+ channel proteins in rat central neurons. Neuron. 1992;9:271–84. https://doi.org/10.1016/0896-6273(92)90166-b.
95. Sheng M, Liao YJ, Jan YN, Jan LY. Presynaptic A-current based on heteromultimeric K+ channels detected in vivo. Nature. 1993;365:72–5. https://doi.org/10.1038/365072a0.
96. Shu Y, Yu Y, Yang J, McCormick DA. Selective control of cortical axonal spikes by a slowly inactivating K+ current. Proc Natl Acad Sci U S A. 2007;104:11453–8. https://doi.org/10.1073/pnas.0702041104.
97. Goldberg EM, Clark BD, Zagha E, Nahmani M, Erisir A, Rudy B. K+ channels at the axon initial segment dampen near-threshold excitability of neocortical fast-spiking GABAergic interneurons. Neuron. 2008;58:387–400. https://doi.org/10.1016/j.neuron.2008.03.003.
98. Gazula VR, Strumbos JG, Mei X, Chen H, Rahner C, Kaczmarek LK. Localization of Kv1.3 channels in presynaptic terminals of brainstem auditory neurons. J Comp Neurol. 2010;518:3205–20. https://doi.org/10.1002/cne.22393.
99. Harvey AL. Twenty years of dendrotoxins. Toxicon. 2001;39:15–26. https://doi.org/10.1016/s0041-0101(00)00162-8.
100. Werkman TR, Gustafson TA, Rogowski RS, Blaustein MP, Rogawski MA. Tityustoxin-K alpha, a structurally novel and highly potent K+ channel peptide toxin, interacts with the alpha-dendrotoxin binding site on the cloned Kv1.2 K+ channel. Mol Pharmacol. 1993;44:430–6.
101. Bartok A, Toth A, Somodi S, Szanto TG, Hajdu P, Panyi G, et al. Margatoxin is a non-selective inhibitor of human Kv1.3 K+ channels. Toxicon. 2014;87:6–16. https://doi.org/10.1016/j.toxicon.2014.05.002.
102. Dodson PD, Barker MC, Forsythe ID. Two heteromeric Kv1 potassium channels differentially regulate action potential firing. J Neurosci. 2002;22:6953–61. https://doi.org/10.1523/JNEUROSCI.22-16-06953.2002.

103. Dodson PD, Billups B, Rusznak Z, Szucs G, Barker MC, Forsythe ID. Presynaptic rat Kv1.2 channels suppress synaptic terminal hyperexcitability following action potential invasion. J Physiol. 2003;550:27–33. https://doi.org/10.1113/jphysiol.2003.046250.
104. Klug A, Trussell LO. Activation and deactivation of voltage-dependent K+ channels during synaptically driven action potentials in the MNTB. J Neurophysiol. 2006;96:1547–55. https://doi.org/10.1152/jn.01381.2005.
105. Zhou J, Brown AM, Lackey EP, Arancillo M, Lin T, Sillitoe RV. Purkinje cell neurotransmission patterns cerebellar basket cells into zonal modules defined by distinct pinceau sizes. elife. 2020;9:e55569. https://doi.org/10.7554/eLife.55569.
106. McNamara NM, Muniz ZM, Wilkin GP, Dolly JO. Prominent location of a K+ channel containing the alpha subunit Kv 1.2 in the basket cell nerve terminals of rat cerebellum. Neuroscience. 1993;57:1039–45. https://doi.org/10.1016/0306-4522(93)90047-j.
107. Wang H, Kunkel DD, Martin TM, Schwartzkroin PA, Tempel BL. Heteromultimeric K+ channels in terminal and juxtaparanodal regions of neurons. Nature. 1993;365:75–9. https://doi.org/10.1038/365075a0.
108. Southan AP, Robertson B. Electrophysiological characterization of voltage-gated K(+) currents in cerebellar basket and purkinje cells: Kv1 and Kv3 channel subfamilies are present in basket cell nerve terminals. J Neurosci. 2000;20:114–22. https://doi.org/10.1523/JNEUROSCI.20-01-00114.2000.
109. Southan AP, Robertson B. Patch-clamp recordings from cerebellar basket cell bodies and their presynaptic terminals reveal an asymmetric distribution of voltage-gated potassium channels. J Neurosci. 1998;18:948–55. https://doi.org/10.1523/JNEUROSCI.18-03-00948.1998.
110. Kole MH, Letzkus JJ, Stuart GJ. Axon initial segment Kv1 channels control axonal action potential waveform and synaptic efficacy. Neuron. 2007;55:633–47. https://doi.org/10.1016/j.neuron.2007.07.031.
111. Yang Q, Chen SR, Li DP, Pan HL. Kv1.1/1.2 channels are downstream effectors of nitric oxide on synaptic GABA release to preautonomic neurons in the paraventricular nucleus. Neuroscience. 2007;149:315–27. https://doi.org/10.1016/j.neuroscience.2007.08.007.
112. Finnegan TF, Chen SR, Pan HL. Mu opioid receptor activation inhibits GABAergic inputs to basolateral amygdala neurons through Kv1.1/1.2 channels. J Neurophysiol. 2006;95:2032–41. https://doi.org/10.1152/jn.01004.2005.
113. Selyanko AA, Hadley JK, Wood IC, Abogadie FC, Jentsch TJ, Brown DA. Inhibition of KCNQ1-4 potassium channels expressed in mammalian cells via M1 muscarinic acetylcholine receptors. J Physiol. 2000;522(Pt 3):349–55. https://doi.org/10.1111/j.1469-7793.2000.t01-2-00349.x.
114. Leao RN, Tan HM, Fisahn A. Kv7/KCNQ channels control action potential phasing of pyramidal neurons during hippocampal gamma oscillations in vitro. J Neurosci. 2009;29:13353–64. https://doi.org/10.1523/JNEUROSCI.1463-09.2009.
115. Miceli F, Cilio MR, Taglialatela M, Bezanilla F. Gating currents from neuronal K(V)7.4 channels: general features and correlation with the ionic conductance. Channels (Austin). 2009;3:274–83.
116. Brown DA, Passmore GM. Neural KCNQ (Kv7) channels. Br J Pharmacol. 2009;156:1185–95. https://doi.org/10.1111/j.1476-5381.2009.00111.x.
117. Huang H, Trussell LO. KCNQ5 channels control resting properties and release probability of a synapse. Nat Neurosci. 2011;14:840–7. https://doi.org/10.1038/nn.2830.
118. Caminos E, Garcia-Pino E, Juiz JM. Loss of auditory activity modifies the location of potassium channel KCNQ5 in auditory brainstem neurons. J Neurosci Res. 2015;93:604–14. https://doi.org/10.1002/jnr.23516.
119. Zhang Y, Li D, Darwish Y, Fu X, Trussell LO, Huang H. KCNQ channels enable reliable presynaptic spiking and synaptic transmission at high frequency. J Neurosci. 2022;42:3305–15. https://doi.org/10.1523/JNEUROSCI.0363-20.2022.

120. Vervaeke K, Gu N, Agdestein C, Hu H, Storm JF. Kv7/KCNQ/M-channels in rat glutamatergic hippocampal axons and their role in regulation of excitability and transmitter release. J Physiol. 2006;576:235–56. https://doi.org/10.1113/jphysiol.2006.111336.
121. Tsentsevitsky AN, Khaziev EF, Kovyazina IV, Petrov AM. GIRK channel as a versatile regulator of neurotransmitter release via L-type Ca(2+) channel-dependent mechanism in the neuromuscular junction. Neuropharmacology. 2022;209:109021. https://doi.org/10.1016/j.neuropharm.2022.109021.
122. Vazquez-Vazquez H, Gonzalez-Sandoval C, Vega AV, Arias-Montano JA, Barral J. Histamine H(3) receptor activation modulates glutamate release in the corticostriatal synapse by acting at Ca(V)2.1 (P/Q-type) calcium channels and GIRK (K(IR)3) potassium channels. Cell Mol Neurobiol. 2022;42:817–28. https://doi.org/10.1007/s10571-020-00980-6.
123. Kaczmarek LK. Slack, slick and sodium-activated potassium channels. ISRN Neurosci. 2013;2013:354262. https://doi.org/10.1155/2013/354262.
124. Yuan A, Santi CM, Wei A, Wang ZW, Pollak K, Nonet M, et al. The sodium-activated potassium channel is encoded by a member of the *Slo* gene family. Neuron. 2003;37:765–73. https://doi.org/10.1016/s0896-6273(03)00096-5.
125. Bhattacharjee A, Gan L, Kaczmarek LK. Localization of the Slack potassium channel in the rat central nervous system. J Comp Neurol. 2002;454:241–54. https://doi.org/10.1002/cne.10439.
126. Bhattacharjee A, Joiner WJ, Wu M, Yang Y, Sigworth FJ, Kaczmarek LK. Slick (Slo2.1), a rapidly-gating sodium-activated potassium channel inhibited by ATP. J Neurosci. 2003;23:11681–91. https://doi.org/10.1523/JNEUROSCI.23-37-11681.2003.
127. Budelli G, Hage TA, Wei A, Rojas P, Jong YJ, O'Malley K, et al. Na^+-activated K^+ channels express a large delayed outward current in neurons during normal physiology. Nat Neurosci. 2009;12:745–50. https://doi.org/10.1038/nn.2313.
128. Lu S, Das P, Fadool DA, Kaczmarek LK. The slack sodium-activated potassium channel provides a major outward current in olfactory neurons of $Kv1.3^{-/-}$ super-smeller mice. J Neurophysiol. 2010;103:3311–9. https://doi.org/10.1152/jn.00607.2009.
129. Martinez-Espinosa PL, Wu J, Yang C, Gonzalez-Perez V, Zhou H, Liang H, et al. Knockout of Slo2.2 enhances itch, abolishes KNa current, and increases action potential firing frequency in DRG neurons. elife. 2015;4:e10013. https://doi.org/10.7554/eLife.10013.
130. Barcia G, Fleming MR, Deligniere A, Gazula VR, Brown MR, Langouet M, et al. *De novo* gain-of-function *KCNT1* channel mutations cause malignant migrating partial seizures of infancy. Nat Genet. 2012;44:1255–9. https://doi.org/10.1038/ng.2441.
131. Heron SE, Smith KR, Bahlo M, Nobili L, Kahana E, Licchetta L, et al. Missense mutations in the sodium-gated potassium channel gene *KCNT1* cause severe autosomal dominant nocturnal frontal lobe epilepsy. Nat Genet. 2012;44:1188–90. https://doi.org/10.1038/ng.2440.
132. Ishii A, Shioda M, Okumura A, Kidokoro H, Sakauchi M, Shimada S, et al. A recurrent *KCNT1* mutation in two sporadic cases with malignant migrating partial seizures in infancy. Gene. 2013;531:467–71. https://doi.org/10.1016/j.gene.2013.08.096.
133. Martin HC, Kim GE, Pagnamenta AT, Murakami Y, Carvill GL, Meyer E, et al. Clinical whole-genome sequencing in severe early-onset epilepsy reveals new genes and improves molecular diagnosis. Hum Mol Genet. 2014;23:3200–11. https://doi.org/10.1093/hmg/ddu030.
134. Vanderver A, Simons C, Schmidt JL, Pearl PL, Bloom M, Lavenstein B, et al. Identification of a novel *de novo* p.Phe932Ile *KCNT1* mutation in a patient with leukoencephalopathy and severe epilepsy. Pediatr Neurol. 2014;50:112–4. https://doi.org/10.1016/j.pediatrneurol.2013.06.024.
135. Yuan A, Dourado M, Butler A, Walton N, Wei A, Salkoff L. SLO-2, a K^+ channel with an unusual Cl^- dependence. Nat Neurosci. 2000;3:771–9. https://doi.org/10.1038/77670.
136. Liu P, Ge Q, Chen B, Salkoff L, Kotlikoff MI, Wang ZW. Genetic dissection of ion currents underlying all-or-none action potentials in *C. elegans* body-wall muscle cells. J Physiol. 2011;589:101–17. https://doi.org/10.1113/jphysiol.2010.200683.

137. Liu Q, Kidd PB, Dobosiewicz M, Bargmann CI. C. elegans AWA olfactory neurons fire calcium-mediated all-or-none action potentials. Cell. 2018;175:57–70. e17. https://doi.org/10.1016/j.cell.2018.08.018.
138. Gao S, Zhen M. Action potentials drive body wall muscle contractions in *Caenorhabditis elegans*. Proc Natl Acad Sci U S A. 2011;108:2557–62. https://doi.org/10.1073/pnas.1012346108.
139. Jiang J, Su Y, Zhang R, Li H, Tao L, Liu Q. C. elegans enteric motor neurons fire synchronized action potentials underlying the defecation motor program. Nat Commun. 2022;13:2783. https://doi.org/10.1038/s41467-022-30452-y.
140. Liu Q, Hollopeter G, Jorgensen EM. Graded synaptic transmission at the *Caenorhabditis elegans* neuromuscular junction. Proc Natl Acad Sci U S A. 2009;106:10823–8. https://doi.org/10.1073/pnas.0903570106.
141. Liu P, Chen B, Wang ZW. Postsynaptic current bursts instruct action potential firing at a graded synapse. Nat Commun. 2013;4:1911. https://doi.org/10.1038/ncomms2925.
142. Liu P, Chen B, Mailler R, Wang ZW. Antidromic-rectifying gap junctions amplify chemical transmission at functionally mixed electrical-chemical synapses. Nat Commun. 2017;8:14818. https://doi.org/10.1038/ncomms14818.
143. Liu P, Chen B, Wang ZW. SLO-2 potassium channel is an important regulator of neurotransmitter release in Caenorhabditis elegans. Nat Commun. 2014;5:5155. https://doi.org/10.1038/ncomms6155.
144. Lucchesi K, Moczydlowski E. Subconductance behavior in a maxi Ca2(+)-activated K+ channel induced by dendrotoxin-I. Neuron. 1990;4:141–8. https://doi.org/10.1016/0896-6273(90)90450-t.
145. Liu P, Jo S, Bean BP. Modulation of neuronal sodium channels by the sea anemone peptide BDS-I. J Neurophysiol. 2012;107:3155–67. https://doi.org/10.1152/jn.00785.2011.
146. Imredy JP, Chen C, MacKinnon R. A snake toxin inhibitor of inward rectifier potassium channel ROMK1. Biochemistry. 1998;37:14867–74. https://doi.org/10.1021/bi980929k.

Regulation of Presynaptic Release Machinery by Cell Adhesion Molecules

Motokazu Uchigashima, Yasunori Hayashi, and Kensuke Futai

Abstract The synapse is a highly specialized asymmetric structure that transmits and stores information in the brain. The size of pre- and postsynaptic structures and function is well coordinated at the individual synapse level. For example, large postsynaptic dendritic spines have a larger postsynaptic density with higher α-amino-3-hydroxy-5-methyl-4-isoxazole propionic acid receptor (AMPAR) number on their surface, while juxtaposing presynaptic terminals have a larger active zone and higher release probability. This indicates that pre- and postsynaptic domains bidirectionally communicate to coordinate assembly of specific molecules on both sides of the synaptic cleft. Cell adhesion molecules (CAMs) that localize at synapses form transsynaptic protein interactions across the synaptic cleft and play important roles in synapse formation and regulation. The extracellular domain of CAMs is essential for specific synapse formation and function. In contrast, the intracellular domain is necessary for binding with synaptic molecules and signal transduction. Therefore, CAMs play an essential role on synapse function and structure. In fact, ample evidence indicates that transsynaptic CAMs instruct and modulate functions at presynaptic sites. This chapter focuses on transsynaptic protein interactions that regulate presynaptic functions emphasizing the role of neuronal CAMs and the intracellular mechanism of their regulation.

M. Uchigashima
Department of Cellular Neuropathology, Brain Research Institute, Niigata University, Niigata, Japan

Y. Hayashi
Department of Pharmacology, Kyoto University Graduate School of Medicine, Kyoto, Japan

K. Futai (✉)
Brudnick Neuropsychiatric Research Institute, Department of Neurobiology, University of Massachusetts Chan Medical School, Worcester, MA, USA
e-mail: kensuke.futai@umassmed.edu

Z.-W. Wang (ed.), *Molecular Mechanisms of Neurotransmitter Release*,
Advances in Neurobiology 33, https://doi.org/10.1007/978-3-031-34229-5_13

Keywords Release probability · Synaptic transmission · Cell adhesion molecules · Cadherin · Catenin · Neuroligin · Neurexin · mGluR · Elfin · Eph receptor · Ephrin · Retrograde messenger · Liquid–liquid phase separation

1 Introduction

The synapse is a highly specialized asymmetric structure that transmits and stores information in the brain. The majority of synapses in the central nervous system (CNS) are chemical synapses, which are physically separated into pre- and postsynaptic structures by the synaptic cleft. Although these structures are discrete sites with specific molecular machinery, their functions are well coordinated at the individual synapse level. For example, in excitatory synapses on hippocampal and cortical neurons, large postsynaptic dendritic spines have a larger postsynaptic density with a greater number of α-amino-3-hydroxy-5-methyl-4-isoxazole propionic acid receptors (AMPARs) on the surface. At the same time, juxtaposing presynaptic terminals have a larger active zone, more docked vesicles, and higher release probability. Intuitively, these observations suggest that larger synapses contribute to high-fidelity synaptic transmission [1–7]. During long-term potentiation (LTP) of synaptic transmission, a persistent expansion of postsynaptic dendritic spines [8, 9] is accompanied by an enlargement of presynaptic structures [10] indicating that pre- and postsynaptic sites coordinate with one another to bring about structural changes. Such coordination of pre- and postsynaptic structure and function ensures more efficient transmission.

Modifications to synaptic elements are not limited in the anterograde direction in which the presynaptic side instructs postsynaptic structure and function. Rather, recent mounting evidence indicates that postsynaptic sites can also retrogradely instruct presynaptic changes. For example, it has been described in cortical and hippocampal circuits that postsynaptic neurons retrogradely regulate presynaptic release probability [11–19]. Hippocampal CA3 neurons project Schaffer collateral fibers and form excitatory synapses with both CA1 pyramidal neurons and inhibitory interneurons. Importantly, the same Schaffer collateral excitatory inputs have different release probabilities depending on the type of postsynaptic neurons they synapse with, indicating that there are target neuron-specific retrograde signals that dictate presynaptic function [12, 14]. Diffusible molecules such as endocannabinoids are considered target cell-specific retrograde messengers (reviews are available from other groups [20, 21]). In addition, recent studies have revealed that CAM-mediated protein complexes also regulate target cell-specific presynaptic function.

During CNS development, CAMs play vital roles in synapse specification and formation by establishing transsynaptic interactions between axonal and dendritic segments [22]. In matured synapses, CAMs are essential for synapse function, plasticity, and maintenance [23–25]. Numerous CAMs, such as cadherin, neuroligin, neurexin, extracellular leucine-rich repeat fibronectin type

III domain-containing protein (Elfn), ephrin, SynCAM, delta glutamate (GluD) receptor, and neuronal pentraxin molecules, generate a vast array of possible combinations between pre- and postsynaptic CAMs [22, 23]. In addition to canonical interactions between pre- and postsynaptic CAMs, non-canonical interactions between presynaptic G-protein-coupled receptors (GPCRs) and postsynaptic CAMs have also been identified [22]. Although some specific transsynaptic interactions of CAMs have been reported to underlie distinct synaptic properties [26–28], elucidating synaptic CAM complexes that dictate synapse identity and function remains a major challenge. Recent multidisciplinary studies integrating electrophysiology, imaging, and mouse genetics have revealed that two CAM-mediated canonical and CAM- and receptor-mediated non-canonical transsynaptic interactions regulate presynaptic functions [22, 23].

Long-term potentiation (LTP) is a phenomenon in which a transient burst of synaptic input causes a long-lasting increase in subsequent synaptic transmission [29]. It is well established that LTP induction requires postsynaptic depolarization combined with the activation of *N*-methyl-*D*-aspartate receptors (NMDARs), and resultant influx of calcium (Ca^{2+}). This triggers a series of biochemical processes including the activation of Ca^{2+}/calmodulin-dependent protein kinase II (CaMKII). Expression of LTP is achieved by increasing the number of AMPA receptors (AMPARs) at the synapse through activity-dependent change in AMPAR trafficking and persistent expansion of synaptic structures, which is known as structural LTP (sLTP) [9, 30, 31]. This indicates that structural elements, including CAMs on both sides of the synaptic cleft, coordinate the assembly of synaptic proteins for activity-dependent structural changes.

In this chapter, we first describe CAMs that regulate presynaptic release machinery. Next, we discuss possible mechanisms underlying CAM-mediated regulation of synapse function and structure during plasticity. Finally, we discuss the possibility of an activity-dependent mechanism that sub-synaptically segregates different CAMs.

2 Roles of Transsynaptic Adhesion Molecules in Presynaptic Functions

Presynaptic cell adhesion molecules (CAMs) directly regulate the presynaptic neurotransmitter release via direct interaction with the active zone proteins. Postsynaptic CAMs can retrogradely modulate presynaptic neurotransmitter release through interacting with presynaptic CAMs and GPCRs, which regulate the presynaptic neurotransmitter release via direct or indirect interaction with the transmitter release machinery. This section summarizes the basic properties of several CAMs such as Neurexin, Cadherin, Elfn, and Ephrin, and their functional roles in the neurotransmitter release.

2.1 Neurexin-Mediated Transsynaptic Signaling

Neurexins (Nrxns) were isolated as a family of brain membrane surface proteins that bind α-latrotoxin, a neurotoxin from black widow spider (*Latrodectus mactans*) that functions as a potent trigger for neurotransmitter release [32]. Nrxns are encoded by three genes (Nrxn1–3) and transcribed into longer α (αNrxn1, αNrxn2, αNrxn3), shorter β (βNrxn1, βNrxn2, βNrxn3), and Nrxn1-specific γ (γNrxn1) isoforms each under different promoter [33, 34]. Nrxns are a single transmembrane molecule composed of an extracellular domain carrying an isoform-specific N-terminus and conserved transmembrane and intracellular domains. Extracellularly, Nrxns have various number of LNS (laminin, neurexin, sex-hormone-binding protein) and EGF (epidermal growth factor)-like domains due to extensive alternative splicing, which can generate thousands of Nrxn isoforms [35–39]. Through these domains, Nrxns can bind to specific postsynaptic binding partners [40–42]. Neuroligins (Nlgns) [43, 44], LRRTMs (leucine-rich repeat transmembrane neuronal proteins) [45, 46], $GABA_A$ receptors [47], cerebellins [48, 49], C1q-like (C1ql) proteins [50], SPARCL1 (secreted protein acidic and rich in cysteines 1, also referred to as Hevin) [51], and latrophilins [52] can bind to the sixth LNS domain present in both αNrxns and βNrxns. Interestingly, a variety of molecules critical for synaptogenesis have been reported to bind to specific Nrxn isoforms. For example, neurexophilins [53] and dystroglycan [54] bind to the second LNS domain specific to αNrxns. lgSF21 can promote presynaptic differentiation of inhibitory synapses through the first LNS domain of αNrxn2 [55]. C1ql2/3 can interact with the fifth splicing site of α/βNrxn3, and recruit kainate receptors to synaptic sites [50]. The extracellular domain of αNrxns may further interact with presynaptic α2δ-1 auxiliary subunit of P/Q-type Ca^{2+} channels (Cav2.1) in a cis-configuration, limiting the mobility of a2δ-1 subunits on the cell surface rather than forming a stable complex with α2δ-1 subunits [56]. Intracellularly, Nrxns bind to CASK (mLin-2) and Mint through a PDZ domain-binding motif [57] and also interact with 4.1 protein characterized by FERM (F for 4.1 protein, E for ezrin, R for radixin, and M for moesin) domain proteins [58]. Importantly, CASK, in turn, interacts with Mint, syntenin, and synaptotagmin. Thus, Nrxn is eventually linked to the presynaptic vesicle release machinery.

Nrxns mediate many regulatory functions [24]. One of the most notable functions of Nrxns is the regulation of presynaptic release. Knockout (KO) of all three Nrxn genes causes a decrease in evoked excitatory postsynaptic current (EPSC) amplitude and an increase in paired-pulse ratio at calyx of Held and cerebellar climbing fiber excitatory synapses or cortical somatostatin-positive (Sst+) inhibitory synapses, suggesting a decrease in presynaptic release probability [59, 60]. shRNA-mediated knockdown (KD) of all Nrxn genes in hippocampal primary cultures also lowers synaptic vesicle exocytosis monitored by a genetically encoded exocytosis sensor synapto-pHluorin [61]. Single KO of Nrxn2 gene reduces spontaneous neurotransmitter release at cortical excitatory synapses without changing synapse density [62]. Specific deletion of α isoform of Nrxn3 gene shows a selective

decrease in miniature inhibitory postsynaptic potential (mIPSP) frequency and evoked inhibitory postsynaptic current (IPSC) amplitude and increase in IPSC paired-pulse ratio in cultured mitral/tufted cells of olfactory bulb, indicating a decrease in presynaptic release probability [63]. Ca^{2+} channel dysfunction in the presynaptic active zone is noted as a major mechanism underlying functional impairment of presynaptic release in Nrxn loss-of-function models. KO of all three Nrxn genes disrupts the spatial coupling of Ca^{2+} channels with synaptic vesicles, and removes P/Q-type Ca^{2+} channels from the active zone at calyx synapses [60]. Furthermore, KO of all three Nrxn genes reduces the function of Ca^{2+}-activated BK potassium channels, whose activation depends on their tight association with presynaptic Ca^{2+} channels [60].

αNrxns and βNrxns may distinctly regulate presynaptic release functions through different molecular mechanisms. αNrxn-specific KO impairs Ca^{2+}-dependent neurotransmitter release mediated by P/Q- or N-type Ca^{2+} channels in the brain stem, which can be rescued by αNrxn1 but not βNrxn1 [64, 65]. These findings are supported by a unique cis interaction between αNrxns and the α2δ-1 auxiliary subunit of P/Q-type Ca^{2+} channels [56]. βNrxn-specific KO also impairs action potential-induced Ca^{2+} influx into presynaptic terminals at excitatory synapses in cortical primary cultures and hippocampal acute slices [66]. However, this impairment is caused partly by an increase in the postsynaptic production of endocannabinoids, which retrogradely inhibit neurotransmitter release via the activation of cannabinoid CB1 receptor [66]. On the other hand, the presynaptic phenotype in Nrxn loss-of-function animals depends on the type of synapses deficient in Nrxns. In pan-Nrxn KO mice, presynaptic release probability is not altered at cortical parvalbumin (Pv)+ inhibitory synapses [59]. Nrxn3 KO does not change presynaptic release probability at hippocampal excitatory and inhibitory synapses and olfactory excitatory synapses [63]. These presynaptic phenotypes vary among brain regions, synapse types, and Nrxn loss-of-function model examined, which can be partly due to the diversity in expression patterns of Nrxn genes and complicated developmental compensatory effects of Nrxns or their binding partners.

Presynaptic functions of Nrxns are also mediated by transsynaptic interactions with postsynaptic binding partners such as Nlgns. Nlgns are encoded by four and five different genes in rodents and humans, respectively. They have one transmembrane region and an extracellular domain that is homologous to acetylcholinesterase but is catalytically inactive. The extracellular domain is crucial for generating an interface for Nrxn binding, which can be regulated by the presence or absence of the insertion at one or two alternative splicing sites for each Nlgn [67]. The corresponding binding interface of Nrxns depends on distinct Nrxn splice variants [24]. Thus, different pairs of Nrxn-Nlgn variants differ in their binding affinities [40, 41]. Intracellularly, Nlgns have a PDZ domain-binding motif that binds to major postsynaptic scaffold proteins, including PSD-95, SAP102, Shank, SSCAM, PICK1 (protein interacting with C-kinase-1), SPAR, and GOPC [68]. Through these interactions, Nrxns and Nlgns bridge the presynaptic release machinery and postsynaptic receptor complex. In an in vitro co-culture assay with neuronal and non-neuronal cells, Nlgns

can induce presynaptic differentiation to recruit presynaptic proteins [69]. Triple KO of Nlgn1–3 reduces the frequencies of both miniature excitatory postsynaptic currents (mEPSCs) and miniature inhibitory postsynaptic currents (mIPSCs). Since synaptic density is normal in triple KO compared to wild-type mice, the decreased frequencies of mEPSCs and mIPSCs reflect reduced presynaptic release probability [70]. In organotypic hippocampal slice cultures, manipulating postsynaptic expression levels of different Nlgns alters presynaptic release probability at specific synapses [27, 71–74]. Simultaneous manipulation of pre- and postsynaptic molecules in organotypic slice cultures is useful to examine functional roles of specific transsynaptic interactions at a given synapse [75, 76]. This approach clarified that Nlgn-mediated alteration of presynaptic release probability is achieved by its Nlgn isoform-specific interactions with presynaptic Nrxns [27, 71, 72]. For example, (i) βNrxn1-AS4 (without the insertion of an exon at the alternative splicing site 4) and Nlgn1+AB (with the insertion of an exon at the alternative splicing sites A and B) pair at hippocampal CA3–CA3 excitatory synapses (Fig. 1a), (ii) αNrxn1-AS4 and Nlgn2+A pair at hippocampal CA1 inhibitory synapses (Fig. 1b), and (iii) αNrxn1+AS4 and Nlgn3Δ (without any exon insertions at any of the alternative splicing sites) pair at hippocampal CA1 inhibitory synapses expressing cholecystokinin, CB1, and vesicular glutamate transporter type 3 (VGluT3) (Fig. 1c) [27, 71, 72]. Such isoform-specific interactions between Nrxns and Nlgn are critical for regulating presynaptic release probability at given synapses. These findings raise the notion that specific Nrxn–Nlgn transsynaptic interactions are responsible for input cell type-dependent molecular mechanisms that control presynaptic release function. Importantly, this view is supported by the distinct expression patterns of Nrxns and Nlgns at individual synapses based on diverse expression patterns of Nrxns in presynaptic neurons across different brain regions and cell types [35, 78, 79] and postsynaptic Nlgn expression that depends on transsynaptic regulation from distinct input cell types [80–85].

Other postsynaptic molecules that bind to Nrxns can be involved in the retrograde modulation of presynaptic release functions via interacting with Nrxns at different synapses. For instance, the deletion of postsynaptic IgSF21, which can bind to αNrxn2, reduces the frequency of mIPSCs and the number of docked synaptic vesicles at hippocampal inhibitory synapses without altering synapse density, suggesting a decrease in presynaptic release probability (Fig. 1d) [55]. Therefore, transsynaptic interactions between αNrxn2 and IgSF21 may contribute to the diversification of presynaptic release function. It has been reported that extracellular C1ql proteins (C1ql2 and C1ql3) and cerebellin1 precursor protein (Cbln1) bridge postsynaptic kainate and delta glutamate (GluD) receptors with presynaptic Nrxns in hippocampal mossy fiber CA3 and cerebellar parallel fiber Purkinje cell synapses, respectively (Fig. 1e, f) [48–50]. Interestingly, reduced release probability has been reported in GluD2 KO mice, which strongly suggests that transsynaptic Nrxn–Cbln1–GluD2 complexes (Fig. 1f) are important for presynaptic structure and/or function [86, 87].

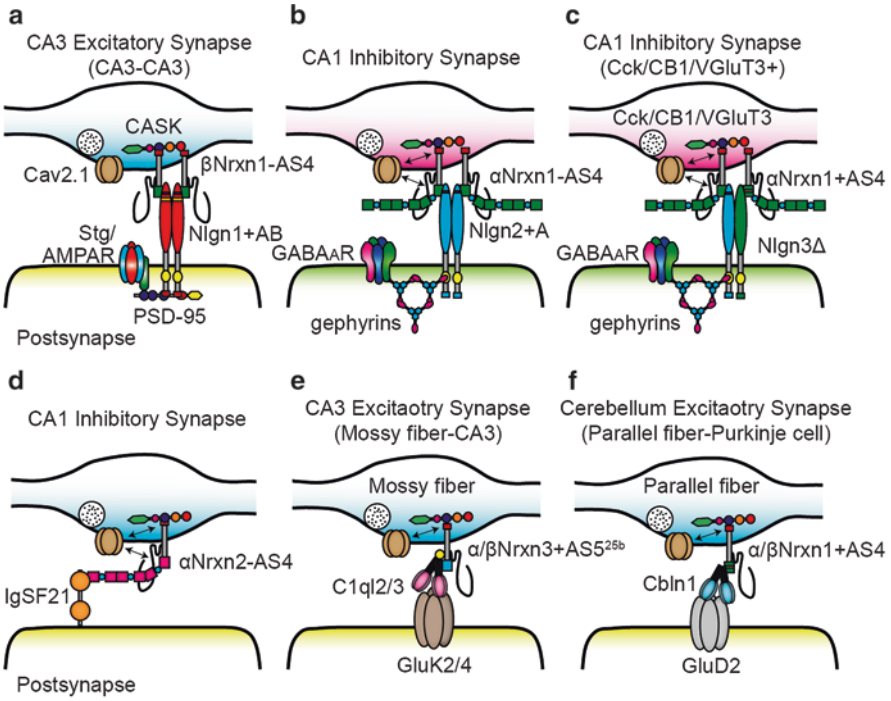

Fig. 1 Schematic diagrams of presynaptic regulation by Nrxn-mediated cis- and transsynaptic protein interactions in the hippocampus. (**a**) Presynaptic βNrxn1-AS4 (βNeurexin1-AS4) and postsynaptic Nlgn1+AB (Neuroligin1+AB) regulate excitatory synaptic transmission in the hippocampal CA3 associational circuit. Nlgn1 forms complexes with AMPARs through PSD-95 and AMPAR auxiliary subunit Stg (stargazin). (**b**) The interaction between presynaptic αNrxn1-AS4 and postsynaptic Nlgn2+A regulates synaptic release at hippocampal CA1 inhibitory synapses. Nlgn2 forms protein complexes with $GABA_AR$s through gephyrin. αNrxn1 regulates P/Q-type Ca^{2+} channel function through cis interactions. (**c**) Postsynaptic Nlgn3Δ regulates presynaptic release through its interaction with presynaptic αNrxn1+AS4 at CA1 Cck/CB1/VGluT3+ inhibitory synapses. (**d**) Postsynaptic IgSF21 regulates inhibitory synaptic function through its interaction with presynaptic αNrxn2 in the hippocampal CA1 region. (**e**) Extracellular C1ql2/3 bridges postsynaptic kainate 2/4 receptors and presynaptic $α/βNrxn3+AS5^{25b}$ at hippocampal mossy fiber CA3 synapses to regulate excitatory synaptic transmission. (**f**) Extracellular Cbln1 bridges postsynaptic GluD2 receptors and presynaptic α/βNrxn1+AS4 at cerebellar parallel fiber Purkinje cell synapses to regulate excitatory synaptic transmission. (Modified from Uchigashima et al. [77])

2.2 Cadherin-Catenin-Mediated Transsynaptic Signaling

The cadherin superfamily consists of more than 100 members in vertebrates [88]. They are classified into subfamilies that are called classical cadherins and non-classical cadherins. Classical cadherins include N-cadherin and E-cadherin, while non-classical cadherins include desmosomal cadherins, protocadherins, Flamingo/CELSRs (*c*adherin, *E*GF-like, *l*aminin A globular-like [LAG], and *s*even-pass

*r*eceptors), and Fat cadherins [88]. All cadherins mediate Ca^{2+}-dependent homophilic adhesions between cells expressing the same class of cadherin through their extracellular domain-containing repetitive cadherin repeats. Among different cadherins, classical cadherins have been the most extensively studied. Their cytoplasmic domain binds to β-catenin and p120 catenin [89, 90]. β-catenin associates with α-catenin, which is known as an actin-binding protein. These protein–protein interactions likely underlie the mechanism of cadherin-mediated synapse formation and spine stability.

The first evidence of retrograde synaptic control by cadherin was observed in a neuronal co-culture differentiated from mouse embryonic stem (ES) cells lacking neural (N)-cadherin (N-cad, also known as cadherin 2), one of the classical cadherins. In the culture, the absence of postsynaptic N-cad enhanced synaptic depression in response to paired-pulse or high-frequency stimulation suggestive of a reduced readily releasable vesicle pool [91]. Interestingly, the same synaptic phenotypes were observed when the deficiency of N-cad was restricted to postsynaptic neurons in experiments of co-culturing wild-type neurons and ES cell-derived N-cad KO neurons, indicating that postsynaptic N-cad retrogradely controls presynaptic release [91]. Likewise, postsynaptic overexpression of a dominant-negative form of N-cad (DN-N-cad), which lacks extracellular cadherin repeats, reduced the number of presynaptic puncta and changed spine morphology concomitant with the reduction in frequency of mEPSC [92, 93]. Also, postsynaptic DN-N-cad overexpression compromised vesicle endocytotic machinery, which reduced the expression of active zone proteins, the number of total and recycling vesicles, and excitatory presynaptic release probability in primary neurons [94]. These studies demonstrate that N-cad is involved in vesicle recruitment from the readily releasable pool to the active zone and in vesicle recycling pathways [91, 93]. However, curiously, presynaptic expression of DN-N-cad or N-cad shRNAi does not change presynaptic release probability. This indicates homophilic interaction between pre- and postsynaptic N-cad is not required for retrograde regulation of transmitter release and suggests that postsynaptic N-cad interacts with another presynaptic molecule(s) in a non-canonical fashion to influence presynaptic release probability though the putative presynaptic molecule(s) is yet to be identified [94].

Postsynaptic AMPAR subunits, GluAs, are considered as non-canonical mediators for N-cad. N-cad forms a protein complex with GluAs in vivo [95], and the extracellular N-terminal domain of GluA2 interacts directly with N-cad in cis and in trans [96]. Importantly, the extracellular N-terminal domain of GluA1, another AMPAR subunit, failed to interact with N-cad in primary excitatory neurons, highlighting the N-cad–GluA2 interaction as a unique transsynaptic mechanism at the synapse. This heterophilic interaction could be an important mechanism for AMPAR trafficking, retrograde regulation of synaptic transmission, and coordination between pre- and postsynaptic structure and functions. Consistently, Vitureira et al. reported that acute postsynaptic GluA2 KD reduced presynaptic release probability and occluded the effects of postsynaptic overexpression of DN-N-cad in primary excitatory neurons, indicating that GluA2 forms a complex with N-cad in cis and

regulates presynaptic release through a retrograde mechanism [94]. On the other hand, acute KD of postsynaptic GluA1, 2, or 3 reduced the size of the readily releasable pool without changing presynaptic release probability through a signaling pathway that does not involve N-cad in primary hippocampal neurons. Therefore, N-cad may contribute to synaptic structure and function through both hemophilic and heterophilic (with GluAs) interactions (Fig. 2) [97].

The intracellular-binding partners of presynaptic N-cad mediate the effect on presynaptic release machinery. Neuron-specific β-catenin KO reduced the number of releasable vesicles and exacerbated synaptic depression during high-frequency stimulation, although interpretation of this result is complicated by the fact that both pre- and postsynaptic β-catenin were knocked out in this study [98]. Consistently, postsynaptic overexpression of β-catenin resulted in an increase in mEPSC frequency, suggesting retrograde regulation by postsynaptic β-catenin/cadherin interactions, although there is an alternative possibility that β-catenin overexpression increased the number of functional synapses [99].

In contrast, cis interactions between presynaptic N-cad and catenin regulate presynaptic release probability through establishing protein complex with the β-catenin-interacting protein p140Cap (p130Cas-associated protein, also known as SRC

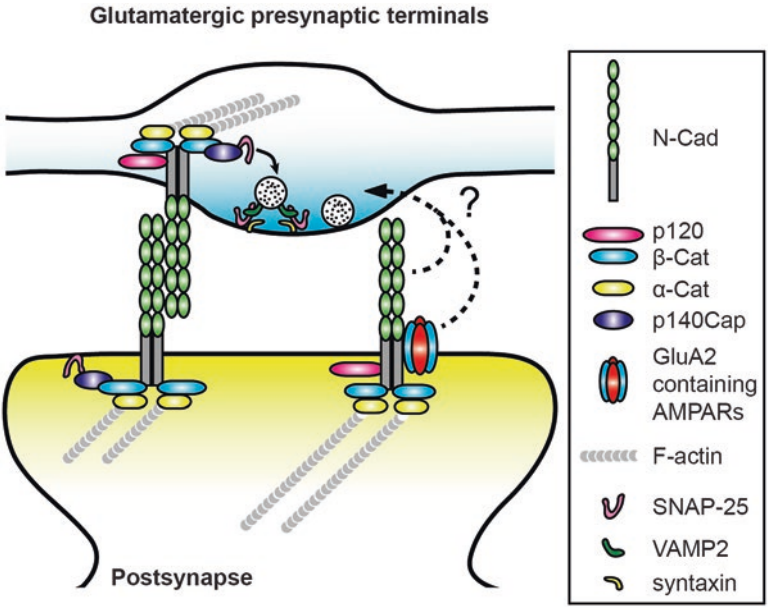

Fig. 2 Schematic diagram of N-cadherin-mediated cis- and transsynaptic regulation of neurotransmitter release at excitatory synapses. Postsynaptic N-cad, β-catenin, and GluA2-containing AMPARs retrogradely regulate excitatory presynaptic release in primary excitatory neurons. In contrast, cis interactions between presynaptic cadherin and β-catenin regulate presynaptic release probability through their interactions with p140Cap

kinase signaling inhibitor 1 [Srcin1] or SNAP-25-interacting protein [SNIP]) in cortical excitatory circuits (Fig. 2) [100]. p140Cap is expressed on both the pre- and postsynaptic sides. On the presynaptic side, p140Cap regulates transmitter release and spine structure through interacting with SNAP-25 while on the postsynaptic side, p140Cap modulates excitatory postsynaptic transmission through interacting with PSD-95 [101, 102]. Li et al. presented that presynaptic but not postsynaptic N-cadherin and β-catenin regulate presynaptic release probability through their interactions with presynaptic p140Cap, suggesting that the N-cad/β-catenin/p140Cap/SNARE protein complex is important for synaptic release.

In summary, both pre- and postsynaptic N-cad are capable of regulating presynaptic release. Further investigation is essential to evaluate how the postsynaptic N-cad/AMPAR complex regulates presynaptic release machinery. It is certainly interesting that postsynaptic N-cad regulates release retrogradely; however, findings are limited to culture systems. A more direct approach, such as acute KD or KO of N-cad in postsynaptic neurons in vivo, is essential to elucidate retrograde N-cad function in native brain circuits.

2.3 Transsynaptic Regulation of Presynaptic Release by mGluR and CAM Interactions

Type III metabotropic glutamate receptors (mGluR6/7/8) are predominantly localized at the presynaptic termini, and modulate neurotransmitter release by activating inhibitory G-proteins ($G_{i/o}$) [103]. Recent evidence has provided that postsynaptic CAMs regulate presynaptic release probability by the activation of type III mGluRs (Fig. 3).

Elfns are primarily expressed at postsynaptic sites and act as target neuron-specific retrograde mediators that regulate presynaptic release machinery. Two Elfn proteins, Elfn1 and Elfn2, consist of a single transmembrane domain and extracellular leucine-rich repeat domain that bind with membrane proteins. Elfn1 is specifically expressed in somatostatin-positive (Sst+) stratum oriens/lacunosum-moleculare (O-LM) inhibitory interneurons but not in parvalbumin-positive (Pv+) interneurons in the hippocampus. Importantly, KD or KO of Elfn1 in either O-LM or cortical Sst+ interneurons robustly reduced synaptic facilitation suggestive of increased presynaptic release by postsynaptic Elfn1 dysfunction. This indicates that Elfn1 negatively regulates presynaptic glutamate release onto Sst+ inhibitory interneurons (Fig. 3a) [104–106]. In addition, overexpression of Elfn1 in Pv+ interneurons, which do not normally express Elfn1, was sufficient to reduce presynaptic release probability, suggesting that Elfn1 is a necessary postsynaptic CAM that can influence target cell-specific release modulation. Importantly, in vitro binding assays elucidated that Elfns directly bind to type III metabotropic glutamate receptors (mGluR) including mGluR6 and mGluR7 [106–109].

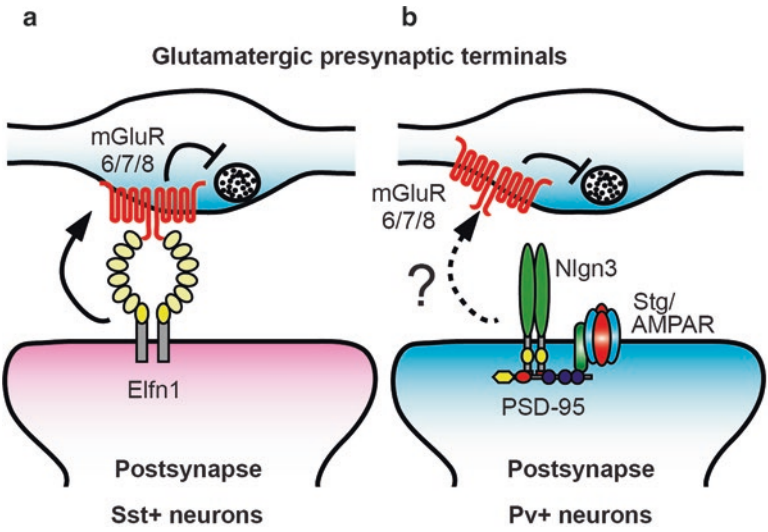

Fig. 3 Schematic diagrams of target neuron-specific regulation of neurotransmitter release at excitatory synapses through mGluRs and CAM interactions. Postsynaptic Nlgn3 (neuroligin 3) (**a**) and Elfn1 (**b**) expressed in Pv+ and Sst+ interneurons, respectively, retrogradely regulate synaptic release of excitatory neurotransmitters through presynaptically expressed type III mGluRs. It is not known whether Nlgn3 physically interacts with presynaptic mGluRs

Interestingly, the formation of the transsynaptic Elfn1-mGluR7 complex activates mGluR7 in a glutamate-independent fashion, which represents a novel GPCR signaling cascade in the brain [105].

In contrast to Elfn1, Elfn2 is highly expressed in excitatory neurons. KO of Elfn2 caused reduced expression of mGluRs in total brain lysate and increased basal excitatory synaptic transmission [107]. The increased basal excitatory synaptic transmission in Elfn2 KO mice might reflect a disruption of mGluR-mediated suppression of synaptic release. It is particularly interesting to test whether other leucine-rich repeat (LRR) family proteins, such as LRRTMs, affect target cell-specific presynaptic modulation.

Nlgn3 is another CAM that regulates neurotransmitter release via interacting with presynaptic type III mGluRs (Fig. 3b). Polepalli et al. demonstrated that Pv+ interneuron-specific Nlgn3 KO impairs type III mGluR-mediated suppressions of EPSC amplitudes and presynaptic release probability at Pv+ interneuron–pyramidal cell excitatory synapses, leading to the alteration of hippocampal network activity that underlies learning and memory [110]. Although a direct interaction between Nlgn3 and type III mGluRs has not been reported yet, this finding supports that type III mGluR-mediated presynaptic functions can be controlled by multiplexed transsynaptic signaling that involves distinct postsynaptic CAMs such as Elfns and Nlgn3.

2.4 Ephrin Receptor–Ephrin Ligand Mediated Transsynaptic Signaling

Ephrin ligand family interacts with its receptor family, Eph. Both ephrin ligands and Eph receptors are divided into two subclasses, A and B. EphrinA ligands are tethered to the membrane through GPI-linkage anchors and specifically bind to EphA receptors, while ephrinB ligands associate with the plasma membrane through a transmembrane domain and preferentially bind to EphB receptors. The intracellular carboxy-terminal tail of Eph receptors contains a tyrosine kinase domain, SAM protein interaction domain, and a consensus motif for binding to PDZ domain-containing proteins. Interestingly, several Eph receptors bind synaptic PDZ domain proteins such as the glutamate receptor-interacting protein 1 (GRIP1), protein interacting with C-kinase-1 (PICK1), syndecan-binding protein syntenin, and Ras-binding protein AF-6 [111, 112]. EphrinB ligands also have PDZ domain-binding motifs in the carboxy-terminal region, which can mediate interactions with syntenin, PICK1, GRIP1, and GRIP2 [112–114]. Thus, Eph receptors and ephrinB ligands are linked to the synaptic scaffold through PDZ-mediated protein interactions. Both EphA and EphB receptors have been detected mainly in postsynaptic sites [111, 115, 116], but some Eph receptors are also expressed in presynaptic terminals [117]. In contrast, the synaptic localization of ephrin ligands differs between subtypes. In the adult hippocampus, ephrinB2 is expressed mainly in CA1 pyramidal cells and is more abundant at postsynaptic sites [118–120] whereas ephrinB3 is expressed in dentate gyrus granule cells and targets presynaptically to the mossy fiber axons and termini [118, 120, 121].

It has been reported that transsynaptic retrograde signaling from postsynaptic EphB receptors to presynaptic ephrinB ligands contributes to the induction of an NMDAR-independent LTP between hippocampal mossy fibers and CA3 pyramidal neurons. Interfering with EphB/ephrinB transsynaptic signaling by the application of soluble EphB2 receptor or ephrinB1 ligand peptides occluded or blocked mossy fiber LTP, while expression of a dominant-negative form of ephrinB3 ligand reduced LTP [121, 122]. Interestingly, ephrinB3 KO mice exhibited normal mossy fiber LTP [121]. This lack of effect may be due to developmentally compensating effects by ephrinBs.

3 Roles of Transsynaptic Interactions in Synaptic Plasticity

A number of studies have shown that LTP is accompanied by synaptic translocation of major players necessary for LTP expression including AMPARs, α-actinin, drebrin, cofilin, CaMKIIα/β, β-catenin, and actin [9, 30, 99, 123, 124]. Furthermore, LTP induction causes the expansion of presynaptic boutons [10] and enlargement of active zones [125, 126]. These observations suggest both pre- and postsynaptic components increase alongside LTP. Therefore, it is likely that CAMs are

translocated to the synapse as part of a process of rebuilding larger postsynaptic structures. Indeed, transsynaptic Nrxn–Nlgn interactions mediate LTP expression in hippocampal CA1 synapses. The extracellular domain of Nlgn1 forms cis- and transsynaptic interactions with postsynaptic NMDARs and presynaptic Nrxns, respectively [127]. Acute KD of Nlgn1 completely blocked LTP in hippocampal dentate gyrus synapses [128], presumably due to reduced NMDAR function. Importantly, Wu et al. replaced endogenous Nlgn1 with a mutated Nlgn1 that cannot interact with βNrxn1 but continues to interact with NMDARs in hippocampal CA1 pyramidal neurons. This Nlgn1 mutant failed to induce LTP, indicating that transsynaptic Nlgn1–βNrxn1 binding is important for LTP [129]. Importantly, sLTP is abolished by application of the extracellular domain of βNrxn1 that blocks βNrxn-mediated transsynaptic interactions [130]. This also supports the significance of Nlgn–βNrxn interaction in LTP. It is widely accepted that the expression of LTP is largely postsynaptic and increases the number of AMPARs in the spines without changing presynaptic release probability [29]. Why is presynaptic βNrxn1 necessary for LTP? Does βNrxn1 simply anchor proper synaptic localization of Nlgn1 or reassemble presynaptic protein complex through cis interaction (see Sect. 2.2)?

The recent development of super-resolution microscopy has revealed the presence of transsynaptic nanocolumns or nanomodules, which represent the alignment of presynaptic transmitter release machinery and postsynaptic receptors within the synaptic contact [23, 131, 132]. Many of the excitatory synapses in hippocampal dissociated culture each contain one nanocolumn with some containing more than one [131]. Because synaptic AMPARs are not saturated with glutamate at the synaptic cleft [133, 134], it is possible that the formation of such nanocolumns enhances synaptic transmission efficacy. Indeed, glycine-induced chemical LTP increases the number of nanocolumns, which allows for the accumulation of more proteins under the alignment [131, 132, 135].

An obvious question is what adjusts pre- and postsynaptic alignment and how neuronal activation can modulate this process. Postsynaptic Nlgn1 and LRRTM both bind presynaptic Nrxn and colocalize with AMPAR nanodomains to potentially mediate the alignment [136, 137]. Nlgn1 can be phosphorylated by CaMKII at its intracellular carboxyl tail. This phosphorylation is necessary for activity-driven surface expression of Nlgn1 [138]. Alternatively, CaMKII has been recently found to form self-condensate in a manner triggered by Ca^{2+}/calmodulin stimulation via liquid–liquid phase separation [139, 140]. Liquid–liquid phase separation is a phenomenon where biological macromolecules such as proteins and nucleic acids, often through multimeric interactions, undergo spontaneous condensation that can generate >100-fold greater concentrations of macromolecules. Indeed, multiple pre- and postsynaptic proteins can undergo this phenomenon [140–143]. Interestingly, CaMKII segregates AMPARs together with Nlgn from NMDARs through a Ca^{2+}/calmodulin-triggered mechanism [139] (Fig. 4a). In this way, liquid–liquid phase separation of CaMKII can generate receptor nanodomains at the synapse where specific CAMs can co-segregate together under the regulation of neuronal activity (Fig. 4b). Such mechanisms might regulate the activity-dependent alignment of components of transsynaptic nanocolumns.

4 Future Directions

Much work has elucidated the functions of CAMs but many unresolved questions remain. First, the crosstalk between different CAM-mediated transsynaptic interactions remains unknown. A single CAM can interact with different binding partners at the synaptic cleft. For instance, postsynaptic Nlgn3 can potentially regulate presynaptic functions via interacting with presynaptic Nrxns, protein tyrosine phosphatase δ, or mGluRs [72, 110, 144]. However, it remains elusive whether these three distinct pathways synergistically contribute to presynaptic functions or compete against each other. Moreover, intracellular singling pathways can be also shared by different CAM-mediated transsynaptic interactions. Further studies are necessary for a better understanding of the crosstalk of CAM-mediated signalings that underlie presynaptic functions.

Second, a number of studies have identified non-canonical transsynaptic interactions between receptors and CAMs such as GluA2-N-cad (Sect. 2.1), Elfn1-mGluR6/7 (Sect. 2.3), and Nlgn3-mGluR (Sect. 2.3) as regulators of synapse function. Additional structural, physiological, and imaging studies are essential to reveal the roles of transsynaptic receptor and CAM complexes on presynaptic function and structure.

Third, the roles of transsynaptic interactions during plasticity are still largely unknown. Although ample studies have elucidated synaptic protein dynamics in dendritic spines during LTP, our knowledge is limited to cis interactions in the postsynaptic density. Much less is known about synaptic dynamics that regulate presynaptic molecular architecture. While it is generally accepted that LTP is expressed postsynaptically during the first hour following stimulation, structural studies have consistently provided evidence for the precise matching of the size and function of the presynaptic active zone and postsynaptic density [4, 7]. Therefore, presynaptic sites should match up with postsynaptic spines at some point. In the future, deciphering the constructive process of synapse modification after LTP induction, from changes in synaptic CAMs to rearrangements of presynaptic structures and vesicular release machinery, will be crucial in elucidating pre- and postsynaptic roles in LTP.

Fourth, recent research has demonstrated that Nlgns expressed in astrocytes regulate synapse development [145]. This indicates that presynaptic Nrxns can form transsynaptic complexes with astrocytic Nlgns as well. It is particularly interesting to highlight the differing roles of postsynaptic and astrocytic Nlgns in presynaptic release and structure.

Fifth, CAM-mediated regulation in modulatory systems is poorly understood. While numerous studies indicate that CAMs regulate fast neurotransmitter release including that of glutamate and GABA, fewer studies have tested CAM functions in central neuromodulatory systems, such as those mediated by dopaminergic and serotonergic signals, which are propagated mainly via volume transmission. Because the expression of CAMs is also detected at dopaminergic synapses [82], pre- and postsynaptic CAMs at these synapses might regulate presynaptic release like that at fast asymmetric synapses. Highlighting the roles of CAMs in modulatory systems will be an intriguing field of investigation.

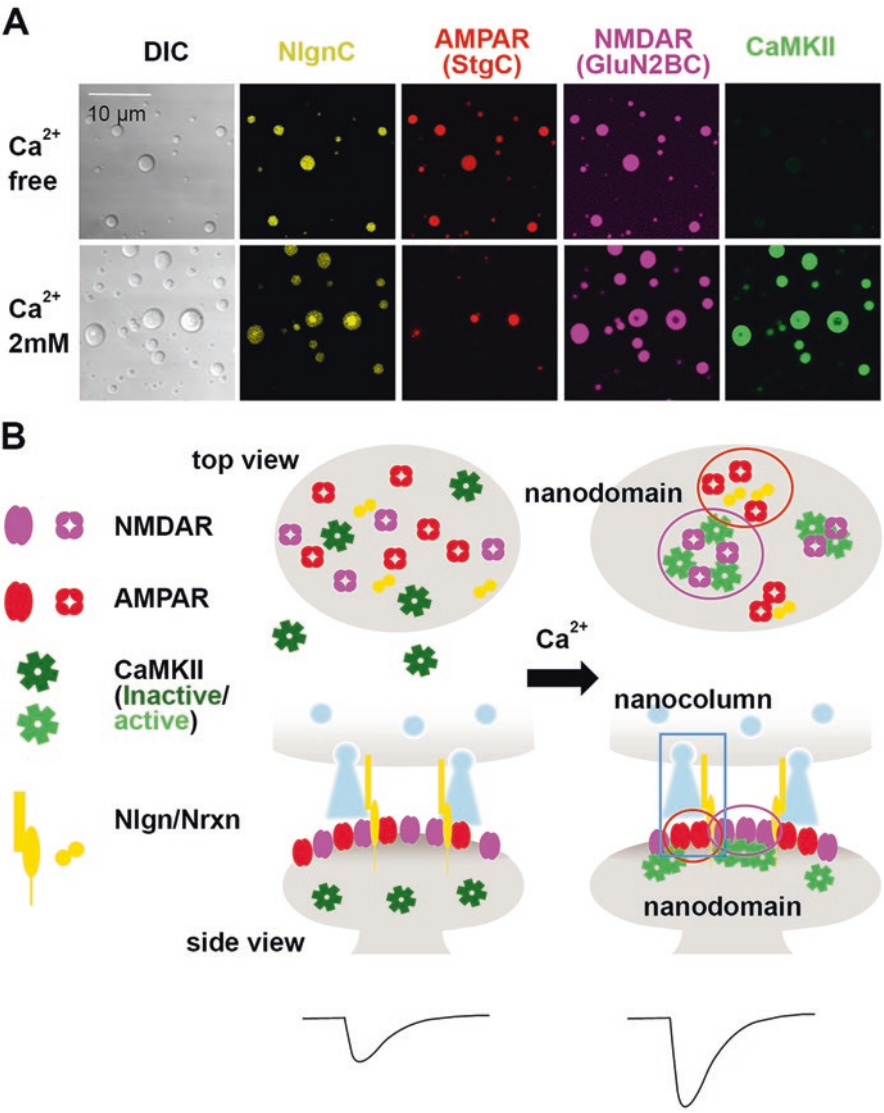

Fig. 4 Formation of synaptic nanocolumns by liquid–liquid phase separation. (**a**) Liquid–liquid phase separation of protein solution containing Nlgn (neuroligin) carboxyl tail (yellow), Stg (stargazin) carboxyl tail (red), NMDAR subunit GluN2B carboxyl tail (magenta), PSD-95 (unstained), calmodulin (unstained), and CaMKII (green). In the absence of Nlgn, AMPARs and NMDARs form homogeneous condensation. CaMKII remains in the diluted phase. Upon stimulation by Ca^{2+}, Nlgn and AMPARs form phase-in-phase surrounded by NMDARs and CaMKII. (**b**) Functional implications of liquid–liquid phase separation. Under resting conditions, AMPARs and NMDARs are mixed. The number of AMPARs beneath the transmitter release site is limited. Upon activation of CaMKII, AMPARs undergo liquid–liquid phase separation with PSD proteins and form nanodomains of AMPARs and NMDARs. Nlgn is condensed together with an AMPAR nanodomain, thereby bringing AMPARs beneath the transmitter release site and forming a synaptic nanodomain. This leads to more efficient synaptic transmission. (Modified from Hosokawa et al. [139])

Acknowledgments We thank Dr. Amy Cheung for comments on the manuscript. M.U. was supported by Grants-in-Aid for Scientific Research from MEXT, Japan (JP20H03349, JP20K21461, and JP20H05918); Y.H. by Grants-in-Aid for Scientific Research from MEXT, Japan (JP15K14330 and JP18H05434); and K.F. by grants from the National Institutes of Health (R01NS085215 and R01MH130582) and Riccio Neuroscience Fund.

References

1. Holderith N, Lorincz A, Katona G, Rozsa B, Kulik A, Watanabe M, et al. Release probability of hippocampal glutamatergic terminals scales with the size of the active zone. Nat Neurosci. 2012;15:988–97. https://doi.org/10.1038/nn.3137.
2. Conti R, Lisman J. The high variance of AMPA receptor- and NMDA receptor-mediated responses at single hippocampal synapses: evidence for multiquantal release. Proc Natl Acad Sci U S A. 2003;100:4885–90. https://doi.org/10.1073/pnas.0630290100.
3. Shepherd GM, Harris KM. Three-dimensional structure and composition of CA3→CA1 axons in rat hippocampal slices: implications for presynaptic connectivity and compartmentalization. J Neurosci. 1998;18:8300–10.
4. Schikorski T, Stevens CF. Quantitative ultrastructural analysis of hippocampal excitatory synapses. J Neurosci. 1997;17:5858–67.
5. Matsuzaki M, Ellis-Davies GC, Nemoto T, Miyashita Y, Iino M, Kasai H. Dendritic spine geometry is critical for AMPA receptor expression in hippocampal CA1 pyramidal neurons. Nat Neurosci. 2001;4:1086–92. https://doi.org/10.1038/nn736.
6. Holler S, Kostinger G, Martin KAC, Schuhknecht GFP, Stratford KJ. Structure and function of a neocortical synapse. Nature. 2021;591:111–6. https://doi.org/10.1038/s41586-020-03134-2.
7. Lisman JE, Harris KM. Quantal analysis and synaptic anatomy--integrating two views of hippocampal plasticity. Trends Neurosci. 1993;16:141–7. https://doi.org/10.1016/0166-2236(93)90122-3.
8. Okamoto K, Bosch M, Hayashi Y. The roles of CaMKII and F-actin in the structural plasticity of dendritic spines: a potential molecular identity of a synaptic tag? Physiology. 2009;24:357–66. https://doi.org/10.1152/physiol.00029.2009.
9. Bosch M, Castro J, Saneyoshi T, Matsuno H, Sur M, Hayashi Y. Structural and molecular remodeling of dendritic spine substructures during long-term potentiation. Neuron. 2014;82:444–59. https://doi.org/10.1016/j.neuron.2014.03.021.
10. Meyer D, Bonhoeffer T, Scheuss V. Balance and stability of synaptic structures during synaptic plasticity. Neuron. 2014;82:430–43. https://doi.org/10.1016/j.neuron.2014.02.031.
11. Koester HJ, Johnston D. Target cell-dependent normalization of transmitter release at neocortical synapses. Science. 2005;308:863–6. https://doi.org/10.1126/science.1100815.
12. Sun HY, Lyons SA, Dobrunz LE. Mechanisms of target-cell specific short-term plasticity at Schaffer collateral synapses onto interneurones versus pyramidal cells in juvenile rats. J Physiol. 2005;568:815–40.
13. Scanziani M, Gahwiler BH, Charpak S. Target cell-specific modulation of transmitter release at terminals from a single axon. Proc Natl Acad Sci U S A. 1998;95:12004–9. https://doi.org/10.1073/pnas.95.20.12004.
14. Sun HY, Dobrunz LE. Presynaptic kainate receptor activation is a novel mechanism for target cell-specific short-term facilitation at Schaffer collateral synapses. J Neurosci. 2006;26:10796–807. https://doi.org/10.1523/JNEUROSCI.2746-06.2006.
15. Losonczy A, Zhang L, Shigemoto R, Somogyi P, Nusser Z. Cell type dependence and variability in the short-term plasticity of EPSCs in identified mouse hippocampal interneurones. J Physiol. 2002;542:193–210. https://doi.org/10.1113/jphysiol.2002.020024.

16. Pouille F, Scanziani M. Routing of spike series by dynamic circuits in the hippocampus. Nature. 2004;429:717–23. https://doi.org/10.1038/nature02615.
17. Reyes A, Lujan R, Rozov A, Burnashev N, Somogyi P, Sakmann B. Target-cell-specific facilitation and depression in neocortical circuits. Nat Neurosci. 1998;1:279–85. https://doi.org/10.1038/1092.
18. Rozov A, Burnashev N, Sakmann B, Neher E. Transmitter release modulation by intracellular Ca2+ buffers in facilitating and depressing nerve terminals of pyramidal cells in layer 2/3 of the rat neocortex indicates a target cell-specific difference in presynaptic calcium dynamics. J Physiol. 2001;531:807–26. https://doi.org/10.1111/j.1469-7793.2001.0807h.x.
19. Thomson AM. Activity-dependent properties of synaptic transmission at two classes of connections made by rat neocortical pyramidal axons in vitro. J Physiol. 1997;502(Pt 1):131–47. https://doi.org/10.1111/j.1469-7793.1997.131bl.x.
20. Katona I, Freund TF. Multiple functions of endocannabinoid signaling in the brain. Annu Rev Neurosci. 2012;35:529–58. https://doi.org/10.1146/annurev-neuro-062111-150420.
21. Chevaleyre V, Takahashi KA, Castillo PE. Endocannabinoid-mediated synaptic plasticity in the CNS. Annu Rev Neurosci. 2006;29:37–76. https://doi.org/10.1146/annurev.neuro.29.051605.112834.
22. de Wit J, Ghosh A. Specification of synaptic connectivity by cell surface interactions. Nat Rev Neurosci. 2016;17:22–35. https://doi.org/10.1038/nrn.2015.3.
23. Biederer T, Kaeser PS, Blanpied TA. Transcellular nanoalignment of synaptic function. Neuron. 2017;96:680–96. https://doi.org/10.1016/j.neuron.2017.10.006.
24. Sudhof TC. Synaptic neurexin complexes: a molecular code for the logic of neural circuits. Cell. 2017;171:745–69. https://doi.org/10.1016/j.cell.2017.10.024.
25. Campbell BFN, Tyagarajan SK. Cellular mechanisms contributing to the functional heterogeneity of GABAergic synapses. Front Mol Neurosci. 2019;12:187. https://doi.org/10.3389/fnmol.2019.00187.
26. Fossati M, Assendorp N, Gemin O, Colasse S, Dingli F, Arras G, et al. Trans-synaptic signaling through the glutamate receptor delta-1 mediates inhibitory synapse formation in cortical pyramidal neurons. Neuron. 2019;104:1081–1094.e1087. https://doi.org/10.1016/j.neuron.2019.09.027.
27. Futai K, Doty CD, Baek B, Ryu J, Sheng M. Specific trans-synaptic interaction with inhibitory interneuronal neurexin underlies differential ability of neuroligins to induce functional inhibitory synapses. J Neurosci. 2013;33:3612–23. https://doi.org/10.1523/JNEUROSCI.1811-12.2013.
28. Chih B, Gollan L, Scheiffele P. Alternative splicing controls selective trans-synaptic interactions of the neuroligin-neurexin complex. Neuron. 2006;51:171–8. https://doi.org/10.1016/j.neuron.2006.06.005.
29. Nicoll RA. A brief history of long-term potentiation. Neuron. 2017;93:281–90. https://doi.org/10.1016/j.neuron.2016.12.015.
30. Matsuzaki M, Honkura N, Ellis-Davies GC, Kasai H. Structural basis of long-term potentiation in single dendritic spines. Nature. 2004;429:761–6. https://doi.org/10.1038/nature02617.
31. Saneyoshi T, Matsuno H, Suzuki A, Murakoshi H, Hedrick NG, Agnello E, et al. Reciprocal activation within a kinase-effector complex underlying persistence of structural LTP. Neuron. 2019;102:1199–1210.e1196. https://doi.org/10.1016/j.neuron.2019.04.012.
32. Ushkaryov YA, Petrenko AG, Geppert M, Sudhof TC. Neurexins: synaptic cell surface proteins related to the alpha-latrotoxin receptor and laminin. Science. 1992;257:50–6.
33. Tabuchi K, Sudhof TC. Structure and evolution of neurexin genes: insight into the mechanism of alternative splicing. Genomics. 2002;79:849–59. https://doi.org/10.1006/geno.2002.6780.
34. Sterky FH, Trotter JH, Lee SJ, Recktenwald CV, Du X, Zhou B, et al. Carbonic anhydrase-related protein CA10 is an evolutionarily conserved pan-neurexin ligand. Proc Natl Acad Sci U S A. 2017;114:E1253–62. https://doi.org/10.1073/pnas.1621321114.

35. Schreiner D, Nguyen TM, Russo G, Heber S, Patrignani A, Ahrne E, et al. Targeted combinatorial alternative splicing generates brain region-specific repertoires of neurexins. Neuron. 2014;84:386–98. https://doi.org/10.1016/j.neuron.2014.09.011.
36. Treutlein B, Gokce O, Quake SR, Sudhof TC. Cartography of neurexin alternative splicing mapped by single-molecule long-read mRNA sequencing. Proc Natl Acad Sci U S A. 2014;111:E1291–9. https://doi.org/10.1073/pnas.1403244111.
37. Ullrich B, Ushkaryov YA, Sudhof TC. Cartography of neurexins: more than 1000 isoforms generated by alternative splicing and expressed in distinct subsets of neurons. Neuron. 1995;14:497–507.
38. Gorecki DC, Szklarczyk A, Lukasiuk K, Kaczmarek L, Simons JP. Differential seizure-induced and developmental changes of neurexin expression. Mol Cell Neurosci. 1999;13:218–27.
39. Puschel AW, Betz H. Neurexins are differentially expressed in the embryonic nervous system of mice. J Neurosci. 1995;15:2849–56.
40. Boucard AA, Chubykin AA, Comoletti D, Taylor P, Sudhof TC. A splice code for trans-synaptic cell adhesion mediated by binding of neuroligin 1 to alpha- and beta-neurexins. Neuron. 2005;48:229–36. https://doi.org/10.1016/j.neuron.2005.08.026.
41. Reissner C, Klose M, Fairless R, Missler M. Mutational analysis of the neurexin/neuroligin complex reveals essential and regulatory components. Proc Natl Acad Sci U S A. 2008;105:15124–9. https://doi.org/10.1073/pnas.0801639105.
42. Koehnke J, Katsamba PS, Ahlsen G, Bahna F, Vendome J, Honig B, et al. Splice form dependence of beta-neurexin/neuroligin binding interactions. Neuron. 2010;67:61–74. https://doi.org/10.1016/j.neuron.2010.06.001.
43. Ichtchenko K, Hata Y, Nguyen T, Ullrich B, Missler M, Moomaw C, et al. Neuroligin 1: a splice site-specific ligand for beta-neurexins. Cell. 1995;81:435–43.
44. Ichtchenko K, Nguyen T, Sudhof TC. Structures, alternative splicing, and neurexin binding of multiple neuroligins. J Biol Chem. 1996;271:2676–82.
45. de Wit J, Sylwestrak E, O'Sullivan ML, Otto S, Tiglio K, Savas JN, et al. LRRTM2 interacts with neurexin1 and regulates excitatory synapse formation. Neuron. 2009;64:799–806. https://doi.org/10.1016/j.neuron.2009.12.019.
46. Ko J, Fuccillo MV, Malenka RC, Sudhof TC. LRRTM2 functions as a neurexin ligand in promoting excitatory synapse formation. Neuron. 2009;64:791–8. https://doi.org/10.1016/j.neuron.2009.12.012.
47. Zhang C, Atasoy D, Arac D, Yang X, Fucillo MV, Robison AJ, et al. Neurexins physically and functionally interact with GABA(A) receptors. Neuron. 2010;66:403–16. https://doi.org/10.1016/j.neuron.2010.04.008.
48. Uemura T, Lee SJ, Yasumura M, Takeuchi T, Yoshida T, Ra M, et al. Trans-synaptic interaction of GluRdelta2 and neurexin through Cbln1 mediates synapse formation in the cerebellum. Cell. 2010;141:1068–79. https://doi.org/10.1016/j.cell.2010.04.035.
49. Matsuda K, Miura E, Miyazaki T, Kakegawa W, Emi K, Narumi S, et al. Cbln1 is a ligand for an orphan glutamate receptor delta2, a bidirectional synapse organizer. Science. 2010;328:363–8. https://doi.org/10.1126/science.1185152.
50. Matsuda K, Budisantoso T, Mitakidis N, Sugaya Y, Miura E, Kakegawa W, et al. Transsynaptic modulation of kainate receptor functions by C1q-like proteins. Neuron. 2016;90:752–67. https://doi.org/10.1016/j.neuron.2016.04.001.
51. Singh SK, Stogsdill JA, Pulimood NS, Dingsdale H, Kim YH, Pilaz LJ, et al. Astrocytes assemble thalamocortical synapses by bridging NRX1alpha and NL1 via Hevin. Cell. 2016;164:183–96. https://doi.org/10.1016/j.cell.2015.11.034.
52. Boucard AA, Ko J, Sudhof TC. High affinity neurexin binding to cell adhesion G-protein-coupled receptor CIRL1/latrophilin-1 produces an intercellular adhesion complex. J Biol Chem. 2012;287:9399–413. https://doi.org/10.1074/jbc.M111.318659.
53. Missler M, Hammer RE, Sudhof TC. Neurexophilin binding to alpha-neurexins. A single LNS domain functions as an independently folding ligand-binding unit. J Biol Chem. 1998;273:34716–23.

54. Sugita S, Saito F, Tang J, Satz J, Campbell K, Sudhof TC. A stoichiometric complex of neurexins and dystroglycan in brain. J Cell Biol. 2001;154:435–45.
55. Tanabe Y, Naito Y, Vasuta C, Lee AK, Soumounou Y, Linhoff MW, et al. IgSF21 promotes differentiation of inhibitory synapses via binding to neurexin2alpha. Nat Commun. 2017;8:408. https://doi.org/10.1038/s41467-017-00333-w.
56. Brockhaus J, Schreitmuller M, Repetto D, Klatt O, Reissner C, Elmslie K, et al. Alpha-neurexins together with alpha2delta-1 auxiliary subunits regulate Ca(2+) influx through Cav2.1 channels. J Neurosci. 2018;38:8277–94. https://doi.org/10.1523/JNEUROSCI.0511-18.2018.
57. Lise MF, El-Husseini A. The neuroligin and neurexin families: from structure to function at the synapse. Cell Mol Life Sci. 2006;63:1833–49. https://doi.org/10.1007/s00018-006-6061-3.
58. Biederer T, Sudhof TC. CASK and protein 4.1 support F-actin nucleation on neurexins. J Biol Chem. 2001;276:47869–76. https://doi.org/10.1074/jbc.M105287200.
59. Chen LY, Jiang M, Zhang B, Gokce O, Sudhof TC. Conditional deletion of all neurexins defines diversity of essential synaptic organizer functions for neurexins. Neuron. 2017;94:611–625.e614. https://doi.org/10.1016/j.neuron.2017.04.011.
60. Luo F, Sclip A, Jiang M, Sudhof TC. Neurexins cluster Ca(2+) channels within the presynaptic active zone. EMBO J. 2020;39:e103208. https://doi.org/10.15252/embj.2019103208.
61. Quinn DP, Kolar A, Wigerius M, Gomm-Kolisko RN, Atwi H, Fawcett JP, et al. Pan-neurexin perturbation results in compromised synapse stability and a reduction in readily releasable synaptic vesicle pool size. Sci Rep. 2017;7:42920. https://doi.org/10.1038/srep42920.
62. Born G, Grayton HM, Langhorst H, Dudanova I, Rohlmann A, Woodward BW, et al. Genetic targeting of NRXN2 in mice unveils role in excitatory cortical synapse function and social behaviors. Front Synaptic Neurosci. 2015;7:3. https://doi.org/10.3389/fnsyn.2015.00003.
63. Aoto J, Foldy C, Ilcus SM, Tabuchi K, Sudhof TC. Distinct circuit-dependent functions of presynaptic neurexin-3 at GABAergic and glutamatergic synapses. Nat Neurosci. 2015;18:997–1007. https://doi.org/10.1038/nn.4037.
64. Missler M, Zhang W, Rohlmann A, Kattenstroth G, Hammer RE, Gottmann K, et al. Alpha-neurexins couple Ca2+ channels to synaptic vesicle exocytosis. Nature. 2003;423:939–48. https://doi.org/10.1038/nature01755.
65. Zhang H, Maximov A, Fu Y, Xu F, Tang TS, Tkatch T, et al. Association of CaV1.3 L-type calcium channels with Shank. J Neurosci. 2005;25:1037–49. https://doi.org/10.1523/JNEUROSCI.4554-04.2005.
66. Anderson GR, Aoto J, Tabuchi K, Foldy C, Covy J, Yee AX, et al. β-Neurexins control neural circuits by regulating synaptic endocannabinoid signaling. Cell. 2015;162:593–606. https://doi.org/10.1016/j.cell.2015.06.056.
67. Sudhof TC. Neuroligins and neurexins link synaptic function to cognitive disease. Nature. 2008;455:903–11. https://doi.org/10.1038/nature07456.
68. Kim E, Sheng M. PDZ domain proteins of synapses. Nat Rev Neurosci. 2004;5:771–81. https://doi.org/10.1038/nrn1517.
69. Scheiffele P, Fan J, Choih J, Fetter R, Serafini T. Neuroligin expressed in nonneuronal cells triggers presynaptic development in contacting axons. Cell. 2000;101:657–69.
70. Varoqueaux F, Aramuni G, Rawson RL, Mohrmann R, Missler M, Gottmann K, et al. Neuroligins determine synapse maturation and function. Neuron. 2006;51:741–54. https://doi.org/10.1016/j.neuron.2006.09.003.
71. Futai K, Kim MJ, Hashikawa T, Scheiffele P, Sheng M, Hayashi Y. Retrograde modulation of presynaptic release probability through signaling mediated by PSD-95-neuroligin. Nat Neurosci. 2007;10:186–95. https://doi.org/10.1038/nn1837.
72. Uchigashima M, Konno K, Demchak E, Cheung A, Watanabe T, Keener DG, et al. Specific Neuroligin3-alphaNeurexin1 signaling regulates GABAergic synaptic function in mouse hippocampus. eLife. 2020;9:e59545. https://doi.org/10.7554/eLife.59545.
73. Uchigashima M, Leung M, Watanabe T, Cheung A, Le T, Pallat S, et al. Neuroligin3 splice isoforms shape inhibitory synaptic function in the mouse hippocampus. J Biol Chem. 2020;295:8589–95. https://doi.org/10.1074/jbc.AC120.012571.

74. Shipman SL, Schnell E, Hirai T, Chen BS, Roche KW, Nicoll RA. Functional dependence of neuroligin on a new non-PDZ intracellular domain. Nat Neurosci. 2011;14:718–26. https://doi.org/10.1038/nn.2825.
75. Keener DG, Cheung A, Futai K. A highly efficient method for single-cell electroporation in mouse organotypic hippocampal slice culture. J Neurosci Methods. 2020;337:108632. https://doi.org/10.1016/j.jneumeth.2020.108632.
76. Keener DG, Cheung A, Futai K. Single-cell electroporation across different organotypic slice culture of mouse hippocampal excitatory and class-specific inhibitory neurons. J Vis Exp. 2020;164:61662. https://doi.org/10.3791/61662doi:10.3791/61662.
77. Uchigashima M, Cheung A, Futai K. Neuroligin-3: a circuit-specific synapse organizer that shapes normal function and autism spectrum disorder-associated dysfunction. Front Mol Neurosci. 2021;14:749164. https://doi.org/10.3389/fnmol.2021.749164.
78. Fuccillo MV, Foldy C, Gokce O, Rothwell PE, Sun GL, Malenka RC, et al. Single-cell mRNA profiling reveals cell-type-specific expression of neurexin isoforms. Neuron. 2015;87:326–40. https://doi.org/10.1016/j.neuron.2015.06.028.
79. Uchigashima M, Cheung A, Suh J, Watanabe M, Futai K. Differential expression of neurexin genes in the mouse brain. J Comp Neurol. 2019;527:1940–65. https://doi.org/10.1002/cne.24664.
80. Song JY, Ichtchenko K, Sudhof TC, Brose N. Neuroligin 1 is a postsynaptic cell-adhesion molecule of excitatory synapses. Proc Natl Acad Sci U S A. 1999;96:1100–5.
81. Takacs VT, Freund TF, Nyiri G. Neuroligin 2 is expressed in synapses established by cholinergic cells in the mouse brain. PLoS One. 2013;8:e72450. https://doi.org/10.1371/journal.pone.0072450.
82. Uchigashima M, Ohtsuka T, Kobayashi K, Watanabe M. Dopamine synapse is a neuroligin-2-mediated contact between dopaminergic presynaptic and GABAergic postsynaptic structures. Proc Natl Acad Sci U S A. 2016;113:4206–11. https://doi.org/10.1073/pnas.1514074113.
83. Budreck EC, Scheiffele P. Neuroligin-3 is a neuronal adhesion protein at GABAergic and glutamatergic synapses. Eur J Neurosci. 2007;26:1738–48. https://doi.org/10.1111/j.1460-9568.2007.05842.x.
84. Hoon M, Soykan T, Falkenburger B, Hammer M, Patrizi A, Schmidt KF, et al. Neuroligin-4 is localized to glycinergic postsynapses and regulates inhibition in the retina. Proc Natl Acad Sci U S A. 2011;108:3053–8. https://doi.org/10.1073/pnas.1006946108.
85. Varoqueaux F, Jamain S, Brose N. Neuroligin 2 is exclusively localized to inhibitory synapses. Eur J Cell Biol. 2004;83:449–56.
86. Kuroyanagi T, Yokoyama M, Hirano T. Postsynaptic glutamate receptor delta family contributes to presynaptic terminal differentiation and establishment of synaptic transmission. Proc Natl Acad Sci U S A. 2009;106:4912–6. https://doi.org/10.1073/pnas.0900892106.
87. Kashiwabuchi N, Ikeda K, Araki K, Hirano T, Shibuki K, Takayama C, et al. Impairment of motor coordination, Purkinje cell synapse formation, and cerebellar long-term depression in GluR delta 2 mutant mice. Cell. 1995;81:245–52. https://doi.org/10.1016/0092-8674(95)90334-8.
88. Takeichi M. The cadherin superfamily in neuronal connections and interactions. Nat Rev Neurosci. 2007;8:11–20. https://doi.org/10.1038/nrn2043.
89. Takeichi M, Abe K. Synaptic contact dynamics controlled by cadherin and catenins. Trends Cell Biol. 2005;15:216–21. https://doi.org/10.1016/j.tcb.2005.02.002.
90. Wheelock MJ, Johnson KR. Cadherins as modulators of cellular phenotype. Annu Rev Cell Dev Biol. 2003;19:207–35. https://doi.org/10.1146/annurev.cellbio.19.011102.111135.
91. Jungling K, Eulenburg V, Moore R, Kemler R, Lessmann V, Gottmann K. N-cadherin transsynaptically regulates short-term plasticity at glutamatergic synapses in embryonic stem cell-derived neurons. J Neurosci. 2006;26:6968–78. https://doi.org/10.1523/JNEUROSCI.1013-06.2006.
92. Togashi H, Abe K, Mizoguchi A, Takaoka K, Chisaka O, Takeichi M. Cadherin regulates dendritic spine morphogenesis. Neuron. 2002;35:77–89. https://doi.org/10.1016/s0896-6273(02)00748-1.

93. Bozdagi O, Valcin M, Poskanzer K, Tanaka H, Benson DL. Temporally distinct demands for classic cadherins in synapse formation and maturation. Mol Cell Neurosci. 2004;27:509–21. https://doi.org/10.1016/j.mcn.2004.08.008.
94. Vitureira N, Letellier M, White IJ, Goda Y. Differential control of presynaptic efficacy by postsynaptic N-cadherin and beta-catenin. Nat Neurosci. 2012;15:81–9. https://doi.org/10.1038/nn.2995.
95. Nuriya M, Huganir RL. Regulation of AMPA receptor trafficking by N-cadherin. J Neurochem. 2006;97:652–61. https://doi.org/10.1111/j.1471-4159.2006.03740.x.
96. Saglietti L, Dequidt C, Kamieniarz K, Rousset MC, Valnegri P, Thoumine O, et al. Extracellular interactions between GluR2 and N-cadherin in spine regulation. Neuron. 2007;54:461–77. https://doi.org/10.1016/j.neuron.2007.04.012.
97. Tracy TE, Yan JJ, Chen L. Acute knockdown of AMPA receptors reveals a trans-synaptic signal for presynaptic maturation. EMBO J. 2011;30:1577–92. https://doi.org/10.1038/emboj.2011.59.
98. Bamji SX, Shimazu K, Kimes N, Huelsken J, Birchmeier W, Lu B, et al. Role of beta-catenin in synaptic vesicle localization and presynaptic assembly. Neuron. 2003;40:719–31. https://doi.org/10.1016/s0896-6273(03)00718-9.
99. Murase S, Mosser E, Schuman EM. Depolarization drives beta-catenin into neuronal spines promoting changes in synaptic structure and function. Neuron. 2002;35:91–105. https://doi.org/10.1016/s0896-6273(02)00764-x.
100. Li MY, Miao WY, Wu QZ, He SJ, Yan G, Yang Y, et al. A critical role of presynaptic cadherin/catenin/p140Cap complexes in stabilizing spines and functional synapses in the neocortex. Neuron. 2017;94:1155–1172.e1158. https://doi.org/10.1016/j.neuron.2017.05.022.
101. Tomasoni R, Repetto D, Morini R, Elia C, Gardoni F, Di Luca M, et al. SNAP-25 regulates spine formation through postsynaptic binding to p140Cap. Nat Commun. 2013;4:2136. https://doi.org/10.1038/ncomms3136.
102. Rizo J, Sudhof TC. The membrane fusion enigma: SNAREs, Sec1/Munc18 proteins, and their accomplices--guilty as charged? Annu Rev Cell Dev Biol. 2012;28:279–308. https://doi.org/10.1146/annurev-cellbio-101011-155818.
103. Niswender CM, Conn PJ. Metabotropic glutamate receptors: physiology, pharmacology, and disease. Annu Rev Pharmacol Toxicol. 2010;50:295–322. https://doi.org/10.1146/annurev.pharmtox.011008.145533.
104. Sylwestrak EL, Ghosh A. Elfn1 regulates target-specific release probability at CA1-interneuron synapses. Science. 2012;338:536–40. https://doi.org/10.1126/science.1222482.
105. Stachniak TJ, Sylwestrak EL, Scheiffele P, Hall BJ, Ghosh A. Elfn1-induced constitutive activation of mGluR7 determines frequency-dependent recruitment of somatostatin interneurons. J Neurosci. 2019;39:4461–74. https://doi.org/10.1523/JNEUROSCI.2276-18.2019.
106. Tomioka NH, Yasuda H, Miyamoto H, Hatayama M, Morimura N, Matsumoto Y, et al. Elfn1 recruits presynaptic mGluR7 in trans and its loss results in seizures. Nat Commun. 2014;5:4501. https://doi.org/10.1038/ncomms5501.
107. Dunn HA, Zucca S, Dao M, Orlandi C, Martemyanov KA. ELFN2 is a postsynaptic cell adhesion molecule with essential roles in controlling group III mGluRs in the brain and neuropsychiatric behavior. Mol Psychiatry. 2019;24:1902–19. https://doi.org/10.1038/s41380-019-0512-3.
108. Dunn HA, Patil DN, Cao Y, Orlandi C, Martemyanov KA. Synaptic adhesion protein ELFN1 is a selective allosteric modulator of group III metabotropic glutamate receptors in trans. Proc Natl Acad Sci U S A. 2018;115:5022–7. https://doi.org/10.1073/pnas.1722498115.
109. Cao Y, Sarria I, Fehlhaber KE, Kamasawa N, Orlandi C, James KN, et al. Mechanism for selective synaptic wiring of rod photoreceptors into the retinal circuitry and its role in vision. Neuron. 2015;87:1248–60. https://doi.org/10.1016/j.neuron.2015.09.002.
110. Polepalli JS, Wu H, Goswami D, Halpern CH, Sudhof TC, Malenka RC. Modulation of excitation on parvalbumin interneurons by neuroligin-3 regulates the hippocampal network. Nat Neurosci. 2017;20:219–29. https://doi.org/10.1038/nn.4471.

111. Buchert M, Schneider S, Meskenaite V, Adams MT, Canaani E, Baechi T, et al. The junction-associated protein AF-6 interacts and clusters with specific Eph receptor tyrosine kinases at specialized sites of cell-cell contact in the brain. J Cell Biol. 1999;144:361–71. https://doi.org/10.1083/jcb.144.2.361.
112. Torres R, Firestein BL, Dong H, Staudinger J, Olson EN, Huganir RL, et al. PDZ proteins bind, cluster, and synaptically colocalize with Eph receptors and their ephrin ligands. Neuron. 1998;21:1453–63. https://doi.org/10.1016/s0896-6273(00)80663-7.
113. Lin D, Gish GD, Songyang Z, Pawson T. The carboxyl terminus of B class ephrins constitutes a PDZ domain binding motif. J Biol Chem. 1999;274:3726–33. https://doi.org/10.1074/jbc.274.6.3726.
114. Bruckner K, Pablo Labrador J, Scheiffele P, Herb A, Seeburg PH, Klein R. EphrinB ligands recruit GRIP family PDZ adaptor proteins into raft membrane microdomains. Neuron. 1999;22:511–24.
115. Murai KK, Nguyen LN, Irie F, Yamaguchi Y, Pasquale EB. Control of hippocampal dendritic spine morphology through ephrin-A3/EphA4 signaling. Nat Neurosci. 2003;6:153–60. https://doi.org/10.1038/nn994.
116. Martone ME, Holash JA, Bayardo A, Pasquale EB, Ellisman MH. Immunolocalization of the receptor tyrosine kinase EphA4 in the adult rat central nervous system. Brain Res. 1997;771:238–50. https://doi.org/10.1016/s0006-8993(97)00792-0.
117. Henderson JT, Georgiou J, Jia Z, Robertson J, Elowe S, Roder JC, et al. The receptor tyrosine kinase EphB2 regulates NMDA-dependent synaptic function. Neuron. 2001;32:1041–56. https://doi.org/10.1016/s0896-6273(01)00553-0.
118. Grunwald IC, Korte M, Wolfer D, Wilkinson GA, Unsicker K, Lipp HP, et al. Kinase-independent requirement of EphB2 receptors in hippocampal synaptic plasticity. Neuron. 2001;32:1027–40. https://doi.org/10.1016/s0896-6273(01)00550-5.
119. Grunwald IC, Korte M, Adelmann G, Plueck A, Kullander K, Adams RH, et al. Hippocampal plasticity requires postsynaptic ephrinBs. Nat Neurosci. 2004;7:33–40. https://doi.org/10.1038/nn1164.
120. Liebl DJ, Morris CJ, Henkemeyer M, Parada LF. mRNA expression of ephrins and Eph receptor tyrosine kinases in the neonatal and adult mouse central nervous system. J Neurosci Res. 2003;71:7–22. https://doi.org/10.1002/jnr.10457.
121. Armstrong JN, Saganich MJ, Xu NJ, Henkemeyer M, Heinemann SF, Contractor A. B-ephrin reverse signaling is required for NMDA-independent long-term potentiation of mossy fibers in the hippocampus. J Neurosci. 2006;26:3474–81. https://doi.org/10.1523/JNEUROSCI.4338-05.2006.
122. Contractor A, Rogers C, Maron C, Henkemeyer M, Swanson GT, Heinemann SF. Trans-synaptic Eph receptor-ephrin signaling in hippocampal mossy fiber LTP. Science. 2002;296:1864–9. https://doi.org/10.1126/science.1069081.
123. Otmakhov N, Tao-Cheng JH, Carpenter S, Asrican B, Dosemeci A, Reese TS, et al. Persistent accumulation of calcium/calmodulin-dependent protein kinase II in dendritic spines after induction of NMDA receptor-dependent chemical long-term potentiation. J Neurosci. 2004;24:9324–31. https://doi.org/10.1523/JNEUROSCI.2350-04.2004.
124. Okamoto K, Nagai T, Miyawaki A, Hayashi Y. Rapid and persistent modulation of actin dynamics regulates postsynaptic reorganization underlying bidirectional plasticity. Nat Neurosci. 2004;7:1104–12. https://doi.org/10.1038/nn1311.
125. Sun Y, Smirnov M, Kamasawa N, Yasuda R. Rapid ultrastructural changes in the PSD and surrounding membrane after induction of structural LTP in single dendritic spines. J Neurosci. 2021;41:7003–14. https://doi.org/10.1523/JNEUROSCI.1964-20.2021.
126. Bell ME, Bourne JN, Chirillo MA, Mendenhall JM, Kuwajima M, Harris KM. Dynamics of nascent and active zone ultrastructure as synapses enlarge during long-term potentiation in mature hippocampus. J Comp Neurol. 2014;522:3861–84. https://doi.org/10.1002/cne.23646.

127. Budreck EC, Kwon OB, Jung JH, Baudouin S, Thommen A, Kim HS, et al. Neuroligin-1 controls synaptic abundance of NMDA-type glutamate receptors through extracellular coupling. Proc Natl Acad Sci U S A. 2013;110:725–30. https://doi.org/10.1073/pnas.1214718110.
128. Shipman SL, Nicoll RA. A subtype-specific function for the extracellular domain of neuroligin 1 in hippocampal LTP. Neuron. 2012;76:309–16. https://doi.org/10.1016/j.neuron.2012.07.024.
129. Wu X, Morishita WK, Riley AM, Hale WD, Sudhof TC, Malenka RC. Neuroligin-1 signaling controls LTP and NMDA receptors by distinct molecular pathways. Neuron. 2019;102:621–635.e623. https://doi.org/10.1016/j.neuron.2019.02.013.
130. Kashiwagi Y, Higashi T, Obashi K, Sato Y, Komiyama NH, Grant SGN, et al. Computational geometry analysis of dendritic spines by structured illumination microscopy. Nat Commun. 2019;10:1285. https://doi.org/10.1038/s41467-019-09337-0.
131. Hruska M, Henderson N, Le Marchand SJ, Jafri H, Dalva MB. Synaptic nanomodules underlie the organization and plasticity of spine synapses. Nat Neurosci. 2018;21:671–82. https://doi.org/10.1038/s41593-018-0138-9.
132. Tang AH, Chen H, Li TP, Metzbower SR, MacGillavry HD, Blanpied TA. A trans-synaptic nanocolumn aligns neurotransmitter release to receptors. Nature. 2016;536:210–4. https://doi.org/10.1038/nature19058.
133. Liu G, Choi S, Tsien RW. Variability of neurotransmitter concentration and nonsaturation of postsynaptic AMPA receptors at synapses in hippocampal cultures and slices. Neuron. 1999;22:395–409. https://doi.org/10.1016/s0896-6273(00)81099-5.
134. Tong G, Jahr CE. Block of glutamate transporters potentiates postsynaptic excitation. Neuron. 1994;13:1195–203. https://doi.org/10.1016/0896-6273(94)90057-4.
135. Xie X, Liaw JS, Baudry M, Berger TW. Novel expression mechanism for synaptic potentiation: alignment of presynaptic release site and postsynaptic receptor. Proc Natl Acad Sci U S A. 1997;94:6983–8. https://doi.org/10.1073/pnas.94.13.6983.
136. Haas KT, Compans B, Letellier M, Bartol TM, Grillo-Bosch D, Sejnowski TJ, et al. Pre-post synaptic alignment through neuroligin-1 tunes synaptic transmission efficiency. eLife. 2018;7:e31755. https://doi.org/10.7554/eLife.31755.
137. Ramsey AM, Tang AH, LeGates TA, Gou XZ, Carbone BE, Thompson SM, et al. Subsynaptic positioning of AMPARs by LRRTM2 controls synaptic strength. Sci Adv. 2021;7:eabf3126. https://doi.org/10.1126/sciadv.abf3126.
138. Bemben MA, Shipman SL, Hirai T, Herring BE, Li Y, Badger JD 2nd, et al. CaMKII phosphorylation of neuroligin-1 regulates excitatory synapses. Nat Neurosci. 2014;17:56–64. https://doi.org/10.1038/nn.3601.
139. Hosokawa T, Liu PW, Cai Q, Ferreira JS, Levet F, Butler C, et al. CaMKII activation persistently segregates postsynaptic proteins via liquid phase separation. Nat Neurosci. 2021;24:777–85. https://doi.org/10.1038/s41593-021-00843-3.
140. Hayashi Y, Ford LK, Fioriti L, McGurk L, Zhang M. Liquid-liquid phase separation in physiology and pathophysiology of the nervous system. J Neurosci. 2021;41:834–44. https://doi.org/10.1523/JNEUROSCI.1656-20.2020.
141. Zeng M, Shang Y, Araki Y, Guo T, Huganir RL, Zhang M. Phase transition in postsynaptic densities underlies formation of synaptic complexes and synaptic plasticity. Cell. 2016;166:1163–1175.e1112. https://doi.org/10.1016/j.cell.2016.07.008.
142. Feng Z, Chen X, Zeng M, Zhang M. Phase separation as a mechanism for assembling dynamic postsynaptic density signalling complexes. Curr Opin Neurobiol. 2019;57:1–8. https://doi.org/10.1016/j.conb.2018.12.001.
143. Zhang H, Ji X, Li P, Liu C, Lou J, Wang Z, et al. Liquid-liquid phase separation in biology: mechanisms, physiological functions and human diseases. Sci China Life Sci. 2020;63:953–85. https://doi.org/10.1007/s11427-020-1702-x.
144. Yoshida T, Yamagata A, Imai A, Kim J, Izumi H, Nakashima S, et al. Canonical versus non-canonical transsynaptic signaling of neuroligin 3 tunes development of sociality in mice. Nat Commun. 2021;12:1848. https://doi.org/10.1038/s41467-021-22059-6.

145. Stogsdill JA, Ramirez J, Liu D, Kim YH, Baldwin KT, Enustun E, et al. Astrocytic neuroligins control astrocyte morphogenesis and synaptogenesis. Nature. 2017;551:192–7. https://doi.org/10.1038/nature24638.

Lipids and Secretory Vesicle Exocytosis

Isaac O. Akefe, Shona L. Osborne, Benjamin Matthews, Tristan P. Wallis, and Frédéric A. Meunier

Abstract In recent years, the number of studies implicating lipids in the regulation of synaptic vesicle exocytosis has risen considerably. It has become increasingly clear that lipids such as phosphoinositides, lysophospholipids, cholesterol, arachidonic acid and myristic acid play critical regulatory roles in the processes leading up to exocytosis. Lipids may affect membrane fusion reactions by altering the physical properties of the membrane, recruiting key regulatory proteins, concentrating proteins into exocytic "hotspots" or by modulating protein functions allosterically. Discrete changes in phosphoinositides concentration are involved in multiple trafficking events including exocytosis and endocytosis. Lipid-modifying enzymes such as the DDHD2 isoform of phospholipase A1 were recently shown to contribute to memory acquisition via dynamic modifications of the brain lipid landscape. Considering the increasing reports on neurodegenerative disorders associated with aberrant intracellular trafficking, an improved understanding of the control of lipid pathways is physiologically and clinically significant and will afford unique insights into mechanisms and therapeutic methods for neurodegenerative diseases. Consequently, this chapter will discuss the different classes of lipids, phospholipase enzymes, the evidence linking them to synaptic neurotransmitter release and how they act to regulate key steps in the multi-step process leading to neuronal communication and memory acquisition.

I. O. Akefe · B. Matthews · T. P. Wallis
Clem Jones Centre for Ageing Dementia Research, Queensland Brain Institute, The University of Queensland, St Lucia, QLD, Australia

S. L. Osborne
ARC Training Centre for Innovation in Biomedical Imaging Technology (CIBIT), The University of Queensland, St Lucia, QLD, Australia

F. A. Meunier (✉)
Clem Jones Centre for Ageing Dementia Research, Queensland Brain Institute, The University of Queensland, St Lucia, QLD, Australia

School of Biomedical Sciences, The University of Queensland, St Lucia, QLD, Australia
e-mail: f.meunier@uq.edu.au

Z.-W. Wang (ed.), *Molecular Mechanisms of Neurotransmitter Release*, Advances in Neurobiology 33, https://doi.org/10.1007/978-3-031-34229-5_14

Keywords Secretory vesicle · Exocytosis · Cholesterol · Phospholipids · Phosphoinositide · Phospholipases · Fatty acids · Sphingolipids · Lipid post-translational modification · Neurotransmission

1 Introduction

Brain cells communicate with each other through the release of neurotransmitter molecules across the synapse, via neuroexocytosis, involving the fusion of neurotransmitter-filled vesicles with the presynaptic membrane [1]. Lipids are the principal components of biological membranes, constituting about half of the brain's dry weight and contributing to the brain's complex structure and function [2, 3]. The main classes of membrane lipid molecules include sphingolipids, sterol lipids, fatty acids, phospholipids, glycerolipids and prenol lipids (Fig. 1a) [4, 5], among which phospholipids are the most abundant [6]. In addition to their structural contribution, phospholipids serve as substrates for various phospholipid-metabolising enzymes, such as phospholipase A (PLA), which hydrolyse phospholipids to release free fatty acids (FFAs) and lysophospholipid (LPL) metabolites capable of recruiting and activating critical proteins, altering basic membrane properties, and functioning as lipid signalling molecules [7, 8]. Exocytosis is a biologically complex process involving the release of neurotransmitters as well as a variety of inter- and intracellular communication mechanisms. While the role of proteins in neurosecretory vesicle cycling has been extensively investigated, the appreciation for lipid involvement has been slower to develop [9]. However, a few important findings have emerged from this growing field, which highlight key roles that membrane lipids play in coordinating the membrane trafficking and signalling events underlying neurotransmitter release [9–12].

The synaptic vesicle (SV) cycle depends upon coordinated membrane fusion and fission events [13–15]. The favoured model for membrane fusion to occur is via the formation of a lipidic hemifusion intermediate [9, 13, 16, 17] (Fig. 1b). According to this model, merging of the two proximal leaflets of the vesicle and plasma membrane bilayers to form the hemifusion intermediate would precede the merging of the two distal leaflets to form the fusion pore [18]. Both fusion and fission require large deformations in membrane curvature. This deformation

Fig. 1 (continued) microdomains that can target and localise certain classes of proteins into functional platforms. (**b**) The favoured model for membrane fusion is via a lipidic hemifusion or stalk intermediate where lipid mixing of the two inner leaflets of the bilayer occurs prior to lipid mixing of the outer bilayers. (**c**) Certain classes of lipids are asymmetrical in shape and thus are unable to form planar structures. Such lipids can be classified into cone-shaped (e.g. phosphatidic acid) and inverted cone-shaped (e.g. lysophosphatidic acid). Such lipids tend to promote either negative or positive curvature as depicted for phosphatidic acid and lysophosphatidic acid. Aq, aqueous

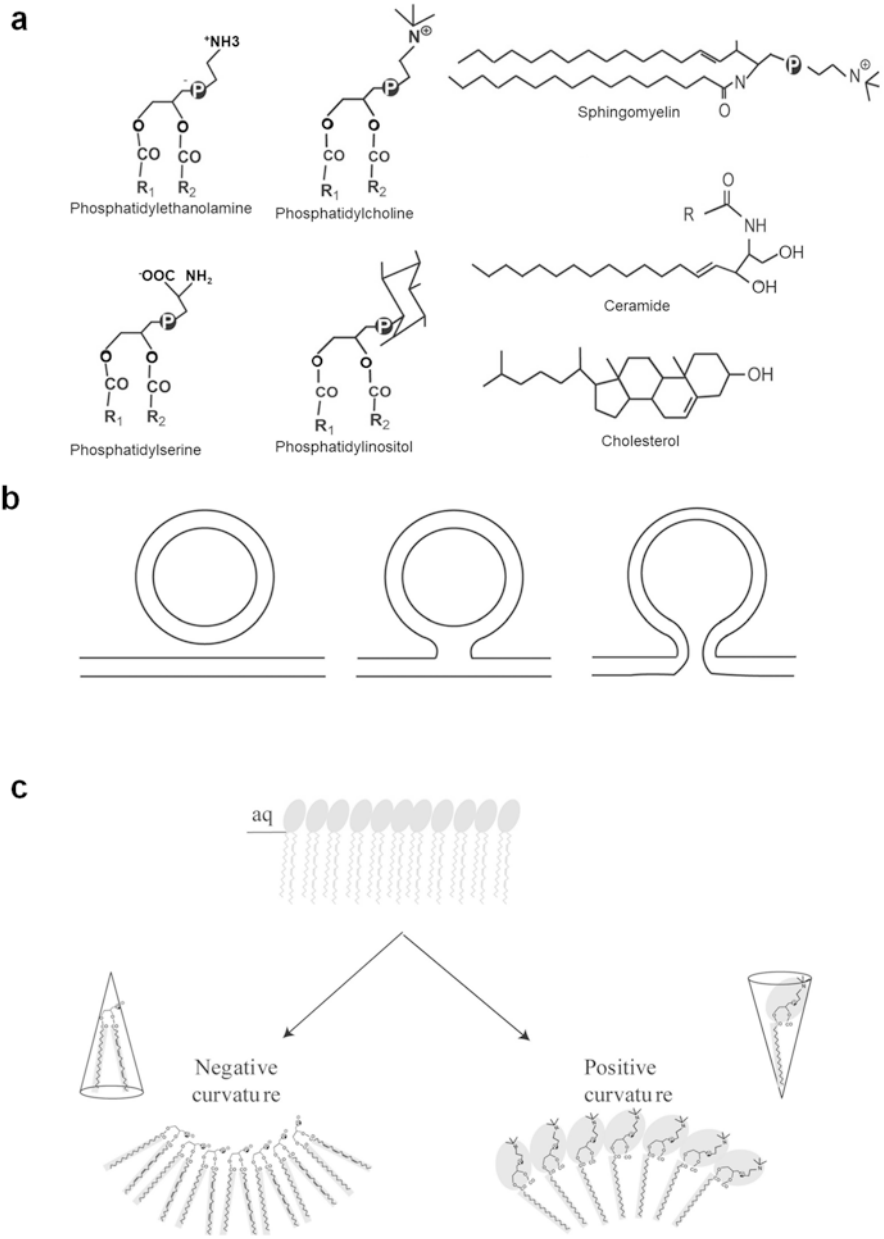

Fig. 1 Lipids and membrane fusion. (**a**) The structure of important classes of lipids is shown. Phospholipids (phosphatidylcholine, phosphatidylethanolamine, phosphatidylinositol and phosphatidylserine) are the most abundant cellular lipids, comprising a headgroup, which identifies the lipid, and two fatty acid chains linked to a glycerophosphate backbone. In addition to structural and other roles, they are precursors for signalling lipids such as phosphoinositides, phosphatidic acid and lysophospholipids. Sphingomyelin, cholesterol and ceramide can aggregate into lipidic

is facilitated by the formation of high local concentrations of lipids with altered shapes (Fig. 1c). Certain lipids have a spontaneous curvature when in a monolayer, either positive (curvature in the direction of the polar headgroup) or negative (curvature in the direction of the hydrophobic tails) [19]. These lipids are classified as inverted cone-shaped and cone-shaped lipids, respectively [20]. Examples that will be discussed include phosphatidic acid (PA), a cone-shaped lipid, and lysophospholipids [3, 6, 21], which are inverted cone-shaped lipids (Fig. 1c).

In addition to structural roles, it is becoming increasingly apparent that lipids can function as bona fide signalling molecules in many intracellular processes including membrane trafficking. Elucidating the complex molecular mechanisms underlying physiological regulation of exocytosis by phospholipids and their metabolites will improve our understanding of neurotransmission, and facilitate the development of new therapeutic agents for certain neurological disorders associated with altered neurotransmitter release [22]. Uncovering the involvement of phospholipase enzymes that dynamically modulate the phospholipid membrane bilayer to impact exocytosis, is essential. Further, how such modifications of the lipidic landscape affect synaptic plasticity leading to learning and memory is also a hot topic. Hence, this chapter focuses on recent findings on the roles of phospholipids and their metabolites, as well as phospholipid-metabolising enzymes, in vesicular exocytosis and memory.

2 Phospholipids and Vesicle Trafficking

Phospholipids constitute the majority of membrane lipids. The term "phospholipids" generally refers to lipids with a phosphate moiety, but is also used more broadly to include ester-linked sphingomyelins, lysophospholipids and diacylglycerophospholipids [7]. All phospholipids are comprised of a glycerol backbone having two ester-linked fatty acyl moieties at the *sn-1* (stereospecific number; The Nomenclature of Lipids, 1967) and *sn-2* positions, and a phosphodiester bond connecting a hydrophilic headgroup such as ethanolamine, choline, inositol or serine at the *sn-3* position (Fig. 2). The specific headgroups are responsible for the unique physical and chemical properties of the distinct phospholipid classes, of which phosphatidylcholine (PC), phosphatidylethanolamine (PE), phosphatidylserine (PS), phosphatidic acid (PA), phosphatidylglycerol (PG) and phosphatidylinositol (PI) are predominant. PC, PE and PS (Fig. 1a) are the most abundant classes detected in mammals [5]. PA, PG and PI are less abundant, although this does not imply a lesser biological significance. At the *sn-1* and *sn-2* positions of glycerol, the fatty acids of phospholipids are esterified and can be classified based on their chain length (number of carbons), and position and number of double bonds [23].

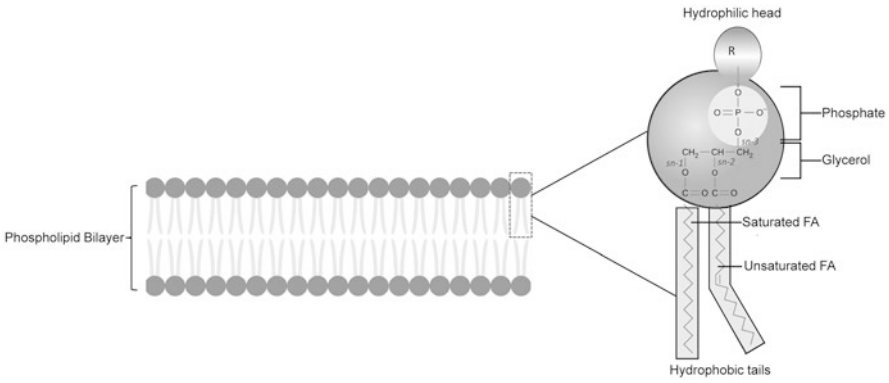

Fig. 2 Phospholipid bilayer. Hydrophobic phospholipid tails orient towards the inner bilayer, and hydrophilic headgroups orient outwards

2.1 Phosphoinositides in Synaptic Vesicle Cycle

Phospholipids consist of two fatty acid side chains, whose composition can vary, linked to a polar headgroup via a glycerol molecule. In the case of phosphatidylinositol (PtdIns), the polar headgroup is an inositol ring linked to the glycerol backbone at the *sn-1* position (Fig. 2). Although PtdIns is only a minor membrane lipid, its phosphorylated derivatives are important regulators of protein functions. PtdIns is unique among phospholipids in that the headgroup can be reversibly phosphorylated on the 3, 4 and 5 positions by a host of phosphatidylinositol kinases (PIKs) producing a family of seven different PtdIns (Fig. 3). This lipid family including PtdIns is refered to as phosphoinositides (PI). PI phosphorylated at the 2 and 6 positions have not been described, and presumably cannot be synthesised due to steric hindrance. High local concentrations of specific PI family members may serve as signals for site-specific recruitment of effectors and for allosteric modulation of protein function. The rapid and reversible phosphorylation of PI makes them ideal candidates for the tight spatio-temporal regulation of both exo- and endocytosis to sustain neurotransmitter release. PI are key signalling molecules in many cellular processes and are the most studied lipid molecules for their roles in the synaptic vesicle cycle. The subcellular localisation and regulated activity of PI-metabolising enzymes are key to understanding the role of PI in exocytosis and will be discussed in detail below.

2.2 Phosphoinositide-Metabolising Enzymes at the Synapse

A large body of work on the role of lipids in exocytosis has come from studies with cell lines such as bovine adrenal chromaffin cells and the rat phaeochromocytoma (PC12) cell line. Earlier work focussed on phosphatidylinositol 4,5-bisphosphate

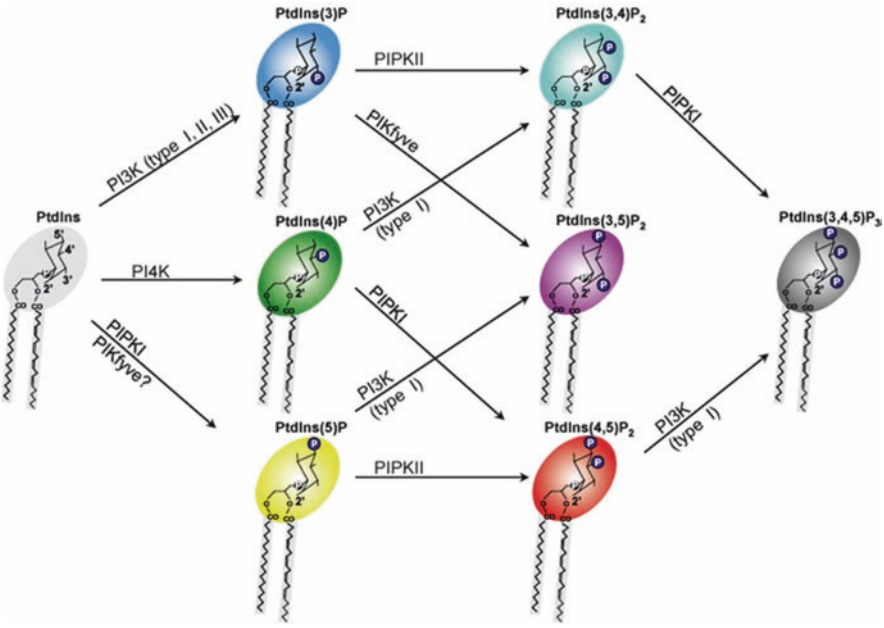

Fig. 3 Phosphoinositides (PI) family. Phosphatidylinositol (PtdIns) consists of two fatty acid side chains linked to the polar inositol headgroup via a glycerophosphate linkage and is mainly found on the cytosolic face of the membrane bilayer. The inositol headgroup can be reversibly phosphorylated by a series of kinases and phosphatases at three positions (3, 4 and 5) to form a family of seven phosphoinositides. PIKfyve, FYVE finger containing phosphoinositide kinase

($PtdIns(4,5)P_2$) with the evidence in support of its roles in exocytosis extended from cell lines to native neurons. More recently, evidence has been building in support of the involvement of other PIs including those synthesised by PI3-kinases (PI3Ks). The contribution of enzymes involved in $PtdIns(4,5)P_2$ metabolism will be discussed first since this is the best studied PtdIns with regard to the synaptic vesicle cycle, followed by PI3K.

2.2.1 $PtdIns(4,5)P_2$ and the Synaptic Vesicle Cycle

A number of enzymes involved in $PtdIns(4,5)P_2$ production are found in neurons, including PI4 kinases (PI4K), PtdIns4P-5 kinases (PI5K) and phosphatases. The major pathways for $PtdIns(4,5)P_2$ metabolism in neurons are illustrated in Fig. 4. The first step is the phosphorylation of PtdIns by a PI4K, generating PtdIns4P. The PtdIns4P then serves as a substrate for a PtdIns4P-5 kinase that adds a phosphate at position 5 to generate $PtdIns(4,5)P_2$. In neurons, there are two isoforms of PI4K implicated in neurotransmitter release: PI4KIIα and PI4KIIIβ.

PI4KIIα is present on synaptic vesicles and can produce PtdIns4P on immunoisolated SVs in vitro [24] despite phosphatidylinositol comprising only a minor

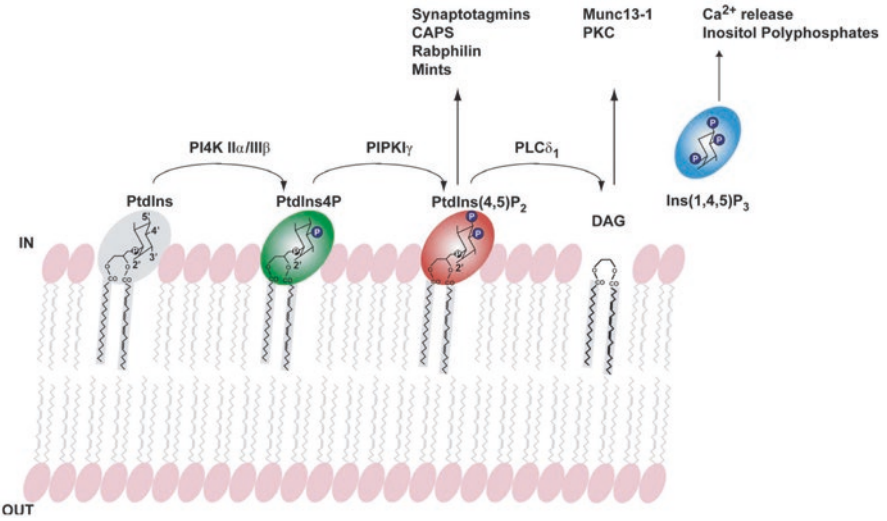

Fig. 4 Phosphoinositides and exocytosis. The major synaptic pathway for synthesis of PtdIns(4,5)P_2 is depicted here since it is the best characterised phosphoinositide functioning in exocytosis and endocytosis. PtdIns(4,5)P_2 functions as a signal to regulate the location and/or function of the synaptic proteins indicated and may also function as a substrate of phospholipase C δ1 (PLCδ1), which cleaves PtdIns(4,5)P_2 generating soluble Ins(1,4,5)P_3 and diacylglycerol (DAG), which remains confined to the bilayer and regulates exocytosis through binding to Munc13-1 and protein kinase C (PKC)

proportion of SV lipid composition (~1% lipid by mass) [25]. However, whether PI4K can generate PtdIns4P on synaptic vesicles in vivo is still unclear. Furthermore, the significance of an SV pool of PtdIns4P is also unclear given that the major PtdIns4P-5 kinase at the synapse, PIPKIγ, is cytosolic and PtdIns(4,5)P_2 on the synaptic plasma membrane is required for exocytosis [26]. One possibility is that PI4KIIα may be activated following fusion of the vesicle membrane with the plasma membrane and prior to endocytosis since PtdIns(4,5)P_2 formation is also crucial for endocytosis.

The localisation and activity of PI4KIIIβ (on the synaptic vesicle membrane) can be regulated, potentially providing an extra level of control for exocytosis. PI4KIIIβ interacts with neuronal calcium sensor-1 (NCS-1, also known as frequenin). In PC12 cells, NCS-1 has been shown to regulate nucleotide-dependent exocytosis via PI4KIIIβ, and both NCS-1 and PI4KIIIβ are transiently recruited to the plasma membrane upon stimulation of exocytosis [27], suggesting that PI4KIIIβ could synthesise the PtdIns4P used by cytosolic PIPKIγ to produce PtdIns(4,5)P_2.

The major PtdIns4P 5-kinase in neurons is PIPKIγ, which is a cytosolic protein. In PIPKI knockout mice, a loss of synaptic PtdIns(4,5)P_2 is correlated with a decrease in the size of the readily releasable pool of SV [28], consistent with a role of PtdIns(4,5)P_2 in priming. PIPKIγ likely synthesises the PtdIns(4,5)P_2 required for

both exocytosis and endocytosis since the knockout mouse shows endocytic defects in addition to the defects in priming [28]. Many of the proteins required for clathrin-mediated endocytosis bind to PtdIns(4,5)P_2. Since neurons in PIPKIγ knockout mice were shown to be lacking endocytic structures, PtdIns(4,5)P_2 appears to be important for the recruitment of endocytic proteins and the process of clathrin-mediated endocytosis [28]. Further evidence for the importance of PtdIns(4,5)P_2 in clathrin-mediated synaptic vesicle endocytosis comes from mice lacking the protein synaptojanin, which is the major PtdIns(4,5)P_2 phosphatase. Neurons in synaptojanin knockout mice exhibit a defect in vesicle uncoating [29].

Once synthesised, PtdIns(4,5)P_2 can be removed either via the action of the PtdIns(4,5)P_2 phosphatase synaptojanin to become PI4P, as is required for clathrin-coated vesicle uncoating, or through the action of a phospholipase C (PLC) to become the classical second messengers Ins(1,4,5)P_3 and diacylgycerol (DAG, Fig. 4).

2.2.2 PI3-Kinases and the Synaptic Vesicle Cycle

PI3-kinases (PI3Ks) are a family of enzymes that phosphorylate PI at 3 positions. There are three classes of enzymes, classes I, II and III, of which class I and class II enzymes have been implicated in the regulation of exocytosis. Class III enzymes are involved in constitutive trafficking through early endosomes and may be involved in synaptic vesicle recycling since recent evidence suggests that synaptic vesicle recycling occurs through PtdIns3P-positive presynaptic endosomes – a process tightly controlled by rab5 [30].

Type I PI3Ks predominantly phosphorylate PtdIns(4,5)P_2 on the plasma membrane to form PtdIns(4,5)P_2, and are the best studied class in all systems [31]. However, their involvement in synaptic processes is questionable. Classically, PI3Ks were studied using the inhibitors wortmannin and LY294002, and an involvement of PI3K was inferred from sensitivity to these generic inhibitors. However, studies using these inhibitors at the synapse have yielded conflicting results. For example, little or no inhibition of exocytosis was observed from both synaptosomes and neurosecretory cells using wortmannin and LY294002 [24, 26, 32–34]. However, wortmannin inhibits both spontaneous and evoked quantal neurotransmitter release at the neuromuscular junction [35], while high doses of LY294002 inhibit synaptic vesicle recycling and increase spontaneous acetylcholine release [36]. These discrepancies may partly be due to the lack of specificity of LY294002, which is known to also block myosin light chain kinase activity. However, it may also be due to the involvement of other PI3Ks such as PI3K-C2α (a Class II PI3K), which is much less sensitive to both inhibitors. In this view, PI3K-C2α was shown to be necessary for the ATP-dependent priming step of exocytosis in neurosecretory cells [37]. Further work has demonstrated that this isoform is recruited to secretory granules and generates PtdIns3P in response to stimulation, suggesting that its activity is regulated by Ca^{2+} [38].

PI3Ks may also play other roles at different stages of the synaptic vesicle cycle. For example, the p85 subunit of type I PI3Kγ interacts with synapsin and plays an important role in regulating vesicle availability from the readily releasable pool [39]. Another type I PI3K, PI3K II, has been implicated in the trafficking and insertion of neuronal calcium channels into the plasma membrane and the subsequent alterations in calcium influx may modulate exocytosis [40]. Inhibition of type I PI3Kδ promotes a transient increase of PtdIns(4,5)P_2 in the plasma membrane of neurosecretory cells and also promotes secretory vesicle docking [41]. In other fields, type I PI3Kδ regulates the trafficking of tumour necrosis factor-alpha (TNF-α) in macrophages [42], and inhibition of PI3Kδ is neuroprotective in a stroke murine model [43]. Further, PI3Kδ might regulate anterograde trafficking of amyloid precursor protein (APP) in neurons because PI3Kδ inhibition can rescue the pathologies associated with the APP/presenilin1 (PS1) murine model of Alzheimer's disease (AD) [40, 44].

2.2.3 Phosphoinositide-Binding Proteins Involved in Exocytosis

PtdIns(4,5)P_2 is mainly localised to the plasma membrane in neurons and neurosecretory cells. Plasma membrane PtdIns(4,5)P_2 is likely to be important for exocytosis since modifying plasma membrane PtdIns(4,5)P_2 levels in chromaffin cells alters secretion by regulating the number of vesicles available for fusion [26]. This effect is regulated via an equilibrium between PI3Kδ and the PI phosphatase PTEN (phosphatase and tensin homolog) [41]. Several presynaptic proteins contain PI-binding motifs and may bind with varying degrees of selectivity to one or more phosphoinositides.

The best studied phosphoinositide-binding motif at the synapse is the C2B domain of synaptotagmin 1, the calcium-sensor for exocytosis (see chapter "Calcium Sensors of Neurotransmitter Release"). Synaptotagmin 1 binds both acidic phospholipids and phosphoinositides, particularly PtdIns(4,5)P_2. There are two phosphoinositide-binding sites in synaptotagmin 1: the first is a calcium-independent site, discrete from the acidic phospholipid-binding sites in the polybasic region on the C2B domain, while the second is a calcium-dependent site mediated through the calcium-binding loops [29]. Other synaptotagmin isoforms, including synaptotagmin 7 and the related synaptotagmin-like protein 4 (granuphilin), also bind PtdIns(4,5)P_2 and may regulate large dense core vesicle (LDCV) exocytosis [45–47].

While synaptotagmin isoforms are important for the exocytosis of both large dense core vesicles and synaptic vesicles, the calcium-dependent activator protein for secretion (CAPS), a cytosolic protein that binds to PtdIns(4,5)P_2, regulates the exocytosis of only LDCVs [48]. Interestingly, besides a reduction in the secretion of LDCVs, heterozygous CAPS-1 knockout mice also show defects in vesicle filling [49], suggesting that CAPS-1 plays multiple roles in the vesicle cycle. Other PtdIns(4,5)P_2-binding proteins include MINTS (Munc18 interacting proteins also called X11-like proteins), annexin and rabphilin. PtdIns(4,5)P_2 binding is critical for a number of endocytic proteins such as the clathrin adaptor proteins AP-2 and AP-180, epsin, amphiphysin and dynamin. Disruption of PtdIns(4,5)P_2-binding

sites prevents their recruitment and inhibits endocytosis [50]. The identification of CAPS-1 as a novel effector of PtdIns(4,5)P_2 on secretory granules suggests that there might be other phosphoinositide-binding proteins to be identified. Given the emerging significance of 3-phosphorylated phosphoinositides in exocytosis, it will be important to identify potential interacting proteins that may mediate the effects of these lipids on the synaptic vesicle cycle.

2.3 Concluding Remarks

Phosphoinositides, in particular PtdIns(4,5)P_2, have multiple functions at the synapse, including regulating exocytosis, endocytosis and calcium channels. To reconcile so many functions with one molecule, one can envisage that it is the localised production of PtdIns(4,5)P_2 in microdomains that are critical for its pleiotropic function. Many phosphoinositide-binding proteins require simultaneous binding to a protein factor and phosphoinositide for correct and efficient localisation and function. Such coincidental detection can explain how PtdIns(4,5)P_2 might coordinate multiple pathways occurring in such a confined localisation. While many questions remain to be addressed, phosphoinositides occupy an important position in the hierarchy of factors regulating the synaptic vesicle cycle.

3 Phospholipid-Metabolising Enzymes

Neurons communicate across the synapse using neurotransmitters, which are released upon fusion of synaptic vesicles with the plasma membrane. While this activity is largely coordinated by well-characterised interactions of the soluble N-ethylmaleimide sensitive factor attachment protein receptor (SNARE) protein complex [51], it also necessitates dynamic remodelling of the properties of the vesicular and synaptic membrane to facilitate fusion [52]. To facilitate vesicle fusion, phospholipids localise and reorganise in the membrane in such a way that conically shaped lipids, PE and PI, accumulate in the regions of high curvature at the fusion site, and lamellar-shaped lipids, such as PC, are prevalent in the low-curvature regions [12]. Membrane remodelling is a consequence of a large range of lipid-modifying enzymes, of which phospholipases are particularly noteworthy.

3.1 Phospholipases and Membrane Processing

Phospholipases are a group of lipolytic enzymes catalysing the hydrolysis of phospholipid ester bonds. They are ubiquitously distributed, regulated by Ca^{2+} or other stimuli, and can be secreted both intracellularly and extracellularly. The four major

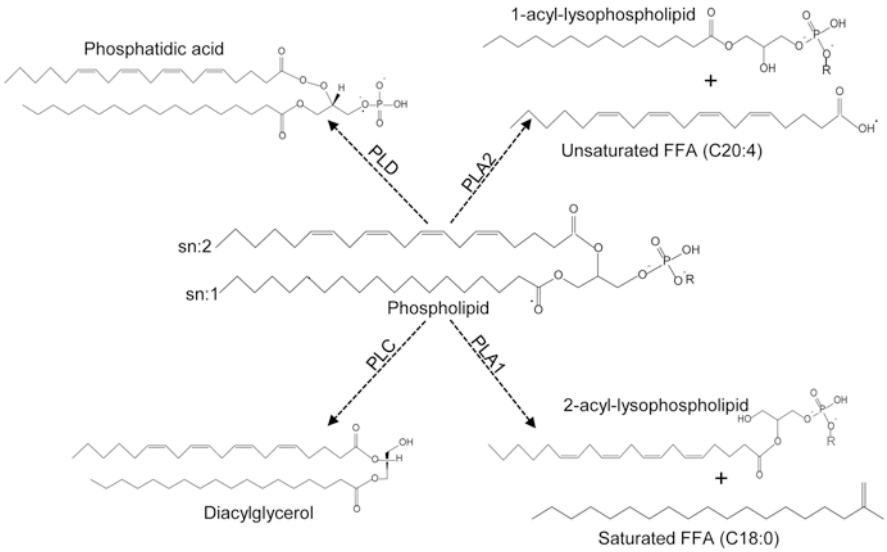

Fig. 5 Phospholipases and their site of action. The different phospholipases act on specific regions of the phospholipid to generate bioactive metabolites, consequently modifying the membrane lipid landscape to impact exocytosis and memory

types of phospholipases (A, B, C and D) are categorised according to the phospholipid site of cleavage (Fig. 5).

Within each of the phospholipase families, there are multiple isoforms with distinct activities and expression patterns in different cell types and organelles [5, 7, 53]. Phospholipase A1 and A2 (PLA1 and PLA2) enzymes catalyse the cleavage of the acyl ester link at the *sn-1* and *sn-2* positions of phospholipid glycerol moieties, respectively, to generate FFAs and either 2-acyl or 1-acyl-lysophospholipids [54]. Phospholipase B (PLB) enzymes are fatty acid ester hydrolases with *sn-1* and *sn-2* activity, as well as lysophospholipase and transacylase activity. Phospholipase C (PLC) enzymes hydrolyse the proximal phosphodiester linkage to generate a free phospho-headgroup and a diacylglycerol (DAG), whereas phospholipase D (PLD) enzymes hydrolyse the distal phosphodiester bond to generate a free headgroup and phosphatidic acid (PA) [54]. Phospholipases therefore play a critical role in dynamically modifying the membrane lipid landscape to generate bioactive metabolites and in directly regulating the process of fusion during exocytosis and neurotransmission [13, 20]. Consequently, genetic mutations in the various phospholipases have been implicated in different neurological disorders in which impaired vesicular trafficking is a major feature (Fig. 6).

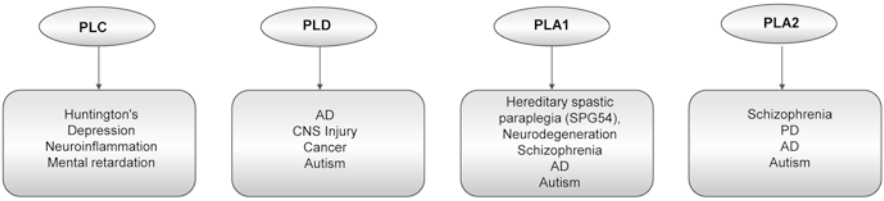

Fig. 6 Implication of specific phospholipases in neurological disorders associated with impairment in vesicular trafficking. Genetic mutation in the various phospholipases have been implicated in different neurological disorders in which impaired vesicular trafficking is a major feature

3.2 Phospholipase D (PLD)

3.2.1 Phospholipase D (PLD) in Phosphatidic Acid (PA) Processing

Phospholipase D hydrolyses phosphatidylcholine to produce phosphatidic acid (PA; Fig. 7a) [55]. Phosphatidic acid can either act as a signalling molecule or alter the biophysical properties of the membrane directly [56]. Phosphatidic acid can also be further hydrolysed by phosphatidic acid hydrolase to remove the phosphate to produce diacylglycerol (Fig. 7) or by PLA2 to remove one fatty acid chain to produce lysophosphatidic acid (discussed further in Sect. 4). There are two mammalian isoforms of PLD: PLD1 and PLD2. Both of them require PtdIns(4,5)P_2 as an essential cofactor for activation while PLD1 activity is additionally regulated by small GTPases including Arf6 [57]. Work with neurosecretory chromaffin cells indicates that PLD1, and in particular $PLD1_b$, is the isoform that regulates exocytosis [58].

3.2.2 Phospholipase D (PLD) in Exocytosis

There is good evidence that PLD is required for exocytosis of LDCV in chromaffin cells. Overexpression of PLD1 (but not PLD2) potentiates exocytosis, whereas either expression of a catalytically inactive PLD1 or knockdown of PLD1 by RNAi inhibits exocytosis [59]. $PLD1_b$ localises to the plasma membrane and is thought to be the isoform responsible for the effect on exocytosis. PLD1 appears to act at a post-docking stage of exocytosis [55, 56, 60]. There are two main hypotheses, not mutually exclusive, that could explain how phosphatidic acid affects exocytosis: (1) Phosphatidic acid may stimulate the activity of PIPKI, which is known to have a facilitating role in exocytosis [26], to promote de novo synthesis of PtdIns(4,5)P_2. Because PtdIns(4,5)P_2 is an essential cofactor for PLD1, the increased PtdIns(4,5)P_2 level may further stimulate the production of phosphatidic acid, forming a positive feedback loop (Fig. 7a). This could act to rapidly produce high local concentrations of PtdIns(4,5)P_2 at sites of exocytosis. (2) Phosphatidic acid may increase the fusogenicity of the membrane at exocytic sites by promoting the formation of a negative curvature and a hemifusion intermediate [55, 56, 61] (Fig. 7b).

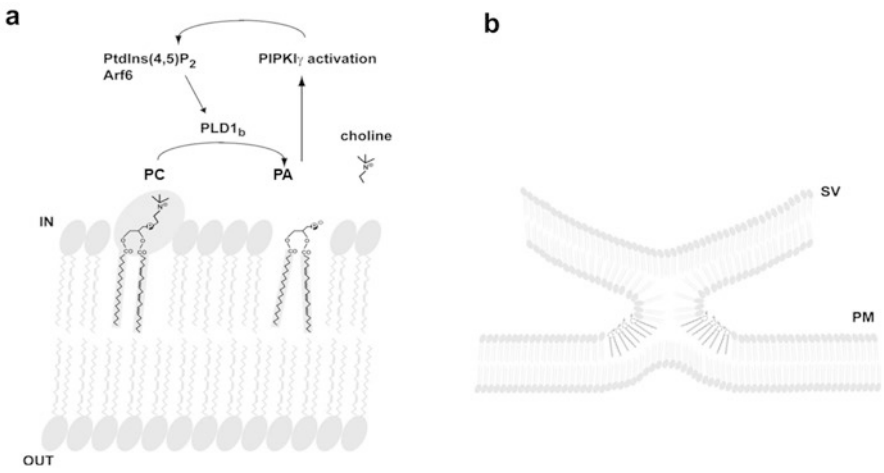

Fig. 7 Phosphatidic acid and exocytosis. (**a**) Phosphatidylcholine (PC) is the major substrate for phospholipase D (PLD). During exocytosis, a PLD, likely $PLD1_b$, acts on PC, liberating phosphatidic acid (PA) and free choline. While no role has been attributed to the soluble choline moiety, PA is known to activate type I phosphatidylinositol kinase, likely PIPKIγ. PtdIns(4,5)P_2 produced by PIPKI is an essential cofactor for $PLD1_b$ activity and stimulates its activity together with the small GTPase Arf6, a possible positive feedback loop for the localised generation of PA. (**b**) PA may also act by promoting deformation of the membrane bilayer. PA is a cone-shaped lipid that promotes negative curvature of the bilayer as is required for formation of a fusion stalk intermediate prior to fusion pore formation and thus may act physically to promote exocytosis. SV, synaptic vesicle; PM, plasma membrane

Microinjection of a catalytically inactive PLD1 inhibited acetylcholine release in *Aplysia* neurons [62], suggesting that PLD1 might play a similar role in synaptic vesicle exocytosis. To substantiate this notion, PLD activity is inhibited by several endocytic proteins in neurons including amphiphysins, synaptojanin and AP-180 [63–65], suggesting that PLD may also be implicated in regulating the endocytic aspects of the vesicle cycle. However, the putative roles of PLD in both neuronal exocytosis and endocytosis require further work to establish.

3.3 Phospholipase C (PLC)

3.3.1 Phospholipase C (PLC) in Phosphoinositide (PI) Processing

PLC cleaves PtdIns(4,5)P_2 to produce diacylglycerol (DAG) and inositol-triphosphate (Ins(1,4,5)P_3 also called IP_3), both being important second messengers. DAG remains confined to the membrane lipid bilayer where it can modulate the activities of protein kinase C (PKC) and Munc13 [17, 66], whereas Ins(1,4,5)P_3 is water soluble, and can either act to promote the release of Ca^{2+} from intracellular stores or be further phosphorylated to become IP_4 (see Fig. 4).

DAG may bind to the C1 domain of both PKC and Munc13. Munc13 is required for SV priming to maintain the readily releasable pool [17, 67]. Although the C1 domain of Munc13 is not essential for its function in priming, it is required for the synaptic potentiation caused by the PKC activator, phorbol ester [68], suggesting it plays a major role in exocytosis. Also, a recent study has highlighted the importance of DAG action on both Munc13 and PKC for the potentiation of exocytosis through a coincidence detection mechanism [69]. PKC has multiple targets at the synapse through which it may regulate exocytosis, including Munc18-1 [70], although recent work in *Caenorhabditis elegans* suggests that PKC-dependent phosphorylation of UNC-18, the worm paralog of mammalian Munc18-1, functions in the exocytosis of large dense core vesicles but not synaptic vesicles [71]. A further, less well-characterised target of DAG at the synapse is protein kinase D (PKD) [72], which also contains a C1 domain. Loss-of-function mutations of the PKD1 domains in *C. elegans* cause movement defects, which could potentially be due to deficient exocytosis [73, 74].

Finally, DAG can be further metabolised by DAG lipase. In *Drosophila*, the protein rolling blackout (RBO) has homology to mammalian DAG lipases and is enriched presynaptically [75]. Temperature-sensitive RBO mutants display a rapid paralysis that is restored upon return to the permissive temperature. In parallel to the loss of function, neurons were shown to become depleted of DAG and to accumulate PtdIns(4,5)P_2 [75]. In the mammalian system, there is no evidence to date of a similar role for a DAG lipase. However, in the striatum, DAG lipase has been shown to be localised postsynaptically where it hydrolyses DAG to produce the endocannabinoid, 2-arachidonoylglycerol (2-AG). 2-AG is the major endocannabinoid mediating retrograde suppression in striatum, possibly through its effect on voltage-dependent calcium channels and/or the presynaptic release machinery [76].

3.3.2 Phospholipase C (PLC) in Exocytosis

The IP_3 released from PtdIns(4,5)P_2 by PLC is water soluble. Its best characterised effect is to promote the release of Ca^{2+} from intracellular stores. However, IP_3 can also be further phosphorylated at the 2, 3 and 6 positions by various inositol polyphosphate kinases to generate various derivatives such as IP_4, IP_5 and IP_6. Inositol polyphosphates can act as signalling molecules on their own right. Several of the higher-order inositol polyphosphates, in particular IP_6, have been implicated in the regulation of exocytosis. IP_6 inhibits neurotransmission by disrupting synaptotagmin 1 binding to PtdIns(4,5)P_2 [77]. It produces this effect by binding to the polybasic patch in synaptotagmin 1's C2B domain. Because PIP_2 binds to the same region in synaptotagmin 1, IP_6 might inhibit the function of synaptotagmin 1 by competing with endogenous PtdIns(4,5)P_2 polybasic region in a similar manner as the syntaxin/SNAP-25 heterodimer [78–81].

3.4 Phospholipase A1 (PLA1)

3.4.1 Phospholipase A1 (PLA1) in Exocytosis

The mammalian PLA1 enzymes possess a common structural motif (Ser-His-Asp catalytic triad) [54]. Notably, all of them contain a DDHD domain, which codes for a serine hydrolase implicated in the pathological mechanism of hereditary spastic paraplegia (HSP). Among 13 isoforms in mammals, 3 work intracellularly, including iPLA1α (PA-preferring phospholipase A1 (PA-PLA1; DDHD1)), iPLA1β (p125) and iPLA1γ (DDHD2) [82] (Fig. 8). Mutations in the *DDHD2* gene are associated with neurological disorders including autism, schizophrenia, spastic ataxia, intellectual disability, mental retardation, learning and memory impairment, and motor neuron disorders such as hereditary spastic paraplegia (HSP) [7, 83–85]. Notably, DDHD2 has been reported to directly impact exocytosis by dynamically modifying the synaptic membrane. DDHD2 also regulates the transport of vesicles at the Golgi and endoplasmic reticulum (ER) interface. The metabolites generated by DDHD2, lysophospholipids (LPLs) and FFAs, are vital lipid mediators associated with various physiological and pathological functions [86]. In particular, DDHD2 and p125 isoforms of PLA1 are commonly found in the Golgi and endoplasmic reticulum (ER) membranes. Both of them possess a WWE domain (which promotes protein–protein interactions), and a sterile alpha motif (SAM). Recent studies from our laboratory [87] showed that neuroexocytic stimulation is accompanied by a significant release of saturated FFAs, strongly suggesting that PLA1 family members are likely engaged in this process. In fact, the level of saturated FFAs generated during exocytosis far exceeds those of unsaturated FFAs such as arachidonic acid (AA). This points to the importance of the DDHD2 in lipid metabolism,

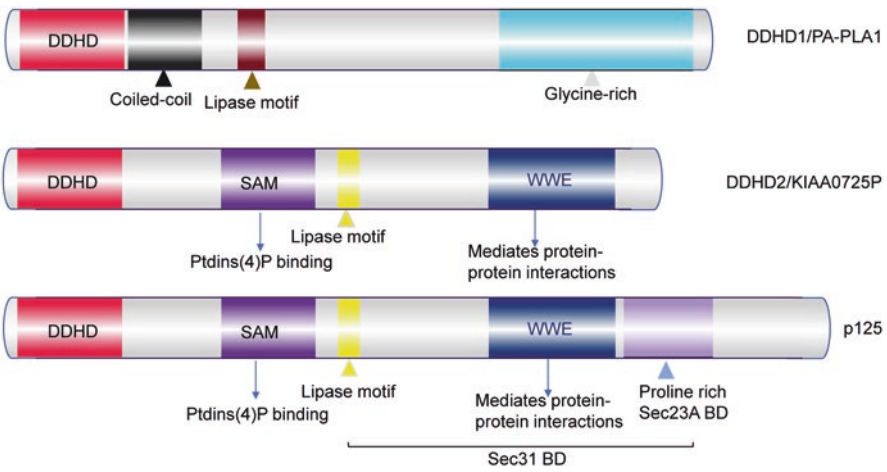

Fig. 8 Schematic representation of the domain structures of intracellular phospholipase A1 isozymes

vesicular cycling and normal function of the brain. In contrast, DDHD1 is primarily cytosolic and lacks both the WWE domain and the SAM [82]. The SAM is crucial for the targeting of DDHD2 to the Golgi/ERGIC (ER-Golgi intermediate compartment) and the binding of DDHD2 to phosphatidylinositol phosphate [82]. Although mutations in either DDHD1 or DDHD2 isozymes may cause hereditary spastic paraplegia, the pathogenic mechanisms might be different because DDHD1 or DDHD2 regulate the metabolism of classes of lipids in the mammalian nervous system [85, 88]. The remaining ten PLA1 isoforms are secreted by the cells and perform a variety of substrate-specific extracellular functions. The extracellular isoforms include hepatic lipase (HL), pancreatic lipase (PL), phosphatidylserine-specific phospholipase A1 (PS-PLA1), membrane-associated phosphatidic acid-selective phospholipase A1α and A1β (mPA-PLA1α and mPA-PLA1β respectively), lipoprotein lipase, endothelial lipase (EL) and pancreatic lipase-related proteins-1, -2 and -3 (PLRP1-3). mPA-PLA1β, PS-PLA1 and mPA-PLA1α display only PLA1 activity, whereas EL, HL and PLRP2 exhibit an additional triacylglycerol-hydrolysing activity [89].

3.5 Phospholipase A2 (PLA2)

3.5.1 Phospholipase A2 (PLA2) in Lysophospholipid (LPL) Processing

Like PLA1, PLA2 exists in several biological isoforms acting either intracellularly or extracellularly [90]. The different PLA2 isoforms hydrolyse the *sn-2* ester bond of phospholipids resulting in production of lysophospholipids (LPLs) and unsaturated FFAs. The primary enzymatic activity of PLA2 on membrane phospholipids is to produce LPLs, which are detergent-like bioactive lipids comprised of glycerol and a polar phosphatidyl headgroup linked to a single fatty acid. Because the polar headgroup is retained in lysophospholipids, they are named according to the headgroup of the parent lipid (e.g. phosphatidylcholine → lysophosphatidylcholine) [91]. Notably, a positive membrane curvature is generated by lysophospholipids, which have an inverted cone form, whereas a negative curvature is promoted by FFAs (Fig. 9). In contrast to FFAs, which can equilibrate between the two sides of the membrane bilayer, lysophospholipids are restricted to the leaflet of the bilayer where they are formed, resulting in an asymmetrical lipid distribution important for membrane dynamics [53, 86, 89].

3.5.2 Phospholipase A2 (PLA2) in Exocytosis

An earlier study by Rigoni et al. [90], on the mechanism of action of snake presynaptic PLA2 neurotoxins (SPANs), provided the strongest evidence for lysophospholipid involvement in intracellular trafficking. By promoting exocytosis and inhibiting endocytosis at the neuromuscular junction, SPANs promote gradual spastic muscle

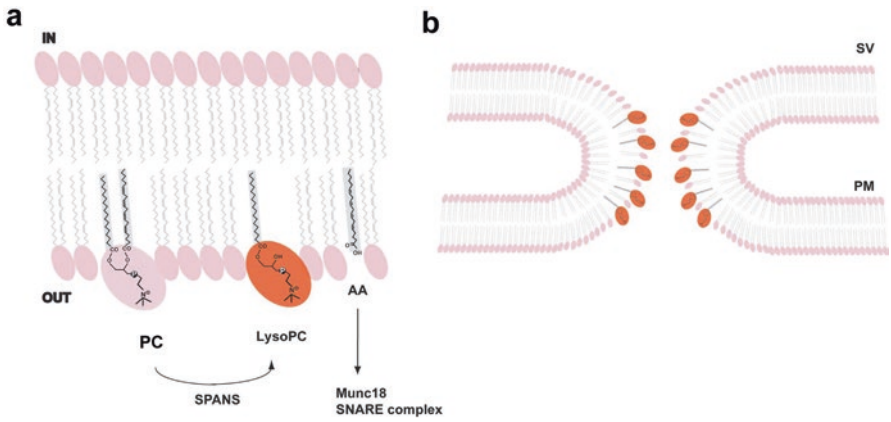

Fig. 9 Lysophosphatidic acid and exocytosis. (**a**) Phosphatidylcholine (PC) is a major substrate for phospholipase A2 and snake presynaptic phospholipase A2 neurotoxins (SPANs), which cleave PC asymmetrically, liberating a free fatty acid from the *sn-2* position (frequently arachidonic acid [AA] as depicted or oleic acid) and lysophosphatidylcholine (LysoPC). (**b**) LysoPC is an inverted cone-shaped lipid that promotes positive curvature of the bilayer. When formed in the outer leaflet of the plasma membrane (e.g. by SPANs), LysoPC would act to promote formation of the fusion pore. Arachidonic acid is a bioactive lipid and in particular may act on exocytosis through Munc18 and promotion of SNARE complex formation. SV, synaptic vesicle; PM, plasma membrane

paralysis, with the initial muscle stimulatory effect aided by arachidonic acid synthesis. A recent study showed that SPANs produce the paralytic effect mainly by acting on phosphatidylcholine to create lysophosphatidylcholine and fatty acids (primarily oleic acid and arachidonic acid) [90]. Application of lysophosphatidylcholine and oleic acid to the nerve terminal causes ultrastructural alterations akin to those caused by SPANs, such as a reduction in the total number of vesicles and appearance of nerve terminal swelling. These abnormalities presumably result from changes in membrane bilayer properties. Specifically, unsaturated FFAs in the inner membrane leaflet produce a negative curvature to promote the formation of a hemifusion intermediate, while inverted cone-shaped lysophospholipids in the outer membrane leaflet promote the formation of the fusion pore. The same lipid distribution is expected to destabilise structures that require positive curvature, such as the invagination needed for endocytosis and membrane fission. This prediction is supported by an observed blockade of endocytosis by SPANs. Microinjection of secretory PLA2 into PC12 cells and hippocampal neurons limits exocytosis, possibly due to the addition of lysophospholipids to the inner leaflet of the bilayer, and the resulting inhibitory effects of lysophospholipids on the formation of the hemifusion intermediate [13].

Lysophosphatidic acid (LysoPA) is produced from PA through the action of lysophosphatidic acid transferase (LPAAT). Like lysophosphatidylcholine and other lysophospholipids, LysoPA functions as a signalling molecule in many biological pathways. As a result, the activity of an LPAAT will predictably change the structure of a lipid from a cone-shaped PA to an inverted cone-shaped LysoPA,

consequently altering properties of the membrane bilayer. Initially, endophilin, a protein involved in endocytosis, was thought to possess LPAAT activity; however, this was later proven to be an artefact of the purification process rather than an innate property of endophilin [92]. However, it is still possible that such activities of LPAAT have a function in membrane dynamics during intracellular trafficking. These findings show that localised and asymmetric alterations in the membrane bilayer's leaflets can significantly alter membrane fusogenicity and consequently impact on synaptic activity [93].

Furthermore, it was recently discovered that AA and its metabolites play a role in modifying synaptic plasticity in *Aplysia* [94, 95]. Furthermore, Williams et al. found that AA was involved in mediating long-term plasticity in the hippocampus [96]. The activity of AA was assigned to presynaptic locations in this early investigation, although the chemical mechanism was not described. PLA2 from various snake and insect venoms has been demonstrated to enhance secretory vesicle fusion in numerous investigations [97] (see also Sect. 3.6). The breakage of the *sn-2* ester link in 1,2-diacyl-3-sn-phosphoglycerides is mediated by PLA2. PLA2-activated neurotoxins release fatty acids such as AA from phospholipids in the plasma membrane and stimulate widespread exocytosis with endocytosis blockage, resulting in a full depletion of synaptic vesicles in presynaptic nerve terminals at the neuromuscular junction [97].

3.6 Concluding Remarks

Membrane remodelling may be caused by a large variety of lipid-modifying enzymes, among which phospholipases are a major player. Phospholipases are ubiquitously distributed across different brain regions. They play a critical role in dynamically modifying the membrane lipid landscape to generate bioactive metabolites and in directly regulating the process of fusion during exocytosis and neurotransmission. Consequently, uncovering their involvement in exocytosis is essential to broaden our knowledge on lipid metabolism, vesicular cycling and normal functioning of the brain.

4 Cholesterol and Exocytosis

4.1 Cholesterol-Metabolising Enzymes

Cholesterol is a 27-carbon molecule that plays a major role in determining the lipid fluidity of the plasma membrane. In most organs, cholesterol is taken up by cells as lipoprotein particles. Due to their sizes, lipoprotein particles are unable to pass the blood-brain barrier. Hence the brain is responsible for the biogenesis of cholesterol, which represents up to 30% of the total lipids of the brain since it is one of the major

components of myelin. A number of metabolic enzymes are required for the de novo synthesis of cholesterol [21]. Briefly, cholesterol synthesis from acetyl-CoA molecules consists of three major steps: (i) synthesis of mevalonate (C6) by the combined actions of acetyl-CoA C-acetyltransferase, hydroxymethylglutaryl-CoA synthase and beta-hydroxy-beta-methylglutaryl-CoA reductase present in the endoplasmic reticulum; (ii) activation of mevalonate to produce isopentenyl-PP (C5) used as an elongation unit to synthesise a squalene (C30); and (iii) demethylation of isopentenyl-PP (C5) to produce cholesterol (C27) [21, 98]. Although cholesterol can be synthesised in a number of embryonic neurons, adult neurons require additional cholesterol synthesised by glial cells as a lipoprotein [99, 100]. Glial-cell-derived cholesterol is essential for synapse formation and maintenance [99, 100]; however, the precise mechanism for its involvement in synapse formation is still unclear.

4.2 Cholesterol Rafts and Exocytosis

Due to the complex mechanisms of cholesterol biosynthesis, transport and delivery, genetic ablation of key metabolic enzymes would not be greatly informative. Much work however has been done on Niemann–Pick type C disease characterised by an abnormal cholesterol accumulation in humans [101]. In this disorder, cholesterol and sphingolipids accumulate in late endosomal compartments without reaching the endoplasmic reticulum resulting in defective cholesterol esterification. Cholesterol has long been known to reduce the fluidity of the plasma membrane, which has major repercussions on the biophysical properties of ion channels and ligand-gated channels. In the last decade, cholesterol as well as other lipids such as sphingolipids have been recognised as major components of lipid rafts [102, 103], which are non-caveolar microdomains in the membrane that are soluble in Triton X-100 but insoluble in Lubrol WX. Flotation assays with neurosecretory cells have revealed that syntaxin and SNAP-25 are enriched in lipid rafts on the plasma membrane [102, 104]. Pharmacological depletion of cholesterol inhibits exocytosis [102, 104], suggesting that lipid rafts may be important to the functions of syntaxin-1 and SNAP-25. SNAP-25 is thought to be a true raft protein partly via its palmitoylation, but it is enigmatic how syntaxin-1 is associated with lipid rafts. Syntaxin-1 might be associated with lipid rafts by binding to SNAP-25, as suggested by perturbation of its clustering to the plasma membrane following botulinum type E treatment, which is known to prevent syntaxin/SNAP-25 interaction [80].

Syntaxin might also associate with lipid rafts via its binding to P/Q-type calcium channels, which exist in lipid rafts [105]. Importantly, another pool of syntaxin that is bound to Munc18a does not associate with lipid rafts [102]. Considering the established role of Munc18 in maintaining syntaxin in a closed conformation, it is tempting to suggest that syntaxin can shuttle between raft and non-raft microdomains and that lipid rafts are necessary for exocytosis. However, even though lipid rafts are undeniably important for exocytosis in neurosecretory cells and various

other cell types [103], a clear model on how lipid rafts and cholesterol play positive roles in exocytosis is yet to emerge. The recent demonstration that cholesterol disrupts a balance between evoked and spontaneous release in hippocampal neurons adds to the complexity of the question suggesting that it is the synchronisation process of neurotransmitter release that is perturbed by cholesterol depletion [100]. Moreover, the high cholesterol level found in synaptic vesicles suggests that lipid rafts could also be present in secretory vesicles. A recent study provided a detailed map of synaptic vesicle lipid compositions, demonstrating a high percentage of cholesterol (~40 mol%) and low levels of phosphatidylinositol [25]. Modelling of the protein components of vesicles assuming a homogeneous distribution indicated that the lipids might not be easily accessible by proteins. However, a high percentage of cholesterol may contribute to clustering of proteins of interest, allowing access to lipids such as phosphatidylinositol (see Sect. 2) and to the high curvature of the synaptic vesicle.

4.3 Concluding Remarks

Exocytosis is inhibited when cholesterol is depleted pharmacologically, showing that lipid rafts are crucial to syntaxin1 and SNAP-25 activities. More research is needed to clarify how cholesterol and/or lipid rafts positively affect exocytosis, and whether their abnormalities are linked to Alzheimer's disease [99, 100].

5 Ceramide and Exocytosis

5.1 Sphingolipid Metabolism

Sphingolipids and their precursor ceramide (*N*-acylsphingosine) act as signalling molecules in a variety of cellular events. Upon various types of stimulation, hydrolysis of sphingomyelin by endogenous sphingomyelinase promotes the formation of ceramide. A ceramidase converts ceramide to sphingosine, which can be further metabolised by sphingosine kinase to sphingosine-1-phosphate, an important regulator of apoptosis, mitosis and motility. Ceramide can be phosphorylated in a Ca^{2+}-dependent manner by a ceramide-kinase located on synaptic vesicles.

5.2 Sphingolipids and Exocytosis

The fact that ceramide-kinase co-purifies with synaptic vesicles and that it is activated by micromolar concentrations of Ca^{2+} suggests that it may play an important role in exocytosis [79, 81]. Interestingly, ceramide-1-phosphate can activate

cytosolic PLA2 to promote the production of arachidonic acid, an important lipid for its role in exocytosis (see Sects. 4 and 7). Ceramide phosphatase activity promotes mast cell degranulation in a Ca^{2+}-dependent manner, and its Ca^{2+}-dependency is mediated through its binding to the Ca^{2+} sensor calmodulin [106]. Genetic evidence points to an important role of ceramide in synaptic transmission in *Drosophila* [107]. In this study, genetic ablation of ceramidase leads to a severe phenotype. A presynaptic impairment of evoked synaptic currents was found and a reduction of readily releasable vesicles associated with fewer vesicles in reserve pool [107]. In PC12 cells, ceramide is produced upon stimulation of exocytosis, and addition of membrane-permeant exogenous ceramide stimulates dopamine release [108]. Following a recent profiling of ceramides involved in excitotoxicity in the brain [9], various ceramide side chains were tested for their effects in exocytosis of PC12 cell, revealing that C2, C6 and C18 ceramide are capable of promoting exocytosis [109]. Sphingosine-1-phosphate was recently shown to act via an autocrine mechanism to promote glutamate exocytosis from hippocampal neurons [110, 111].

5.3 Concluding Remarks

At this stage, it is not clear how ceramide or sphingosine are involved in exocytosis, but both have been associated with lipid rafts and could contribute to the negative curvature necessary to generate membrane fusion [16, 107].

6 Fatty acid Metabolism and Exocytosis

Ever more detailed analyses of brain lipids and lipid metabolites have allowed a transition from the traditional protein-centric notion of neurotransmission to a more holistic viewpoint encompassing tightly regulated protein–protein, protein–lipid and lipid–lipid interactions, which are all critical for neuronal communication [112]. Phospholipase A activity uses phospholipids as substrates to produce lysophospholipids (LPL) and free fatty acids (FFAs; see Sect. 3) [113]. Fatty acids were previously considered to merely play a structural role in the membrane by being the hydrophobic lipid chains of phospholipids. However, investigations into the role of lipids in exocytosis have revealed that fatty acids also play active roles in exocytosis. These fatty acids possess signalling and receptor mobility functions that have been suggested to be fundamental in inflammation, synapse formation, vesicle fusion and neurotransmission. Free fatty acids and especially polyunsaturated fatty acids (PUFAs) released from phospholipids in the plasma membrane through the action of various phospholipases also play important roles in exocytosis, synaptic vesicle cycling and long-term potentiation (memory) [114–116]. Furthermore, FFAs are capable of regulating neurotransmission by modulating membrane curvature, fluidity and fusogenicity [117]. PUFAs, which contain more than one double

bond in their backbone (such as arachidonic acid [AA] C20:4 and docosahexaenoic acid [DHA] C22:6), play major roles in SNARE-mediated synaptic transmission, as the non-covalent interaction of AA has been shown to induce a transformation in the conformation of syntaxin1, thereby enabling the formation of a Munc18-syntaxin1-SNAP-25 tripartite complex [118]. This chapter will discuss the roles of saturated and unsaturated FFAs in vesicular cycling.

6.1 Polyunsaturated Fatty Acid-Metabolising Enzymes

Mammalian neurons cannot synthesise omega-3 (n-3) fatty acids, which has fuelled much research into how brain function and development may benefit from dietary omega-3 precursors such as oleic acid. The concentrations of long-chain PUFAs of the n-6 and n-3 series in neurons depend on food intake of their precursors such as linoleic (18:2 n-6) and alpha linolenic acids (18:3 n-3), and preformed PUFAs such as AA (20:4 n-6), eicosapentaenoic acid (EPA; 20:5 n-3) and docosahexaenoic acid (22:6 n-3). Once in neurons, a variety of desaturase and elongase enzymes can produce and maintain a well-balanced concentration of various PUFAs [119]. Notably, increased dietary intake of n-3 PUFA is positively correlated with cognitive performance in rodents and humans [11, 120–124].

6.1.1 Arachidonic Acid in Exocytosis

Several early studies using pharmacological approaches have highlighted positive roles of AA in neuroexocytosis. Piomelli et al. found that AA and its metabolites promote synaptic plasticity in *Aplysia* [94, 95]. Williams et al. showed that AA plays a role in long-term synaptic plasticity in the hippocampus [96]. In this study, activity of AA was attributed to presynaptic sites although the molecular mechanism was not defined. Numerous studies have shown that PLA2 from various snake and insect venoms promotes fusion of secretory vesicles [97] (see also Sect. 3.6). PLA2 is responsible for the cleavage of the *sn-2* ester bond of 1,2-diacyl-3-*sn*-phosphoglycerides. Neurotoxins harbouring PLA2 activities can release fatty acids such as AA from phospholipids in the plasma membrane and promote extensive exocytosis, which, when accompanied by a blockade of endocytosis, can cause a complete depletion of synaptic vesicles in presynaptic motor nerve terminals at the neuromuscular junction [97]. Morgan and Burgoyne (1990) found that stimulation of exocytosis in neurosecretory cells causes concomitant increases in endogenous AA production and catecholamine secretion [125]. However, application of the PKC inhibitor staurosporine inhibited AA production completely with minimal effects on catecholamine secretion and exocytosis [125], which has raised doubts over the putative active role of AA in exocytosis. In *Caenorhabditis elegans*, null mutations of *fat-3*, a gene encoding the PUFA synthesising enzyme Δ6-fatty-acid desaturase, cause great decreases in motility, the amplitude of evoked postsynaptic current and

the frequency of miniature postsynaptic currents at the neuromuscular junction, and the numbers of docked and total synaptic vesicles in motor neurons [126]. These studies prompted more careful examinations of which PUFA is critically involved in exocytosis and by which mechanism. Latham et al. (2007) screened a variety of PUFA molecules for their effects on secretion and found that only AA can significantly potentiate catecholamine secretion from bovine chromaffin cells. Importantly, AA can also increase SNARE complex formation dose-dependently, suggesting that it might act on the mechanism of exocytosis [127]. Rickman and Davletov (2005) found that various PUFAs and detergents can revert a negative regulatory effect of Munc18a on exocytosis [128, 129]. This was further substantiated with the demonstration that AA allows Munc18a to bind to the SNARE complex, suggesting that Munc18a, like other related Munc/sec proteins, is capable of directly binding and promoting the formation of the SNARE complex [15]. SNARE binding to Munc18a is only revealed in the presence of AA suggesting that AA is a critical component allowing a switch in Munc18a function.

AA can be found as either free molecule (free fatty acids) or as a component of phospholipids. In this view, it is interesting to note that Munc18a binding to the syntaxin 1 N-terminal peptide occurs on the plasma membrane, suggesting that the plasma membrane provides a lipid environment that favours a "productive" Munc18a mode that facilitates SNARE-mediated endocytosis. This contrasts with the "inhibitory" mode where Munc18a binds the closed conformation of syntaxin 1 (which occurs inside the cell, presumably in the endoplasmic reticulum and the Golgi) [130]. Moreover, in fusion-competent membrane sheets, Munc18a allows the t-SNARE complex of syntaxin 1 and SNAP-25 to form as an acceptor intermediate for the vesicle-bound v-SNARE protein: vesicle associated membrane protein 2 (VAMP2) [131]. Whether this effect is mediated by free AA or the AA moieties of plasma membrane phospholipids remains an open question. These combined findings suggest that AA serves as a switch for Munc18a by acting as either free molecule or side chain of phospholipids (Fig. 7). Further research into this molecular switch could reveal how Munc18a tightly controls exocytosis both negatively (to avoid ectopic fusion events) and positively (to promote exocytosis of secretory vesicles with the plasma membrane).

6.1.2 Docosahexaenoic Acid in Neuroexocytosis

Docosahexaenoic acid (DHA) is another major PUFA in the human brain and a vital structural element of neuronal membranes. It facilitates the formation of SNARE-complex, which is imperative for neurite outgrowth-dependent plasticity as well as the fusion of synaptic vesicles with the plasma membrane [132]. Dietary deficiency in DHA in rats has been shown to induce a considerable reduction in levels of the NR2B subunit of the *N*-methyl-*D*-aspartate (NMDA) receptor [133]. In addition, exogenous supplementation with arachidonic acid or DHA has also been demonstrated to partially improve synaptic vesicle recycling potential in lipoprotein lipase (LPL)-deficient mice [8]. Likewise, consumption of diets rich in PUFAs has been

shown to enhance the expression of the Munc18-2 gene, indicating a plausible correlation between SNARE proteins and the FFAs [134]. Notably, elevated levels of endogenous DHA have been demonstrated to enhance learning and memory performance [135], as well as synaptogenesis, via the up-regulation of syntaxin-3, glutamate alpha-amino-3-hydroxy-5-methyl-4-isoxazole-propionic acid (AMPA) receptor subunit (GluR1), GAP-43, synapsin-1, filamentous actin and postsynaptic density protein-95 (PSD-95), in the hippocampus of adult transgenic gerbils and mice [136, 137]. In addition, Luchtman and Song reported that DHA (n-3 PUFA) may protect neurons by reducing the levels of reactive oxygen species (ROS) generated from brain lipid peroxidation during the initial period of Alzheimer's disease (AD) [135, 138, 139]. Thus, the PUFA DHA plays a crucial role in vesicular trafficking and memory function.

6.1.3 Eicosapentaenoic Acid in Neuroexocytosis

Eicosapentaenoic acid (EPA) and alpha-linolenic acid (ALA) have been demonstrated to co-function in sustaining glucose uptake in brain cells to reinforce optimal cognitive function [140]. Similarly, n-3 FFAs have been demonstrated to bolster synaptic plasticity for spatial memory formation via up-regulation of cyclic adenosine monophosphate (AMP) response element-binding protein (CREB) and calcium-calmodulin-dependent protein kinase II (CaMKII) levels, leading to improved long term potentiation (LTP)-stimulated dendritic spine formation, and increase in the number of c-Fos-positive neurons and secretion of brain-derived neurotrophic factor (BDNF) [136, 141, 142]. Furthermore, dietary supplementation with EPA in γ-irradiation-damaged rats has also been shown to improve cognitive performance, sustain LTP and lessen the levels of ROS and apoptotic hippocampal neurons [143]. However, the specific types of phospholipids and saturated FFA modifications occurring in specialised brain regions during memory acquisition remain unclear. This further suggests that the production of FFAs may be associated with synaptic function and tightly controlled by the presynaptic exocytic machinery in general.

6.1.4 Saturated FFAs in Association with Neuroexocytosis and Memory

Stimulation of neuroexocytosis is accompanied by a substantial increase in saturated FFAs [87]. Moreover, we have shown that acquisition/consolidation of long term fear memory in rats is also correlated with strong saturated FFA increases, particularly of myristic acid (C14:0) [144], suggesting that PLA1 family members are activated during these processes. This supports the importance of other phospholipid processing pathways aside from the classical PLA2-mediated release of unsaturated FFAs from the *sn-2* position of canonical phospholipids, and further suggests a critical role for PLA1 in lipid metabolism, membrane trafficking, long term potentiation and normal brain function. It is therefore conceivable that saturated FFAs may be cleaved by PLA1 at the *sn-1* position of canonical

phospholipids (saturated *sn-1* acyl, unsaturated *sn-2* acyl) [53]. Furthermore, the demonstration that mutations in the *DDHD2* gene alters Golgi-to-ER membrane trafficking further corroborates its critical role in essential cellular processes associated with memory and motor function [145, 146]. Supporting evidence from previous studies also show that genetic mutation in the *DDHD2* gene is associated with intellectual disabilities, cognitive deficits and accumulation of lipid droplets in the brain [83, 85, 146]. This indicates that the DDHD2 isozyme may be playing a critical role in regulating the activity-dependent generation of distinct saturated FFAs, which mediate intra- and intercellular activities (including exocytosis) that are important to neuronal function and memory in the mammalian brain [86].

In line with the potential of palmitic and myristic acids to drive protein acylation, it is conceivable that the increase in these saturated FFAs during memory may be required for generating substrates for post-translational modifications (myristoylation and palmitoylation), which, in turn, may alter the structure and function of neuronal membranes to impact learning and memory.

6.2 Concluding Remarks

Increasing evidence supports a role of saturated FFAs generated by the activity of PLA1 in neuroexocytosis and memory. Accordingly, this suggests that the *DDHD2* gene may be an important pharmacological target for regulating key fatty acid signalling pathways and a better understanding of the DDHD2-regulated lipid pathways in the central nervous system (CNS) may offer novel insights into the mechanism and therapeutic strategies for neurodegenerative diseases. Consequently, more studies are required to elucidate the potential association between synaptic protein acylation and saturated FFA generation during neuroexocytosis and memory formation.

7 Lipid Post-translational Modification and Intracellular Trafficking

Free fatty acids have been shown to be fundamental in inflammation, synapse formation, vesicle fusion and neurotransmission. Free fatty acids, and especially polyunsaturated fatty acids, play important roles in exocytosis, inflammation, synapse formation, vesicle fusion, neurotransmission, synaptic vesicle cycling and memory [114–116]. Furthermore, FFAs play a key role in regulating the nanostructural configuration of the plasma membrane [147, 148] via transbilayer covalent (e.g. myristoylation, palmitoylation) and non-covalent interaction with proteins implicated in cognitive and memory decline during ageing and in the pathophysiology of many neurodegenerative disorders [3, 6, 114, 121, 149, 150]. We discuss in this section palmitoylation, a post-translational modification to attach fatty acids covalently to cysteine residues in certain proteins of critical importance in exocytosis.

7.1 Protein Lipidations

Protein lipidations are characterised according to the chemistry of the modifications, with *N*-lipidations occurring on amines on the N-terminus and lysine residues, *S*-lipidations occurring on the thiol (SH) group of cysteine residues and *O*-lipidations occurring on the hydroxyl group of serine, threonine and tyrosine residues. The two most predominant lipids involved in protein modifications are myristic and palmitic acids [151, 152]. Lipid post-translational modifications involving the addition of a fatty acid myristoyl or palmitoyl moiety (C14 or C16 chain, respectively) to exocytic proteins such as SNARE proteins, play crucial roles in regulating enzymatic activity, modifying protein stability and mediating protein–protein interactions during intracellular trafficking and neuroexocytosis [153]. These specific FFAs have also been demonstrated to undergo the greatest activity-dependent mobilisation during neuroexocytosis and memory in our laboratory [87, 144]. Basically, palmitoylation is a dynamic process, while myristoylation is irreversible and controls basal membrane interactions. This implies that saturated FFAs may be playing a key role in intracellular trafficking, synaptic plasticity and neurotransmission. Although the mechanism by which these FFAs contribute to memory formation is still largely unknown, several studies have demonstrated the relevance of co- and post-translational protein myristoylation and palmitoylation to intracellular trafficking, synaptic plasticity and memory [154]. Myristoyl and palmitoyl acyl transferases (MATs and PATs, respectively) are responsible for catalysing the transfer of myristate and palmitate molecules, respectively [155]; however, due to the possibility of palmitoylation and myristoylation occurring spontaneously on highly reactive cysteine residues [60], the requirement of these enzymes to complete post-translational modifications has been queried [156].

7.1.1 Protein Palmitoylation

Although *O*-lipidation of threonine and serine residues, as well as amide-linked N-terminal palmitoylation, has been documented in the literature, the majority of palmitoyl modifications occur as *S*-lipidation of cysteines [151]. The thioester linkage is notably more labile than the ester and amide bonds of other protein lipidations due to the low electronegativity of sulphur and the lack of valence electron delocalisation across the bond. As a result, *S*-palmitoylations are easily removed by palmitoyl thioesterases, allowing for dynamic lipid addition and removal to actively migrate proteins between the cytosol and plasma membrane. Palmitoyl acyl transferases, called zDHHC proteins due to a conserved zinc binding and DHHC amino acid sequence in the catalytic domain, catalyse *S*-palmitoyl modifications, as shown in Fig. 10. The zinc finger DHHC-type group of enzymes has been shown to mediate post-translational modifications associated with lipids and essentially regulate synaptic development, as well as the morphology and functions of neurons [157–160]. In neurons, SNAP-25, VAMP2 and synaptotagmin undergo post-translational

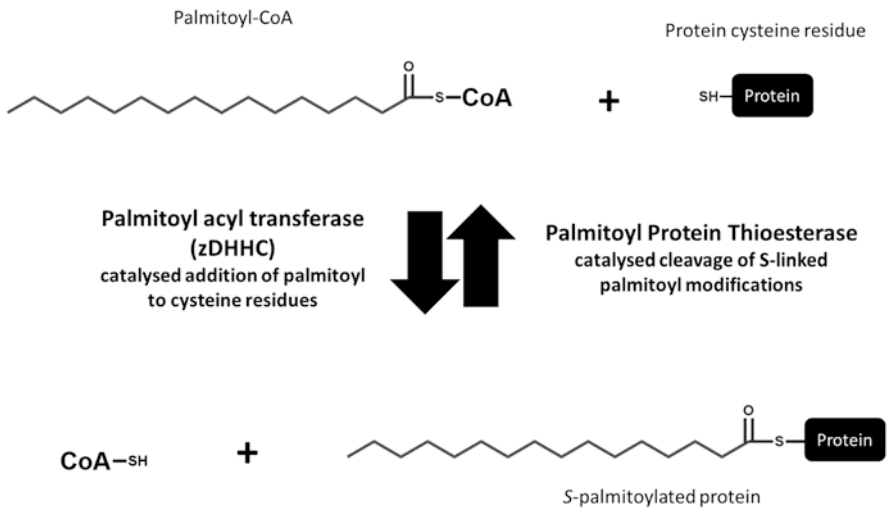

Fig. 10 S-palmitoylation reaction. Palmitoyl acyl transferases, also known as zDHHC proteins due to a conserved zinc binding and DHHC amino acid sequence in the catalytic domain, catalyse S-palmitoyl modifications

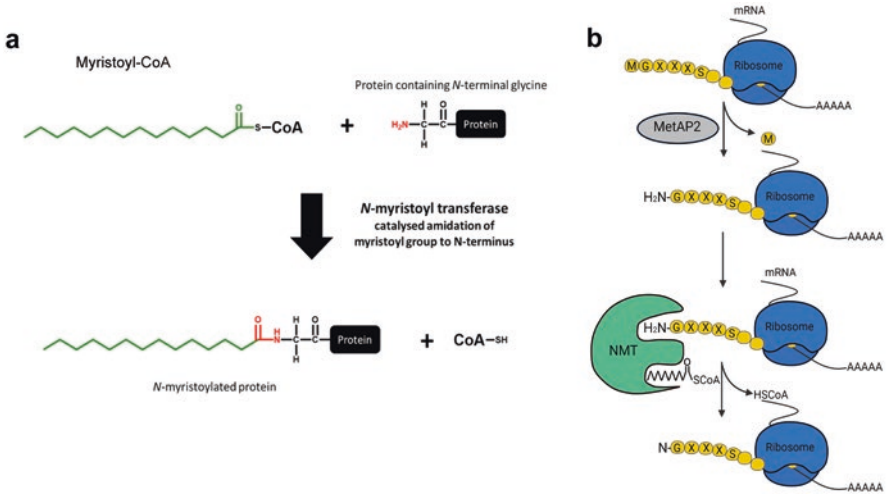

Fig. 11 (**a**) N-myristoylation reaction. (**b**) Protein N-myristoylation is a non-reversible modification, generally occurring co-translationally during protein synthesis. (Figure (**b**) was sourced from Yuan et al. [164])

modifications [156, 161–163], which increase protein hydrophobicity, making membrane insertion easier (Fig. 11a). However, palmitoylation-deficient mutations in SNAP-25 did not affect either its plasma membrane targeting or its interaction with syntaxin 1 [165]. Interestingly, this research found a clear inhibition of

exocytosis as well as a blockade of SNARE disassembly, implying that SNAP-25 palmitoylation may play a key role in exocytosis [165]. This theory is supported by the fact that SNAP-25A, which is typically produced during development but lacks the cysteine for palmitoylation, is substantially less effective at mediating exocytosis [166]. Aside from palmitoylation, the precise sequence of the palmitoylated cysteines in SNAP-25 is crucial for optimal exocytosis. Further, palmitoylation has lately been proposed as a way to improve protein–protein interaction [163].

7.1.2 Protein Myristylation

N-lipidations are the most common myristoyl modifications in proteins, occurring largely on the N-terminal amine of glycine (G) residues through the activity of *N*-myristoyl transferase (NMT) enzymes (Fig. 11). Recent data suggest that NMTs can also myristoylate lysine (K) residues [167, 168]. The *N*-myristoyltransferases NMT1 and NMT2 play a crucial role in the myristoylation of proteins. The myristoylation of G-proteins typically occurs with adenosine ribosylation factor (ARF) GTPases myristoylated to modify their membrane interactions, involving vesicular trafficking and phospholipase activation, among other functions. Furthermore, myristoylation of ARF6 at a lysine residue could be dynamically and specifically removed by the histone deacylase SIRT2 in a GTP-dependent manner.

In contrast to palmitoylation, N-terminal myristoylation occurs as an essentially non-reversible co-translational step during protein synthesis (Fig. 11b). The exposure of cryptic myristoylation sites after protein cleavage, such as through caspase proteolytic activity during apoptosis, has been identified as a source of post-translational N-terminal glycine myristoylation [169]. Hence, considering the possibility of myristic and palmitic acid to undergo protein acylation, it is conceivable that the increase in saturated FFAs in response to memory formation serves to generate substrates for such post-translational modifications, which in turn mediate learning and memory by modulating the structure and function of neurons.

7.2 Concluding Remarks

S-palmitoylation is currently the most studied form of protein lipidation in neuroexocytosis and memory processes. *S*-palmitoylation may occur in several synaptic proteins critical for vesicular transport across the synaptic membrane. Palmitoylation and de-palmitoylation of AMPA glutamate receptors during long term potentiation and depression processes directly mediate their localisation to the synaptic membrane. Myristoyl modifications, on the other hand, are thought to be long-lasting constitutive co-translational processes that occur during protein synthesis [170]. Since a variety of proteins critical to synaptic plasticity (e.g. kinases, phosphatases, G-protein-coupled receptors and cell signalling mediators) are myristoylated, and

proper myristoylation is required for cellular function, myristoylation likely plays important roles in memory-related processes. Early research on the signalling protein myristoylated alanine-rich protein C kinase substrate (MARCKS) suggests that myristoylation is more dynamic than previously thought, with evidence suggesting activity-dependent cleavage and post-translational addition of the protein's N-terminal myristoyl group. These findings suggest that activity-dependent *N*-myristoylation may play a more dynamic function in neuronal biology.

8 FFAs at the Nexus of Vesicular Trafficking, Ageing and Neurodegenerative Diseases

Free fatty acids have been implicated in the pathogenesis of several conditions, including Alzheimer's disease, that are characterised by aberrant vesicular trafficking [135]. Recently, Snowden et al. reported that the metabolism of unsaturated FFAs in the brains of AD patients is substantially dysregulated [150]. Intriguingly, administration of a diet comprising high DHA/arachidonic acid ratios may allow these metabolites to cross the blood-brain barrier and subsequently incorporate into neuronal membrane phospholipids to enhance brain function and potentially slow the progression of AD [171]. Moreover, administration of DHA to healthy people may enhance the expression of sorting protein (SorLA/LR11), which is diminished in Alzheimer's disease [172]. Additionally, consumption of a DHA-rich diet has been shown to preclude memory decline in the Senescence Accelerated Mouse Prone (SAMP) 8 mouse model by preventing the accumulation of amyloid and reducing the levels of lipid peroxidation and oxidative damage [129, 135, 173, 174]. Similarly, reduced levels of DHA were noticed in the hippocampus of patients with Alzheimer's pathology [175, 176]. Likewise, several beneficial effects of EPA supplementation have been observed, including decreased levels of amyloid-β, interferon-γ and interleukin-1β, major histocompatibility complex molecule II, and age-related overexpression of CD40, which have been attributed to anti-inflammatory effects of EPA [177]. Additionally, dietary AA may amplify amyloid-β oligomer neurotoxicity and impair cognition in humans [178]. DHA, AA and other PUFAs are present at high concentrations in the brain [179], predominantly ester linked into phospholipids in the neuronal cell membrane, where their unsaturated disposition enhances membrane fluidity.

In amyotrophic lateral sclerosis (ALS), DHA concentrations are substantially decreased in the brain, which causes a decrease in membrane fluidity and a concomitant decrease in the mobility of membrane proteins and associated signalling lipids, altering their function, and leading to disease via modification of signalling pathways [149]. Aberrant fatty acid metabolism has also been flagged to trigger diminished fluidity of membranes in the spinal cord and brain of the ALS model mouse, especially as the disease progresses over time [180, 181].

Similarly, aberrant metabolism of lipids has been recently implicated in different subtypes of hereditary spastic paraplegia (HSP) characterised by distortion in myelin formation, mitochondrial dysfunction and intracellular membrane trafficking defects as the major pathological signs [10]. Furthermore, ageing has been proven to trigger alterations in membrane lipid composition, thereby contributing to both altered neuronal survival and age-dependent decline in cognition [182]. These age-associated perturbations are linked to the loss of neuronal function by considerably reducing synaptic vesicle docking and fusion, release of neurotransmitters, postsynaptic signalling and synaptic strength, and long term potentiation [3]. The accompanying symptoms of these changes include a decline in cognition, executive function, short-term recollection, episodic memory and spatial memory. Interestingly, increased dietary n-3 PUFAs aid in improving the performance of learning and memory via reversal of age-associated alterations in synaptic plasticity, as a compensation for the age-linked decline in DHA, consequently enhancing learning and memory [14, 173, 183].

9 Final Conclusions

Research into the molecular mechanisms of exocytosis and endocytosis has long focussed on presynaptic proteins and has led to important discoveries as to how key proteins can locally control lipid composition and fusogenicity. As indispensable components of the membrane bilayer, lipids have properties that also allow them to regulate exocytosis: lipids can directly change the intrinsic fusion properties of membranes, recruit and/or activate many different proteins to create a suitable environment for vesicular exocytosis. More recent work has revealed that certain lipids can orchestrate membrane fusion by interacting with microdomains both on the plasma membrane and on synaptic vesicles whose lipid and protein composition is critical for exocytosis and endocytosis. Some lipids, such as PtdIns(4,5)P_2, have long been known to be intrinsically linked to the very late events in membrane fusion. But the focus on presynaptic lipids has recently shifted to the next level with reports that lipids present on or near the plasma membrane of neurosecretory cells can regulate the functions of SNARE proteins in exocytosis by modifying the functions of Munc18-1, as described above. Emerging evidence suggests that in addition to other phospholipases, the DDHD2 isoform of PLA1 is involved in cognitive function via interactions with Munc18 for the generation of saturated FFAs (particularly myristic acid) and in dynamic modification of the lipid landscape across the different brain regions classically involved in learning and memory. With the current increase in reports of neurodegenerative disorders associated with vesicular transport defects, an improved understanding of the regulation of lipid metabolism is physiologically and clinically significant and may offer novel insights into mechanisms and therapeutic strategies for neurodegenerative diseases.

References

1. Garcia-Morales V, Montero F, Gonzalez-Forero D, Rodriguez-Bey G, Gomez-Perez L, Medialdea-Wandossell MJ, et al. Membrane-derived phospholipids control synaptic neurotransmission and plasticity. PLoS Biol. 2015;13:e1002153. https://doi.org/10.1371/journal.pbio.1002153.
2. Bruce KD, Zsombok A, Eckel RH. Lipid processing in the brain: a key regulator of systemic metabolism. Front Endocrinol (Lausanne). 2017;8:60. https://doi.org/10.3389/fendo.2017.00060.
3. Egawa J, Pearn ML, Lemkuil BP, Patel PM, Head BP. Membrane lipid rafts and neurobiology: age-related changes in membrane lipids and loss of neuronal function. J Physiol. 2016;594:4565–79. https://doi.org/10.1113/JP270590.
4. Fahy E, Subramaniam S, Murphy RC, Nishijima M, Raetz CR, Shimizu T, et al. Update of the LIPID MAPS comprehensive classification system for lipids. J Lipid Res. 2009;50(Suppl):S9–S14. https://doi.org/10.1194/jlr.R800095-JLR200.
5. Wang HJ, Hsu FF. Structural characterization of phospholipids and sphingolipids by in-source fragmentation MALDI/TOF mass spectrometry. Anal Bioanal Chem. 2022;414:2089–102. https://doi.org/10.1007/s00216-021-03843-1.
6. de Mendoza D, Pilon M. Control of membrane lipid homeostasis by lipid-bilayer associated sensors: a mechanism conserved from bacteria to humans. Prog Lipid Res. 2019;76:100996. https://doi.org/10.1016/j.plipres.2019.100996.
7. Joensuu M, Wallis TP, Saber SH, Meunier FA. Phospholipases in neuronal function: a role in learning and memory? J Neurochem. 2020;153:300–33. https://doi.org/10.1111/jnc.14918.
8. Liu X, Zhang B, Yang H, Wang H, Liu Y, Huang A, et al. Impaired synaptic vesicle recycling contributes to presynaptic dysfunction in lipoprotein lipase-deficient mice. Neuroscience. 2014;280:275–81. https://doi.org/10.1016/j.neuroscience.2014.07.080.
9. Garcia-Martinez V, Gimenez-Molina Y, Villanueva J, Darios FD, Davletov B, Gutierrez LM. Emerging evidence for the modulation of exocytosis by signalling lipids. FEBS Lett. 2018;592:3493–503. https://doi.org/10.1002/1873-3468.13178.
10. Darios F, Mochel F, Stevanin G. Lipids in the physiopathology of hereditary spastic paraplegias. Front Neurosci. 2020;14:74. https://doi.org/10.3389/fnins.2020.00074.
11. Chianese R, Coccurello R, Viggiano A, Scafuro M, Fiore M, Coppola G, et al. Impact of dietary fats on brain functions. Curr Neuropharmacol. 2018;16:1059–85. https://doi.org/10.2174/1570159X15666171017102547.
12. Bennett SA, Valenzuela N, Xu H, Franko B, Fai S, Figeys D. Using neurolipidomics to identify phospholipid mediators of synaptic (dys)function in Alzheimer's disease. Front Physiol. 2013;4:168. https://doi.org/10.3389/fphys.2013.00168.
13. Wei S, Ong WY, Thwin MM, Fong CW, Farooqui AA, Gopalakrishnakone P, et al. Group IIA secretory phospholipase A2 stimulates exocytosis and neurotransmitter release in pheochromocytoma-12 cells and cultured rat hippocampal neurons. Neuroscience. 2003;121:891–8. https://doi.org/10.1016/s0306-4522(03)00525-6.
14. Martin TF. Role of PI(4,5)P(2) in vesicle exocytosis and membrane fusion. Subcell Biochem. 2012;59:111–30. https://doi.org/10.1007/978-94-007-3015-1_4.
15. Kasula R, Chai YJ, Bademosi AT, Harper CB, Gormal RS, Morrow IC, et al. The Munc18-1 domain 3a hinge-loop controls syntaxin-1A nanodomain assembly and engagement with the SNARE complex during secretory vesicle priming. J Cell Biol. 2016;214:847–58. https://doi.org/10.1083/jcb.201508118.
16. Rogasevskaia T, Coorssen JR. Sphingomyelin-enriched microdomains define the efficiency of native Ca(2+)-triggered membrane fusion. J Cell Sci. 2006;119:2688–94. https://doi.org/10.1242/jcs.03007.
17. Basu J, Betz A, Brose N, Rosenmund C. Munc13-1 C1 domain activation lowers the energy barrier for synaptic vesicle fusion. J Neurosci. 2007;27:1200–10. https://doi.org/10.1523/JNEUROSCI.4908-06.2007.

18. Megighian A, Rigoni M, Caccin P, Zordan MA, Montecucco C. A lysolecithin/fatty acid mixture promotes and then blocks neurotransmitter release at the Drosophila melanogaster larval neuromuscular junction. Neurosci Lett. 2007;416:6–11. https://doi.org/10.1016/j.neulet.2007.01.040.
19. Vitale N. Synthesis of fusogenic lipids through activation of phospholipase D1 by GTPases and the kinase RSK2 is required for calcium-regulated exocytosis in neuroendocrine cells. Biochem Soc Trans. 2010;38:167–71. https://doi.org/10.1042/BST0380167.
20. Darios F, Connell E, Davletov B. Phospholipases and fatty acid signalling in exocytosis. J Physiol. 2007;585:699–704. https://doi.org/10.1113/jphysiol.2007.136812.
21. Dietschy JM, Turley SD. Thematic review series: brain Lipids. Cholesterol metabolism in the central nervous system during early development and in the mature animal. J Lipid Res. 2004;45:1375–97. https://doi.org/10.1194/jlr.R400004-JLR200.
22. Lanoue V, Chai YJ, Brouillet JZ, Weckhuysen S, Palmer EE, Collins BM, et al. STXBP1 encephalopathy: connecting neurodevelopmental disorders with alpha-synucleinopathies? Neurology. 2019;93:114–23. https://doi.org/10.1212/WNL.0000000000007786.
23. Fahy E, Subramaniam S, Brown HA, Glass CK, Merrill AH Jr, Murphy RC, et al. A comprehensive classification system for lipids. J Lipid Res. 2005;46:839–61. https://doi.org/10.1194/jlr.E400004-JLR200.
24. Wiedemann C, Schafer T, Burger MM, Sihra TS. An essential role for a small synaptic vesicle-associated phosphatidylinositol 4-kinase in neurotransmitter release. J Neurosci. 1998;18:5594–602.
25. Takamori S, Holt M, Stenius K, Lemke EA, Gronborg M, Riedel D, et al. Molecular anatomy of a trafficking organelle. Cell. 2006;127:831–46. https://doi.org/10.1016/j.cell.2006.10.030.
26. Milosevic I, Sorensen JB, Lang T, Krauss M, Nagy G, Haucke V, et al. Plasmalemmal phosphatidylinositol-4,5-bisphosphate level regulates the releasable vesicle pool size in chromaffin cells. J Neurosci. 2005;25:2557–65. https://doi.org/10.1523/JNEUROSCI.3761-04.2005.
27. de Barry J, Janoshazi A, Dupont JL, Procksch O, Chasserot-Golaz S, Jeromin A, et al. Functional implication of neuronal calcium sensor-1 and phosphoinositol 4-kinase-beta interaction in regulated exocytosis of PC12 cells. J Biol Chem. 2006;281:18098–111. https://doi.org/10.1074/jbc.M509842200.
28. Di Paolo G, Moskowitz HS, Gipson K, Wenk MR, Voronov S, Obayashi M, et al. Impaired PtdIns(4,5)P2 synthesis in nerve terminals produces defects in synaptic vesicle trafficking. Nature. 2004;431:415–22. https://doi.org/10.1038/nature02896.
29. Cremona O, Di Paolo G, Wenk MR, Luthi A, Kim WT, Takei K, et al. Essential role of phosphoinositide metabolism in synaptic vesicle recycling. Cell. 1999;99:179–88. https://doi.org/10.1016/s0092-8674(00)81649-9.
30. Wucherpfennig T, Wilsch-Brauninger M, Gonzalez-Gaitan M. Role of Drosophila Rab5 during endosomal trafficking at the synapse and evoked neurotransmitter release. J Cell Biol. 2003;161:609–24. https://doi.org/10.1083/jcb.200211087.
31. Hawkins PT, Anderson KE, Davidson K, Stephens LR. Signalling through Class I PI3Ks in mammalian cells. Biochem Soc Trans. 2006;34:647–62. https://doi.org/10.1042/BST0340647.
32. Chasserot-Golaz S, Hubert P, Thierse D, Dirrig S, Vlahos CJ, Aunis D, et al. Possible involvement of phosphatidylinositol 3-kinase in regulated exocytosis: studies in chromaffin cells with inhibitor LY294002. J Neurochem. 1998;70:2347–56. https://doi.org/10.1046/j.1471-4159.1998.70062347.x.
33. Martin TFJ. Phosphoinositides as spatial regulators of membrane traffic. Curr Opin Neurobiol. 1997;7:331–8. https://doi.org/10.1016/S0959-4388(97)80060-8.
34. Wiedemann C, Schafer T, Burger MM. Chromaffin granule-associated phosphatidylinositol 4-kinase activity is required for stimulated secretion. EMBO J. 1996;15:2094–101. https://doi.org/10.1002/j.1460-2075.1996.tb00563.x.

35. Hong SJ, Chang CC. Inhibition of quantal release from motor nerve by wortmannin. Br J Pharmacol. 1999;128:142–8. https://doi.org/10.1038/sj.bjp.0702754.
36. Rizzoli SO, Betz WJ. Effects of 2-(4-morpholinyl)-8-phenyl-4H-1-benzopyran-4-one on synaptic vesicle cycling at the frog neuromuscular junction. J Neurosci. 2002;22:10680–9.
37. Meunier FA, Osborne SL, Hammond GR, Cooke FT, Parker PJ, Domin J, et al. Phosphatidylinositol 3-kinase C2alpha is essential for ATP-dependent priming of neurosecretory granule exocytosis. Mol Biol Cell. 2005;16:4841–51. https://doi.org/10.1091/mbc.e05-02-0171.
38. Wen PJ, Osborne SL, Morrow IC, Parton RG, Domin J, Meunier FA. Ca2+-regulated pool of phosphatidylinositol-3-phosphate produced by phosphatidylinositol 3-kinase C2α on neurosecretory vesicles. Mol Biol Cell. 2008;19:5593–603. https://doi.org/10.1091/mbc.E08-06-0595.
39. Cousin MA, Malladi CS, Tan TC, Raymond CR, Smillie KJ, Robinson PJ. Synapsin I-associated phosphatidylinositol 3-kinase mediates synaptic vesicle delivery to the readily releasable pool. J Biol Chem. 2003;278:29065–71. https://doi.org/10.1074/jbc.M302386200.
40. Viard P, Butcher AJ, Halet G, Davies A, Nurnberg B, Heblich F, et al. PI3K promotes voltage-dependent calcium channel trafficking to the plasma membrane. Nat Neurosci. 2004;7:939–46. https://doi.org/10.1038/nn1300.
41. Wen PJ, Osborne SL, Zanin M, Low PC, Wang HT, Schoenwaelder SM, et al. Phosphatidylinositol(4,5)bisphosphate coordinates actin-mediated mobilization and translocation of secretory vesicles to the plasma membrane of chromaffin cells. Nat Commun. 2011;2:491. https://doi.org/10.1038/ncomms1500.
42. Low PC, Misaki R, Schroder K, Stanley AC, Sweet MJ, Teasdale RD, et al. Phosphoinositide 3-kinase delta regulates membrane fission of Golgi carriers for selective cytokine secretion. J Cell Biol. 2010;190:1053–65. https://doi.org/10.1083/jcb.201001028.
43. Low PC, Manzanero S, Mohannak N, Narayana VK, Nguyen TH, Kvaskoff D, et al. PI3Kdelta inhibition reduces TNF secretion and neuroinflammation in a mouse cerebral stroke model. Nat Commun. 2014;5:3450. https://doi.org/10.1038/ncomms4450.
44. Martinez-Marmol R, Mohannak N, Qian L, Wang T, Gormal RS, Ruitenberg MJ, et al. p110delta PI3-kinase inhibition perturbs APP and TNFalpha trafficking, reduces plaque burden, dampens neuroinflammation, and prevents cognitive decline in an Alzheimer's disease mouse model. J Neurosci. 2019;39:7976–91. https://doi.org/10.1523/JNEUROSCI.0674-19.2019.
45. Osborne SL, Wallis TP, Jimenez JL, Gorman JJ, Meunier FA. Identification of secretory granule phosphatidylinositol 4,5-bisphosphate-interacting proteins using an affinity pulldown strategy. Mol Cell Proteomics. 2007;6:1158–69. https://doi.org/10.1074/mcp.M600430-MCP200.
46. Vevea JD, Kusick GF, Courtney KC, Chen E, Watanabe S, Chapman ER. Synaptotagmin 7 is targeted to the axonal plasma membrane through gamma-secretase processing to promote synaptic vesicle docking in mouse hippocampal neurons. eLife. 2021;10:e67261. https://doi.org/10.7554/eLife.67261.
47. Guan Z, Quinones-Frias MC, Akbergenova Y, Littleton JT. Drosophila Synaptotagmin 7 negatively regulates synaptic vesicle release and replenishment in a dosage-dependent manner. eLife. 2020;9:e55443. https://doi.org/10.7554/eLife.55443.
48. Speese S, Petrie M, Schuske K, Ailion M, Ann K, Iwasaki K, et al. UNC-31 (CAPS) is required for dense-core vesicle but not synaptic vesicle exocytosis in Caenorhabditis elegans. J Neurosci. 2007;27:6150–62. https://doi.org/10.1523/JNEUROSCI.1466-07.2007.
49. Speidel D, Bruederle CE, Enk C, Voets T, Varoqueaux F, Reim K, et al. CAPS1 regulates catecholamine loading of large dense-core vesicles. Neuron. 2005;46:75–88. https://doi.org/10.1016/j.neuron.2005.02.019.
50. Haucke V. Phosphoinositide regulation of clathrin-mediated endocytosis. Biochem Soc Trans. 2005;33:1285–9. https://doi.org/10.1042/BST20051285.

51. Gu Y, Huganir RL. Identification of the SNARE complex mediating the exocytosis of NMDA receptors. Proc Natl Acad Sci U S A. 2016;113:12280–5. https://doi.org/10.1073/pnas.1614042113.
52. Jarsch IK, Daste F, Gallop JL. Membrane curvature in cell biology: an integration of molecular mechanisms. J Cell Biol. 2016;214:375–87. https://doi.org/10.1083/jcb.201604003.
53. Richmond GS, Smith TK. Phospholipases A(1). Int J Mol Sci. 2011;12:588–612. https://doi.org/10.3390/ijms12010588.
54. Aloulou A, Rahier R, Arhab Y, Noiriel A, Abousalham A. Phospholipases: an overview. In: Sandoval G, editor. Lipases and phospholipases: methods and protocols. New York: Springer; 2018. p. 69–105. https://doi.org/10.1007/978-1-4939-8672-9_3.
55. Tanguy E, Wolf A, Montero-Hadjadje M, Gasman S, Bader MF, Vitale N. Phosphatidic acid: mono- and poly-unsaturated forms regulate distinct stages of neuroendocrine exocytosis. Adv Biol Regul. 2021;79:100772. https://doi.org/10.1016/j.jbior.2020.100772.
56. Tanguy E, Wang Q, Vitale N. Role of phospholipase D-derived phosphatidic acid in regulated exocytosis and neurological disease. Handb Exp Pharmacol. 2020;259:115–30. https://doi.org/10.1007/164_2018_180.
57. Nelson RK, Frohman MA. Physiological and pathophysiological roles for phospholipase D. J Lipid Res. 2015;56:2229–37. https://doi.org/10.1194/jlr.R059220.
58. Bader MF, Doussau F, Chasserot-Golaz S, Vitale N, Gasman S. Coupling actin and membrane dynamics during calcium-regulated exocytosis: a role for Rho and ARF GTPases. Biochim Biophys Acta. 2004;1742:37–49. https://doi.org/10.1016/j.bbamcr.2004.09.028.
59. Zeniou-Meyer M, Zabari N, Ashery U, Chasserot-Golaz S, Haeberle AM, Demais V, et al. Phospholipase D1 production of phosphatidic acid at the plasma membrane promotes exocytosis of large dense-core granules at a late stage. J Biol Chem. 2007;282:21746–57. https://doi.org/10.1074/jbc.M702968200.
60. Vitale N, Caumont AS, Chasserot-Golaz S, Du G, Wu S, Sciorra VA, et al. Phospholipase D1: a key factor for the exocytotic machinery in neuroendocrine cells. EMBO J. 2001;20:2424–34. https://doi.org/10.1093/emboj/20.10.2424.
61. Tanguy E, Wolf A, Wang Q, Chasserot-Golaz S, Ory S, Gasman S, et al. Phospholipase D1-generated phosphatidic acid modulates secretory granule trafficking from biogenesis to compensatory endocytosis in neuroendocrine cells. Adv Biol Regul. 2022;83:100844. https://doi.org/10.1016/j.jbior.2021.100844.
62. Humeau Y, Vitale N, Chasserot-Golaz S, Dupont JL, Du G, Frohman MA, et al. A role for phospholipase D1 in neurotransmitter release. Proc Natl Acad Sci U S A. 2001;98:15300–5. https://doi.org/10.1073/pnas.261358698.
63. Lee C, Kim SR, Chung JK, Frohman MA, Kilimann MW, Rhee SG. Inhibition of phospholipase D by amphiphysins. J Biol Chem. 2000;275:18751–8. https://doi.org/10.1074/jbc.M001695200.
64. Cao M, Wu Y, Ashrafi G, McCartney AJ, Wheeler H, Bushong EA, et al. Parkinson Sac domain mutation in synaptojanin 1 impairs clathrin uncoating at synapses and triggers dystrophic changes in dopaminergic axons. Neuron. 2017;93:882–896.e885. https://doi.org/10.1016/j.neuron.2017.01.019.
65. Mani M, Lee SY, Lucast L, Cremona O, Di Paolo G, De Camilli P, et al. The dual phosphatase activity of synaptojanin1 is required for both efficient synaptic vesicle endocytosis and reavailability at nerve terminals. Neuron. 2007;56:1004–18. https://doi.org/10.1016/j.neuron.2007.10.032.
66. Jang H-J, Yang YR, Cocco L, Ryu SH, Suh P-G. Phosphoinositide-specific phospholipase C (PI-PLC). In: Choi S, editor. Encyclopedia of signaling molecules. Cham: Springer International Publishing; 2018. p. 3973–88. https://doi.org/10.1007/978-3-319-67199-4_101584.
67. Bauer CS, Woolley RJ, Teschemacher AG, Seward EP. Potentiation of exocytosis by phospholipase C-coupled G-protein-coupled receptors requires the priming protein Munc13-1. J Neurosci. 2007;27:212–9. https://doi.org/10.1523/JNEUROSCI.4201-06.2007.

68. Rhee SG. Regulation of phosphoinositide-specific phospholipase C. Annu Rev Biochem. 2001;70:281–312. https://doi.org/10.1146/annurev.biochem.70.1.281.
69. Wierda KD, Toonen RF, de Wit H, Brussaard AB, Verhage M. Interdependence of PKC-dependent and PKC-independent pathways for presynaptic plasticity. Neuron. 2007;54:275–90. https://doi.org/10.1016/j.neuron.2007.04.001.
70. Nili U, de Wit H, Gulyas-Kovacs A, Toonen RF, Sorensen JB, Verhage M, et al. Munc18-1 phosphorylation by protein kinase C potentiates vesicle pool replenishment in bovine chromaffin cells. Neuroscience. 2006;143:487–500. https://doi.org/10.1016/j.neuroscience.2006.08.014.
71. Sieburth D, Madison JM, Kaplan JM. PKC-1 regulates secretion of neuropeptides. Nat Neurosci. 2007;10:49–57. https://doi.org/10.1038/nn1810.
72. Zhang X, Connelly J, Chao Y, Wang QJ. Multifaceted functions of protein kinase D in pathological processes and human diseases. Biomol Ther. 2021;11:483. https://doi.org/10.3390/biom11030483.
73. Feng H, Ren M, Wu SL, Hall DH, Rubin CS. Characterization of a novel protein kinase D: Caenorhabditis elegans DKF-1 is activated by translocation-phosphorylation and regulates movement and growth in vivo. J Biol Chem. 2006;281:17801–14. https://doi.org/10.1074/jbc.M511899200.
74. Lv D, Chen H, Feng Y, Cui B, Kang Y, Zhang P, et al. Small-molecule inhibitor targeting protein kinase D: a potential therapeutic strategy. Front Oncol. 2021;11:680221. https://doi.org/10.3389/fonc.2021.680221.
75. Huang FD, Matthies HJ, Speese SD, Smith MA, Broadie K. Rolling blackout, a newly identified PIP2-DAG pathway lipase required for Drosophila phototransduction. Nat Neurosci. 2004;7:1070–8. https://doi.org/10.1038/nn1313.
76. Uchigashima M, Narushima M, Fukaya M, Katona I, Kano M, Watanabe M. Subcellular arrangement of molecules for 2-arachidonoyl-glycerol-mediated retrograde signaling and its physiological contribution to synaptic modulation in the striatum. J Neurosci. 2007;27:3663–76. https://doi.org/10.1523/JNEUROSCI.0448-07.2007.
77. Llinas R, Sugimori M, Lang EJ, Morita M, Fukuda M, Niinobe M, et al. The inositol high-polyphosphate series blocks synaptic transmission by preventing vesicular fusion: a squid giant synapse study. Proc Natl Acad Sci U S A. 1994;91:12990–3. https://doi.org/10.1073/pnas.91.26.12990.
78. Li L, Liu H, Krout M, Richmond JE, Wang Y, Bai J, et al. A novel dual Ca2+ sensor system regulates Ca2+-dependent neurotransmitter release. J Cell Biol. 2021;220:e202008121. https://doi.org/10.1083/jcb.202008121.
79. Wu Z, Dharan N, McDargh ZA, Thiyagarajan S, O'Shaughnessy B, Karatekin E. The neuronal calcium sensor Synaptotagmin-1 and SNARE proteins cooperate to dilate fusion pores. eLife. 2021;10:e68215. https://doi.org/10.7554/eLife.68215.
80. Rickman C, Archer DA, Meunier FA, Craxton M, Fukuda M, Burgoyne RD, et al. Synaptotagmin interaction with the syntaxin/SNAP-25 dimer is mediated by an evolutionarily conserved motif and is sensitive to inositol hexakisphosphate. J Biol Chem. 2004;279:12574–9. https://doi.org/10.1074/jbc.M310710200.
81. Bykhovskaia M. SNARE complex alters the interactions of the Ca(2+) sensor synaptotagmin 1 with lipid bilayers. Biophys J. 2021;120:642–61. https://doi.org/10.1016/j.bpj.2020.12.025.
82. Inoue H, Baba T, Sato S, Ohtsuki R, Takemori A, Watanabe T, et al. Roles of SAM and DDHD domains in mammalian intracellular phospholipase A1 KIAA0725p. Biochim Biophys Acta. 2012;1823:930–9. https://doi.org/10.1016/j.bbamcr.2012.02.002.
83. Alrayes N, Mohamoud HS, Jelani M, Ahmad S, Vadgama N, Bakur K, et al. Truncating mutation in intracellular phospholipase A(1) gene (DDHD2) in hereditary spastic paraplegia with intellectual disability (SPG54). BMC Res Notes. 2015;8:271. https://doi.org/10.1186/s13104-015-1227-4.
84. Bertran-Gonzalez J, Laurent V, Chieng BC, Christie MJ, Balleine BW. Learning-related translocation of delta-opioid receptors on ventral striatal cholinergic interneurons mediates choice between goal-directed actions. J Neurosci. 2013;33:16060–71. https://doi.org/10.1523/JNEUROSCI.1927-13.2013.

85. Inloes JM, Hsu KL, Dix MM, Viader A, Masuda K, Takei T, et al. The hereditary spastic paraplegia-related enzyme DDHD2 is a principal brain triglyceride lipase. Proc Natl Acad Sci U S A. 2014;111:14924–9. https://doi.org/10.1073/pnas.1413706111.
86. Yung YC, Stoddard NC, Chun J. LPA receptor signaling: pharmacology, physiology, and pathophysiology. J Lipid Res. 2014;55:1192–214. https://doi.org/10.1194/jlr.R046458.
87. Narayana VK, Tomatis VM, Wang T, Kvaskoff D, Meunier FA. Profiling of free fatty acids using stable isotope tagging uncovers a role for saturated fatty acids in neuroexocytosis. Chem Biol. 2015;22:1552–61. https://doi.org/10.1016/j.chembiol.2015.09.010.
88. Inoue T, Hashimoto M, Katakura M, Hossain S, Matsuzaki K, Shido O. Effect of chronic administration of arachidonic acid on the performance of learning and memory in aged rats. Food Nutr Res. 2019;63:10.29219/fnr.v29263.21441. https://doi.org/10.29219/fnr.v63.1441.
89. Aoki J, Inoue A, Makide K, Saiki N, Arai H. Structure and function of extracellular phospholipase A1 belonging to the pancreatic lipase gene family. Biochimie. 2007;89:197–204. https://doi.org/10.1016/j.biochi.2006.09.021.
90. Rigoni M, Caccin P, Gschmeissner S, Koster G, Postle AD, Rossetto O, et al. Equivalent effects of snake PLA2 neurotoxins and lysophospholipid-fatty acid mixtures. Science. 2005;310:1678–80. https://doi.org/10.1126/science.1120640.
91. Caccin P, Rigoni M, Bisceglie A, Rossetto O, Montecucco C. Reversible skeletal neuromuscular paralysis induced by different lysophospholipids. FEBS Lett. 2006;580:6317–21. https://doi.org/10.1016/j.febslet.2006.10.039.
92. Gallop JL, Butler PJ, McMahon HT. Endophilin and CtBP/BARS are not acyl transferases in endocytosis or Golgi fission. Nature. 2005;438:675–8. https://doi.org/10.1038/nature04136.
93. Basak S, Mallick R, Banerjee A, Pathak S, Duttaroy AK. Maternal supply of both arachidonic and docosahexaenoic acids is required for optimal neurodevelopment. Nutrients. 2021;13:2061. https://doi.org/10.3390/nu13062061.
94. Piomelli D, Shapiro E, Feinmark SJ, Schwartz JH. Metabolites of arachidonic acid in the nervous system of Aplysia: possible mediators of synaptic modulation. J Neurosci. 1987;7:3675–86.
95. Piomelli D, Volterra A, Dale N, Siegelbaum SA, Kandel ER, Schwartz JH, et al. Lipoxygenase metabolites of arachidonic acid as second messengers for presynaptic inhibition of Aplysia sensory cells. Nature. 1987;328:38–43. https://doi.org/10.1038/328038a0.
96. Williams JH, Errington ML, Lynch MA, Bliss TV. Arachidonic acid induces a long-term activity-dependent enhancement of synaptic transmission in the hippocampus. Nature. 1989;341:739–42. https://doi.org/10.1038/341739a0.
97. Pellett S, Tepp WH, Johnson EA. Botulinum neurotoxins A, B, C, E, and F preferentially enter cultured human motor neurons compared to other cultured human neuronal populations. FEBS Lett. 2019;593:2675–85. https://doi.org/10.1002/1873-3468.13508.
98. Zhang J, Liu Q. Cholesterol metabolism and homeostasis in the brain. Protein Cell. 2015;6:254–64. https://doi.org/10.1007/s13238-014-0131-3.
99. Feringa FM, van der Kant R. Cholesterol and Alzheimer's disease; from risk genes to pathological effects. Front Aging Neurosci. 2021;13:690372. https://doi.org/10.3389/fnagi.2021.690372.
100. Berghoff SA, Spieth L, Saher G. Local cholesterol metabolism orchestrates remyelination. Trends Neurosci. 2022;45:272–83. https://doi.org/10.1016/j.tins.2022.01.001.
101. Rituper B, Gucek A, Lisjak M, Gorska U, Sakanovic A, Bobnar ST, et al. Vesicle cholesterol controls exocytotic fusion pore. Cell Calcium. 2022;101:102503. https://doi.org/10.1016/j.ceca.2021.102503.
102. Chamberlain LH, Burgoyne RD, Gould GW. SNARE proteins are highly enriched in lipid rafts in PC12 cells: implications for the spatial control of exocytosis. Proc Natl Acad Sci U S A. 2001;98:5619–24. https://doi.org/10.1073/pnas.091502398.
103. Salaun C, James DJ, Chamberlain LH. Lipid rafts and the regulation of exocytosis. Traffic. 2004;5:255–64. https://doi.org/10.1111/j.1600-0854.2004.0162.x.

104. Lang T, Bruns D, Wenzel D, Riedel D, Holroyd P, Thiele C, et al. SNAREs are concentrated in cholesterol-dependent clusters that define docking and fusion sites for exocytosis. EMBO J. 2001;20:2202–13. https://doi.org/10.1093/emboj/20.9.2202.
105. Taverna E, Saba E, Rowe J, Francolini M, Clementi F, Rosa P. Role of lipid microdomains in P/Q-type calcium channel (Cav2.1) clustering and function in presynaptic membranes. J Biol Chem. 2004;279:5127–34. https://doi.org/10.1074/jbc.M308798200.
106. Mitsutake S, Igarashi Y. Calmodulin is involved in the Ca2+-dependent activation of ceramide kinase as a calcium sensor. J Biol Chem. 2005;280:40436–41. https://doi.org/10.1074/jbc.M501962200.
107. Rohrbough J, Rushton E, Palanker L, Woodruff E, Matthies HJ, Acharya U, et al. Ceramidase regulates synaptic vesicle exocytosis and trafficking. J Neurosci. 2004;24:7789–803. https://doi.org/10.1523/JNEUROSCI.1146-04.2004.
108. Jeon HJ, Lee DH, Kang MS, Lee MO, Jung KM, Jung SY, et al. Dopamine release in PC12 cells is mediated by Ca(2+)-dependent production of ceramide via sphingomyelin pathway. J Neurochem. 2005;95:811–20. https://doi.org/10.1111/j.1471-4159.2005.03403.x.
109. Hori M, Gokita M, Yasue M, Honda T, Kohama T, Mashimo M, et al. Down-regulation of ceramide kinase via proteasome and lysosome pathways in PC12 cells by serum withdrawal: its protection by nerve growth factor and role in exocytosis. Biochim Biophys Acta, Mol Cell Res. 1867;2020:118714. https://doi.org/10.1016/j.bbamcr.2020.118714.
110. Kajimoto T, Okada T, Yu H, Goparaju SK, Jahangeer S, Nakamura S. Involvement of sphingosine-1-phosphate in glutamate secretion in hippocampal neurons. Mol Cell Biol. 2007;27:3429–40. https://doi.org/10.1128/MCB.01465-06.
111. Jiang ZJ, Delaney TL, Zanin MP, Haberberger RV, Pitson SM, Huang J, et al. Extracellular and intracellular sphingosine-1-phosphate distinctly regulates exocytosis in chromaffin cells. J Neurochem. 2019;149:729–46. https://doi.org/10.1111/jnc.14703.
112. Wenk MR, De Camilli P. Protein-lipid interactions and phosphoinositide metabolism in membrane traffic: insights from vesicle recycling in nerve terminals. Proc Natl Acad Sci U S A. 2004;101:8262–9. https://doi.org/10.1073/pnas.0401874101.
113. Kihara Y, Maceyka M, Spiegel S, Chun J. Lysophospholipid receptor nomenclature review: IUPHAR Review 8. Br J Pharmacol. 2014;171:3575–94. https://doi.org/10.1111/bph.12678.
114. Joffre C. Polyunsaturated fatty acid metabolism in the brain and brain cells. In: Bosch-Bouju C, Layé S, Pallet V, editors. Feed your mind – how does nutrition modulate brain function throughout life? IntechOpen; 2019. https://doi.org/10.5772/intechopen.88232.
115. Falomir-Lockhart LJ, Cavazzutti GF, Gimenez E, Toscani AM. Fatty acid signaling mechanisms in neural cells: fatty acid receptors. Front Cell Neurosci. 2019;13:162. https://doi.org/10.3389/fncel.2019.00162.
116. Barber CN, Raben DM. Lipid metabolism crosstalk in the brain: glia and neurons. Front Cell Neurosci. 2019;13:212. https://doi.org/10.3389/fncel.2019.00212.
117. Graham TR, Kozlov MM. Interplay of proteins and lipids in generating membrane curvature. Curr Opin Cell Biol. 2010;22:430–6. https://doi.org/10.1016/j.ceb.2010.05.002.
118. Connell E, Darios F, Broersen K, Gatsby N, Peak-Chew SY, Rickman C, et al. Mechanism of arachidonic acid action on syntaxin-Munc18. EMBO Rep. 2007;8:414–9. https://doi.org/10.1038/sj.embor.7400935.
119. Lauritzen L, Hansen HS, Jorgensen MH, Michaelsen KF. The essentiality of long chain n-3 fatty acids in relation to development and function of the brain and retina. Prog Lipid Res. 2001;40:1–94. https://doi.org/10.1016/s0163-7827(00)00017-5.
120. Queiroz MP, Lima MDS, Barbosa MQ, de Melo M, Bertozzo C, de Oliveira MEG, et al. Effect of conjugated linoleic acid on memory and reflex maturation in rats treated during early life. Front Neurosci. 2019;13:370. https://doi.org/10.3389/fnins.2019.00370.
121. Derbyshire E. Brain health across the lifespan: a systematic review on the role of omega-3 fatty acid supplements. Nutrients. 2018;10:1094. https://doi.org/10.3390/nu10081094.

122. Kalmijn S, van Boxtel MP, Ocke M, Verschuren WM, Kromhout D, Launer LJ. Dietary intake of fatty acids and fish in relation to cognitive performance at middle age. Neurology. 2004;62:275–80. https://doi.org/10.1212/01.wnl.0000103860.75218.a5.
123. Yurko-Mauro K, Alexander DD, Van Elswyk ME. Docosahexaenoic acid and adult memory: a systematic review and meta-analysis. PLoS One. 2015;10:e0120391. https://doi.org/10.1371/journal.pone.0120391.
124. Suzuki H, Park SJ, Tamura M, Ando S. Effect of the long-term feeding of dietary lipids on the learning ability, fatty acid composition of brain stem phospholipids and synaptic membrane fluidity in adult mice: a comparison of sardine oil diet with palm oil diet. Mech Ageing Dev. 1998;101:119–28. https://doi.org/10.1016/s0047-6374(97)00169-3.
125. Morgan A, Burgoyne RD. Relationship between arachidonic acid release and Ca2(+)-dependent exocytosis in digitonin-permeabilized bovine adrenal chromaffin cells. Biochem J. 1990;271:571–4. https://doi.org/10.1042/bj2710571.
126. Lesa GM, Palfreyman M, Hall DH, Clandinin MT, Rudolph C, Jorgensen EM, et al. Long chain polyunsaturated fatty acids are required for efficient neurotransmission in C. elegans. J Cell Sci. 2003;116:4965–75. https://doi.org/10.1242/jcs.00918.
127. Latham CF, Osborne SL, Cryle MJ, Meunier FA. Arachidonic acid potentiates exocytosis and allows neuronal SNARE complex to interact with Munc18a. J Neurochem. 2007;100:1543–54. https://doi.org/10.1111/j.1471-4159.2006.04286.x.
128. Rickman C, Davletov B. Arachidonic acid allows SNARE complex formation in the presence of Munc18. Chem Biol. 2005;12:545–53. https://doi.org/10.1016/j.chembiol.2005.03.004.
129. Fonteh AN, Cipolla M, Chiang AJ, Edminster SP, Arakaki X, Harrington MG. Polyunsaturated fatty acid composition of cerebrospinal fluid fractions shows their contribution to cognitive resilience of a pre-symptomatic Alzheimer's disease cohort. Front Physiol. 2020;11:83. https://doi.org/10.3389/fphys.2020.00083.
130. Han GA, Malintan NT, Saw NM, Li L, Han L, Meunier FA, et al. Munc18-1 domain-1 controls vesicle docking and secretion by interacting with syntaxin-1 and chaperoning it to the plasma membrane. Mol Biol Cell. 2011;22:4134–49. https://doi.org/10.1091/mbc.E11-02-0135.
131. Zilly FE, Sorensen JB, Jahn R, Lang T. Munc18-bound syntaxin readily forms SNARE complexes with synaptobrevin in native plasma membranes. PLoS Biol. 2006;4:e330. https://doi.org/10.1371/journal.pbio.0040330.
132. Walczewska A, Stepien T, Bewicz-Binkowska D, Zgorzynska E. The role of docosahexaenoic acid in neuronal function. Postepy Hig Med Dosw (Online). 2011;65:314–27. https://doi.org/10.5604/17322693.945763.
133. Sharma S, Ying Z, Gomez-Pinilla F. A pyrazole curcumin derivative restores membrane homeostasis disrupted after brain trauma. Exp Neurol. 2010;226:191–9. https://doi.org/10.1016/j.expneurol.2010.08.027.
134. Barceló-Coblijn G, Kitajka K, Puskás LG, Hőgyes E, Zvara A, Hackler L, et al. Gene expression and molecular composition of phospholipids in rat brain in relation to dietary n-6 to n-3 fatty acid ratio. Biochim Biophys Acta. 2003;1632:72–9. https://doi.org/10.1016/s1388-1981(03)00064-7.
135. Sun GY, Simonyi A, Fritsche KL, Chuang DY, Hannink M, Gu Z, et al. Docosahexaenoic acid (DHA): an essential nutrient and a nutraceutical for brain health and diseases. Prostaglandins Leukot Essent Fatty Acids. 2018;136:3–13. https://doi.org/10.1016/j.plefa.2017.03.006.
136. Cansev M, Wurtman RJ, Sakamoto T, Ulus IH. Oral administration of circulating precursors for membrane phosphatides can promote the synthesis of new brain synapses. Alzheimers Dement. 2008;4:S153–68. https://doi.org/10.1016/j.jalz.2007.10.005.
137. He C, Qu X, Cui L, Wang J, Kang JX. Improved spatial learning performance of fat-1 mice is associated with enhanced neurogenesis and neuritogenesis by docosahexaenoic acid. Proc Natl Acad Sci U S A. 2009;106:11370–5. https://doi.org/10.1073/pnas.0904835106.
138. Pan Y, Khalil H, Nicolazzo JA. The impact of docosahexaenoic acid on Alzheimer's disease: is there a role of the blood-brain barrier? Curr Clin Pharmacol. 2015;10:222–41. https://doi.org/10.2174/1574884710031508201515 32.

139. Markesbery WR, Kryscio RJ, Lovell MA, Morrow JD. Lipid peroxidation is an early event in the brain in amnestic mild cognitive impairment. Ann Neurol. 2005;58:730–5. https://doi.org/10.1002/ana.20629.
140. Freemantle E, Vandal M, Tremblay-Mercier J, Tremblay S, Blachere JC, Begin ME, et al. Omega-3 fatty acids, energy substrates, and brain function during aging. Prostaglandins Leukot Essent Fatty Acids. 2006;75:213–20. https://doi.org/10.1016/j.plefa.2006.05.011.
141. Kawashima A, Harada T, Kami H, Yano T, Imada K, Mizuguchi K. Effects of eicosapentaenoic acid on synaptic plasticity, fatty acid profile and phosphoinositide 3-kinase signaling in rat hippocampus and differentiated PC12 cells. J Nutr Biochem. 2010;21:268–77. https://doi.org/10.1016/j.jnutbio.2008.12.015.
142. Wu A, Ying Z, Gomez-Pinilla F. Docosahexaenoic acid dietary supplementation enhances the effects of exercise on synaptic plasticity and cognition. Neuroscience. 2008;155:751–9. https://doi.org/10.1016/j.neuroscience.2008.05.061.
143. Lonergan PE, Martin DS, Horrobin DF, Lynch MA. Neuroprotective effect of eicosapentaenoic acid in hippocampus of rats exposed to gamma-irradiation. J Biol Chem. 2002;277:20804–11. https://doi.org/10.1074/jbc.M202387200.
144. Wallis TP, Venkatesh BG, Narayana VK, Kvaskoff D, Ho A, Sullivan RK, et al. Saturated free fatty acids and association with memory formation. Nat Commun. 2021;12:3443. https://doi.org/10.1038/s41467-021-23840-3.
145. Yadav PK, Rajasekharan R. Misregulation of a DDHD domain-containing lipase causes mitochondrial dysfunction in yeast. J Biol Chem. 2016;291:18562–81. https://doi.org/10.1074/jbc.M116.733378.
146. Park CY, Zhou J, Wong AK, Chen KM, Theesfeld CL, Darnell RB, et al. Genome-wide landscape of RNA-binding protein target site dysregulation reveals a major impact on psychiatric disorder risk. Nat Genet. 2021;53:166–73. https://doi.org/10.1038/s41588-020-00761-3.
147. Raghupathy R, Anilkumar AA, Polley A, Singh PP, Yadav M, Johnson C, et al. Transbilayer lipid interactions mediate nanoclustering of lipid-anchored proteins. Cell. 2015;161:581–94. https://doi.org/10.1016/j.cell.2015.03.048.
148. Lamidi IY, Mikail HG, Adamu S, Akefe IO, Tijjani MB, Salihu SI, et al. Flavonoid fractions of diosmin and hesperidin mitigate lead acetate-induced biochemical, oxidative stress, and histopathological alterations in Wistar rats. Toxicol Res. 2021;37:473–84. https://doi.org/10.1007/s43188-020-00084-9.
149. Tracey TJ, Steyn FJ, Wolvetang EJ, Ngo ST. Neuronal lipid metabolism: multiple pathways driving functional outcomes in health and disease. Front Mol Neurosci. 2018;11:10. https://doi.org/10.3389/fnmol.2018.00010.
150. Snowden SG, Ebshiana AA, Hye A, An Y, Pletnikova O, O'Brien R, et al. Association between fatty acid metabolism in the brain and Alzheimer disease neuropathology and cognitive performance: a nontargeted metabolomic study. PLoS Med. 2017;14:e1002266. https://doi.org/10.1371/journal.pmed.1002266.
151. Jiang H, Zhang X, Chen X, Aramsangtienchai P, Tong Z, Lin H. Protein lipidation: occurrence, mechanisms, biological functions, and enabling technologies. Chem Rev. 2018;118:919–88. https://doi.org/10.1021/acs.chemrev.6b00750.
152. Ji B, Skup M. Roles of palmitoylation in structural long-term synaptic plasticity. Mol Brain. 2021;14:8. https://doi.org/10.1186/s13041-020-00717-y.
153. Chen B, Sun Y, Niu J, Jarugumilli GK, Wu X. Protein lipidation in cell Signaling and diseases: function, regulation, and therapeutic opportunities. Cell Chem Biol. 2018;25:817–31. https://doi.org/10.1016/j.chembiol.2018.05.003.
154. Zamzow DR, Elias V, Acosta VA, Escobedo E, Magnusson KR. Higher levels of protein palmitoylation in the frontal cortex across aging were associated with reference memory and executive function declines. eNeuro. 2019;6:ENEURO.0310-18.2019. https://doi.org/10.1523/ENEURO.0310-18.2019.

155. Huang K, Yanai A, Kang R, Arstikaitis P, Singaraja RR, Metzler M, et al. Huntingtin-interacting protein HIP14 is a palmitoyl transferase involved in palmitoylation and trafficking of multiple neuronal proteins. Neuron. 2004;44:977–86. https://doi.org/10.1016/j.neuron.2004.11.027.
156. Veit M. Palmitoylation of the 25-kDa synaptosomal protein (SNAP-25) in vitro occurs in the absence of an enzyme, but is stimulated by binding to syntaxin. Biochem J. 2000;345(Pt 1):145–51.
157. Shah BS, Shimell JJ, Bamji SX. Regulation of dendrite morphology and excitatory synapse formation by zDHHC15. J Cell Sci. 2019;132:jcs230052. https://doi.org/10.1242/jcs.230052.
158. Matt L, Kim K, Chowdhury D, Hell JW. Role of palmitoylation of postsynaptic proteins in promoting synaptic plasticity. Front Mol Neurosci. 2019;12:8. https://doi.org/10.3389/fnmol.2019.00008.
159. Globa AK, Bamji SX. Protein palmitoylation in the development and plasticity of neuronal connections. Curr Opin Neurobiol. 2017;45:210–20. https://doi.org/10.1016/j.conb.2017.02.016.
160. Salaun C, Greaves J, Tomkinson NCO, Chamberlain LH. The linker domain of the SNARE protein SNAP25 acts as a flexible molecular spacer that ensures efficient S-acylation. J Biol Chem. 2020;295:7501–15. https://doi.org/10.1074/jbc.RA120.012726.
161. Veit M, Becher A, Ahnert-Hilger G. Synaptobrevin 2 is palmitoylated in synaptic vesicles prepared from adult, but not from embryonic brain. Mol Cell Neurosci. 2000;15:408–16. https://doi.org/10.1006/mcne.1999.0830.
162. Veit M, Sollner TH, Rothman JE. Multiple palmitoylation of synaptotagmin and the t-SNARE SNAP-25. FEBS Lett. 1996;385:119–23. https://doi.org/10.1016/0014-5793(96)00362-6.
163. Washbourne P. Greasing transmission: palmitoylation at the synapse. Neuron. 2004;44:901–2. https://doi.org/10.1016/S0896-6273(04)00799-8.
164. Yuan M, Song ZH, Ying MD, Zhu H, He QJ, Yang B, et al. N-myristoylation: from cell biology to translational medicine. Acta Pharmacol Sin. 2020;41:1005–15. https://doi.org/10.1038/s41401-020-0388-4.
165. Washbourne P, Cansino V, Mathews JR, Graham M, Burgoyne RD, Wilson MC. Cysteine residues of SNAP-25 are required for SNARE disassembly and exocytosis, but not for membrane targeting. Biochem J. 2001;357:625–34. https://doi.org/10.1042/0264-6021:3570625.
166. Sorensen JB, Nagy G, Varoqueaux F, Nehring RB, Brose N, Wilson MC, et al. Differential control of the releasable vesicle pools by SNAP-25 splice variants and SNAP-23. Cell. 2003;114:75–86. https://doi.org/10.1016/s0092-8674(03)00477-x.
167. Kosciuk T, Price IR, Zhang X, Zhu C, Johnson KN, Zhang S, et al. NMT1 and NMT2 are lysine myristoyltransferases regulating the ARF6 GTPase cycle. Nat Commun. 2020;11:1067. https://doi.org/10.1038/s41467-020-14893-x.
168. Kosciuk T, Lin H. N-myristoyltransferase as a glycine and lysine myristoyltransferase in cancer, immunity, and infections. ACS Chem Biol. 2020;15:1747–58. https://doi.org/10.1021/acschembio.0c00314.
169. Vilas GL, Corvi MM, Plummer GJ, Seime AM, Lambkin GR, Berthiaume LG. Posttranslational myristoylation of caspase-activated p21-activated protein kinase 2 (PAK2) potentiates late apoptotic events. Proc Natl Acad Sci U S A. 2006;103:6542–7. https://doi.org/10.1073/pnas.0600824103.
170. Xiong WH, Qin M, Zhong H. Myristoylation alone is sufficient for PKA catalytic subunits to associate with the plasma membrane to regulate neuronal functions. Proc Natl Acad Sci U S A. 2021;118:e2021658118. https://doi.org/10.1073/pnas.2021658118.
171. Thomas MH, Pelleieux S, Vitale N, Olivier JL. Dietary arachidonic acid as a risk factor for age-associated neurodegenerative diseases: potential mechanisms. Biochimie. 2016;130:168–77. https://doi.org/10.1016/j.biochi.2016.07.013.
172. Ma QL, Teter B, Ubeda OJ, Morihara T, Dhoot D, Nyby MD, et al. Omega-3 fatty acid docosahexaenoic acid increases SorLA/LR11, a sorting protein with reduced expression in sporadic Alzheimer's disease (AD): relevance to AD prevention. J Neurosci. 2007;27:14299–307. https://doi.org/10.1523/JNEUROSCI.3593-07.2007.

173. Giacobbe J, Benoiton B, Zunszain P, Pariante CM, Borsini A. The anti-inflammatory role of omega-3 polyunsaturated fatty acids metabolites in pre-clinical models of psychiatric, neurodegenerative, and neurological disorders. Front Psych. 2020;11:122. https://doi.org/10.3389/fpsyt.2020.00122.
174. Hashimoto M, Hossain S, Agdul H, Shido O. Docosahexaenoic acid-induced amelioration on impairment of memory learning in amyloid beta-infused rats relates to the decreases of amyloid beta and cholesterol levels in detergent-insoluble membrane fractions. Biochim Biophys Acta. 2005;1738:91–8. https://doi.org/10.1016/j.bbalip.2005.11.011.
175. Mohajeri MH, Troesch B, Weber P. Inadequate supply of vitamins and DHA in the elderly: implications for brain aging and Alzheimer-type dementia. Nutrition. 2015;31:261–75. https://doi.org/10.1016/j.nut.2014.06.016.
176. Akefe IO, Ayo JO, Sinkalu VO, Nevels M. Assortment of kaempferol and zinc gluconate improves noise-induced biochemical imbalance and deficits in body weight gain. Exp Results. 2021;2:e37. https://doi.org/10.1017/exp.2021.30.
177. Szabo Z, Marosvolgyi T, Szabo E, Bai P, Figler M, Verzar Z. The potential beneficial effect of EPA and DHA supplementation managing cytokine storm in coronavirus disease. Front Physiol. 2020;11:752. https://doi.org/10.3389/fphys.2020.00752.
178. Thomas MH, Paris C, Magnien M, Colin J, Pelleieux S, Coste F, et al. Dietary arachidonic acid increases deleterious effects of amyloid-beta oligomers on learning abilities and expression of AMPA receptors: putative role of the ACSL4-cPLA2 balance. Alzheimers Res Ther. 2017;9:69. https://doi.org/10.1186/s13195-017-0295-1.
179. Bazinet RP, Laye S. Polyunsaturated fatty acids and their metabolites in brain function and disease. Nat Rev Neurosci. 2014;15:771–85. https://doi.org/10.1038/nrn3820.
180. Miana-Mena FJ, Piedrafita E, Gonzalez-Mingot C, Larrode P, Munoz MJ, Martinez-Ballarin E, et al. Levels of membrane fluidity in the spinal cord and the brain in an animal model of amyotrophic lateral sclerosis. J Bioenerg Biomembr. 2011;43:181–6. https://doi.org/10.1007/s10863-011-9348-5.
181. Area-Gomez E, Larrea D, Yun T, Xu Y, Hupf J, Zandkarimi F, et al. Lipidomics study of plasma from patients suggest that ALS and PLS are part of a continuum of motor neuron disorders. Sci Rep. 2021;11:13562. https://doi.org/10.1038/s41598-021-92112-3.
182. Ledesma MD, Martin MG, Dotti CG. Lipid changes in the aged brain: effect on synaptic function and neuronal survival. Prog Lipid Res. 2012;51:23–35. https://doi.org/10.1016/j.plipres.2011.11.004.
183. Dyall SC, Michael GJ, Whelpton R, Scott AG, Michael-Titus AT. Dietary enrichment with omega-3 polyunsaturated fatty acids reverses age-related decreases in the GluR2 and NR2B glutamate receptor subunits in rat forebrain. Neurobiol Aging. 2007;28:424–39. https://doi.org/10.1016/j.neurobiolaging.2006.01.002.

Index

Z.-W. Wang (ed.), *Molecular Mechanisms of Neurotransmitter Release*, Advances in Neurobiology 33, https://doi.org/10.1007/978-3-031-34229-5